
THE UNIVERSITY
*of* EDINBURGH


THE UNIVERSITY
*of* EDINBURGH

---

# *Regulation of Calcium Signalling in Murine Corticotrophs*

---

Mengdie DENG

(Supervisor: Michael Shipston)

Presented for the Degree of Doctor of Philosophy

The University of Edinburgh

2019

# *Declaration*

I declare that, except where explicitly stated otherwise in the text, the word described herein is my own, carried out at the Centre for Discovery Brain Sciences, The University of Edinburgh. This thesis was composed by myself and has not been submitted for any other degree or professional qualification.

Mengdie DENG

March 2019

# *Acknowledgements*

I would like to extend thanks to so many people who generously helped and supported me throughout my PhD study.

Firstly, I would like to express my sincere thanks to my supervisor Prof. Michael Shipston for his tremendous support throughout the four years of my PhD. His feedback and guidance helped me direct my research all the time as well as the thesis write-up. His motivation, experience and knowledge are so valuable that really shapes my development as a researcher and formulate my attitude for my career. It's really my pleasure to have this opportunity to work in his lab, which will be the most memorable days in my lifetime.

I am hugely appreciative to Dr Nicola Romanò. I am particularly indebted to Nicola for his guidance in calcium imaging experiments, complicated data analysis and endless patience to my incessant questions. Without your support, I would not be able to achieve success in this work.

I would like to give particular thanks to my fellow labmates. Thanks to Dr Peter J. Duncan and Heather McClafferty for providing me lab training and assistance with biochemical experiments. I have very fond memories of my time in the office with you.

Thanks to Dr Paul Le Tissier for his advice and encouragement that always inspired me when I was in a jam. I am also grateful to all past and present members of the Centre for Discovery Brain Sciences who provided technical support.

Finally, but by no means least, I must express my profound gratitude to my parents for providing me with incredible support and continuing encouragement throughout my studies. I am also grateful to my friends who have all been supportive along the way. This work would not have been possible without the support from my family and friends. Thank you.

# Abstract

Anterior pituitary corticotrophs, the central components of the hypothalamic-pituitary-adrenal (HPA) axis, are important for controlling the neuroendocrine response to stress. In response to a stressor, corticotrophin-releasing hormone (CRH) and arginine vasopressin (AVP) are released from the hypothalamic neuroendocrine neurones and act synergistically on corticotrophs to stimulate the release of adrenocorticotrophin hormone (ACTH). In turn, ACTH stimulates the secretion of glucocorticoids from adrenal glands that exerts negative feedback on the HPA axis. CRH and AVP have been shown to stimulate different patterns of electrical excitability in corticotrophs, with CRH inducing electrical bursting behaviour that is dependent upon large conductance voltage- and calcium-activated potassium (BK) channels whereas AVP-induced spiking is BK channel independent. Although CRH and AVP are known to control intracellular free calcium ($[Ca^{2+}]_i$) by different signalling pathways, several important questions remain. Firstly, most previous studies have examined CRH and/or AVP-evoked changes in calcium signalling in response to a single supraphysiological concentration of secretagogue whereas *in vivo* corticotrophs must respond to repeated changes in CRH and AVP. Secondly, although CRH and AVP synergise at the level of ACTH secretion, whether synergy is also observed at the level of intracellular free calcium is essentially unknown. Thirdly, although CRH and AVP regulate different patterns of electrical excitability, whether CRH-, or AVP-induced calcium signalling

is modified by BK channels is not known. Fourthly, BK channels are subject to regulation by post-translational modifications, such as S-acylation by zDHHC23, however, whether S-acylation controls CRH-induced calcium signalling is not known.

To address these questions and to test the overarching hypothesis that CRH-, but not AVP-induced $[Ca^{2+}]_i$ signalling is dependent upon functional BK channels, a new lentiviral-mediated POMC-GCaMP6s reporter was developed and tested to allow specific labelling of live murine corticotrophs *in vitro* for calcium imaging recordings. $[Ca^{2+}]_i$ signalling was characterised in wild-type corticotrophs under basal conditions and following repeated exposure to pulses of physiological levels of CRH (0.2 nM) and/or AVP (2 nM). Murine wild-type corticotrophs showed highly variable spontaneous $[Ca^{2+}]_i$ signalling. Stimulation with CRH induced a significant sustained and repeatable increase of $[Ca^{2+}]_i$ that lasted longer than the exposure to CRH. In contrast, AVP evoked two phenotypes of $[Ca^{2+}]_i$ responses, oscillations and sustained increases, that were highly reproducible. No significant differences were observed between corticotrophs from male or female mice. Synergistic $[Ca^{2+}]_i$ responses between CRH and AVP were observed in ~ 30% of female wild-type corticotrophs, although this was not significantly different at the population level. However, this was never observed in male corticotrophs.

To test the role of BK channels in $[Ca^{2+}]_i$ responses, we took both genetic and pharmacological approaches. Genetic deletion of BK channels displayed sex differences in regulating corticotroph spontaneous $[Ca^{2+}]_i$ signalling. Repeated CRH stimulation induced significantly reduced $[Ca^{2+}]_i$ responses in male, but not female, BK-KO corticotrophs compared to wild-type controls. However, CRH-evoked $[Ca^{2+}]_i$ signalling was unaffected by acute pharmacological inhibition of BK channels with paxilline suggesting a compensatory mechanism may underlie the change in CRH-evoked $[Ca^{2+}]_i$ responses in BK-KO corticotrophs. Genetic deletion of BK channels had no impact on $[Ca^{2+}]_i$ responses to repeated AVP stimulation in either male or female corticotrophs.

Genetic deletion of the S-acyl transferase zDHHC23 had no significant effect on spontaneous $[Ca^{2+}]_i$ signalling. Both male and female zDHHC23-KO corticotrophs showed a progressive attenuation in $[Ca^{2+}]_i$ responses to repeated CRH stimulation. However, compared to wild-type corticotrophs, $[Ca^{2+}]_i$ responses evoked by repeated CRH or AVP stimulation were unaffected by knockout of zDHHC23 in either male or female corticotrophs.

In conclusion, development of the lentiviral POMC-GCaMP6 calcium reporter allowed analysis of spontaneous and secretagogue-evoked $[Ca^{2+}]_i$ responses

specifically in corticotrophs *in vitro*. CRH evoked sustained elevations of $[Ca^{2+}]_i$ whereas AVP evoked two patterns of $[Ca^{2+}]_i$ response: sustained elevation and oscillation. No significant differences were observed between wild-type male and female corticotrophs although synergy between CRH and AVP was only observed in female corticotrophs. Genetic deletion of BK channels reduced CRH- but not AVP-induced $[Ca^{2+}]_i$ signalling in male but not female corticotrophs. However, this is likely a compensatory mechanism as acute pharmacological inhibition of BK channels in wild-type corticotrophs did not show the same effect. zDHHC23 plays a minor role in regulating $[Ca^{2+}]_i$ signalling in corticotrophs.

Further studies are warranted to investigate the link between changes in electrical excitability, calcium signalling and the control of ACTH release in corticotrophs. The approach developed here should allow us to probe the mechanism of $[Ca^{2+}]_i$ signalling and its regulation that is central to understand the physiological role of corticotrophs and the control of the stress axis.

# Lay Summary

In the 21st century, stress is a pervasive feature of fast-paced life. A variety of situations and events can cause stress, such as injury, noise, fear, financial difficulty and unemployment. Although people can cope with a certain amount of stress in different ways, long-term excessive stress can have a negative impact on their mental and physical health that may eventually lead to a diverse range of stress-related illnesses, including cardiovascular disease, epilepsy, diabetes, hypertension, depression and anxiety disorders. Therefore, understanding how the response to stress is controlled is important for long-term health and well-being.

In response to stress, two hormones, CRH and AVP, are released from the brain to stimulate the secretion of the stress hormone ACTH from cells (corticotrophs) in the pituitary gland at the base of the brain. ACTH stimulates the adrenal gland to secrete steroid hormones that exert powerful effects on most cells in the body. The two brain hormones regulate different patterns of electrical activity of corticotrophs through different molecular signalling pathways. Importantly, activation of these signalling pathways ultimately controls the levels of an important signalling molecule in corticotrophs, calcium ions, that control the release of ACTH. We already know that the movement of potassium ions across the cell membrane through ion channel pores, called BK channels, is important for controlling CRH-, but not AVP-induced electrical

excitability in corticotrophs. However, whether BK channels are also important for controlling CRH-, or AVP-induced calcium signalling is not known. Furthermore, many proteins, including BK channels, are controlled by the addition of fat. It is unknown whether the enzymes that control the addition of fat to BK channels is important for controlling calcium signalling in corticotrophs.

To address these questions, I first engineered a fluorescent protein that responds to calcium by emitting light. This allows specific labelling of live murine corticotrophs *in vitro* to investigate calcium signalling in cells. Most previous studies examined corticotroph calcium signalling in response to a single supraphysiological concentration of brain hormones whereas *in vivo* corticotrophs must respond to repeated pulses of brain hormone. In this study, I established a repeated stimulation protocol that allows robust and repeatable calcium responses to pulses of hormones at physiological concentrations. This replicates the typical secretion pulse of two brain hormones *in vivo*, which may provide valuable insight into how corticotrophs coordinate adaptive responses to different stress. The experimental results suggested that BK channels *per se*, rather than the key enzyme controls the addition of fat to BK channels, play an important role in controlling CRH-, but not AVP-induced calcium signalling in corticotrophs. This study also suggested sex differences in controlling calcium signalling in corticotrophs as the effect of loss of BK channels was only seen

in corticotrophs from male mice.

As the regulation of the calcium signalling pathway may be important for controlling the secretion of the stress hormone and coordination of appropriate stress responses, it is vital to understand the regulation of corticotroph calcium signalling. Further study of the link between the changes in electrical excitability, calcium signalling, and stress hormone secretion would lead to a greater understanding of their role in regulating stress and potentially lead to novel therapeutic targets and drugs for stress-related disorders.

# *Abbreviations*

| | |
|---|---|
| **AC** | adenylate cyclase |
| **ACTH** | adrenocorticotrophic hormone |
| **AD** | Alzheimer's disease |
| **ADH** | antidiuretic hormone |
| **AIC** | Akaike Information Criterion |
| **AM** | acetoxymethyl esters |
| **AP** | action potential |
| **APT** | acyl protein thioesterase |
| **AUC** | area under the curve |
| **AVP** | arginine vasopressin |
| **BAPTA** | 1,2- bis(o-aminophenoxy)ethane-N,N,-N',N'-tetraacetic acid |
| **BIC** | Bayesian Information Criterion |
| **BK channel** | large conductance calcium- and voltage-activated potassium channel |
| **bp** | base pair |
| **BSA** | bovine serum albumin |
| **CAD** | coronary artery disease |
| **CaM** | calmodulin |
| **cAMP** | adenosine-3',5'-cyclic monophosphate (cyclic AMP) |
| **$Ca_v$** | voltage-gated calcium channels (VGCC) |
| **CBG** | corticosteroid binding globulin |
| **cpEGFP** | circularly permuted enhanced green fluorescent protein |
| **CHD** | coronary heart disease |
| **CICR** | calcium-induced calcium release |
| **CRH** | corticotropin-releasing hormone |
| **CRHR1** | CRH receptor type 1 |

| | |
|---|---|
| **CRHR2** | CRH receptor type 2 |
| **CVD** | cardiovascular diseases |
| **DABCO** | 1,4-diazabizyclo[2.2.2]octane |
| **DAG** | diacylglycerol |
| **DEPC** | diethyl pyrocarbonate |
| **DMEM** | Dulbecco's Modified Eagle Medium |
| **DMSO** | dimethyl sulphoxide |
| **DNA** | deoxyibosenucleic acid |
| **DNAse** | deoxyribonuclease |
| **dNTP** | deoxynucleotides triphosphate namely dATP, dCTP, dGTP, dTTP |
| **EDTA** | ethylene diaminetetraacetic acid |
| **EMMs** | estimated marginal means |
| **ER** | endoplasmic reticulum |
| **eYFP** | enhanced yellow fluorescent protein |
| **FRET** | Förester resonance energy transfer |
| **FSH** | follicle-stimulating hormone |
| **GC** | glucocorticoid |
| **GECIs** | genetically encoded calcium indicators |
| **GFP** | green fluorescent protein |
| **GH** | growth hormone |
| **GPCR** | G protein-coupled receptor |
| **GR** | glucocorticoid receptor |
| **HEPES** | N-[2-hydroxyethyl]piperazine-N'-[2-ethanesulphonic acid] |
| **HotSHOT** | hot sodium hydroxide and tris |
| **HPA axis** | hypothalamic-pituitary-adrenal axis |
| **IBD** | inflammatory bowel disease |

| | |
|---|---|
| **IBS** | irritable bowel syndrome |
| **IHD** | ischemic heart disease |
| **IK channel** | intermediate conductance calcium-activated potassium channel |
| **$IP_3$** | inositol 1,4,5-triphosphate |
| **$IP_3R$** | $IP_3$ receptor |
| **ITS** | insulin-transferrin-sodium selenite |
| **$K_{Ca}$** | calcium-activated potassium channel |
| **$K_{ir}$** | inward-rectifier potassium channel |
| **KO** | knockout |
| **LH** | luteinizing hormone |
| **$MC_2$-R** | melanocortin receptor 2 |
| **MDD** | major depressive disorders |
| **mPVN** | magnocellular neurons of PVN |
| **MR** | mineralocorticoid receptor |
| **MSH** | melanocyte stimulating hormone |
| **Mw** | molecular weight |
| **$Na_v$** | voltage-gated $Na^+$ channels |
| **NMDG** | N-methyl-D-glucamine |
| **OGB-1** | Oregon Green BAPTA-1 |
| **PBS** | phosphate buffered saline |
| **PCR** | polymerase chain reaction |
| **$PIP_2$** | phosphatidylinositol 4,5-biphosphate |
| **PKA** | protein kinase A |
| **PKC** | protein kinase C |
| **PLC** | phospholipase C |
| **POMC** | proopiomelanocortin |

| | |
|---|---|
| **PPT** | palmitoyl-protein thioesterase |
| **pPVN** | parvicellular neurons of PVN |
| **PRL** | prolactin |
| **PTM** | post-translational modification |
| **PVN** | paraventricular nucleus |
| **RCK** | regulator of $K^+$ conductance |
| **RNA** | ribose nucleic acid |
| **RyR** | ryanodine receptor |
| **SAM system** | sympathetic–adrenomedullary system |
| **SCN** | suprachiasmatic nucleus |
| **SEM** | standard error of mean |
| **SK channel** | small conductance calcium-activated potassium channel |
| **SON** | supraoptic nucleus |
| **STREX** | stress regulated, or stress axis related exon |
| **STREX channel** | BK channel splice variant that expresses the STREX insert |
| **TBE** | Tris, boric acid, EDTA buffer |
| **$T_m$** | melting temperature |
| **TRAM-34** | 1-[(2-Chlorophenyl)diphenylmethyl]-1H-pyrazole |
| **TREK-1** | TWIK-related potassium channel |
| **TSH** | thyroid-stimulating hormone |
| **TTX** | tetrodotoxin |
| **V1a** | AVP receptor 1a subtype |
| **V1b** | AVP receptor 1b subtype |
| **V2** | AVP receptor 2 subtype |
| **ZERO channel** | BK channel splice variant lacking splice inserts |
| **zDHHC** | zinc-finger containing palmitoyl acyl-transferases |

# *List of Figures and Tables*

**Chapter 1: Introduction 1**

Figure 1.1 The hypothalamic-pituitary-adrenal (HPA) axis 5
Figure 1.2 CRH and AVP act synergistically to regulate ACTH secretion 12
Figure 1.3 Two distinct patterns of electrical activity in corticotrophs 14
Figure 1.4 Schematic illustrating the topology of the BK channel and two S-acylated sites in the pore-forming α-subunit 25
Figure 1.5 Schematic diagram of the ion channels in corticotroph model 28
Figure 1.6 Reversible enzymatic regulation of S-acylation 32

**Chapter 2: Materials and Methods 41**

Table 2.1 List of drugs and dilutions 46
Table 2.2 Primers used for BK-KO genotyping 50
Figure 2.1 Cycling parameters for BK-KO genotyping 50
Table 2.3 Primers used for zDHHC23-KO genotyping 52
Figure 2.2 Cycling parameters for zDHHC23-KO genotyping 53
Figure 2.3 BK-KO genotyping PCR products separated by agarose gel electrophoresis 56
Figure 2.4 zDHHC23-KO genotyping PCR products separated by agarose gel electrophoresis 57
Figure 2.5 Protocols for calcium imaging 66
Figure 2.6 Criteria of a valid calcium imaging recording 68
Figure 2.7 Measurement parameters of calcium imaging recordings 71

**Chapter 3: Calcium signalling in wild-type corticotrophs 75**

Figure 3.1 Identification and labelling of murine corticotrophs by lentiviral transduction of POMC-GCaMP6s reporter 81
Figure 3.2 Definition of spontaneous $[Ca^{2+}]_i$ signalling 84
Figure 3.3 Spontaneous $[Ca^{2+}]_i$ active time is significantly higher in male than female in wild-type corticotrophs 85
Figure 3.4 Representative examples of spontaneous $[Ca^{2+}]_i$ in wild-type corticotrophs 87

Figure 3.5 The maximum amplitude of spontaneous $[Ca^{2+}]_i$ signalling is not different in male and female wild-type corticotrophs 89
Figure 3.6 Stimulation with CRH results in $[Ca^{2+}]_i$ increase in wild-type corticotrophs 90
Figure 3.7 Repeated CRH induces $[Ca^{2+}]_i$ responses in male wild-type corticotrophs 93
Figure 3.8 Stable AUC (10 min) and AUC (peak) of $[Ca^{2+}]_i$ responses in male wild-type corticotrophs to repeated CRH 95
Figure 3.9 Attenuation of peak but not time to peak of $[Ca^{2+}]_i$ responses in male wild-type corticotrophs to repeated CRH 96
Figure 3.10 Response duration and peak duration of $[Ca^{2+}]_i$ responses in male wild-type corticotrophs to repeated CRH 97
Figure 3.11 Time gap of $[Ca^{2+}]_i$ responses in male wild-type corticotrophs to repeated CRH 98
Figure 3.12 Repeated CRH induces $[Ca^{2+}]_i$ responses in female wild-type corticotrophs 100
Figure 3.13 AUC (10 min) but not AUC (peak) of $[Ca^{2+}]_i$ responses is stable in female wild-type corticotrophs to repeated CRH 101
Figure 3.14 Attenuation of peak but not time to peak of $[Ca^{2+}]_i$ responses in female wild-type corticotrophs to repeated CRH 102
Figure 3.15 Response duration and peak duration of $[Ca^{2+}]_i$ responses in female wild-type corticotrophs to repeated CRH 103
Figure 3.16 Time gap of $[Ca^{2+}]_i$ responses in female wild-type corticotrophs to repeated CRH 104
Figure 3.17 No significant sex difference in CRH-induced AUC (10 min) or AUC (peak) of $[Ca^{2+}]_i$ responses in wild-type corticotrophs 106
Figure 3.18 No significant sex difference in CRH-induced peak, time to peak or response duration of $[Ca^{2+}]_i$ responses in wild-type corticotrophs 107
Figure 3.19 No significant sex difference in CRH-induced peak duration or time gap of $[Ca^{2+}]_i$ responses in wild-type corticotrophs 108
Figure 3.20 Nifedipine inhibits CRH-induced $[Ca^{2+}]_i$ response in male wild-type corticotrophs 110
Figure 3.21 Nifedipine significantly reduced CRH-induced AUC (10 min) and AUC (peak) of $[Ca^{2+}]_i$ responses in male wild-type corticotrophs

112

Figure 3.22 Nifedipine significantly reduced CRH-induced peak of $[Ca^{2+}]_i$ responses in male wild-type corticotrophs 113

Figure 3.23 Stimulation with AVP results in two phenotypes of $[Ca^{2+}]_i$ responses in wild-type corticotrophs 115

Figure 3.24 Repeated AVP induces consistent $[Ca^{2+}]_i$ responses in male wild-type corticotrophs 117

Figure 3.25 Stable AUC (10 min) and AUC (peak) of $[Ca^{2+}]_i$ responses in male wild-type corticotrophs to repeated AVP 119

Figure 3.26 Peak and time to peak of $[Ca^{2+}]_i$ responses in male wild-type corticotrophs to repeated AVP 120

Figure 3.27 Response duration and peak duration of $[Ca^{2+}]_i$ responses in male wild-type corticotrophs to repeated AVP 121

Figure 3.28 Time gap of $[Ca^{2+}]_i$ responses in male wild-type corticotrophs to repeated AVP 122

Figure 3.29 Repeated AVP induces consistent $[Ca^{2+}]_i$ responses in female wild-type corticotrophs 124

Figure 3.30 Stable AUC (10 min) and AUC (peak) of $[Ca^{2+}]_i$ responses in female wild-type corticotrophs to repeated AVP 126

Figure 3.31 Attenuation of peak but not time to peak of $[Ca^{2+}]_i$ responses in female wild-type corticotrophs to repeated AVP 127

Figure 3.32 Response duration and peak duration of $[Ca^{2+}]_i$ responses in female wild-type corticotrophs to repeated AVP 128

Figure 3.33 Time gap of $[Ca^{2+}]_i$ responses in female wild-type corticotrophs to repeated AVP 129

Figure 3.34 No significant sex difference in AVP-induced AUC (10 min) or AUC (peak) of $[Ca^{2+}]_i$ responses in wild-type corticotrophs 131

Figure 3.35 Female wild-type corticotrophs have longer response duration but not peak or time to peak of $[Ca^{2+}]_i$ responses to repeated AVP compared to males 132

Figure 3.36 No significant sex difference in AVP-induced peak duration or time gap of $[Ca^{2+}]_i$ responses in wild-type corticotrophs 133

Figure 3.37 CRH, AVP and CRH/AVP induce $[Ca^{2+}]_i$ responses in male wild-type corticotrophs 136

Figure 3.38 AVP, CRH and CRH/AVP induce $[Ca^{2+}]_i$ responses in male wild-type

corticotrophs 137
Figure 3.39 No synergistic $[Ca^{2+}]_i$ response between CRH and AVP in male wild-type corticotrophs 139
Figure 3.40 CRH/AVP induces longer response duration but not peak or time to peak of $[Ca^{2+}]_i$ responses in male wild-type corticotrophs 140
Figure 3.41 CRH/AVP induces longer peak duration but not time gap of $[Ca^{2+}]_i$ responses in male wild-type corticotrophs 141
Figure 3.42 CRH, AVP and CRH/AVP induce $[Ca^{2+}]_i$ responses in female wild-type corticotrophs 144
Figure 3.43 AVP, CRH and CRH/AVP induce $[Ca^{2+}]_i$ responses in female wild-type corticotrophs 145
Figure 3.44 No synergistic $[Ca^{2+}]_i$ response between CRH and AVP in female wild-type corticotrophs 147
Figure 3.45 Peak, time to peak and response duration of $[Ca^{2+}]_i$ responses to CRH, AVP and CRH/AVP in female wild-type corticotrophs 148
Figure 3.46 AVP induces longer time gap but not peak duration of $[Ca^{2+}]_i$ response in female wild-type corticotrophs 149
Figure 3.47 No significant sex difference in AUC (10 min) or AUC (peak) of $[Ca^{2+}]_i$ responses to CRH, AVP and CRH/AVP in wild-type corticotrophs 151
Figure 3.48 No significant sex difference in peak, time to peak, response duration or peak duration of $[Ca^{2+}]_i$ responses to CRH, AVP and CRH/AVP in wild-type corticotrophs 152
Figure 3.49 No significant sex difference in time gap of $[Ca^{2+}]_i$ responses to CRH, AVP and CRH/AVP in wild-type corticotrophs 153

**Chapter 4: Calcium signalling in BK-KO corticotrophs 163**

Figure 4.1 Spontaneous $[Ca^{2+}]_i$ active time is significantly higher in female than male in BK-KO corticotrophs 168
Figure 4.2 The maximum amplitude of spontaneous $[Ca^{2+}]_i$ signalling is not different between male and female BK-KO corticotrophs 170
Figure 4.3 Genetic deletion of BK channels results in an increase in spontaneous $[Ca^{2+}]_i$ active time in female corticotrophs 171
Figure 4.4 Repeated CRH induces $[Ca^{2+}]_i$ responses in male BK-KO

corticotrophs 174
Figure 4.5 Stable AUC (10 min) and AUC (peak) $[Ca^{2+}]_i$ responses in male BK-KO corticotrophs to repeated CRH 176
Figure 4.6 Peak and time to peak of $[Ca^{2+}]_i$ responses in male BK-KO corticotrophs to repeated CRH 177
Figure 4.7 Response duration and peak duration of $[Ca^{2+}]_i$ responses in male BK-KO corticotrophs to repeated CRH 178
Figure 4.8 Time gap of $[Ca^{2+}]_i$ responses in male BK-KO corticotrophs to repeated CRH 179
Figure 4.9 Repeated CRH induces $[Ca^{2+}]_i$ responses in female BK-KO corticotrophs 181
Figure 4.10 Attenuated AUC (peak) but not AUC (10 min) of $[Ca^{2+}]_i$ responses in female BK-KO corticotrophs to repeated CRH 182
Figure 4.11 Peak and time to peak of $[Ca^{2+}]_i$ responses in female BK-KO corticotrophs to repeated CRH 183
Figure 4.12 Response duration and peak duration of $[Ca^{2+}]_i$ responses in female BK-KO corticotrophs to repeated CRH 184
Figure 4.13 Time gap of $[Ca^{2+}]_i$ responses in female BK-KO corticotrophs to repeated CRH 185
Figure 4.14 Female BK-KO corticotrophs have higher AUC (10 min) and AUC (peak) of $[Ca^{2+}]_i$ responses to repeated CRH compared to males 187
Figure 4.15 Female BK-KO corticotrophs have higher peak but not time to peak or response duration of $[Ca^{2+}]_i$ responses to repeated CRH compared to males 188
Figure 4.16 No significant sex difference in CRH-induced peak duration or time gap of $[Ca^{2+}]_i$ responses in BK-KO corticotrophs 189
Figure 4.17 Suppressed AUC (10 min) and AUC (peak) of $[Ca^{2+}]_i$ responses in male BK-KO corticotrophs to repeated CRH compared to male wild-type corticotrophs 191
Figure 4.18 Suppressed peak but not time to peak or response duration of $[Ca^{2+}]_i$ responses in male BK-KO corticotrophs to repeated CRH compared to male wild-type corticotrophs 192
Figure 4.19 No significant differences in CRH-induced peak duration and time gap $[Ca^{2+}]_i$ responses between male wild-type and BK-KO corticotrophs 193

Figure 4.20 Paxilline has no significant inhibition on CRH-induced $[Ca^{2+}]_i$ response in male BK-KO corticotrophs 195
Figure 4.21 Pharmacological inhibition of BK channels has no significant effect on CRH-induced AUC (10 min) and AUC (peak) of $[Ca^{2+}]_i$ responses in male corticotrophs 197
Figure 4.22 Pharmacological inhibition of BK channels has no significant effect on CRH-induced peak of $[Ca^{2+}]_i$ responses in male corticotrophs 198
Figure 4.23 No significant differences in CRH-induced AUC (10 min) or AUC (peak) of $[Ca^{2+}]_i$ responses between female wild-type and BK-KO corticotrophs 200
Figure 4.24 No significant differences in CRH-induced peak, time to peak or response duration of $[Ca^{2+}]_i$ responses between female wild-type and BK-KO corticotrophs 201
Figure 4.25 No significant differences in CRH-induced peak duration or time gap of $[Ca^{2+}]_i$ responses between female wild-type and BK-KO corticotrophs 202
Figure 4.26 Paxilline has no significant inhibition on CRH-induced $[Ca^{2+}]_i$ response in female BK-KO corticotrophs 204
Figure 4.27 Pharmacological inhibition of BK channels has no significant effect on CRH-induced AUC (10 min) and AUC (peak) of $[Ca^{2+}]_i$ responses in female corticotrophs 205
Figure 4.28 Pharmacological inhibition of BK channels has no significant effect on CRH-induced peak of $[Ca^{2+}]_i$ responses in female corticotrophs 206
Figure 4.29 Repeated AVP induces repeatable $[Ca^{2+}]_i$ responses in male BK-KO corticotrophs 210
Figure 4.30 Stable AUC (10 min) and AUC (peak) of $[Ca^{2+}]_i$ responses in male BK-KO corticotrophs to repeated AVP 211
Figure 4.31 Peak and time to peak of $[Ca^{2+}]_i$ responses in male BK-KO corticotrophs to repeated AVP 212
Figure 4.32 Response duration and peak duration of $[Ca^{2+}]_i$ responses in male BK-KO corticotrophs to repeated AVP 213
Figure 4.33 Time gap of $[Ca^{2+}]_i$ responses in male BK-KO corticotrophs to repeated AVP 214

Figure 4.34 Repeated AVP induces repeatable $[Ca^{2+}]_i$ responses in female BK-KO corticotrophs 216
Figure 4.35 Stable AUC (10 min) and AUC (peak) of $[Ca^{2+}]_i$ responses in female BK-KO corticotrophs to repeated AVP 218
Figure 4.36 Peak and time to peak of $[Ca^{2+}]_i$ responses in female BK-KO corticotrophs to repeated AVP 219
Figure 4.37 Response duration and peak duration of $[Ca^{2+}]_i$ responses in female BK-KO corticotrophs to repeated AVP 220
Figure 4.38 Time gap of $[Ca^{2+}]_i$ responses in female BK-KO corticotrophs to repeated AVP 221
Figure 4.39 No significant sex difference in AVP-induced AUC (10 min) or AUC (peak) of $[Ca^{2+}]_i$ responses in BK-KO corticotrophs 223
Figure 4.40 Female BK-KO corticotrophs have longer response duration but not peak or time to peak of $[Ca^{2+}]_i$ responses to repeated AVP compared to males 224
Figure 4.41 Female BK-KO corticotrophs have longer peak duration but not time gap of $[Ca^{2+}]_i$ responses to repeated AVP compared to males 225
Figure 4.42 No significant differences in AVP-induced AUC (10 min) or AUC (peak) of $[Ca^{2+}]_i$ responses between male wild-type and BK-KO corticotrophs 227
Figure 4.43 No significant differences in AVP-induced peak, time to peak or response duration of $[Ca^{2+}]_i$ responses between male wild-type and BK-KO corticotrophs 228
Figure 4.44 No significant differences in AVP-induced peak duration or time gap of $[Ca^{2+}]_i$ responses between male wild-type and BK-KO corticotrophs 229
Figure 4.45 No significant differences in AVP-induced AUC (10 min) or AUC (peak) of $[Ca^{2+}]_i$ responses between female wild-type and BK-KO corticotrophs 230
Figure 4.46 Female BK-KO corticotrophs have longer response duration but not peak or time to peak of $[Ca^{2+}]_i$ responses to repeated AVP compared to female wild-type corticotrophs 231
Figure 4.47 Female BK-KO corticotrophs have longer peak duration but not time gap of $[Ca^{2+}]_i$ responses to repeated AVP compared to female wild-type corticotrophs 232

Figure 4.48 CRH, AVP and CRH/AVP induce $[Ca^{2+}]_i$ responses in female BK-KO corticotrophs 236
Figure 4.49 AVP, CRH and CRH/AVP induce $[Ca^{2+}]_i$ responses in female BK-KO corticotrophs 237
Figure 4.50 No synergistic $[Ca^{2+}]_i$ responses to CRH/AVP in female BK-KO corticotrophs 239
Figure 4.51 CRH induces longer response duration but not peak or time to peak of $[Ca^{2+}]_i$ responses in female BK-KO corticotrophs 240
Figure 4.52 Peak duration and time gap of $[Ca^{2+}]_i$ responses to CRH, AVP and CRH/AVP in female BK-KO corticotrophs 241
Table 4.1 Summary of major findings in results 242

**Chapter 5: Calcium signalling in zDHHC23-KO corticotrophs 257**

Figure 5.1 The active time of spontaneous $[Ca^{2+}]_i$ signalling is not different between male and female zDHHC23-KO corticotrophs 262
Figure 5.2 The maximum amplitude of spontaneous $[Ca^{2+}]_i$ signalling is not different between male and female zDHHC23-KO corticotrophs 264
Figure 5.3 Genetic deletion of zDHHC23 has no effect on spontaneous $[Ca^{2+}]_i$ signalling in corticotrophs 266
Figure 5.4 Progressive attenuation of $[Ca^{2+}]_i$ responses in male zDHHC23-KO corticotrophs to repeated CRH 268
Figure 5.5 Attenuation of AUC (10 min) and AUC (peak) of $[Ca^{2+}]_i$ responses in male zDHHC23-KO corticotrophs to repeated CRH 270
Figure 5.6 Attenuation of peak but not time to peak of $[Ca^{2+}]_i$ responses in male zDHHC23-KO corticotrophs to repeated CRH 271
Figure 5.7 Response duration and peak duration of $[Ca^{2+}]_i$ responses in male zDHHC23-KO corticotrophs to repeated CRH 272
Figure 5.8 Time gap of $[Ca^{2+}]_i$ responses in male zDHHC23-KO corticotrophs to repeated CRH 273
Figure 5.9 Progressive attenuation of $[Ca^{2+}]_i$ responses in female zDHHC23-KO corticotrophs to repeated CRH 275
Figure 5.10 Attenuation of AUC (10 min) and AUC (peak) of $[Ca^{2+}]_i$ responses in female zDHHC23-KO corticotrophs to repeated CRH 276

Figure 5.11 Attenuation of peak but not time to peak of $[Ca^{2+}]_i$ responses in female zDHHC23-KO corticotrophs to repeated CRH 277

Figure 5.12 Response duration and peak duration of $[Ca^{2+}]_i$ responses in female zDHHC23-KO corticotrophs to repeated CRH 278

Figure 5.13 Time gap of $[Ca^{2+}]_i$ responses in female zDHHC23-KO corticotrophs to repeated CRH 279

Figure 5.14 AUC (peak) but not AUC (10 min) of $[Ca^{2+}]_i$ responses to repeated CRH are significantly different between female and male zDHHC23-KO corticotrophs 281

Figure 5.15 Female zDHHC23-KO corticotrophs have higher response duration but not peak or time to peak of $[Ca^{2+}]_i$ responses to repeated CRH compared to males 282

Figure 5.16 No significant sex difference in CRH-induced peak duration or time gap $[Ca^{2+}]_i$ responses in zDHHC23-KO corticotrophs 283

Figure 5.17 No significant differences in CRH-induced AUC (10 min) or AUC (peak) of $[Ca^{2+}]_i$ responses between male wild-type and zDHHC23-KO corticotrophs 285

Figure 5.18 No significant differences in CRH-induced peak, time to peak or response duration of $[Ca^{2+}]_i$ responses between male wild-type and zDHHC23-KO corticotrophs 286

Figure 5.19 No significant differences in CRH-induced peak duration or time gap of $[Ca^{2+}]_i$ responses between male wild-type and zDHHC23-KO corticotrophs 287

Figure 5.20 No significant differences in CRH-induced AUC (10 min) and AUC (peak) of $[Ca^{2+}]_i$ responses between female wild-type and zDHHC23-KO corticotrophs 289

Figure 5.21 No significant differences in CRH-induced peak, time to peak or response duration of $[Ca^{2+}]_i$ responses between female wild-type and zDHHC23-KO corticotrophs 290

Figure 5.22 No significant differences in CRH-induced peak duration or time gap of $[Ca^{2+}]_i$ responses between female wild-type and zDHHC23-KO corticotrophs 291

Figure 5.23 Repeated AVP induces repeatable $[Ca^{2+}]_i$ responses in male zDHHC23-KO corticotrophs 294

Figure 5.24 Stable AUC (10 min) and AUC (peak) of $[Ca^{2+}]_i$ responses in male

zDHHC23-KO corticotrophs to repeated AVP 296
Figure 5.25 Peak and time to peak of $[Ca^{2+}]_i$ responses in male zDHHC23-KO corticotrophs to repeated AVP 297
Figure 5.26 Response duration and peak duration of $[Ca^{2+}]_i$ responses in male zDHHC23-KO corticotrophs to repeated AVP 298
Figure 5.27 Time gap of $[Ca^{2+}]_i$ responses in male zDHHC23-KO corticotrophs to repeated AVP 299
Figure 5.28 Repeated AVP induces repeatable $[Ca^{2+}]_i$ responses in female zDHHC23-KO corticotrophs 301
Figure 5.29 Stable AUC (10 min) and AUC (peak) of $[Ca^{2+}]_i$ responses in female zDHHC23-KO corticotrophs to repeated AVP 302
Figure 5.30 Peak and time to peak of $[Ca^{2+}]_i$ responses in female zDHHC23-KO corticotrophs to repeated AVP 303
Figure 5.31 Response duration and peak duration of $[Ca^{2+}]_i$ responses in female zDHHC23-KO corticotrophs to repeated AVP 304
Figure 5.32 Time gap of $[Ca^{2+}]_i$ responses in female zDHHC23-KO corticotrophs to repeated AVP 305
Figure 5.33 No significant sex difference in AVP-induced AUC (10 min) or AUC (peak) of $[Ca^{2+}]_i$ responses in zDHHC23-KO corticotrophs 307
Figure 5.34 No significant sex difference in AVP-induced peak, time to peak or response duration of $[Ca^{2+}]_i$ responses in zDHHC23-KO corticotrophs 308
Figure 5.35 No significant sex difference in AVP-induced peak duration or time gap of $[Ca^{2+}]_i$ responses in zDHHC23-KO corticotrophs 309
Figure 5.36 No significant differences in AVP-induced AUC (10 min) or AUC (peak) $[Ca^{2+}]_i$ responses between male wild-type and zDHHC23-KO corticotrophs 311
Figure 5.37 No significant differences in AVP-induced peak, time to peak or response duration $[Ca^{2+}]_i$ responses between male wild-type and zDHHC23-KO corticotrophs 312
Figure 5.38 No significant differences in AVP-induced peak duration or time gap $[Ca^{2+}]_i$ responses between male wild-type and zDHHC23-KO corticotrophs 313
Figure 5.39 No significant differences in AVP-induced AUC (10 min) or AUC (peak) of $[Ca^{2+}]_i$ responses between female wild-type and

zDHHC23-KO corticotrophs 315
Figure 5.40 No significant differences in AVP-induced peak, time to peak or response duration of $[Ca^{2+}]_i$ responses between female wild-type and zDHHC23-KO corticotrophs 316
Figure 5.41 No significant differences in AVP-induced peak duration or time gap of $[Ca^{2+}]_i$ responses between female wild-type and zDHHC23-KO corticotrophs 317
Figure 5.42 CRH, AVP and CRH/AVP induce $[Ca^{2+}]_i$ responses in male zDHHC23-KO corticotrophs 320
Figure 5.43 AVP, CRH and CRH/AVP induce $[Ca^{2+}]_i$ responses in male zDHHC23-KO corticotrophs 321
Figure 5.44 No synergistic $[Ca^{2+}]_i$ response to CRH/AVP in male zDHHC23-KO corticotrophs 323
Figure 5.45 Peak, time to peak and response duration of $[Ca^{2+}]_i$ responses to CRH, AVP and CRH/AVP in male zDHHC23-KO corticotrophs 324
Figure 5.46 Peak duration and time gap of $[Ca^{2+}]_i$ responses to CRH, AVP and CRH/AVP in male zDHHC23-KO corticotrophs 325
Figure 5.47 CRH, AVP and CRH/AVP induce $[Ca^{2+}]_i$ responses in female zDHHC23-KO corticotrophs 327
Figure 5.48 AVP, CRH and CRH/AVP induce $[Ca^{2+}]_i$ responses in female zDHHC23-KO corticotrophs 328
Figure 5.49 No synergistic $[Ca^{2+}]_i$ responses to CRH/AVP in female zDHHC23-KO corticotrophs 330
Figure 5.50 Peak, time to peak and response duration of $[Ca^{2+}]_i$ responses to CRH, AVP and CRH/AVP in female zDHHC23-KO corticotrophs 331
Figure 5.51 Peak duration and time gap of $[Ca^{2+}]_i$ responses to CRH, AVP and CRH/AVP in female zDHHC23-KO corticotrophs 332
Figure 5.52 No significant sex difference in AUC (10 min) or AUC (peak) of $[Ca^{2+}]_i$ responses to CRH, AVP and CRH/AVP in zDHHC23-KO corticotrophs 334
Figure 5.53 No significant sex difference in peak, time to peak, response duration or peak duration of $[Ca^{2+}]_i$ responses to CRH, AVP and CRH/AVP in zDHHC23-KO corticotrophs 335
Figure 5.54 No significant sex difference in time gap of $[Ca^{2+}]_i$ responses to CRH,

AVP and CRH/AVP in zDHHC23-KO corticotrophs 336

**Chapter 6: General discussion and future work 343**

Figure 6.1 Schematic diagram of different timescale between global $[Ca^{2+}]_i$ signalling and electrical activity in corticotrophs 347

# Table of Contents

**Declaration** i
**Acknowledgements** ii
**Abstract** iv
**Lay Summary** viii
**Abbreviations** xi
**List of Figures and Tables** xv
**Table of Contents** xxvii

**Chapter 1: Introduction** 1

1.1 Stress and health 2
1.2 The hypothalamic-pituitary-adrenal (HPA) axis 4
1.3 Anterior pituitary corticotrophs in the control of the HPA axis 9
*1.3.1 The regulation of corticotrophs 9*
*1.3.2 Calcium signalling in corticotrophs 13*
*1.3.3 Excitability of corticotrophs 21*
*1.3.4 The role of BK channels in corticotroph excitability 24*
1.4 S-acylation controls BK channel properties and function 29
*1.4.1 S-acylation and its enzymatic regulation 29*
*1.4.2 Regulation of BK channels by S-acylation 31*
1.5 Sex differences in HPA axis 35
1.6 Hypothesis, aims and objectives 38

**Chapter 2: Materials and Methods** 41

2.1 Materials 42
2.2 Animals 47
*2.2.1 Animals 47*
*2.2.2 Mouse PCR genotyping 47*
2.3 Generation of POMC-GCaMP6s lentivirus 55
2.4 Primary cell culture and lentiviral transduction of mouse anterior pituitary cells 58

*2.4.1 Isolation and culture of mouse anterior pituitary cells* *58*
*2.4.2 Lentiviral transduction of mouse anterior pituitary cells* *59*
*2.4.3 Validation and quantification of lentiviral transduction* *60*
2.5 Calcium imaging 62
*2.5.1 Calcium imaging recordings* *62*
*2.5.2 Calcium imaging protocols* *63*
2.6 Data analysis 67
*2.6.1 Acquisition of data from images* *67*
*2.6.2 Measurement parameters* *67*
*2.6.3 Statistical analysis* *72*

**Chapter 3: Calcium signalling in wild-type corticotrophs 75**

3.1 Introduction 76
*3.1.1 Identification of corticotrophs* *76*
*3.1.2 Calcium signalling in corticotrophs* *77*
3.2 Results 79
*3.2.1 Identification and labelling of mouse corticotrophs with a lentiviral POMC-GCaMP6s reporter* *79*
*3.2.2 Wild-type corticotrophs show variable spontaneous $[Ca^{2+}]_i$ signalling* *80*
*3.2.3 CRH stimulation increases $[Ca^{2+}]_i$ signalling in wild-type corticotrophs* *88*
*3.2.4 AVP-induced $[Ca^{2+}]_i$ responses are consistent in wild-type corticotrophs* *111*
*3.2.5 Do wild-type corticotrophs display synergy between CRH and AVP at the level of intracellular free calcium?* *130*
3.3 Discussion 154
*3.3.1 Specific labelling of murine corticotrophs and spontaneous $[Ca^{2+}]_i$ in wild-type murine corticotrophs* *155*
*3.3.2 CRH induces sustained $[Ca^{2+}]_i$ increase in wild-type corticotrophs* *157*
*3.3.3 AVP induces two patterns of $[Ca^{2+}]_i$ responses* *158*
*3.3.4 Lack of synergistic $[Ca^{2+}]_i$ responses to CRH and AVP* *159*
3.4 Chapter summary 160

**Chapter 4: Calcium signalling in BK-KO corticotrophs 163**

4.1 Introduction 164

*4.1.1 BK channels regulate corticotroph activity 164*

4.2 Results 166

*4.2.1 Genetic deletion of BK channels differentially controls spontaneous $[Ca^{2+}]_i$ signalling in male and female corticotrophs 166*

*4.2.2 CRH-induced $[Ca^{2+}]_i$ responses are suppressed in male but not female BK-KO corticotrophs 172*

*4.2.3 Genetic deletion of BK channels has no significant effect on AVP-induced $[Ca^{2+}]_i$ responses in male and female corticotrophs 207*

*4.2.4 Do BK-KO corticotrophs display synergy between CRH and AVP at the level of intracellular free calcium? 233*

4.3 Discussion 243

*4.3.1 CRH-induced $[Ca^{2+}]_i$ responses are suppressed in male BK-KO corticotrophs but not affected by acute pharmacological inhibition of BK channels in wild-type corticotrophs 243*

*4.3.2 AVP-induced $[Ca^{2+}]_i$ responses are unaffected by genetic deletion of BK channels in both male and female corticotrophs 251*

4.4 Chapter summary 254

**Chapter 5: Calcium signalling in zDHHC23-KO corticotrophs 257**

5.1 Introduction 258

*5.1.1 S-acylation is regulated by zDHHCs 258*

*5.1.2 BK channels are modulated by S-acylation 259*

5.2 Results 261

*5.2.1 Genetic deletion of zDHHC23 has no effect on spontaneous $[Ca^{2+}]_i$ in corticotrophs 261*

*5.2.2 Progressive attenuation of $[Ca^{2+}]_i$ responses to repeated CRH stimulation in zDHHC23-KO corticotrophs 265*

*5.2.3 Genetic deletion of zDHHC23 has no significant effect on AVP-induced $[Ca^{2+}]_i$ responses in male and female corticotrophs 288*

*5.2.4 Do zDHHC23-KO corticotrophs show synergy between CRH and AVP at the level of intracellular free calcium? 314*

5.3 Discussion 337

*5.3.1 Progressive attenuation of CRH-induced $[Ca^{2+}]_i$ responses in zDHHC23-KO corticotrophs 338*
*5.3.2 Does zDHHC23 control the pattern of AVP-evoked $[Ca^{2+}]_i$ responses in corticotrophs? 340*
5.4 Chapter summary 342

**Chapter 6: General discussion and future work 343**
6.1 Hypothesis and aims 344
6.2 Discussion and future work 344
*6.2.1 CRH-induced $[Ca^{2+}]_i$ responses are suppressed in male BK-KO corticotrophs 344*
*6.2.2 Genetic deletion of BK channels or zDHHC23 have no effect on AVP-induced $[Ca^{2+}]_i$ responses in corticotrophs 351*
*6.2.3 Lack of synergistic $[Ca^{2+}]_i$ responses to CRH and AVP 352*
6.3 Conclusion 355

**References 359**

**Appendices 373**
I. The UI script 374
II. The Sever script 376

# Chapter One: Introduction

# Chapter 1: Introduction

## 1.1 Stress and health

In the 21st century, stress is a ubiquitous condition in our daily life. Everyone experiences different stressful situations. A recent survey found that 74% of people in the UK felt overwhelmed in dealing with stress (Mental Health Foundation, 2018) and this has led to an increasing number of stress-related illnesses.

How to define stress? The modern concept of stress recognizes stress as a real or sensed threat to disrupt homeostasis, which is a dynamic state of equilibrium in living organisms. Any situations or events causing stress are known as a stressor. Stressors can be generally divided into two broad categories: physiological stressors including pain, injury, noise and temperature extremes; and psychological stressors such as anxiety, frustration, interpersonal issues and unemployment. Both types of stressors can result in an elevated release of glucocorticoids, which act to increase the level of blood glucose as well as regulate multiple physiological functions including fat and protein metabolism (Herman *et al.*, 2003; Spiga *et al.*, 2014). Glucocorticoids thus also play an important role in human energy balance and dysregulation of glucocorticoid secretion may contribute to the development of obesity and metabolic syndrome (Nieuwenhuizen & Rutters, 2008).

Acute stress might be good for humans by providing positive stimuli to emotional and intellectual growth and development (Chrousos & Gold, 1992). However, chronic stress has a negative impact on both physical and psychological health. Existing evidence suggests a consistent association between stress and the risk of cardiovascular disease, and chronic stress also predicts the emergence of coronary heart disease (CHD) (Krantz & McCeney, 2002; Steptoe & Mika Kivimäki, 2012). Exposure to stress may alter brain-gut interactions which leads to a range of gastrointestinal disorders such as irritable bowel syndrome (IBS) and inflammatory bowel disease (IBD) (Konturek *et al.*, 2011). Long-term stress can also dysregulate the human immune system (Morey *et al.*, 2015), which may also be linked to the onset of depression (Slavich & Irwin, 2014). Stress is also a major contributing factor to major depressive disorders with approximately 80% of community cases of major depression being preceded by stressors (Mazure, 1998; Stroud *et al.*, 2008). Moreover, stress has been suggested to contribute to the initiation and development of selected cancer types (Heffner *et al.*, 2003; Antoni *et al.*, 2006).

Stress evokes adaptive physiological and behavioural responses to reinstate the internal environment, which is important in ensuring the survival of organisms. The activation of the sympathetic-adrenomedullary (SAM) and hypothalamic-pituitary-adrenal (HPA) neuroendocrine systems leads to the release of catecholamines

and glucocorticoids (GCs, specifically cortisol in humans and corticosterone in rodents) respectively to regulate many physiological functions.

## 1.2 The hypothalamic-pituitary-adrenal (HPA) axis

The hypothalamic-pituitary-adrenal (HPA) axis is the major neuroendocrine system activated in response to stress and maintains body homeostasis (Figure 1.1). Physical or emotional stressors are perceived and conveyed via numerous neural pathways in the brain that eventually activate the paraventricular nucleus (PVN) of the hypothalamus (Herman *et al.*, 2003). The excitation of PVN neurons results in the release of corticotrophin releasing hormone (CRH) and arginine vasopressin (AVP) into the pituitary portal circulation. CRH and AVP act synergistically on anterior pituitary corticotrophs to enhance the secretion of adrenocorticotrophin hormone (ACTH) (Gillies *et al.*, 1982; Lamberts *et al.*, 1984).

The pituitary gland is located within a protective recess of the sphenoid bone (sella turcica) underneath the hypothalamus at the base of the brain. The pituitary gland is connected to the hypothalamus by the pituitary stalk and comprised of two functionally and morphologically distinct structures: the adenohypophysis (including anterior and intermediate lobes) and the neurohypophysis (posterior lobe). In contrast to the presence of a clearly defined intermediate lobe in mice and rats, it is largely absent in

## Figure 1.1

### The hypothalamic-pituitary-adrenal (HPA) axis

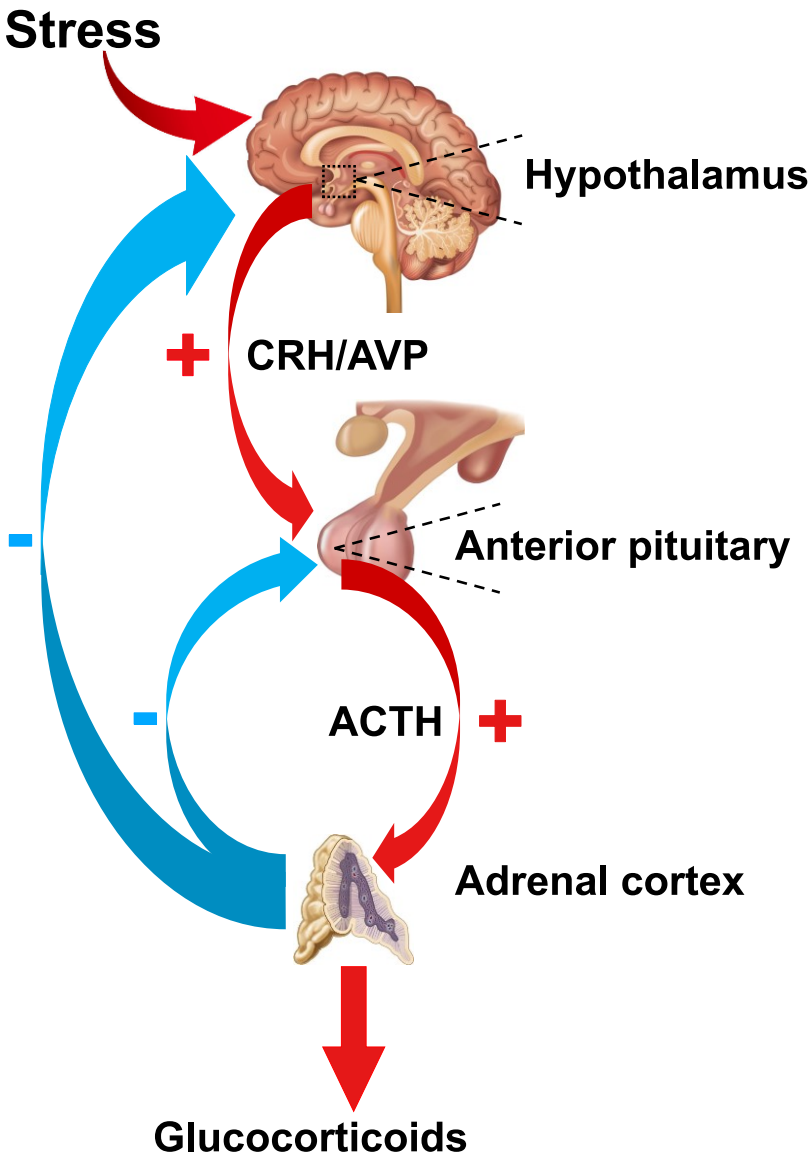


**Figure 1.1 The hypothalamic-pituitary-adrenal (HPA) axis.** The HPA axis is the major neuroendocrine system activated in response to stress. Following stimulation, corticotrophin-releasing hormone (CRH) and arginine vasopressin (AVP) are released from hypothalamic neuroendocrine neurones, which stimulate the synthesis and secretion of the stress hormone adrenocorticotrophin (ACTH) from corticotrophs in the anterior pituitary gland. ACTH then stimulates the synthesis and release of glucocorticoids from the adrenal cortex. In turn, glucocorticoids exert a negative feedback of the HPA axis at the level of both the pituitary and the hypothalamus.

humans. The anterior and intermediate lobes are derived from oral ectoderm and forms Rathke's pouch, whereas the posterior lobe is neuroectodermal origin (Kelberman *et al.*, 2009; Stojilkovic *et al.*, 2010). The posterior lobe secretes antidiuretic hormone (ADH, also known as vasopressin) and oxytocin, which are synthesized and released from neurones of the supraoptic and paraventricular nuclei of the hypothalamus respectively. The intermediate lobe produces and releases melanocyte-stimulating hormone (MSH) from melanotrophs. The anterior lobe is composed of five endocrine cell types with different relative proportions: somatotrophs (up to 50%), lactotrophs (10–25%), gonadotrophs (10–15%), thyrotrophs (< 10%) and corticotrophs (2–15%), with each cell type secreting different hormones: growth hormone (GH), prolactin (PRL), luteinizing hormone (LH) and follicle-stimulating hormone (FSH), thyroid-stimulating hormone (TSH) and ACTH respectively. The anterior lobe also contains 5–10% of non-endocrine folliculostellate cells (Ooi *et al.*, 2004; Yeung *et al.*, 2006; Stojilkovic *et al.*, 2010).

ACTH, a 39 amino acid peptide, is produced as a part of large precursor proopiomelanocortin (POMC), a 241 amino acid peptide (Raffin-Sanson *et al.*, 2003). Following CRH and/or AVP stimulation, ACTH is released from corticotrophs and transported via the systemic circulation to stimulate the synthesis and secretion of glucocorticoids from the zona fasciculata of the adrenal by acting on type 2

melanocortin receptors (MC2-R). Approximately 90–95% of plasma cortisol in humans is bound to proteins including corticosteroid binding globulin (CBG) and serum albumin, while only 5–10% of the total plasma cortisol circulates in an unbound state which is biologically active (Kudielka & Kirschbaum, 2005). Glucocorticoids are involved in the physiological adaptations to cope with stress and exert a negative feedback of the HPA axis at the level of both the pituitary and the hypothalamus. Two types of glucocorticoid receptor are involved in the feedback mechanisms: a high affinity mineralocorticoid receptor (MR, type I), which is present in the hypothalamus and highly expressed in the hippocampus; and a low-affinity glucocorticoid receptor (GR, type II), which is expressed throughout the brain but mainly in hypothalamic neurons and corticotrophs (Ratka *et al.*, 1989; Joëls & de Kloet, 1992). Feedback inhibition of HPA axis is principally mediated via the GRs, which are activated through binding of glucocorticoids and then translocate into the nucleus to regulate relevant transcription factors to alter the transcription of glucocorticoid-sensitive genes (Papadimitriou & Priftis, 2009).

Glucocorticoid negative feedback can be divided into three time domains: fast (within seconds to minutes), intermediate (minutes to 2–3 hours) and slow (over hours to days) (Keller-Wood & Dallman, 1984; Shipston, 1995). Previous studies have reported that glucocorticoids rapidly regulate ACTH release though a non-genomic signalling

pathways, including regulation of ion channel activity (Loechner *et al.*, 1999) and mediated by one or more membrane-associated glucocorticoid receptors (Tasker *et al.*, 2006). Compared to controls, injection of corticosterone immediately before CRH resulted in a significant reduction in CRH-induced plasma ACTH levels in rats, which provides evidence of a rapid and non-genomic effect of glucocorticoids (Hinz & Hirschelmann, 2000). Glucocorticoids have been shown to regulate BK channel activity in AtT20 cells through a non-genomic mechanism as well (Huang *et al.*, 2006). A wide body of evidence reveals that intermediate effects of glucocorticoids involve predominantly genomic mechanisms to inhibit secretagogue-evoked ACTH secretion. In large part, this appears to be downstream of the protein kinase A (PKA) or protein kinase C (PKC) signalling pathways through acting at or beyond intracellular free calcium mobilization (Shipston, 1995). Slow glucocorticoid negative feedback involves the inhibition of the POMC gene transcription (Autelitano *et al.*, 1989) and the reduction of ACTH expression in corticotrophs (Lundblad & Roberts, 1988; Engler *et al.*, 1999). In addition, glucocorticoids have been implicated in contributing to the downregulation of CRH expression in the PVN as well as CRH receptors in corticotrophs (Pozzoli *et al.*, 1996; Herman *et al.*, 2003).

Under basal conditions, glucocorticoids are normally released following a robust ultradian and circadian rhythm. The circadian rhythm of the HPA axis is primarily

regulated by the suprachiasmatic nucleus (SCN) with a daily peak during the active time which is daytime in humans and night-time in mice and rats. The rapid ultradian oscillations of glucocorticoid levels are thought to originate from the dynamics of feedback between the adrenal gland and pituitary corticotrophs (Walker *et al.*, 2010; Spiga *et al.*, 2014; Oster *et al.*, 2017).

## 1.3 Anterior pituitary corticotrophs in the control of the HPA axis

### 1.3.1 The regulation of corticotrophs

ACTH-producing corticotrophs, the central components of the HPA axis, are vital for mediating the neuroendocrine response to stress. Corticotrophs receive excitatory neuropeptide (CRH and AVP) signals from the hypothalamus to stimulate the secretion of ACTH. ACTH subsequently stimulates synthesis and release of glucocorticoids from the adrenal gland, which in turn exerts negative feedback on corticotrophs to inhibit the HPA axis. Therefore, it is important to understand the regulation of corticotrophs.

In response to stress, hypothalamic hormones CRH and AVP are released into the portal blood circulation from PVN neurones. The portal plasma concentration of CRH and AVP is approximately 0.2 nM and 2 nM respectively during stress (Gibbs & Vale,

1982; Sheward & Fink, 1991). CRH and AVP activate distinct G-protein-coupled receptors on anterior pituitary corticotrophs to stimulate ACTH release. CRH is a highly conserved peptide hormone composed of 41 amino acids which was first discovered and characterized in 1983 (Vale *et al.*, 1983). CRH neurons are situated in the parvicellular division of the PVN (pPVN) in the hypothalamus and project axons to the median eminence to secret CRH into the portal circulation (Majzoub, 2006). Two major subtypes of CRH receptor termed CRH receptor 1 (CRHR1) and CRH receptor 2 (CRHR2) belong to the G protein-coupled receptors (GPCRs) family B. CRH exerts its physiological effect exclusively via CRHR1 in corticotrophs to regulate the HPA axis (Bale & Vale, 2004; Papadimitriou & Priftis, 2009) (Figure 1.2). CRHR1 couples to the stimulatory Gαs G-protein pathway leading to an activation of adenylate cyclase (AC), subsequently inducing the accumulation of cyclic adenosine monophosphate (cAMP) and activation of protein kinase A (PKA) (Murat *et al.*, 2012). PKA-dependent phosphorylation of L-type $Ca^{2+}$ channels has been suggested to drive an influx of extracellular $Ca^{2+}$ which is essential for ACTH secretion (Kuryshev *et al.*, 1995, 1996; Lee & Tse, 1997). However, some studies have also implicated calcium-induced calcium release (CICR) resulting in the release of $Ca^{2+}$ from the intracellular stores as a result of activation of ryanodine receptors (RyRs) (Soares *et al.*, 2005). The RyR inhibitor ruthenium red induced a significant reduction in CRH-induced ACTH release in AtT20 cells suggesting CICR is also involved in the

regulation of CRH-induced ACTH secretion (Yamamori *et al.*, 2004).

AVP is a 9 amino acid peptide which is synthesized and secreted by magnocellular neurons in the paraventricular nucleus (mPVN) and supraoptic nucleus (SON) of the hypothalamus as well as CRH-producing parvicellular neurons of the PVN (Antoni, 1993). AVP produced by pPVN neurons is secreted into the hypophyseal portal circulation to regulate the HPA axis. Three specific receptor subtypes, V1a, V1b (or V3) and V2 belong to the GPCRs family A and regulate the physiological effects of AVP (Papadimitriou & Priftis, 2009; Goncharova, 2013). AVP stimulates the release of ACTH through binding to V1b receptors located on corticotrophs (Figure 1.2). V1b is coupled to the Gαq pathway which results in an activation of phospholipase C (PLC), leading to the cleavage of phosphatidylinositol 4,5-biphosphate ($PIP_2$) to generate inositol 1,4,5-triphosphate ($IP_3$), which binds to $IP_3$ receptors ($IP_3R$) on the endoplasmic reticulum (ER) to release $Ca^{2+}$ from intracellular stores, and diacylglycerol (DAG), which activates protein kinase C (PKC) (Tse & Lee, 1998; Murat *et al.*, 2012). Other studies have demonstrated that AVP, at supraphysiological concentrations, evokes transient and plateau phases of ACTH secretion, with the transient phase largely resulting from intracellular $Ca^{2+}$ release while the plateau phase primarily involves extracellular $Ca^{2+}$ entry via voltage-gated $Ca^{2+}$ channels (VGCC) through a PKC-mediated pathway (Tse & Lee, 1998).

## Figure 1.2

### CRH and AVP act synergistically to regulate ACTH secretion

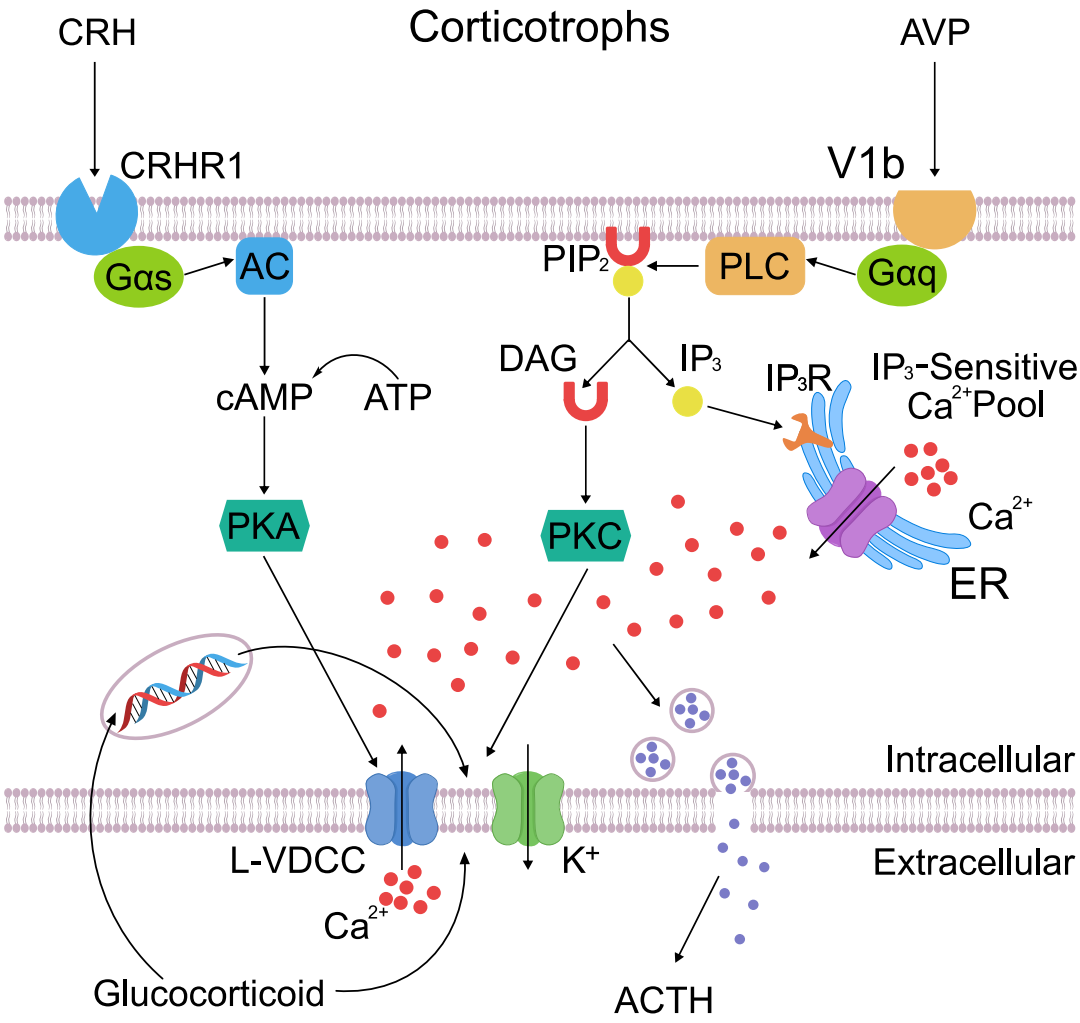


**Figure 1.2 CRH and AVP act synergistically to regulate ACTH secretion.** CRH and AVP activate distinct G-protein coupled receptors to stimulate ACTH secretion. CRH acts on CRH receptor 1 (CRHR1) which couples to the Gαs pathway to activate adenylate cyclase (AC), increase cyclic adenosine monophosphate (cAMP) and activate protein kinase A (PKA). AVP acts on AVP receptor V1b coupled to the Gαq pathway leading to cleavage of phosphatidylinositol 4,5-biphosphate ($PIP_2$) to generate inositol 1,4,5-triphosphate ($IP_3$) and diacylglycerol (DAG). $IP_3$ stimulates calcium release from the endoplasmic reticulum (ER) stores whereas DAG activates protein kinase C (PKC). PKA and PKC control the activity of ion channels to promote an increase of intracellular free calcium which triggers ACTH release. Glucocorticoids regulates ACTH secretion through both non-genomic and genomic signalling pathways.

In comparison to AVP, CRH is a more potent secretagogue in most species including humans, non-human primates, rats, horses but not sheep. Importantly, CRH and AVP have been demonstrated to act synergistically to stimulate the secretion of ACTH (Antoni, 1993; Favrod-Coune *et al.*, 1993; Aguilera, 1998). The synergistic effect of AVP on CRH-induced cAMP accumulation results in a synergistic release of ACTH. Furthermore, it has also been demonstrated that the PKC-dependent reduction of TREK channels contributes to the synergy between CRH and AVP (Stojilkovic *et al.*, 2010; Lee *et al.*, 2015). However, whether CRH and AVP synergy is also observed at the level of electrical activity and intracellular free calcium in corticotrophs is very poorly understood.

### 1.3.2 Calcium signalling in corticotrophs

Many endocrine pituitary cells are able to fire action potentials spontaneously, like neurons, which are associated with the rise of intracellular free calcium ($[Ca^{2+}]_i$) (Stojilkovic *et al.*, 2010). The pattern of electrical activity varies among pituitary cells and two distinct types are observed in corticotrophs: single action potentials (spikes) and pseudo-plateau bursting (Liang *et al.*, 2011; Duncan *et al.*, 2015; Fletcher *et al.*, 2017) (Figure 1.3). However, the link between these distinct patterns of electrical activity and associated elevation of $[Ca^{2+}]_i$ in corticotrophs remains unclear. In part, this has been because of the challenge of unambiguously identifying corticotrophs in

## Figure 1.3

### Two distinct patterns of electrical activity in corticotrophs

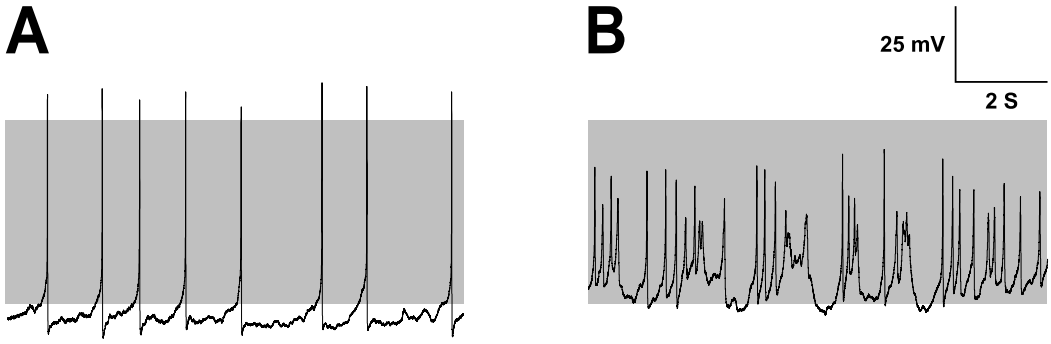


**Figure 1.3 Two distinct patterns of electrical activity in corticotrophs.** Two distinct patterns of electrical activity are observed in corticotrophs: **(A)** single spiking and **(B)** pseudo-plateau bursting evoked by CRH/AVP. Grey shading indicates membrane potential between −50 mv to +10 mv. Images are adapted from Duncan *et al.*, 2015.

real-time assays.

#### 1.3.2.1 Identification of corticotrophs

In many previous studies, the AtT20 cell line, which is derived from a radiation-induced anterior pituitary tumour, has been widely used to investigate the function of corticotrophs (Surprenant, 1982; Ooi *et al.*, 2004). AtT20 cells maintain many properties and functions of primary pituitary corticotrophs, however, AtT20 cells lack AVP receptors and several ionic mechanisms appear to be different from native corticotrophs (Woods *et al.*, 1992). Some experiments have also been carried out on the cells from human pituitary corticotroph tumours (Mollard *et al.*, 1987; Takano *et al.*, 1996). However, the number of studies that have analysed individual identified normal corticotrophs has until recently been very limited.

As indicated before, the anterior pituitary gland is made up of five types of hormone secreting cells with corticotrophs only comprising ~10% of the population, which makes it difficult to identify and distinguish live corticotrophs from the mixed cell populations. Several methods have been used in previous studies to identify and label corticotrophs from primary cell cultures. Biotinylated CRH peptides has been used to identify corticotrophs *in vitro* (Childs *et al.*, 1987). Treatment with high concentrations of CRH results in an increase in corticotroph volume, which allows the purification

of corticotrophs by centrifugal elutriation (Ritchie *et al.*, 1996; Kuryshev *et al.*, 1997). In addition, corticotrophs are identified based on the expression of ACTH that can be detected using the reverse haemolytic plaque assay (Lee & Tse, 1997). *Post hoc* staining of fixed cells for ACTH immunoreactivity can also be used for the identification of corticotrophs (Brunton *et al.*, 2007). However, all these studies have obvious drawbacks: a large majority of experiments are stimulated with CRH and AVP that are several orders of magnitude higher than those reported *in vivo*; prior exposure to a high dose of CRH makes it difficult to investigate the spontaneous activity in the absence of secretagogues; and all these approaches do not allow analysis of behaviour before stimulation/identification in real time *in vitro*.

#### 1.3.2.2 Measuring intracellular calcium in corticotrophs

Previous studies have exploited transgenic mice constitutively expressing green fluorescent protein (GFP) under control of the *Pomc* promoter or expressed enhanced yellow fluorescent protein (eYFP) with a lentiviral transduction system to label corticotrophs *in vitro*, which allow the identification of corticotrophs without compromising normal cell functions (Lee *et al.*, 2011; Liang *et al.*, 2011). A recent study used BK-POMC-GFP mice, which expressed green fluorescent protein (GFP) under the *Pom*c promoter to identify corticotrophs in culture (Duncan *et al.*, 2015). However, they are not the ideal tools to identify and label corticotrophs when we want

to investigate $[Ca^{2+}]_i$ signalling in corticotrophs at the same time, as they are not able to bind $Ca^{2+}$ and indicate $[Ca^{2+}]_i$ dynamic changes by changing their fluorescence properties. Importantly, these new labelling approaches provide us a new insight to integrate the lentiviral mediated transduction system with genetically encoded calcium indicators to identify corticotrophs when investigating $[Ca^{2+}]_i$ signalling.

As described above (see 1.3.1), CRH and AVP activate different calcium signalling pathways in corticotrophs. CRH primarily evokes calcium influx through L-type calcium channels whereas AVP primarily stimulates elevations in $[Ca^{2+}]_i$ through a combination of both release of calcium from $IP_3$-sensitive intracellular stores and influx of calcium via VGCC. In order to measure dynamic changes in $[Ca^{2+}]_i$ in corticotrophs, a variety of calcium indicators, which are based on fluorescent molecules whose fluorescence properties change depending on $Ca^{2+}$ binding, can be used. There are two classes of calcium indicators: synthetic (chemically synthesized) calcium indicators and genetically encoded calcium indicators (GECIs) (Horikawa, 2015; Lock *et al.*, 2015).

Chemical synthetic calcium indicators are small molecules with a fluorescent chromophore that are able to chelate $Ca^{2+}$ with highly selectivity like 1,2-bis(o-aminophenoxy)ethane-N,N,-N',N'-tetraacetic acid (BAPTA), including

fura-2, indo-1, fluo-4 and Oregon Green BAPTA-1 (OGB-1) (Perry *et al.*, 2015). The advantages of small molecule dyes include readily available from commercial sources; ease for intracellular loading by using their acetoxymethyl esters (AM) instead of gene transfer; high sensitivity and fast response kinetics, high spatiotemporal resolution of imaging and in several cases allowing ratiometric imaging to avoid artefacts from dye accumulation. However, there are also several drawbacks of chemical calcium indicators, such as unable to specifically target subpopulations of cells; poor loading into some cell types; suffer from deleterious compartmentalization and poor retention; photobleaching and leakage of dyes occurring over long-term imaging (Palmer & Tsien, 2006; Horikawa, 2015; Suzuki *et al.*, 2016).

GECIs are fluorescent proteins having a specific $Ca^{2+}$ responsive element which modifies the spectral properties of the fluorescent proteins upon $Ca^{2+}$ binding. GECIs can be divided into three categories: (i) bioluminescent sensors, such as aequorin; (ii) indicators based on the efficiency change of Förster resonance energy transfer (FRET) between two fluorescent proteins; (iii) indicators based on changes in fluorescence intensity of a single fluorescent protein (Horikawa, 2015; Perry *et al.*, 2015). Compared to synthetic chemical calcium indicators, GECIs provide the following advantages: (i) allows selectively targeting to distinct population of cells and subcellular compartments using cell specific promoters or expressing specific

targeting sequences; (ii) incorporated into transgenic or transduced mice/organisms to avoid loading exogenous dyes; (iii) enabling a micro-domain or nano-domain of $Ca^{2+}$ dynamic measurement in the immediate vicinity of a given protein and (vi) suitable for long-term and non-invasive imaging (Palmer & Tsien, 2006; Lock *et al.*, 2015; Suzuki *et al.*, 2016; Garcia *et al.*, 2017). Although some predecessors of GECIs have significant limitations ranging from low brightness, low sensitivity and very slow kinetics, most recently developed GECIs exhibit improved brightness and speed, dynamic range, thermal stability as well as folding efficiency (Mao *et al.*, 2008).

The GCaMP family, single fluorescent protein-based indicators, are one of the most widely used GECIs. GCaMPs are composed of a circularly permuted enhanced green fluorescent protein (cpEGFP), a calcium binding protein calmodulin (CaM) at the C-terminus and CaM binding motif M13 peptide, which is derived from skeletal muscle myosin light chain kinase, at the N-terminus. Upon $Ca^{2+}$ binding, the C- and N-terminus associate to induce the interaction between the CaM motif and M13 peptide. The conformational changes in the CaM/M13 complex cause an increase in fluorescence intensity of the cpEGFP-based chromophore (Nakai *et al.*, 2001; Akerboom *et al.*, 2009; Chen *et al.*, 2013*b*). The most recently developed GCaMP derivatives in 2013 are GCaMP6s, 6m and 6f (for slow, medium and fast kinetics, respectively), which have improved fluorescence intensity and signal-to-noise ratio

compared to previous versions, with sensitivity comparable to synthetic $Ca^{2+}$ indicators (Chen *et al.*, 2013*b*; Ding *et al.*, 2014). Of particular interest is GCaMP6s that shows the highest $Ca^{2+}$ sensitivity but slow response kinetics, which may have more utility in monitoring cytosolic $Ca^{2+}$ changes, such as in corticotrophs, where fast kinetics are not necessary. In addition, chronic imaging of GCaMP6s-expressing neurons has been shown up to 2 months without disturbing their physiological function suggesting the superiority of GCaMP6s in non-invasive imaging over extended time periods (Chen *et al.*, 2013*b*; Garcia *et al.*, 2017).

In this Thesis, GCaMP6s was chosen as the calcium indicator of choice to allow real time identification and analysis of calcium signals of corticotrophs by exploiting a genetic approach to express the calcium indicator under the control of a minimal *Pomc* promoter. A previous study utilized lentiviral mediated transduction of primary murine pituitary cells with a fluorescent enhanced yellow fluorescent protein (eYFP) under the control of the minimal *Pomc* promoter as an efficient and specific approach to identify and label corticotrophs *in vitro* (Liang *et al.*, 2011). Importantly, this study also revealed that lentiviral mediated transduction of corticotrophs with POMC-eYFP reporter does not compromise the viability and function of corticotrophs, which allows the systematic analysis of murine corticotroph properties. Furthermore, most previous studies of calcium imaging in corticotrophs only recorded for a short period of time in

response to a single stimulation with secretagogues. However, CRH release is pulsatile with a mean ultradian frequency of ~ three pulses per hour (Ixart *et al.*, 1991). To imitate a typical CRH exposure at physiologically relevant concentrations, a chronic imaging time frame is required to monitor $Ca^{2+}$ dynamics in response to multiple exposures. Thus, a key aim of the Thesis was to develop a lentiviral system to express GCaMP6s in corticotrophs under the control of a minimal *Pomc* promoter to allow identification and long-term imaging of corticotrophs *in vitro*.

### 1.3.3 Excitability of corticotrophs

Numerous ion channels are expressed in corticotrophs that are important in regulating their electrical activity. Voltage-gated $Na^+$ channels ($Na_v$) generate the fast upstroke of the action potential and control the maximum spike amplitude in most nerve, muscle and neuroendocrine cells (Stojilkovic *et al.*, 2010). Previous studies have indicated that all pituitary cells including corticotrophs express $Na_v$ channels that are sensitive to tetrodotoxin (TTX), a voltage-gated $Na^+$ channel blocker. However, inhibition of $Na_v$ channels with TTX has no consistent effect on spontaneous action potentials of corticotrophs, whereas removal of extracellular $Na^+$ with the large impermeant organic cation N-methyl-D-glucamine ($NMDG^+$) results in cessation of spontaneous action potential firing (Liang *et al.*, 2011). Moreover, a background $Na^+$ conductance can be recorded at the potassium reversal potential, suggesting a background $Na^+$

conductance is crucial in maintaining the resting membrane potential of murine corticotrophs (Stojilkovic *et al.*, 2010; Liang *et al.*, 2011). Furthermore, inward-rectifier $K^+$ channels ($K_{ir}$) have been shown to contribute to the regulation of resting membrane potential in rat but not murine corticotrophs (Kuryshev *et al.*, 1997; Liang *et al.*, 2011). TWIK-related $K^+$ channel (TREK)-1have been identified to play a role in controlling the resting membrane potential in murine corticotrophs (Lee *et al.*, 2011).

Voltage-gated $Ca^{2+}$ channels ($Ca_v$, also known as VGCC) are composed of five subunits: one large α1 subunit and four smaller ancillary subunits, α2, β, γ and δ (Stojilkovic, 2008). Electrophysiologically, two major types of $Ca_v$ channels have been identified: high-voltage-activated (HVA) $Ca_v$ channels require moderate to strong depolarisation to open and are distinguished by their single-channel conductance, pharmacology and metabolic regulation, including L-, N-, P/Q- and R-type $Ca^{2+}$ channels; low-voltage-activated (LVA) $Ca_v$ channels, also referred to transient or T-type $Ca^{2+}$ channels, require less membrane depolarisation to activate, which followed by a rapid and complete inactivation and a strong membrane hyperpolarization is required to release them from inactivation (Stojilkovic, 2008; Stojilkovic *et al.*, 2010). The functional expression of VGCC has been well established in corticotrophs. CRH-induced $[Ca^{2+}]_i$ increase in corticotrophs is due to the firing of calcium-dependent action potentials, which are primarily dependent on $Ca^{2+}$ influx via

L-type $Ca^{2+}$ channels (Kuryshev *et al.*, 1996). Activation of T-type $Ca^{2+}$ channels have also been proposed in regulating membrane potential and helping initiate $Ca^{2+}$ dependent action potentials (Guérineau *et al.*, 1991; LeBeau *et al.*, 1997). P/Q-type $Ca^{2+}$ channels have been proposed to drive the depolarization needed to generate action potentials and regulate spontaneous electrical activity in corticotrophs (Fiordelisio *et al.*, 2007).

Calcium-activated $K^+$ channels ($K_{Ca}$) comprise three families: (i) one family includes three small conductance calcium-activated potassium (SK) channels ($K_{Ca}$2.1, 2.2, and 2.3); (ii) the intermediate conductance calcium-activated potassium (IK) channels ($K_{Ca}$3.1) and (iii) large conductance calcium- and voltage-activated potassium (BK) channels (Stojilkovic *et al.*, 2010). Pharmacological inhibition of IK channels with an IK channel blocker, TRAM-34, results in an increase in corticotroph excitability associated with a transition to a pseudo-plateau bursting. In murine corticotrophs, genetic deletion of IK channels shows an enhanced level of plasma ACTH and corticosterone under restraint stress compared to wild-type controls. Moreover, CRH and AVP mRNA expression is significantly elevated in mice lacking IK channels (Liang *et al.*, 2011). These data suggested that IK channels play a role in controlling the corticotroph excitability and ACTH secretion and may also contribute to regulate HPA stress axis function.

### 1.3.4 The role of BK channels in corticotroph excitability

BK channels are composed of four pore-forming α-subunits which assemble as tetramers to form functional channels and are encoded by a single gene (KCNMA1) in all organisms. The pore-forming α-subunit of BK channel consists of seven transmembrane domains (S0-S6), with a pore-gate domain between S5 and S6 domains and a voltage sensor domain comprised of S1-S4 domains, an extracellular amino ($NH_2$ or N-) terminus at the S0 domain and a large intracellular carboxyl (COOH or C-) terminus containing two regulators of $K^+$ conductance (RCK1 and RCK2). Calcium binding sites called "calcium bowls" are located within the C-terminus which is important for $Ca^{2+}$ sensitivity of the channels (Meera *et al.*, 1997; Coetzee *et al.*, 1999). The diversity of BK channel properties and function may be achieved by assembly with tissue specific auxiliary β-subunits (β1-β4) (Behrens *et al.*, 2000; Orio *et al.*, 2002) and γ-subunits (Yan & Aldrich, 2012) as well as various splice variants of the α-subunit (Lagrutta *et al.*, 1994; Tseng-Crank *et al.*, 1994; Xie & McCobb, 1998; Zarei *et al.*, 2001; Fury *et al.*, 2002; Chen *et al.*, 2005) (Figure 1.4). BK channels are widely expressed in virtually all mammalian cells and play important roles in a diverse range of physiological processes including smooth muscle contraction (Wellman & Nelson, 2003), blood flow (Sausbier *et al.*, 2005), hormone secretion (Ghatta *et al.*, 2006), neuronal excitation (Sausbier *et al.*, 2004) and neurotransmitter release (Wang *et al.*, 2001). Malfunction of BK channels can lead to

## Figure 1.4

### Schematic illustrating the topology of the BK channel and two S-acylated sites in the pore-forming α-subunit

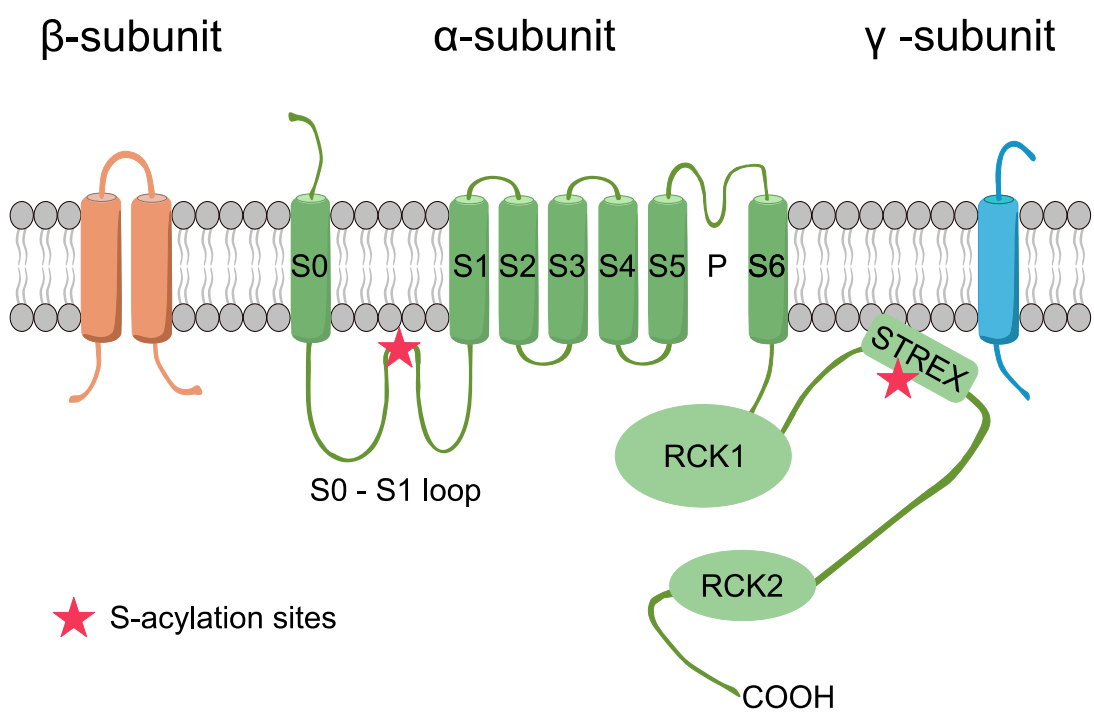


**Figure 1.4 Schematic illustrating the topology of the BK channel and two S-acylated sites in the pore-forming α-subunit.** The pore forming α-subunit of BK channels consists of seven transmembrane domains (S0-S6), an extracellular amino (NH2) terminus and a large intracellular carboxyl (COOH) terminus containing two regulators of $K^+$ conductance RCK1 and RCK2. The regulatory β- and γ-subunits are also illustrated. BK channel α-subunits are S-acylated at two distinct sites: the intracellular S0-S1 loop and the alternatively spliced stress axis-regulated exon (STREX) insert in the linker between the two RCK domains in the C-terminus.

epilepsy (Du *et al.*, 2005), asthma (Seibold *et al.*, 2008), obesity (Jiao *et al.*, 2011), hypertension (Brenner *et al.*, 2000) and many other disorders.

Alternative splicing is a regulated process to produce multiple transcripts from a single gene through combining exons in different ways. The α-subunits of BK channels, only encoded by KCNMA1, undergoes extensive alternative pre-mRNA splicing to generate BK channel variants with distinct properties, which is important in diversifying channel function. Previous studies have demonstrated that two major splice variants are predominantly expressed in the pituitary and adrenal glands. The STREX (stress axis-regulated exon) variant containing a cysteine-rich domain of 58 amino acids insert increases $Ca^{2+}$ sensitivity, and ZERO channels, which do not express STREX splice insert (Saito *et al.*, 1997; Xie & McCobb, 1998). Removal of the anterior pituitary gland results in a reduced expression of STREX splice variants in the adrenal gland (Xie & McCobb, 1998). Alternative splicing of BK channels determines their sensitivity to protein phosphorylation to control channel regulation. ZERO variants of BK channels are activated by PKA whereas STREX-containing BK channels are inhibited by PKA dependent phosphorylation, which is due to the dissociation of STREX domain from the plasma membrane (Tian *et al.*, 2001, 2008). In addition, the presence of STREX determines PKC regulation of BK channels. PKC phosphorylation inhibits ZERO channels, however, STREX splice variant is entirely

resistant to PKC phosphorylation unless the channels have been previously inhibited by PKA (Zhou *et al.*, 2012).

Previous studies have shown a paradoxical role of BK channels in generating spontaneous pseudo-plateau bursting in anterior pituitary somatotrophs and gonadotrophs (Van Goor *et al.*, 2001*a*; Tabak *et al.*, 2011). Anterior pituitary corticotrophs, also express BK channels but exhibit primarily spontaneous single spikes which can transit to pseudo-plateau bursting when stimulated with CRH (Duncan *et al.*, 2015). However, CRH and AVP evoke distinct patterns of electrical excitability with AVP promoting an increase in spiking frequency through a BK-independent pathway (Duncan *et al.*, 2015). A simplified mathematical model used in previous studies (Duncan *et al.*, 2015, 2016) has suggested six major ionic currents expressed in corticotrophs including L-type $Ca^{2+}$ current, inward rectifier $K^+$ current, delayed rectifier $K^+$ current, BK-near current, BK-far current and nonselective current (Figure 1.5). Two functional populations of BK channels are predicted by the model: BK channels in close proximity to VGCC (BK-near) and the other BK channels located far from the VGCC (BK-far). The fast activation of BK-near channels caused by the high concentration of micro-domain $[Ca^{2+}]_i$ close to VGCC has been demonstrated to be necessary in promoting pseudo-plateau bursting (Tabak *et al.*, 2011). In contrast, BK-far channels, responding to the slowly increased bulk cytosolic

# Figure 1.5

## Schematic diagram of the ion channels in corticotroph model

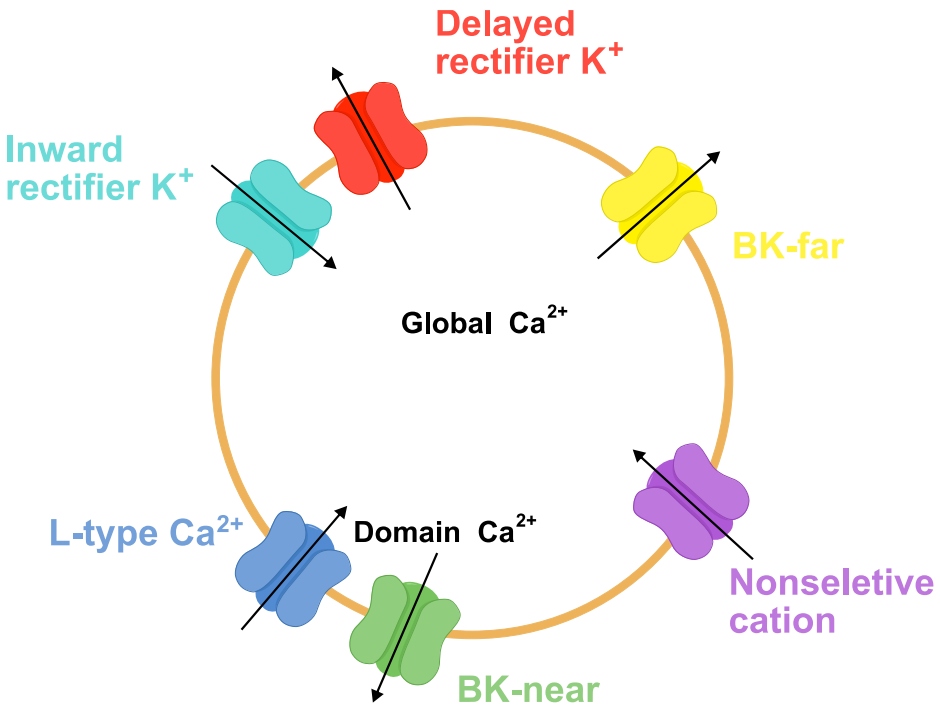


**Figure 1.5 Schematic diagram of the ion channels in corticotroph model.** Six ionic currents are expressed in corticotrophs including L-type $Ca^{2+}$ current, inward rectifier $K^+$ current, delayed rectifier $K^+$ current, BK-near current, BK-far current and nonselective current.

$[Ca^{2+}]_i$, predominantly control the termination of bursting (Tsaneva-Atanasova *et al.*, 2007). However, the molecular biology of these populations has not been established. This may represent different splice variants of BK channels or other calcium-activated potassium channels, such as IK or SK channels. Importantly, pseudo-plateau bursting has been proposed to increase $[Ca^{2+}]_i$ to a greater extent than during single spiking, and thus proposed to drive a higher level of hormone secretion (Van Goor *et al.*, 2001*b*; Stojilkovic *et al.*, 2005). However, a more recent study, has revealed that spiking may be just as effective as bursting at evoking hormone release if the release sites are close to $Ca^{2+}$ channels or at higher spiking frequencies (Tagliavini *et al.*, 2016).

Although loss of BK channels in mice leads to a stress hyporesponsiveness with attenuated acute restraint stress induced plasma ACTH and corticosterone levels compared to controls, which may involve effects at both the level of the corticotroph and the hypothalamus (Brunton *et al.*, 2007). However, whether BK channels also play an important role in CRH-, or AVP-induced $[Ca^{2+}]_i$ signalling in corticotrophs is unknown.

## 1.4 S-acylation controls BK channel properties and function

### 1.4.1 S-acylation and its enzymatic regulation

Most proteins, including ion channels, are regulated by a diverse range of post-translational modifications (PTMs), such as lipid modifications and phosphorylation. Lipid modifications attach lipids and lipid-like groups onto proteins, which increase protein hydrophobicity, affect protein structure and the affinity of proteins for membranes (Resh, 2006*a*; Chamberlain & Shipston, 2015). There are three most common lipid modifications: N-myristoylation, prenylation and S-acylation. N-myristoylation is the addition of a 14-carbon saturated fatty acid myristate to the N-terminal glycine through an amide bond. Prenylation is the addition of a 15-carbon (farnesyl) or 20-carbon (geranylgeranyl) isoprenoid to the COOH-terminal cysteine residues of the protein though a thioether bond. S-acylation involves the attachment of a lipid (typically but not exclusively palmitate, a 16-carbon saturated fatty acid) to intracellular cysteine residues of a target protein via a thioester linkage. Importantly, S-acylation, unlike the other two irreversible lipid modifications N-myristoylation and prenylation, is the only fully reversible post-translational lipid modification of proteins. This ubiquitous PTM provides a dynamic mechanism in regulating protein properties and functions across species: from yeast to man (Resh, 2006*b*; Shipston, 2011; Chamberlain & Shipston, 2015). S-acylation of most proteins is enzymatically mediated by a large family of transmembrane zinc-finger containing protein palmitoyl acyl-transferases (zDHHC family). To date, 23/24 zDHHCs genes have been identified in mammals. zDHHCs

have a highly conserved Asp-His-His-Cys (DHHC) signature sequence within a cysteine rich stretch of ~50 amino acids critical for catalytic activity (Shipston, 2011; Chamberlain & Shipston, 2015). In addition, increasing evidence suggests distinct zDHHC enzymes display substrate specificity for proteins (Greaves & Chamberlain, 2011). Subcellular localization and tissue specific distribution of zDHHCs are also demonstrated, with the majority of zDHHCs localized to the endoplasmic reticular (ER) and/or Golgi membranes and a few localized in the plasma membrane (Ohno *et al.*, 2006). Conversely, enzymes that control the de-acylation of proteins have not been clearly defined. The cytosolic acyl protein thioesterase 1 (APT1), APT2, the palmitoyl protein thioesterase 1 (PPT1) and PPT2 are most likely responsible for the de-acylation process (Figure 1.6). PPT1 is primarily expressed in lysosomes that probably involves in de-acylation of proteins during degradation (Shipston, 2013, 2014*a*; Chamberlain & Shipston, 2015).

### 1.4.2 Regulation of BK channels by S-acylation

S-acylation has been shown to play a diverse role in the regulation of multiple ion channels including: the modulation of L-type $Ca^{2+}$ channels function via the $\beta_{2a}$ subunit (Chien *et al.*, 1996), the regulation of voltage sensing of the voltage-gated Kv1.1 channel through protein-membrane interaction (Gubitosi-Klug *et al.*, 2005) and the phosphorylation-dependent regulation and trafficking of BK channels

# Figure 1.6

## Reversible enzymatic regulation of S-acylation

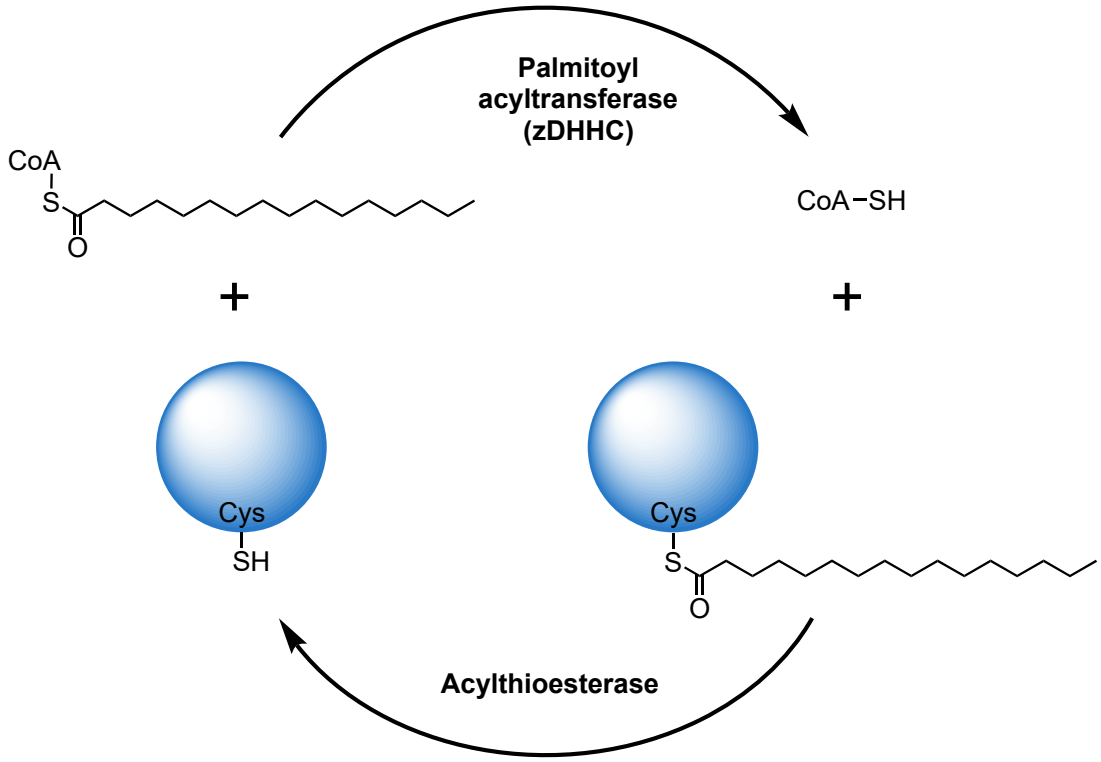


**Figure 1.6 Reversible enzymatic regulation of S-acylation.** S-acylation is controlled by a large family of transmembrane zinc-finger containing protein palmitoyl acyl-transferases (zDHHC family) and de-acylation is primarily regulated by acyl protein thioesterase.

(Tian *et al.*, 2001, 2004, 2008; Zhou *et al.*, 2001). Both the BK channel pore-forming α-subunit and regulatory β-subunits are S-acylated. In particular, the pore-forming α-subunit is S-acylated at two distinct sites: cysteine residues within the intracellular loop between transmembrane domains S0 and S1 (S0-S1 loop) and the alternatively spliced STREX insert in the intracellular linker between the two RCK domains in the C-terminus (Shipston, 2013) (Figure 1.4).

Increasing evidence suggests each S-acylation site is regulated by different zDHHCs due to their substrate specificity. zDHHCs 3, 5, 7, 9 and 17 have been identified as potential enzymes in regulating the S-acylation of the STREX domain, with zDHHC17 showing greatest selectivity for this site (Tian *et al.*, 2010). The S-acylation of the S0-S1 loop of the BK channels is predominately controlled by zDHHC22 and zDHHC23, and overexpression of zDHHC23 increases the cell surface expression of S0-S1 loop (Jeffries *et al.*, 2010; Tian *et al.*, 2012). APT1 and a splice variant APTL1 but not APT2 de-acylate BK channels at the S0-S1 loop (Tian *et al.*, 2012). S-acylation of the BK channel S0-S1 loop is an important determinant in cell surface expression, whereas S-acylation of the STREX domain regulates the BK channel activity mediated by AGC family protein kinase dependent phosphorylation. S-acylation of S0-S1 loop allows the association of isolated S0-S1 linker with the plasma membrane to control surface expression without having an impact on S-acylation of the alternatively spliced

STREX insert (Jeffries *et al.*, 2010). The S-acylated STREX domain prevents the inhibition of STREX containing BK channels through PKC pathway. However, de-acylation of STREX insert or PKA-mediated dissociation of STREX variants from the plasma membrane inhibits BK channel activity via PKC-dependent phosphorylation (Zhou *et al.*, 2010, 2012). Importantly, the zDHHCs controlling the S-acylation of S0-S1 loop or STREX domain are also expressed at multiple cellular compartments including ER, Golgi and/or plasma membrane suggesting that the modulation of BK channel occurs at multiple sites and different stages in the trafficking pathways (Shipston, 2014*a*). Furthermore, S-acylation of β4-subunits controls surface delivery of BK channels through masking an α-subunit trafficking motif, which provide a dynamic mechanism for specific splice variants surface trafficking (Chen *et al.*, 2013*a*). Although the role of zDHHCs-mediated S-acylation in controlling BK channel properties and regulation have been described, the functional relevance is largely unknown. As zDHHC23 is highly expressed in murine corticotrophs, compared to other pituitary cell types, and zDHHC23 controls surface expression of BK channels, we hypothesised that zDHHC23 may control BK channel dependent excitability and accompanied calcium signals in corticotrophs. Thus, we examined the effect of the deletion of zDHHC23 on intracellular calcium responses in corticotrophs.

## 1.5 Sex differences in HPA axis

Remarkably, underrepresentation of females in animal models is very common and male bias is most obvious in neuroscience studies (Beery & Zucker, 2011). Men or male rodents are considered as representatives of the species to generalize findings to females and differences from the male are often regarded as abnormal/atypical (Beery & Zucker, 2011; Bangasser & Wiersielis, 2018). However, numerous studies have revealed sex-specific prevalence rates for many diseases in humans, including several stress-related disorders. Women are at two-fold higher risk to develop stress- and anxiety-related psychiatric disorders, whereas men are more likely to show antisocial behaviour or substance abuse (Weich *et al.*, 2001; Maeng & Milad, 2015). Major depressive disorders (MDD) are also sexually dimorphic, where women are 2–3 times likely to develop MMD with higher symptom severity, greater functional impairment as well as responding differently to treatment compared to men (Labonté *et al.*, 2017). Concerning cardiovascular diseases (CVD), while men are prone to occlusive coronary artery disease (CAD), women have a higher incidence of ischemic heart disease (IHD) (Regitz-Zagrosek & Kararigas, 2017). Rates of chronic pain and autoimmune disease are also higher in women than in man (Sorge & Totsch, 2017). Furthermore, women's susceptibility in stress responses may mediate increased risk for Alzheimer's disease (AD) (Yan *et al.*, 2018). Interestingly, several studies conclude that women subjectively experience more stress than men with higher stress vulnerability and

longer life expectancy (Kudielka & Kirschbaum, 2005). In this case, sex-specific stress responses may contribute to the sex-specific prevalence rates of diseases.

Do males and females differ in their response to stress? Increasing evidence suggests sex differences in HPA axis function. Compared to males, females show a higher level of glucocorticoid secretion following HPA axis stimulation in animal studies (Haleem *et al.*, 1988; Yoshimura *et al.*, 2003). Moreover, sexual dimorphism has been demonstrated at the level of ACTH secretion as adult men have higher and more frequent ACTH pulses while a higher sensitivity to ACTH is observed in female adrenal cortex (Kudielka & Kirschbaum, 2005). CRH neurons show increased CRHR1 signalling and reduced CRHR1 internalization in female rats (Bourke *et al.*, 2012). Bourke and colleagues also suggest that a faster reduction of ACTH and cortisol in female rats after CRH stimulation may alter the negative feedback of HPA axis. Acute stress results in the longer activation of HPA axis in females (Haleem *et al.*, 1988). The activity of HPA axis may vary in female rats upon the different phases of oestrous cycles due to the gonadal steroid mediated release of CRH and AVP (Panagiotakopoulos & Neigh, 2014). Furthermore, following chronic stress, males display a higher level of GABA and increased dopaminergic activity in the frontal cortex and amygdala, whereas females exhibit increased levels of serotonin (5-HT) and norepinephrine (NE), which suggested that chronic stress affects females and

males differently (Luine, 2002).

Currently, whether sexual dimorphism of HPA axis function also occurs at the level of corticotrophs remains unclear. In large part this is because in most previous rodent studies on corticotroph function; in particular *in vitro*, the sex of animal used in corticotroph studies is not reported. Furthermore, in many *in vitro* studies, data are reported from mixed populations of female and male corticotrophs with no identification of sex prior to study. This is important as studies have suggested differences between male and female pituitary cells. For example, sex steroids are implicated in the regulation of ion channel expression, including VGCC, L-type $Ca^{2+}$ currents are higher in female cultured rat melanotrophs, while oestrogen treatment can upregulates the expression of L-type $Ca^{2+}$ channels in male cells (Fiordelisio *et al.*, 2007). This may affect $Ca^{2+}$ signalling differentially in male and female cells. Previous studies have suggested a probable sexually dimorphic mechanism in $[Ca^{2+}]_i$ signalling of rat corticotrophs (Guérineau *et al.*, 1991; Romanò *et al.*, 2017). Romanò and colleagues observed that only 30% of corticotrophs from male rats showed spontaneous $[Ca^{2+}]_i$ signalling whereas Guérineau *et al*. reported that 65% of female rat corticotrophs displayed spontaneous $[Ca^{2+}]_i$ signalling. However, the $[Ca^{2+}]_i$ signalling have not been systematically analysed in mouse corticotrophs between males and females. As the regulation of $Ca^{2+}$ signalling pathway may be vital for

coordination of appropriate HPA axis stress responses, in this Thesis $[Ca^{2+}]_i$ signalling has been systematically determined in male and female corticotrophs respectively.

## 1.6 Hypothesis, aims and objectives

Anterior pituitary corticotrophs, a key component of the HPA axis, integrate the inputs from the hypothalamic secretagogues (CRH and AVP) with the negative feedback from the adrenal glucocorticoids to control HPA axis function. Corticotrophs are electrically excitable with CRH and AVP stimulating increases in $[Ca^{2+}]_i$ via different calcium signalling pathways.

BK channels have been shown to be essential for the transition to bursting following CRH stimulation and bursting is believed to have higher capacity to drive $Ca^{2+}$ influx than single spiking. Moreover, AVP stimulates an increase in spiking frequency that is independent of BK channels function. Therefore, it is hypothesized that genetic deletion, or pharmacological blockade, of BK channels will result in the attenuation of CRH-induced, but not AVP-induced, $[Ca^{2+}]_i$ responses. Furthermore, as BK channel surface expression is controlled by zDHHC23, the genetic deletion of zDHHC23 in corticotrophs is also predicted to attenuate CRH-induced $[Ca^{2+}]_i$ signalling. As corticotrophs may display sexual dimorphism, analysis will be performed independently in both male and female corticotrophs at physiological levels of CRH (0.2 nM) and/or AVP (2 nM) (Gibbs & Vale, 1982; Sheward & Fink, 1991).

The aim of this Thesis is thus to investigate the hypothesis that: *CRH-, but not AVP-evoked $[Ca^{2+}]_i$ responses in murine corticotrophs are dependent upon the function of BK channels.*

To address this hypothesis, $[Ca^{2+}]_i$ responses to CRH and AVP are investigated in both male and female corticotrophs with the following major aims:

In Chapter Three, I first develop and test a new POMC-GCaMP6s reporter using the lentivirus transduction system to allow specific labelling of live corticotrophs *in vitro* for calcium imaging recordings. Using this approach, $[Ca^{2+}]_i$ responses in wild-type corticotrophs are characterised under basal conditions and following CRH and/or AVP stimulation including analysis of CRH/AVP synergy at the level of $[Ca^{2+}]_i$.

In Chapter Four, the role of BK channels in controlling spontaneous and secretagogue-evoked $[Ca^{2+}]_i$ signalling in corticotrophs are investigated when BK channels are genetically deleted, or pharmacological blocked by a specific inhibitor, paxilline.

In Chapter Five, $[Ca^{2+}]_i$ signalling in corticotrophs in which the S-acyl transferase zDHHC23, that controls BK channel surface expression, is genetically deleted is

examined.

Importantly, a repeated stimulation protocol is developed throughout the study to replicate typical secretion pulse of hypothalamic hormones. Most previous studies investigated CRH and/or AVP-evoked $[Ca^{2+}]_i$ signalling in response to a single supraphysiological concentration of secretagogue whereas *in vivo* corticotrophs must respond to repeated changes in CRH and AVP. Compared to the single stimulus used in most previous studies, repeated stimulation of corticotrophs at physiologically relevant concentrations may provide new insights into how corticotrophs coordinate appropriate and adaptive responses to distinct stressors.

# Chapter Two:

# Materials and Methods

# Chapter 2: Materials and Methods

## 2.1 Materials

### 2.1.1 General materials and reagents

Unless otherwise indicated, general chemical reagents and solvents used in this study were from Sigma-Aldrich Company and of analytical grade quality.

### 2.1.2 Molecular biology reagents

Abcam Inc., Cambridge, MA, USA

Chicken Anti-GFP antibody (ab13970)

Goat Anti-Chicken IgY H&L (Alexa Fluor® 488) (ab150169)

Rabbit Anti-ACTH antibody (ab74976)

Invitrogen Ltd., Paisley, UK

Deoxyribonucleotides (dNTPs): 100 mM each of dATP, dTTP, dCTP and dGTP (10297018)

F(ab')2-Goat anti-Rabbit IgG (H+L) Secondary Antibody, Alexa Fluor 546 (A11071)

SYBR® Safe DNA Gel Stain (S33102)

TO-PRO™-3 Iodide (642/661) - 1 mM Solution in DMSO (T3605)

UltraPure™ Agarose (16500500)

Promega, Madison, WI, USA

GoTaq® G2 DNA Polymerase: includes GoTaq® G2 DNA Polymerase 500 units, 5X Green GoTaq® Reaction Buffer, 5X Colourless GoTaq® Reaction Buffer (M7845)

Sigma-Aldrich Company Ltd., Gillingham, UK

Betaine solution (B0300)

Bovine Serum Albumin: heat shock fraction (A7906)

Dimethyl sulfoxide (DMSO) (D2650)

Mowiol® 4-88 (81381)

PCR primers: made up to 100 µM stocks in TE buffer (10 mM Tris, 1 mM EDTA in $dH_2O$).

### 2.1.3 Cell culture reagents

Gibco® Life Technologies, Paisley, UK

Gibco® Dulbecco's Modified Eagle Medium (DMEM + 4.5 g/L high-glucose, +L-Glutamine, +25 mM HEPES, −Pyruvate) (42430-025)

Sigma-Aldrich Company Ltd., Gillingham, UK

Antibiotic Antimycotic Solution (100x), Stabilized: Contains 10000 units penicillin, 10 mg streptomycin and 25 µg amphotericin B per ml (A5955)

Aprotinin from bovine lung (10820)

Bovine Serum Albumin (BSA) solution: 30% in DPBS (A9576)

Deoxyribonuclease I from bovine pancreas (D5025)

Fibronectin from bovine plasma (F1141)

ITS liquid media supplement (100x): Contains 1.0 mg/ml recombinant human insulin, 0.55 mg/ml human transferrin and 0.5 µg/ml sodium selenite (I3146)

Trypsin inhibitor from *Glycine max* (soybean) (T6522)

Thermo Scientific, Paisley, UK

GeneRuler 1 kb DNA Ladder (SM0311)

Worthington Biochemical Corporation, Lakewood, NJ, USA

Trypsin (LS003702)

### 2.1.4 Peptides and channel inhibitors

Bachem AG, Bubendorf, Switzerland

Corticotrophin-releasing hormone (CRH); human, rat (H-2435)

Sigma-Aldrich Company Ltd., Gillingham, UK

[$Arg^8$]-Vasopressin (AVP) acetate salt (V9879)

Dimethyl sulfoxide (DMSO) (D8418)

Paxilline (P2928)

Nifedipine (N7634)

Peptide hormones CRH and AVP were used to stimulate corticotrophs at physiologically relevant concentrations (0.2 nM CRH and 2 nM AVP) (Gibbs & Vale, 1982; Sheward & Fink, 1991) which allowed us to investigate the secretagogue-induced $[Ca^{2+}]_i$ signalling in corticotrophs. Stock solutions were made up in 0.01 N HCl and 0.0001 N L-Ascorbic acid and stored at −80 ºC. Ion channel blockers nifedipine and paxilline were used to study the role of specific ion channels in regulating corticotroph $[Ca^{2+}]_i$ signalling. Stock solutions were made in DMSO, then aliquoted and stored at -20 ºC (Table 2.1). Everyday a fresh aliquot of each drug was used. Stock solutions were diluted to their working concentrations with Ringer's solution containing (in mM) 125 NaCl, 2.5 KCl, 1.25 $NaH_2PO_4$, 12 $NaHCO_3$, 2 $CaCl_2$, 1 $MgCl_2$ and 2 glucose with the pH adjusted to 7.3 and osmolarity adjusted with NaCl between 300 and 305 mOsmol/l.

# Table 2.1

## List of drugs and dilutions

| Drug | Stock concentration | Working concentration | Storage |
|---|---|---|---|
| AVP | 1 mM | 2 nM | 10 µl/aliquot<br>−80 ºC |
| CRH | 0.1 mM | 0.2 nM | 10 µl/aliquot<br>−80 ºC |
| Nifedipine | 125 mM | 2.5 µM | 20 µl/aliquot<br>−20 ºC |
| Paxilline | 10 mM | 1 µM | 20 µl/aliquot<br>−20 ºC |

# 2.2 Animals

## 2.2.1 Animals

Wild-type mice were on a C57/BL6 background. Mice lacking the pore forming exon of α-subunit in the BK channel (BK-KO mice) were generated on the same C57/BL6 background as described (Sausbier *et al.*, 2004). Mice with a genetic deletion of zDHHC23 (zDHHC23-KO mice) were generated by Knockout Mouse Project (KOMP, www.komp.org, $Zdhhc23^{tm1(KOMP)Vlcg}$) and backcrossed for at least 10 generations with mice on a C57/BL6 background. Mice were caged in groups of two to four under standard laboratory conditions (lights on at 07.00 h, lights off at 19.00 h, 21ºC, with tap water and chow available *ad libitum*). Mice used for anterior pituitary cell culture were aged between 2 and 5 months and were matched by age and sex. Tissue collection was performed between 09.30h and 11.30h in accordance with United Kingdom Home Office requirements.

## 2.2.2 Mouse PCR genotyping

### 2.2.2.1 Preparation of DNA from ear clip samples with Hot Sodium Hydroxide and Tris (HotSHOT)

The Hot Sodium Hydroxide and Tris (HotSHOT) method was used to isolate mouse genomic DNA from ear clips (2 mm diameter) for genotyping (Truett *et al.*, 2000). Alkaline lysis reagent with 25 mM NaOH, 0.2 mM disodium EDTA, pH 12 was

prepared by dissolving the salts in water without adjusting the pH. Neutralizing reagent with 40 mM Tris-HCl and a pH of 5 was prepared by dissolving Tris-HCl in water without adjusting the pH. Both the alkaline lysis and neutralizing reagents were made up as 10x stocks and diluted with $dH_2O$ on the day of use. 75 µl alkaline lysis reagent was added to each ear clip sample and heated to 95°C for 1 h. After heating, samples were then cooled to 4°C and 75 µl neutralizing reagent were added to each sample. The combination of two reagents resulted in a solution composed of 20 mM Tris-HCl and 0.1 mM EDTA (pH 8.1) which was similar to a common DNA storage buffer.

#### 2.2.2.2 Amplification of DNA using polymerase chain reaction

The polymerase chain reaction (PCR) is a technique used to exponentially amplify a single copy or a few copies of specific segment of genomic DNA. During this study, mice used for anterior pituitary cell culture were selected based on their BK and zDHHC23 genotype respectively. GeneAmp® PCR System 2720 thermal cycler (Applied Biosciences) was employed for the PCR reactions.

To identify the BK genotype for each mouse, primers (Table 2.2) and cycling parameters (Figure 2.1) were used in PCR reactions. Two forward primers were designed corresponding to the wild-type and knockout allele (F1 and F2 respectively) and a reverse primer (R) common to both alleles. The PCR reaction consisted of

10-30 ng DNA template, 500 nM of each primer (Eurofins), 2 µl of 10x PCR buffer, 1.5 mM $MgCl_2$, 2 mM each of dATP, dTTP, dCTP and dGTP, 1-2.5 U of Taq DNA polymerase (Invitrogen), made up to a final volume of 20 µl with DEPC-treated (0.05% v/v diethyl pyrocarbonate in $dH_2O$) water. The standard protocol started with 10 minutes at 94 ºC to denature the template, followed by 37 cycles of a denaturing step (45 seconds at 94 ºC), an annealing step (30 seconds at 52 ºC) and an elongation step (30 seconds at 72 ºC). Annealing temperature was chosen to be 5–6 ºC lower than the melting temperatures ($T_m$) of the primers. After the final cycle, the reaction was concluded with 10 minutes at 72 ºC and then held at 4 ºC (Figure 2.1). A negative control was always set up in parallel replacing the DNA template with equivalent volume of DEPC-treated water to check the contamination. Genotyping was performed by a lab member, Dr Peter J. Duncan.

The "Touchdown" PCR method was used to determine the zDHHC23 genotype for each mouse with appropriate primers (Table 2.3) and cycling parameters (Figure 2.2). Two PCR reactions were performed, where one set of forward and reserve primers were designed corresponding to wild-type genotype (Reg-zDHHC23-wtF and Reg-zDHHC23-wtR) and the other set of forward and reserve primers were designed corresponding to zDHH23-KO genotype (Reg-NeoF and Reg-zDHHC23-R). Each PCR reaction consisted of 10-30 ng DNA template, 6.5 µl of 5M betaine, 0.325 µl of

## Table 2.2

### Primers used for BK-KO genotyping

| Name | Target Gene | Tm (ºC) | Sequence (5' – 3') |
|---|---|---|---|
| BK F1 | BK-KO | 59.4 | TGG TCT TCT TCA TCC TCG GG |
| BK F2 | BK-KO | 57.9 | AAG GGC CAT TTT GAA GTC |
| BK R | BK-KO | 59.4 | CCA GCC ACA GTG TTT GTT GG |

## Figure 2.1

### Cycling parameters for BK-KO genotyping

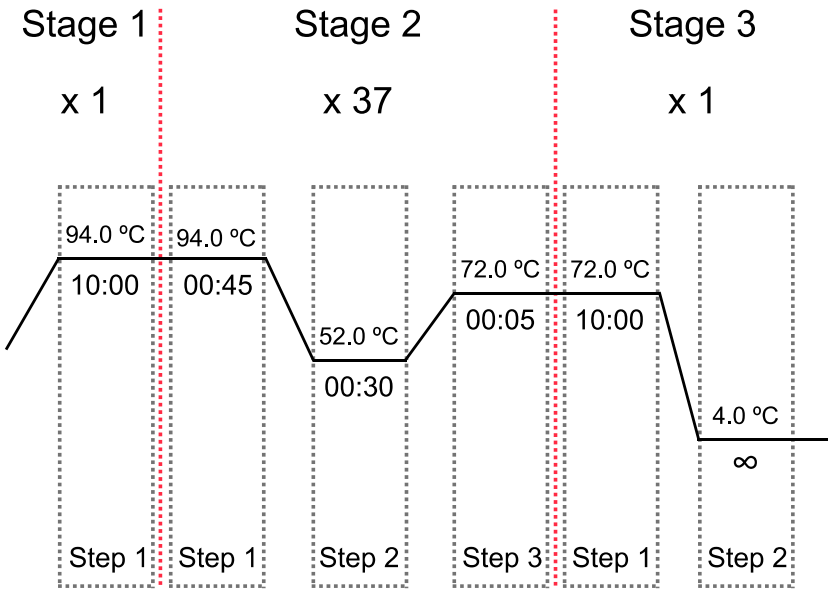


**Figure 2.1 Cycling parameters for BK-KO genotyping.** BK-KO genotyping started with a denaturing stage at 94 ºC for 10 minutes. Next stage was programmed as a denaturing step (45 seconds at 94 ºC), an annealing step (30 seconds at 52 ºC) and an elongation step (30 seconds at 72 ºC) for 37 cycles. After the final cycle PCR reaction was completed with a 10 minute extension at 72 ºC and held at 4 ºC.

DMSO, 200 nM of each primer (Sigma), 0.2 mM each of dATP, dTTP, dCTP and dGTP (Invitrogen), 5 µl of 5X GoTaq reaction buffer containing 1.5 mM $MgCl_2$ (Promega), 1U of Taq DNA polymerase (Promega), made up to a final volume of 25 µl with DEPC-treated (0.05% v/v diethyl pyrocarbonate in $dH_2O$) water.

The "Touchdown" PCR protocol started with the initial denaturation for 5 minutes at 94 ºC to denature the template. In the first 10 cycles, denaturation lasted for 15 seconds at 94 ºC; the annealing temperature was decreased 1 ºC every cycle from 65 ºC for 30 seconds and the extension was at 72 ºC for 40 seconds. In the subsequent 30 cycles, the cycling program was set as a denaturing step (15 seconds at 94 ºC), an annealing step (30 seconds at 55 ºC) and an elongation step (40 seconds at 72 ºC). The initial temperature selected for the annealing step was 65°C so that the annealing temperature was progressively decreased to 55°C by the end of this stage (Korbie & Mattick, 2008). The gradually reduced annealing temperature increased the specificity and sensitivity of the PCR reaction. After the final cycle, a final extension of 5 minutes at 72 ºC was performed and then held at 4 ºC (Figure 2.2).

Positive and negative controls were always set up for each genotype. A plasmid template from wild-type or heterozygote mice were used to replace the DNA template as a positive control. DEPC-treated water was used instead of the DNA template as a

## Table 2.3

### Primers used for zDHHC23-KO genotyping

| Name | Target Gene | Tm (ºC) | Sequence (5' – 3') |
|---|---|---|---|
| Reg-zDHHC23-wtF | Wild-type | 71.8 | AGT AAG CAT TTG GAA ATG GGC CAC C |
| Reg-zDHHC23-wtR | Wild-type | 66.9 | AGT GAA GGG AGT CTT AGC ACT CAG C |
| Reg-NeoF | zDHHC23-KO | 71.0 | GCA GCC TCT GTT CCA CAT ACA CTT CA |
| Reg-zDHHC23-R | zDHHC23-KO | 62.9 | AAT TGA AAG GAG GGC GAG AAA TGC C |

# Figure 2.2

## Cycling parameters for zDHHC23-KO genotyping

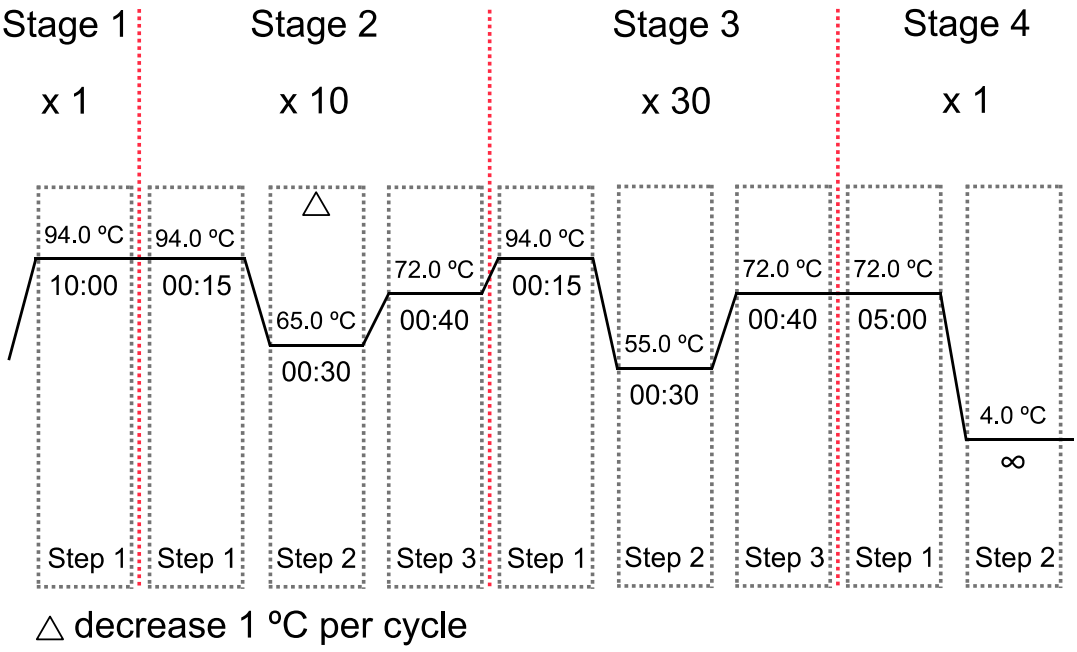


**Figure 2.2 Cycling parameters for zDHHC23-KO genotyping.** zDHHC23-KO genotyping started with a denaturing stage at 94 ºC for 5 minutes. The second stage was programmed as the denaturation (15 seconds at 94 ºC), the annealing step (the temperature decreased 1 ºC every cycle from 65 ºC for 30 seconds) and the extension (40 seconds at 72 ºC) for 10 cycles. The third stage cycling program was set as a denaturing step (15 seconds at 94 ºC), an annealing step (30 seconds at 55 ºC) and an elongation step (40 seconds at 72 ºC) for 30 cycles. After the final cycle, PCR reaction was completed with a 5 minute extension at 72 ºC and held at 4 ºC.

negative control to confirm the contamination.

#### 2.2.2.3 Agarose gel electrophoresis of DNA

Gel electrophoresis was used to separate and analyse the PCR amplified DNA according to molecular weight on a gel composed of 1% - 1.5% agarose (w/v; Invitrogen). 1x TBE buffer (45 mM Tris, 49 mM Boric acid and 1.6 mM EDTA) was used to make to gel and 0.01% SYBR® Safe (Invitrogen) DNA gel stain was added and mixed well in the gel to allow the visualization of DNA under ultraviolet (UV) light. 5 µl of DNA samples were loaded into each lane and with one lane loading 6 µl of GeneRuler 1 kb DNA Ladder (Thermo Scientific) to allow molecular weights to be determined. Electrophoresis was performed in 1x TBE buffer for 20-30 minutes at a constant voltage of 120 V with PowerPac™ Basic Power Supply (Bio-Rad). Gels were imaged under UV illumination using the GeneGenius Bio Imaging System (SYNGENE) and images were captured using GeneSnap (SYNGENE).

BK-KO genotype was identified with three primers: two forward primers corresponding to wild-type and knockout alleles, and one common reverse primer. When determining the BK-KO genotype, wild-type mice (+/+) show a single band around 480 bp, BK knockout mice (−/−) show a single band around 170 bp, and heterozygotes (+/−) show two bands (Figure 2.3). zDHHC23-KO genotype was

identified with four primers: a set of forward and reverse primers corresponding to wild-type genes and the other set of forward and reverse primers corresponding to knockout genes. When determining the zDHHC23-KO genotype, wild-type mice (+/+) was positive (+) for wild-type primers showing a single band around 300 bp and negative (−) showing no bands for knockout primers. zDHHC23 knockout mice (−/−) was negative (−) showing no bands for wild-type primers and positive (+) for knockout primes showing a single band around 460 bp. Heterozygotes (+/−) showed a single band for each set of primers (Figure 2.4).

## 2.3 Generation of POMC-GCaMP6s lentivirus

The POMC-GCaMP6s reporter was constructed using a pLenti backbone from Addgene plasmid No.20946, whose coding region was replaced with a genetically encoded calcium indicator GCaMP6s from Addgene plasmid No.40753 under the control of the minimal rat *Pomc* promoter (Romanò *et al.*, 2017). This ensures specific expression in corticotrophs (Hammer *et al.*, 1990). The SURF facility of the University of Edinburgh or VectorBuilder Inc. packed the lentivirus for us. Multiple batches of virus were generated and used throughout this study, with the titre of virus ranging from 6.30 x $10^8$ to 1.81 x $10^{11}$ TU/ml. Fresh aliquots of lentivirus were diluted with culture medium to transduce each preparation of mouse primary anterior pituitary cells (See 2.4.2). The final titre of virus used for transduction ranged from 2.63 x $10^4$

## Figure 2.3

### BK-KO genotyping PCR products separated by agarose gel electrophoresis

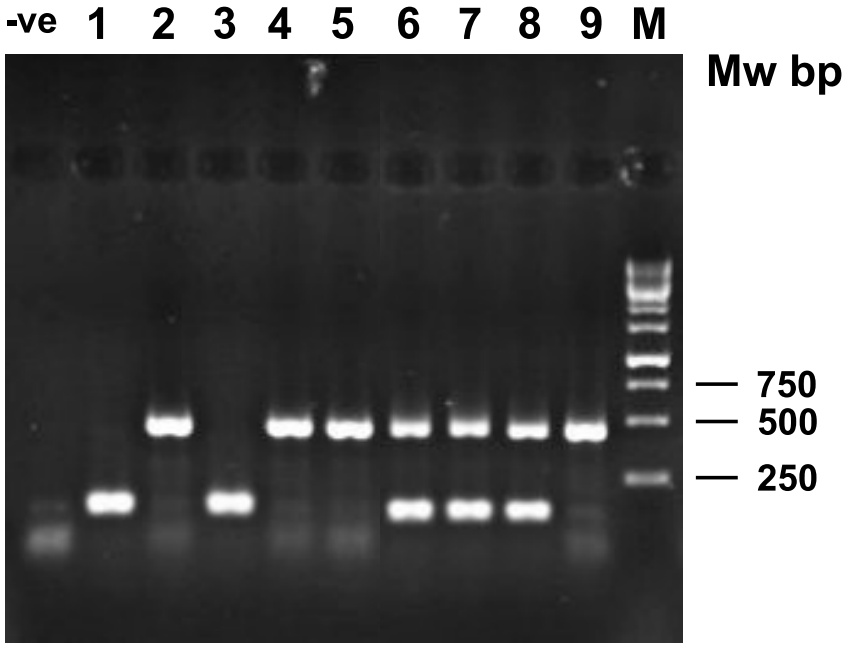


**Figure 2.3 BK-KO genotyping PCR products separated by agarose gel electrophoresis.** Each numbered lane represented a mouse. When determining the BK-KO genotype, wild-type mice (+/+) showed a single band around 480 bp, BK knockout mice (−/−) showed a single band around 170bp and heterozygotes (+/−) showed two bands. −ve represented a negative control; M represented a 1kb DNA ladder.

## Figure 2.4

### zDHHC23-KO genotyping PCR products separated by agarose gel electrophoresis

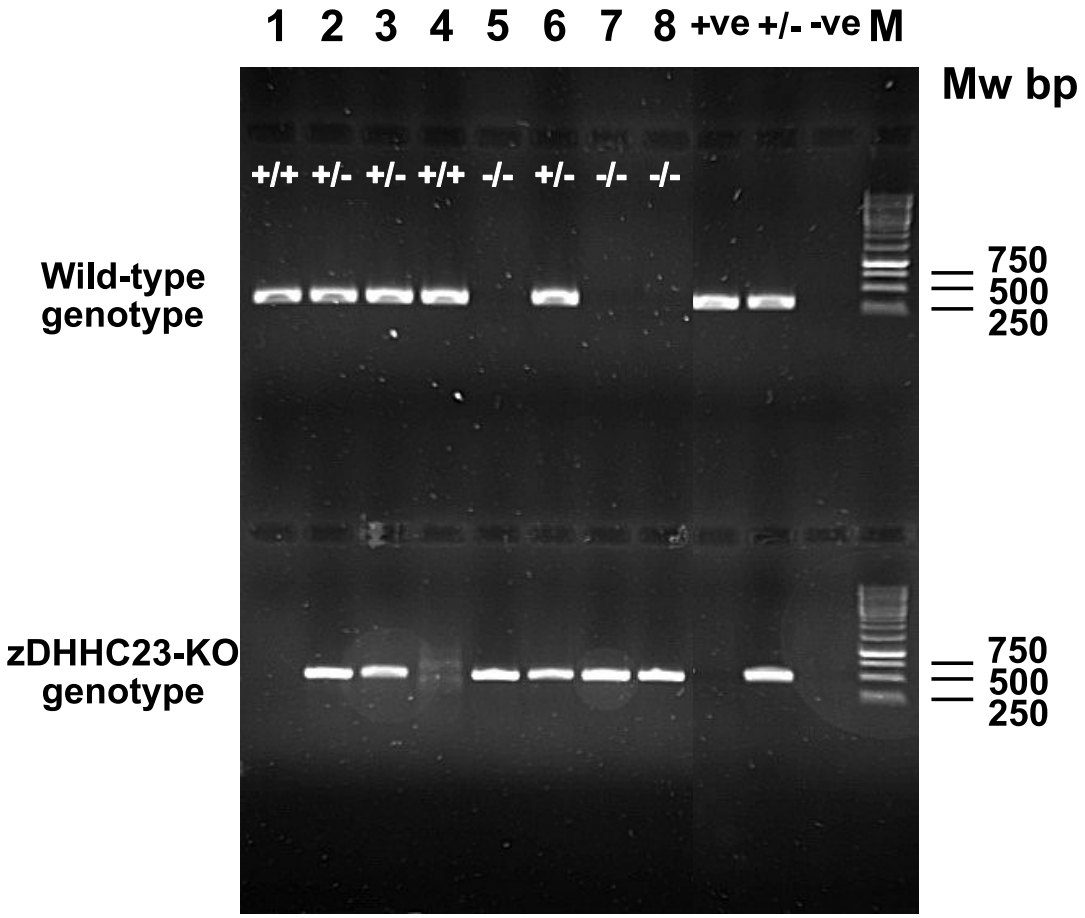


**Figure 2.4 zDHHC23-KO genotyping PCR products separated by agarose gel electrophoresis.** Each numbered lane represented a mouse. When determining the zDHHC23-KO genotype, wild-type mice (+/+) was positive (+) for wild-type primers showing a single band around 300 bp and negative (−) showing no bands for knockout primers. zDHHC23 knockout mice (−/−) was negative (−) showing no bands for wild-type primers and positive (+) for knockout primes showing a single band around 460 bp. Heterozygotes (+/−) showed a single band for each set of primers. +ve represented a positive control; +/− represented a heterozygote control; −ve represented a negative control. M represented a 1kb DNA ladder.

to 2.87 x 106 TU/ml.

## 2.4 Primary cell culture and lentiviral transduction of mouse anterior pituitary cells

### 2.4.1 Isolation and culture of mouse anterior pituitary cells

For each preparation, three genotyped mice (either male or female) were killed by cervical dislocation. After removing heads and scalps, the anterior pituitary was gently removed from the skull. The anterior lobes were isolated, the posterior lobe was gently removed and the intermediate zone was dissected out to avoid contamination from POMC-expressing melanotrophs. The isolated anterior pituitary lobes were placed in a dish with DMEM (+4.5 g/L high-glucose, +L-Glutamine, +25 mM HEPES, −Pyruvate; Gibco) and then chopped with a single edged razor blade in both directions (dish rotated by 90º).

The chopped anterior lobes were transferred into a tube with a digestion solution made of DMEM containing 0.25% (w/v) Trypsin (Worthington) and 36 Kunitz units/ml DNAse I and incubated at 37 ºC for 20–25 minutes in a water bath. The tube was shaken every 5 minutes to ensure a complete and equivalent digestion. The tube was left for 5 minutes to allow tissue pieces to settle to the bottom after the digestion and the supernatant was aspirated. 1 ml of inhibition solution consisted of DMEM

containing 0.25 mg/ml Soybean Trypsin inhibitor, 100 kallikrein units Aprotinin (200x dilution of Sigma stock), 36 Kunitz units/ml DNAse I was added to stop the digestion and the tissue pieces were triturated using a 1ml Pipetman tip (Gilson) approximately 40 times. Another 4 ml of inhibition solution were added into the tube and the cell suspension was filtered over a cell strainer with 70 µm nylon mesh (Falcon$^{TM}$, BD Biosciences). The cell suspension was then diluted with an equal volume of culture medium containing DMEM with ITS (10 µg/ml insulin, 5.5 µg/ml transferrin, 30 nM sodium selenite), 0.3% bovine serum albumin (BSA; w/v), 4.2 µg/ml fibronectin and antibiotic/antimycotic (100× dilution of Sigma stock) and centrifuged at 100 ***g*** for 10 minutes at room temperature (RT). To disperse single pituitary cells, the supernatant was removed without disturbing the pellet which was then triturated with 1 ml culture medium for approximately 40 times. Another 1.5 ml of culture medium were added to make up the final cell suspension. One 12 mm coverslip was added to each well in a 12-well plate and 200 µl of the final cell suspension was plated onto the coverslips. The 12-well plate was left for 20 minutes to allow the pituitary cells to settle down and 1 ml of culture medium was then added to each well. Primary pituitary cells were incubated at 37 ºC in 95% air/5% $CO_2$.

### 2.4.2 Lentiviral transduction of mouse anterior pituitary cells

After incubating for 4–6 h in culture medium, primary pituitary cells were transduced

with POMC-GCaMP6s lentivirus. The culture medium was then replaced with fresh antibiotic/antimycotic free culture medium after 24 h transduction and the medium was then changed with a culture medium free of antibiotic/antimycotic every two days. Corticotrophs usually displayed fluorescence 48–72 h post-transduction.

## 2.4.3 Validation and quantification of lentiviral transduction

### 2.4.3.1 Immunostaining and imaging

Mouse anterior pituitary cells cultured on glass coverslips 48–72 h after lentiviral transduction were washed with phosphate buffered saline (PBS, containing 137 mM NaCl, 2.7 mM KCl, 10 mM $Na_2HPO_4$ and 1.8 mM $KH_2PO_4$) 3 times and then fixed with 4% formaldehyde solution for 30 minutes at room temperature (RT). The formaldehyde was aspirated, cells were washed with PBS 3 times, incubated in permeabilization buffer (0.3% Triton X-100 in PBS) for 1 hour at RT and then in blocking buffer (0.3% Triton X-100, 3% BSA in PBS) for 1 hour at RT. Primary rabbit anti-ACTH antibody (1:1000, Abcam) and primary chicken anti-GFP antibody (1:2000, Abcam) were diluted in blocking solution and incubated at 4 ºC overnight. The next day pituitary cells were washed 3 times with PBS and then incubated with secondary antibodies (goat anti-rabbit IgG conjugated with Alexa Fluor 546, 1:1000, Invitrogen; goat anti-chicken IgY conjugated with Alexa Fluor® 488, 1:1000, Abcam) diluted in blocking buffer for 1 hour at RT. After washing with PBS 3 times, cells were

incubated for 1–2 min with TO-PRO-3 Iodide for nuclei staining. Subsequently, cells were rinsed rapidly in distilled water, drained and then finally mounted on glass slides with Mowiol 4-88 mounting medium (Calbiochem) containing 1,4-diazabizyclo[2.2.2]octane (DABCO, Sigma) as anti-fading agent. Cells were left overnight to dry in the dark and stored at 4 ºC before image acquisition.

Z-stack confocal images were obtained using a Nikon A1R confocal laser microscope system (Nikon Corp., Tokyo, Japan) equipped with a 20x Plan Apochromat VC (NA = 0.75) objective lens. To image GCaMP6s (Alexa Fluor® 488 antibody), 488 nm laser was used for excitation and emission was collected using a 525/50 nm bandpass filter. For ACTH (Alexa Fluor 546 antibody), excitation was performed by a 561 nm laser and fluorescence was detected through a 595/50 nm bandpass filter. TO-PRO was excited with a 640 nm laser, emission was recorded at 700/75 nm. The multitracking function was used to minimize the cross-talk between different fluorophores. Images were acquired with Nikon NIS Elements software and processed with Fiji software (Schindelin *et al.*, 2012).

#### 2.4.3.2 Quantification of POMC-GCaMP6s reporter expression

The expression of GCaMP6s reporter was controlled by the minimal rat *Pomc* promoter using lentivirus-mediated cell transduction in murine primary pituitary cell

cultures. The efficiency and specificity of lentiviral-mediated transduction of corticotrophs with GCaMP6s was quantified:

For efficiency, the percentage of total anterior pituitary cells that were immunohistochemically identified as corticotrophs (ACTH positive) that also expressed GCaMP6s, was determined.

$$\text{Efficiency (\%)} = \frac{\text{ACTH and GCaMP6s positive cells}}{\text{ACTH positive cells}} * 100\%$$

Specificity was determined by calculating the percentage of all anterior pituitary cells that expressed GCaMP6s that were also immunohistochemically identified as corticotrophs (ACTH positive).

$$\text{Specificity (\%)} = \frac{\text{ACTH and GCaMP6s positive cells}}{\text{GCaMP6s positive cells}} * 100\%$$

## 2.5 Calcium imaging

### 2.5.1 Calcium imaging recordings

Calcium imaging recordings were performed on single isolated corticotrophs cultured on glass coverslips post-transduction (typically 48h–72h). A coverslip was placed in the centre of a circular recording chamber with two parallel silica inserts to keep the

coverslip stable and allow the linear flow of solution. The chamber was mounted on a heated stage (37 ± 1 ℃) that warmed the solution in the chamber to 30 ± 1 ℃. During recording, corticotrophs were continuously perfused with oxygenated Ringer's solution at a rate of 1–2 ml/minute with all treatments applied at the same flow rate. Isolated cells expressing POMC-CaMP6s lentivirus were imaged with an Olympus IX81 epi-fluorescence microscope (Olympus, Tokyo, Japan), equipped with an MT20 xenon lamp, an EM-CCD digital camera (Hamamatsu Photonics, Hamamatsu City, Japan), a VCM-D1 Uniblitz shutter driver (Vincent Associates, NY, USA), which was linked to a computer. Hardware control was performed using Cell^R imaging software. Images were captured every second using either a 488 nm laser or 492 nm filter for excitation and a 547/31 nm bandpass filter for emission.

## 2.5.2 Calcium imaging protocols

### 2.5.2.1 CRH and AVP physiological concentrations and patterns of release

The physiological concentrations of CRH and AVP in the pituitary portal circulation of mice is are not well characterized. In anaesthetised rats, during stress CRH concentrations are typically reported between 0.11 ± 0.01 nM and 0.19 ± 0.04 nM (Gibbs & Vale, 1982; Sheward & Fink, 1991) with AVP at 1.81 ± 0.38 nM (Sheward & Fink, 1991). In this PhD study, 0.2 nM CRH and 2 nM AVP were assumed to be

within the physiological range, albeit of a stressed and anesthetized rat, and hence were used. Importantly these concentrations are in accordance with those used in previous electrophysiological and calcium imaging studies in both primary rat and mouse corticotrophs (Duncan *et al.*, 2015; Romanò *et al.*, 2017). The actual patterns of CRH or AVP release in the pituitary portal circulation are also not well characterised. In a previous study in rats, the average frequency of CRH pulsatile release was approximately every 20 minutes with pulse duration being variable between 2.5 to 10 minutes based on push pull sampling of every 2.5 minutes or 5 minutes (Ixart *et al.*, 1991). In this PhD study, a three minute duration square wave pulse of CRH and/or AVP was used to replicate a typical release pulse and the stimulus was applied every 25 minutes to ensure complete washout and recovery to baseline before exposure to the next stimulus.

#### 2.5.2.2 Repeated stimulation protocol

Initial calcium imaging recordings were performed with a repeated stimulation protocol (Figure 2.5A, based on that reported in Romanò *et al.*, 2017). Spontaneous intracellular free calcium ($[Ca^{2+}]_i$) signalling was recorded for 15–20 minutes. Cells were then exposed to a stimulus for three minutes, which was repeated three times at 25 minutes intervals. Finally, cells were treated with 30 mM potassium chloride for one minute to confirm cell viability (Figure 2.5A). During this study, some

experiments were performed to investigate the synergistic effect of CRH and AVP at the level of $[Ca^{2+}]_i$. These recordings also followed a similar repeated stimulation protocol, where cells were exposed to either CRH or AVP in a random order, followed by the combined stimulus (CRH + AVP).

#### 2.5.2.3 Ion channel blocking protocol

Based on the repeated stimulation protocol, an ion channel blocking protocol was developed to examine the role of specific ion channels (Figure 2.5B). Starting with 15–20 minutes basal recording to define spontaneous $[Ca^{2+}]_i$ signalling, corticotrophs were then exposed to a stimulus of interest for three minutes. The second three minute stimulation was applied to corticotrophs in the presence of an ion channel blocker, which was applied 10 minutes before and after the second stimulus to ensure the blockade of specific ion channels. After a 25 minute washout period, cells were exposed to the stimulus for the third time to confirm whether the effects of the blocker were reversible. Calcium imaging recording was completed with a one minute 30 mM potassium chloride stimulus to verify cell viability (Figure 2.5B).

# Figure 2.5

## Protocols for calcium imaging

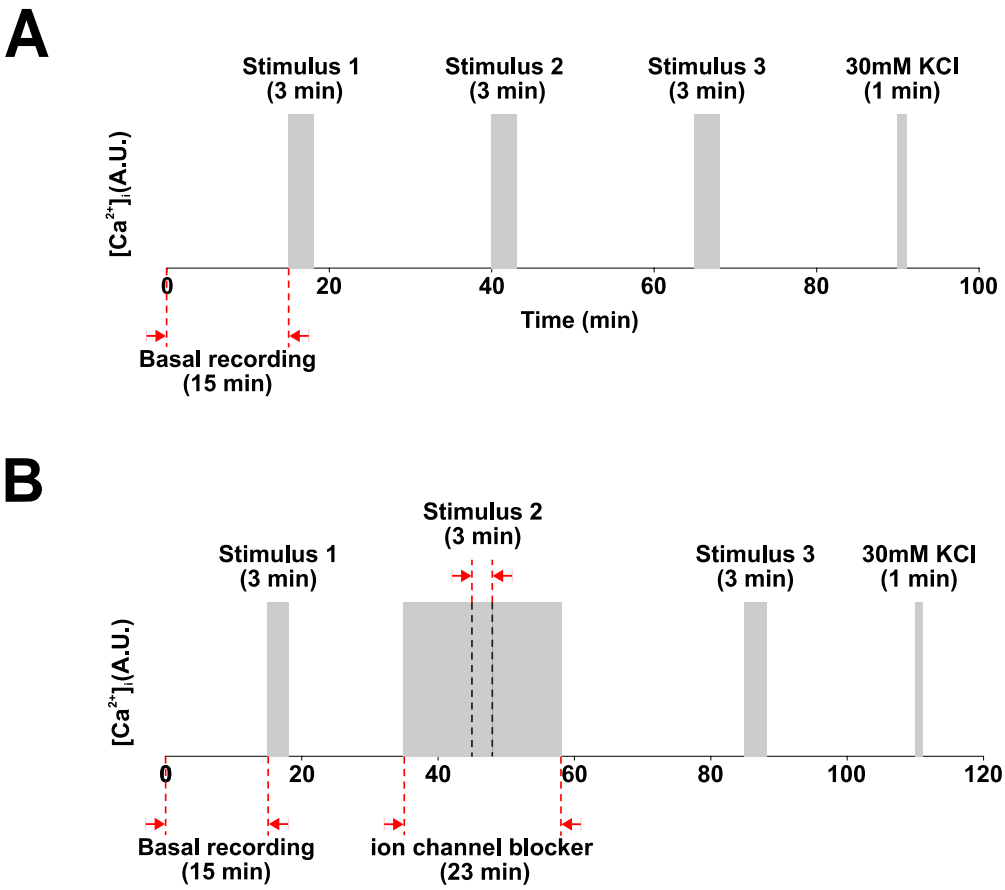


**Figure 2.5 Protocols for calcium imaging. (A)** Repeated stimulation protocol: cells were exposed to a stimulus for three minutes that was repeated three times at 25 minutes intervals. When investigating synergy between CRH and AVP, cells were exposed to either CRH or AVP in a random order, followed by the combined stimulus. **(B)** Ion channel blocking protocol: cells were first exposed to a stimulus for three minutes. The second three minute stimulation was applied to corticotrophs in the presence of an ion channel blocker, applied 10 minutes before and after the second stimulus. After a 25 minute washout period, cells were exposed to the stimulus for a third time to determine reversibility.

# 2.6 Data analysis

## 2.6.1 Acquisition of data from images

After collecting the calcium images using Cell^R imaging software, fluorescent intensity was calculated with Fiji and background noise was subtracted using a region of interest not containing any cell. Extracted calcium imaging traces were then analysed using custom scripts written in R by Dr Nicola Romanò (See Appendices I and II).

## 2.6.2 Measurement parameters

### 2.6.2.1 Criteria for inclusion of data

Corticotrophs were exposed to stimuli three times during calcium imaging recordings. For inclusion in the data analyses, only the cells that responded to the three consecutive stimuli as well as responding to 30 mM potassium chloride, to verify cell viability at the end of recording were included (Figure 2.6A). An example of a recording that was excluded because it did not met the inclusion criteria is given above is shown in Figure 2.6B.

# Figure 2.6

## Criteria of a valid calcium imaging recording

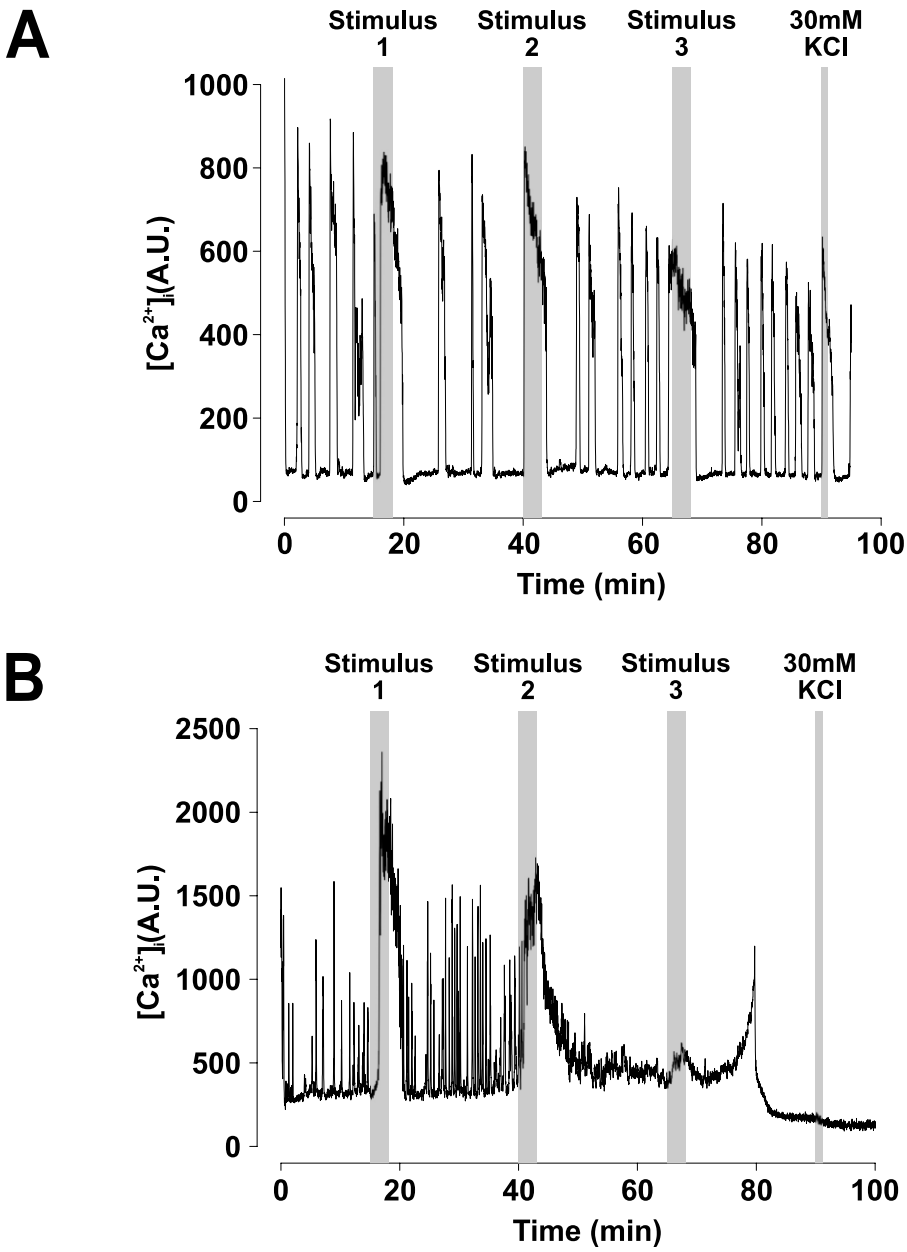


**Figure 2.6 Criteria of a valid calcium imaging recording. (A)** A valid calcium imaging recording includes clear and effective calcium responses to all stimuli and an effective response to 30 mM KCl. **(B)** Cells showing no clear and effective responses to all three stimuli or KCl are excluded.

#### 2.6.2.2 Measurement parameters

In this Thesis, the POMC-GCaMP6s calcium indicator rather than a ratiometric dye was used to allow the identification and analysis of intracellular free calcium level in corticotrophs. The absolute basal level of calcium signal is dependent on the expression level of POMC-GCaMP6s in each cell. Thus, instead of defining the absolute basal calcium level, which was the minimum value in the calcium imaging experiment, I measured spontaneous and secretagogue-induced $[Ca^{2+}]_i$ responses relative to the basal calcium level in each cell.

Spontaneous $[Ca^{2+}]_i$ signalling was defined by spontaneous active time and maximum amplitude (see 3.2.2). The data were presented as a probability density function (p.d.f.) histogram with the Y-axis indicating the probability density (of either the percentage of active time or of the maximum amplitude). It is important to note that the p.d.f. shows the probability per unit value of the observed variable. In other words, to obtain the probability that the variable is between two values a and b we should integrate (i.e. calculate the area under the curve) the p.d.f. between a and b. This implies that the area under the curve of the whole p.d.f. (i.e. its integral between $-\infty$ and $+\infty$) needs to be 1, since a probability cannot be greater than 1. However, for an interval [a,b] smaller than 1, the p.d.f. can take values greater than 1, provided that the area under the curve in [a,b] is $< 1$.

To quantify the intensity of $[Ca^{2+}]_i$ responses to different secretagogues, several parameters were used (Figure 2.7), including:

- **AUC (10 min)**: area under the curve (AUC) for a 10 minute window from the time secretagogues arrived in the bath. This is based on previous observations in mouse corticotrophs for the typical duration of membrane excitability to a 3 min pulse exposure to CRH (0.2 nM) or AVP (2 nM) (Duncan *et al.*, 2015).
- **AUC (peak)**: AUC measured from the start of secretagogue exposure to first point after stimulus $[Ca^{2+}]_i$ response returns to baseline.
- **Peak**: the highest point after secretagogue arrival in the bath during the 10 minute recording window.
- **Time to peak**: time from secretagogues arrived in the bath to peak, measuring the time needed to reach the maximum $[Ca^{2+}]_i$ level change.
- **Response duration**: time from secretagogue arrival in the bath to first point after stimulus $[Ca^{2+}]_i$ response returns to baseline.
- **Peak duration**: time from the start of secretagogue exposure to first point after stimulus $[Ca^{2+}]_i$ response returns to baseline.
- **Time gap**: time between secretagogue arrival in the bath and start of the response.

# Figure 2.7

## Measurement parameters of calcium imaging recordings

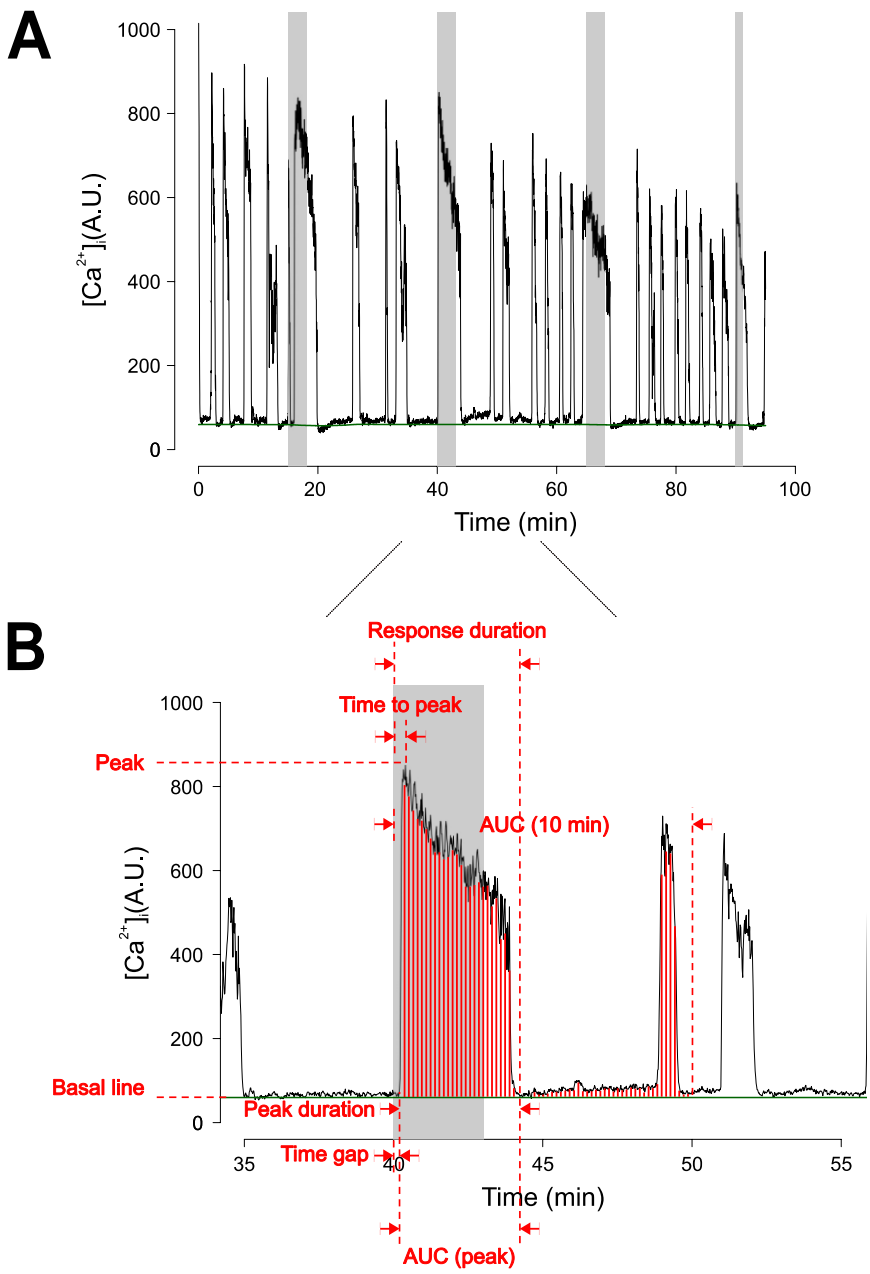


**Figure 2.7 Measurement parameters of calcium imaging recordings. (A)** A representative calcium imaging trace following repeated stimulation protocol. **(B)** Area under the curve (AUC) (10min), AUC (peak), peak, time to peak, response duration, peak duration, and time gap were measured parameters. Grey shading indicates the three minute duration of exposure to stimulus.

### 2.6.3 Statistical analysis

The data were expressed as mean ± SEM (standard error of the mean), N = number of independent experiments, and n = number of independent cells. All data was presented using R (R Development Core Team) and GraphPad Prism v7.00 (GraphPad Software, Inc). All statistical analysis was performed using R, with significant differences defined by * $p < 0.05$, ** $p < 0.01$ and *** $p < 0.001$.

In this study, all calcium imaging experiments used a repeated stimulation protocol, which allowed analysis of repeated $[Ca^{2+}]_i$ responses to same/different stimuli in the same cell. Thus, all measuring parameters were compared using mixed effects models with the *nlme* R package. In the mixed effects models, genotype of the mouse, sex of the mouse and the stimulus were used as fixed factors; the cell, the experiment, and experiment date were used as random factors. Estimated marginal means (EMMs) were then utilized to compare the $[Ca^{2+}]_i$ responses to repeated or different stimuli in corticotrophs isolated from mice of different genotypes. To improve model fitting and more reliable estimates, the data from different genotypes and sexes were analysed together (that is, all data presented in Chapters 3, 4 and 5 were analyzed together), which allowed us to use all the data collected to increase the sample size and account for the correlations between the data. In this case, we also estimated fewer parameters and reduced the likelihood of Type I Errors when making multiple comparisons.

Since the absolute values of the AUC (10 min), AUC (peak) and peak were variable depending on the expression level of the non-ratiometric POMC-GCaMP6s reporter, statistical analysis was performed on log-transformed data. When comparing the normal mixed effects model and mixed effects logit model, Akaike Information Criterion (AIC) and Bayesian Information Criterion (BIC) indicated that the mixed effects logit model was better fitted. However, no differences were observed in other measuring parameters including time to peak, response duration, peak duration and time gap. Therefore, statistical analysis for AUC (10 min), AUC (peak) and peak were performed using mixed effects logit models followed by EMMs, while the other parameters were analyzed with mixed effects models with EMMs test.

# Chapter Three:

# Calcium signalling in wild-type corticotrophs

# Chapter 3: Calcium signalling in wild-type corticotrophs

## 3.1 Introduction

In this chapter, the first aim was to exploit a lentiviral transduction system that allows specific labelling of live murine corticotrophs *in vitro*. Next, calcium imaging experiments were performed on corticotrophs isolated from male and female wild-type mice respectively to explore spontaneous intracellular free calcium ($[Ca^{2+}]_i$) of corticotrophs and characterise $[Ca^{2+}]_i$ signalling following CRH or AVP stimulation in terms of their typical pulsatile release and physiological concentrations. Furthermore, experiments were also performed in both sexes to investigate whether CRH and AVP act in a synergistic manner at the level of intracellular free calcium.

### 3.1.1 Identification of corticotrophs

The anterior pituitary gland consists of five types of hormone secreting cells with corticotrophs only comprising ~10% of the population, which presents the challenge of specific identification of live corticotrophs from the variety of cell populations. Methods used in previous studies to identify corticotrophs from primary cell cultures have several drawbacks including prior exposure to high dose of CRH and stimulation with higher concentrations of CRH up to 100 nM that is far beyond the physiological

range (Guérineau *et al.*, 1991; Lee & Tse, 1997), which makes it difficult to explore the spontaneous $[Ca^{2+}]_i$ signalling of corticotrophs and replicate a typical stress response *in vivo.* A lentiviral-mediated POMC-eYFP reporter generated by Liang and colleagues allowed the identification and systematic analysis of electrical properties of corticotrophs (Liang *et al.*, 2011), however, it's not suitable for calcium imaging study. Integration of the lentivirus transduction system and calcium imaging indicators may provide a new tool to specifically label corticotrophs *in vitro* when investigating the $[Ca^{2+}]_i$ signalling.

In this chapter, a labelling approach using lentiviral mediated transduction of primary murine pituitary cells *in vitro* with the latest calcium indicator GCaMP6s driven by the minimal rat *Pomc* promoter was examined.

### 3.1.2 Calcium signalling in corticotrophs

It has been demonstrated that corticotrophs are electrically excitable and fire action potentials which causes transient elevation in $[Ca^{2+}]_i$ (Stojilkovic *et al.*, 2010). Hypothalamic hormones CRH and AVP stimulate ACTH secretion from corticotrophs through different calcium signalling pathways. CRH, the predominant secretagogue, acts on corticotrophs via CRHR1 to activate the Gαs pathway resulting in an accumulation of cAMP and an activation of PKA, with subsequent influx of

extracellular $Ca^{2+}$ via L-type $Ca^{2+}$ channels (Kuryshev *et al.*, 1995; Murat *et al.*, 2012). AVP, on the contrary, acts on corticotrophs via V1b coupled to the Gαq pathway leading to the activation of PKC and the generation of $IP_3$ triggering the release of $Ca^{2+}$ from $IP_3$-sensitive intracellular stores (Tse & Lee, 1998). Since CRH and AVP regulate corticotrophs through different mechanisms, it is necessary to examine both pathways when attempting to examine secretagogue-induced $[Ca^{2+}]_i$ signalling in corticotrophs.

Two distinct patterns of electrical activity have been observed in secretory cells from anterior pituitary lobe: single spikes and pseudo-plateau bursting (Stojilkovic *et al.*, 2010). Previous studies revealed that pseudo-plateau bursting behaviour has a higher capacity to drive $Ca^{2+}$ influx than large amplitude single-spike action potentials. Pseudo-plateau bursting action potentials are believed to generate sufficient calcium signals to trigger hormone secretion (Van Goor *et al.*, 2001*b*; Stojilkovic *et al.*, 2005). Other studies indicated that corticotrophs primarily fire spontaneous single spike activity that could become pseudo-plateau bursting when stimulated (Kuryshev *et al.*, 1997; Duncan *et al.*, 2015, 2016). CRH and AVP have been reported to promote different patterns of corticotroph electrical activity with CRH driving the transition to bursting whereas AVP induces the increase in spiking frequency and increase $[Ca^{2+}]_i$ in corticotrophs (Leong, 1988; Duncan *et al.*, 2015). The $Ca^{2+}$ mobilization of

transforming single spiking into bursting in corticotrophs following CRH stimulation may play a vital role in triggering ACTH secretion. However, the mechanism underlying the $[Ca^{2+}]_i$ signalling remains elusive. In addition, CRH and AVP have been demonstrated to act synergistically to regulate ACTH release, however, synergy has not been investigated at the level of intracellular free calcium.

In this chapter, calcium imaging experiments were performed to define spontaneous $[Ca^{2+}]_i$ of corticotrophs and characterise $[Ca^{2+}]_i$ signalling regulated by CRH and AVP. The synergy between CRH and AVP was also investigated at the level of $[Ca^{2+}]_i$. Considering the possible sex differences in the HPA stress axis, all experiments were carried out in male and female wild-type corticotrophs respectively.

## 3.2 Results

### 3.2.1 Identification and labelling of mouse corticotrophs with a lentiviral POMC-GCaMP6s reporter

The anterior pituitary is made up of multiple cell types with corticotrophs representing only 5–10% of the cell population. To allow specific targeting of corticotrophs *in vitro* for calcium imaging experiments, genetically encoded calcium indicator GCaMP6s was expressed under the control of a minimal rat *Pomc* promoter using lentivirus-mediated cell transduction of isolated mouse anterior pituitary cultures

(Figure 3.1A). To determine the efficiency and specificity of lentiviral-mediated GCaMP6s expression in murine corticotrophs, isolated and dispersed cells were dual labelled for ACTH and GCaMP6s using immunohistochemistry. About 53 ± 8.0% of anterior pituitary cells that were immunohistochemically identified as corticotrophs (ACTH positive, ACTH+) also expressed GCaMP6s, which demonstrated the efficiency of lentiviral-mediated expression of GCaMP6s with the specific *Pomc* promoter (Figure 3.1B). Importantly, 83 ± 4.9% of GCaMP6s positive cells were immunohistochemically identified as corticotrophs (ACTH+) revealing good specificity of the minimal *Pomc* promoter for driving the expression of GCaMP6s in corticotrophs. Thus, POMC-GCaMP6s lentivirus is a useful tool to identify and label mouse anterior pituitary corticotrophs *in vitro* (Figure 3.1C).

### 3.2.2 Wild-type corticotrophs show variable spontaneous $[Ca^{2+}]_i$ signalling

In order to investigate the effects of CRH and/or AVP on $[Ca^{2+}]_i$ signalling in corticotrophs, it was first essential to determine spontaneous $[Ca^{2+}]_i$ signalling of corticotrophs under basal conditions. Calcium imaging experiments were performed following the protocol in Section 2.5.1 and corticotrophs continuously perfused with Ringer's solution (in mM, 125 NaCl, 2.5 KCl, 1.25 $NaH_2PO_4$, 12 $NaHCO_3$, 1 $MgCl_2$, 2 $CaCl_2$, pH 7.3, osmolarity between 300 and 305 mOsmol/l).

## Figure 3.1

### Identification and labelling of murine corticotrophs by lentiviral transduction of POMC-GCaMP6s reporter

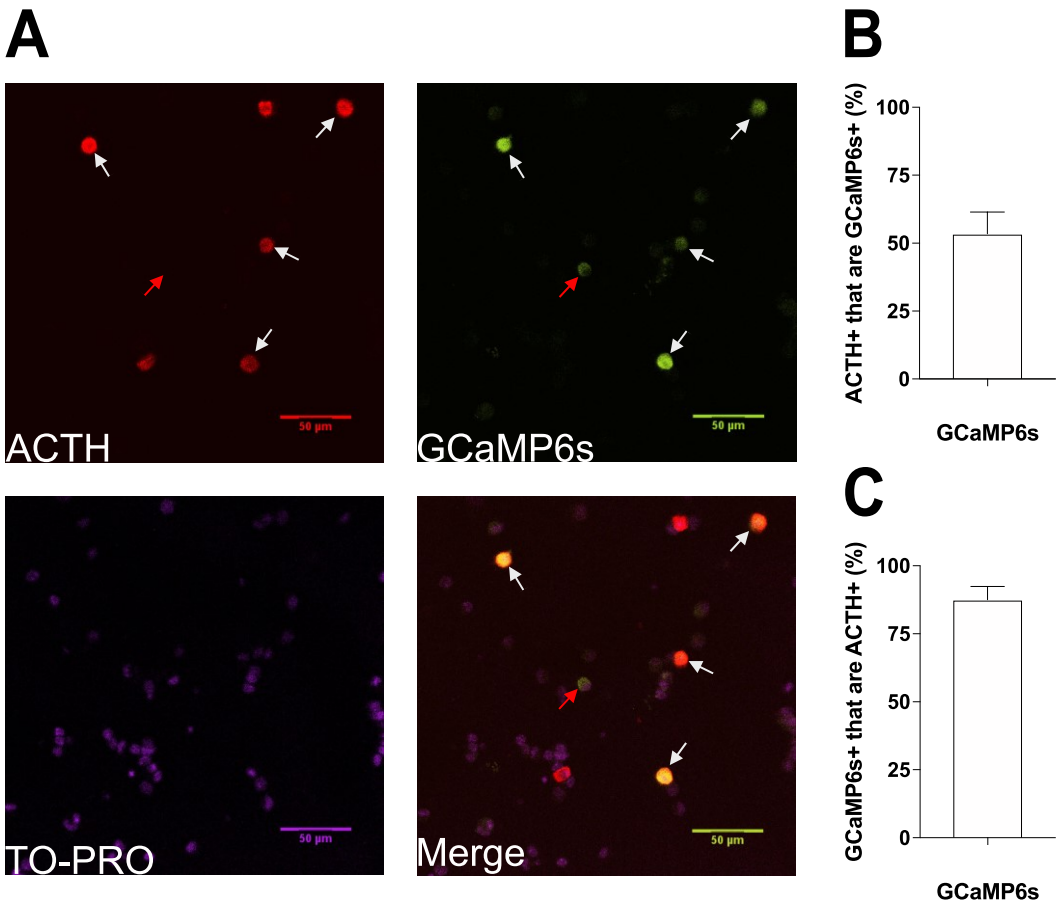


**Figure 3.1 Identification and labelling of murine corticotrophs by lentiviral transduction of POMC-GCaMP6s reporter. (A)** Representative confocal sections of primary anterior pituitary cells following transduction with POMC-GCaMP6s lentivirus. The ACTH immunoreactivity (left top panel), GCaMP6s signal (right top panel), nuclei stained with TO-PRO (left bottom panel) and merged images (right bottom panel) are shown. Arrows show cells positive for ACTH (red), GCaMP6s (green) and merged images. Scale bars are 50 µm. **(B)** Quantification of percentage of cells immunoreactive for ACTH (ACTH+) that are also labelled with GCaMP6s (GCaMP6s+) reveals efficiency of transduction. **(C)** Quantification of percentage of cells labelled with GCaMP6s (GCaMP6s+) that are also immunoreactive for ACTH (ACTH+) reveals specificity. All data are means ± SEM, N > 3 independent experiments.

Previous studies have revealed that a sexually dimorphic mechanism probably exist in both calcium signalling and electrical activity of corticotrophs (Guérineau *et al.*, 1991; Liang *et al.*, 2011; Romanò *et al.*, 2017). Thus, corticotrophs isolated from male and female wild-type mice were investigated respectively.

In calcium imaging experiments using the POMC-GCaMP6s reporter, the absolute fluorescent intensity depends on both the intracellular free calcium concentration and the expression level of GCaMP6s. To analyse and quantify spontaneous $[Ca^{2+}]_i$ signalling of corticotrophs, calcium imaging traces were normalized between a value of 0 to 1 where 1 is the peak of the response to stimulus in the experiment and 0 is the baseline intensity under non-stimulated conditions in the same cell (Figure 3.2). Thus, the change of spontaneous $[Ca^{2+}]_i$ signalling could be compared between cells.

A "15% threshold" method was used to categorize and analyse spontaneous $[Ca^{2+}]_i$ signalling over a five minute period of "baseline" before the cells were exposed to any treatments. During the 5 min "baseline" period, the time during which the $[Ca^{2+}]_i$ signalling was above 15% of the peak of the subsequent response to stimulation with CRH (or AVP) (normalized to 1), was called active time and expressed as a percentage of the total "baseline" period (5 min). When the active time was 0%, the cell was defined as no spontaneous $[Ca^{2+}]_i$ signalling (Figure 3.2A). Cells displaying

spontaneous $[Ca^{2+}]_i$ signalling could thus be categorized based on the percentage of "active time" for each cell (Figure 3.2B).

The active time of spontaneous $[Ca^{2+}]_i$ signalling in all wild-type corticotrophs ranged from 0% to 100% with a mean of 45.2 ± 2.2% (n = 121 from 56 experiments) and the distribution was slightly skewed to the right (Figure 3.3A&B). To examine whether there were differences in spontaneous $[Ca^{2+}]_i$ signalling between male and female wild-type corticotrophs, active time was analysed as a function of sex. The spontaneous active time in female wild-type corticotrophs was 39.9 ± 3.0% (n = 72 from 28 experiments), whereas the mean of male wild-type corticotrophs was 53.0 ± 3.1% (n = 49 from 28 experiments) (Figure 3.3A), which is significantly ($p < 0.05$) longer compared to females. The distribution of active time in female wild-type corticotrophs was negatively skewed while in male wild-type corticotrophs was close to normal distribution (Figure 3.3C&D). This indicated that there was a high degree of variability as well as sex differences in the active time of spontaneous $[Ca^{2+}]_i$ signalling in wild-type corticotrophs.

Using the "15% threshold" definition of spontaneous $[Ca^{2+}]_i$ signalling, only 3.3% (4 out of 121 cells) of wild-type corticotrophs were silent (Figure 3.4A) with the rest displaying different patterns of spontaneous $[Ca^{2+}]_i$ signalling under basal conditions.

# Figure 3.2

## Definition of spontaneous $[Ca^{2+}]_i$ signalling

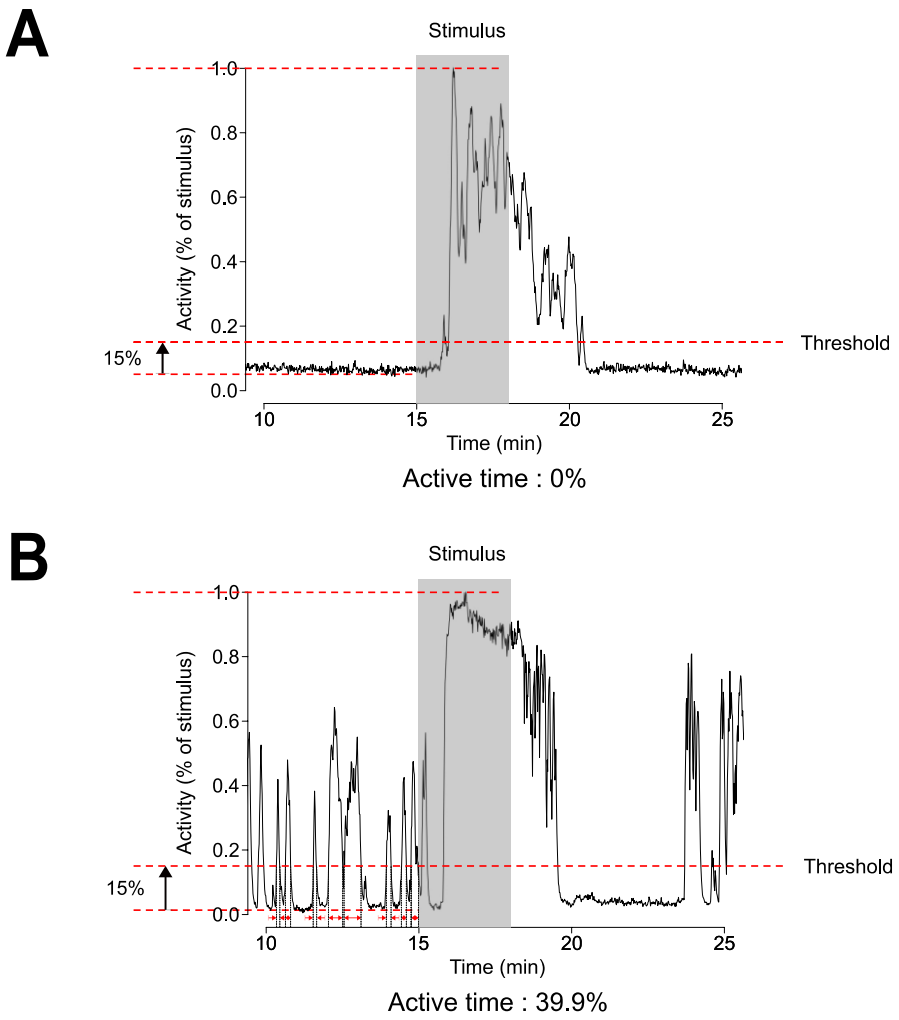


**Figure 3.2 Definition of spontaneous $[Ca^{2+}]_i$ signalling.** Spontaneous $[Ca^{2+}]_i$ signalling was defined by "15% threshold" method. During the 5 min "baseline" period, the time during which the $[Ca^{2+}]_i$ was above 15% of the peak of the response to stimulus (normalized as 1) was called active time and expressed as a percentage of the total "baseline" period (5 min). **(A)** The cells whose active time were 0% were defined as no spontaneous $[Ca^{2+}]_i$ signalling. **(B)** The cells whose active time were more than 0% was defined as displaying spontaneous $[Ca^{2+}]_i$ signalling could be categorized based on the percentage of "active time" for each cell.

## Figure 3.3

### Spontaneous $[Ca^{2+}]_i$ active time is significantly higher in male than female in wild-type corticotrophs

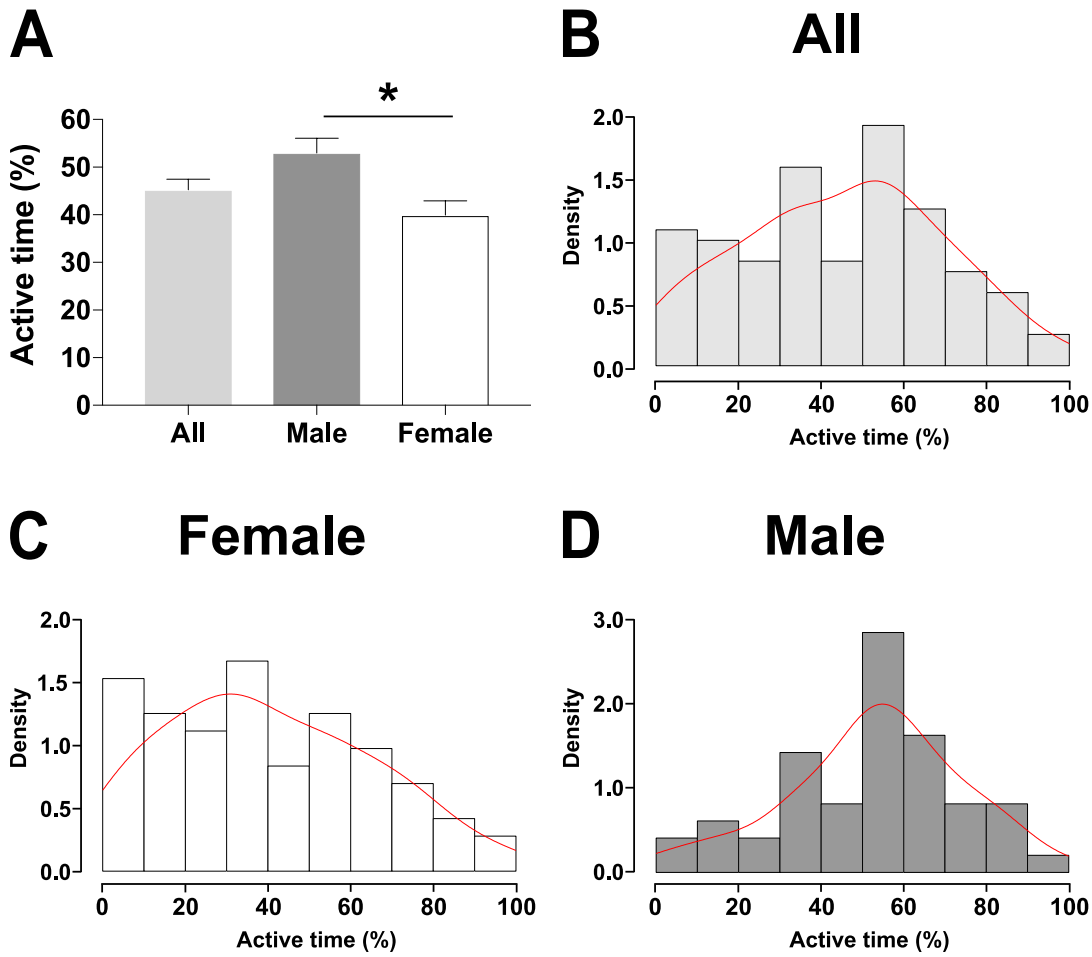


**Figure 3.3 Spontaneous $[Ca^{2+}]_i$ active time is significantly higher in male than female in wild-type corticotrophs. (A)** The mean active time of spontaneous $[Ca^{2+}]_i$ signalling in all wild-type corticotrophs. **(B)** The distribution of spontaneous $[Ca^{2+}]_i$ active time in all wild-type corticotrophs. The distribution of spontaneous $[Ca^{2+}]_i$ active time in **(C)** female and **(D)** male wild-type corticotrophs. Red line indicates the fit of distribution density. * $p < 0.05$ (female n = 72, male n = 49, mixed effects model). All data are means ± SEM, N > 3 independent experiments.

The amplitude, duration, frequency and kinetics of spontaneous $[Ca^{2+}]_i$ signalling were highly variable, the vast majority of cells exhibited two types of calcium behaviour: 46.3% of wild-type corticotrophs displayed high or low frequency of $Ca^{2+}$ oscillation (Figure 3.4B) and 43.8% of cells showed sustained $Ca^{2+}$ elevation that lasted for several minutes (Figure 3.4C). Besides, a small proportion of cells (6.6%) showed low amplitude, complex patterns of $[Ca^{2+}]_i$ changes during five minutes of recording (Figure 3.4D). Importantly, all patterns of spontaneous $[Ca^{2+}]_i$ signalling were found both in female (left panel) and male (right panel) wild-type corticotrophs.

The calcium imaging traces were normalized between 0 and 1 (the peak of the response to stimulus) which allowed us to compare the relative change in maximum amplitude of spontaneous $[Ca^{2+}]_i$ signalling in wild-type corticotrophs. The maximum amplitude was expressed as a percentage of the peak of the response to stimulus. The spontaneous $[Ca^{2+}]_i$ signalling in all wild-type corticotrophs had a maximum amplitude of 69.8 ± 1.7% (n = 121 from 56 experiments) which was positively skewed (Figure 3.5A&B). The maximum amplitude of spontaneous $[Ca^{2+}]_i$ signalling in female wild-type corticotrophs was 68.6 ± 2.3% (n = 72 from 28 experiments), which was not significantly different from male corticotrophs with a mean of 71.5 ± 1.5% (n = 49 from 28 experiments) in spontaneous $[Ca^{2+}]_i$ maximum amplitude (Figure 3.5A). The distribution of spontaneous maximum amplitude was skewed to the right in both male

## Figure 3.4

### Representative examples of spontaneous $[Ca^{2+}]_i$ in wild-type corticotrophs

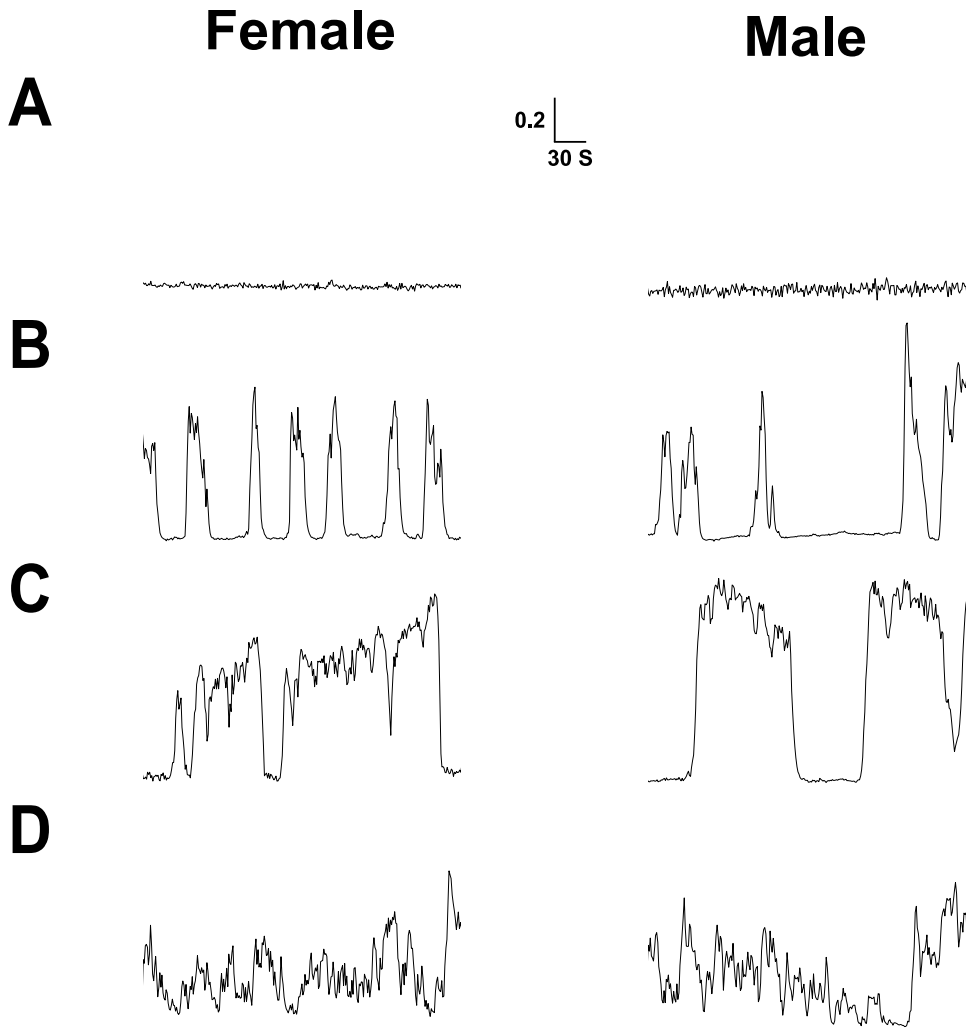


**Figure 3.4 Representative examples of spontaneous $[Ca^{2+}]_i$ signalling in wild-type corticotrophs.** Corticotrophs exhibited different types of spontaneous $[Ca^{2+}]_i$ signalling, including **(A)** silent, **(B)** $Ca^{2+}$ oscillation, **(C)** sustained $Ca^{2+}$ elevation and **(D)** low amplitude and complex pattern. All patterns of spontaneous $[Ca^{2+}]_i$ signalling were found in female (left panel) and male (right panel). Traces are shown as normalized between 0 and 1, where 0 equals to baseline intensity and 1 is the peak of the response to stimulus.

and female wild-type corticotrophs (Figure 3.5C&D) indicating there were no significant differences in maximum amplitude of spontaneous $[Ca^{2+}]_i$ signalling.

### 3.2.3 CRH stimulation increases $[Ca^{2+}]_i$ signalling in wild-type corticotrophs

CRH is released from hypothalamic neurones to stimulate corticotrophs in response to stress *in vivo*. After determining the spontaneous $[Ca^{2+}]_i$ in wild-type corticotrophs under basal conditions, it was then important to investigate how $[Ca^{2+}]_i$ was regulated by CRH stimulation. In order to replicate a typical CRH pulse under stressful conditions in terms of its physiologically relevant concentration, pulse duration and pulse frequency, wild-type corticotrophs were stimulated with a three minute duration of 0.2 nM CRH every 25 minutes for three times with continuous calcium imaging recording (Gibbs & Vale, 1982; Ixart *et al.*, 1991). A typical response to 0.2 nM CRH observed was a significant and sustained increase of $[Ca^{2+}]_i$ that remained elevated even after CRH was washed out (Figure 3.6).

To quantify the CRH-induced $[Ca^{2+}]_i$ responses, several parameters were measured as mentioned in Section **Error! Reference source not found.**, including AUC (10 min), A UC (peak), peak, time to peak, response duration, peak duration and time gap.

## Figure 3.5

### The maximum amplitude of spontaneous $[Ca^{2+}]_i$ signalling is not different in male and female wild-type corticotrophs

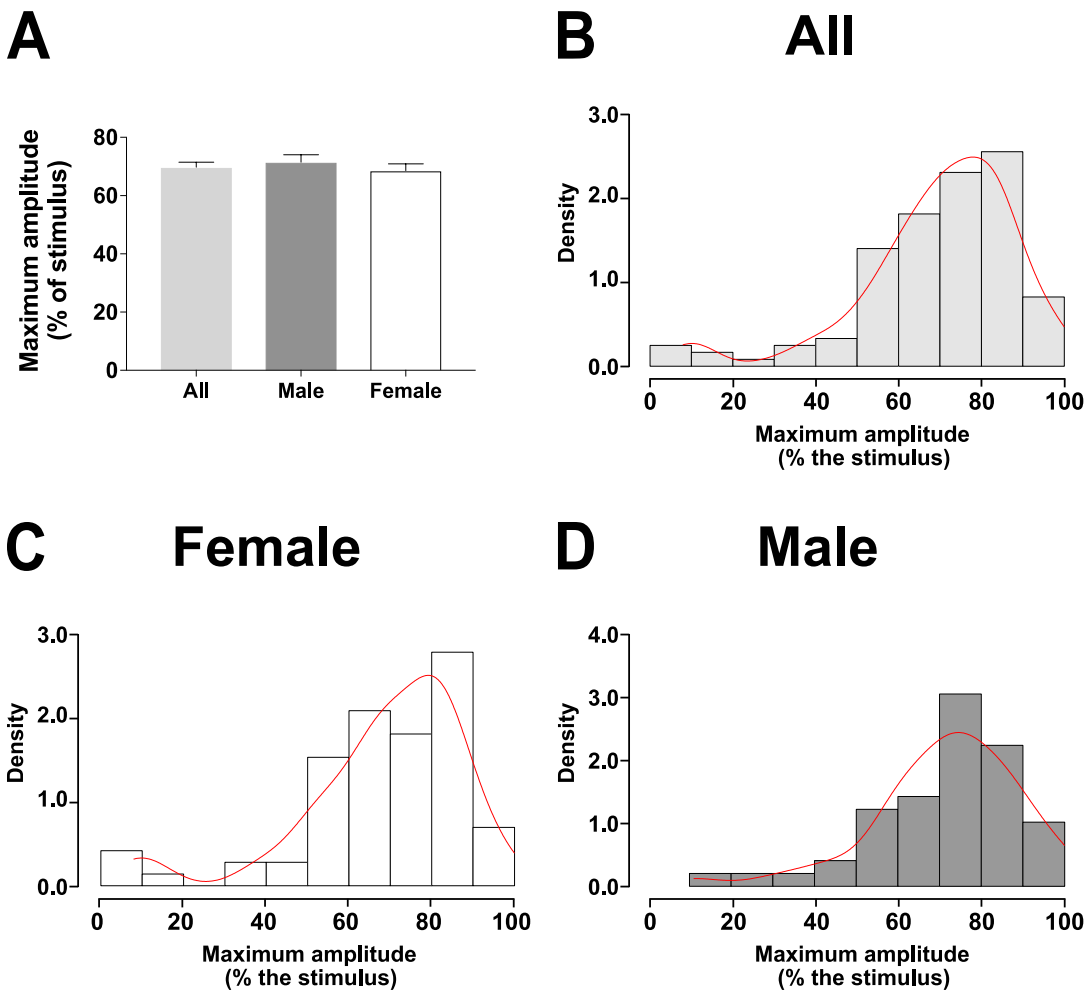


**Figure 3.5 The maximum amplitude of spontaneous $[Ca^{2+}]_i$ signalling is not different in male and female wild-type corticotrophs. (A)** The mean maximum amplitude of spontaneous $[Ca^{2+}]_i$ signalling in all wild-type corticotrophs. **(B)** The distribution of spontaneous $[Ca^{2+}]_i$ maximum amplitude in all wild-type corticotrophs. The distributions of spontaneous $[Ca^{2+}]_i$ maximum amplitude in **(C)** female and **(D)** male wild-type corticotrophs (female n = 72, male n = 49, mixed effects model). Red line indicates the fit of distribution density. All data are means ± SEM, N > 3 independent experiments.

# Figure 3.6

## Stimulation with CRH results in $[Ca^{2+}]_i$ increase in wild-type corticotrophs

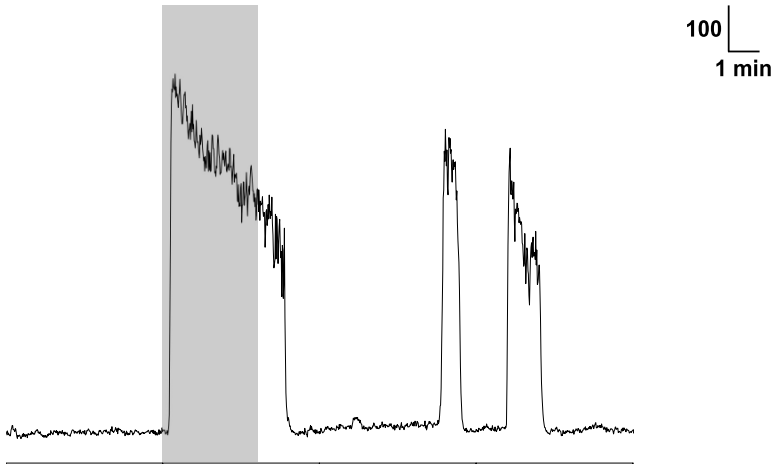


**Figure 3.6 Stimulation with CRH results in $[Ca^{2+}]_i$ increase in wild-type corticotrophs.** Representative calcium imaging trace of 0.2 nM CRH-induced $[Ca^{2+}]_i$ responses in wild-type corticotrophs: sustained elevation of $[Ca^{2+}]_i$. Grey shading indicates the three minute duration of exposure to 0.2 nM CRH.

The CRH-induced $[Ca^{2+}]_i$ responses were investigated in male and female wild-type corticotrophs respectively. Only relevant data from wild-type corticotrophs are presented in this chapter. The analysis of these data was done in conjunction with the analyses for Chapters Four and Five (see 2.6.3).

#### 3.2.3.1 CRH-induced $[Ca^{2+}]_i$ responses are consistent in male wild-type corticotrophs

Calcium imaging recordings were obtained from male wild-type corticotrophs (n = 12 from 8 experiments) following repeated stimulation protocol: calcium imaging experiments were performed starting with 15–20 minutes of basal recording, following by a three minute duration of exposure to 0.2 nM CRH and repeated three times at 25 minutes intervals, then finally treated with a one minute 30 mM potassium chloride stimulus to confirm cell viability at the end of recording.

As described before, the vast majority of corticotrophs displayed spontaneous $[Ca^{2+}]_i$ signalling, whereas only a few of cells were quiescent. With three minutes of 0.2 nM CRH stimulation, all corticotrophs responded with a rapid and significant elevation in $[Ca^{2+}]_i$, followed by returning to baseline in several different ways. In some cells, the $[Ca^{2+}]_i$ started to decrease during the CRH stimulus but returned to baseline after the end of the stimulus; in some other cells, the response was sustained during the CRH

exposure, but the $[Ca^{2+}]_i$ decreased to baseline rapidly after withdrawal of CRH; the response of a few cells ended during the stimulus and the $[Ca^{2+}]_i$ returned to baseline before the end of the stimulus. At the end, treatment with 30 mM potassium chloride for one minute resulted in a rapid rise in the amplitude of $[Ca^{2+}]_i$ signal indicating corticotrophs were viable at the end of recording (Figure 3.7A).

The superposition of calcium imaging traces of typical experiments in male wild-type corticotrophs shown in Figure 3.7B. Following repeated 0.2 nM CRH stimuli, some male wild-type corticotrophs showed reduced $[Ca^{2+}]_i$ responses (Figure 3.7B, top) whereas the others showed robust and similar $[Ca^{2+}]_i$ responses (Figure 3.7B, bottom). Importantly, this suggests that the repeated stimulus protocol allows reproducible $[Ca^{2+}]_i$ responses to repeated CRH pulses at physiological concentrations with frequency of pulses similar to those reported *in vivo*.

The effects of repeated 0.2 nM CRH stimulation on $[Ca^{2+}]_i$ responses in male wild-type corticotrophs were characterized in terms of different parameters mentioned above. As the absolute values of AUC and peak are highly variable depending on the expression level of POMC-GCaMP6s reporter, the statistical calculations of AUC (10 min), AUC (peak) and peak were performed on log-transformed data. The statistical calculations of other parameters were performed on raw data. Each parameter is shown

## Figure 3.7

### Repeated CRH induces $[Ca^{2+}]_i$ responses in male wild-type corticotrophs

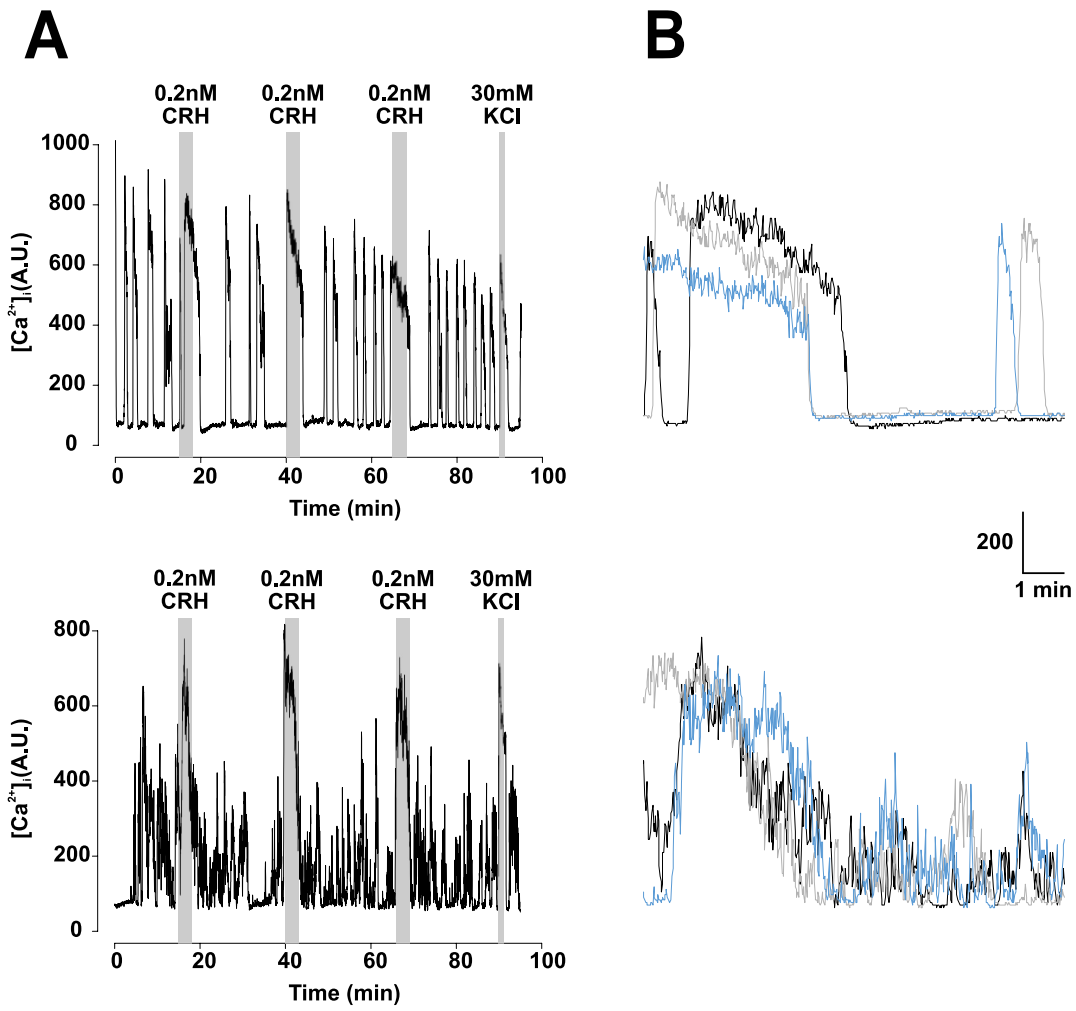


**Figure 3.7 Repeated CRH induces $[Ca^{2+}]_i$ responses in male wild-type corticotrophs. (A)** Representative calcium imaging traces of male wild-type corticotrophs exposed to 0.2 nM CRH for three minutes and repeated three times at 25 minutes intervals. 30 mM potassium chloride was applied at the end for one minute. **(B)** Superposition of extracts of the two traces shown in A, showing $[Ca^{2+}]_i$ changes in male wild-type corticotrophs with repeated 0.2 nM CRH stimulation. Black line shows response to the first stimulus (starting at 15 min), grey line shows response to the second stimulus (starting at 40 min), and blue line shows response to the third stimulus (starting at 65 min).

in three different ways: (i) raw data in log transformation, (ii) the track between each individual cell and (iii) the normalization to Stimulus 1.

Statistical analysis revealed that although AUC (10 min) and AUC (peak) showed a declining trend following repeated CRH stimulation, it failed to show any significant difference between Stimulus 1 and Stimulus 3 ($p = 0.07$ and $p = 0.05$ respectively). (Figure 3.8). Repeated CRH stimulation resulted in a significant reduction in peak (Figure 3.9A) between Stimulus 1 and Stimulus 3 ($p < 0.001$), Stimulus 2 and Stimulus 3 ($p < 0.01$). Time to peak (Figure 3.9B), response duration (Figure 3.10A), peak duration (Figure 3.10B) and time gap (Figure 3.11) were not significantly different between repeated CRH stimulation.

Although peak showed significant reduction following repeated CRH stimulation, AUC (10 min) and AUC (peak) $[Ca^{2+}]_i$ responses were stable. These results suggest that $[Ca^{2+}]_i$ responses to repeated CRH stimulation were relatively consistent in male corticotrophs.

#### 3.2.3.2 CRH-induced $[Ca^{2+}]_i$ responses are consistent in female wild-type corticotrophs

Calcium imaging recordings were obtained from female wild-type corticotrophs

## Figure 3.8

**Stable AUC (10 min) and AUC (peak) of $[Ca^{2+}]_i$ responses in male wild-type corticotrophs to repeated CRH**

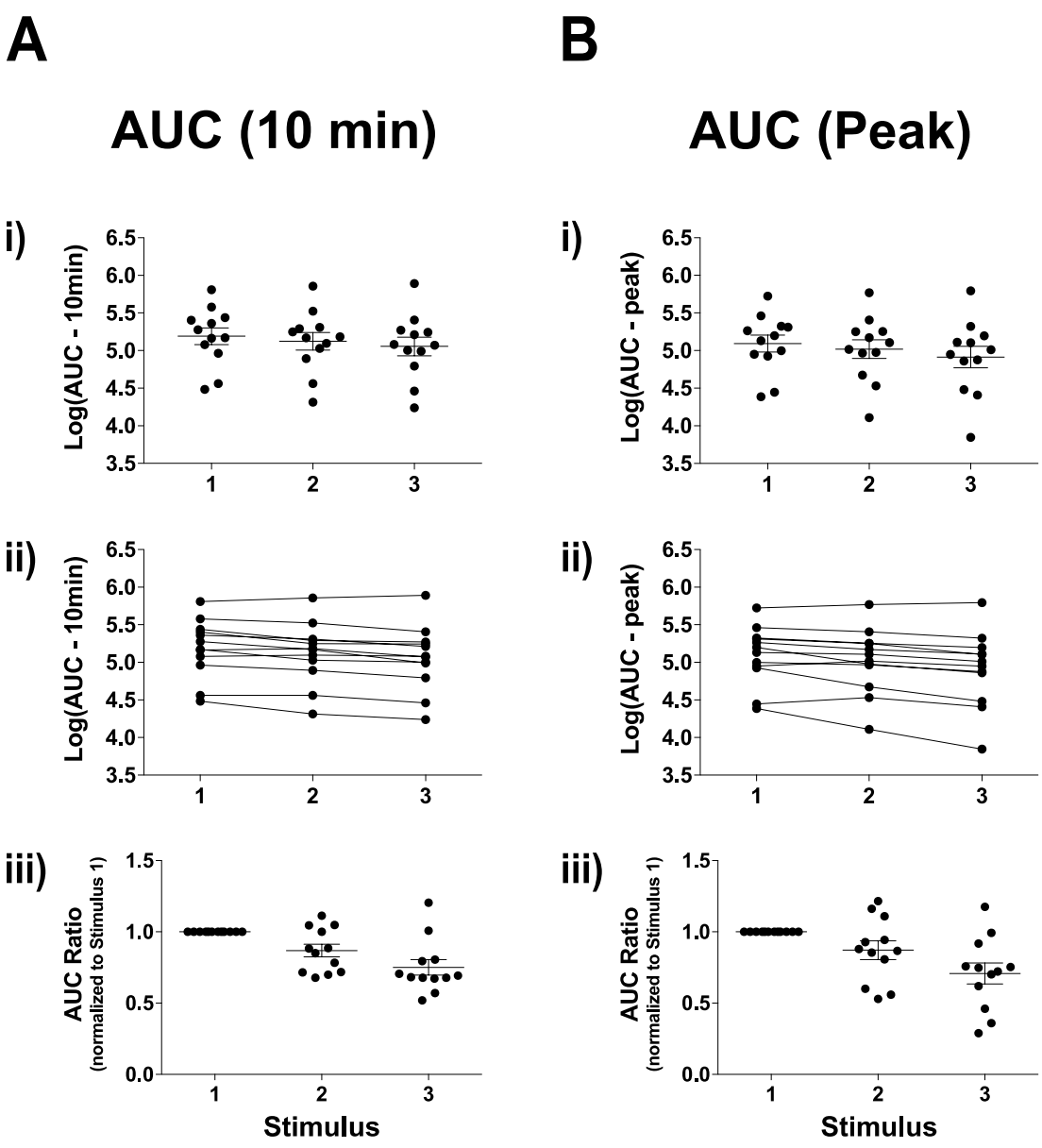


**Figure 3.8 Stable AUC (10 min) and AUC (peak) of $[Ca^{2+}]_i$ responses in male wild-type corticotrophs to repeated CRH.** Quantification of effects of repeated exposure to 0.2 nM CRH in **(A)** AUC (10 min) and **(B)** AUC (peak) (n = 12 from 8 experiments, mixed effects models). All data are means ± SEM.

## Figure 3.9

### Attenuation of peak but not time to peak of $[Ca^{2+}]_i$ responses in male wild-type corticotrophs to repeated CRH

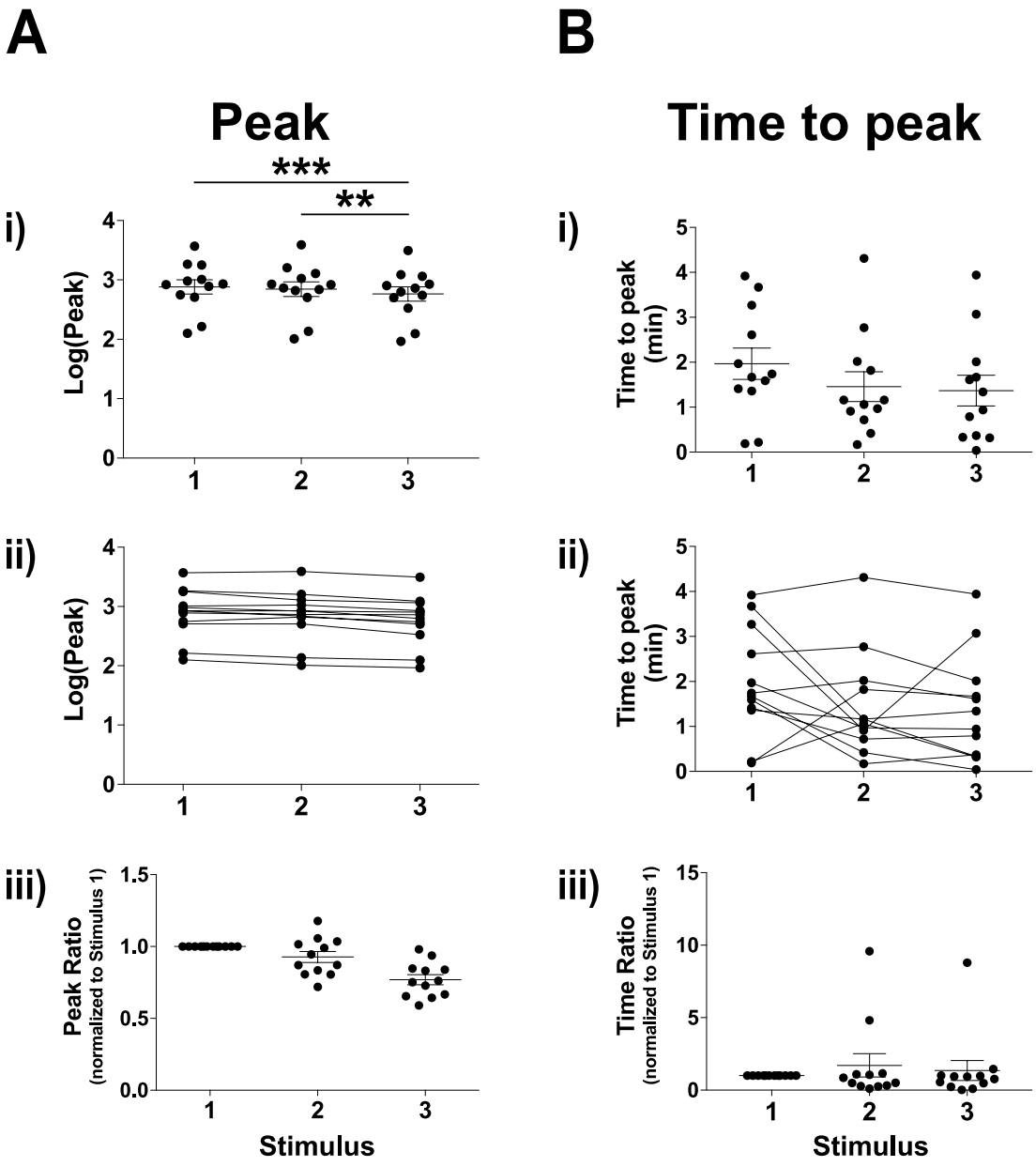


**Figure 3.9 Attenuation of peak but not time to peak of $[Ca^{2+}]_i$ responses in male wild-type corticotrophs to repeated CRH.** Quantification of effects of repeated exposure to 0.2 nM CRH in **(A)** peak and **(B)** time to peak. ** $p < 0.01$ and *** $p < 0.001$ ($n = 12$ from 8 experiments, mixed effects model). All data are means ± SEM.

## Figure 3.10

**Response duration and peak duration of $[Ca^{2+}]_i$ responses in male wild-type corticotrophs to repeated CRH**

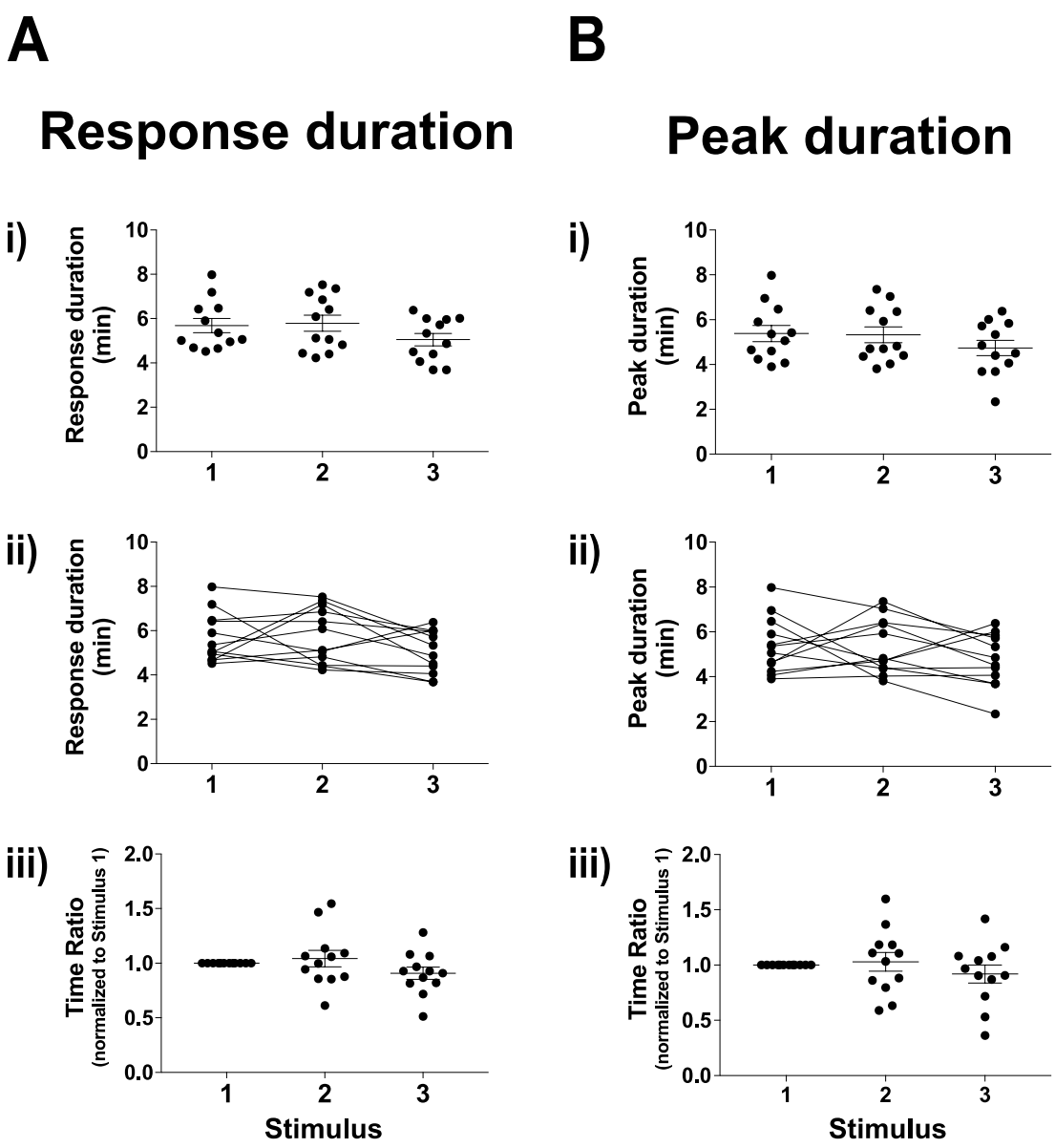


**Figure 3.10 Response duration and peak duration of $[Ca^{2+}]_i$ responses in male wild-type corticotrophs to repeated CRH.** Quantification of effects of repeated exposure to 0.2 nM CRH in **(A)** response duration and **(B)** peak duration (n = 12 from 8 experiments, mixed effects model). All data are means ± SEM.

## Figure 3.11

### Time gap of $[Ca^{2+}]_i$ responses in male wild-type corticotrophs to repeated CRH

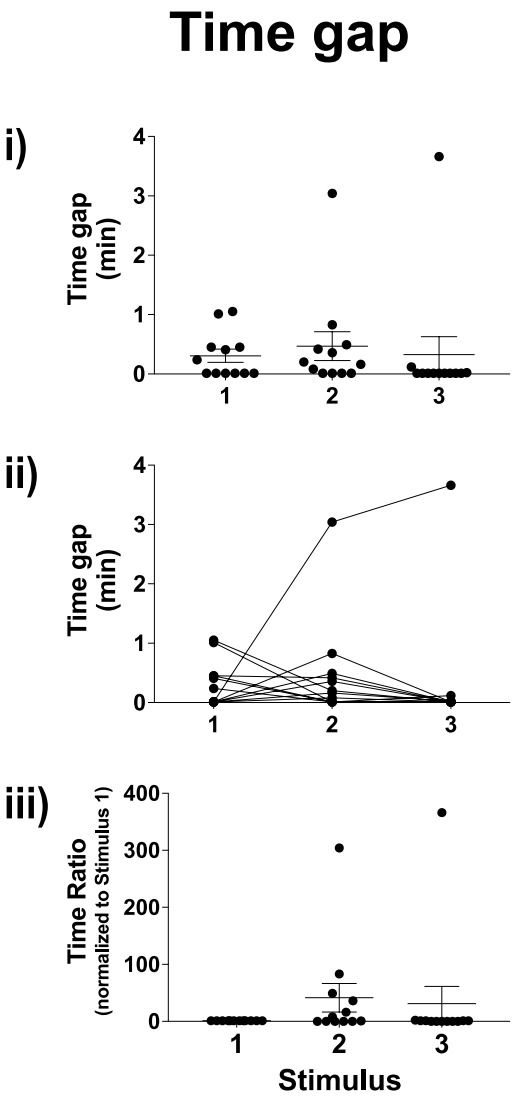


**Figure 3.11 Time gap of $[Ca^{2+}]_i$ responses in male wild-type corticotrophs to repeated CRH.** Quantification of effects of repeated exposure to 0.2 nM CRH in time gap (n = 12 from 8 experiments, mixed effects model). All data are means ± SEM.

(n = 14 from 7 experiments) following the same protocol used in male wild-type corticotrophs. Following stimulation with 0.2 nM CRH for three minutes, all female corticotrophs showed a rapid and significant increase in $[Ca^{2+}]_i$ response compared to basal $[Ca^{2+}]_i$ level. The $[Ca^{2+}]_i$ signalling remained elevated even after withdrawal of CRH before returning to baseline (Figure 3.12A). The superposition of calcium imaging traces revealed that repeated 0.2 nM CRH stimulation resulted in repeatable $[Ca^{2+}]_i$ responses in female wild-type corticotrophs (Figure 3.12B).

To quantify the repeated 0.2 nM CRH induced $[Ca^{2+}]_i$ responses in female wild-type corticotrophs, the same parameters were measured as in male wild-type corticotrophs. Log transformation was performed in AUC (10 min), AUC (peak) and peak whereas the raw data was used in other parameters when performing statistical analysis. Repeated CRH stimulation significantly ($p < 0.05$) reduced AUC (peak) of Stimulus 3 compared to Stimulus 1 (Figure 3.13B). Peak was also significantly decreased between Stimulus 1 and Stimulus 3 ($p < 0.001$), Stimulus 2 and Stimulus 3 ($p < 0.05$) (Figure 3.14A). AUC (10 min) (Figure 3.13A), time to peak (Figure 3.14B), response duration, peak duration (Figure 3.15) and time gap (Figure 3.16) showed no statistically significant differences following repeated CRH stimulation.

In contrast to the consistency of AUC (10 min), the significant reduction observed in

# Figure 3.12

## Repeated CRH induces $[Ca^{2+}]_i$ responses in female wild-type corticotrophs

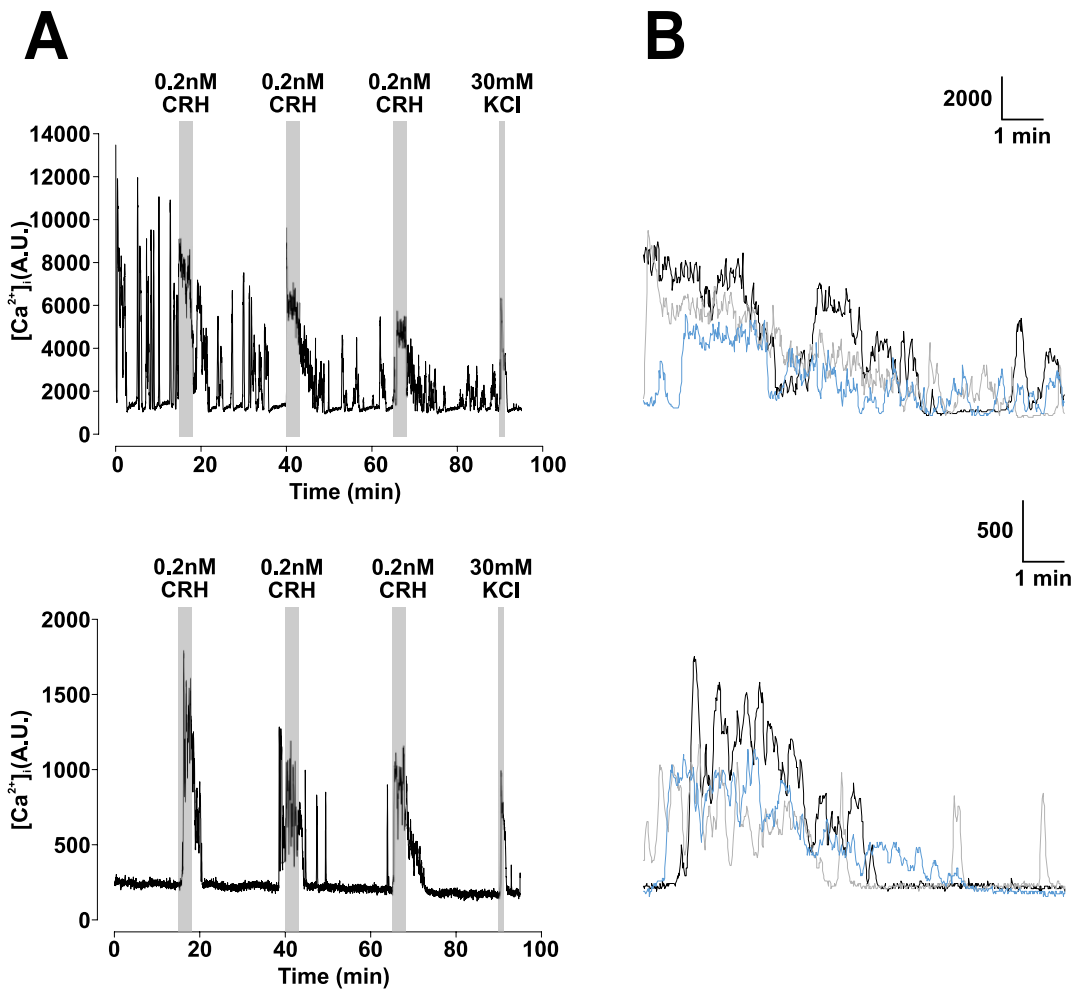


**Figure 3.12 Repeated CRH induces $[Ca^{2+}]_i$ responses in female wild-type corticotrophs. (A)** Representative calcium imaging traces of female wild-type corticotrophs exposed to 0.2 nM CRH for three minutes and repeated three times at 25 minutes intervals. 30 mM potassium chloride was applied at the end for one minute. **(B)** Superposition of extracts of the two traces shown in A, showing $[Ca^{2+}]_i$ changes in female wild-type corticotrophs with repeated 0.2 nM CRH stimulation. Black line shows response to the first stimulus (starting at 15 min), grey line shows response to the second stimulus (starting at 40 min), and blue line shows response to the third stimulus (starting at 65 min).

## Figure 3.13

**AUC (10 min) but not AUC (peak) of $[Ca^{2+}]_i$ responses is stable in female wild-type corticotrophs to repeated CRH**

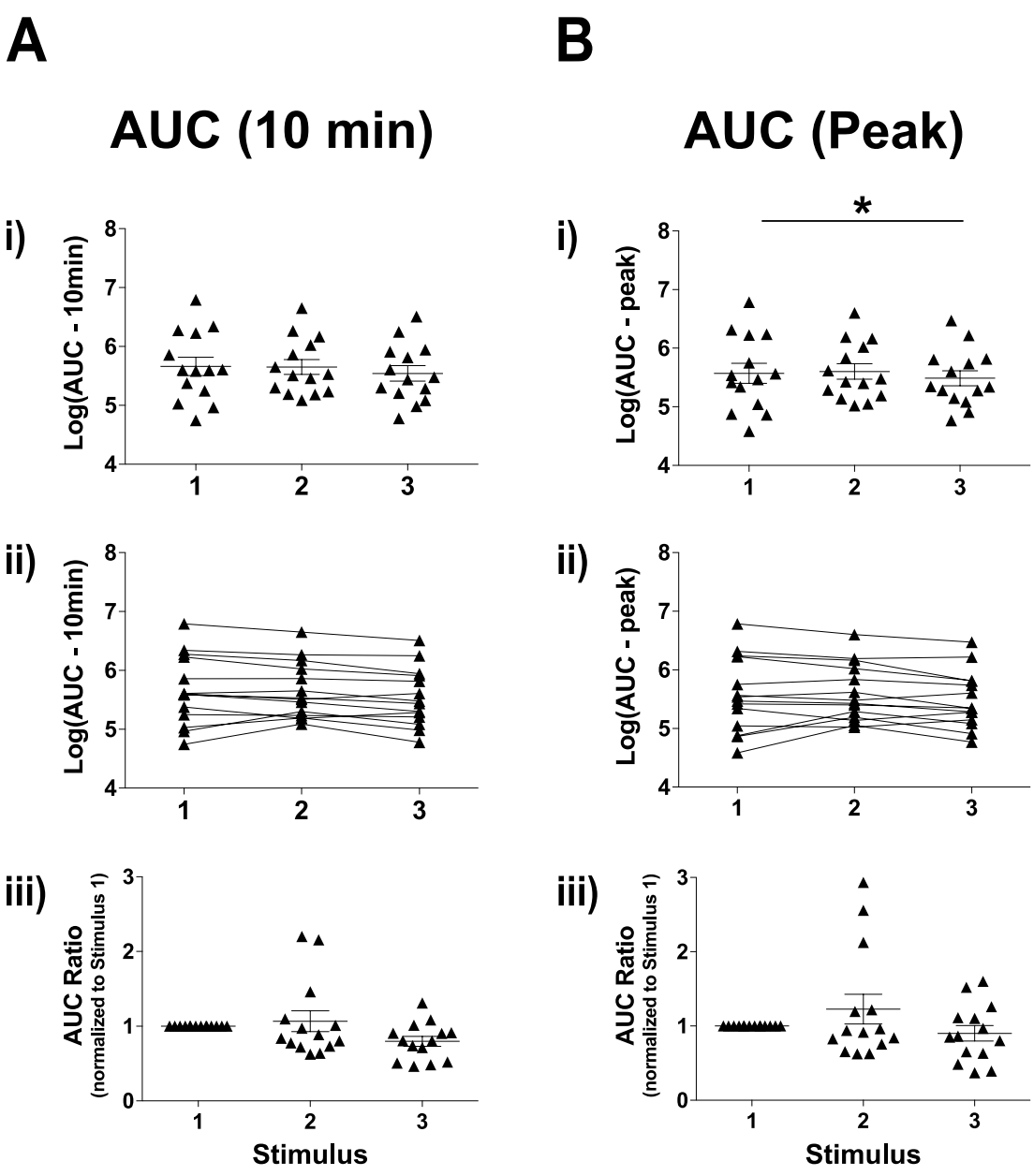


**Figure 3.13 AUC (10 min) but not AUC (peak) of $[Ca^{2+}]_i$ responses is stable in female wild-type corticotrophs to repeated CRH.** Quantification of effects of repeated exposure to 0.2 nM CRH in **(A)** AUC (10 min) and **(B)** AUC (peak). * $p < 0.05$ ($n = 14$ from 7 experiments, mixed effects model). All data are means ± SEM.

## Figure 3.14

### Attenuation of peak but not time to peak of $[Ca^{2+}]_i$ responses in female wild-type corticotrophs to repeated CRH

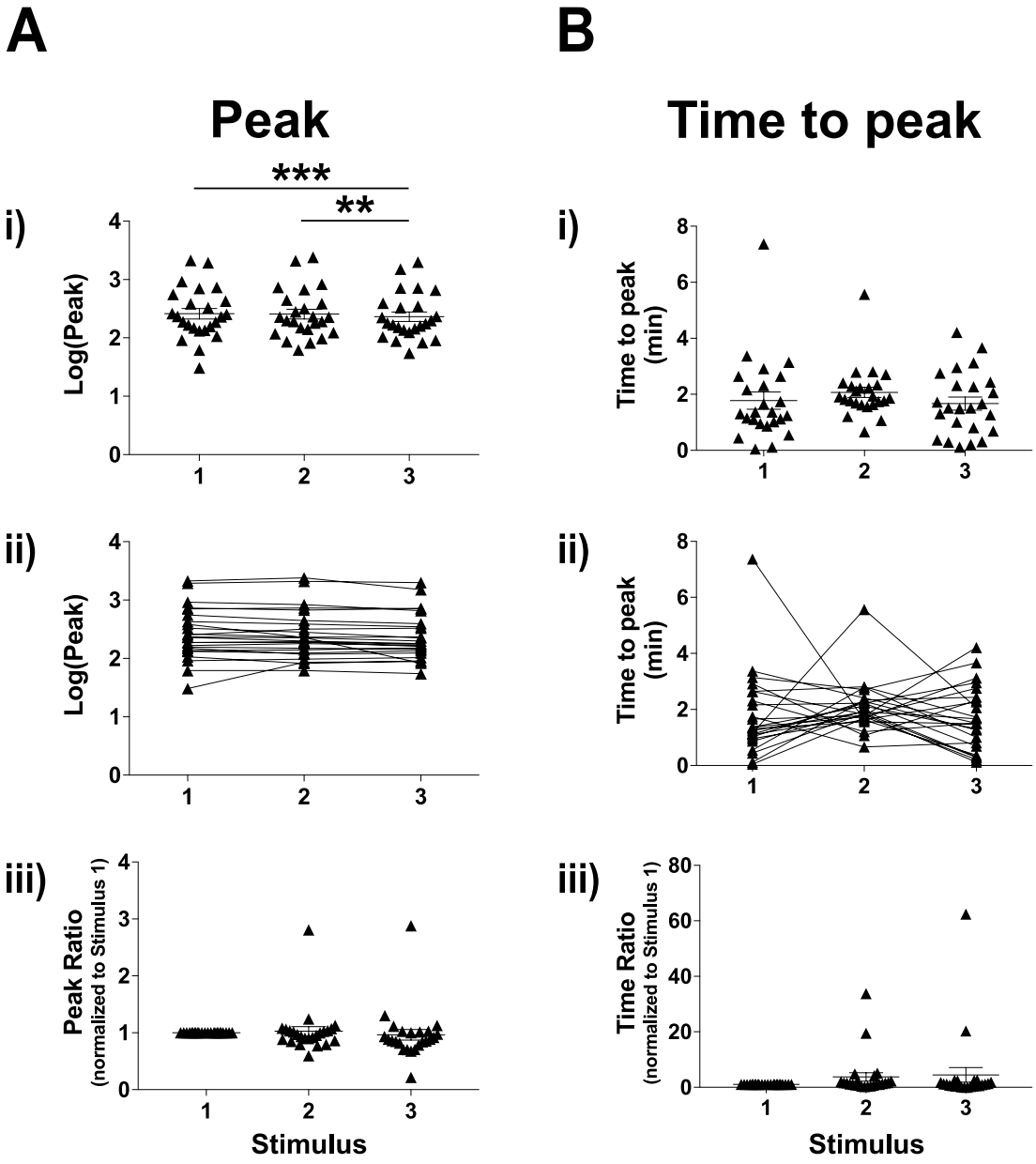


**Figure 3.14 Attenuation of peak but not time to peak of $[Ca^{2+}]_i$ responses in female wild-type corticotrophs to repeated CRH.** Quantification of effects of repeated exposure to 0.2 nM CRH in **(A)** peak and **(B)** time to peak. ** $p < 0.01$ and *** $p < 0.001$ (n = 14 from 7 experiments, mixed effects model). All data are means ± SEM.

## Figure 3.15

### Response duration and peak duration of $[Ca^{2+}]_i$ responses in female wild-type corticotrophs to repeated CRH

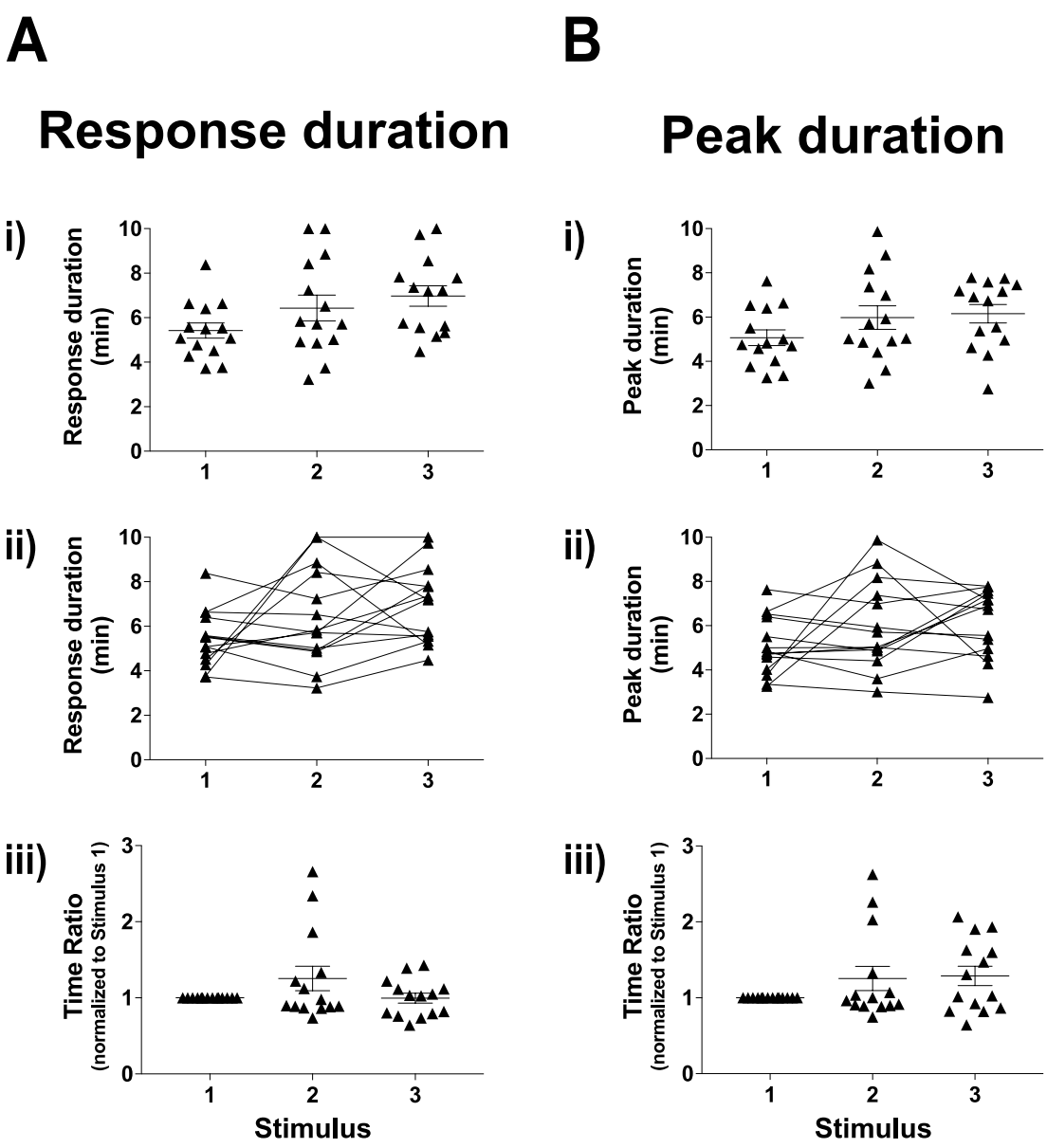


**Figure 3.15 Response duration and peak duration of $[Ca^{2+}]_i$ responses in female wild-type corticotrophs to repeated CRH.** Quantification of effects of repeated exposure to 0.2 nM CRH in **(A)** peak and **(B)** time to peak (n = 14 from 7 experiments, mixed effects model). All data are means ± SEM.

## Figure 3.16

**Time gap of $[Ca^{2+}]_i$ responses in female wild-type corticotrophs to repeated CRH**

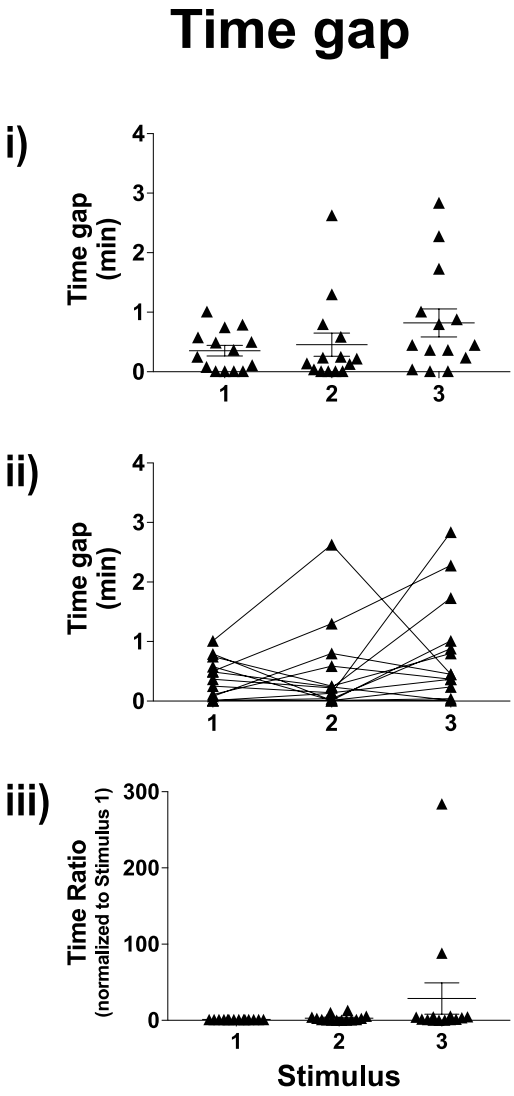


**Figure 3.16 Time gap of $[Ca^{2+}]_i$ responses in female wild-type corticotrophs to repeated CRH.** Quantification of effects of repeated exposure to 0.2 nM CRH in time gap (n = 14 from 7 experiments, mixed effects model). All data are means ± SEM.

AUC (peak) might be due to the decline of peak. These results suggest that $[Ca^{2+}]_i$ response to repeated 0.2 nM CRH is consistent in female wild-type corticotrophs.

#### 3.2.3.3 CRH-induced $[Ca^{2+}]_i$ responses are not significantly different between male and female wild-type corticotrophs

Although both male and female wild-type corticotrophs displayed a reduction in CRH-induced AUC (peak) and peak of $[Ca^{2+}]_i$ responses, we investigated whether there were differences between male and female wild-type corticotrophs in CRH-induced $[Ca^{2+}]_i$ responses.

Statistical analysis revealed that although female wild-type corticotrophs tended to have higher $[Ca^{2+}]_i$ responses in AUC (10 min), AUC (peak) (Figure 3.17) and peak (Figure 3.18A), they were not significantly different between male and female wild-type corticotrophs. There were no significant differences between male and female wild-type corticotrophs in time to peak (Figure 3.18B), response duration (Figure 3.18C), peak duration and time gap (Figure 3.19) either.

In summary, there were no significant differences between male and female wild-type corticotrophs in CRH-induced $[Ca^{2+}]_i$ responses**.**

## Figure 3.17

### No significant sex difference in CRH-induced AUC (10 min) or AUC (peak) of $[Ca^{2+}]_i$ responses in wild-type corticotrophs

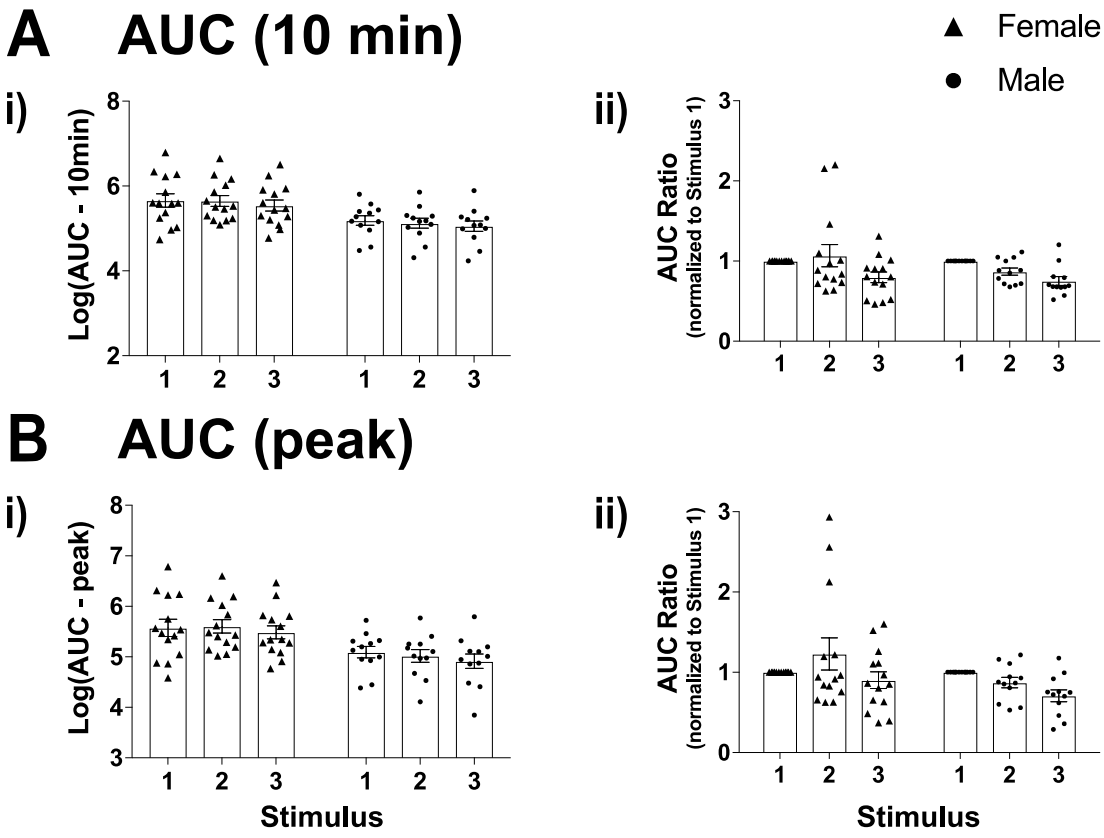


**Figure 3.17 No significant sex difference in CRH-induced AUC (10 min) or AUC (peak) of $[Ca^{2+}]_i$ responses in wild-type corticotrophs.** Quantification of effects of repeated exposure to 0.2 nM CRH in **(A)** AUC (10 min) and **(B)** AUC (peak) (male n = 12 from 8 experiments, female n = 14 from 7 experiments, mixed effects model). All data are means ± SEM.

## Figure 3.18

**No significant sex difference in CRH-induced peak, time to peak or response duration of $[Ca^{2+}]_i$ responses in wild-type corticotrophs**

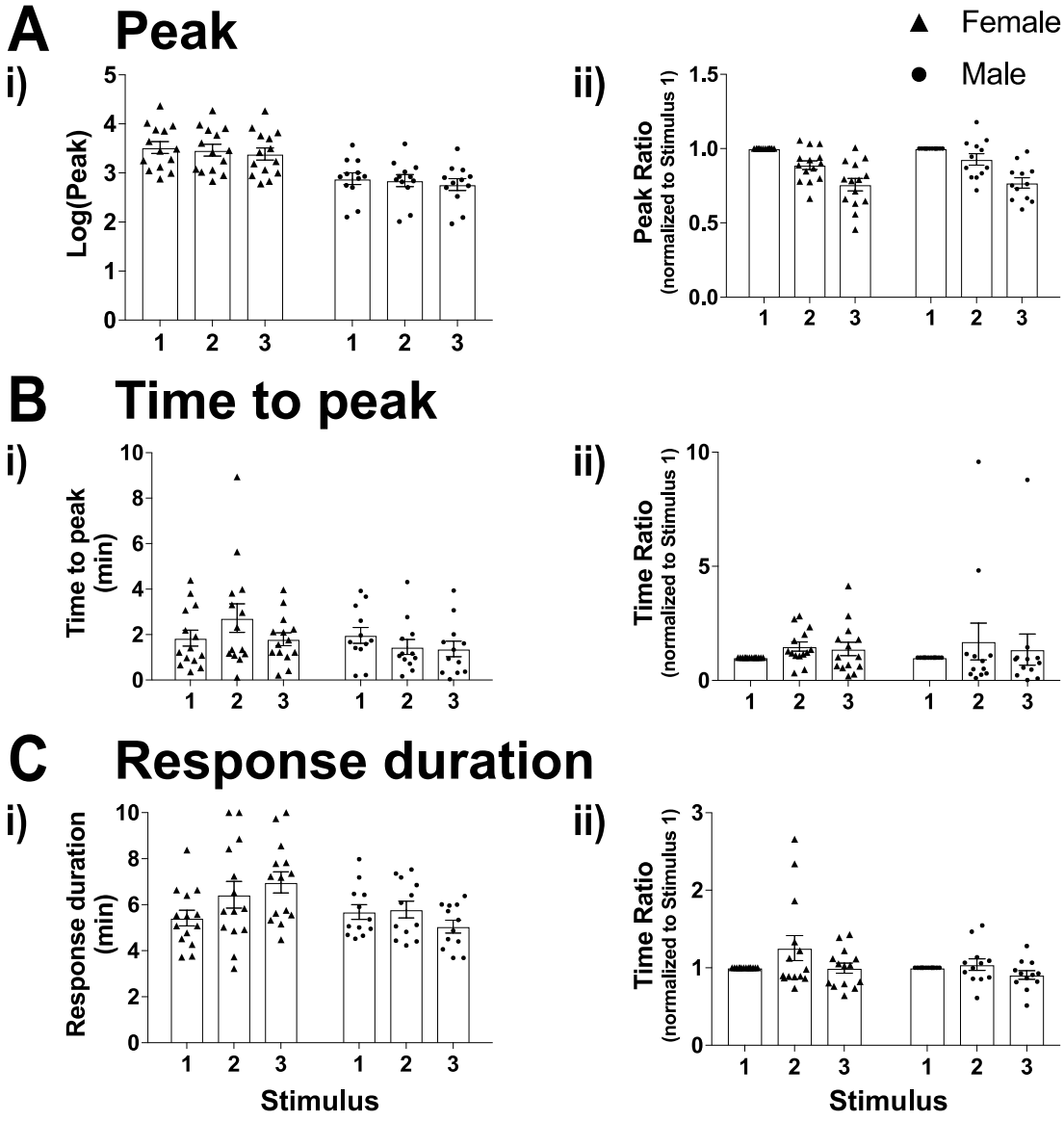


**Figure 3.18 No significant sex difference in CRH-induced peak, time to peak or response duration of $[Ca^{2+}]_i$ responses in wild-type corticotrophs.** Quantification of effects of repeated exposure to 0.2 nM CRH in **(A)** peak, **(B)** time to peak and **(C)** response duration (male n = 12 from 8 experiments, female n = 14 from 7 experiments, mixed effects model). All data are means ± SEM.

## Figure 3.19

### No significant sex difference in CRH-induced peak duration or time gap of $[Ca^{2+}]_i$ responses in wild-type corticotrophs

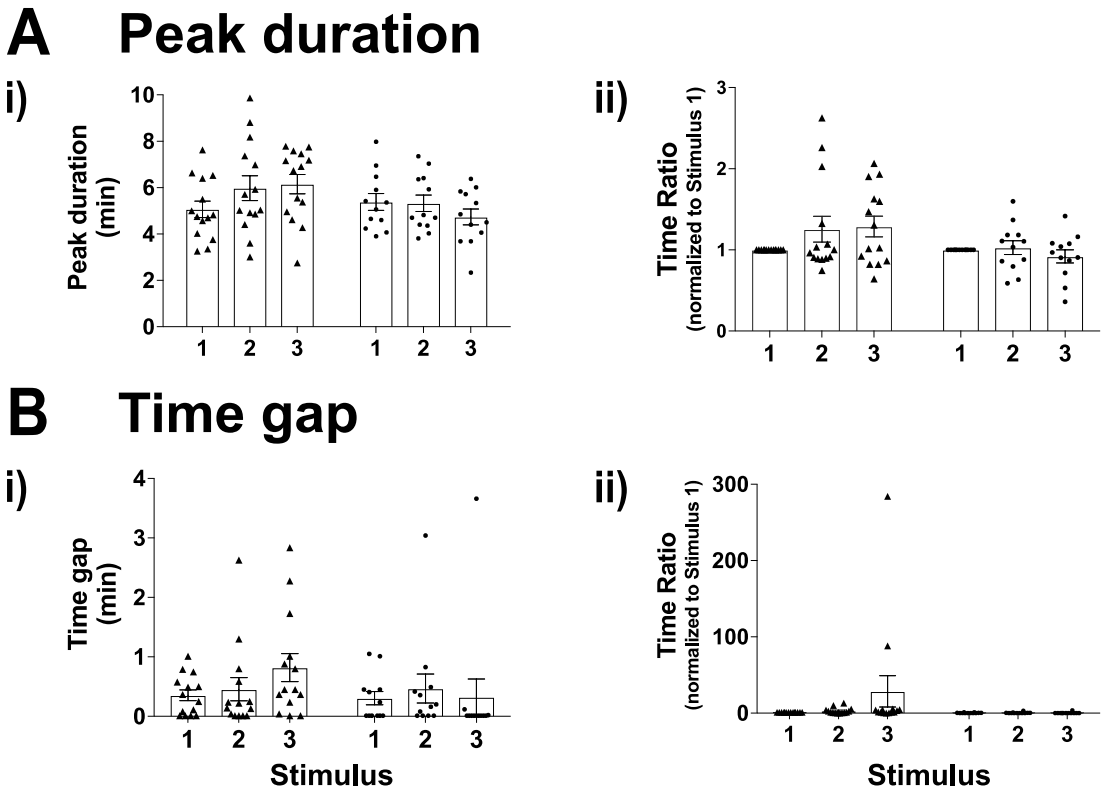


**Figure 3.19 No significant sex difference in CRH-induced peak duration or time gap of $[Ca^{2+}]_i$ responses in wild-type corticotrophs.** Quantification of effects of repeated exposure to 0.2 nM CRH in **(A)** peak duration and **(B)** time gap (male n = 12 from 8 experiments, female n = 14 from 7 experiments, mixed effects model). All data are means ± SEM.

#### 3.2.3.4 CRH-induced $[Ca^{2+}]_i$ responses are nifedipine-sensitive

To examine whether CRH-induced $[Ca^{2+}]_i$ responses are regulated by an influx of extracellular $Ca^{2+}$ through L-type voltage gated calcium channels, calcium imaging experiments were performed on male wild-type corticotrophs (n = 9 from 2 experiments) treated with 0.2 nM CRH in the presence of the L-type calcium channel blocker nifedipine (2.5 μM).

Following the ion channel blocking protocol (see 2.5.2.3), male wild-type corticotrophs were stimulated with 0.2 nM CRH for three minutes and repeated three times after 15–20 minutes basal recording. The second CRH stimulation was applied in the presence of 2.5 μM nifedipine and nifedipine was applied 10 minutes before and after the stimulation to ensure the blockade of calcium channels. Following a 25 minute washout period, corticotrophs were treated with CRH for the third time and finally a one minute 30 mM potassium chloride to verify cell viability (Figure 3.20A). Stimulation with CRH alone induced significant elevation of $[Ca^{2+}]_i$ in corticotrophs. Spontaneous $[Ca^{2+}]_i$ signalling and CRH-induced $[Ca^{2+}]_i$ responses were both inhibited in the presence of nifedipine (Figure 3.20B). Following nifedipine washout, the spontaneous $[Ca^{2+}]_i$ signalling did not restore completely and the $[Ca^{2+}]_i$ response to CRH was not fully recovered either, 7 out of 9 cells showed partial recover and the remaining 2 cells did not recover at all.

# Figure 3.20

## Nifedipine inhibits CRH-induced $[Ca^{2+}]_i$ response in male wild-type corticotrophs

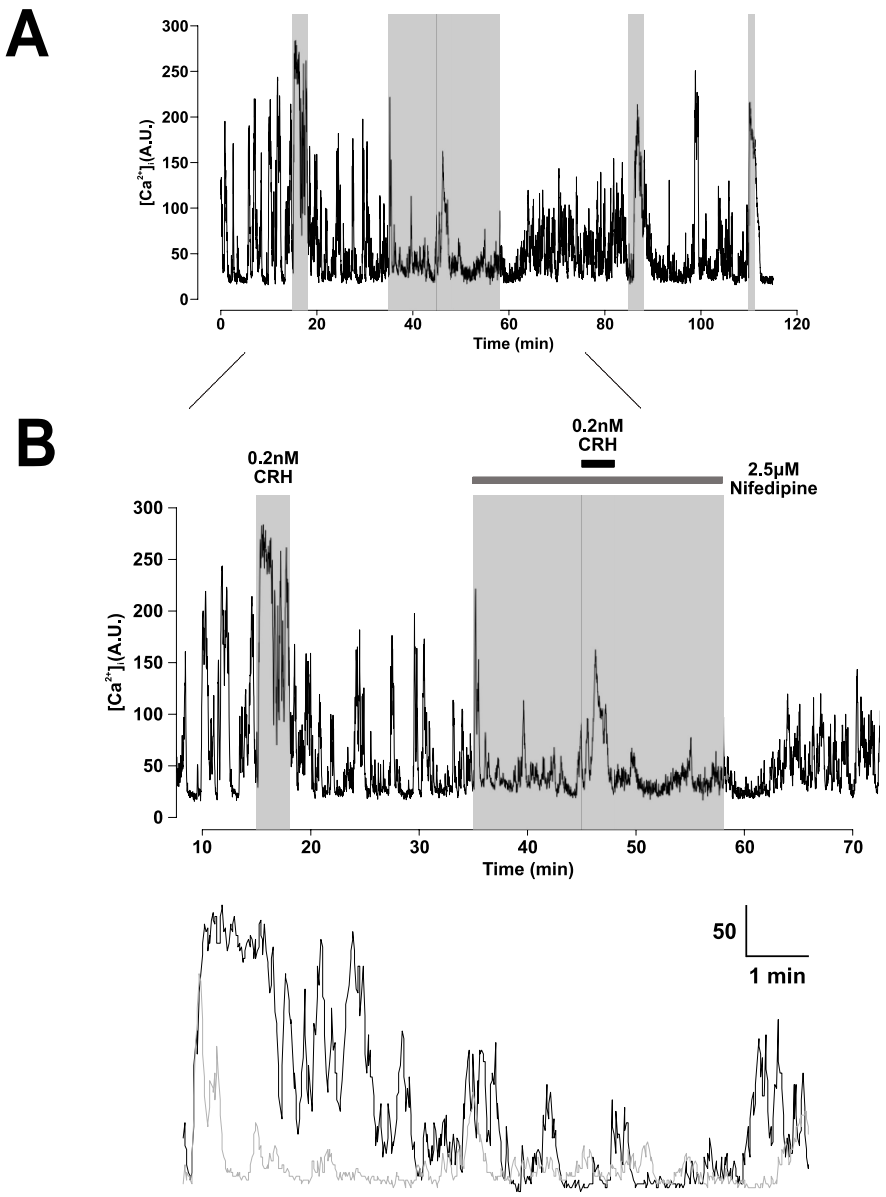


**Figure 3.20 Nifedipine inhibits CRH-induced $[Ca^{2+}]_i$ response in male wild-type corticotrophs. (A)** Representative calcium imaging traces of the effects of nifedipine on CRH-induced $[Ca^{2+}]_i$ response in male wild-type corticotrophs. **(B)** Superposition of extracts of the trace shown in A, showing $[Ca^{2+}]_i$ changes in male wild-type corticotrophs. Black line shows $[Ca^{2+}]_i$ response to the 0.2 nM CRH alone, grey line shows $[Ca^{2+}]_i$ response to 0.2 nM CRH in the presence of 2.5 μM nifedipine.

The effects of nifedipine on CRH-induced $[Ca^{2+}]_i$ signalling were evaluated by AUC (10 min), AUC (peak) and peak. Treatment with 2.5 μM nifedipine resulted in a significant ($p < 0.001$) reduction in AUC (10 min) and AUC (peak). After washout nifedipine, the $[Ca^{2+}]_i$ response to the third CRH stimulation was significantly ($p < 0.001$) smaller in AUC (10 min) and AUC (peak) compared to the first CRH stimulation (Figure 3.21). Peak was also significantly ($p < 0.001$) reduced when treated with nifedipine and showed significant ($p < 0.001$) smaller $[Ca^{2+}]_i$ response to the third CRH stimulation (Figure 3.22). These results revealed that the elevation of $[Ca^{2+}]_i$ was largely abolished by L-type calcium channel blocker nifedipine and the effects of nifedipine were not fully reversible upon washout.

In summary, CRH-evoked $[Ca^{2+}]_i$ responses were nifedipine-sensitive and elevated $[Ca^{2+}]_i$ responses were largely driven by an influx of extracellular calcium.

### 3.2.4 AVP-induced $[Ca^{2+}]_i$ responses are consistent in wild-type corticotrophs

After characterizing both spontaneous and CRH-evoked $[Ca^{2+}]_i$ signalling in wild-type corticotrophs, experiments were designed to investigate the $[Ca^{2+}]_i$ signalling in corticotrophs exposed to 2 nM AVP, which is physiological relevant concentration in portal circulation (Sheward & Fink, 1991).

## Figure 3.21

**Nifedipine significantly reduced CRH-induced AUC (10 min) and AUC (peak) of $[Ca^{2+}]_i$ responses in male wild-type corticotrophs**

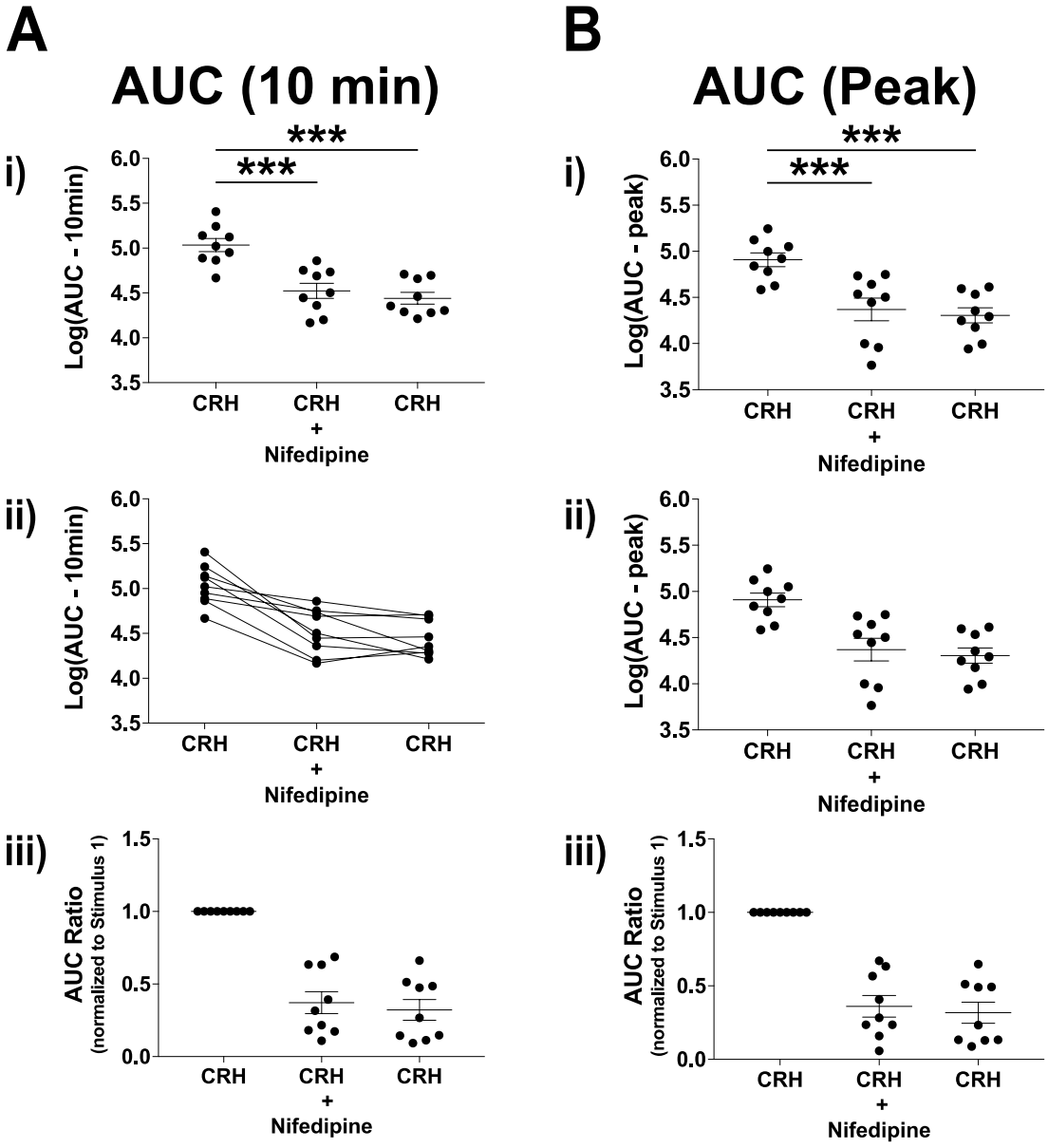


**Figure 3.21 Nifedipine significantly reduced CRH-induced AUC (10 min) and AUC (peak) of $[Ca^{2+}]_i$ response in male wild-type corticotrophs.** Quantification of effects of repeated exposure to 0.2 nM CRH in the presence of nifedipine in (A) AUC (10 min) and (B) AUC (peak). *** $p < 0.001$ (n = 9 from 2 experiments, mixed effects model). All data are means ± SEM.

## Figure 3.22

### Nifedipine significantly reduced CRH-induced peak of $[Ca^{2+}]_i$ responses in male wild-type corticotrophs

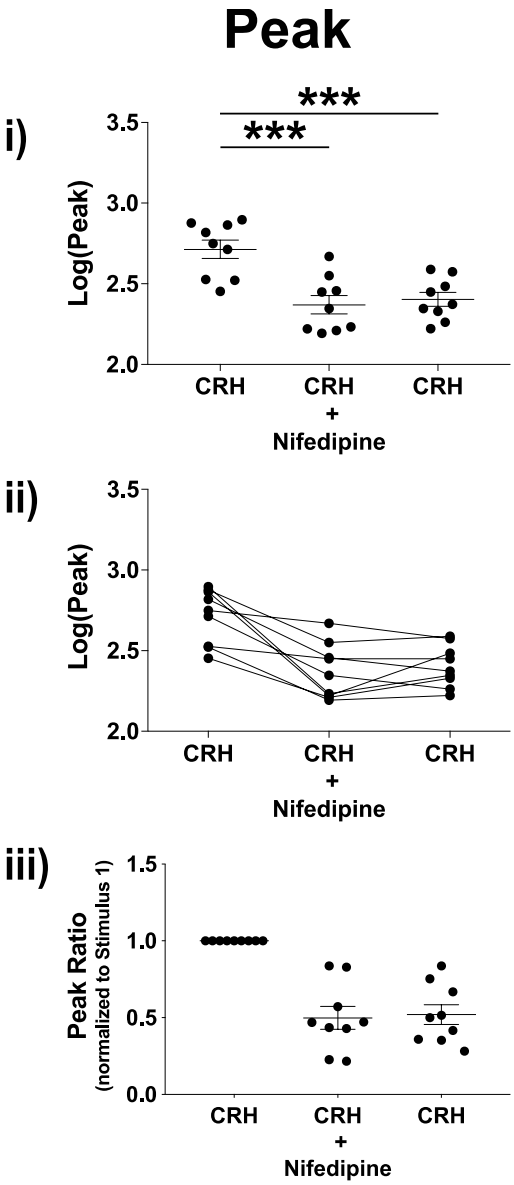


**Figure 3.22 Nifedipine significantly reduced CRH-induced peak of $[Ca^{2+}]_i$ response in male wild-type corticotrophs.** Quantification of effects of repeated exposure to 0.2 nM CRH in the presence of nifedipine in peak. *** $p < 0.001$ ($n = 9$ from 2 experiments, mixed effects model). All data are means ± SEM.

Wild-type corticotrophs were stimulated with a 2 nM AVP pulse for three minutes every 25 minutes with continuous calcium imaging recording. Two typical $[Ca^{2+}]_i$ responses to AVP were observed in corticotrophs: 60% (24/40) of cells displayed similar responses to 0.2 nM CRH, with a sustained elevation of $[Ca^{2+}]_i$ for several minutes (Figure 3.23A); the other 40% (16/40) of corticotrophs exhibited a rhythmic and oscillatory $[Ca^{2+}]_i$ behaviour, accompanied with an increased amplitude of $[Ca^{2+}]_i$ (Figure 3.23B).

The parameters used to quantify AVP-induced $[Ca^{2+}]_i$ responses are the same as used in CRH-induced $[Ca^{2+}]_i$ responses, which are AUC (10 min), AUC (peak), peak, time to peak, response duration, peak duration and time gap. It was more difficult to clearly define the start and the end of the $[Ca^{2+}]_i$ response in corticotrophs showing oscillatory $[Ca^{2+}]_i$ behaviour, which might lead to measurement error in AUC (peak) and peak duration. The statistical analysis of AUC (10 min), AUC (peak) and peak were performed on log-transformed data due to the variability of absolute values and the statistical calculation of other parameters used raw data. To examine whether there were sex differences in AVP-induced $[Ca^{2+}]_i$ responses, calcium imaging experiments were performed on corticotrophs isolated from male and female wild-type corticotrophs respectively.

## Figure 3.23

### Stimulation with AVP results in two phenotypes of $[Ca^{2+}]_i$ responses in wild-type corticotrophs

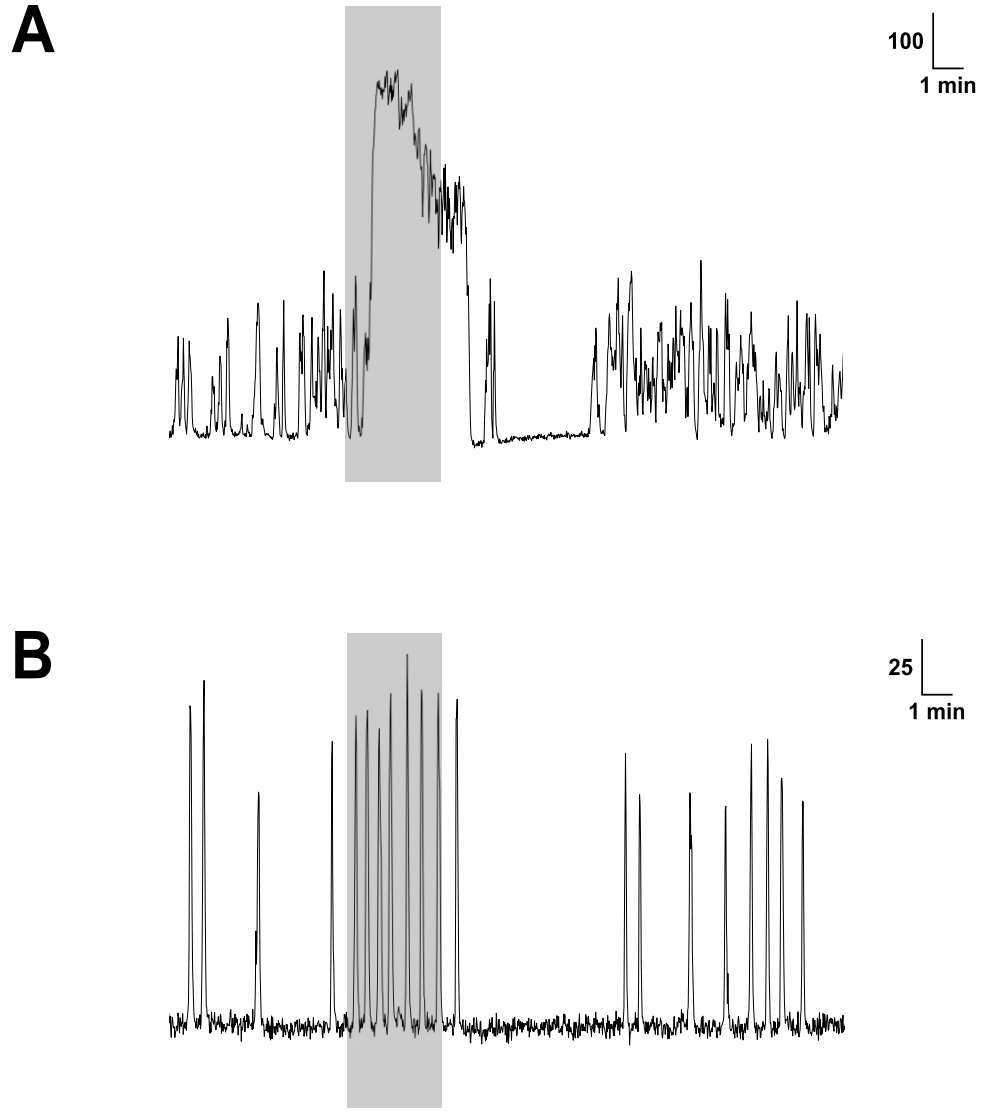


**Figure 3.23 Stimulation with AVP results in two phenotypes of $[Ca^{2+}]_i$ responses in wild-type corticotrophs.** Representative calcium imaging traces of two phenotype of 2 nM AVP-induced $[Ca^{2+}]_i$ responses in wild-type corticotrophs: **(A)** a sustained elevation of $[Ca^{2+}]_i$ and **(B)** a rhythmic and oscillatory $[Ca^{2+}]_i$ behaviour, accompanied with an increased peak of $[Ca^{2+}]_i$. Grey shading indicates the three minute duration of exposure to 2 nM AVP.

#### 3.2.4.1 AVP-induced $[Ca^{2+}]_i$ responses are consistent in male wild-type corticotrophs

Calcium imaging recordings were obtained from male wild-type corticotrophs (n = 16 from 9 experiments). Following 15–20 minutes recording under basal condition, corticotrophs were stimulated for three minutes with 2 nM AVP and repeated every 25 minutes for three times with continuous calcium imaging recording, then treated with 30 mM potassium chloride stimulus for one minute to validate cell viability at the end of recording.

Prior to AVP stimulation, all corticotrophs displayed some spontaneous $[Ca^{2+}]_i$ signalling. Although none of them was absolutely silent, but a small minority (< 10%) with active time lower than 5%. When stimulated with 2 nM AVP, two phenotypes of $[Ca^{2+}]_i$ responses were observed in male wild-type corticotrophs. In 12 out of 16 cells, the $[Ca^{2+}]_i$ was raised and sustained for several minutes and returned to baseline later (Figure 3.24A, top). The other 4 cells showed increased amplitude of $[Ca^{2+}]_i$ together with an oscillatory behaviour (Figure 3.24A, bottom). For any given cell, the $[Ca^{2+}]_i$ responses to repeated AVP stimulation were highly reproducible and consistent (Figure 3.24B).

Since there were two phenotypes of $[Ca^{2+}]_i$ responses when stimulated with 2 nM AVP,

## Figure 3.24

### Repeated AVP induces consistent $[Ca^{2+}]_i$ responses in male wild-type corticotrophs

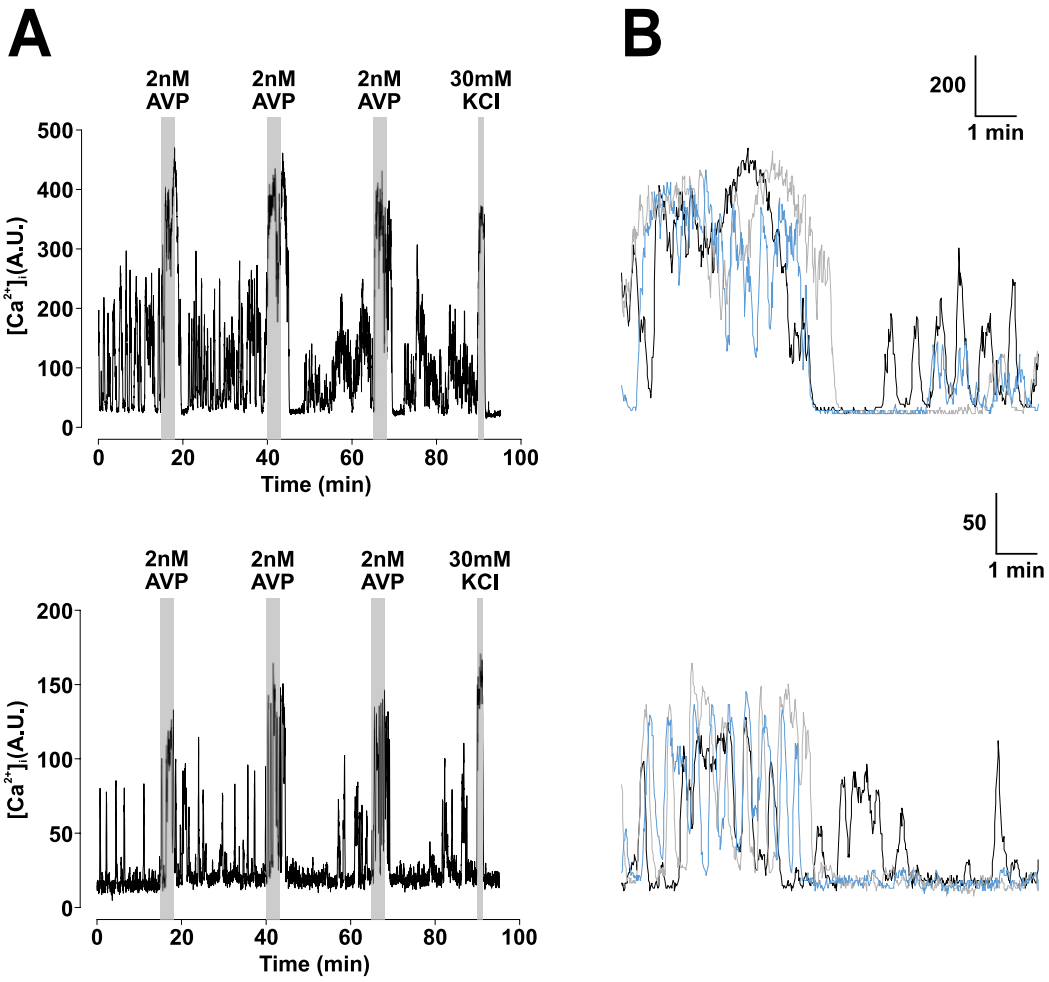


**Figure 3.24 Repeated AVP induces consistent $[Ca^{2+}]_i$ responses in male wild-type corticotrophs. (A)** Representative calcium imaging traces of male wild-type corticotrophs exposed to 2 nM AVP for three minutes and repeated three times at 25 minutes intervals. 30 mM potassium chloride was applied at the end for one minute. **(B)** Superposition of extracts of the two traces shown in A, showing $[Ca^{2+}]_i$ changes in male wild-type corticotrophs with repeated 2 nM AVP stimulation. Black line shows response to the first stimulus (starting at 15 min), grey line shows response to the second stimulus (starting at 40 min), and blue line shows response to the third stimulus (starting at 65 min).

all corticotrophs were first separated into two groups based on their responding phenotypes, sustained increase of $[Ca^{2+}]_i$ and oscillatory $[Ca^{2+}]_i$ behaviour, to examine whether there was any significant difference between them in all parameters. None of these parameters showed significant differences between the two phenotypes of $[Ca^{2+}]_i$ responses (data not shown), thus statistical analysis was performed on all male wild-type corticotrophs together.

Statistical analysis revealed that there were no significant differences between repeated AVP stimulation for AUC (10 min), AUC (peak) (Figure 3.25), peak, time to peak (Figure 3.26), response duration, peak duration (Figure 3.27) or time gap (Figure 3.28). These results suggest that $[Ca^{2+}]_i$ responses evoked by repeated 2 nM AVP stimulation were highly reproducible and consistent in male wild-type corticotrophs.

#### 3.2.4.2 Attenuated peak of $[Ca^{2+}]_i$ responses to repeated AVP stimulation in female wild-type corticotrophs

The calcium imaging experiments were repeated in corticotrophs isolated from female wild-type mice (n = 24 from 8 experiments) following the same protocol used in male wild-type corticotrophs.

Upon stimulation of 2 nM AVP, all female wild-type corticotrophs showed an increase

## Figure 3.25

**Stable AUC (10 min) and AUC (peak) of $[Ca^{2+}]_i$ responses in male wild-type corticotrophs to repeated AVP**

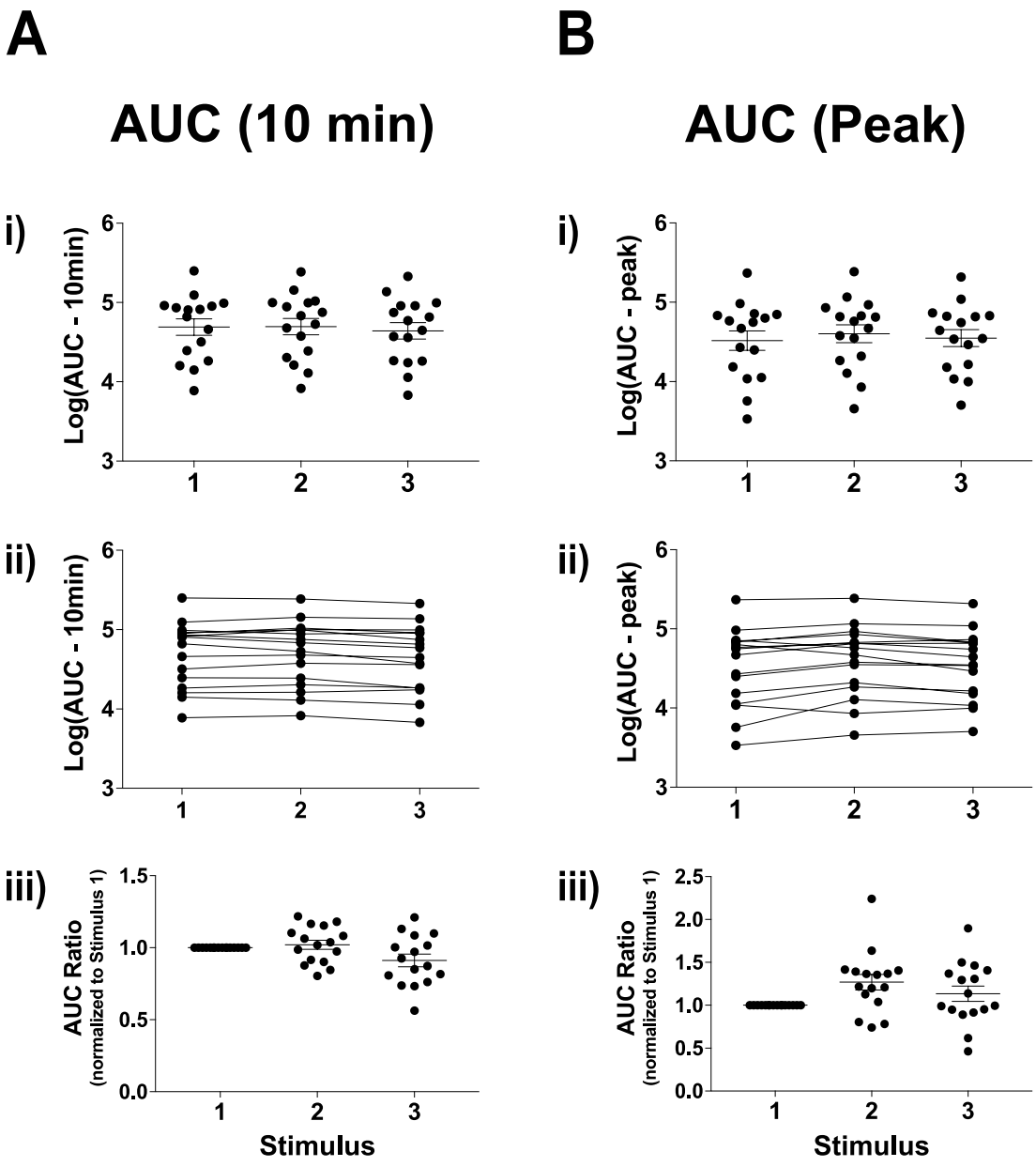


**Figure 3.25 Stable AUC (10 min) and AUC (peak) of $[Ca^{2+}]_i$ responses in male wild-type corticotrophs to repeated AVP.** Quantification of effects of repeated exposure to 2 nM AVP in **(A)** AUC (10 min) and **(B)** AUC (peak) (n = 16 from 9 experiments, mixed effects model). All data are means ± SEM.

## Figure 3.26

**Peak and time to peak of $[Ca^{2+}]_i$ responses in male wild-type corticotrophs to repeated AVP**

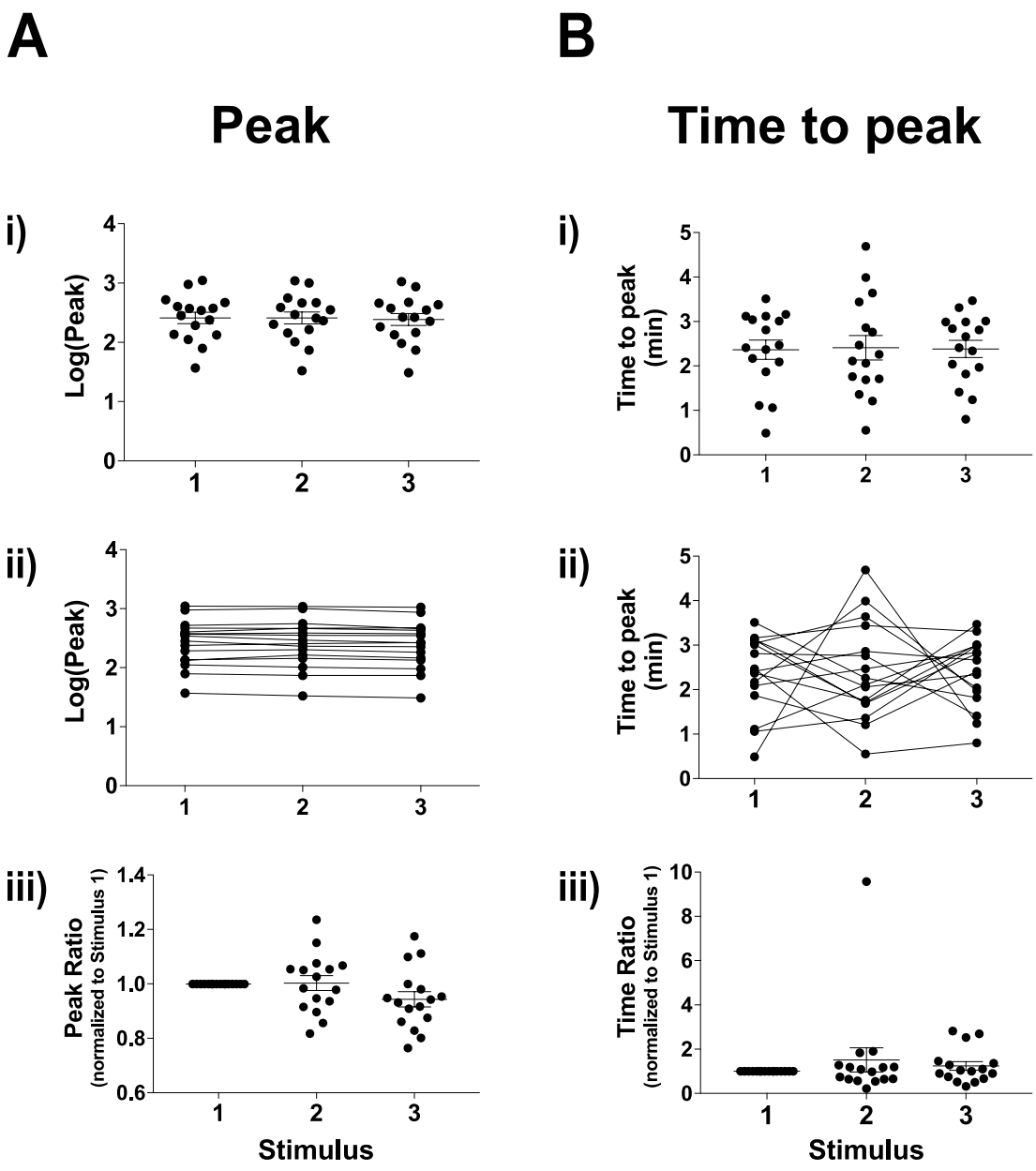


**Figure 3.26 Peak and time to peak of $[Ca^{2+}]_i$ responses in male wild-type corticotrophs to repeated AVP.** Quantification of effects of repeated exposure to 2 nM AVP in **(A)** peak and **(B)** time to peak (n = 16 from 9 experiments, mixed effects model). All data are means ± SEM.

## Figure 3.27

### Response duration and peak duration of $[Ca^{2+}]_i$ responses in male wild-type corticotrophs to repeated AVP

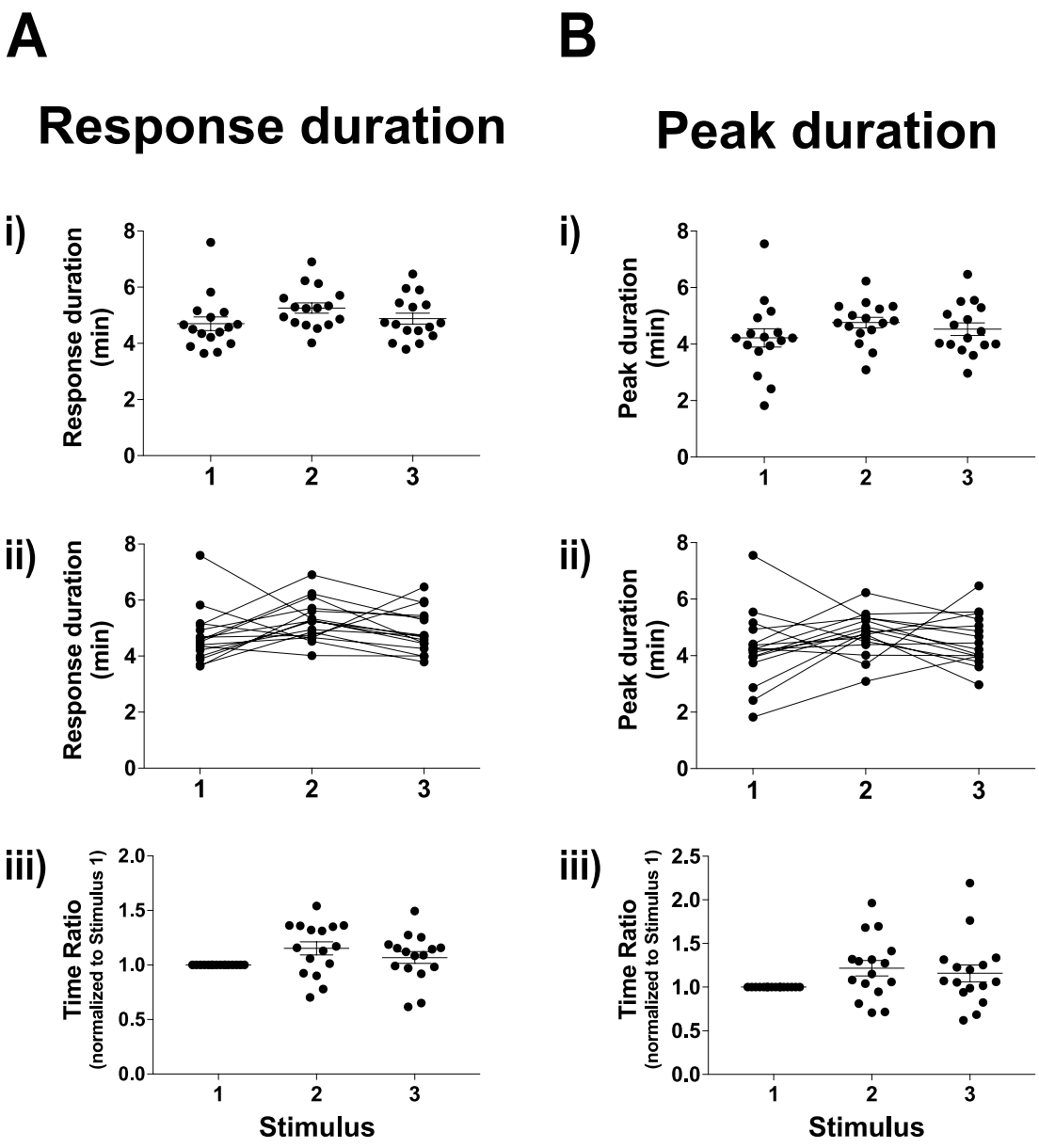


**Figure 3.27 Response duration and peak duration of $[Ca^{2+}]_i$ responses in male wild-type corticotrophs to repeated AVP.** Quantification of effects of repeated exposure to 2 nM AVP in **(A)** response duration and **(B)** peak duration (n = 16 from 9 experiments, mixed effects model). All data are means ± SEM.

## Figure 3.28

### Time gap of $[Ca^{2+}]_i$ responses in male wild-type corticotrophs to repeated AVP

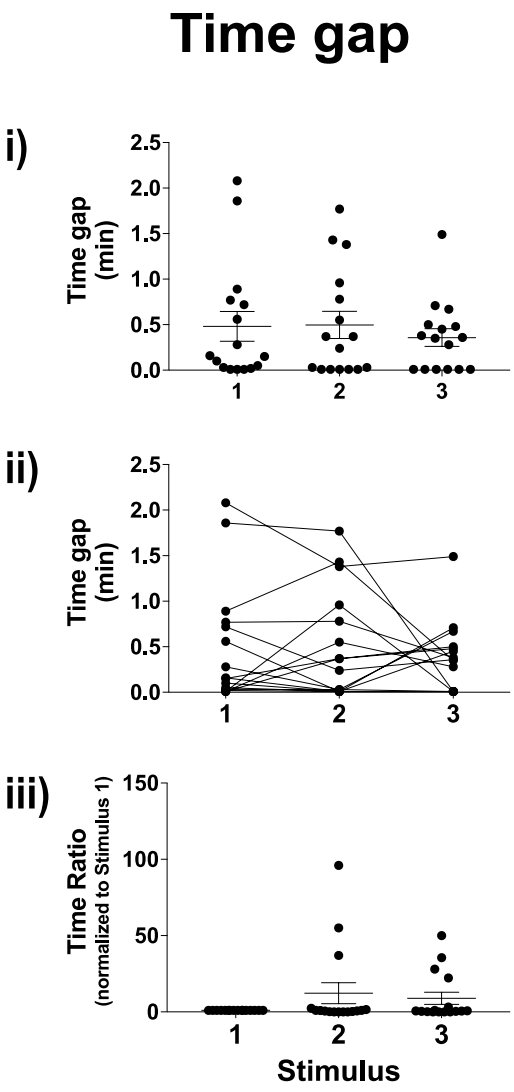


**Figure 3.28 Time gap of $[Ca^{2+}]_i$ responses in male wild-type corticotrophs to repeated AVP.** Quantification of effects of repeated exposure to 2 nM AVP in time gap (n = 16 from 9 experiments, mixed effects model). All data are means ± SEM.

in $[Ca^{2+}]_i$ responses and both phenotypes of AVP-induced $[Ca^{2+}]_i$ responses were observed as in male wild-type corticotrophs. In 12 out of 24 cells, a sustained $[Ca^{2+}]_i$ elevation was observed (Figure 3.29A, top). In remaining 12 cells, $[Ca^{2+}]_i$ had high frequency oscillations, accompanied with an increase in $[Ca^{2+}]_i$ amplitude (Figure 3.29A, bottom). Superposition of calcium imaging traces revealed that $[Ca^{2+}]_i$ responses to repeated 2 nM AVP stimulation were highly repeatable and consistent in female wild-type corticotrophs in both phenotypes of $[Ca^{2+}]_i$ response (Figure 3.29B).

All calcium imaging recordings were then classified into two groups according to their $[Ca^{2+}]_i$ responding phenotypes to examine all measurement parameters as in wild-type male corticotrophs. Statistical analysis revealed that there were no significant differences between AVP-induced sustained $[Ca^{2+}]_i$ elevation and oscillatory $[Ca^{2+}]_i$ behaviour in any parameter in female wild-type corticotrophs (data not shown). Thus, the statistical analysis of the effects of AVP on $[Ca^{2+}]_i$ responses was performed on all female wild-type corticotrophs together.

Statistical analysis revealed that there were no significant differences in AUC (10 min) or AUC (peak) following AVP stimulation in female wild-type corticotrophs (Figure 3.30). Repeated AVP stimulation significantly ($p < 0.05$) reduced peak in Stimulus 3 compared to Stimulus 1 (Figure 3.31A). Time to peak (Figure 3.31B), response

# Figure 3.29

## Repeated AVP induces consistent $[Ca^{2+}]_i$ responses in female wild-type corticotrophs

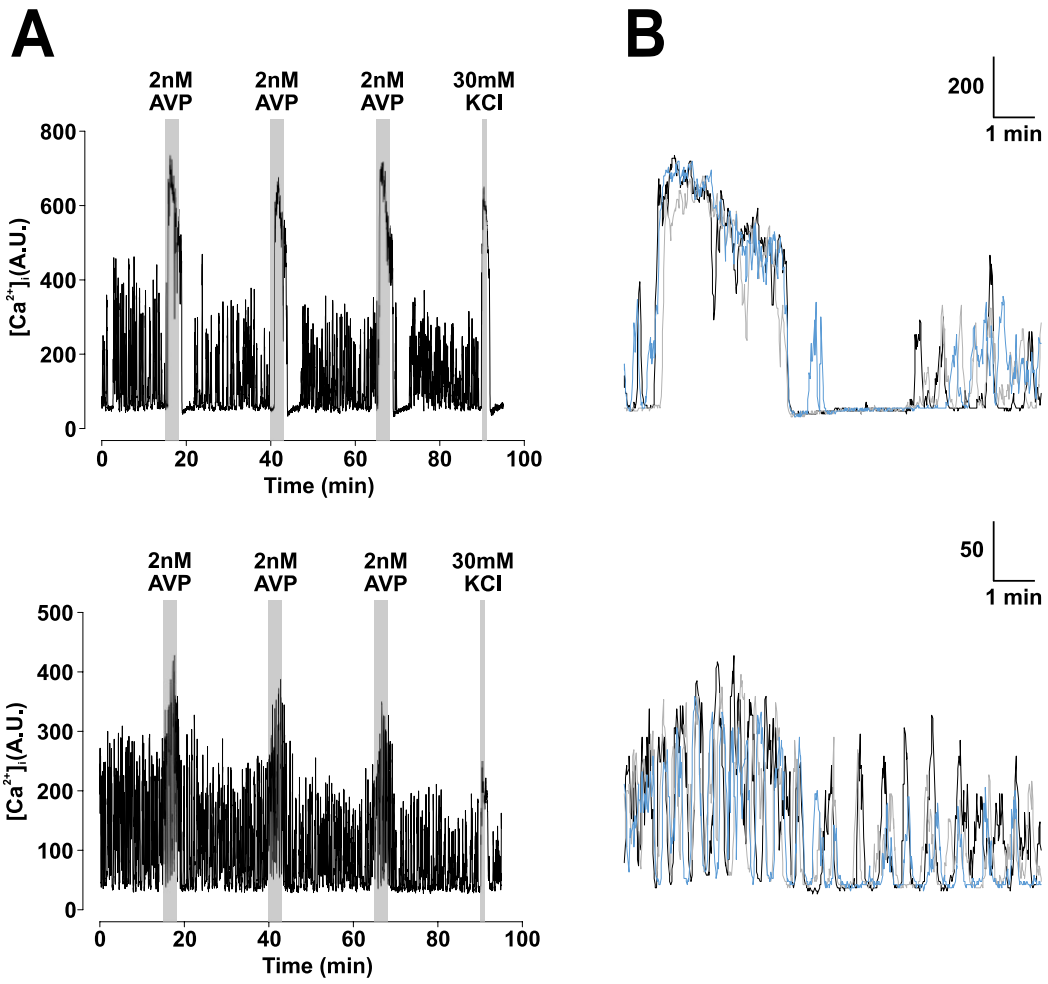


**Figure 3.29 Repeated AVP induces consistent $[Ca^{2+}]_i$ responses in female wild-type corticotrophs. (A)** Representative calcium imaging traces of female wild-type corticotrophs exposed to 2 nM AVP for three minutes and repeated three times at 25 minutes intervals. 30 mM potassium chloride was applied at the end for one minute. **(B)** Superposition of extracts of the two traces shown in A, showing $[Ca^{2+}]_i$ changes in female wild-type corticotrophs with repeated 2 nM AVP stimulation. Black line shows response to the first stimulus (starting at 15 min), grey line shows response to the second stimulus (starting at 40 min), and blue line shows response to the third stimulus (starting at 65 min).

duration, peak duration (Figure 3.32) and time gap showed no statistically significant differences between repeated AVP stimulation (Figure 3.33). These results suggested that AVP-induced $[Ca^{2+}]_i$ responses were highly repeatable and stable in female wild-type corticotrophs.

#### 3.2.4.3 Female wild-type corticotrophs have longer response duration to repeated AVP stimulation compared to males

Although both male and female wild-type corticotrophs displayed stable $[Ca^{2+}]_i$ responses to repeated AVP stimulation, we examined whether there were differences between male and female corticotrophs.

AVP evoked two phenotypes of $[Ca^{2+}]_i$ responses that were both found in male and female wild-type corticotrophs. As shown before, there were no significant differences between two phenotypes of $[Ca^{2+}]_i$ responses in both sexes. Thus, the effects of 2 nM AVP on $[Ca^{2+}]_i$ responses were compared on all calcium imaging recordings without classification between male and female wild-type corticotrophs.

There were no statistically significant differences between male and female wild-type corticotrophs in AVP-evoked $[Ca^{2+}]_i$ responses for AUC (10 min), AUC (peak) (Figure 3.34), peak or time to peak (Figure 3.35A&B). However, female corticotrophs showed

## Figure 3.30

**Stable AUC (10 min) and AUC (peak) of $[Ca^{2+}]_i$ responses in female wild-type corticotrophs to repeated AVP**

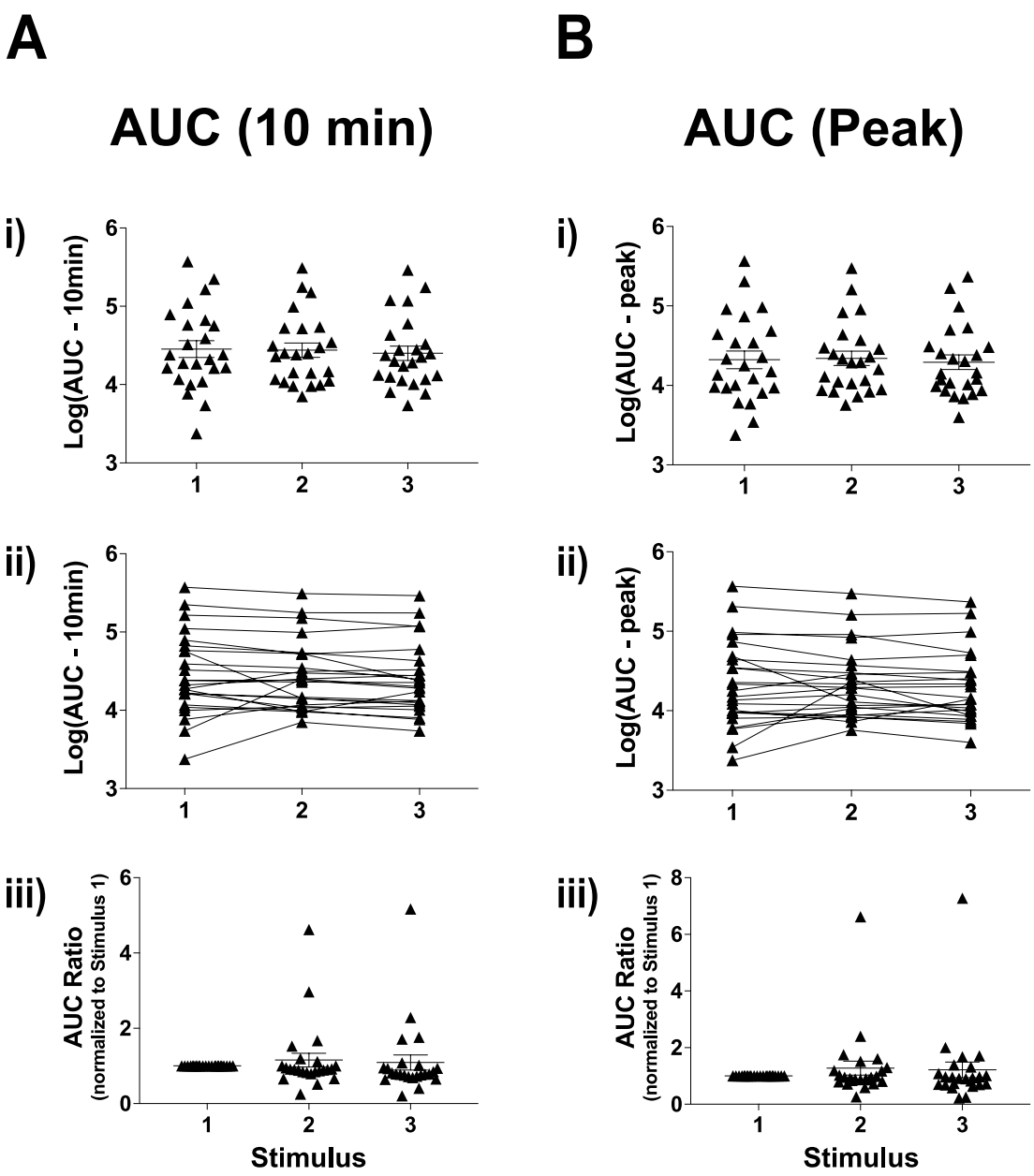


**Figure 3.30 Stable AUC (10 min) and AUC (peak) of $[Ca^{2+}]_i$ responses in female wild-type corticotrophs to repeated AVP.** Quantification of effects of repeated exposure to 2 nM AVP in **(A)** AUC (10 min) and **(B)** AUC (peak) (n = 24 from 8 experiments, mixed effects model). All data are means ± SEM.

## Figure 3.31

### Attenuation of peak but not time to peak of $[Ca^{2+}]_i$ responses in female wild-type corticotrophs to repeated AVP

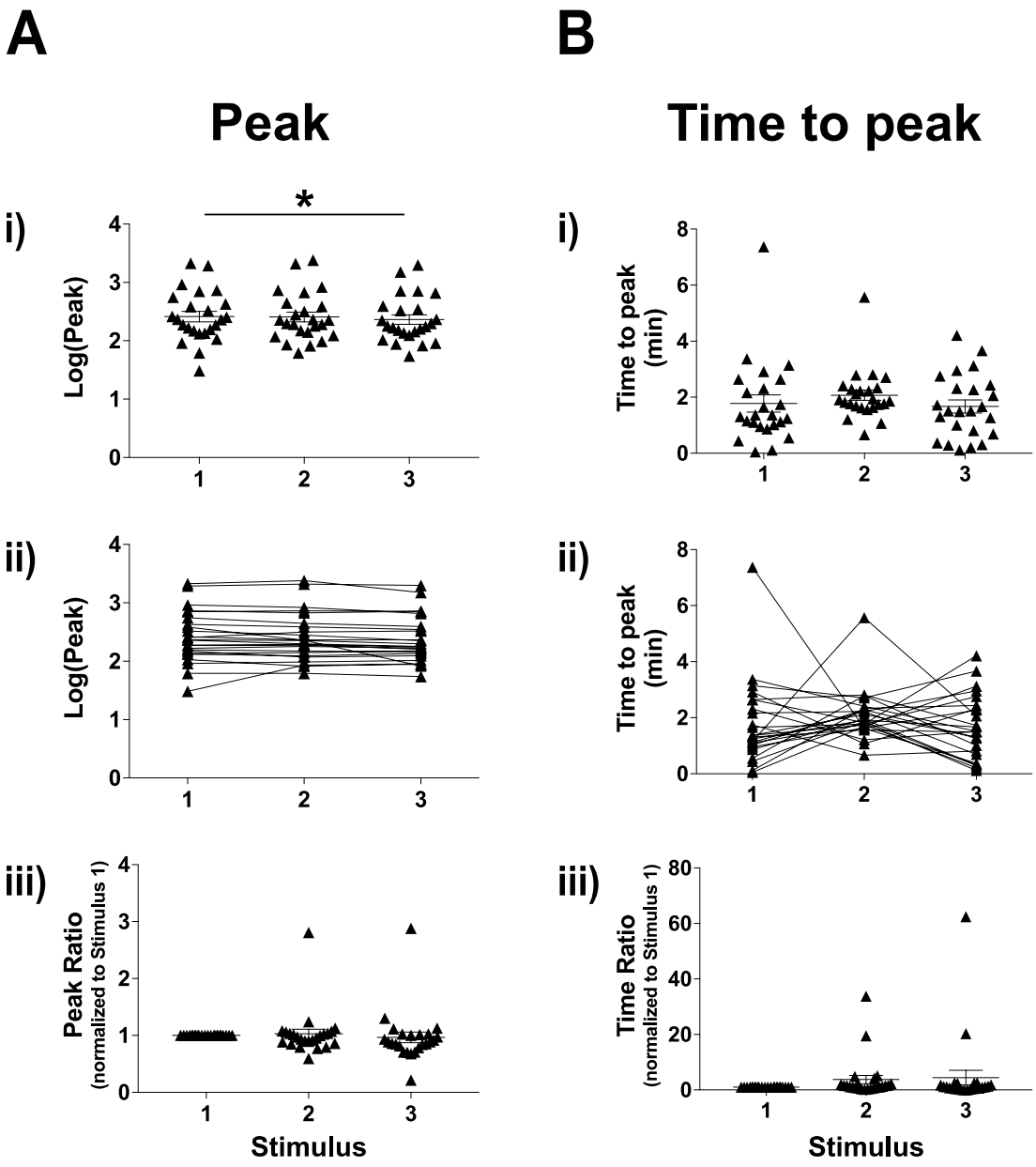


**Figure 3.31 Attenuation of peak but not time to peak of $[Ca^{2+}]_i$ responses in female wild-type corticotrophs to repeated AVP.** Quantification of effects of repeated exposure to 2 nM AVP in **(A)** peak and **(B)** time to peak. * $p < 0.05$ (n = 24 from 8 experiments, mixed effects model). All data are means ± SEM.

## Figure 3.32

### Response duration and peak duration of $[Ca^{2+}]_i$ responses in female wild-type corticotrophs to repeated AVP

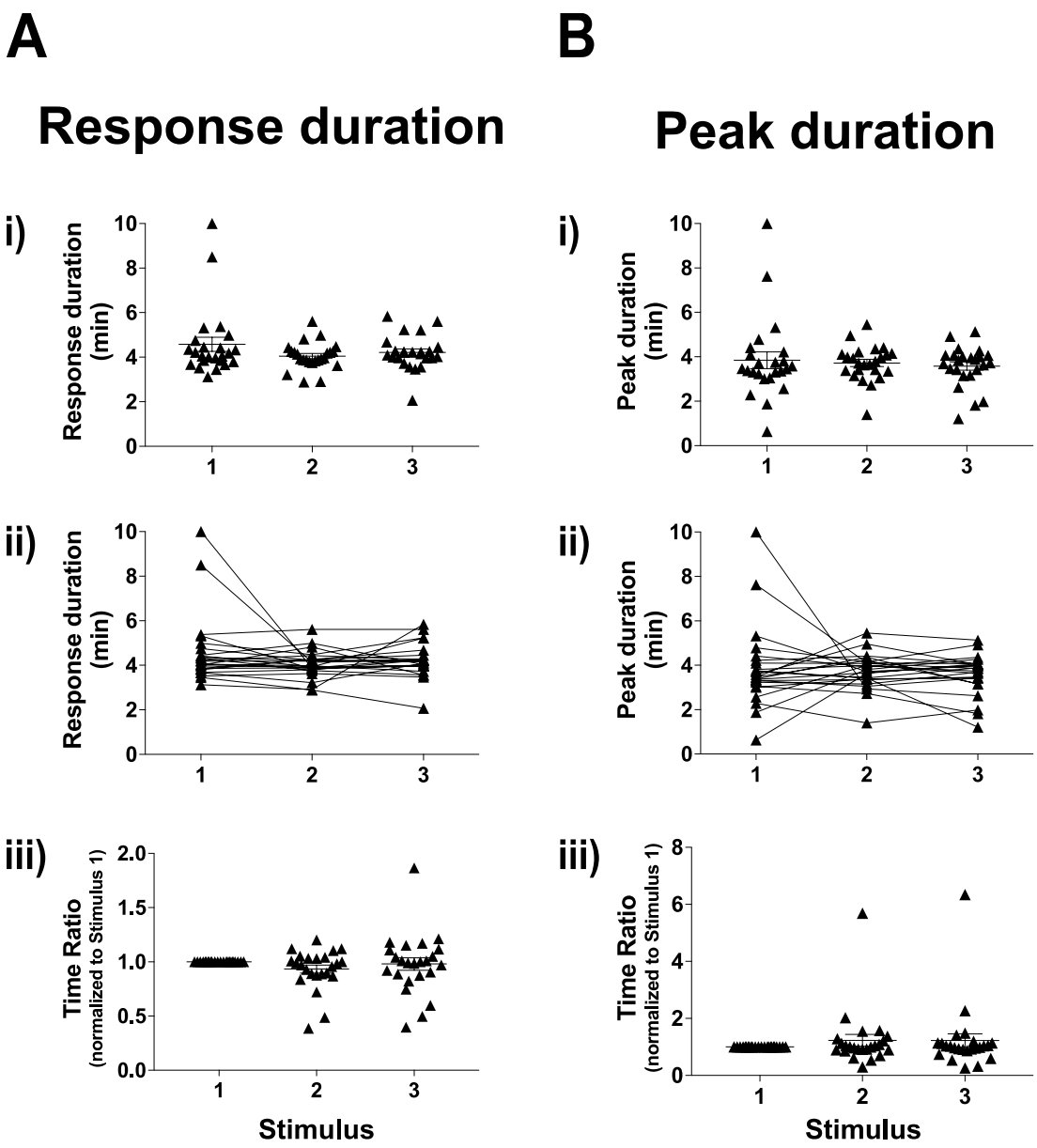


**Figure 3.32 Response duration and peak duration of $[Ca^{2+}]_i$ responses in female wild-type corticotrophs to repeated AVP.** Quantification of effects of repeated exposure to 2 nM AVP in **(A)** response duration and **(B)** peak duration (n = 24 from 8 experiments, mixed effects model). All data are means ± SEM.

## Figure 3.33

### Time gap of $[Ca^{2+}]_i$ responses in female wild-type corticotrophs to repeated AVP

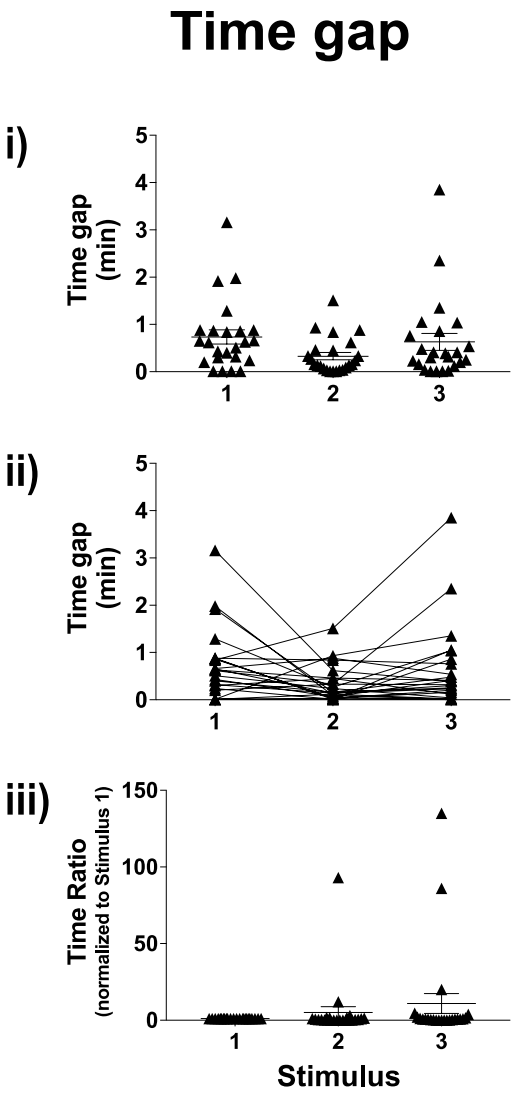


**Figure 3.33 Time gap of $[Ca^{2+}]_i$ responses in female wild-type corticotrophs to repeated AVP.** Quantification of effects of repeated exposure to 2 nM AVP in time gap (n = 24 from 8 experiments, mixed effects model). All data are means ± SEM.

a significant ($p < 0.05$) longer response duration compared to males in Stimulus 2 (Figure 3.35C). Peak duration and time gap (Figure 3.36) were not significantly different between male and female wild-type corticotrophs either.

In summary, there were no major sex differences in wild-type corticotrophs in $[Ca^{2+}]_i$ response to repeated 2nM AVP stimulation.

### 3.2.5 Do wild-type corticotrophs display synergy between CRH and AVP at the level of intracellular free calcium?

Previous studies have reported that CRH and AVP stimulate corticotrophs in a synergistic way to increase the secretion of ACTH, in part through synergy at the level of cAMP accumulation (Gillies *et al.*, 1982; Lamberts *et al.*, 1984). Stimulation of corticotrophs with CRH and AVP individually both increased $[Ca^{2+}]_i$. After the characterisation of CRH- or AVP-induced $[Ca^{2+}]_i$ in wild-type corticotrophs, the following experiments were designed to investigate whether there was synergy between CRH and AVP at the level of $[Ca^{2+}]_i$.

## Figure 3.34

### No significant sex difference in AVP-induced AUC (10 min) or AUC (peak) of $[Ca^{2+}]_i$ responses in wild-type corticotrophs

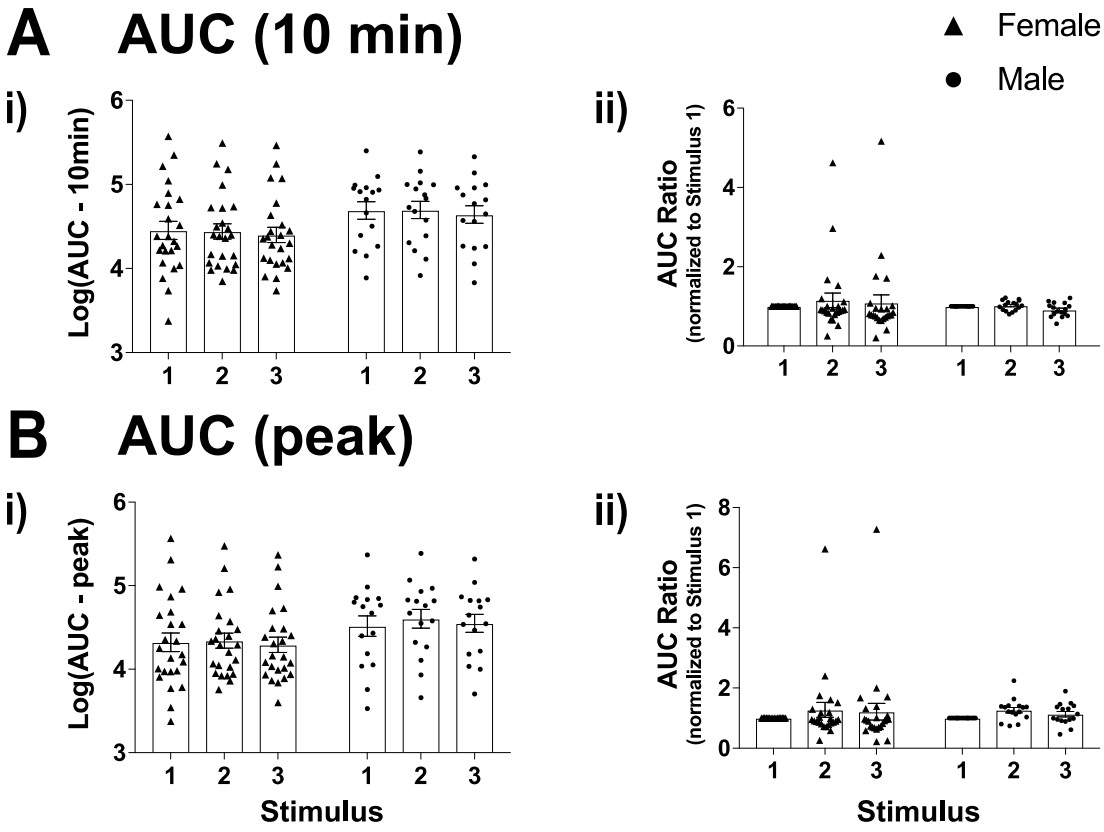


**Figure 3.34 No significant sex differences in AVP-induced AUC (10 min) or AUC (peak) of $[Ca^{2+}]_i$ responses in wild-type corticotrophs.** Quantifications of effects of repeated exposure to 2 nM AVP in (A) AUC (10 min) and (B) AUC (peak) (male n = 16 from 9 experiments, female n = 24 from 8 experiments, mixed effects model). All data are means ± SEM.

## Figure 3.35

**Female wild-type corticotrophs have longer response duration but not peak or time to peak of $[Ca^{2+}]_i$ responses to repeated AVP compared to males**

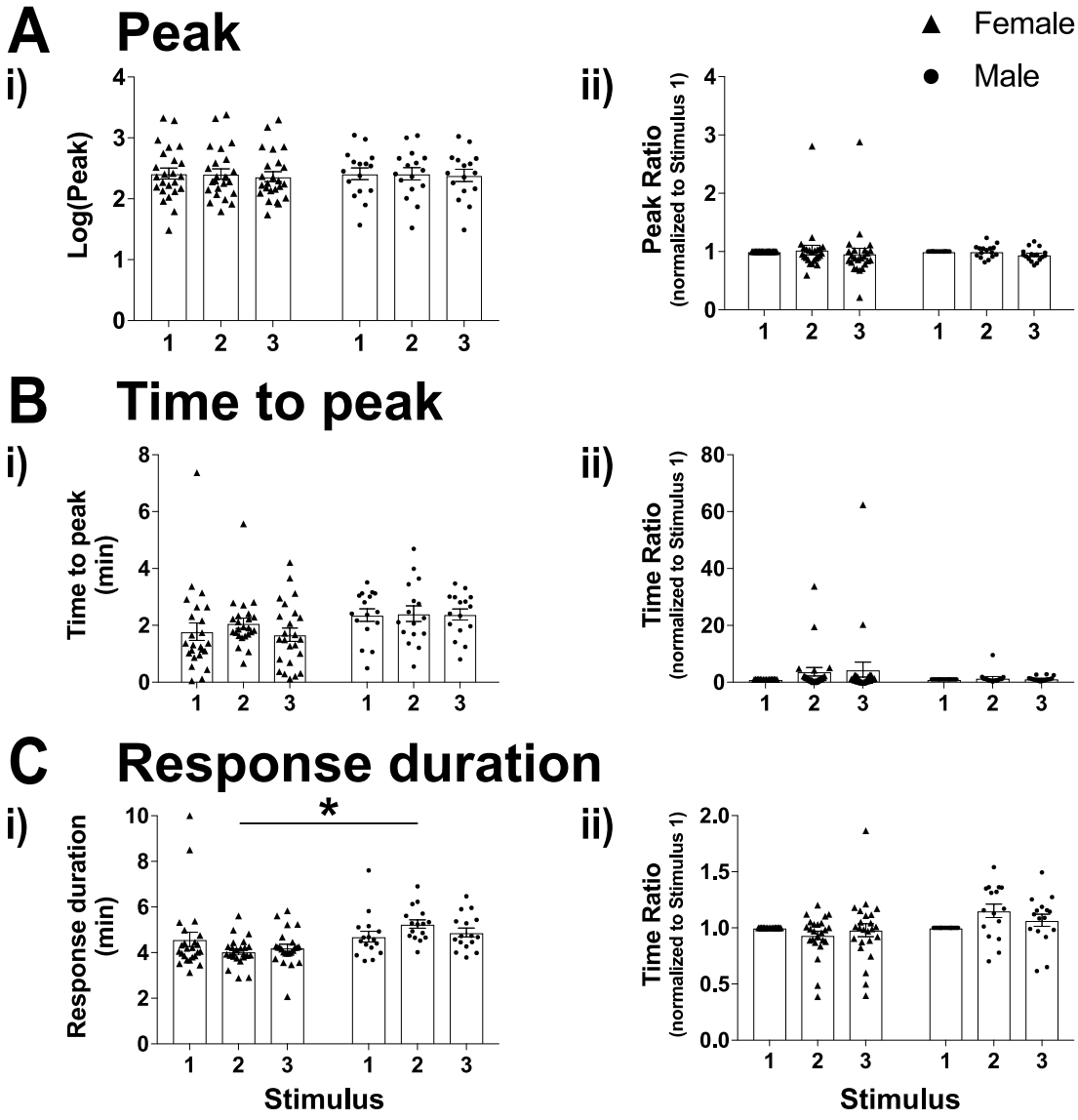


**Figure 3.35 Female wild-type corticotrophs have longer response duration but not peak or time to peak of $[Ca^{2+}]_i$ responses to repeated AVP compared to males.** Quantification of effects of repeated exposure to 2 nM AVP in **(A)** peak, **(B)** time to peak and **(C)** response duration. * $p < 0.05$ (male n = 16 from 9 experiments, female n = 24 from 8 experiments, mixed effects model). All data are means ± SEM.

## Figure 3.36

### No significant sex difference in AVP-induced peak duration or time gap of $[Ca^{2+}]_i$ responses in wild-type corticotrophs

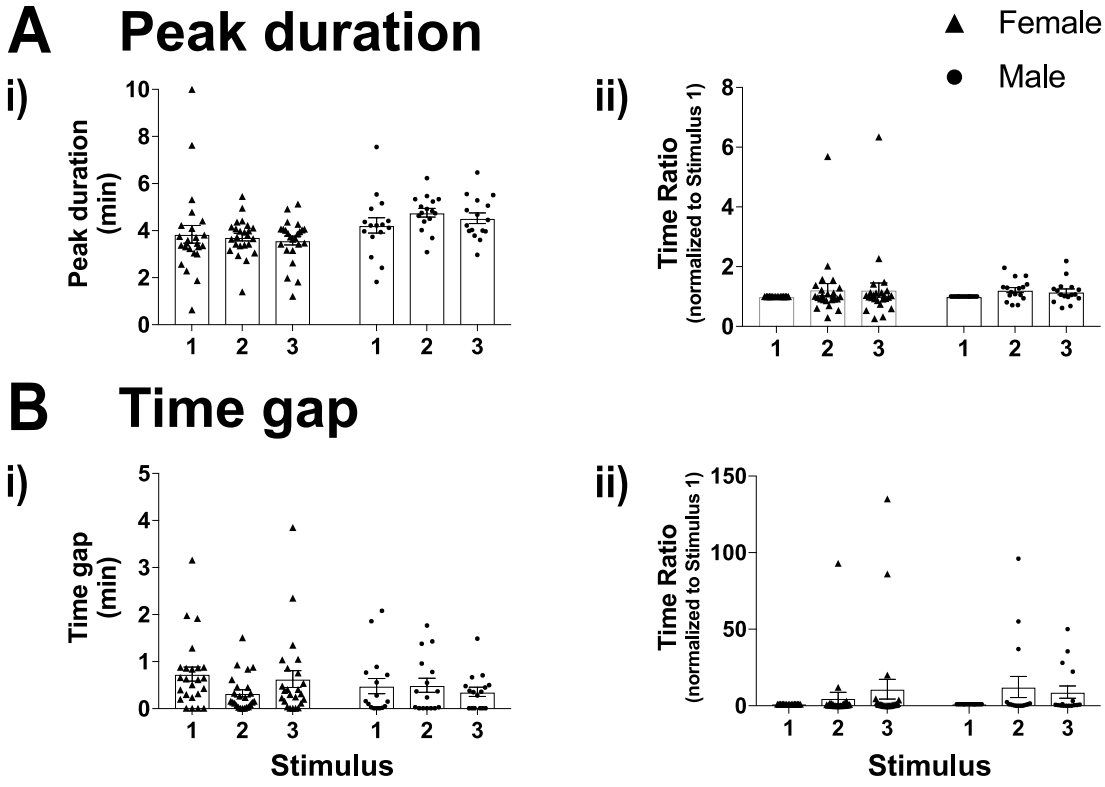


**Figure 3.36 No significant sex difference in AVP-induced peak duration or time gap of $[Ca^{2+}]_i$ responses in wild-type corticotrophs.** Quantification of effects of repeated exposure to 2 nM AVP in **(A)** peak duration and **(B)** time gap (male n = 16 from 9 experiments, female n = 24 from 8 experiments, mixed effects model). All data are means ± SEM.

### 3.2.5.1 No synergistic $[Ca^{2+}]_i$ response between CRH and AVP in male wild-type corticotrophs

Calcium imaging experiments were performed on male wild-type corticotrophs following the repeated stimulation protocol (see 2.5.2.1): spontaneous $[Ca^{2+}]_i$ signalling was recorded for 15 minutes, then corticotrophs were stimulated with 0.2 nM CRH and 2 nM AVP separately followed by the combination of two single stimuli. Each stimulation lasted for three minutes with a 25 minute interval. Finally, corticotrophs were exposed to 30 mM potassium chloride for one minute to confirm cell viability at the end of recording. To counteract the possible influence caused by the sequence of exposure to CRH and AVP, the order of two single stimuli was randomized (CRH, AVP, combination, n = 8 or AVP, CRH, combination, n = 3 from 6 experiments).

All male wild-type corticotrophs responded to 0.2 nM CRH with a significant and sustained elevation of $[Ca^{2+}]_i$ regardless of the exposure order, which was the same as the responses to repeated CRH stimulation. When stimulated with 2 nM AVP, two phenotypes of $[Ca^{2+}]_i$ responses observed before were both found in corticotrophs no matter what the exposure sequence was. In 6 out of 11 cells, the sustained $[Ca^{2+}]_i$ increase was observed and the other 5 cells showed an oscillatory $[Ca^{2+}]_i$ behaviour when stimulated with AVP. Stimulation with the combination of 0.2 nM CRH and

2 nM AVP, male wild-type corticotrophs always displayed a rapid and significant elevation of $[Ca^{2+}]_i$ and sustained for a few minutes (Figure 3.37A & Figure 3.38A). Extracts of calcium imaging traces suggested the $[Ca^{2+}]_i$ responses to two single stimuli and combined stimulus were highly coincident, no matter what the exposure sequence was and what the phenotypes of AVP-induced calcium responses were (Figure 3.37B & Figure 3.38B).

To determine whether CRH and AVP act in a synergistic manner at the level of $[Ca^{2+}]_i$ in male wild-type corticotrophs, the AUC of the combined stimulus was compared to the sum of the AUC of the two single stimuli. If the AUC of the combined stimulus is larger than the sum of the AUC of the two single stimuli indicating the corticotroph shows synergistic $[Ca^{2+}]_i$ response. As AVP-induced oscillatory $[Ca^{2+}]_i$ responses always showed smaller AUC compared to sustained elevation of $[Ca^{2+}]_i$ during peak duration, sustained increase of $[Ca^{2+}]_i$ (n = 8) and oscillatory $[Ca^{2+}]_i$ behaviour (n = 3) were compared to examine whether there were significant differences between the two phenotypes of $[Ca^{2+}]_i$ responses in AUC (10 min) and AUC (peak). Neither AUC (10 min) nor AUC (peak) showed statistically significant differences between the two phenotypes of $[Ca^{2+}]_i$ responses (data not shown), thus statistical analysis of AUC (10 min) and AUC (peak) was performed on all male wild-type corticotrophs together. The effects of two single stimuli and combined stimulus on $[Ca^{2+}]_i$ responses were also

## Figure 3.37

### CRH, AVP and CRH/AVP induce $[Ca^{2+}]_i$ responses in male wild-type corticotrophs

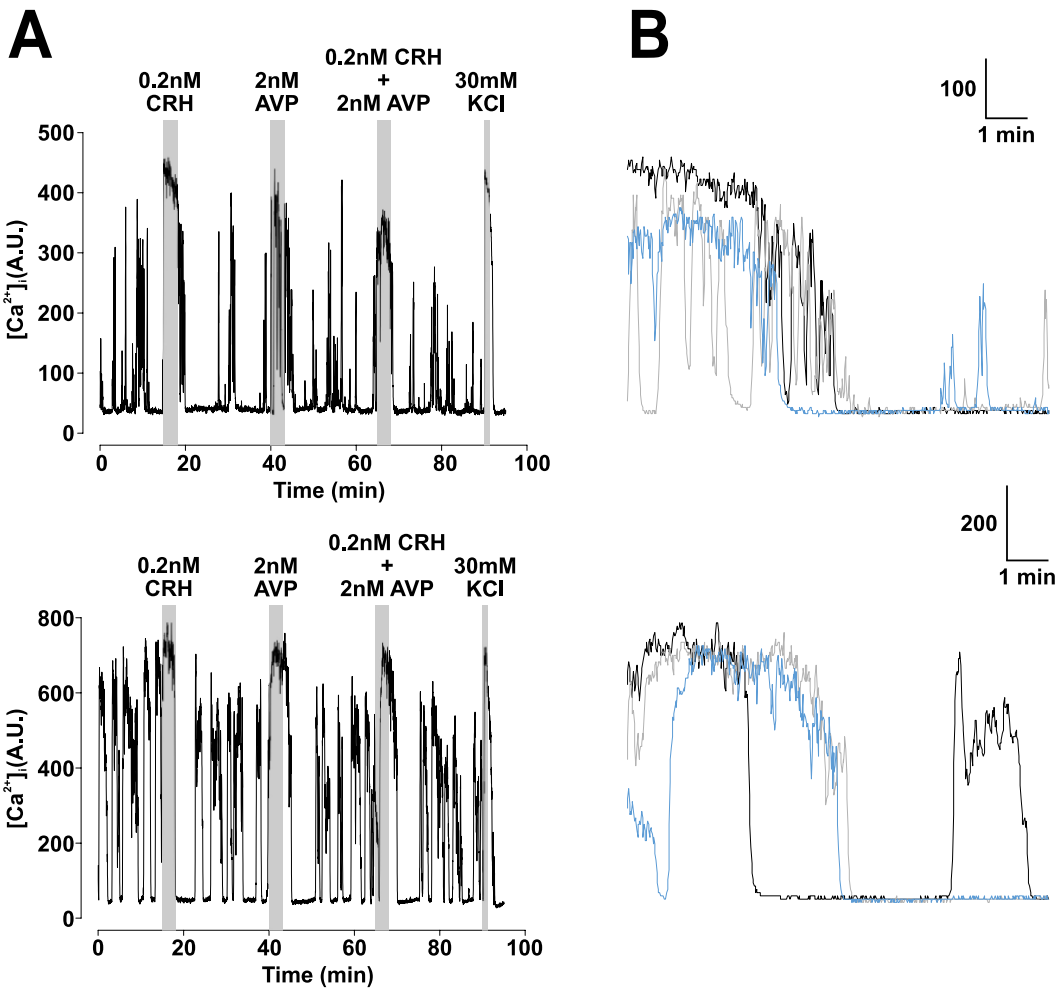


**Figure 3.37 CRH, AVP and CRH/AVP induce $[Ca^{2+}]_i$ responses in male wild-type corticotrophs.** **(A)** Representative calcium imaging traces of male wild-type corticotrophs exposed to 0.2 nM CRH, 2 nM AVP and 0.2 nM CRH together with 2 nM AVP at 25 minutes intervals. 30 mM potassium chloride was applied at the end for one minute. **(B)** Superposition of extracts of the two traces shown in A, showing $[Ca^{2+}]_i$ changes in male wild-type corticotrophs with stimuli. Black line shows response to 0.2 nM CRH (starting at 15 min), grey line shows response to 2 nM AVP (starting at 40 min), and blue line shows response to the combined stimulus (starting at 65 min).

## Figure 3.38

### AVP, CRH and CRH/AVP induce $[Ca^{2+}]_i$ responses in male wild-type corticotrophs

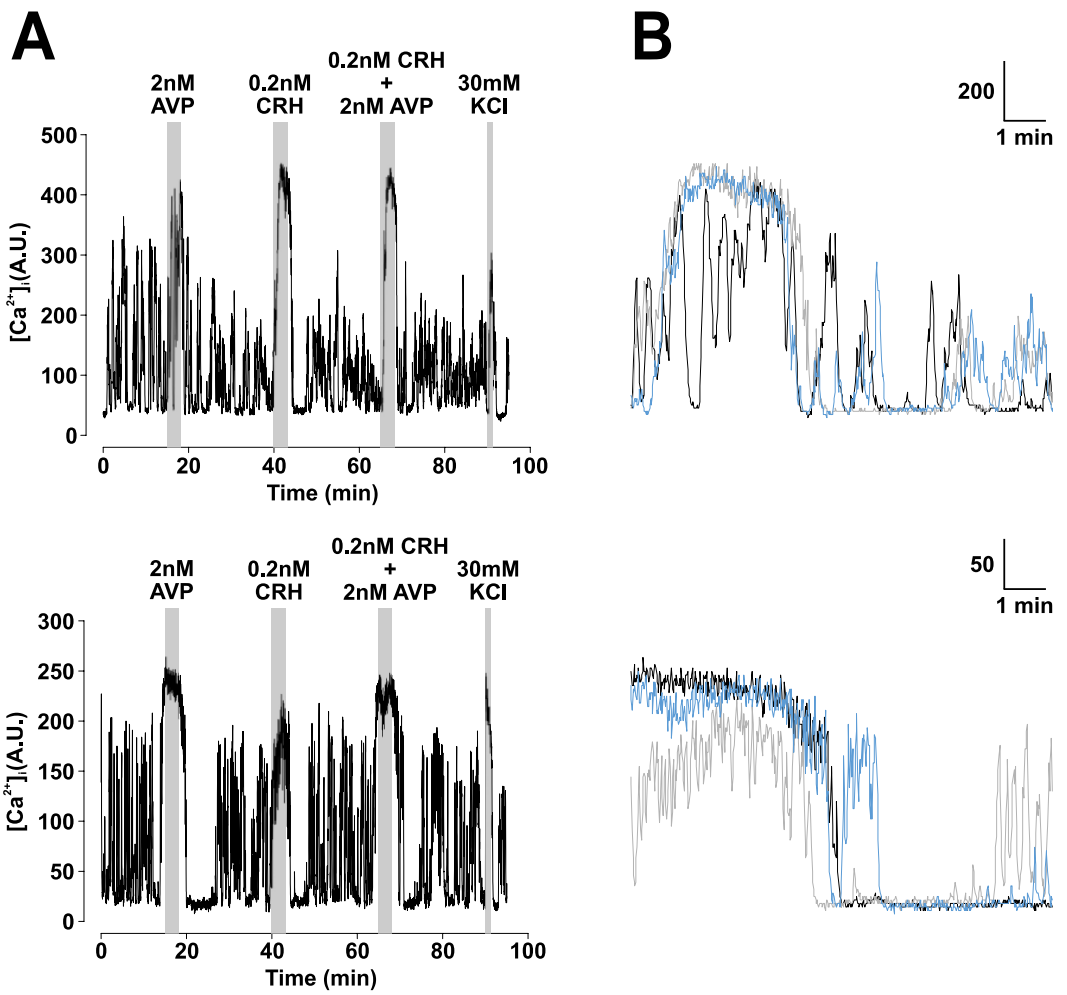


**Figure 3.38 AVP, CRH and CRH/AVP induce $[Ca^{2+}]_i$ responses in male wild-type corticotrophs. (A)** Representative calcium imaging traces of male wild-type corticotrophs exposed to 2 nM AVP, 0.2 nM CRH, and 0.2 nM CRH together with 2 nM AVP at 25 minutes intervals. 30 mM potassium chloride was applied at the end for one minute. **(B)** Superposition of extracts of the two traces shown in A, showing $[Ca^{2+}]_i$ changes in male wild-type corticotrophs with stimuli. Black line shows response to 2 nM AVP (starting at 15 min), grey line shows response to 0.2 nM CRH (starting at 40 min), and blue line shows response to the combined stimulus (starting at 65 min).

characterized in peak, time to peak, response duration, peak duration and time gap. The statistical analysis of AUC (10 min), AUC (peak) and peak were performed on log-transformed data and other parameters were analysed on raw data.

There were no statistically significant differences among the $[Ca^{2+}]_i$ responses induced by CRH, AVP and the combined stimulus in AUC (10 min) or AUC (peak). However, the combined stimulus was significantly ($p < 0.001$) smaller than the sum of the two single stimuli in both AUC (10 min) and AUC (peak), indicating none of these corticotrophs showed synergy between CRH and AVP at the level of $[Ca^{2+}]_i$ (Figure 3.39). Peak and time to peak were not significantly different following the three stimuli (Figure 3.40A&B). Stimulation with CRH and AVP together resulted in a significantly ($p < 0.001$) longer response duration (Figure 3.40C) and peak duration (Figure 3.41A) compared to CRH but not AVP stimulus. No significant differences were observed in time peak (Figure 3.41B) between CRH-, AVP- and CRH/AVP-induced $[Ca^{2+}]_i$ responses.

These results suggested that there was no synergistic $[Ca^{2+}]_i$ response to CRH/ AVP in male wild-type corticotrophs. CRH/AVP induced longer response duration and peak duration compared to CRH stimulus alone.

## Figure 3.39

### No synergistic $[Ca^{2+}]_i$ response between CRH and AVP in male wild-type corticotrophs

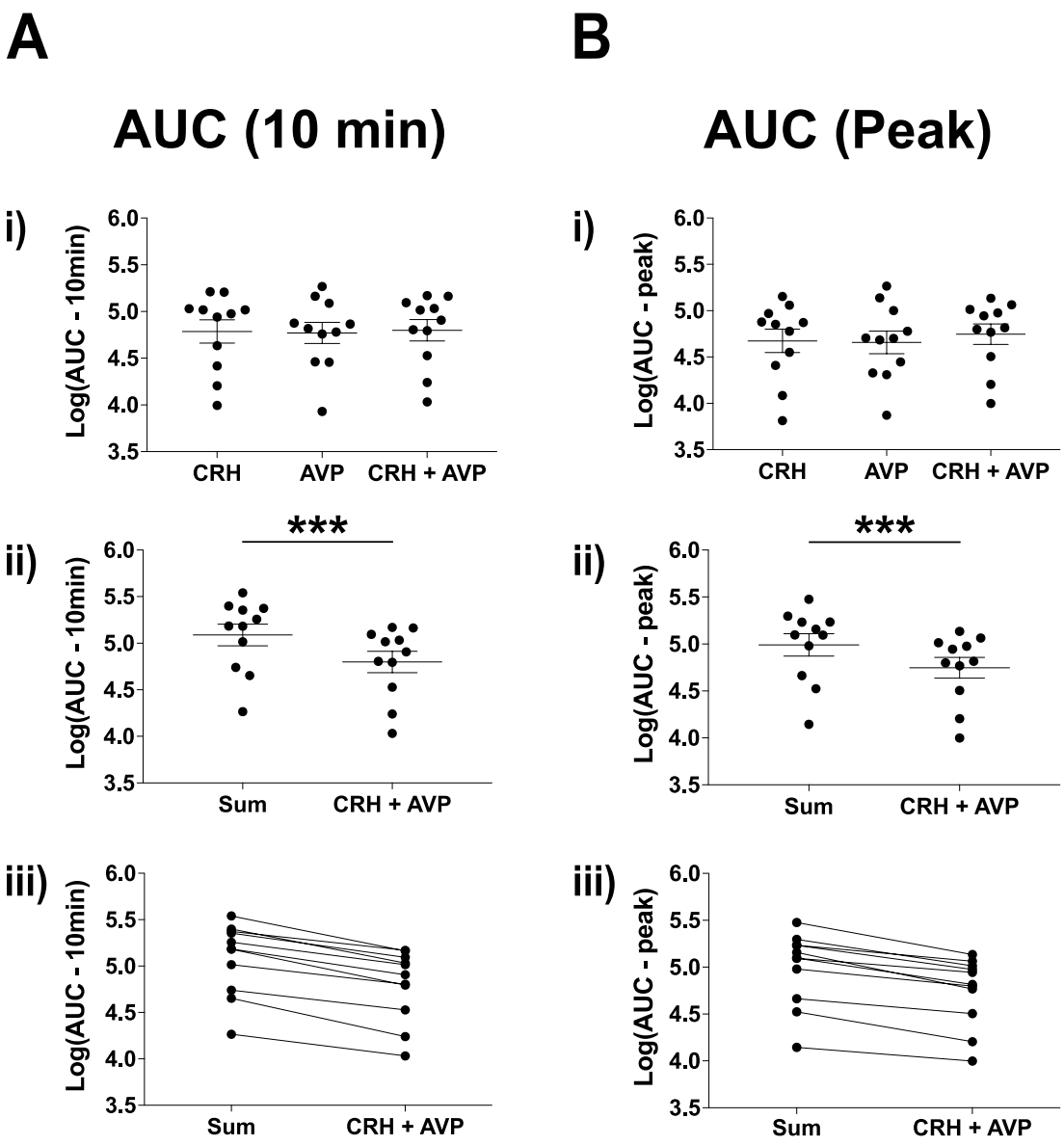


**Figure 3.39 No synergistic $[Ca^{2+}]_i$ response between CRH and AVP in male wild-type corticotrophs.** Quantification of effects of exposure to 0.2 nM CRH, 2 nM AVP and the combination of the two in **(A)** AUC (10 min) and **(B)** AUC (peak). The comparison of the AUC of the combined stimulus and the sum of the two single stimuli was used as a measurement of synergy. *** $p < 0.001$ (n = 11 from 6 experiments, mixed effects model). All data are means ± SEM.

## Figure 3.40

**CRH/AVP induces longer response duration but not peak or time to peak of $[Ca^{2+}]_i$ responses in male wild-type corticotrophs**

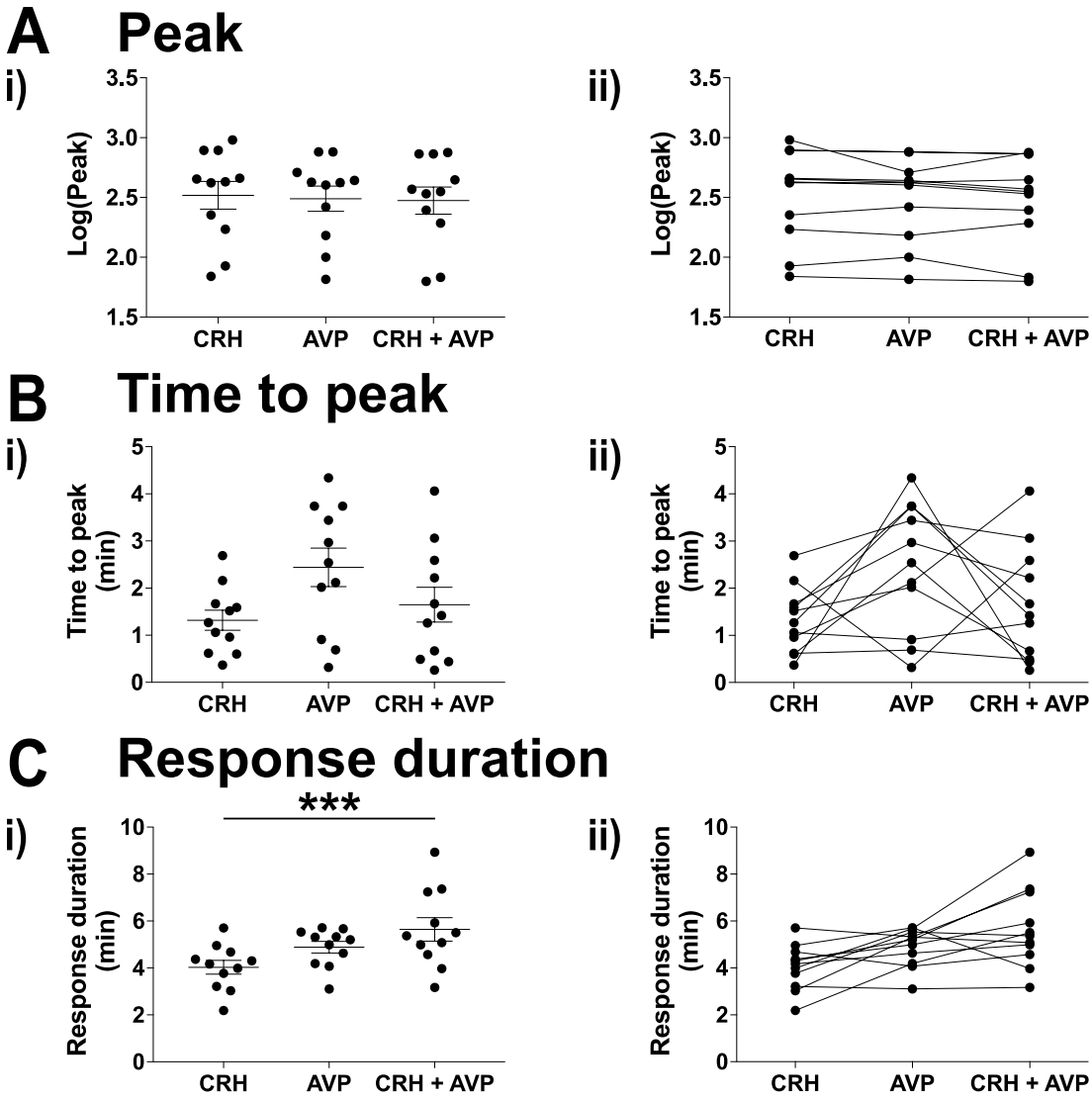


**Figure 3.40 CRH/AVP induces longer response duration but not peak or time to peak of $[Ca^{2+}]_i$ responses in male wild-type corticotrophs.** Quantification of effects of exposure to 0.2 nM CRH, 2 nM AVP and the combination of the two in **(A)** peak, **(B)** time to peak and **(C)** response duration. *** $p < 0.001$ (n = 11 from 6 experiments, mixed effects model). All data are means ± SEM.

## Figure 3.41

**CRH/AVP induces longer peak duration but not time gap of $[Ca^{2+}]_i$ responses in male wild-type corticotrophs**

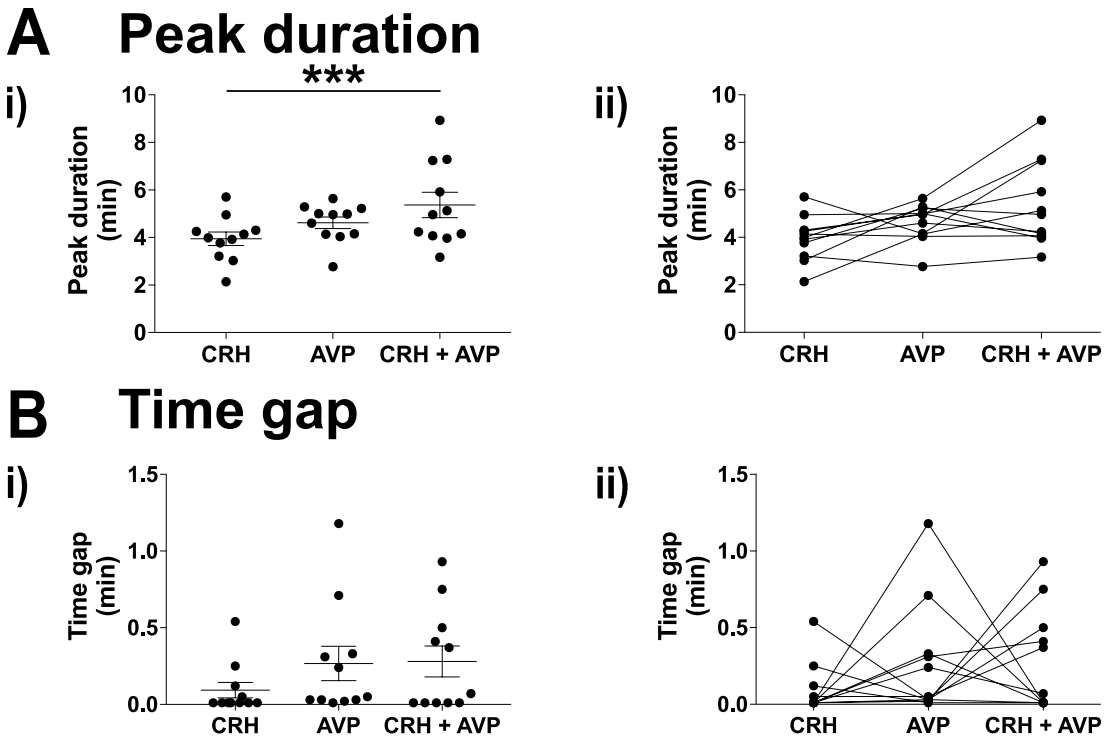


**Figure 3.41 CRH/AVP induces longer peak duration but not time gap of $[Ca^{2+}]_i$ responses in male wild-type corticotrophs.** Quantification of effects of exposure to 0.2 nM CRH, 2 nM AVP and the combination of the two in **(A)** peak duration and **(B)** time gap. *** $p < 0.001$ (n = 11 from 6 experiments, mixed effects model). All data are means ± SEM.

### 3.2.5.2 No synergistic $[Ca^{2+}]_i$ response between CRH and AVP in female wild-type corticotrophs at the population level

Calcium imaging experiments were performed on female wild-type corticotrophs isolated following the same protocol used in male wild-type corticotrophs. The order of CRH and AVP was random to minimize the possible impact resulted from the sequence of exposure to two single stimuli (CRH, AVP, combination, n = 8 or AVP, CRH, combination, n = 7 from 5 experiments).

When stimulated with 0.2 nM CRH, 2 nM AVP and the combined stimulus sequentially (n = 8), all 8 corticotrophs showed sustained increase of $[Ca^{2+}]_i$ to CRH stimulus, 5 out of 8 cells had sustained elevation of $[Ca^{2+}]_i$ to AVP stimulus and the other 3 cells displayed oscillatory $[Ca^{2+}]_i$ behaviour. All 8 cells showed a significant and rapid increase of $[Ca^{2+}]_i$ following combination stimulus (Figure 3.42A). When the order of stimulus was 2 nM AVP, 0.2 nM CRH and the combination of the two (n = 7), 1 out of 7 corticotrophs responding to all three stimuli with oscillatory $[Ca^{2+}]_i$ behaviour, which was not observed in wild-type corticotrophs exposed to repeated CRH stimulation. In the remaining 6 cells, all cells responded to CRH and the combination of the two single stimuli with sustained $[Ca^{2+}]_i$ increase, with 3 of them showing $[Ca^{2+}]_i$ oscillation and the rest 3 cells showing sustained $[Ca^{2+}]_i$ responses to AVP stimulus (Figure 3.43B). Although two phenotypes of $[Ca^{2+}]_i$ responses were

observed in all stimuli, extracts of calcium imaging traces suggested that $[Ca^{2+}]_i$ responses to two single stimuli and combined stimulus were highly coincident regardless of the order of stimulus (Figure 3.42B & Figure 3.43B).

The synergistic $[Ca^{2+}]_i$ responses and the effects of two single stimuli and combined stimulus on $[Ca^{2+}]_i$ responses were assessed with the same parameters used in male wild-type corticotrophs. Statistical analysis revealed that female wild-type corticotrophs showed no significant differences between AVP-induced sustained elevation of $[Ca^{2+}]_i$ ($n = 8$) and oscillatory $[Ca^{2+}]_i$ behaviour ($n = 7$) in either AUC (10 min) or AUC (peak) (data not shown). Thus, statistical analysis was performed on all female wild-type corticotrophs together.

AVP-induced AUC (10 min) $[Ca^{2+}]_i$ responses was significantly lower than $[Ca^{2+}]_i$ responses induced by CRH ($p < 0.01$) and the combined stimulus ($p < 0.01$). AVP-induced AUC (peak) was also significantly lower than CRH ($p < 0.05$) and the combined stimulus ($p < 0.001$). Importantly, the combined stimulus was significantly smaller than the sum of the two single stimuli in both AUC (10 min) ($p < 0.001$) and AUC (peak) ($p < 0.01$), which suggests that there was no synergistic $[Ca^{2+}]_i$ responses CRH and AVP in female wild-type corticotrophs (Figure 3.44). Although the synergy was not observed when considering the population, in 4 out of 15 cells (26.7%) the

# Figure 3.42

## CRH, AVP and CRH/AVP induce $[Ca^{2+}]_i$ responses in female wild-type corticotrophs

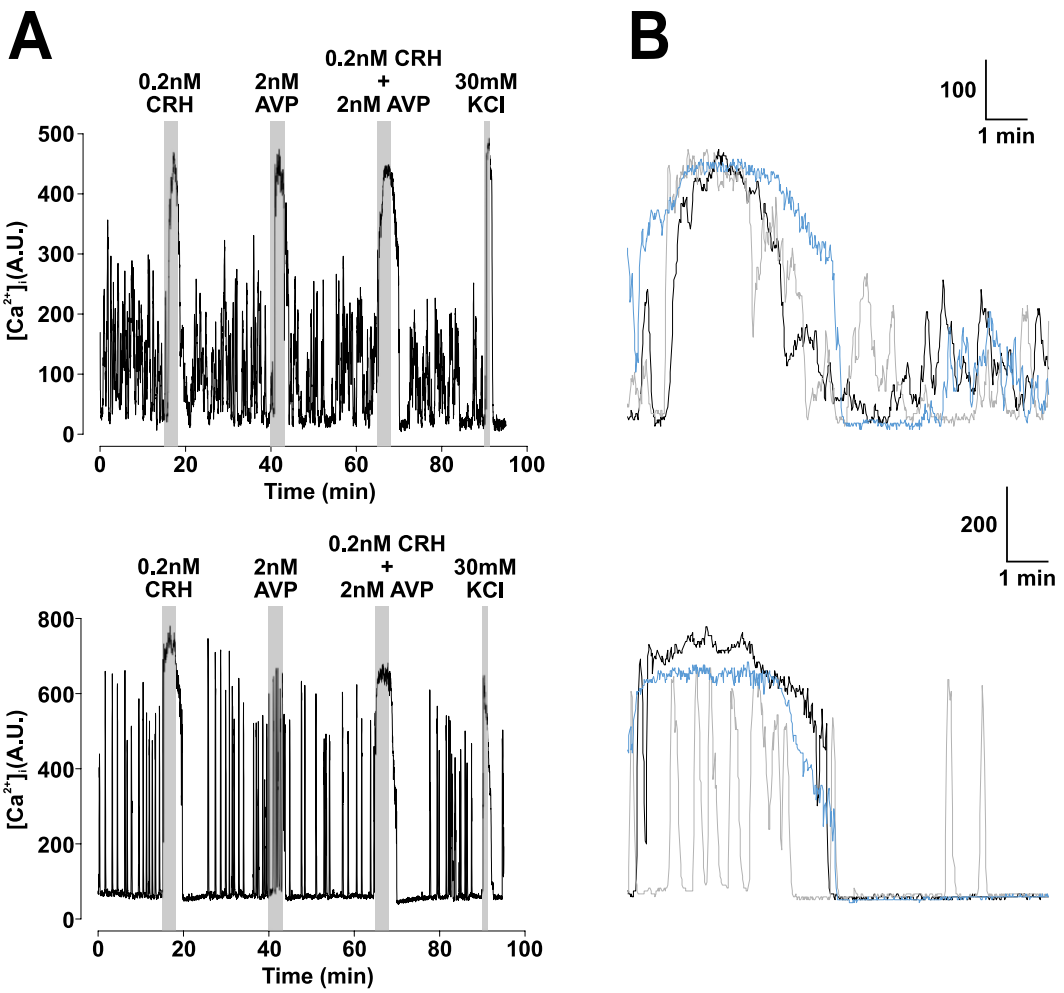


**Figure 3.42 CRH, AVP and CRH/AVP induce $[Ca^{2+}]_i$ responses in female wild-type corticotrophs. (A)** Representative calcium imaging traces of female wild-type corticotrophs exposed to 0.2 nM CRH, 2 nM AVP and 0.2 nM CRH together with 2 nM AVP at 25 minutes intervals. 30 mM potassium chloride was applied at the end for one minute. **(B)** Superposition of extracts of the two traces shown in A, showing $[Ca^{2+}]_i$ changes in female wild-type corticotrophs with stimuli. Black line shows response to 0.2 nM CRH (starting at 15 min), grey line shows response to 2 nM AVP (starting at 40 min), and blue line shows response to the combined stimulus (starting at 65 min).

## Figure 3.43

### AVP, CRH and CRH/AVP induce $[Ca^{2+}]_i$ responses in female wild-type corticotrophs

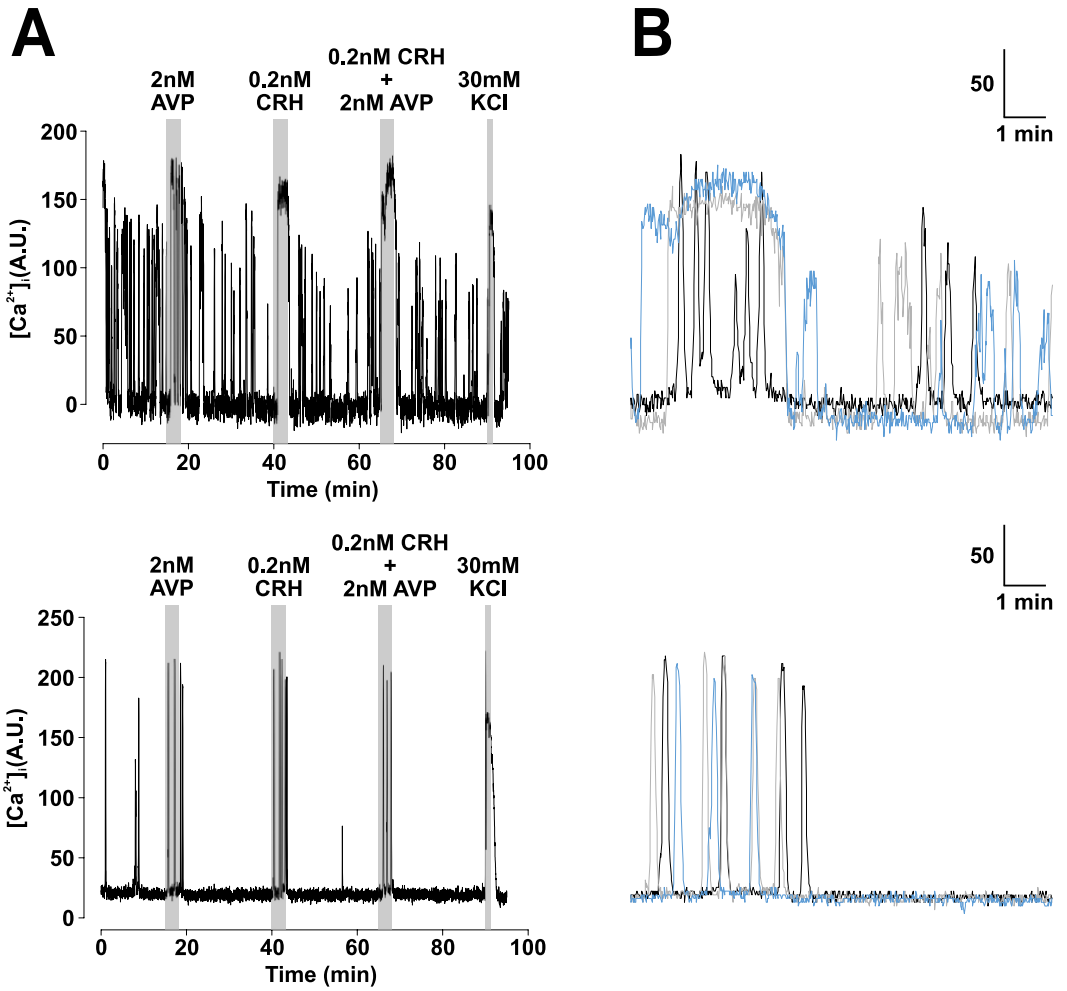


**Figure 3.43 AVP, CRH and CRH/AVP induce $[Ca^{2+}]_i$ responses in female wild-type corticotrophs. (A)** Representative calcium imaging traces of female wild-type corticotrophs exposed to 2 nM AVP, 0.2 nM CRH and 0.2 nM CRH together with 2 nM AVP at 25 minutes intervals. 30 mM potassium chloride was applied at the end for one minute. **(B)** Superposition of extracts of the two traces shown in A, showing $[Ca^{2+}]_i$ changes in female wild-type corticotrophs with stimuli. Black line shows response to 2 nM AVP (starting at 15 min), grey line shows response to 0.2 nM CRH (starting at 40 min), and blue line shows response to the combined stimulus (starting at 65 min).

AUC (peak) but not AUC (10 min) of the combined stimulus was larger than the sum of the two single stimuli. Peak, time to peak, response duration (Figure 3.45) and peak duration (Figure 3.46A) were not significantly different among CRH-, AVP- and CRH/AVP-induced $[Ca^{2+}]_i$ responses. Stimulation with AVP showed a significantly longer time gap compared to CRH stimulus ($p < 0.01$) and the combined stimulus ($p < 0.001$) (Figure 3.46A).

These results suggested that there was no synergistic $[Ca^{2+}]_i$ response between CRH and AVP in female wild-type corticotrophs at the level of population, however, a proportion of corticotrophs (26.7%) showed synergistic $[Ca^{2+}]_i$ response at the level of single cell. AVP-induced significantly smaller AUC (10 min) and AUC (peak) but longer time gap compared to CRH stimulus and the combined stimulus.

#### 3.2.5.3 CRH/AVP-induced $[Ca^{2+}]_i$ responses are not significantly different between male and female wild-type corticotrophs

Although no synergistic $[Ca^{2+}]_i$ responses between CRH and AVP were observed in either male or female wild-type corticotrophs at the population level, we investigated whether there were differences between male and female wild-type corticotrophs.

## Figure 3.44

**No synergistic $[Ca^{2+}]_i$ response between CRH and AVP in female wild-type corticotrophs**

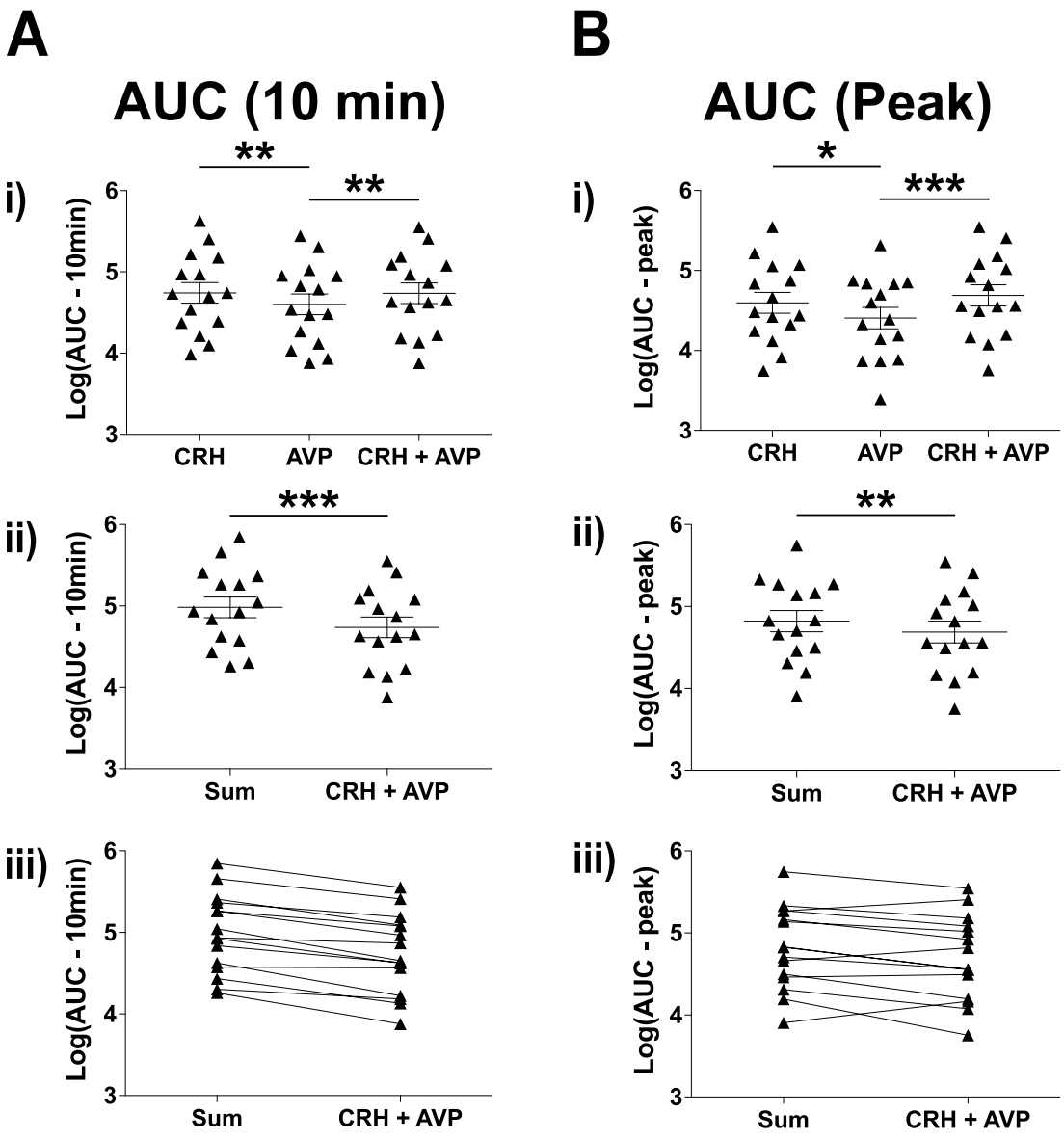


**Figure 3.44 No synergistic $[Ca^{2+}]_i$ response between CRH and AVP in female wild-type corticotrophs.** Quantification of effects of exposure to 0.2 nM CRH, 2 nM AVP and the combination of the two in **(A)** AUC (10 min) and **(B)** AUC (peak). The comparison of the AUC of the combined stimulus and the sum of the two single stimuli was used as a measurement of synergy. * $p < 0.05$, ** $p < 0.01$ and *** $p < 0.001$ ($n = 15$ from 5 experiments, mixed effects model). All data are means ± SEM.

## Figure 3.45

### Peak, time to peak and response duration of $[Ca^{2+}]_i$ responses to CRH, AVP and CRH/AVP in female wild-type corticotrophs

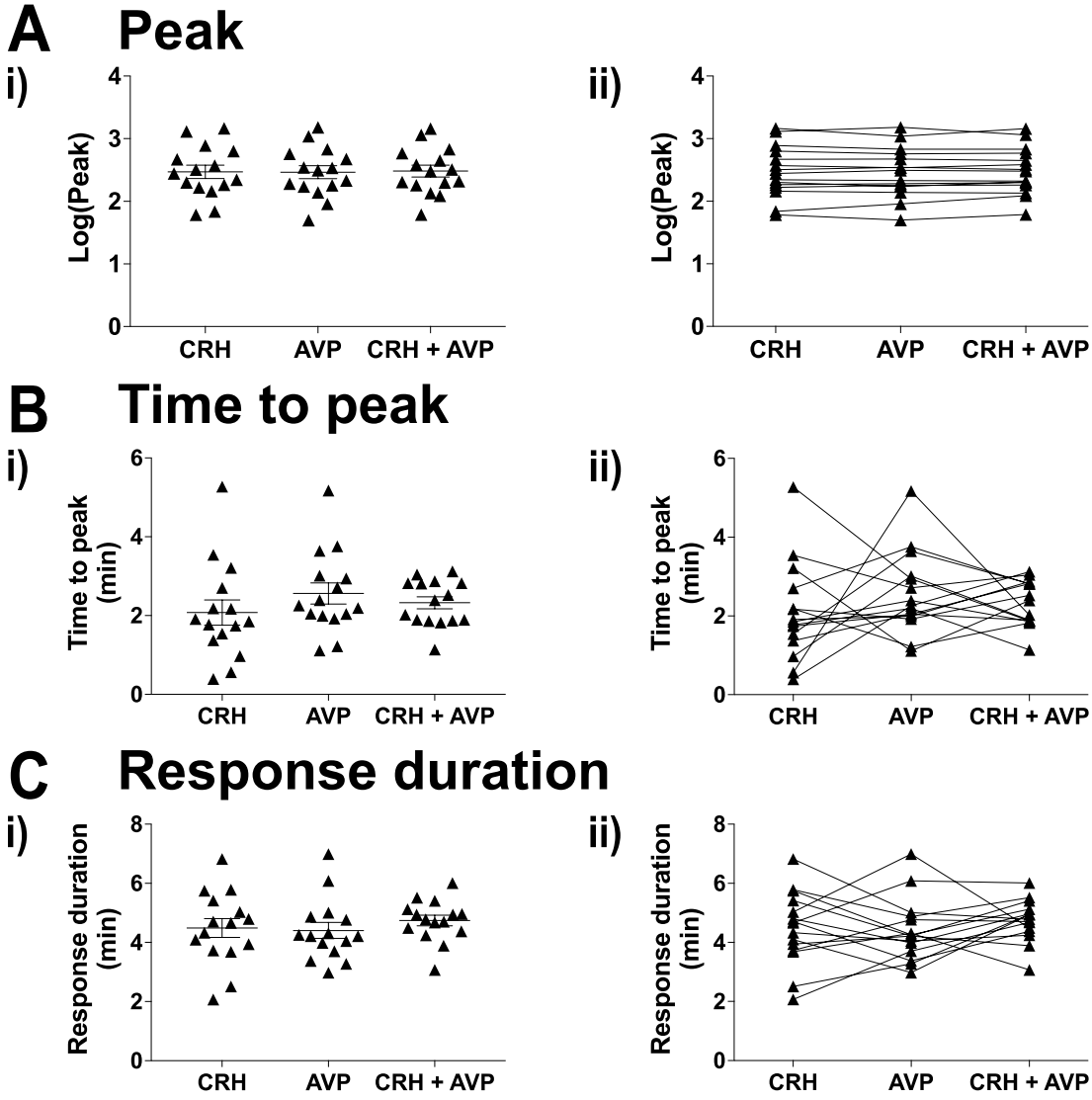


**Figure 3.45 Peak, time to peak and response duration of $[Ca^{2+}]_i$ responses to CRH, AVP and CRH/AVP in female wild-type corticotrophs.** Quantification of effects of exposure to 0.2 nM CRH, 2 nM AVP and the combination of the two in **(A)** peak, **(B)** time to peak and **(C)** response duration (n = 15 from 5 experiments, mixed effects model). All data are means ± SEM.

## Figure 3.46

### AVP induces longer time gap but not peak duration of $[Ca^{2+}]_i$ response in female wild-type corticotrophs

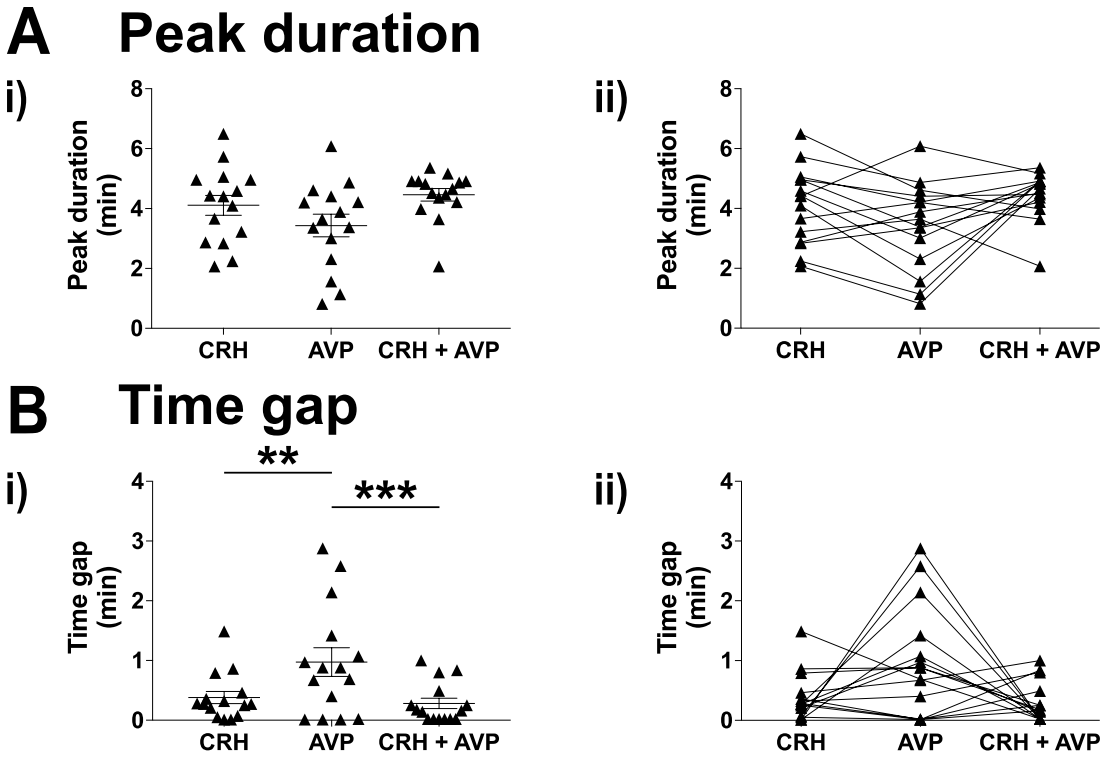


**Figure 3.46 AVP induces longer time gap but not peak duration of $[Ca^{2+}]_i$ responses in female wild-type corticotrophs.** Quantification of effects of exposure to 0.2 nM CRH, 2 nM AVP and the combination of the two in **(A)** peak duration and **(B)** time gap. ** $p < 0.01$ and *** $p < 0.001$ ($n = 15$ from 5 experiments, mixed effects model). All data are means ± SEM.

Statistical analysis revealed that there were no significant differences between male and female wild-type corticotrophs in AUC (10 min) and AUC (peak), although female corticotrophs tended to have higher variability (Figure 3.47). Peak, time to peak, response duration and peak duration failed to show any significant sex difference either (Figure 3.48). Male corticotrophs displayed longer mean time gap following two single stimuli and the combined stimulus compared to females with statistical analysis approaching significance ($p = 0.08$) (Figure 3.49).

In summary, there were no statistically significant differences between male and female wild-type corticotrophs in $[Ca^{2+}]_i$ responses induced by CRH, AVP and the combination of the two.

## Figure 3.47

**No significant sex difference in AUC (10 min) or AUC (peak) of $[Ca^{2+}]_i$ responses to CRH, AVP and CRH/AVP in wild-type corticotrophs**

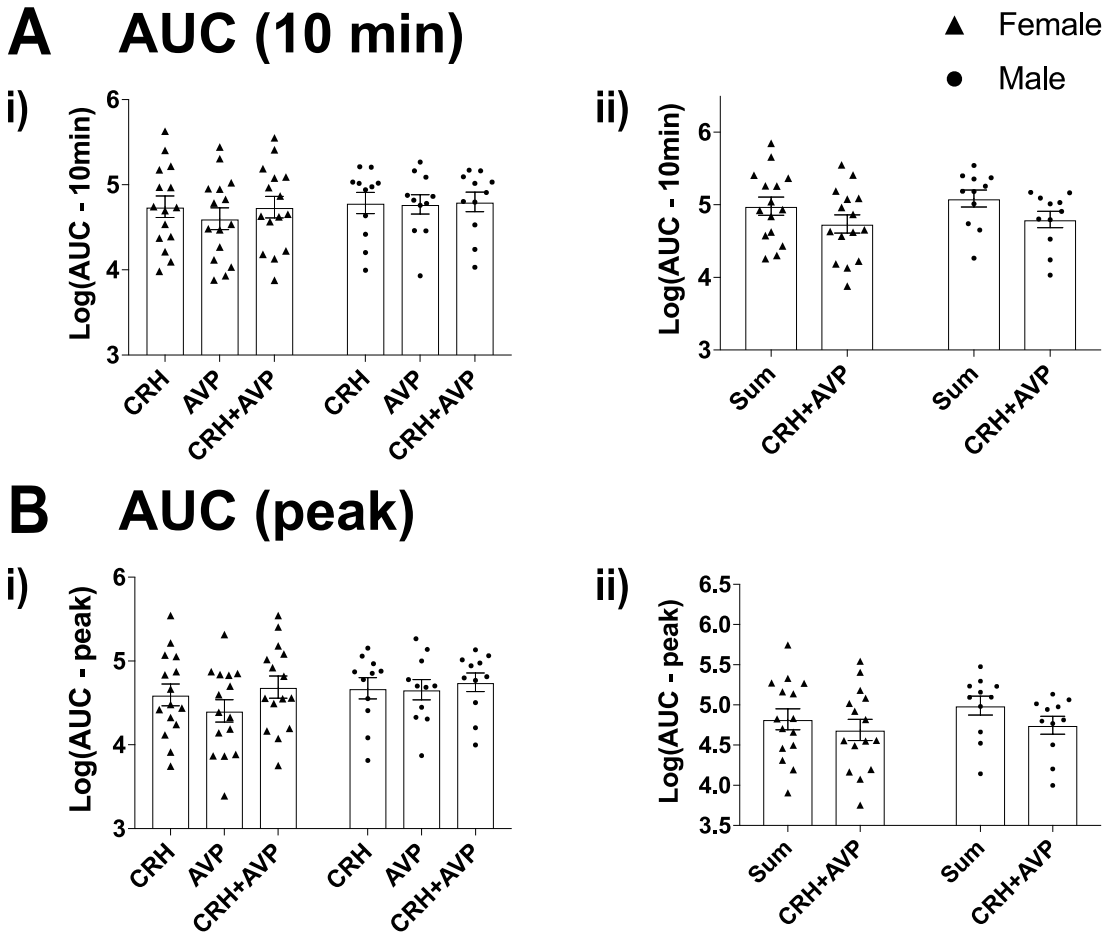


**Figure 3.47 No significant sex difference in AUC (10 min) or AUC (peak) of $[Ca^{2+}]_i$ responses to CRH, AVP and CRH/AVP in wild-type corticotrophs.** Quantification of effects of exposure to 0.2 nM CRH, 2 nM AVP and the combination of the two in **(A)** AUC (10 min) and **(B)** AUC (peak) (male n = 11 from 6 experiments, female n = 15 from 5 experiments, mixed effects model). All data are means ± SEM.

## Figure 3.48

**No significant sex difference in peak, time to peak, response duration or peak duration of $[Ca^{2+}]_i$ responses to CRH, AVP and CRH/AVP in wild-type corticotrophs**

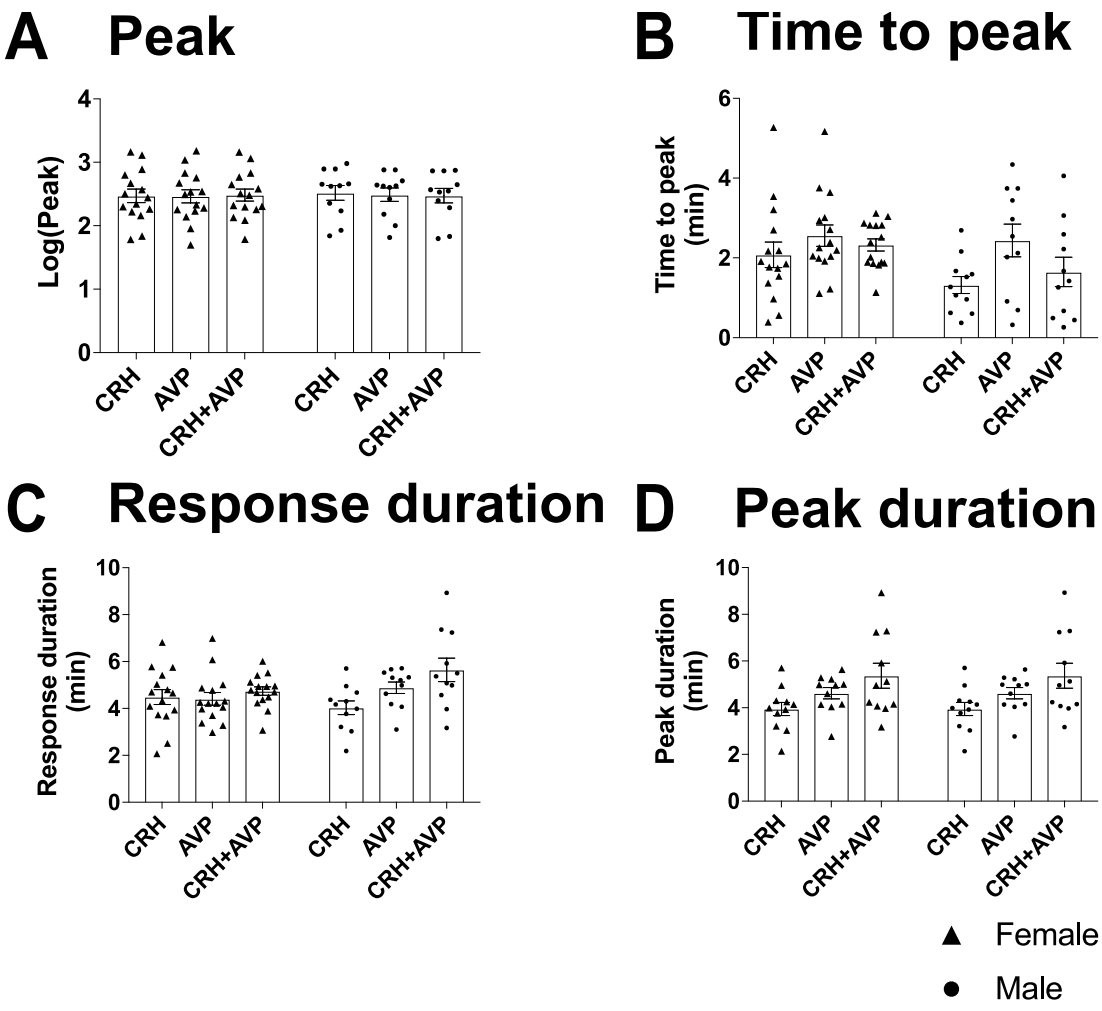


**Figure 3.48 No significant sex difference in peak, time to peak, response duration or peak duration of $[Ca^{2+}]_i$ responses to CRH, AVP and CRH/AVP in wild-type corticotrophs.** Quantification of effects of exposure to 0.2 nM CRH, 2 nM AVP and the combination of the two in **(A)** peak, **(B)** time to peak, **(C)** response duration and **(D)** peak duration (male n = 11 from 6 experiments, female n = 15 from 5 experiments, mixed effects model). All data are means ± SEM.

# Figure 3.49

## No significant sex difference in time gap of $[Ca^{2+}]_i$ responses to CRH, AVP and CRH/AVP in wild-type corticotrophs

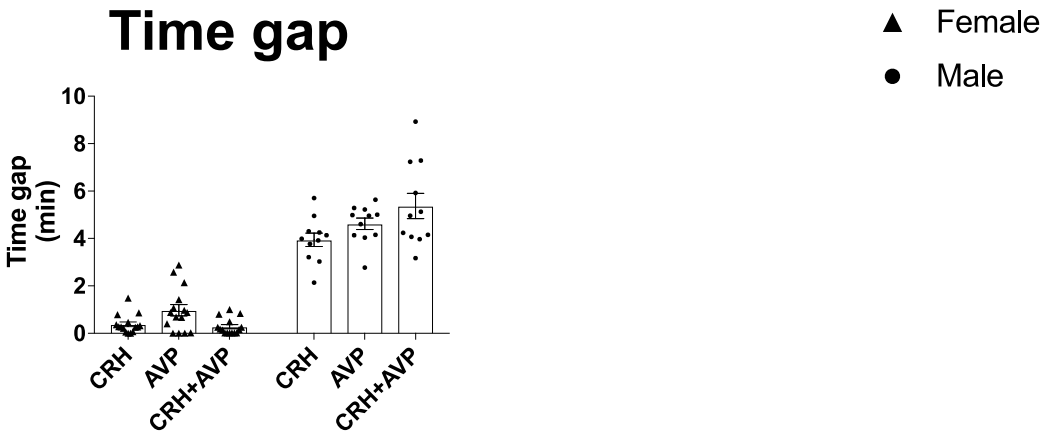


**Figure 3.49 No significant sex difference in time gap of $[Ca^{2+}]_i$ responses to CRH, AVP and CRH/AVP in wild-type corticotrophs.** Quantification of effects of exposure to 0.2 nM CRH, 2 nM AVP and the combination of the two in time gap (male n = 11 from 6 experiments, female n = 15 from 5 experiments, mixed effects model). All data are means ± SEM.

## 3.3 Discussion

In this chapter, I exploited a genetic approach for expression of the GCaMP6s calcium sensor specifically in murine anterior pituitary corticotrophs by using lentiviral driven expression under the control of a minimal rat *Pomc* promoter. This allowed robust real-time identification of murine corticotrophs and examination of spontaneous, CRH- and AVP-induced $[Ca^{2+}]_i$ responses in murine corticotrophs. Importantly, these studies allowed robust and repeatable $[Ca^{2+}]_i$ responses to pulses of secretagogues at physiological concentrations with frequency of pulses similar to those reported *in vivo*. Wild-type corticotrophs displayed robust and sustained $[Ca^{2+}]_i$ responses to CRH, whereas AVP evoked two patterns of $[Ca^{2+}]_i$ responses, sustained elevation and oscillatory behaviour. The $[Ca^{2+}]_i$ responses to CRH and AVP were similar in male and female wild-type corticotrophs whereas spontaneous $[Ca^{2+}]_i$ signalling was significantly higher in male corticotrophs. Although synergistic $[Ca^{2+}]_i$ responses was observed in a small proportion of corticotrophs from female wild-type mice, synergy was not observed in males. This characterisation provides a platform to further interrogate the regulation of $[Ca^{2+}]_i$ signalling in murine corticotrophs as addressed in Chapter Four and Chapter Five.

### 3.3.1 Specific labelling of murine corticotrophs and spontaneous $[Ca^{2+}]_i$ in wild-type murine corticotrophs

By using lentiviral-mediated transduction of isolated mouse anterior pituitary cultures, the genetically encoded calcium indicator GCaMP6s was expressed under the control of a minimal rat *Pomc* promoter. This allowed labelling of live corticotrophs with 83% specificity and 53% efficiency as determined by co-localisation with ACTH. Importantly, in all analysed corticotrophs *a priori* identification of corticotrophs using POMC-GCaMP6s responded to CRH and/or AVP suggesting that the specificity of labelling likely represent an underestimate in the immunohistochemical analysis. Indeed, previous studies from the Shipston laboratory, expressing eYFP under the control of the same minimal promoter revealed a specificity greater than 99.5%. Importantly, lentiviral expression has no significant effect on basal or secretaogue-evoked ACTH secretion or electrical properties (Liang *et al.*, 2011) supporting that lentiviral mediated-transduction has no significant effect on corticotroph viability or physiology. Thus, this approach could be used to target corticotrophs *in vitro* for calcium imaging experiments.

To determine spontaneous $[Ca^{2+}]_i$ signalling, a "15% threshold" method was used to define whether the corticotrophs were active or silent over the five minute period of "baseline" recording before exposure to any secretagogue. This is important as the vast

majority of previous studies on corticotrophs have used high concentrations of secretagogues to isolate and/or identify cells prior to analysis. Calcium imaging experiments performed in this PhD revealed that the vast majority (> 95%) of mouse corticotrophs displayed spontaneous $[Ca^{2+}]_i$ signalling while only a small proportion of them was absolutely silent. This was different from previous studies on male rat pituitary corticotrophs where only 30% of cells showed spontaneous $[Ca^{2+}]_i$ transients (Romanò *et al.*, 2017). Spontaneous $[Ca^{2+}]_i$ signalling in murine corticotrophs were highly variable between cells and all spontaneously active corticotrophs could be classified into three categories: high or low frequency of $[Ca^{2+}]_i$ oscillation, sustained elevation of $[Ca^{2+}]_i$ as well as low amplitude and complex patterns of $[Ca^{2+}]_i$ changes that was only seen in a small proportion of cells (< 5%). Importantly, all patterns of spontaneous $[Ca^{2+}]_i$ signalling were found in both female and male wild-type corticotrophs. However, the distribution and mean of spontaneous active time in male wild-type corticotrophs were significantly ($p < 0.01$) higher compared to females, although the maximum amplitude of spontaneous $[Ca^{2+}]_i$ signalling was not significantly different between male and female corticotrophs. Whether the variety of spontaneous $[Ca^{2+}]_i$ signalling that could be categorized into subtypes suggest potential distinct subpopulation of corticotrophs or reflect stochastic variability in corticotrophs behaviour is not known. To address this, an approach would be to analyse corticotroph $[Ca^{2+}]_i$ responses in pituitary slices instead of pituitary cultures to

compare $[Ca^{2+}]_i$ signalling of corticotrophs from different regions of the anterior pituitary gland to determine whether there is heterogeneity of corticotroph behaviour when in a network of cells.

### 3.3.2 CRH induces sustained $[Ca^{2+}]_i$ increase in wild-type corticotrophs

Following three minutes of 0.2 nM CRH stimulation, wild-type corticotrophs responded with a significant and rapid sustained elevation of global $[Ca^{2+}]_i$ signalling that continued for several minutes even after the removal of secretagogue. Importantly, the majority of analysed parameters were stable with repeated exposure to CRH in both male and female corticotrophs although there was a significant decrease in peak of $[Ca^{2+}]_i$ responses in corticotrophs from both sexes by the third pulse. In addition, there were no significant differences in CRH-induced $[Ca^{2+}]_i$ responses between male and female wild-type corticotrophs. L-type calcium channel blocker nifedipine largely abolished both spontaneous $[Ca^{2+}]_i$ and CRH-evoked $[Ca^{2+}]_i$ responses in male wild-type corticotrophs suggesting that these $[Ca^{2+}]_i$ responses were driven predominantly by an influx of extracellular calcium as previously reported (Guérineau *et al.*, 1991; Kuryshev *et al.*, 1996; Romanò *et al.*, 2017).

### 3.3.3 AVP induces two patterns of $[Ca^{2+}]_i$ responses

Wild-type corticotrophs stimulated with a 2 nM AVP pulse for three minutes exhibited two phenotypes of $[Ca^{2+}]_i$ responses: sustained elevation of $[Ca^{2+}]_i$ for several minutes, similar to that observed with CRH stimulation, and oscillatory $[Ca^{2+}]_i$ behaviour accompanied with increased amplitude of $[Ca^{2+}]_i$ "oscillations". Importantly, these distinct patterns were deterministic — in the same corticotroph repeated exposure to AVP always produced the same $[Ca^{2+}]_i$ response phenotype.

AVP-induced increases in $[Ca^{2+}]_i$ is dependent on two mechanisms: calcium released from $IP_3$-regulated internal stores and influx through L-type calcium channels. In pituitary corticotrophs, AVP activates V1b G-protein-coupled membrane receptor that activates PLC, leading to the increase of $IP_3$ and the formation of DAG with subsequent activation of PKC (Antoni, 1993; Corcuff *et al.*, 1993; Stojilkovic *et al.*, 2010). Most previous studies have used AVP at supraphysiological (10–100 nM) and reported a biphasic pattern of $[Ca^{2+}]_i$ response (transient and plateau phase) in corticotrophs with $IP_3$-mediated $[Ca^{2+}]_i$ release controlling the transient phase and $Ca^{2+}$ entry though voltage-gated calcium channel (VGCC) required for the plateau phase of AVP-induced $Ca^{2+}$ signal (Tse & Lee, 1998). The AVP-induced oscillatory $[Ca^{2+}]_i$ response reported in this Thesis is reminiscent of GnRH-evoked $[Ca^{2+}]_i$ responses in pituitary gonadotrophs dependent upon release of $Ca^{2+}$ from $IP_3$-sensitive calcium

stores (Tse & Hille, 1992; Stojilkovic, 2012). Further studies to interrogate the relative contribution of $Ca^{2+}$ influx via VGCC versus $IP_3$-mediated $[Ca^{2+}]_i$ release are required, for example using pharmacological inhibitors to address this issue. Furthermore, whether these distinct phenotypes reflect different subpopulations of corticotrophs or reflect variations in the size of the intracellular $IP_3$-sensetive calcium store between corticotrophs remains to be determined.

### 3.3.4 Lack of synergistic $[Ca^{2+}]_i$ responses to CRH and AVP

In corticotrophs, CRH acts in synergy with AVP to increase the secretion of ACTH. This synergy has been considered to occur at multiple levels of the CRH- and AVP-signalling pathways. For example, at the level of second messenger, cAMP accumulation induced by CRH via CRHR1 receptor is potentiated by AVP likely though the regulation of a $Ca^{2+}$ dependent adenylate cyclase and control of phosphodiesterase activity (Abou-Samra *et al.*, 1987; Stojilkovic *et al.*, 2010; Antoni, 2012). In addition, the synergy between CRH and AVP may involve the molecular interaction (heterodimerization) between CRHR1 and V1b receptors (Murat *et al.*, 2012). However, whether synergy occurs at the level of $[Ca^{2+}]_i$ is largely unexplored. The ability to expose corticotrophs to repeated pulses of secretagogue allowed me to directly test if synergy also occurs at the level of $[Ca^{2+}]_i$. Calcium imaging data showed that a three minute exposure of CRH/AVP resulted in a rapid and significant sustained

increase of $[Ca^{2+}]_i$ for several minutes. No significant synergistic $[Ca^{2+}]_i$ response was observed between CRH and AVP in any male wild-type corticotroph. Although there was no significant synergistic $[Ca^{2+}]_i$ response in female wild-type corticotrophs at the population level, 26.7% (4 out of 15 cells) of single corticotrophs displayed synergistic $[Ca^{2+}]_i$ responses to CRH and AVP stimulation. A recent study reported similar results that no synergistic $[Ca^{2+}]_i$ response was seen at the population level, however, ~ 30% of male rat corticotrophs examined showed synergy to CRH and AVP at the level of single cells (Romanò *et al.*, 2017). There were no significant differences between male and female wild-type corticotrophs in $[Ca^{2+}]_i$ responses induced by CRH, AVP and the combination of the two either.

These results showed that there was no significant synergistic $[Ca^{2+}]_i$ response to CRH and AVP at the population level in either male or female wild-type corticotrophs, but 26.7% of female corticotrophs elicited synergistic $[Ca^{2+}]_i$ responses. Again, whether this proportion of corticotrophs that display synergy represents a distinct population or reflects variation in signalling pathways remains to be addressed.

## 3.4 Chapter summary

A lentiviral-mediated POMC-GCaMP6s transduction was developed to identify and label mouse anterior pituitary corticotrophs *in vitro*. Wild-type corticotrophs showed

highly variable spontaneous $[Ca^{2+}]_i$ signalling that probably suggest the existence of potential subpopulation of corticotrophs. CRH induced sustained and significant elevation of $[Ca^{2+}]_i$ that is nifedipine-sensitive and depends on an influx of extracellular $Ca^{2+}$. In particular, repeated CRH stimulation evoked robust and repeatable $[Ca^{2+}]_i$ responses which had a reduction in peak of $[Ca^{2+}]_i$ responses and no significant sex differences were observed. Stimulation with AVP resulted in two phenotypes of $[Ca^{2+}]_i$ response: sustained elevation of $[Ca^{2+}]_i$ and oscillatory $[Ca^{2+}]_i$ behaviour. Repeated AVP stimulation evoked highly reproducible and deterministic $[Ca^{2+}]_i$ responses in both male and female wild-type corticotrophs, although male wild-type corticotrophs had longer response duration compared to females. There were no significant synergistic $[Ca^{2+}]_i$ responses to CRH and AVP in either male or female wild-type corticotrophs.

# Chapter Four:

# Calcium signalling in BK-KO corticotrophs

# Chapter 4: Calcium signalling in BK-KO corticotrophs

## 4.1 Introduction

In this chapter, the aim was to investigate the role of large conductance calcium- and voltage-activated potassium (BK) channels in regulating intracellular free calcium ($[Ca^{2+}]_i$) responses in corticotrophs. Calcium imaging recordings were first obtained from male and female BK channel knockout (BK-KO) corticotrophs respectively to determine the role of BK channels in spontaneous $[Ca^{2+}]_i$ signalling, CRH- or AVP-induced elevation of $[Ca^{2+}]_i$ as well as the synergy between CRH and AVP in corticotrophs. Secondly, the experiments were designed to examine whether pharmacological blockade of BK channels with the specific BK channel blocker paxilline had similar effect as genetic deletion of BK channels in corticotrophs.

### 4.1.1 BK channels regulate corticotroph activity

Previous investigation of the role of BK channels in the regulation of the HPA axis indicated that, compared to wild-type mice, plasma ACTH and corticosterone are significantly decreased in female BK channel knockout mice following acute restraint stress (Brunton *et al.*, 2007). These studies, using mice with a global deletion of BK channels revealed that this stress hyporespensiveness is likely a result of changes in

properties at multiple levels of the HPA axis. Importantly, recent *in vitro* studies in male murine corticotrophs revealed that the CRH-dependent transition from action potential spiking to bursting is dependent on functional BK channels, whereas AVP promotes an increase in spiking frequency alone via a BK-independent pathway (Duncan *et al.*, 2015; Fletcher *et al.*, 2017).

Interestingly, a shift of firing patterns from spiking to plateau-bursting in gonadotrophs has been implicated in triggering luteinizing hormone secretion (Van Goor *et al.*, 2001*b*). Bursting behaviour is suggested to be more capable of driving the influx of extracellular $Ca^{2+}$ than spiking, which is believed to result in a higher level of $[Ca^{2+}]_i$ to drive hormone secretion (Van Goor *et al.*, 2001*b*; Stojilkovic *et al.*, 2005). However, recent modelling studies revealed that the pattern of spiking activity can also result in highly efficient global calcium signalling (Tagliavini *et al.*, 2016). The patterns of $Ca^{2+}$ entry driven by action potentials and their relationships are likely to be important for ACTH secretion.

In this chapter, calcium imaging experiments were performed to determine the role of BK channels in regulating spontaneous $[Ca^{2+}]_i$ and CRH- or AVP-evoked $[Ca^{2+}]_i$ signalling in corticotrophs with both genetic and pharmacological approaches. We hypothesised that corticotrophs isolated from BK-KO mice would show an attenuated

$[Ca^{2+}]_i$ responses to CRH but not AVP, and this would be mimicked in wild-type corticotrophs treated with the specific BK channel blocker paxilline. As CRH and AVP did not display significant synergistic $[Ca^{2+}]_i$ responses in wild-type corticotrophs at the level of the population, we predicted that synergy would also be absent in BK-KO corticotrophs. All experiments were performed on corticotrophs isolated from BK-KO mice of both sexes according to the potential sexual dimorphism in response to stress.

## 4.2 Results

### 4.2.1 Genetic deletion of BK channels differentially controls spontaneous $[Ca^{2+}]_i$ signalling in male and female corticotrophs

To investigate the role of BK channels in regulating spontaneous $[Ca^{2+}]_i$ signalling, the basal $[Ca^{2+}]_i$ of corticotrophs isolated form BK-KO mice were continuously recorded for five minutes before exposure to secretagogues. The active time and maximum amplitude of spontaneous $[Ca^{2+}]_i$ signalling were analysed between sexes. Only data from BK-KO corticotrophs and the comparison between wild-type and BK-KO corticotrophs are presented in this chapter. The analysis of these data was done in conjunction with the analyses for Chapters Three and Five (see 2.6.3).The active time of spontaneous $[Ca^{2+}]_i$ signalling was 49.8 ± 3.6% when comparing all male and female corticotrophs with a skewed distribution to lower values (n = 71 cells from 29

experiments). Importantly, the active time was 32.1 ± 6.1% in male BK-KO corticotrophs (n = 18 from 12 experiments), which was significantly lower ($p < 0.01$) than female BK-KO corticotrophs with an active time of 55.8 ± 4.1% (n = 53 from 17 experiments) (Figure 4.1A&B). The distribution of spontaneous active time in male corticotrophs was significantly skewed to the left compared to female corticotrophs (Figure 4.1C&D).

Using the "15% threshold" definition revealed that 5.6% (4 out of 71 cells) of all BK-KO corticotrophs were silent during the basal recoding period, 47.9% of cells displayed oscillatory $[Ca^{2+}]_i$ behaviour, 32.4% of cells had sustained $[Ca^{2+}]_i$ elevation and the rest 10 out of 71 cells (14.1%) showed a low amplitude and complex pattern of calcium behaviour (Figure 4.3A). In female BK-KO corticotrophs, oscillatory $[Ca^{2+}]_i$ behaviour and sustained $[Ca^{2+}]_i$ elevation were 35.9% and 39.6% respectively. However, 72.2% of male BK-KO corticotrophs displayed oscillatory $[Ca^{2+}]_i$ behaviour and only 22.2% of cells showed sustained $[Ca^{2+}]_i$ elevation. In addition, no silent cells were found in male BK-KO corticotrophs. The differences between male and female BK-KO corticotrophs in spontaneous $[Ca^{2+}]_i$ signalling patterns might due to the relatively low number of male BK-KO corticotrophs analysed (n = 18). Next, the maximum amplitude of spontaneous $[Ca^{2+}]_i$ signalling between BK-KO corticotrophs was compared using normalized calcium imaging traces as before. The maximum

## Figure 4.1

### Spontaneous $[Ca^{2+}]_i$ active time is significantly higher in female than male in BK-KO corticotrophs

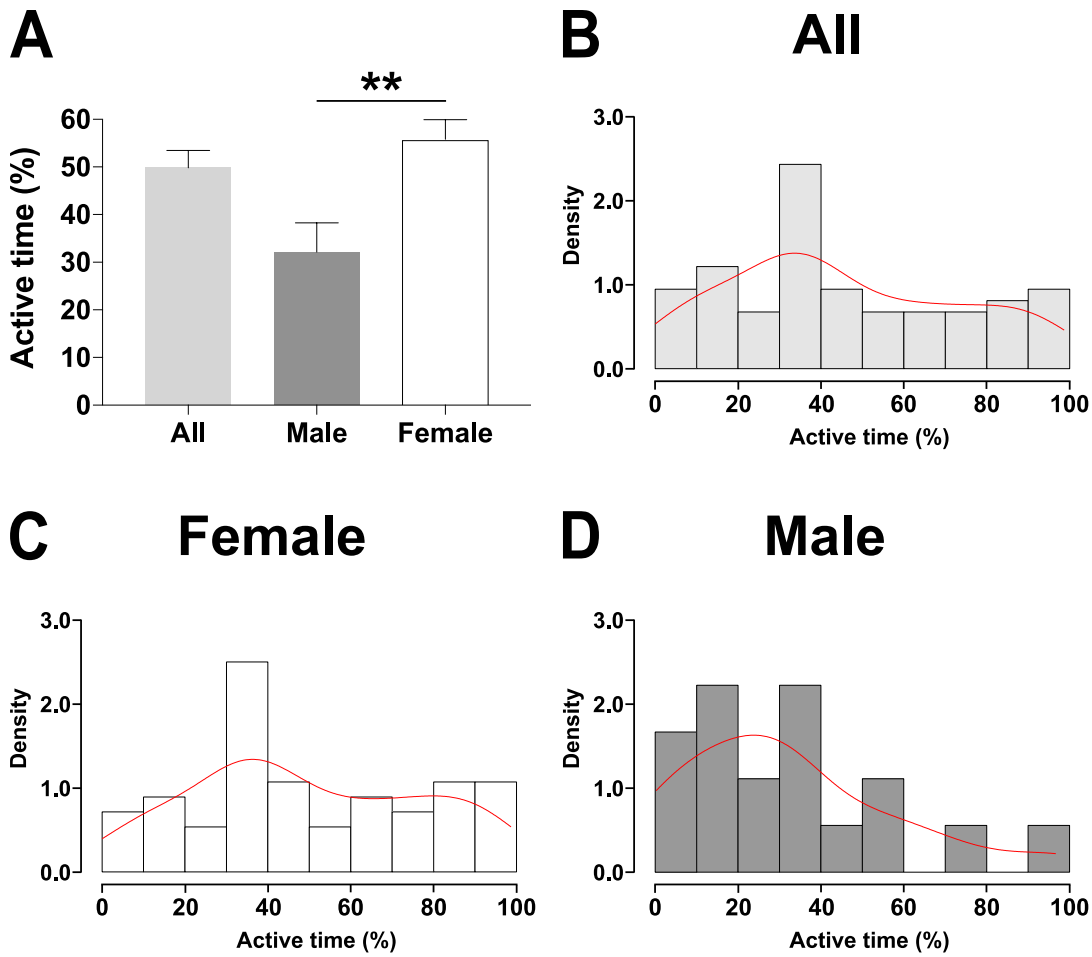


**Figure 4.1 Spontaneous $[Ca^{2+}]_i$ active time is significantly higher in female than male in BK-KO corticotrophs. (A)** The mean active time of spontaneous $[Ca^{2+}]_i$ signalling in all BK-KO corticotrophs. **(B)** The distribution of spontaneous $[Ca^{2+}]_i$ active time in all BK-KO corticotrophs. The distribution of spontaneous $[Ca^{2+}]_i$ active time in **(C)** female and **(D)** male BK-KO corticotrophs. ** $p < 0.01$ (female n = 53, male n = 18, mixed effects model). Red line indicates the fit of distribution density. All data are means ± SEM, N > 3 independent experiments.

amplitude of spontaneous $[Ca^{2+}]_i$ signalling in all BK-KO corticotrophs was 64.1 ± 3.0% (n = 71 from 29 experiments) showing a positive skewed distribution (Figure 4.2A&B). The spontaneous $[Ca^{2+}]_i$ signalling in female BK-KO corticotrophs had a maximum amplitude of 63.7 ± 3.6% (n = 53 from 17 experiments), which was not significantly different from male BK-KO corticotrophs with a maximum amplitude of 65.2 ± 5.2% (n = 18 from 12 experiments) (Figure 4.2A). The maximum amplitude displayed a highly positive skewed distribution in both male and female BK-KO corticotrophs (Figure 4.2C&D). These results demonstrated that there were no significant sex differences in maximum amplitude of spontaneous $[Ca^{2+}]_i$ signalling in BK-KO corticotrophs.

To determine the role of BK channels in spontaneous $[Ca^{2+}]_i$ signalling, statistical analysis was performed between wild-type and BK-KO corticotrophs for active time and maximum amplitude. When combining data from both male and female corticotrophs, the active time in wild-type corticotrophs was 45.2 ± 2.2% (n = 121 from 56 experiments) revealing no significant differences compared to BK-KO corticotrophs with the active time of 49.8 ± 3.6% (n = 71 from 29 experiments) (Figure 4.3B). There were no significant differences in maximum amplitude either (mean of 69.8 ± 1.5% in wild-type and 64.1 ± 3.0% in BK-KO corticotrophs respectively) (Figure 4.3C). However, compared to female wild-type corticotrophs, the spontaneous

## Figure 4.2

### The maximum amplitude of spontaneous $[Ca^{2+}]_i$ signalling is not different between male and female BK-KO corticotrophs

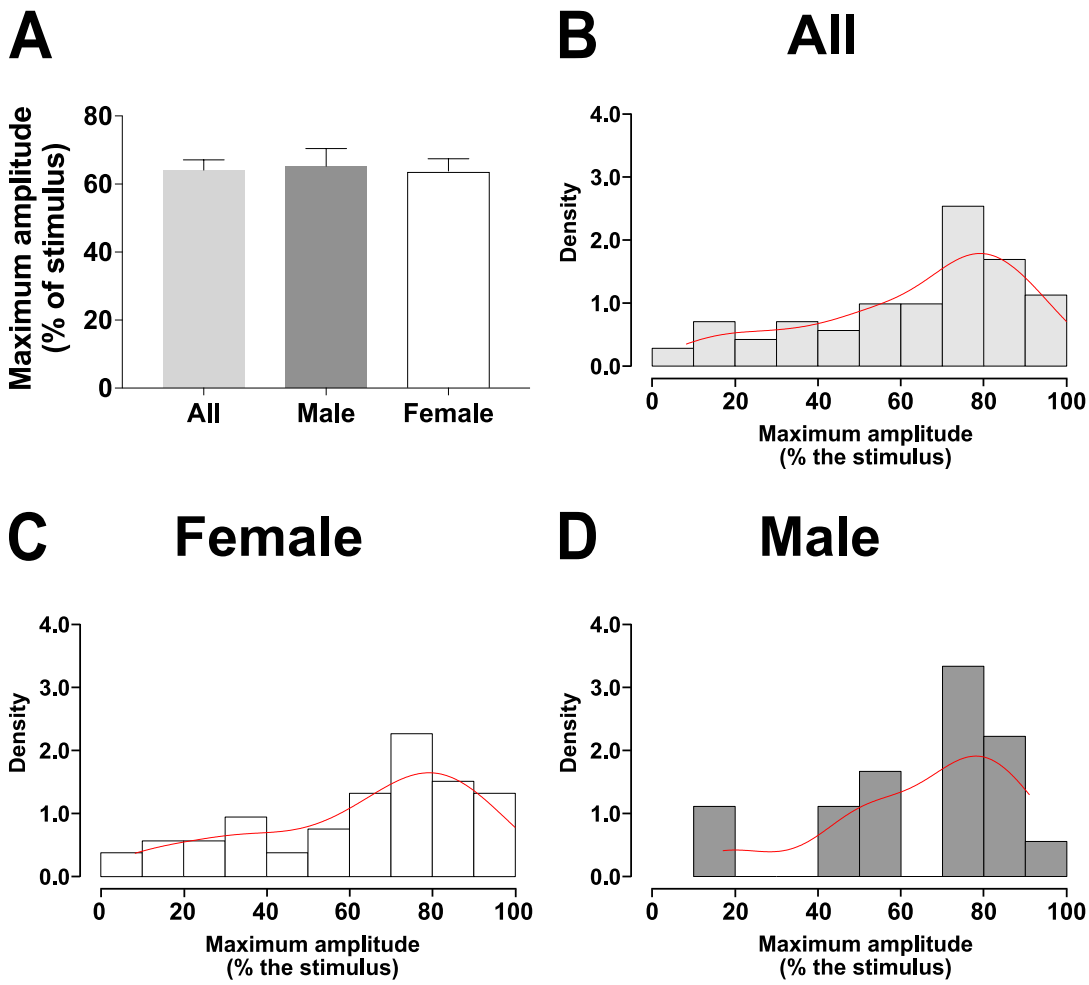


**Figure 4.2 The maximum amplitude of spontaneous $[Ca^{2+}]_i$ signalling is not different between male and female BK-KO corticotrophs. (A)** The mean maximum amplitude of spontaneous $[Ca^{2+}]_i$ signalling in all BK-KO corticotrophs. **(B)** The distribution of spontaneous $[Ca^{2+}]_i$ maximum amplitude in all BK-KO corticotrophs. The distributions of spontaneous $[Ca^{2+}]_i$ maximum amplitude in **(C)** female and **(D)** male BK-KO corticotrophs (female n = 53, male n = 31, mixed effects model). Red line indicates the fit of distribution density. All data are means ± SEM, N > 3 independent experiments.

## Figure 4.3

### Genetic deletion of BK channels results in an increase in spontaneous $[Ca^{2+}]_i$ active time in female corticotrophs

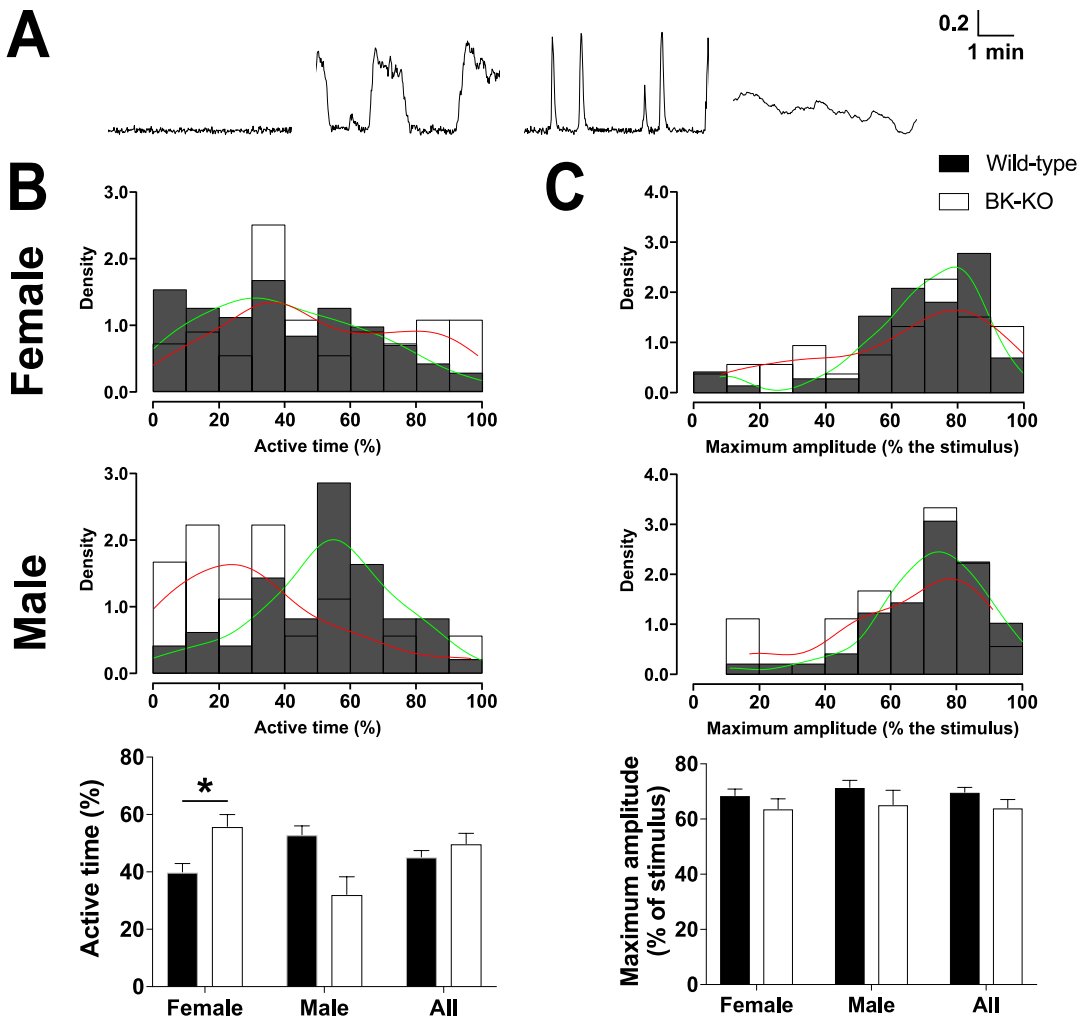


**Figure 4.3 Genetic deletion of BK channels results in an increase in spontaneous $[Ca^{2+}]_i$ active time in female corticotrophs. (A)** All patterns of spontaneous $[Ca^{2+}]_i$ signalling were seen in BK-KO corticotrophs. **(B)** The distribution and mean of spontaneous $[Ca^{2+}]_i$ active time in male and female wild-type and BK-KO corticotrophs. **(C)** The distribution and mean of spontaneous $[Ca^{2+}]_i$ maximum amplitude in male and female wild-type and BK-KO corticotrophs. * $p < 0.05$ (wild-type n = 121, BK-KO n = 71, mixed effects model). Green line and red line indicate the fit of distribution density of wild-type and BK-KO corticotrophs respectively. All data are means ± SEM, N > 3 independent experiments.

active time was significantly longer ($p < 0.05$) and distribution skewed to the right in female BK-KO corticotrophs, although there were no statistical differences in maximum amplitude. In contrast, male BK-KO corticotrophs showed a shorter active time that approach to significance ($p = 0.07$) with a distribution skewed to the left compared to wild-type. No significant difference were observed between them in maximum amplitude.

In conclusion, these results indicated sex differences in spontaneous $[Ca^{2+}]_i$ signalling in male and female BK-KO corticotrophs. Deletion of BK channels led to a significant increase in the active time of spontaneous $[Ca^{2+}]_i$ signalling in female corticotrophs, with the maximum amplitude of spontaneous $[Ca^{2+}]_i$ signalling independent of BK channels in both sexes.

### 4.2.2 CRH-induced $[Ca^{2+}]_i$ responses are suppressed in male but not female BK-KO corticotrophs

To address whether BK channels also play a role in CRH-evoked $[Ca^{2+}]_i$ responses, we characterised $[Ca^{2+}]_i$ responses to repeated CRH stimulation in male and female corticotrophs in which BK channels were genetically deleted.

#### 4.2.2.1 CRH-induced $[Ca^{2+}]_i$ responses are consistent in male BK-KO corticotrophs

Calcium imaging experiments were performed on male BK-KO corticotrophs (n = 12 from 8 experiments) using the same repeated stimulation protocol as for wild-type corticotrophs (see 3.2.3.1).

Upon repeated exposure to 0.2 nM CRH for three minutes, all corticotrophs displayed a rapid and significant $[Ca^{2+}]_i$ elevation that returned to the basal level a few minutes later. It's interesting to note that in 1 out of 12 cells (8.3%), CRH-induced oscillatory $[Ca^{2+}]_i$ behaviour, something that was never observed in male wild-type corticotrophs (Figure 4.4A). However, whether this reflects a potential effect of loss of BK channels cannot be determined due to the low numbers observed. Superposition of calcium imaging traces indicated consistent and robust changes in $[Ca^{2+}]_i$ in response to the three CRH exposures in male BK-KO corticotrophs (Figure 4.4B).

The effects of 0.2 nM CRH on $[Ca^{2+}]_i$ in male BK-KO corticotrophs were evaluated using the same parameters as for wild-type corticotrophs including AUC (10min), AUC (peak), peak, time to peak, response duration, peak duration and time gap. Log transformation was performed on AUC (10min), AUC (peak) and peak as before. Overall, there were no significant differences between three stimuli for AUC (10 min),

# Figure 4.4

## Repeated CRH induces $[Ca^{2+}]_i$ responses in male BK-KO corticotrophs

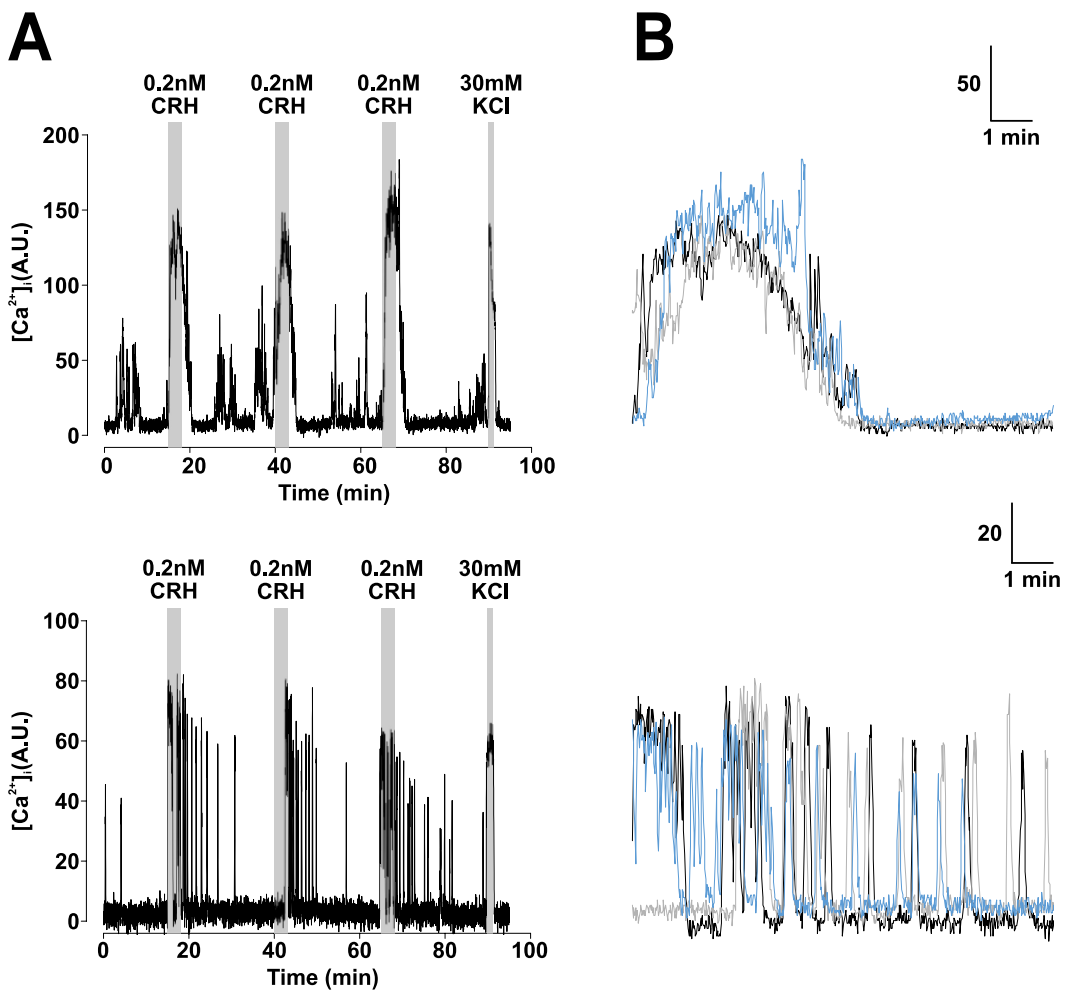


**Figure 4.4 Repeated CRH induces $[Ca^{2+}]_i$ responses in male BK-KO corticotrophs. (A)** Representative calcium imaging traces of male BK-KO corticotrophs exposed to 0.2 nM CRH for three minutes and repeated three times at 25 minutes intervals. 30 mM potassium chloride was applied at the end for one minute. **(B)** Superposition of extracts of the two traces shown in A, showing $[Ca^{2+}]_i$ changes in male BK-KO corticotrophs with repeated 0.2 nM CRH stimulation. Black line shows response to the first stimulus (starting at 15 min), grey line shows response to the second stimulus (starting at 40 min), and blue line shows response to the third stimulus (starting at 65 min).

AUC (peak) (Figure 4.5), peak, time to peak (Figure 4.6), response duration or peak duration (Figure 4.7). However, a significantly ($p < 0.05$) shorter time gap between Stimulus 2 and Stimulus 3 was observed (Figure 4.8).

These results suggest that the $[Ca^{2+}]_i$ responses are largely consistent upon repeated 0.2 nM CRH stimulation in male BK-KO corticotrophs.

#### 4.2.2.2 Attenuated AUC (peak) of $[Ca^{2+}]_i$ responses to repeated CRH stimulation in female BK-KO corticotrophs

Calcium imaging recordings were obtained from female BK-KO corticotrophs (n = 20 from 6 experiments) following the same experimental protocol used in male corticotrophs.

Similar to male BK-KO corticotrophs, two phenotypes of $[Ca^{2+}]_i$ responses were observed: 18 out of 20 cells (90.0%) showed sustained elevation of $[Ca^{2+}]_i$ (Figure 4.9A, top) and the other 2 cells (10.0%) exhibited oscillatory $[Ca^{2+}]_i$ behaviour (Figure 4.9A, bottom). As for male wild-type corticotrophs this oscillatory $[Ca^{2+}]_i$ response was never observed in female wild-type corticotrophs again suggesting BK channels may play a role in modulating the pattern of $[Ca^{2+}]_i$ dynamics. Two phenotypes of $[Ca^{2+}]_i$ responses were both repetitive upon repeated CRH stimulation in female

## Figure 4.5

### Stable AUC (10 min) and AUC (peak) $[Ca^{2+}]_i$ responses in male BK-KO corticotrophs to repeated CRH

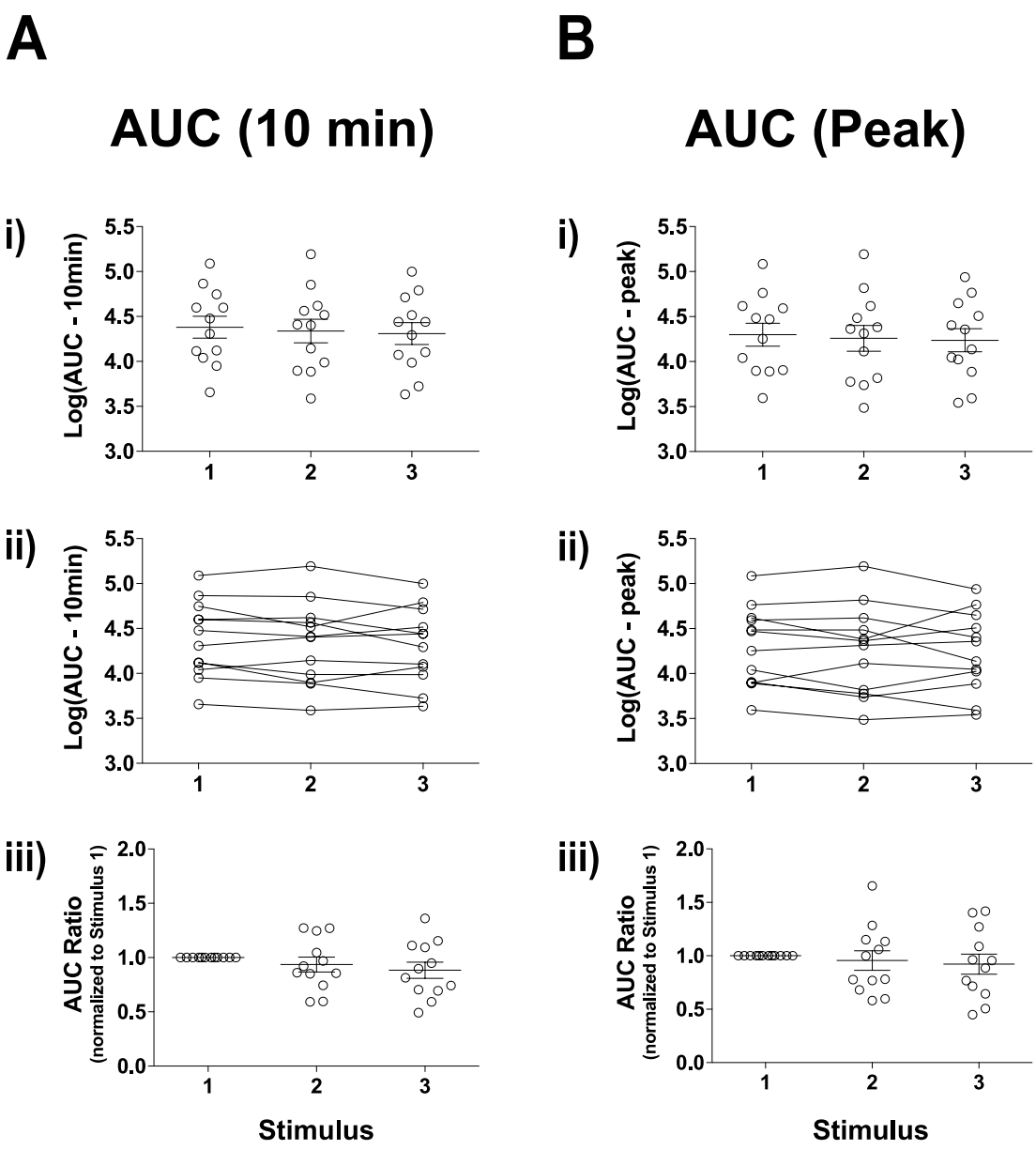


**Figure 4.5 Stable AUC (10 min) and AUC (peak) $[Ca^{2+}]_i$ responses in male BK-KO corticotrophs to repeated CRH.** Quantification of effects of repeated exposure to 0.2 nM CRH in **(A)** AUC (10 min) and **(B)** AUC (peak) (n = 12 from 8 experiments, mixed effects model). All data are means ± SEM.

## Figure 4.6

**Peak and time to peak of $[Ca^{2+}]_i$ responses in male BK-KO corticotrophs to repeated CRH**

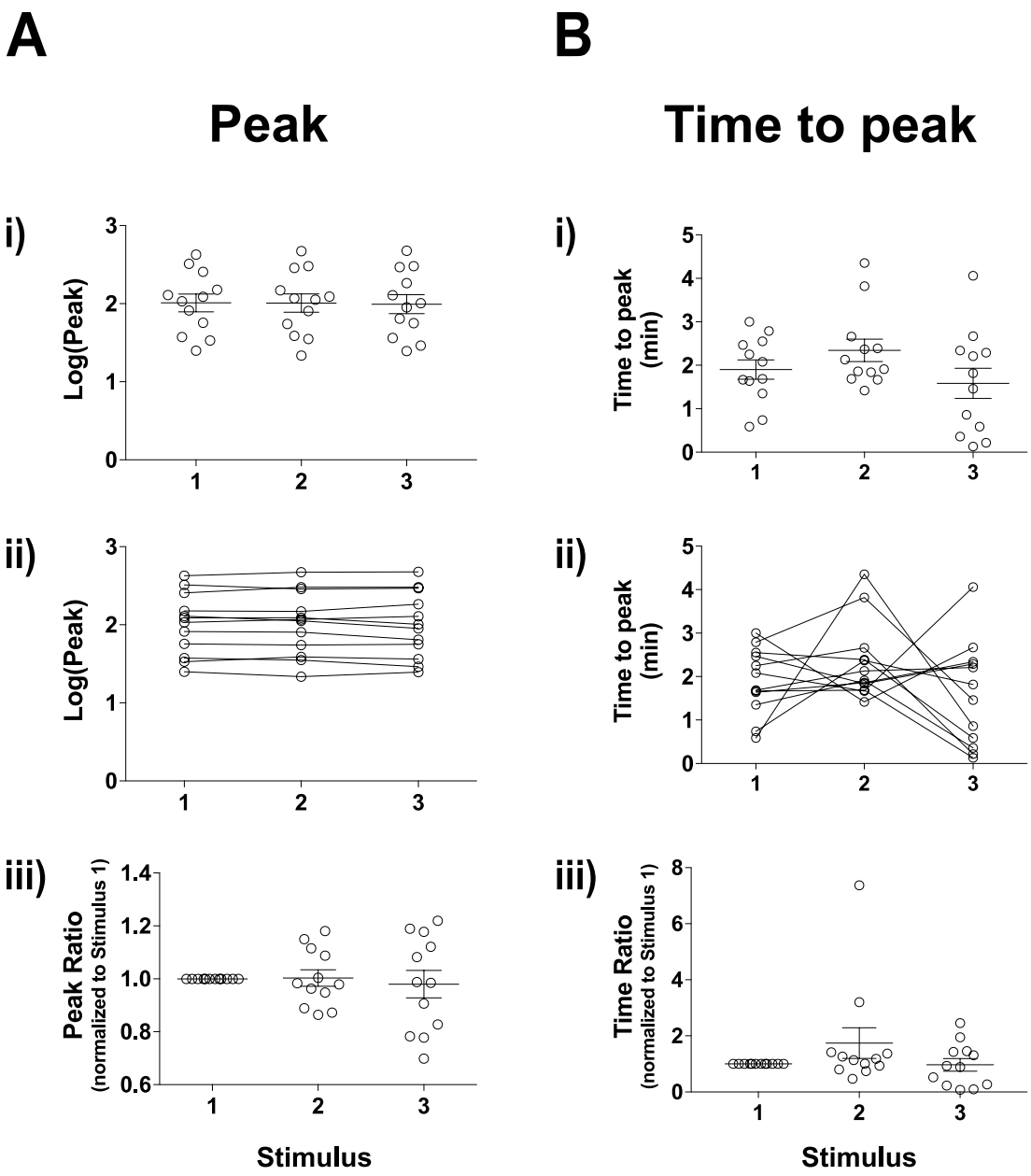


**Figure 4.6 Peak and time to peak of $[Ca^{2+}]_i$ responses in male BK-KO corticotrophs to repeated CRH.** Quantification of effects of repeated exposure to 0.2 nM CRH in **(A)** peak and **(B)** time to peak (n = 12 from 8 experiments, mixed effects model). All data are means ± SEM.

## Figure 4.7

### Response duration and peak duration of $[Ca^{2+}]_i$ responses in male BK-KO corticotrophs to repeated CRH

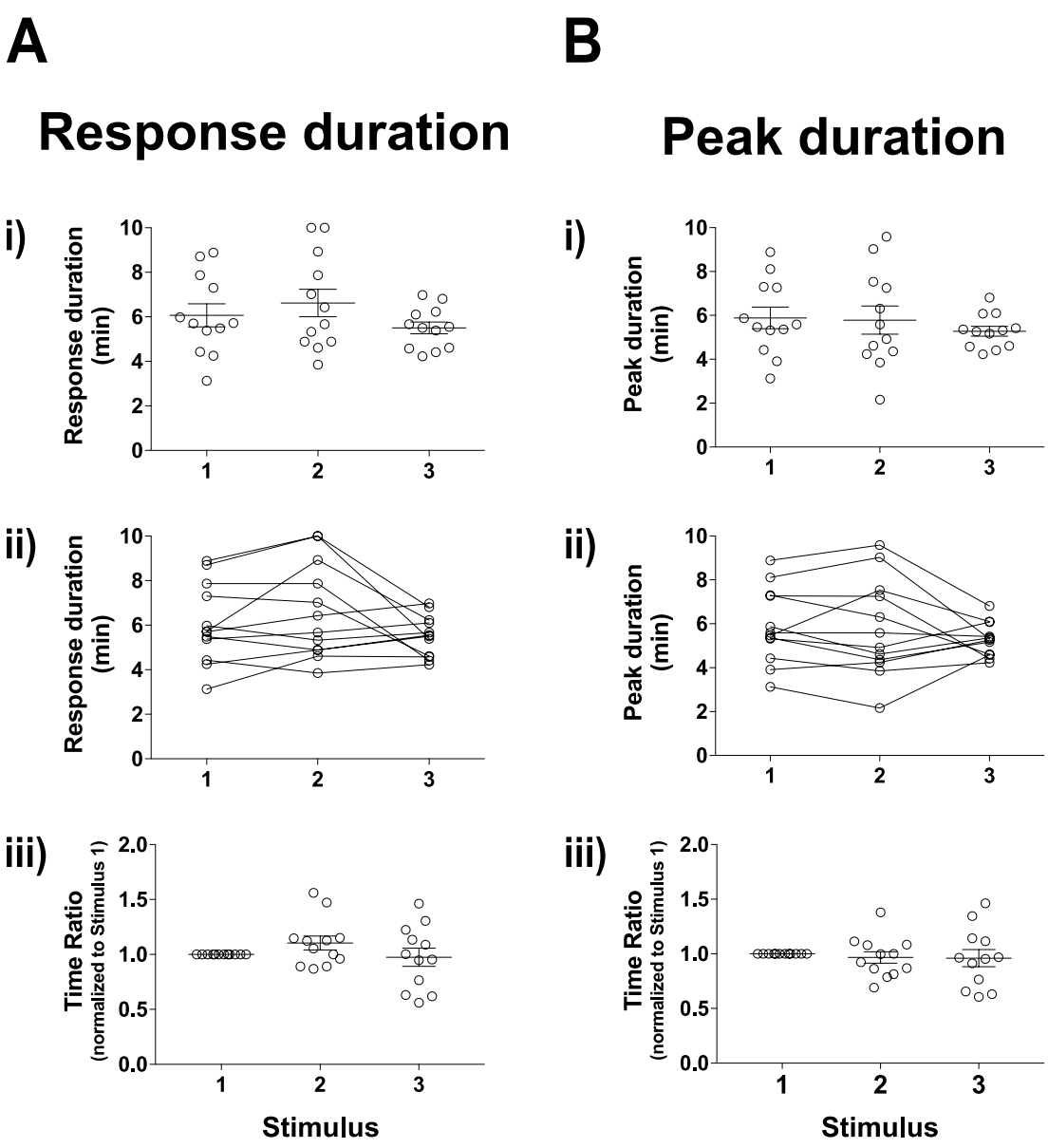


**Figure 4.7 Response duration and peak duration of $[Ca^{2+}]_i$ responses in male BK-KO corticotrophs to repeated CRH.** Quantification of effects of repeated exposure to 0.2 nM CRH in **(A)** response duration and **(B)** peak duration (n = 12 from 8 experiments, mixed effects model). All data are means ± SEM.

## Figure 4.8

### Time gap of $[Ca^{2+}]_i$ responses in male BK-KO corticotrophs to repeated CRH

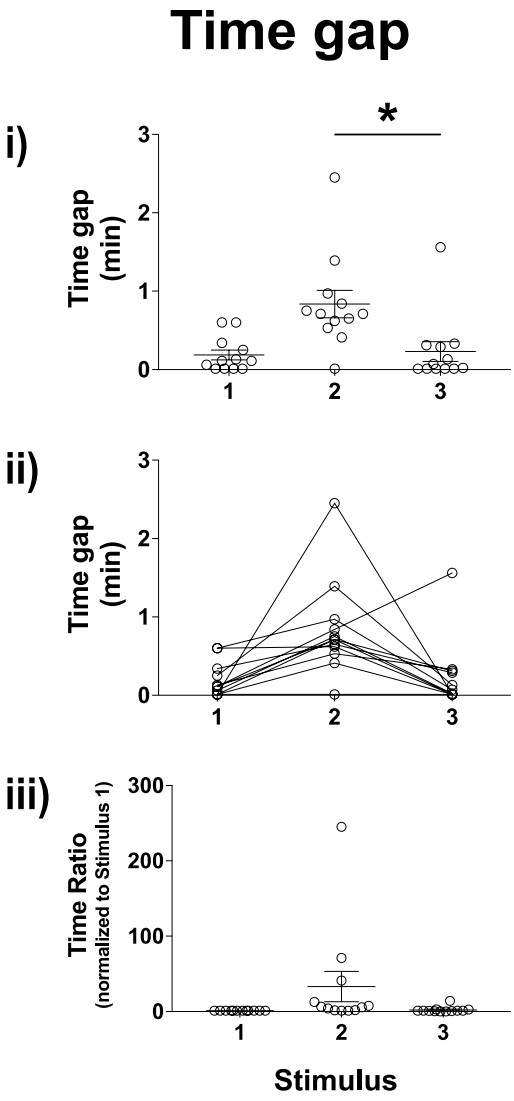


**Figure 4.8 Time gap of $[Ca^{2+}]_i$ responses in male BK-KO corticotrophs to repeated CRH.** Quantification of effects of repeated exposure to 0.2 nM CRH in time gap. * $p < 0.05$ ($n = 12$ from 8 experiments, mixed effects model). All data are means ± SEM.

BK-KO corticotrophs (Figure 4.9B).

In contrast to the stable $[Ca^{2+}]_i$ responses to repeated CRH stimulation observed in male BK-KO corticotrophs, $[Ca^{2+}]_i$ responses in female BK-KO corticotrophs were significantly attenuated in AUC (peak) ($p < 0.05$) but not AUC (10 min) (Figure 4.10) by Stimulus 3 compared to Stimulus 1. However, there were no significant differences between $[Ca^{2+}]_i$ responses for peak, time to peak (Figure 4.11), response duration, peak duration (Figure 4.12) or time gap (Figure 4.13) between Stimulus 1 and Stimulus 3 in female BK-KO corticotrophs.

Although AUC (peak) showed significant reduction following repeated CRH stimulation, AUC (10 min) and peak of $[Ca^{2+}]_i$ responses were stable. These data suggest that stimulation with repeated 0.2 nM CRH could largely induce robust $[Ca^{2+}]_i$ responses in female BK-KO corticotrophs.

#### 4.2.2.3 Female BK-KO corticotrophs have higher AUC (10 min), AUC (peak) and peak of $[Ca^{2+}]_i$ responses to repeated CRH stimulation compared to males

Attenuation of AUC (peak) of $[Ca^{2+}]_i$ responses to repeated CRH stimulation was observed in female but not male BK-KO corticotrophs suggesting that there were sex

## Figure 4.9

### Repeated CRH induces $[Ca^{2+}]_i$ responses in female BK-KO corticotrophs

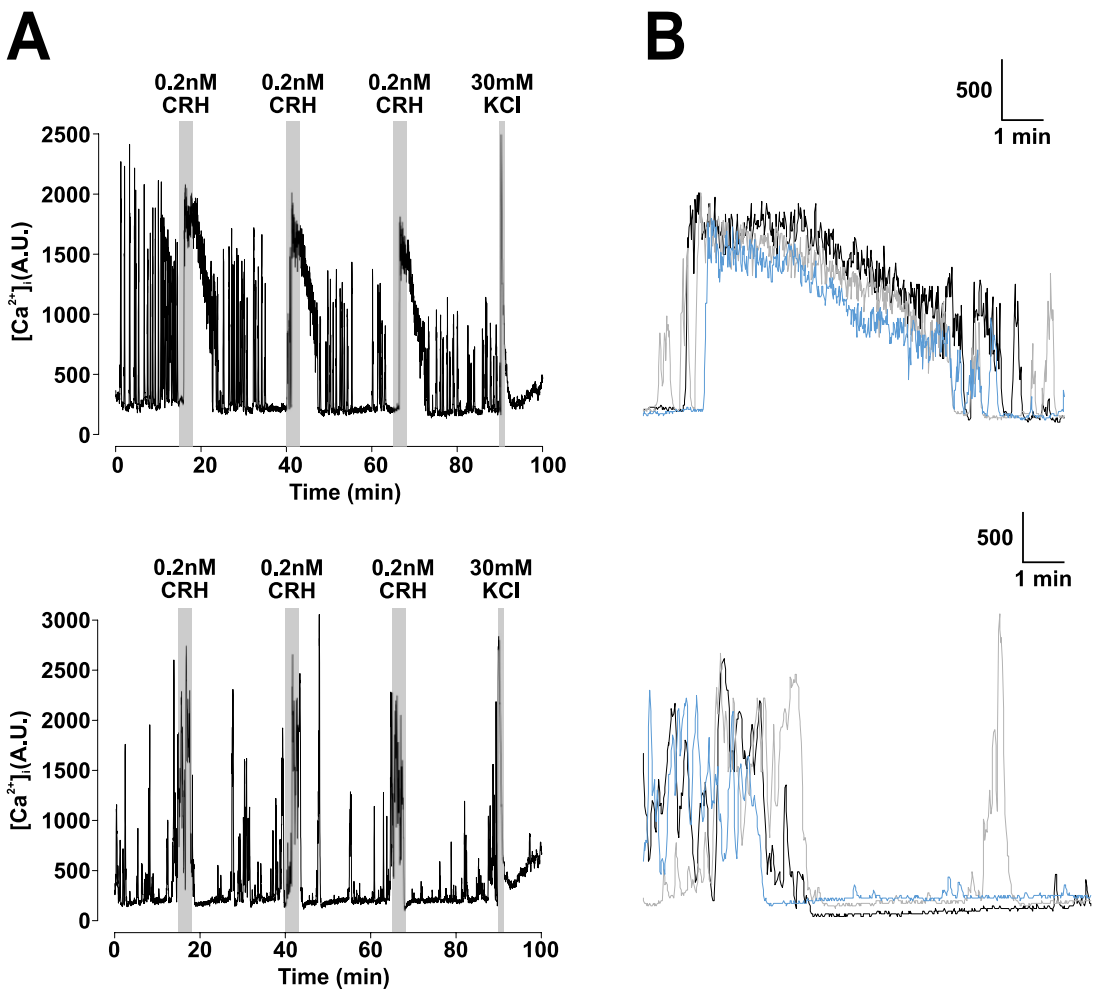


**Figure 4.9 Repeated CRH induces $[Ca^{2+}]_i$ responses in female BK-KO corticotrophs. (A)** Representative calcium imaging traces of female BK-KO corticotrophs exposed to 0.2 nM CRH for three minutes and repeated three times at 25 minutes intervals. 30 mM potassium chloride was applied at the end for one minute. **(B)** Superposition of extracts of the two traces shown in A, showing $[Ca^{2+}]_i$ changes in female BK-KO corticotrophs with repeated 0.2 nM CRH stimulation. Black line shows response to the first stimulus (starting at 15 min), grey line shows response to the second stimulus (starting at 40 min), and blue line shows response to the third stimulus (starting at 65 min).

## Figure 4.10

**Attenuated AUC (peak) but not AUC (10 min) of $[Ca^{2+}]_i$ responses in female BK-KO corticotrophs to repeated CRH**

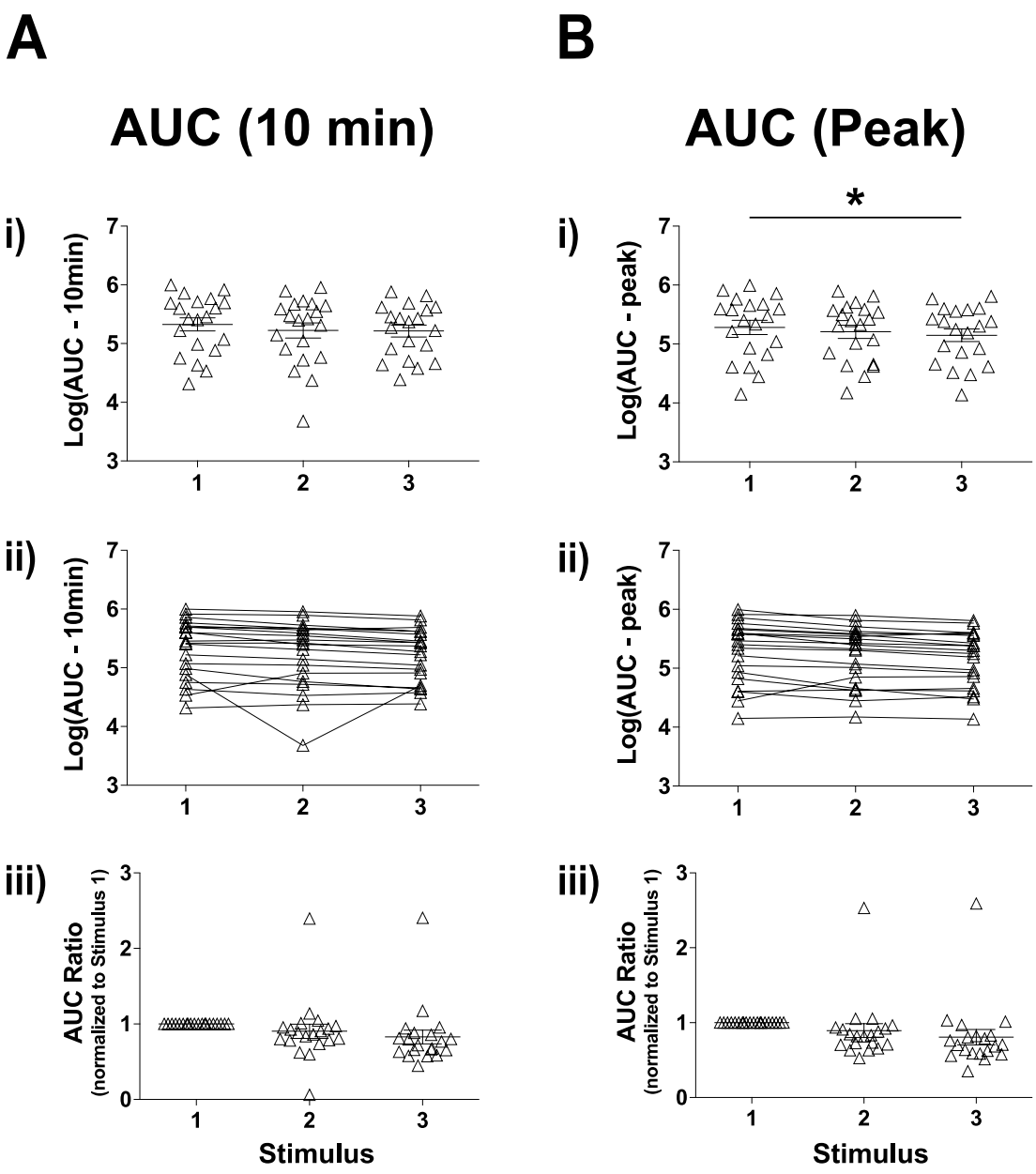


**Figure 4.10 Attenuated AUC (peak) but not AUC (10 min) of $[Ca^{2+}]_i$ responses in female BK-KO corticotrophs to repeated CRH.** Quantification of effects of repeated exposure to 0.2 nM CRH in **(A)** AUC (10 min) and **(B)** AUC (peak). * $p < 0.05$ (n = 20 from 6 experiments, mixed effects model). All data are means ± SEM.

## Figure 4.11

**Peak and time to peak of $[Ca^{2+}]_i$ responses in female BK-KO corticotrophs to repeated CRH**

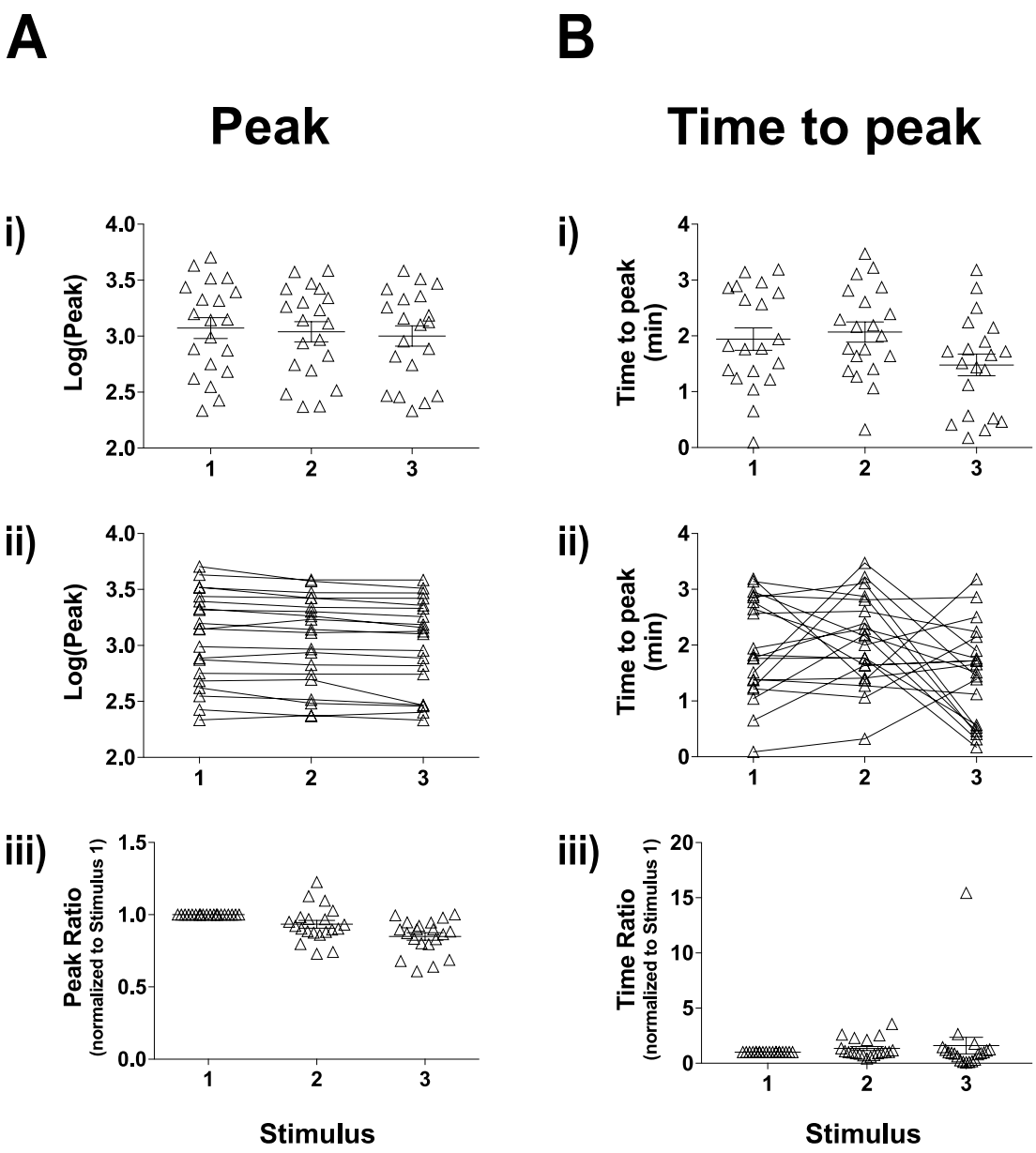


**Figure 4.11 Peak and time to peak of $[Ca^{2+}]_i$ responses in female BK-KO corticotrophs to repeated CRH.** Quantification of effects of repeated exposure to 0.2 nM CRH in **(A)** peak and **(B)** time to peak (n = 20 from 6 experiments, mixed effects model). All data are means ± SEM.

## Figure 4.12

### Response duration and peak duration of $[Ca^{2+}]_i$ responses in female BK-KO corticotrophs to repeated CRH

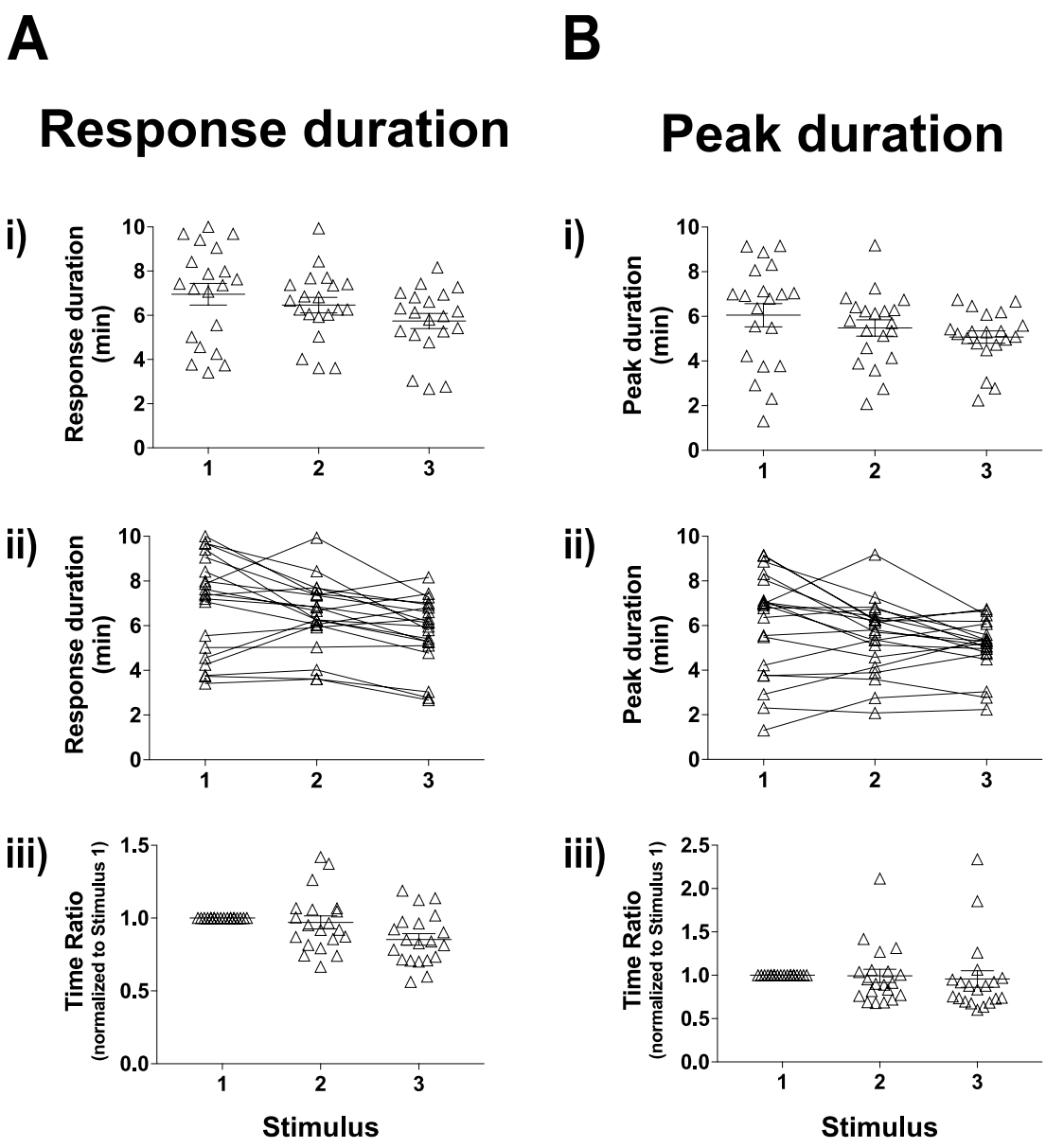


**Figure 4.12 Response duration and peak duration of $[Ca^{2+}]_i$ responses in female BK-KO corticotrophs to repeated CRH.** Quantification of effects of repeated exposure to 0.2 nM CRH in **(A)** response duration and **(B)** peak duration (n = 20 from 6 experiments, mixed effects model). All data are means ± SEM.

## Figure 4.13

### Time gap of $[Ca^{2+}]_i$ responses in female BK-KO corticotrophs to repeated CRH

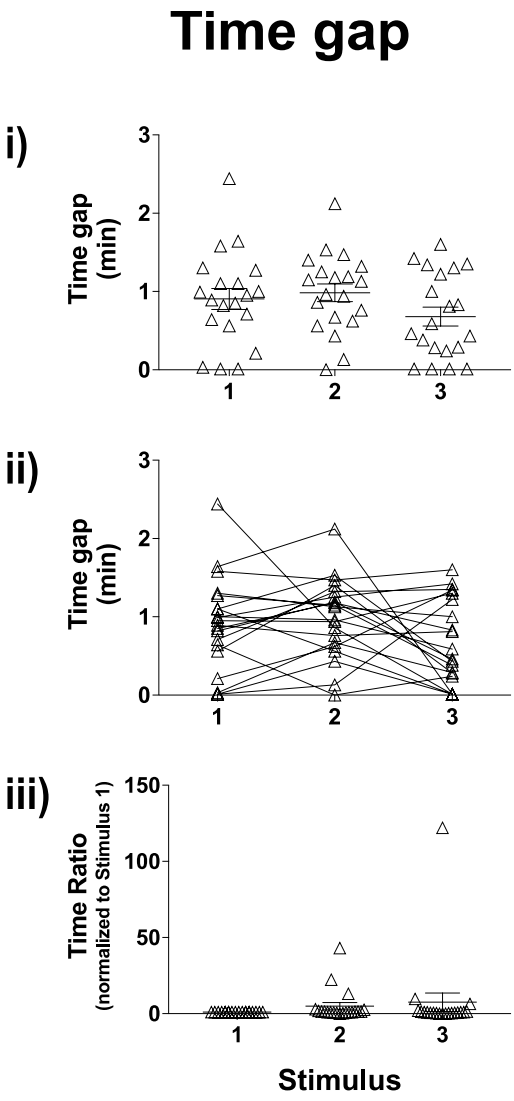


**Figure 4.13 Time gap of $[Ca^{2+}]_i$ responses in female BK-KO corticotrophs to repeated CRH.** Quantification of effects of repeated exposure to 0.2 nM CRH in time gap (n = 20 from 6 experiments, mixed effects model). All data are means ± SEM.

differences in BK-KO corticotrophs. Statistical analysis of each parameter was then performed between male and female BK-KO corticotrophs to determine the sex differences at the level of CRH-evoked $[Ca^{2+}]_i$ responses.

Female BK-KO corticotrophs displayed significantly ($p < 0.01$) larger AUC (10 min) and AUC (peak) in all three CRH stimuli compared to males (Figure 4.14). Female BK-KO corticotrophs also showed significantly ($p < 0.001$) higher peak than male in each stimulus responding to repeated CRH stimulation (Figure 4.15A). However, there were no statistically significant differences between male and female BK-KO corticotrophs in time to peak, response duration (Figure 4.15B&C), peak duration or time gap (Figure 4.16).

The sex differences observed in AUC (10 min), AUC (peak) and peak may suggest that deletion of BK channels affect male and female corticotrophs in different ways in responses to CRH stimulation.

#### 4.2.2.4 CRH-induced $[Ca^{2+}]_i$ responses are suppressed in male BK-KO corticotrophs compared to male wild-type corticotrophs

Although consistent $[Ca^{2+}]_i$ responses induced by repeated CRH stimulation were observed in both male wild-type and BK-KO corticotrophs, statistical analysis of each

## Figure 4.14

**Female BK-KO corticotrophs have higher AUC (10 min) and AUC (peak) of $[Ca^{2+}]_i$ responses to repeated CRH compared to males**

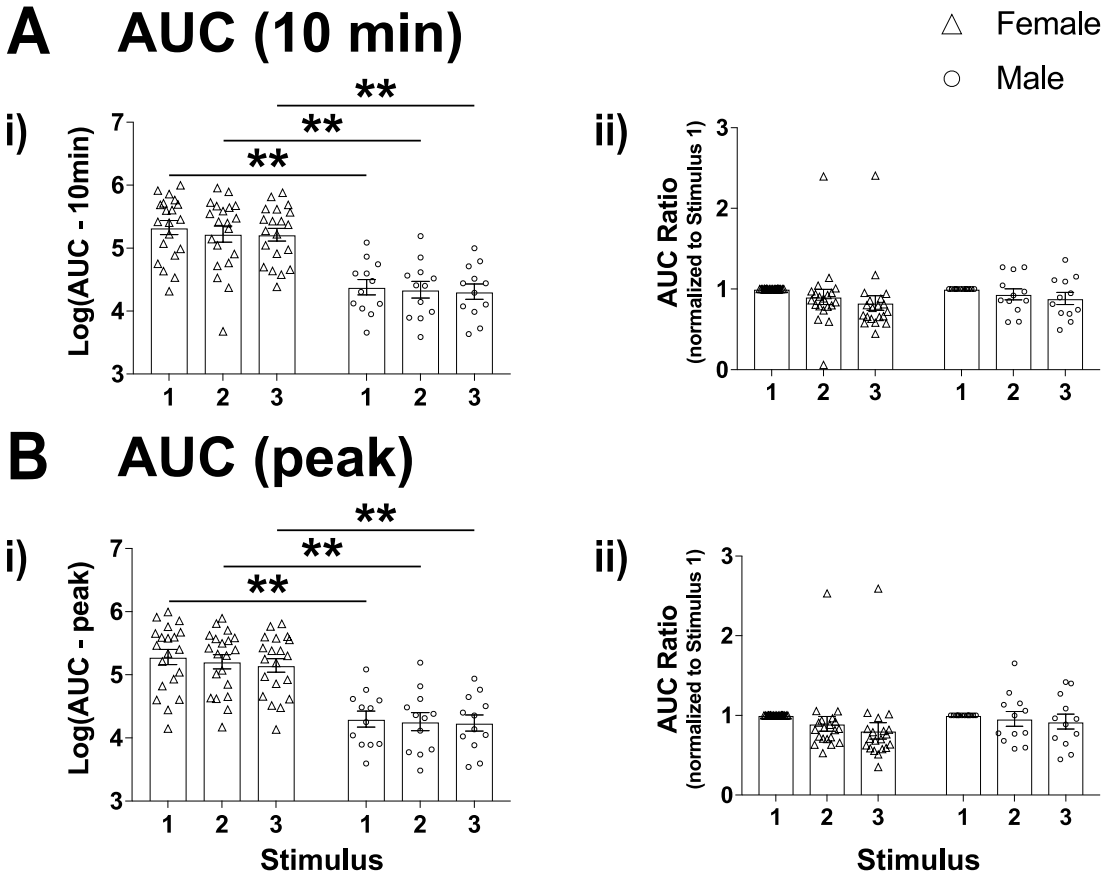


**Figure 4.14 Female BK-KO corticotrophs have higher AUC (10 min) and AUC (peak) of $[Ca^{2+}]_i$ responses to repeated CRH compared to males.** Quantification of effects of repeated exposure to 0.2 nM CRH in **(A)** AUC (10 min) and **(B)** AUC (peak). ** $p < 0.01$ (male n = 12 from 8 experiments, female n = 20 from 6 experiments, mixed effects model). All data are means ± SEM.

## Figure 4.15

**Female BK-KO corticotrophs have higher peak but not time to peak or response duration of $[Ca^{2+}]_i$ responses to repeated CRH compared to males**

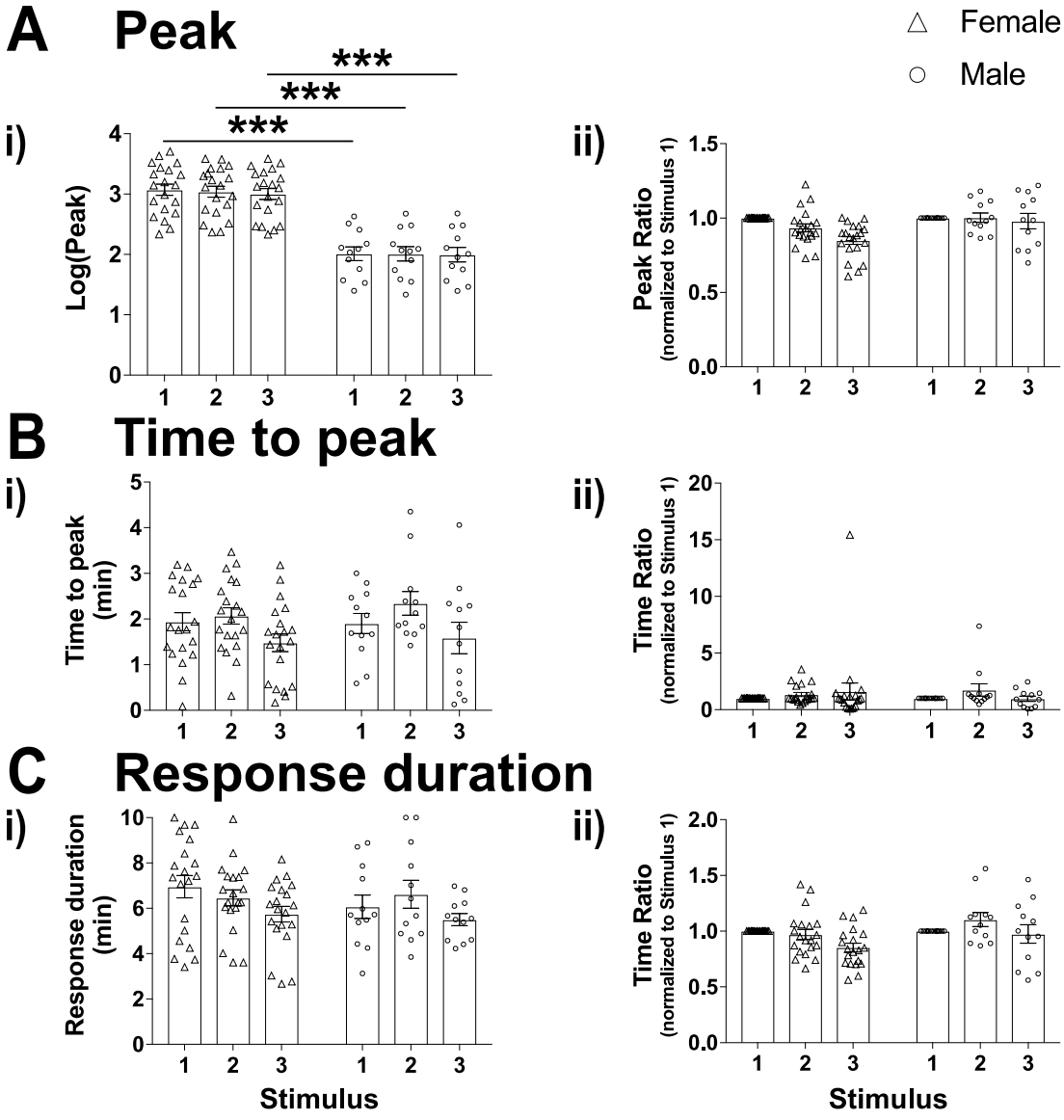


**Figure 4.15 Female BK-KO corticotrophs have higher peak but not time to peak or response duration of $[Ca^{2+}]_i$ responses to repeated CRH compared to males.** Quantification of effects of repeated exposure to 0.2 nM CRH in **(A)** peak, **(B)** time to peak and **(C)** response duration. *** $p < 0.001$ (male n = 12 from 8 experiments, female n = 20 from 6 experiments, mixed effects model). All data are means ± SEM.

## Figure 4.16

### No significant sex difference in CRH-induced peak duration or time gap of $[Ca^{2+}]_i$ responses in BK-KO corticotrophs

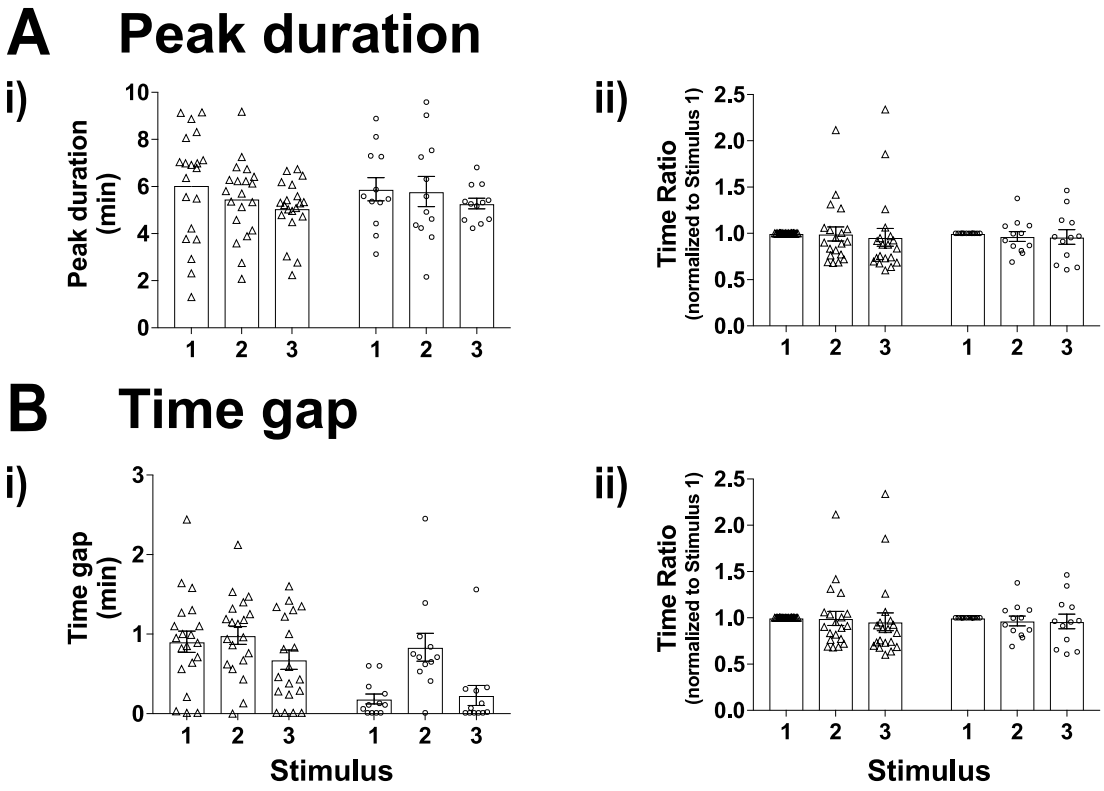


**Figure 4.16 No significant sex difference in CRH-induced peak duration or time gap of $[Ca^{2+}]_i$ responses in BK-KO corticotrophs.** Quantification of effects of repeated exposure to 0.2 nM CRH in **(A)** peak duration and **(B)** time gap (male n = 12 from 6 experiments, female n = 20 from 6 experiments, mixed effects model). All data are means ± SEM.

parameter was performed between male wild-type and BK-KO corticotrophs to examine whether genetic deletion of BK channels have effect on the $[Ca^{2+}]_i$ responses induced by repeated 0.2 nM CRH stimulation in male corticotrophs. Compared to male wild-type corticotrophs, AUC (10 min) and AUC (peak) were significantly ($p < 0.01$) suppressed in all three stimuli following repeated CRH stimulation in male BK-KO corticotrophs (Figure 4.17). CRH-induced peak was also significantly suppressed in Stimulus 1 ($p < 0.001$), Stimulus 2 ($p < 0.001$) and Stimulus 3 ($p < 0.01$) in male BK-KO corticotrophs (Figure 4.18A). There were no significant differences between male wild-type and BK-KO corticotrophs in time to peak (Figure 4.18B), response duration (Figure 4.18C), peak duration or time gap (Figure 4.19).

Overall, these results suggest that genetic deletion of BK channels suppressed the $[Ca^{2+}]_i$ responses to repeated CRH stimulation in male corticotrophs.

#### 4.2.2.5 CRH-induced $[Ca^{2+}]_i$ responses are not affected by pharmacological inhibition of BK channels in male corticotrophs

Previous experiments suggest that genetic deletion of BK channels significantly suppressed $[Ca^{2+}]_i$ responses to repeated CRH stimulation in male corticotrophs. To examine whether pharmacological inhibition of BK channels have similar effects on male corticotrophs, calcium imaging experiments were performed on male wild-type

## Figure 4.17

**Suppressed AUC (10 min) and AUC (peak) of $[Ca^{2+}]_i$ responses in male BK-KO corticotrophs to repeated CRH compared to male wild-type corticotrophs**

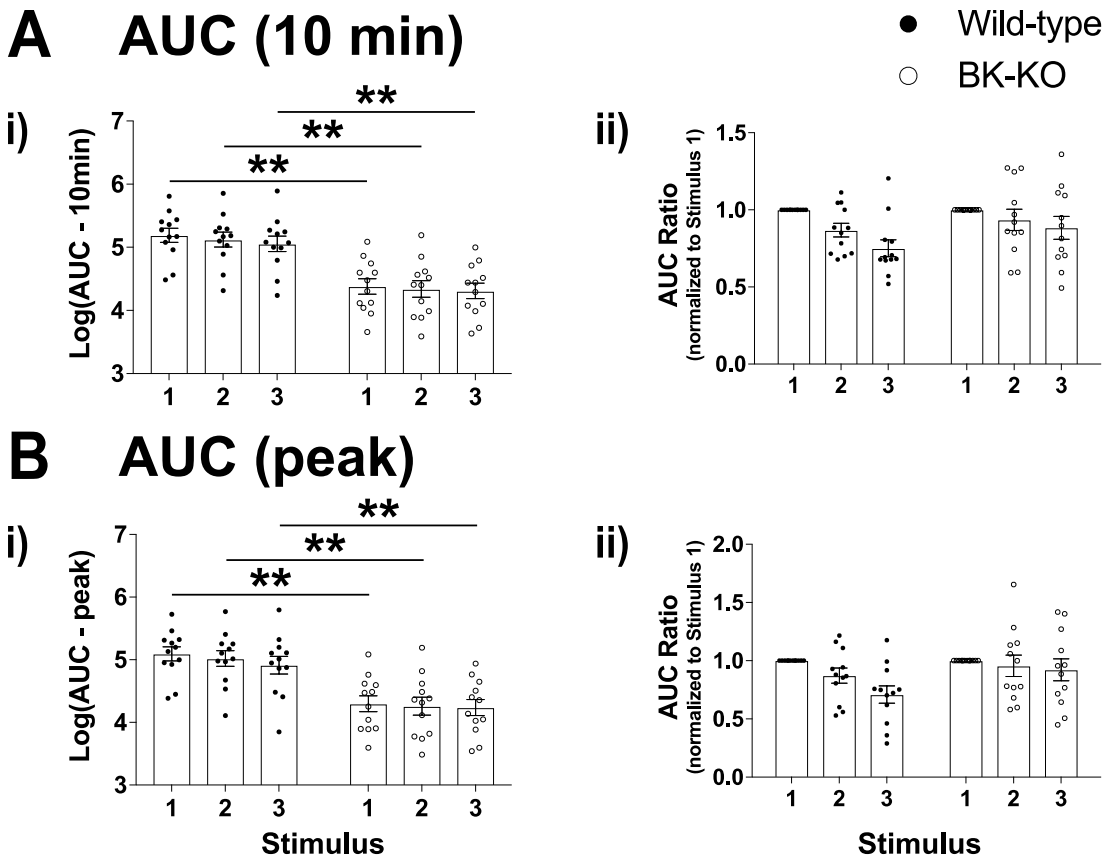


**Figure 4.17 Suppressed AUC (10 min) and AUC (peak) of $[Ca^{2+}]_i$ responses in male BK-KO corticotrophs to repeated CRH compared to male wild-type corticotrophs.** Quantification of effects of repeated exposure to 0.2 nM CRH in **(A)** AUC (10 min) and **(B)** AUC (peak). ** $p < 0.01$ (wild-type n = 12 from 8 experiments, BK-KO n = 12 from 8 experiments, mixed effects model). All data are means ± SEM.

## Figure 4.18

### Suppressed peak but not time to peak or response duration of $[Ca^{2+}]_i$ responses in male BK-KO corticotrophs to repeated CRH compared to male wild-type corticotrophs

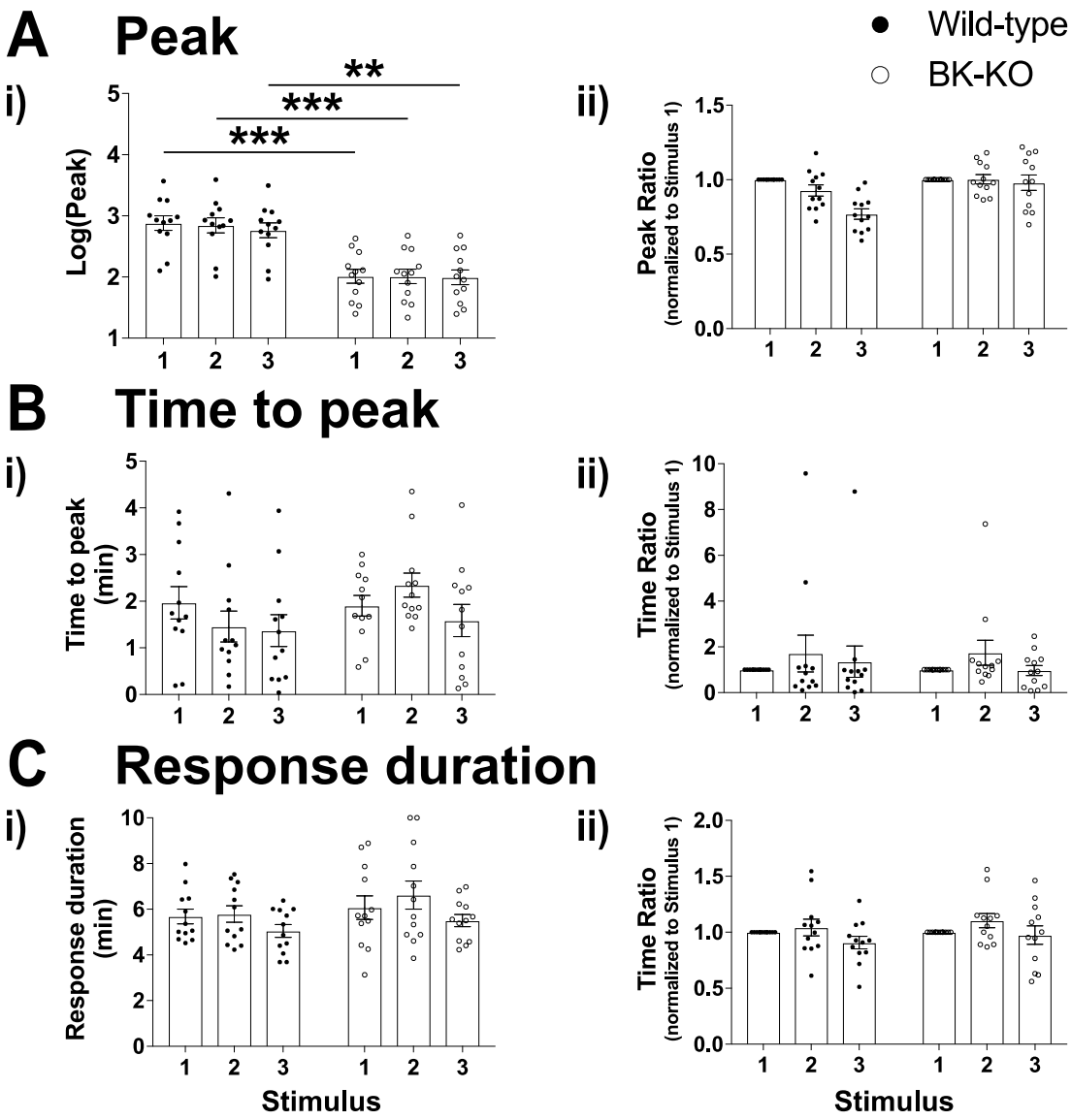


**Figure 4.18 Suppressed peak but not time to peak or response duration of $[Ca^{2+}]_i$ responses in male BK-KO corticotrophs to repeated CRH compared to male wild-type corticotrophs.** Quantification of effects of repeated exposure to 0.2 nM CRH in **(A)** peak, **(B)** time to peak and **(C)** response duration. ** $p < 0.01$, *** $p < 0.001$ (wild-type n = 12 from 8 experiments, BK-KO n = 12 from 8 experiments, mixed effects model). All data are means ± SEM.

## Figure 4.19

**No significant differences in CRH-induced peak duration and time gap $[Ca^{2+}]_i$ responses between male wild-type and BK-KO corticotrophs**

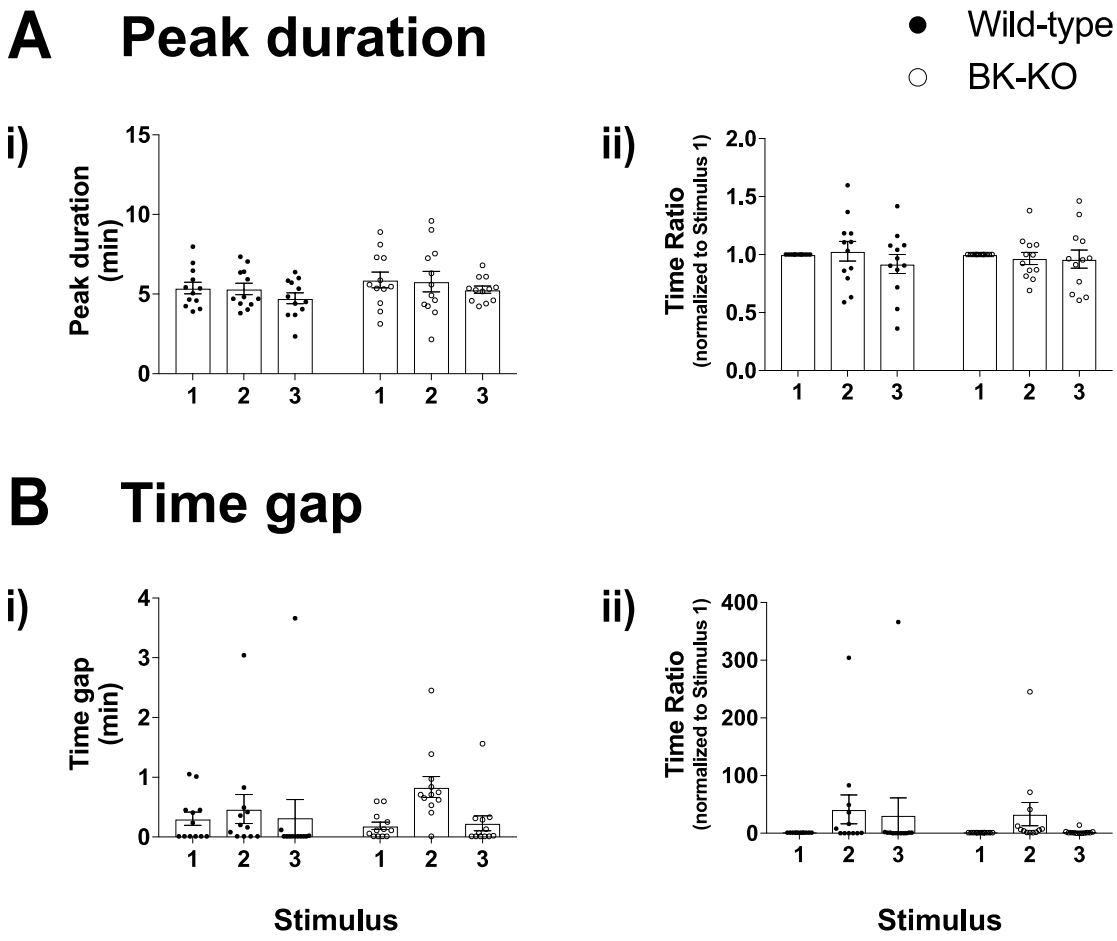


**Figure 4.19 No significant differences in CRH-induced peak duration and time gap $[Ca^{2+}]_i$ responses between male wild-type and BK-KO corticotrophs.** Quantification of effects of repeated exposure to 0.2 nM CRH in **(A)** peak duration and **(B)** time gap (wild-type n = 12 from 8 experiments, BK-KO n = 12 from 8 experiments, mixed effects model). All data are means ± SEM.

corticotrophs (n = 10 from 5 experiments) treated with 0.2 nM CRH in the presence of specific BK channel blocker paxilline (1 μM).

Following the ion channel blocking protocol (see 2.5.2.3), male wild-type corticotrophs were stimulated with 0.2 nM CRH for three minutes and repeated three times after 15–20 minutes spontaneous $[Ca^{2+}]_i$ signalling recording. The second CRH stimulation was applied in the presence of 1 μM paxilline and paxilline was applied 10 minutes before and after the stimulation to ensure the blockade of BK channels. Following by a 25 minute washout period, corticotrophs were treated with CRH for the third time and finally a one minute 30 mM potassium chloride to verify cell viability (Figure 4.20A). Stimulation with CRH alone induced significant increase of $[Ca^{2+}]_i$ in male wild-type corticotrophs. However, CRH-induced $[Ca^{2+}]_i$ response was not affected when BK channels were pharmacologically blocked by paxilline (Figure 4.20B). Following paxilline washout, the $[Ca^{2+}]_i$ response to CRH was similar to the first stimulus.

Analysis of 5 min "baseline" period before the second CRH stimulus suggested that paxilline had no significant effect on either spontaneous $[Ca^{2+}]_i$ active time or maximum amplitude compared to the spontaneous $[Ca^{2+}]_i$ signalling before the first CRH stimulus in male wild-type corticotrophs (data not shown). The effects of

## Figure 4.20

## Paxilline has no significant inhibition on CRH-induced $[Ca^{2+}]_i$ response in male BK-KO corticotrophs

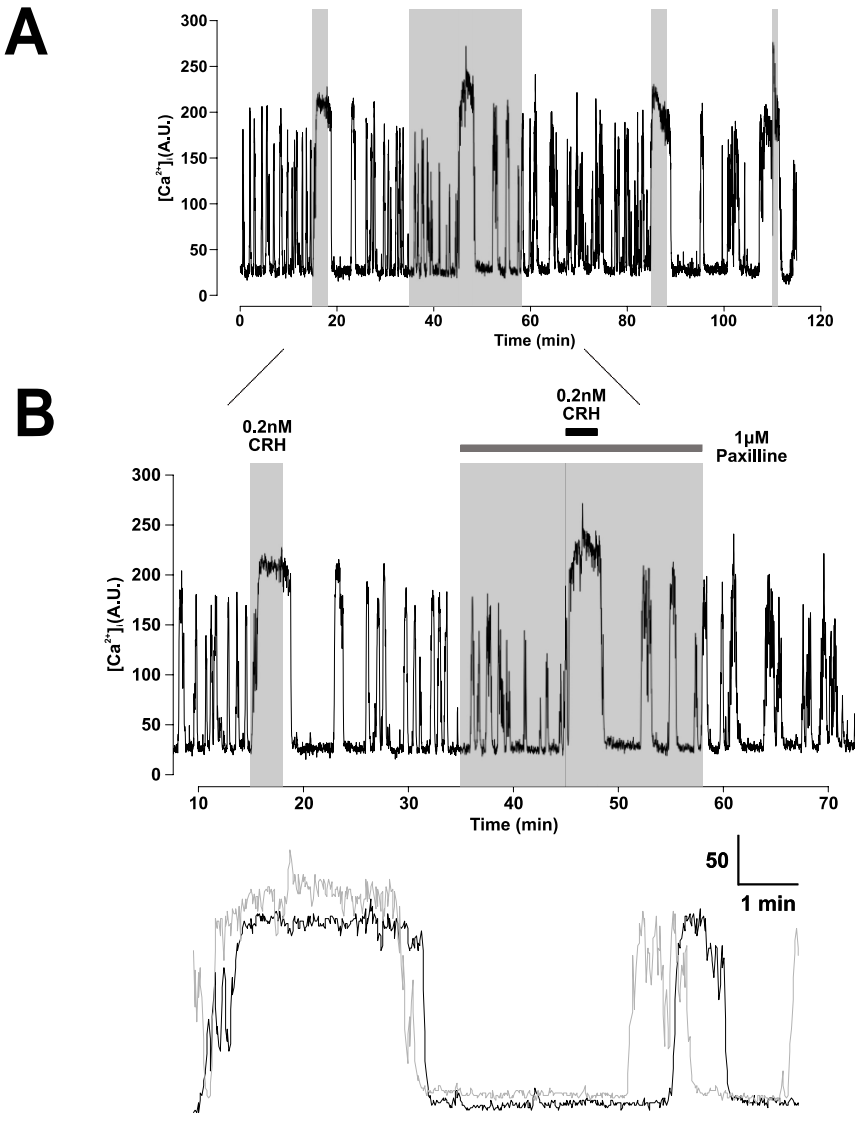


**Figure 4.20 Paxilline has no significant inhibition on CRH-induced $[Ca^{2+}]_i$ response in male BK-KO corticotrophs. (A)** Representative calcium imaging traces of the effects of paxilline on $[Ca^{2+}]_i$ responses to 0.2 nM CRH in male BK-KO corticotrophs. **(B)** Superposition of extracts of the trace shown in A, showing $[Ca^{2+}]_i$ changes in male BK-KO corticotrophs. Black line shows the response to 0.2 nM CRH alone, grey line shows the response to 0.2 nM CRH in the presence of 1 μM paxilline.

paxilline on CRH induced $[Ca^{2+}]_i$ responses were evaluated by AUC (10 min), AUC (peak) and peak. Statistical analysis revealed that paxilline had no significant inhibition effect on CRH-induced AUC (10 min), AUC (peak) (Figure 4.21) or peak (Figure 4.22) in male wild-type corticotrophs, which is different from genetic deletion of BK channels in male corticotrophs. Interestingly, in comparison to stimulation with CRH alone, 5 out of 10 (50%) cells showed larger AUC (peak) and 4 of them also showed larger AUC (10 min) in the presence of paxilline. In addition, higher peak was observed in 70% (7 out of 10) of cells when treated with paxilline.

These results suggest that spontaneous and CRH-induced $[Ca^{2+}]_i$ responses in male wild-type corticotrophs was not affected by pharmacological inhibition of BK channels with paxilline.

#### 4.2.2.6 CRH-induced $[Ca^{2+}]_i$ responses are not significantly different between female wild-type and BK-KO corticotrophs

The same statistical analysis was then performed between female wild-type and BK-KO corticotrophs to examine whether genetic deletion of BK channels had effects on CRH-induced $[Ca^{2+}]_i$ responses in female corticotrophs.

Unlike the suppressed $[Ca^{2+}]_i$ responses in AUC (10 min), AUC (peak) and peak

## Figure 4.21

**Pharmacological inhibition of BK channels has no significant effect on CRH-induced AUC (10 min) and AUC (peak) of $[Ca^{2+}]_i$ responses in male corticotrophs**

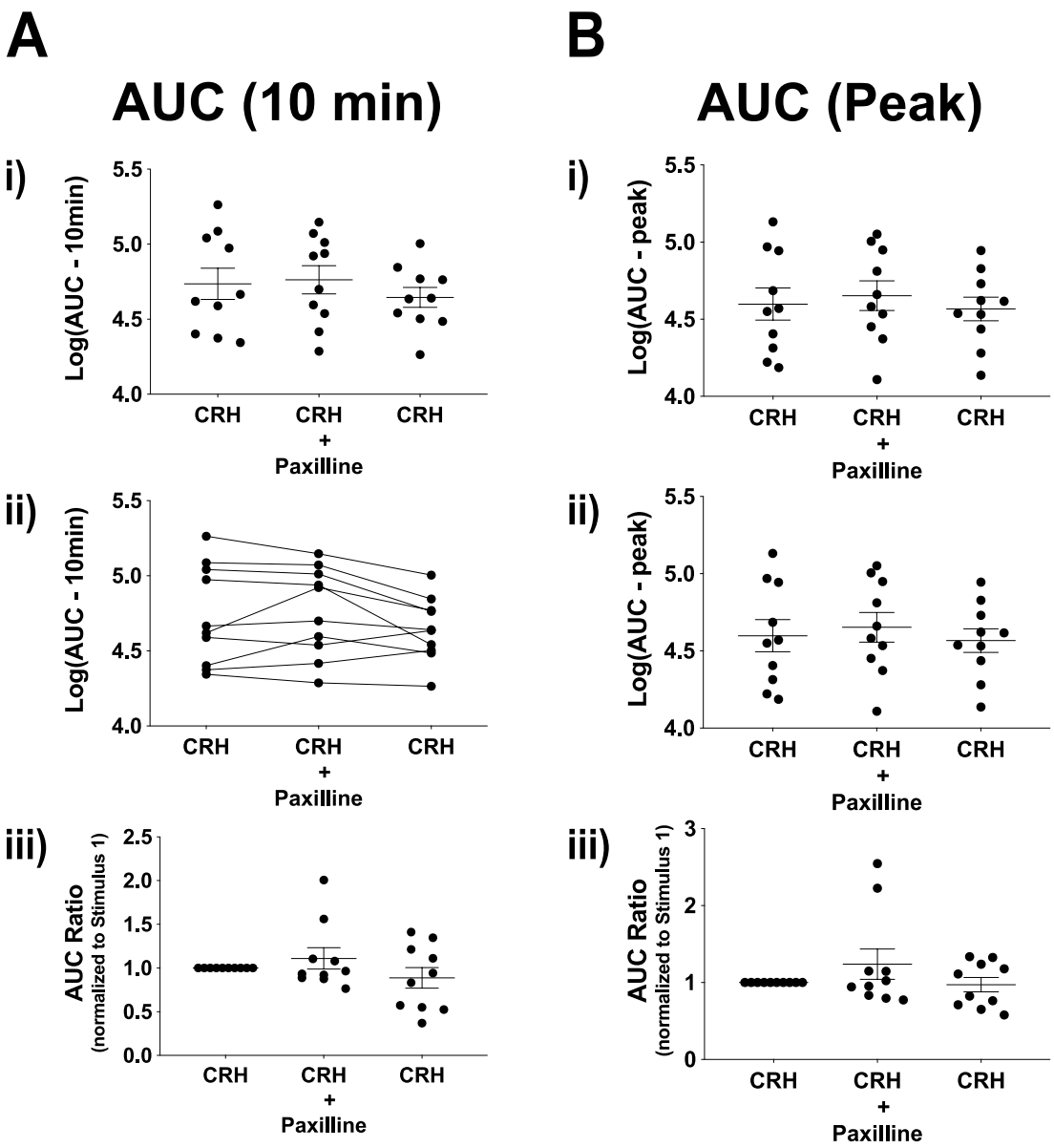


**Figure 4.21 Pharmacological inhibition of BK channels has no significant effect on CRH-induced AUC (10 min) and AUC (peak) of $[Ca^{2+}]_i$ responses in male corticotrophs.** Quantification of effects of repeated exposure to 0.2 nM CRH in **(A)** AUC (10 min) and **(B)** AUC (peak) (n = 10 from 5 experiments, mixed effects model). All data are means ± SEM.

# Figure 4.22

## Pharmacological inhibition of BK channels has no significant effect on CRH-induced peak of $[Ca^{2+}]_i$ responses in male corticotrophs

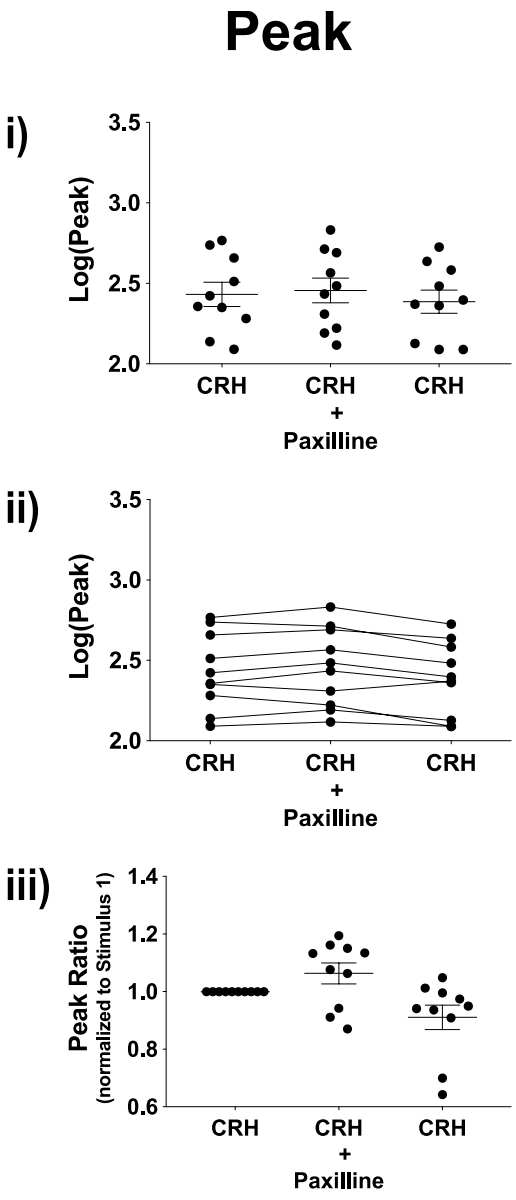


**Figure 4.22 Pharmacological inhibition of BK channels has no significant effect on CRH-induced peak of $[Ca^{2+}]_i$ responses in male corticotrophs.** Quantification of effects of repeated exposure to 0.2 nM CRH in peak (n = 10 from 5 experiments, mixed effects model). All data are means ± SEM.

observed in male BK-KO corticotrophs, there were no significant differences in these parameters at each CRH stimulus between female wild-type and BK-KO corticotrophs (Figure 4.23 and Figure 4.24A). Female wild-type and BK-KO corticotrophs also had no significant differences in time to peak, response duration (Figure 4.24B&C), peak duration or time gap (Figure 4.25) following repeated CRH stimulation, although female wild-type corticotrophs tended to have higher variability.

In summary, these results suggest that genetic deletion of BK channels had no significant effect on $[Ca^{2+}]_i$ responses to repeated CRH stimulation in female corticotrophs, which is different from male corticotrophs.

#### 4.2.2.7 CRH-induced $[Ca^{2+}]_i$ responses are not affected by pharmacological inhibition of BK channels in female corticotrophs

Although pharmacological inhibition of BK channels had no significant effect on CRH-induced $[Ca^{2+}]_i$ responses in male wild-type corticotrophs, we investigated whether pharmacological inhibition of BK channels would affect CRH-induced $[Ca^{2+}]_i$ responses in female wild-type corticotrophs.

Calcium imaging recordings were obtained from female wild-type corticotrophs (n = 19 from 8 experiments) following the same ion channel blocking protocol used

## Figure 4.23

**No significant differences in CRH-induced AUC (10 min) or AUC (peak) of $[Ca^{2+}]_i$ responses between female wild-type and BK-KO corticotrophs**

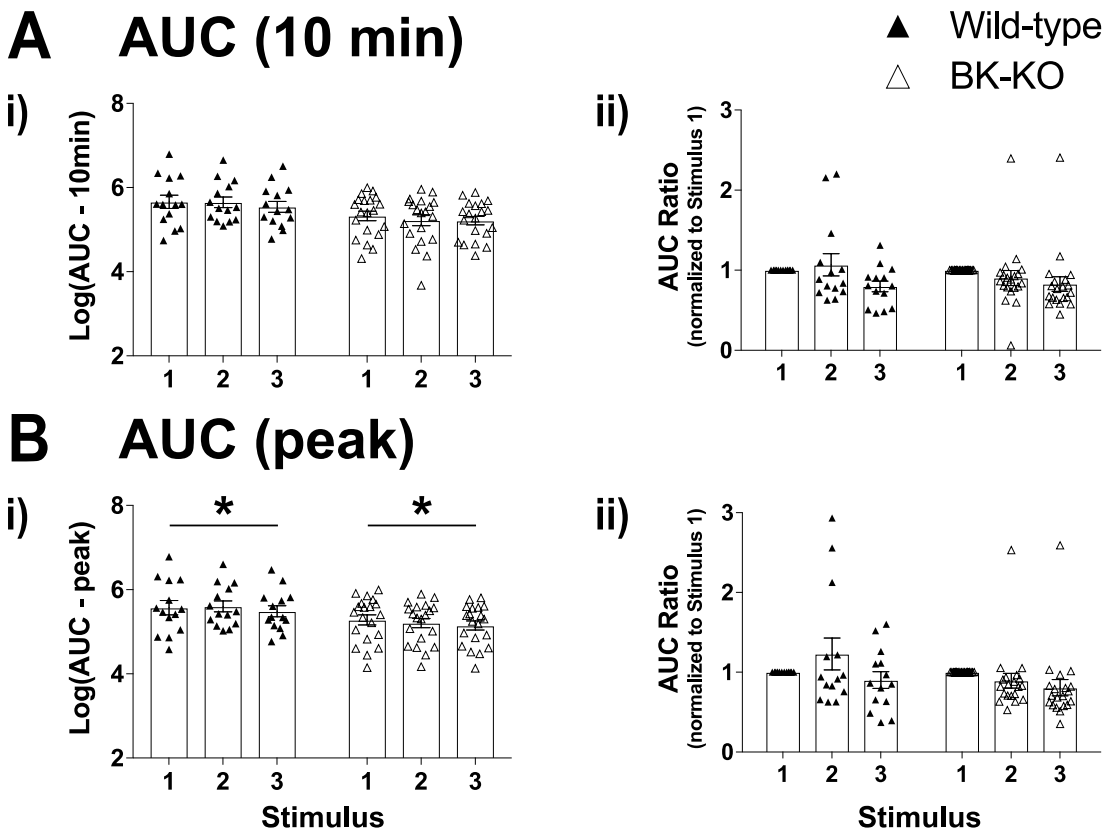


**Figure 4.23 No significant differences in CRH-induced AUC (10 min) or AUC (peak) of $[Ca^{2+}]_i$ responses between female wild-type and BK-KO corticotrophs.** Quantification of effects of repeated exposure to 0.2 nM CRH in **(A)** AUC (10 min) and **(B)** AUC (peak). * $p < 0.05$ (wild-type n = 14 from 7 experiments, BK-KO n = 20 from 6 experiments, mixed effects model). All data are means ± SEM.

## Figure 4.24

**No significant differences in CRH-induced peak, time to peak or response duration of $[Ca^{2+}]_i$ responses between female wild-type and BK-KO corticotrophs**

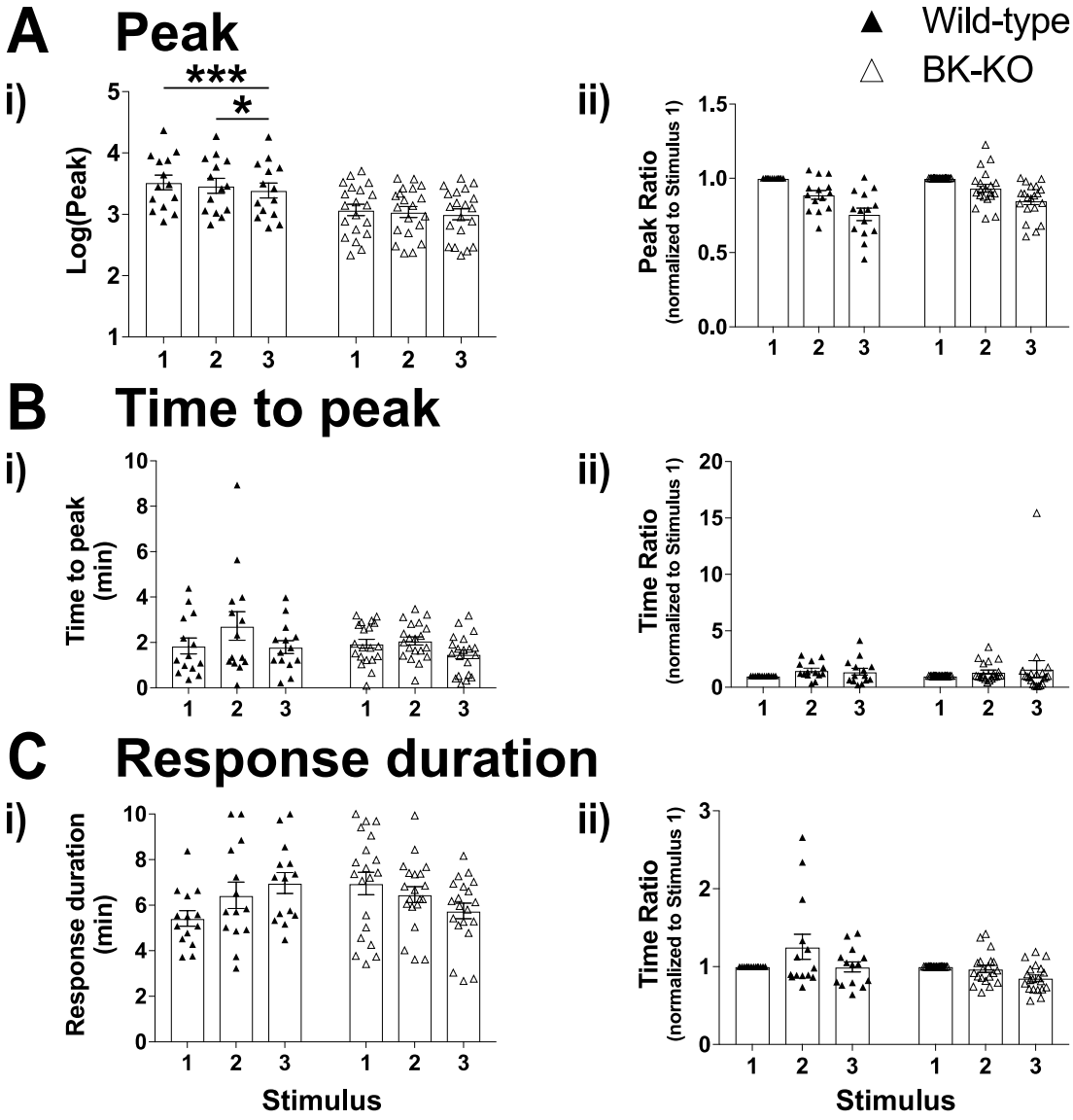


**Figure 4.24 No significant differences in CRH-induced peak, time to peak or response duration of $[Ca^{2+}]_i$ responses between female wild-type and BK-KO corticotrophs.** Quantification of effects of repeated exposure to 0.2 nM CRH in **(A)** peak, **(B)** time to peak and **(C)** response duration. *** $p < 0.001$ (wild-type n = 14 from 7 experiments, BK-KO n = 20 from 6 experiments, mixed effects model). All data are means ± SEM.

## Figure 4.25

**No significant differences in CRH-induced peak duration or time gap of $[Ca^{2+}]_i$ responses between female wild-type and BK-KO corticotrophs**

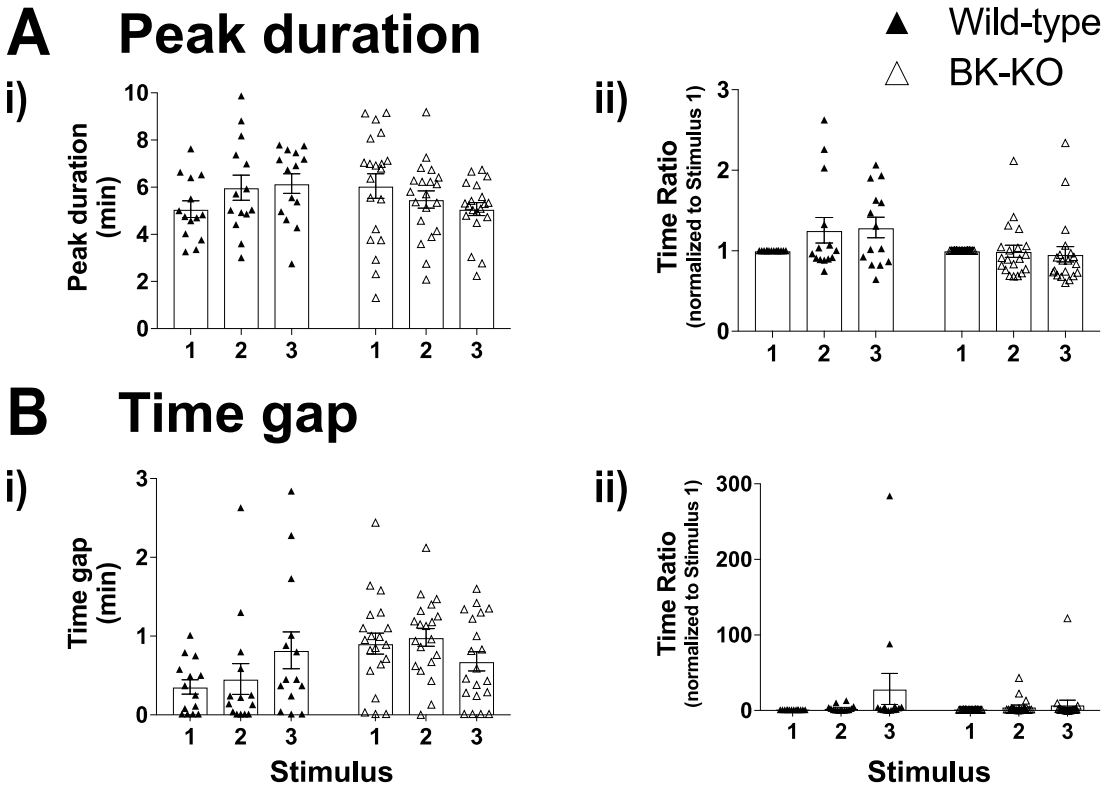


**Figure 4.25 No significant differences in CRH-induced peak duration or time gap of $[Ca^{2+}]_i$ responses between female wild-type and BK-KO corticotrophs.** Quantification of effects of repeated exposure to 0.2 nM CRH in **(A)** peak duration and **(B)** time gap (wild-type n = 14 from 7 experiments, BK-KO n = 20 from 6 experiments, mixed effects model). All data are means ± SEM.

in male wild-type corticotrophs. Stimulation with CRH alone, female wild-type corticotrophs displayed significant and sustained elevation of $[Ca^{2+}]_i$ (Figure 4.26A). However, stimulation with CRH did not show significant effect on $[Ca^{2+}]_i$ responses in female wild-type corticotrophs when BK channels were pharmacological blocked by paxilline (Figure 4.26B). After washing out paxilline, all corticotrophs responded to CRH with similar $[Ca^{2+}]_i$ responses as seen in the first stimulus.

Compared to the spontaneous $[Ca^{2+}]_i$ signalling under 5 min "baseline" period before the first CRH stimulus, neither spontaneous $[Ca^{2+}]_i$ active time nor maximum amplitude before the second CRH stimulus was affected by treatment with paxilline in female wild-type corticotrophs (data not shown). Statistical analysis revealed that blockade of BK channels with paxilline had no significant inhibition effect on CRH-induced AUC (10 min), AUC (peak) (Figure 4.27) or peak (Figure 4.28) in female wild-type corticotrophs. It is worth noting that, compared to stimulation with CRH alone, larger AUC (10 min) was observed in 47.4% of (9 out of 19) cells when treated with paxilline, with 8 of them also showing larger AUC (10 min). 52.6% (10 out of 19) of cells exhibited higher peak in the presence of paxilline.

These data suggest that pharmacological inhibition of BK channels with paxilline had no significant inhibition effect on CRH-induced $[Ca^{2+}]_i$ responses in female wild-type

# Figure 4.26

# Paxilline has no significant inhibition on CRH-induced $[Ca^{2+}]_i$ response in female BK-KO corticotrophs

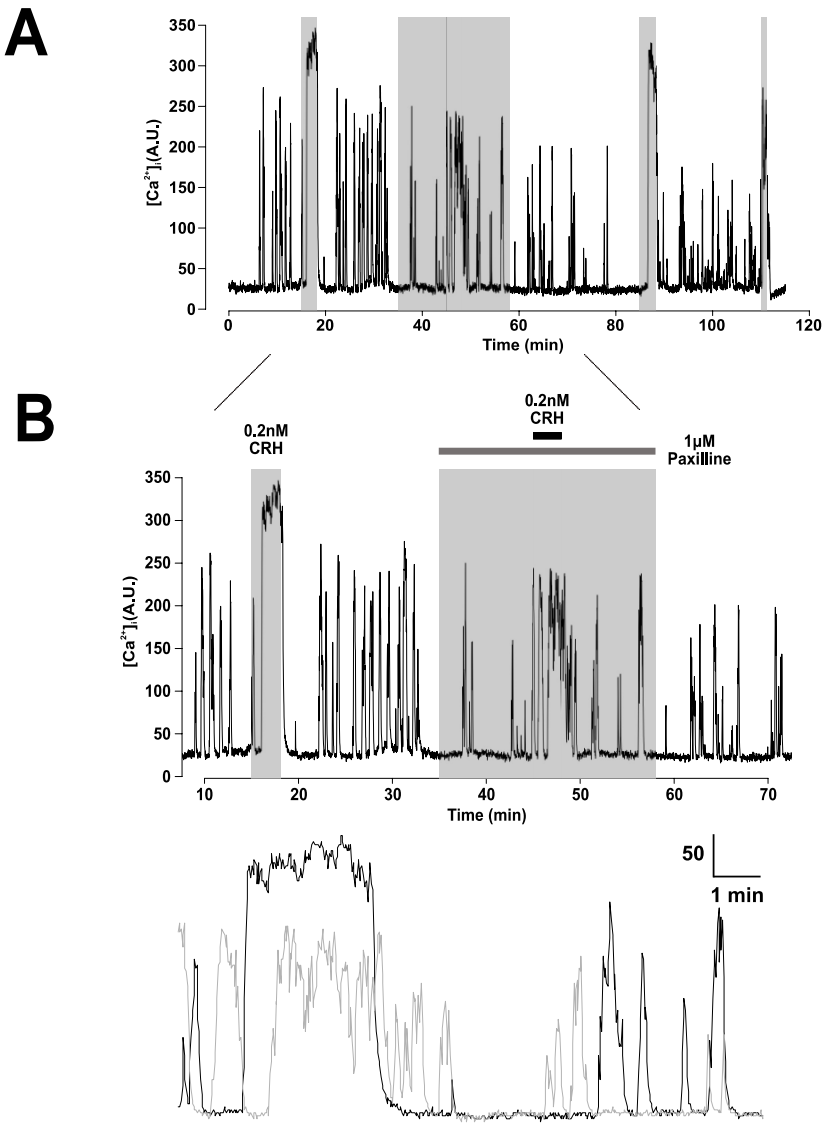


**Figure 4.26 Paxilline has no significant inhibition on CRH-induced $[Ca^{2+}]_i$ response in female BK-KO corticotrophs. (A)** Representative calcium imaging traces of the effects of paxilline on $[Ca^{2+}]_i$ responses to 0.2 nM CRH in female BK-KO corticotrophs. **(B)** Superposition of extracts of the trace shown in A, showing $[Ca^{2+}]_i$ changes in female BK-KO corticotrophs. Black line shows the response to 0.2 nM CRH alone, grey line shows the response to 0.2 nM CRH in the presence of 1 μM paxilline.

## Figure 4.27

**Pharmacological inhibition of BK channels has no significant effect on CRH-induced AUC (10 min) and AUC (peak) of $[Ca^{2+}]_i$ responses in female corticotrophs**

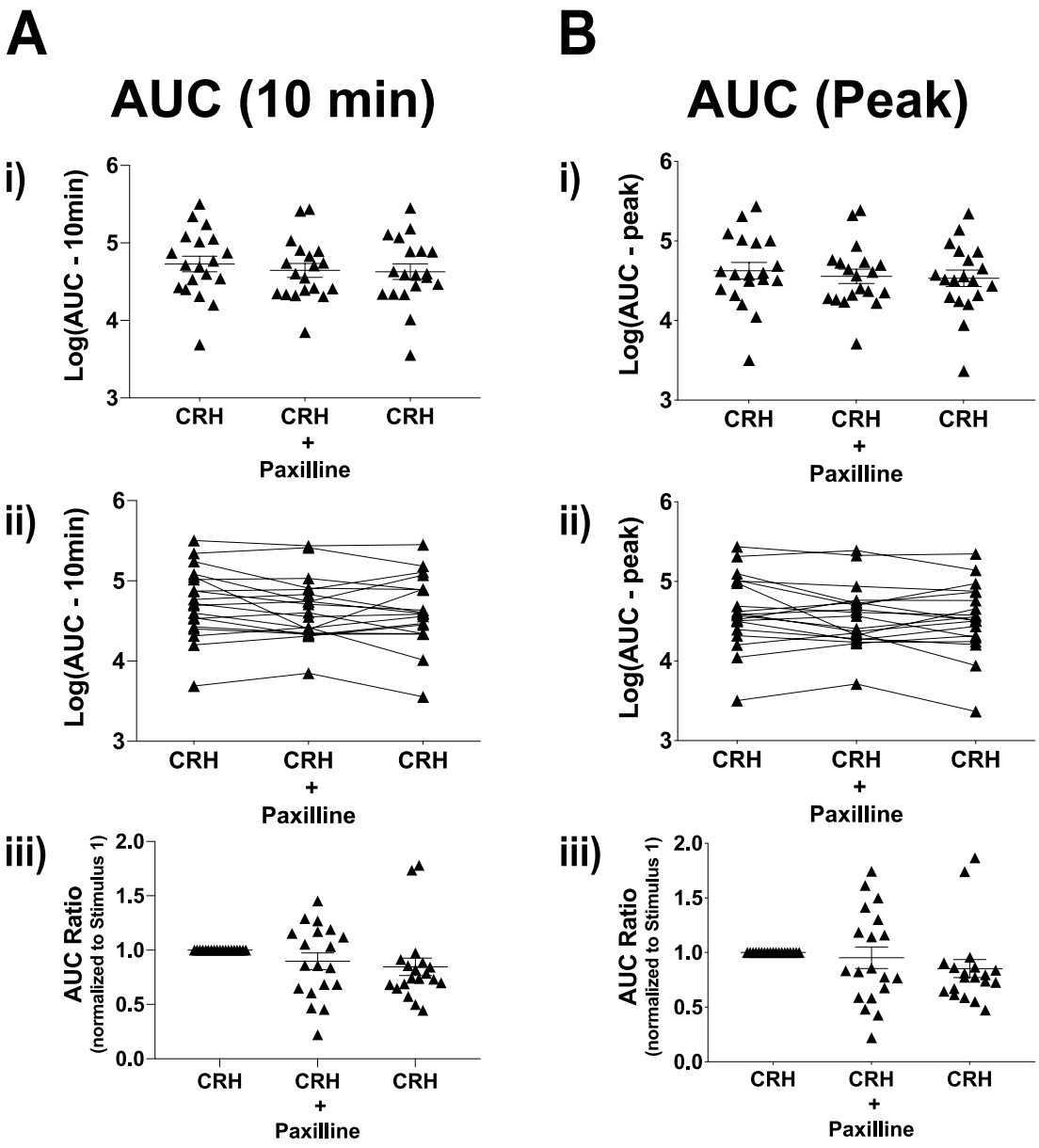


**Figure 4.27 Pharmacological inhibition of BK channels has no significant effect on CRH-induced AUC (10 min) and AUC (peak) of $[Ca^{2+}]_i$ responses in female corticotrophs.** Quantification of effects of paxilline on exposure to 0.2 nM CRH in **(A)** AUC (10 min) and **(B)** AUC (peak) (n = 19 from 8 experiments, mixed effects model). All data are means ± SEM.

## Figure 4.28

**Pharmacological inhibition of BK channels has no significant effect on CRH-induced peak of $[Ca^{2+}]_i$ responses in female corticotrophs**

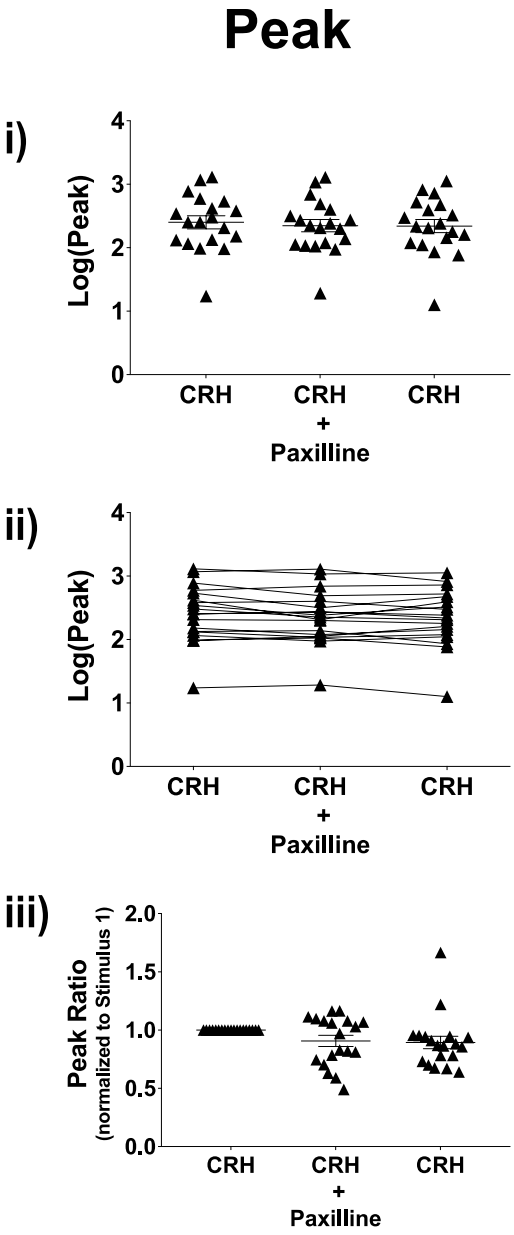


**Figure 4.28 Pharmacological inhibition of BK channels has no significant effect on CRH-induced peak of $[Ca^{2+}]_i$ responses in female corticotrophs.** Quantification of effects of paxilline on exposure to 0.2 nM CRH in peak (n = 19 from 8 experiments, mixed effects model). All data are means ± SEM.

corticotrophs, which is similar to female BK-KO corticotrophs.

In summary, global genetic deletion of BK channels resulted in statistically significant reduction of AUC (10 min), AUC (peak) and peak in male but not female corticotrophs. This suggest that functional BK channels are essential in regulating CRH-induced $[Ca^{2+}]_i$ responses in murine corticotrophs with sex differences. However, CRH-induced $[Ca^{2+}]_i$ responses were unaffected by pharmacological inhibition of BK channels with paxilline suggesting a compensatory mechanism may underlie the changes in CRH-evoked $[Ca^{2+}]_i$ responses in BK-KO corticotrophs.

### 4.2.3 Genetic deletion of BK channels has no significant effect on AVP-induced $[Ca^{2+}]_i$ responses in male and female corticotrophs

BK channels have been suggested to play an important role in regulating spontaneous and CRH-evoked $[Ca^{2+}]_i$ signalling in murine corticotrophs, experiments were then carried out to examine whether genetic deletion of BK channels would affect AVP-induced $[Ca^{2+}]_i$ responses in corticotrophs.

Two phenotypes of $[Ca^{2+}]_i$ responses observed in wild-type corticotrophs were also found in BK-KO corticotrophs. Following repeated 2 nM AVP stimulation, 66.7%

(12/18) of cells displayed sustained elevation of $[Ca^{2+}]_i$ and 22.2% (4/18) of cells showed oscillatory$[Ca^{2+}]_i$ behaviour in all three stimuli. The remaining 2 cells (11.1%) exhibited sustained $[Ca^{2+}]_i$ increase as well as oscillated $[Ca^{2+}]_i$ behaviour in one single cell among three times $[Ca^{2+}]_i$ responses to repeated AVP stimulation. Interestingly, the mixture of two phenotypes of $[Ca^{2+}]_i$ responses to AVP was never observed in one single cell isolated from wild-type mice. More importantly, the oscillatory $[Ca^{2+}]_i$ behaviour was less likely to appear in all BK-KO corticotrophs (22.2%) compared to wild-type (40.0%). These results suggest that BK channels may contribute to regulate the patterns of $[Ca^{2+}]_i$ responses in corticotrophs. Next, the quantification of AVP-evoked $[Ca^{2+}]_i$ responses was performed on male and female BK-KO corticotrophs respectively and the effects of 2 nM AVP on $[Ca^{2+}]_i$ responses in BK-KO corticotrophs were quantified with the same parameters as used in wild-type corticotrophs.

#### 4.2.3.1 Repeated AVP evokes robust $[Ca^{2+}]_i$ responses in male BK-KO corticotrophs

Calcium imaging experiments were performed on male BK-KO corticotrophs (n = 6 from 3 experiments) following the same repeated stimulation protocol used previously for wild-type corticotrophs (see 3.2.4.1).

Stimulation with repeated 2 nM AVP, 2 out of 6 cells showed sustained elevation of $[Ca^{2+}]_i$ (Figure 4.29A, top) and 3 cells had repetitive oscillatory $[Ca^{2+}]_i$ responses (Figure 4.29A, bottom). The remaining 1 cell displayed both sustained $[Ca^{2+}]_i$ increase and oscillatory $[Ca^{2+}]_i$ behaviour following repeated AVP stimulation (data not shown). The mixture of two phenotypes of $[Ca^{2+}]_i$ responses was not observed in the same corticotroph from male wild-type mice. Superposition of extracts of representative calcium imaging traces shown in Figure 4.29B suggested that no matter what types of $[Ca^{2+}]_i$ responses male BK-KO corticotrophs exhibited, either of them was highly reproducible and consistent.

To examine whether the two phenotypes of $[Ca^{2+}]_i$ responses and the mixture of them have significant differences in response to AVP, all parameters were analysed among them. Statistical analysis revealed that none of them had significant differences in any parameters (data not shown). Therefore, statistical analysis was performed on all male BK-KO corticotrophs together. AUC (10 min), AUC (peak) (Figure 4.30), peak, time to peak (Figure 4.31), response duration, peak duration (Figure 4.32) and time gap (Figure 4.33) showed no statistically significant differences following repeated AVP stimulation.

These results revealed that male BK-KO corticotrophs were able to induce consistent

# Figure 4.29

## Repeated AVP induces repeatable $[Ca^{2+}]_i$ responses in male BK-KO corticotrophs

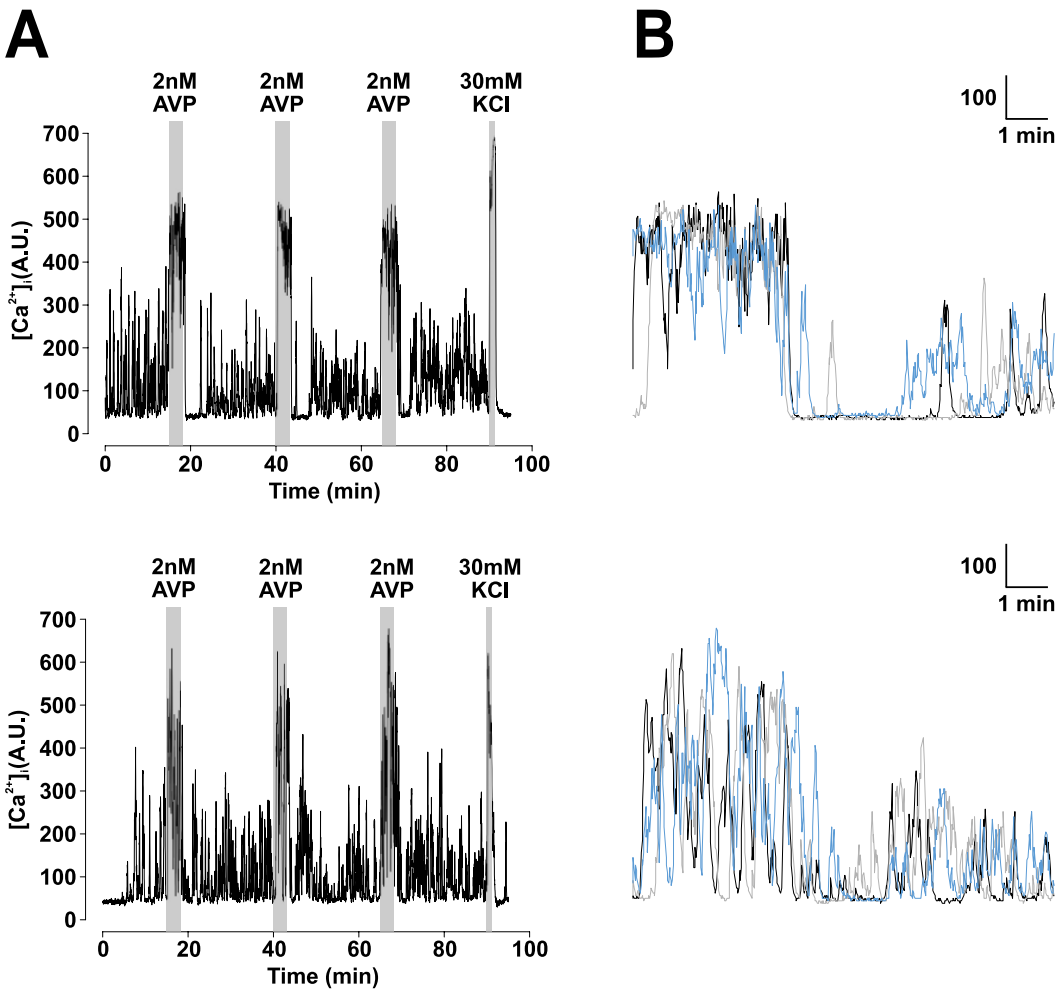


**Figure 4.29 Repeated AVP induces repeatable $[Ca^{2+}]_i$ responses in male BK-KO corticotrophs. (A)** Representative calcium imaging traces of male BK-KO corticotrophs exposed to 2 nM AVP for three minutes and repeated three times at 25 minutes intervals. 30 mM potassium chloride was applied at the end for one minute. **(B)** Superposition of extracts of the two traces shown in A, showing $[Ca^{2+}]_i$ changes in male BK-KO corticotrophs with repeated 2 nM AVP stimulation. Black line shows response to the first stimulus (starting at 15 min), grey line shows response to the second stimulus (starting at 40 min), and blue line shows response to the third stimulus (starting at 65 min).

## Figure 4.30

**Stable AUC (10 min) and AUC (peak) of $[Ca^{2+}]_i$ responses in male BK-KO corticotrophs to repeated AVP**

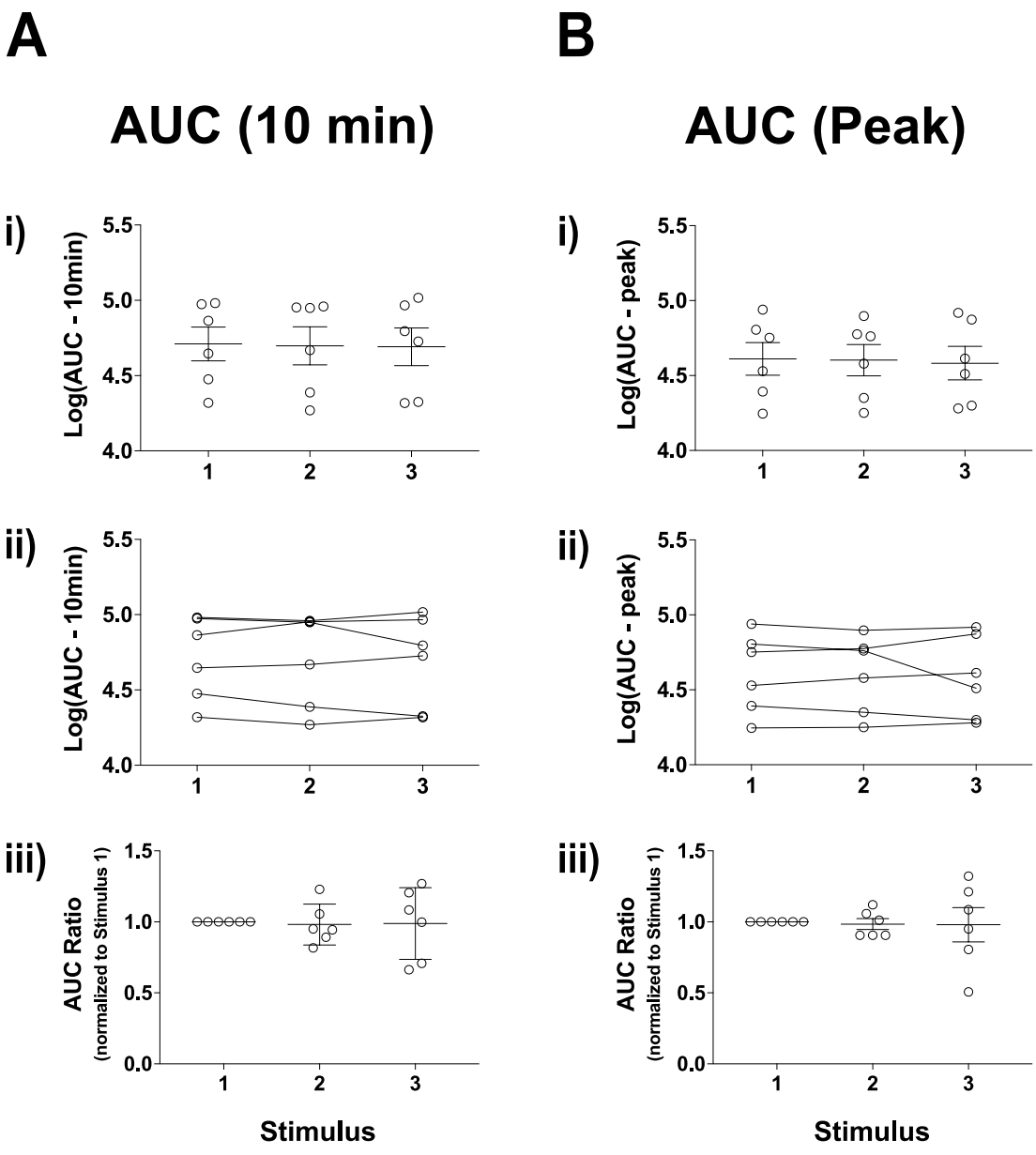


**Figure 4.30 Stable AUC (10 min) and AUC (peak) of $[Ca^{2+}]_i$ responses in male BK-KO corticotrophs to repeated AVP.** Quantification of effects of repeated exposure to 2 nM AVP in **(A)** AUC (10 min) and **(B)** AUC (peak) (n = 6 from 3 experiments, mixed effects model). All data are means ± SEM.

## Figure 4.31

**Peak and time to peak of $[Ca^{2+}]_i$ responses in male BK-KO corticotrophs to repeated AVP**

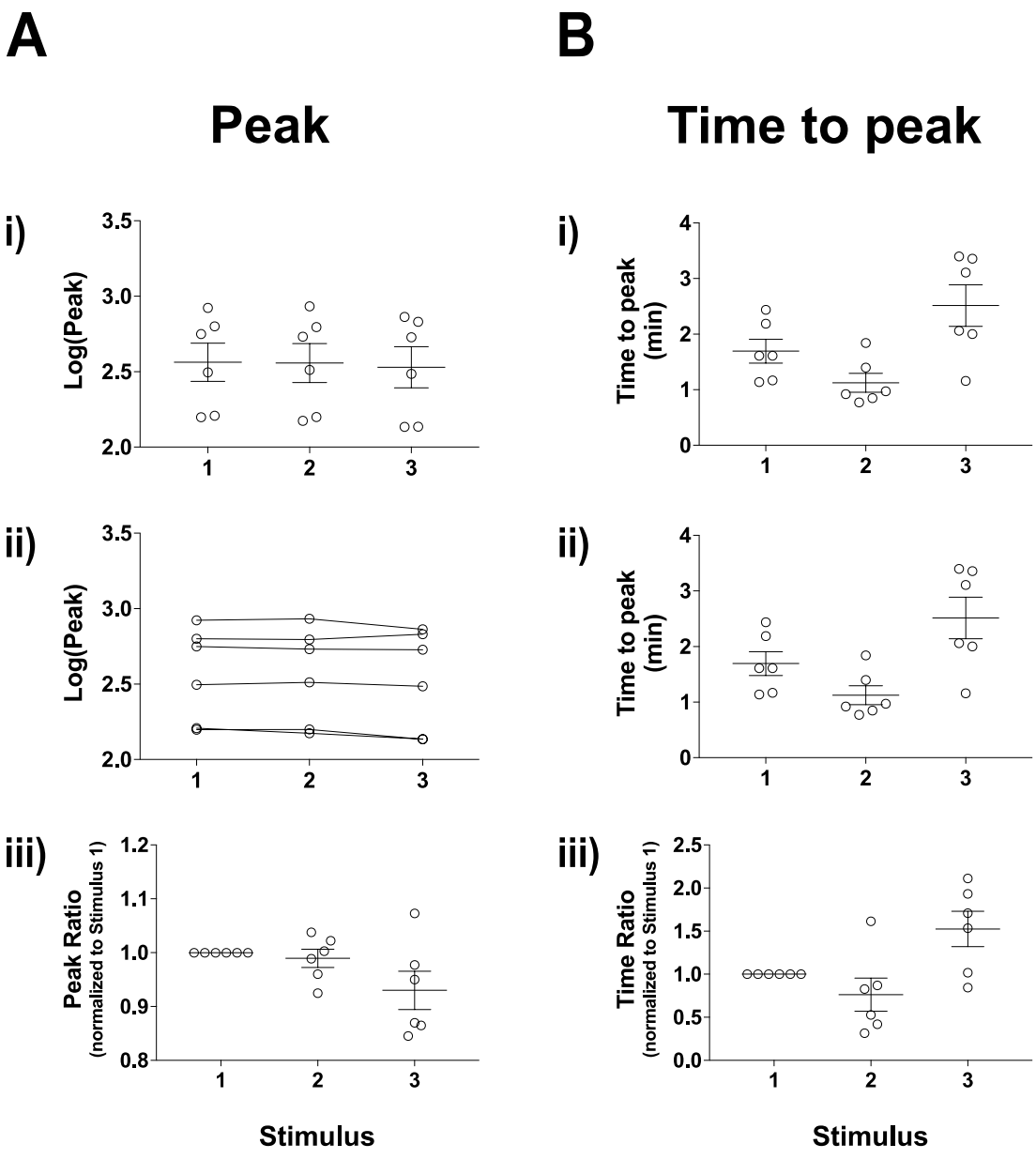


**Figure 4.31 Peak and time to peak of $[Ca^{2+}]_i$ responses in male BK-KO corticotrophs to repeated AVP.** Quantification of effects of repeated exposure to 2 nM AVP in **(A)** peak and **(B)** time to peak (n = 6 from 3 experiments, mixed effects model). All data are means ± SEM.

## Figure 4.32

**Response duration and peak duration of $[Ca^{2+}]_i$ responses in male BK-KO corticotrophs to repeated AVP**

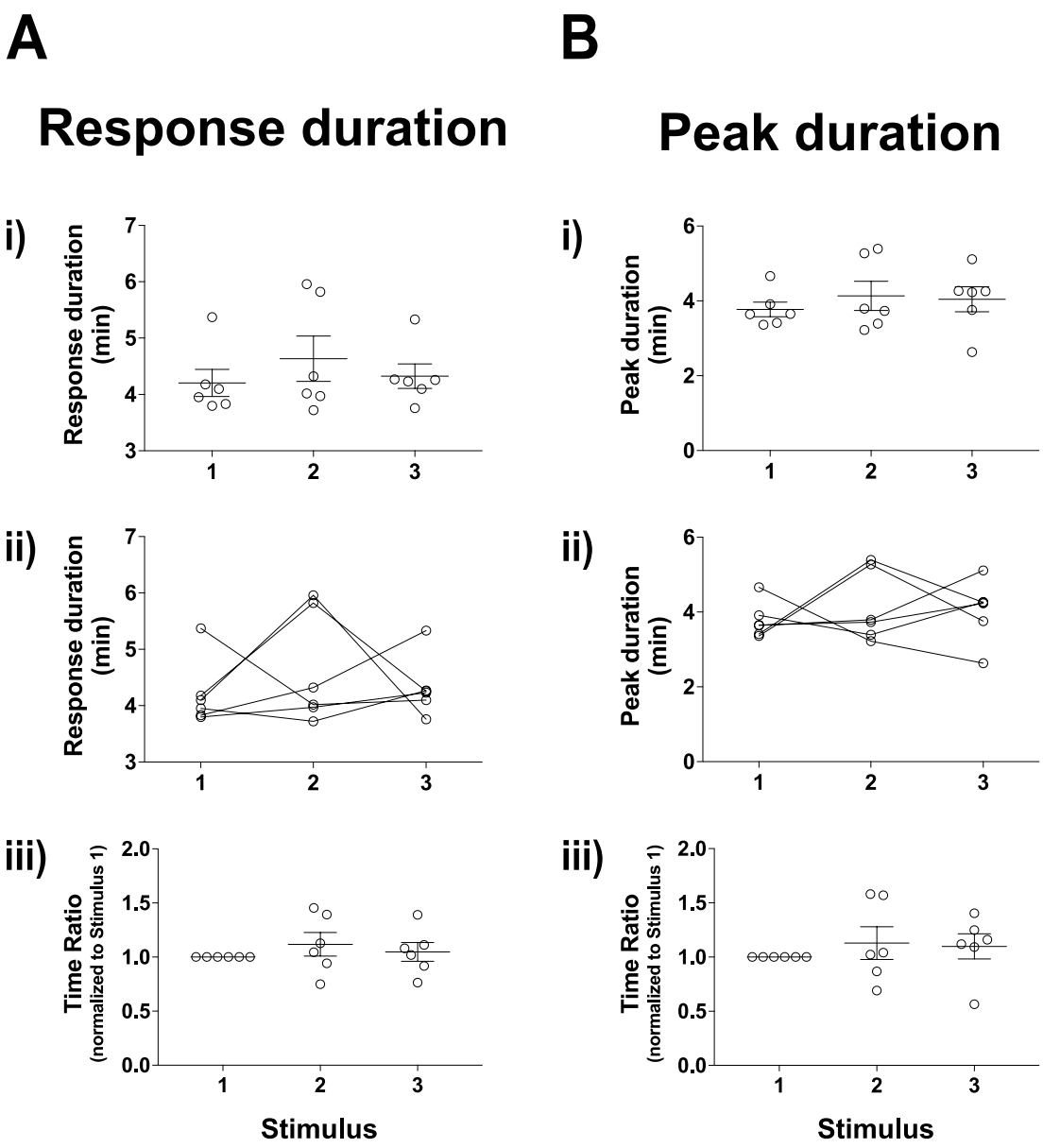


**Figure 4.32 Response duration and peak duration of $[Ca^{2+}]_i$ responses in male BK-KO corticotrophs to repeated AVP.** Quantification of effects of repeated exposure to 2 nM AVP in **(A)** response duration and **(B)** peak duration (n = 6 from 3 experiments, mixed effects model). All data are means ± SEM.

# Figure 4.33

## Time gap of $[Ca^{2+}]_i$ responses in male BK-KO corticotrophs to repeated AVP

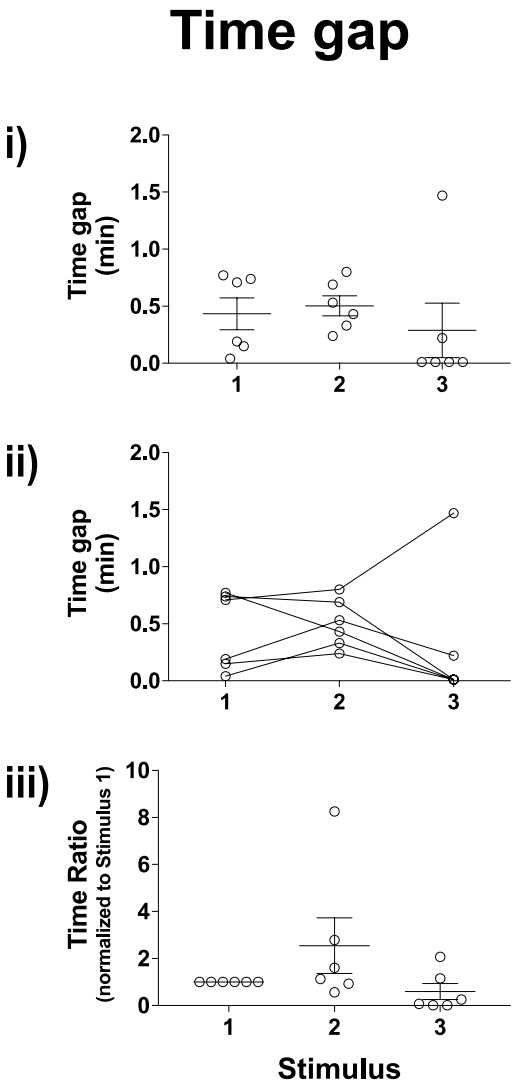


**Figure 4.33 Time gap of $[Ca^{2+}]_i$ responses in male BK-KO corticotrophs to repeated AVP.** Quantification of effects of repeated exposure to 2 nM AVP in time gap (n = 6 from 3 experiments, mixed effects model). All data are means ± SEM.

and repetitive $[Ca^{2+}]_i$ responses when stimulated with repeated 2 nM AVP.

#### 4.2.3.2 Repeated AVP evokes robust $[Ca^{2+}]_i$ responses in female BK-KO corticotrophs

Calcium imaging experiments were performed on female BK-KO corticotrophs (n = 12 from 5 experiments) following the same protocol used in male BK-KO corticotrophs.

Similar to male BK-KO corticotrophs, two phenotypes of $[Ca^{2+}]_i$ responses and the mixture of the two phenotypes were observed in female BK-KO corticotrophs when stimulated with 2 nM AVP. 10 out of 12 cells (83.3%) displayed sustained elevation of $[Ca^{2+}]_i$, whereas oscillatory $[Ca^{2+}]_i$ behaviour and the mixture was only found in 1 single cell (Figure 4.34A). However, 50% of cells responded with a sustained increase $[Ca^{2+}]_i$ and the other 50% showed oscillatory $[Ca^{2+}]_i$ responses in female wild-type corticotrophs. Only 8.3% of female corticotrophs (1/12) showed oscillatory $[Ca^{2+}]_i$ behaviour with genetic deletion of BK channels. In addition, the mixture of the two response patterns was not observed in single female wild-type corticotrophs. The differences between both male and female wild-type and BK-KO corticotrophs suggest that BK channels may be involved in controlling AVP-induced $[Ca^{2+}]_i$ responding patterns in corticotrophs. Extracts of representative calcium traces

# Figure 4.34

## Repeated AVP induces repeatable $[Ca^{2+}]_i$ responses in female BK-KO corticotrophs

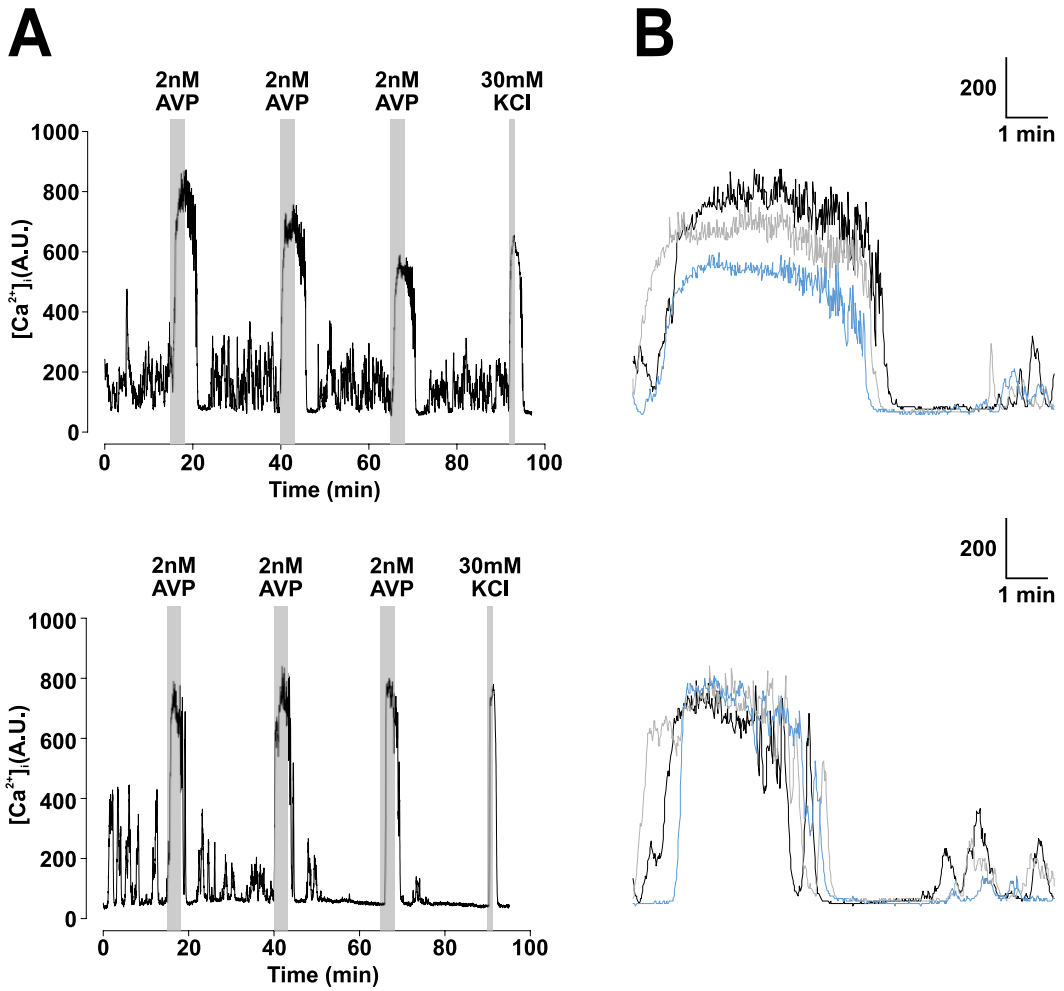


**Figure 4.34 Repeated AVP induces repeatable $[Ca^{2+}]_i$ responses in female BK-KO corticotrophs. (A)** Representative calcium imaging traces of female BK-KO corticotrophs exposed to 2 nM AVP for three minutes and repeated three times at 25 minutes intervals. 30 mM potassium chloride was applied at the end for one minute. **(B)** Superposition of extracts of the two traces shown in A, showing $[Ca^{2+}]_i$ changes in female BK-KO corticotrophs with repeated 2 nM AVP stimulation. Black line shows response to the first stimulus (starting at 15 min), grey line shows response to the second stimulus (starting at 40 min), and blue line shows response to the third stimulus (starting at 65 min).

coincided nicely to each other indicated that $[Ca^{2+}]_i$ responses to repeated 2 nM AVP stimulation were robust and repeatable in female BK-KO corticotrophs (Figure 4.34B).

Two responding phenotypes and the mixture of the two were compared to identify any possible statistical difference. No significant differences were found among sustained elevation of $[Ca^{2+}]_i$, oscillatory $[Ca^{2+}]_i$ behaviour and the mixture (data not shown). Thus, the effects of repeated AVP on $[Ca^{2+}]_i$ responses in female BK-KO corticotrophs were quantified on all calcium recordings together. Statistical analysis revealed that there were no significant differences between repeated AVP stimulation for AUC (10 min), AUC (peak) (Figure 4.35), peak, time to peak (Figure 4.36), response duration, peak duration (Figure 4.37) or time gap (Figure 4.38).

These results suggest that $[Ca^{2+}]_i$ responses evoked by repeated 2 nM AVP stimulation were stable and reproducible in female BK-KO corticotrophs.

#### 4.2.3.3 Female BK-KO corticotrophs have longer response duration and peak duration to repeated AVP stimulation compared to males

Although both male and female BK-KO corticotrophs showed highly consistent and reproducible $[Ca^{2+}]_i$ responses to repeated AVP stimulation, we examined whether there were differences between male and female BK-KO corticotrophs. Statistical

## Figure 4.35

**Stable AUC (10 min) and AUC (peak) of $[Ca^{2+}]_i$ responses in female BK-KO corticotrophs to repeated AVP**

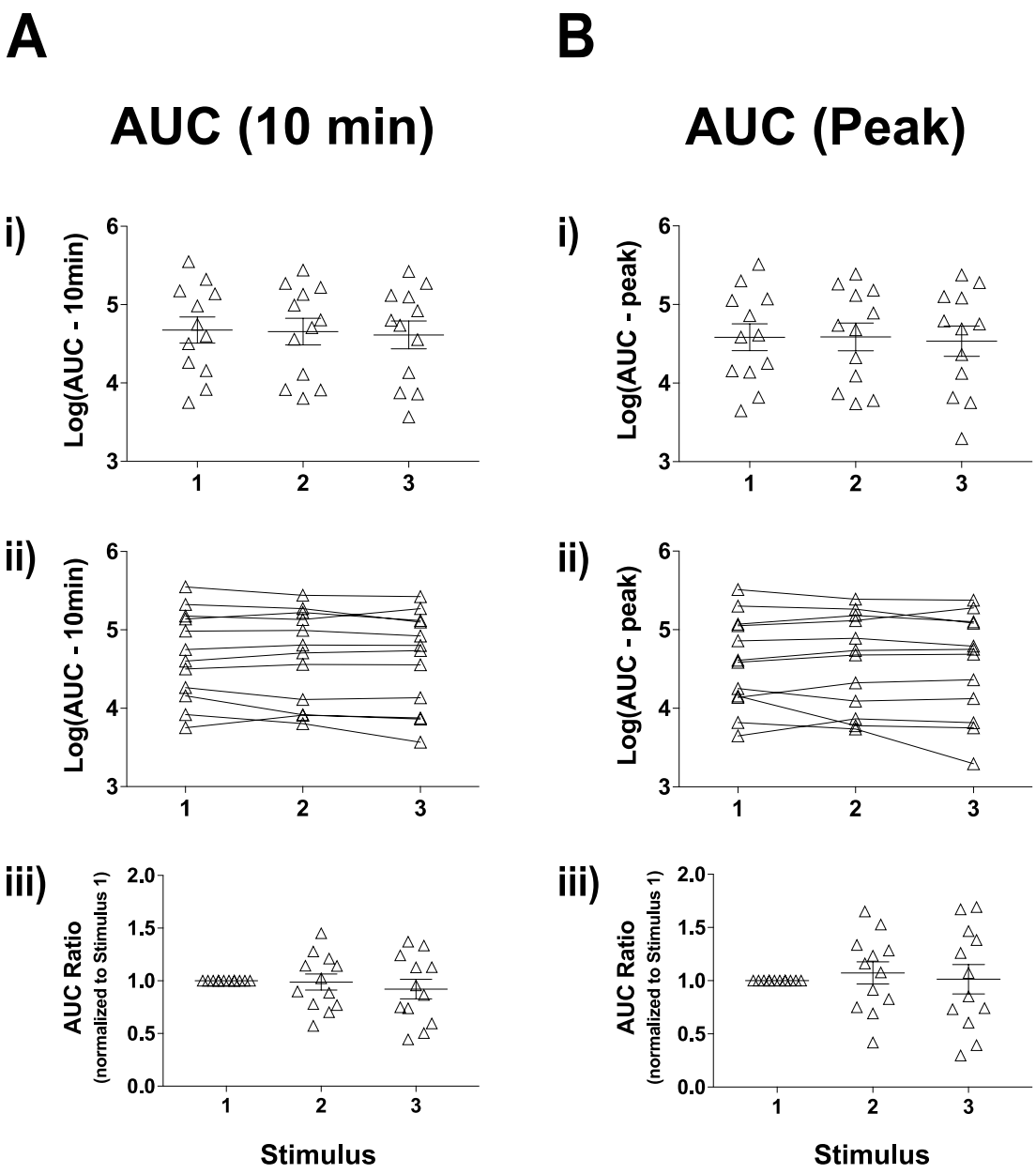


**Figure 4.35 Stable AUC (10 min) and AUC (peak) of $[Ca^{2+}]_i$ responses in female BK-KO corticotrophs to repeated AVP.** Quantification of effects of repeated exposure to 2 nM AVP in **(A)** AUC (10 min) and **(B)** AUC (peak) (n = 12 from 5 experiments, mixed effects model). All data are means ± SEM.

## Figure 4.36

**Peak and time to peak of $[Ca^{2+}]_i$ responses in female BK-KO corticotrophs to repeated AVP**

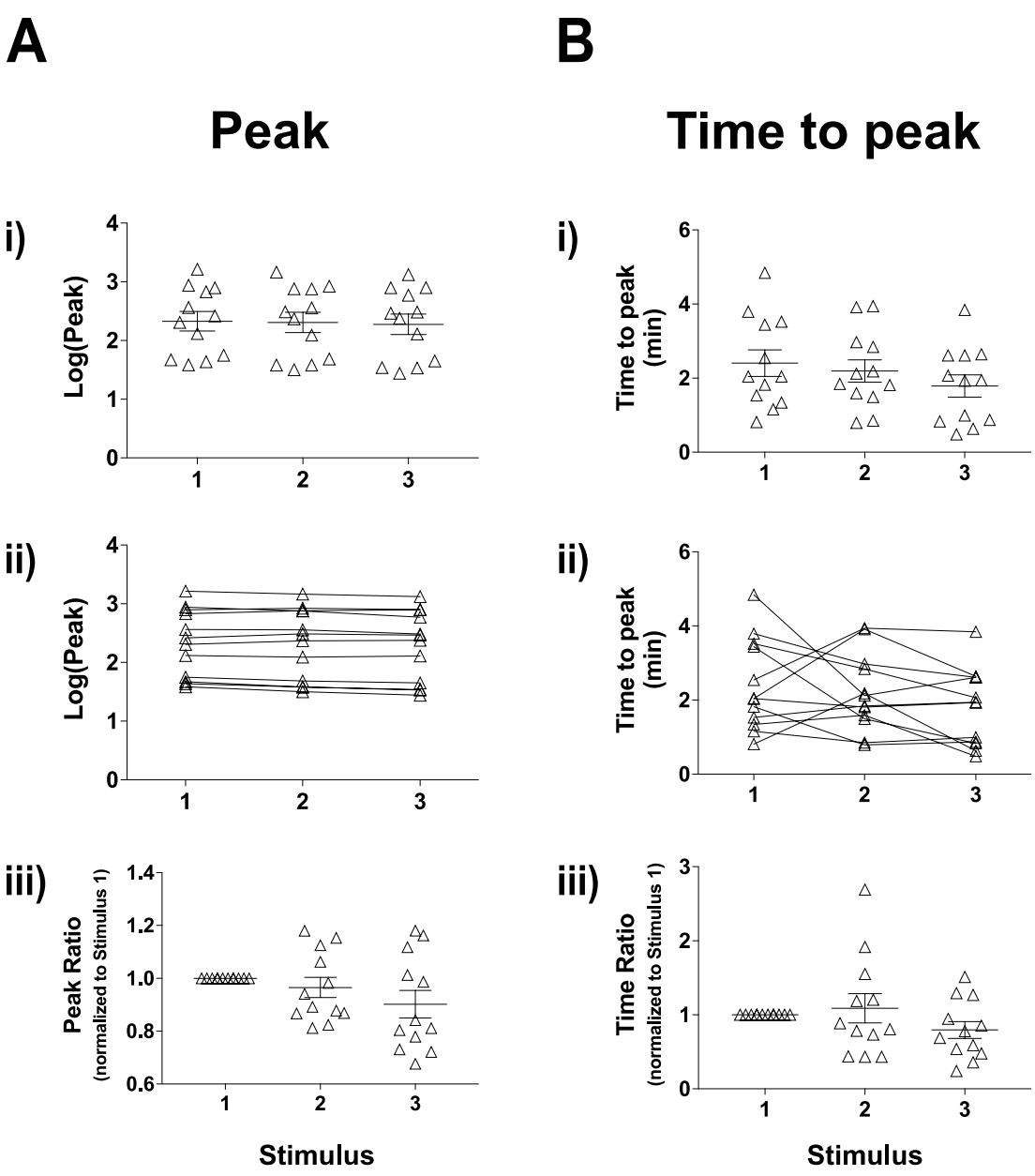


**Figure 4.36 Peak and time to peak of $[Ca^{2+}]_i$ responses in female BK-KO corticotrophs to repeated AVP.** Quantification of effects of repeated exposure to 2 nM AVP in **(A)** peak and **(B)** time to peak (n = 12 from 5 experiments, mixed effects model). All data are means ± SEM.

## Figure 4.37

### Response duration and peak duration of $[Ca^{2+}]_i$ responses in female BK-KO corticotrophs to repeated AVP

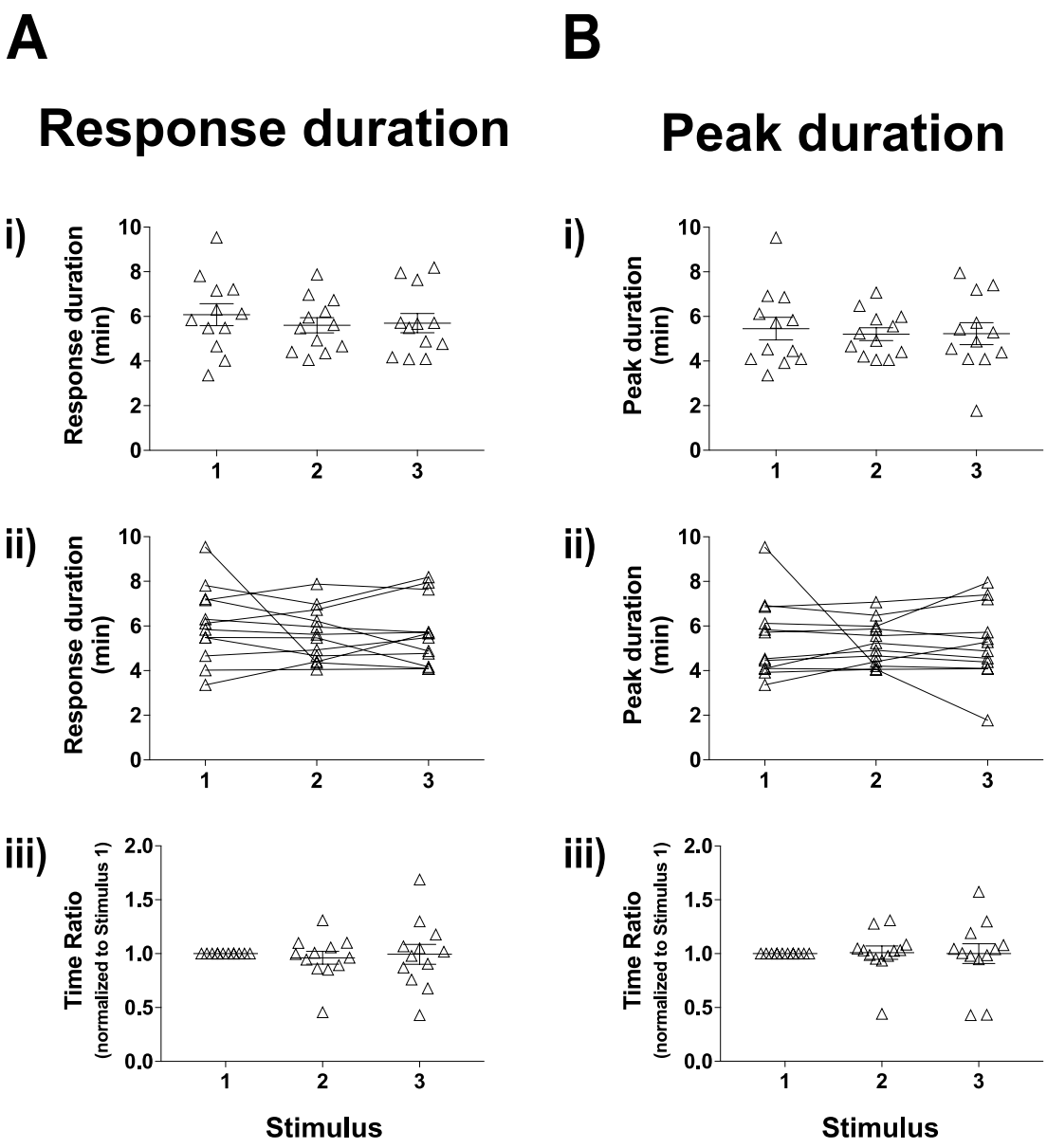


**Figure 4.37 Response duration and peak duration of $[Ca^{2+}]_i$ responses in female BK-KO corticotrophs to repeated AVP.** Quantification of effects of repeated exposure to 2 nM AVP in **(A)** response duration and **(B)** peak duration (n = 12 from 5 experiments, mixed effects model). All data are means ± SEM.

## Figure 4.38

### Time gap of $[Ca^{2+}]_i$ responses in female BK-KO corticotrophs to repeated AVP

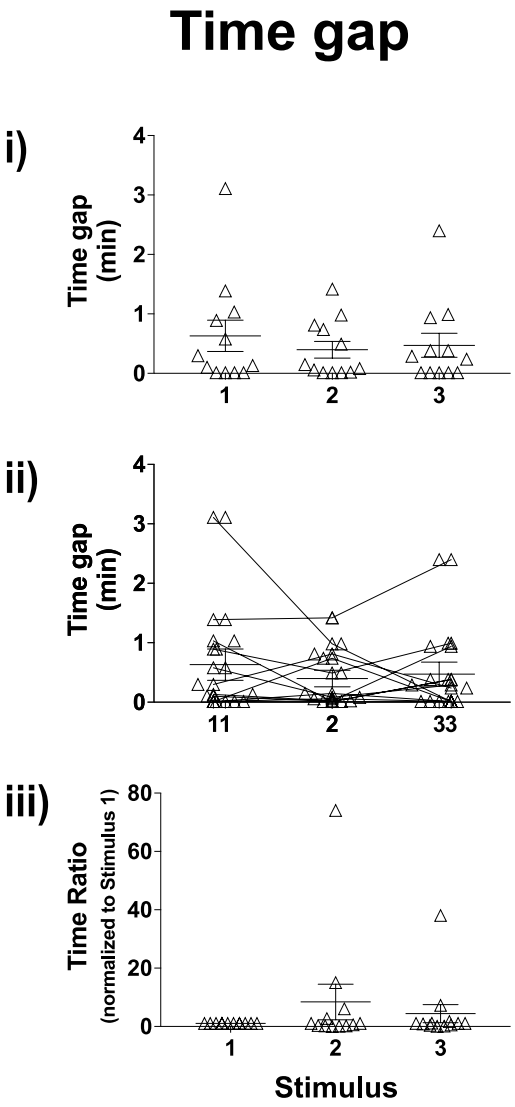


**Figure 4.38 Time gap of $[Ca^{2+}]_i$ responses in female BK-KO corticotrophs to repeated AVP.** Quantification of effects of repeated exposure to 2 nM AVP in time gap (n = 12 from 5 experiments, mixed effects model). All data are means ± SEM.

analysis of all parameters indicated that there were no significant differences between two $[Ca^{2+}]_i$ response phenotypes as well as their mixture (data not shown). Therefore, all calcium imaging experiments were analysed together to determine whether there were sex differences in AVP-induced $[Ca^{2+}]_i$ responses in BK-KO corticotrophs. Following repeated AVP stimulation, female and male BK-KO corticotrophs showed no statistically significant differences in AUC (10 min), AUC (peak) (Figure 4.39), peak, time to peak (Figure 4.40A&B) or time gap (Figure 4.41B). However, there were some significant differences, in particular with lower values in male BK-KO corticotrophs for response duration ($p < 0.01$) (Figure 4.40C) and peak duration ($p < 0.05$) (Figure 4.41A) compared to females in Stimulus 1.

Overall, there were no major sex differences in AVP-induced $[Ca^{2+}]_i$ responses in corticotrophs with a genetic deletion of BK channels.

#### 4.2.3.4 Genetic deletion of BK channels has no significant effect on AVP-induced $[Ca^{2+}]_i$ responses in male corticotrophs

Both male wild-type and BK-KO corticotrophs displayed highly reproducible $[Ca^{2+}]_i$ responses to repeated AVP stimulation. To investigate whether genetic deletion of BK channels would affect AVP-induced $[Ca^{2+}]_i$ responses in male corticotrophs, comparison and statistical analysis of each parameter were performed between male

## Figure 4.39

### No significant sex difference in AVP-induced AUC (10 min) or AUC (peak) of $[Ca^{2+}]_i$ responses in BK-KO corticotrophs

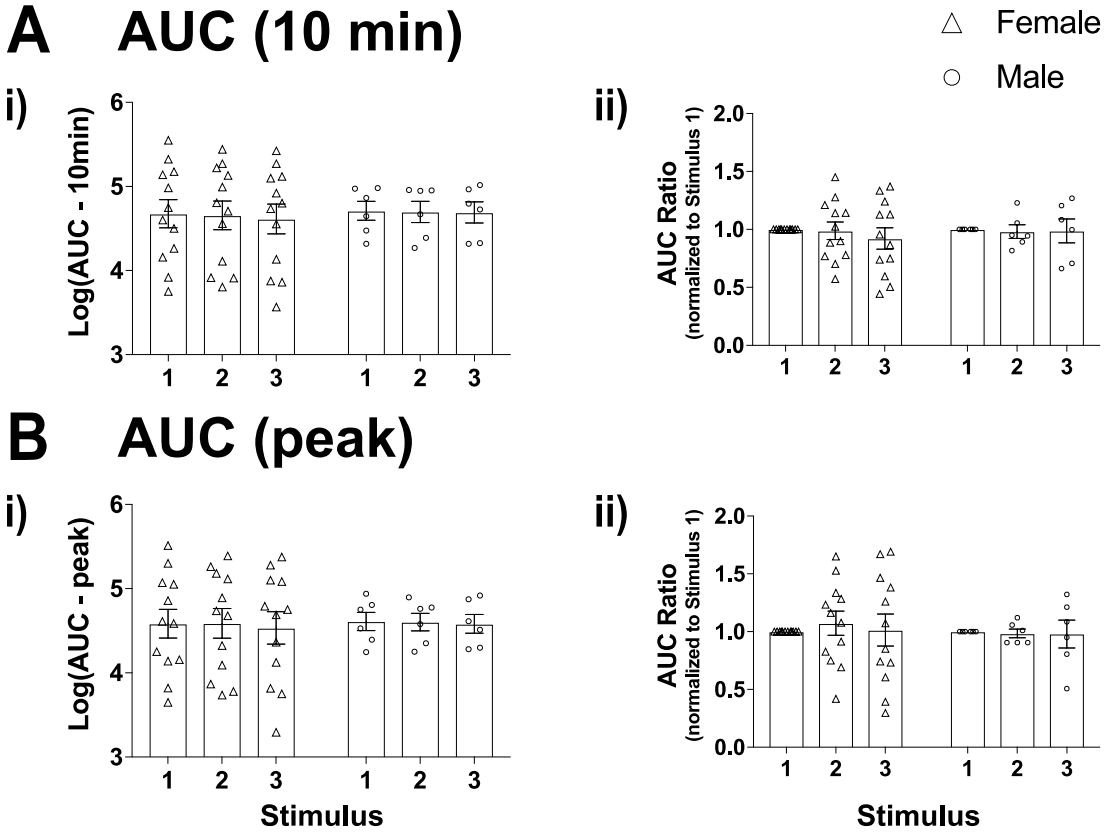


**Figure 4.39 No significant sex difference in AVP-induced AUC (10 min) or AUC (peak) of $[Ca^{2+}]_i$ responses in BK-KO corticotrophs.** Quantification of effects of repeated exposure to 2 nM AVP in **(A)** AUC (10 min) and **(B)** AUC (peak) (male n = 6 from 3 experiments, female n = 12 from 5 experiments, mixed effects model). All data are means ± SEM.

## Figure 4.40

**Female BK-KO corticotrophs have longer response duration but not peak or time to peak of $[Ca^{2+}]_i$ responses to repeated AVP compared to males**

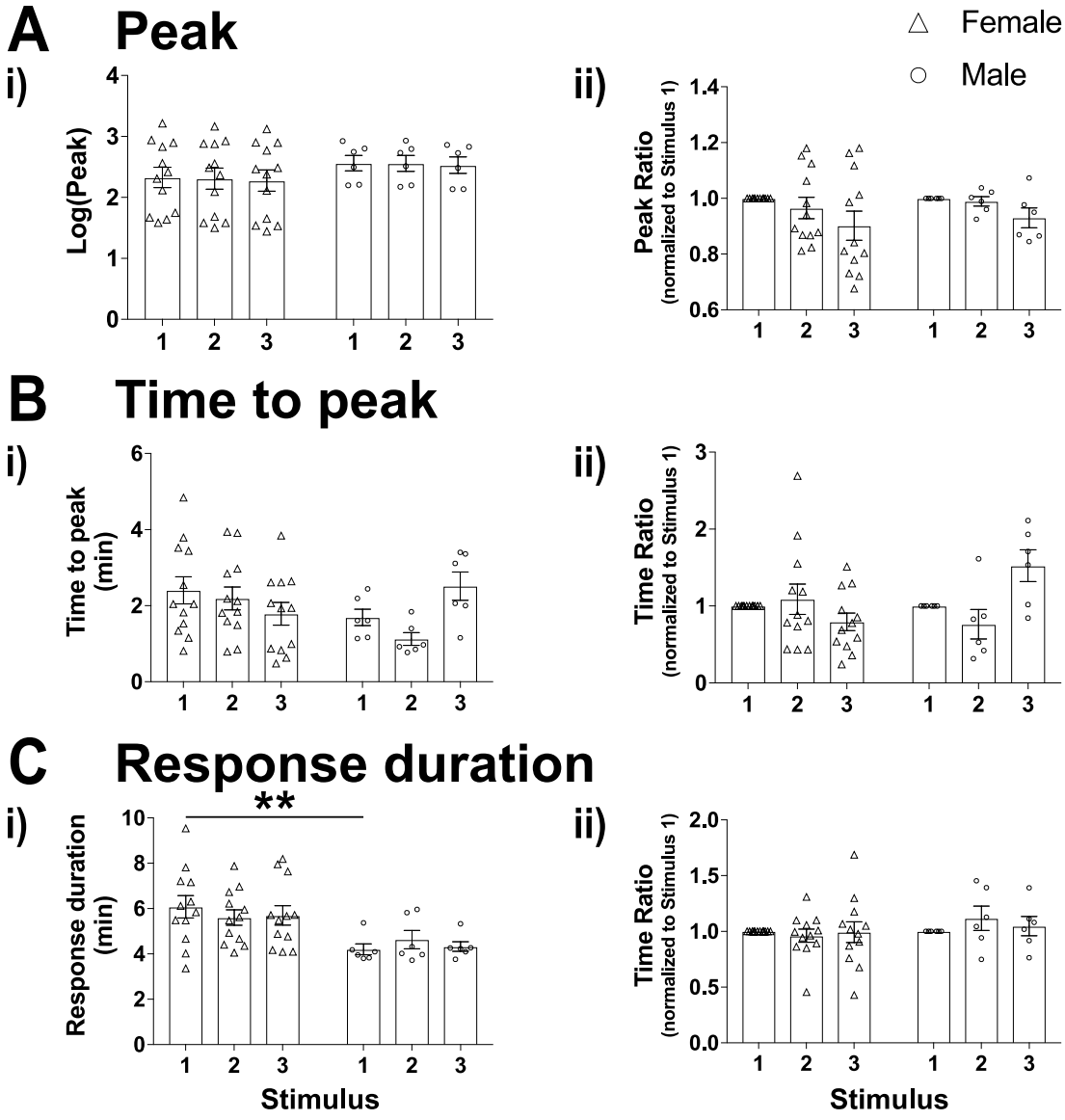


**Figure 4.40 Female BK-KO corticotrophs have longer response duration but not peak or time to peak of $[Ca^{2+}]_i$ responses to repeated AVP compared to males.** Quantification of effects of repeated exposure to 2 nM AVP in **(A)** peak, **(B)** time to peak and **(C)** response duration. ** $p < 0.01$ (male n = 6 from 3 experiments, female n = 12 from 5 experiments, mixed effects model). All data are means ± SEM.

## Figure 4.41

**Female BK-KO corticotrophs have longer peak duration but not time gap of $[Ca^{2+}]_i$ responses to repeated AVP compared to males**

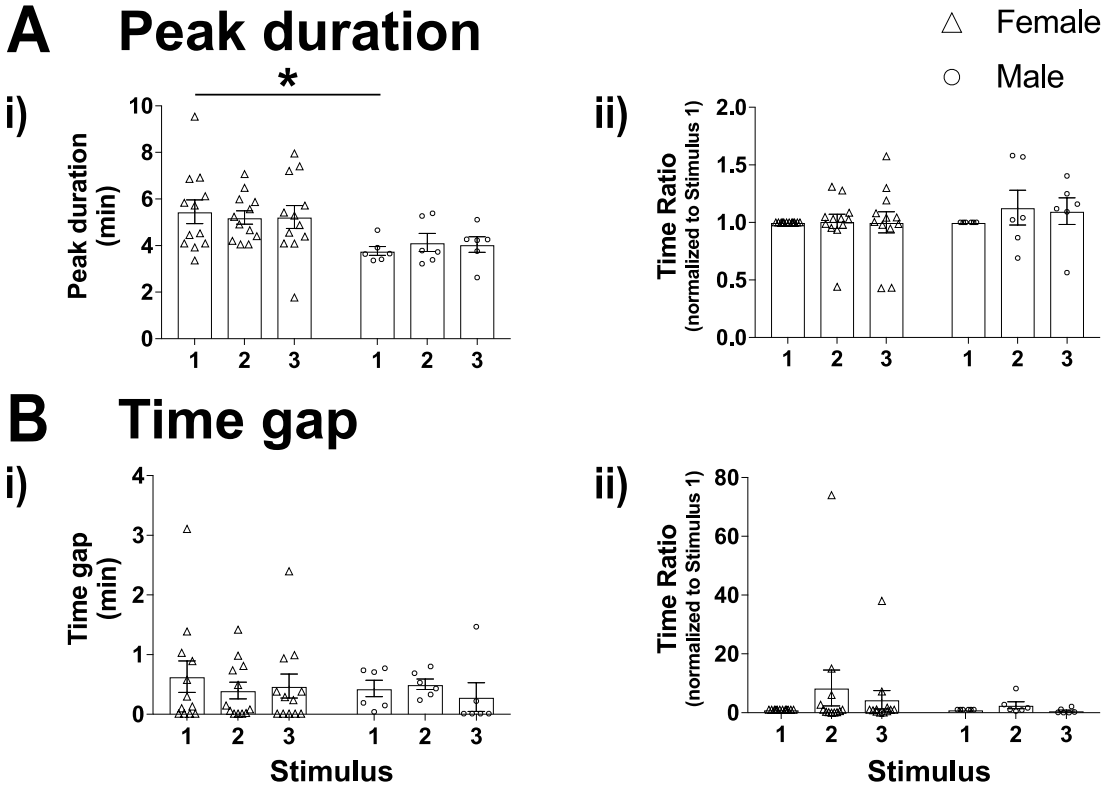


**Figure 4.41 Female BK-KO corticotrophs have longer peak duration but not time gap of $[Ca^{2+}]_i$ responses to repeated AVP compared to males.** Quantification of effects of repeated exposure to 2 nM AVP in **(A)** peak duration and **(B)** time gap. * $p < 0.05$ (male n = 6 from 3 experiments, female n = 12 from 5 experiments, mixed effects model). All data are means ± SEM.

wild-type and BK-KO male corticotrophs.

Statistical analysis revealed that there were no significant differences in AUC (10 min), AUC (peak) (Figure 4.42), peak, time to peak, response duration (Figure 4.43), peak duration or time to peak (Figure 4.44) between male wild-type and BK-KO corticotrophs.

This suggests that genetic deletion of BK channels did not have a significant effect on $[Ca^{2+}]_i$ responses to repeated AVP stimulation in male corticotrophs.

#### 4.2.3.5 AVP-induced response duration and peak duration of $[Ca^{2+}]_i$ responses are significantly different between female wild-type and BK-KO corticotrophs

As observed in male wild-type and BK-KO corticotrophs, there were no significant differences in AUC (10 min), AUC (peak) (Figure 4.45), peak, time to peak (Figure 4.46A&B) or time gap (Figure 4.47B) either. However, female BK-KO corticotrophs displayed significantly ($p < 0.01$) longer response duration (Figure 4.46C) and peak duration (Figure 4.47A) at each stimulus compared to female wild-type corticotrophs.

These results suggest that although female BK-KO corticotrophs could evoke robust

## Figure 4.42

**No significant differences in AVP-induced AUC (10 min) or AUC (peak) of $[Ca^{2+}]_i$ responses between male wild-type and BK-KO corticotrophs**

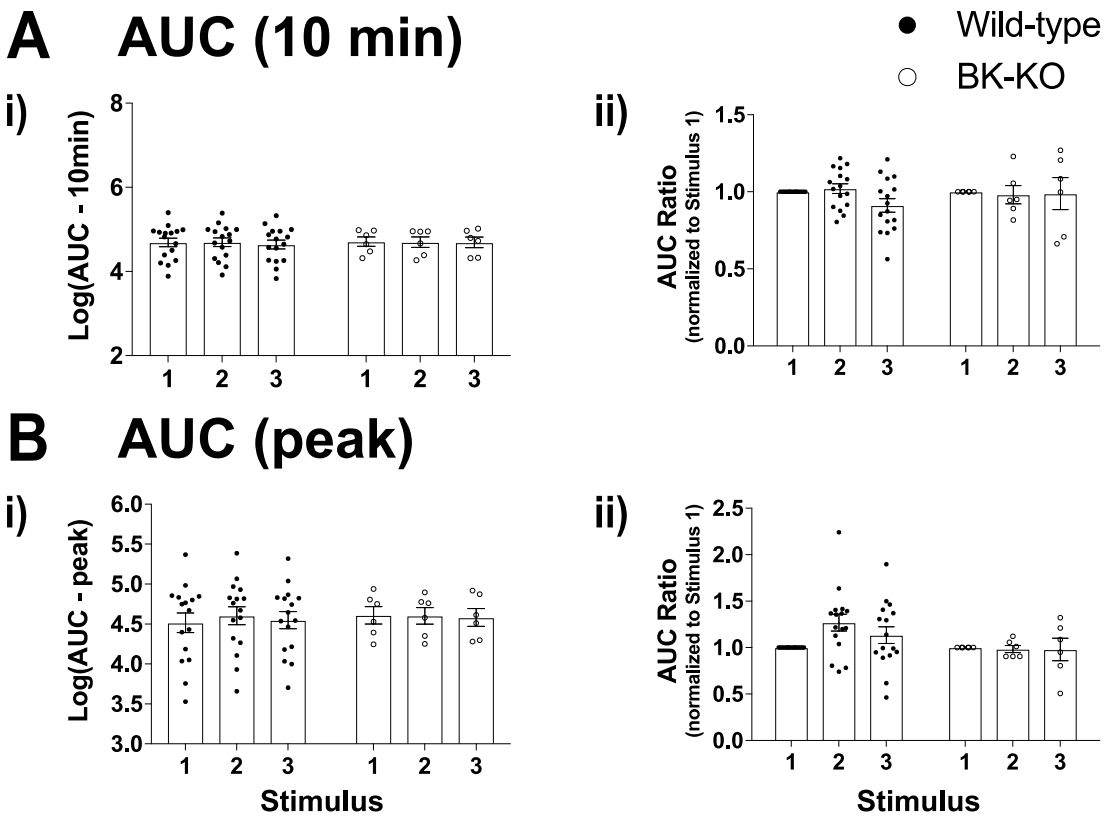


**Figure 4.42 No significant differences in AVP-induced AUC (10 min) and AUC (peak) of $[Ca^{2+}]_i$ responses between male wild-type and BK-KO corticotrophs.** Quantification of effects of repeated exposure to 2 nM AVP in **(A)** AUC (10 min) and **(B)** AUC (peak) (wild-type n = 16 from 9 experiments, BK-KO n = 6 from 3 experiments, mixed effects model). All data are means ± SEM.

## Figure 4.43

**No significant differences in AVP-induced peak, time to peak or response duration of $[Ca^{2+}]_i$ responses between male wild-type and BK-KO corticotrophs**

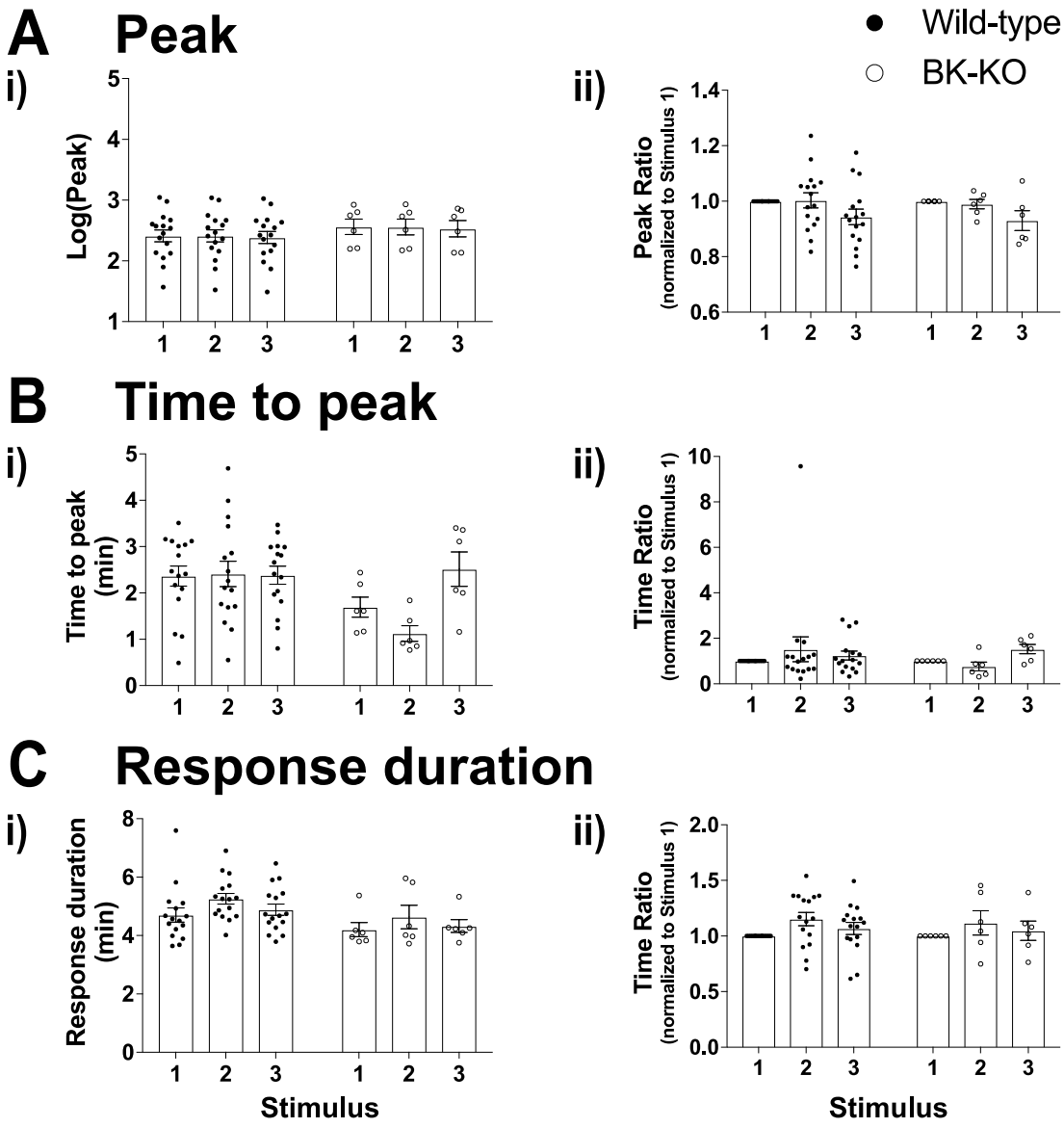


**Figure 4.43 No significant differences in AVP-induced peak, time to peak or response duration of $[Ca^{2+}]_i$ responses between male wild-type and BK-KO corticotrophs.** Quantification of effects of repeated exposure to 2 nM AVP in **(A)** peak, **(B)** time to peak and (C) response duration (wild-type n = 16 from 9 experiments, BK-KO n = 6 from 3 experiments, mixed effects model). All data are means ± SEM.

## Figure 4.44

**No significant differences in AVP-induced peak duration or time gap of $[Ca^{2+}]_i$ responses between male wild-type and BK-KO corticotrophs**

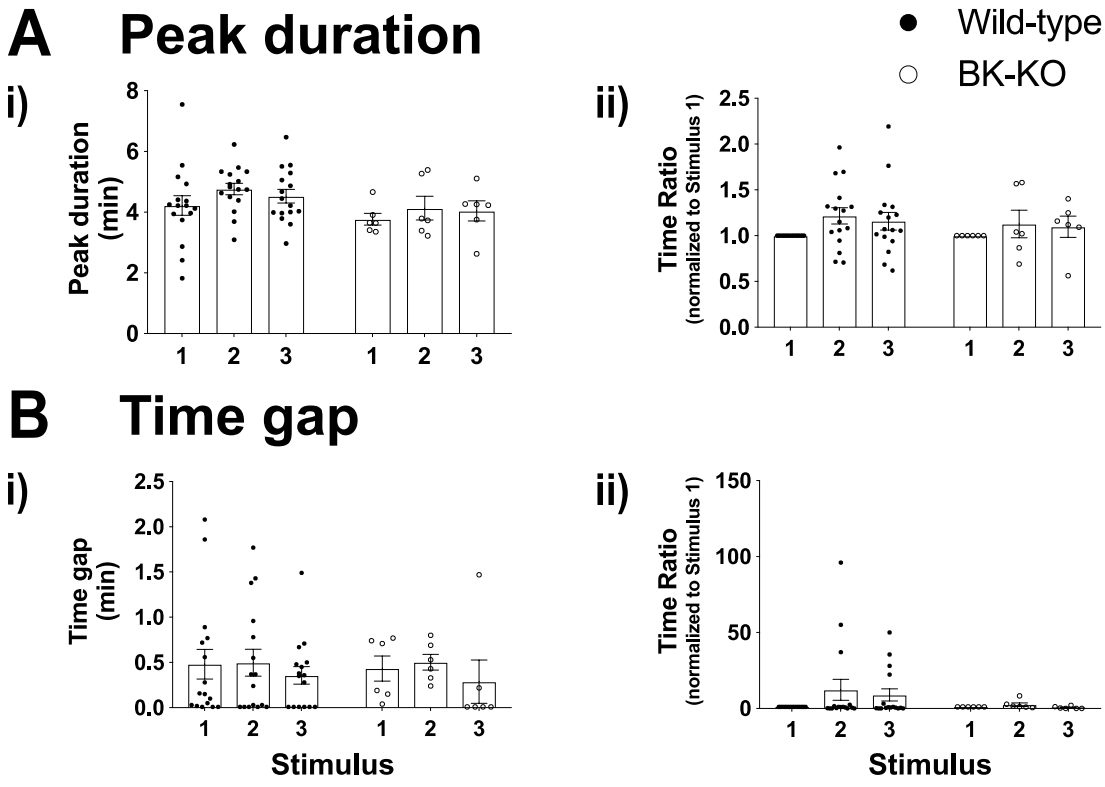


**Figure 4.44 No significant differences in AVP-induced peak duration or time gap of $[Ca^{2+}]_i$ responses between male wild-type and BK-KO corticotrophs.** Quantification of effects of repeated exposure to 2 nM AVP in **(A)** peak duration and **(B)** time gap (wild-type n = 16 from 9 experiments, BK-KO n = 6 from 3 experiments, mixed effects model). All data are means ± SEM.

## Figure 4.45

**No significant differences in AVP-induced AUC (10 min) or AUC (peak) of $[Ca^{2+}]_i$ responses between female wild-type and BK-KO corticotrophs**

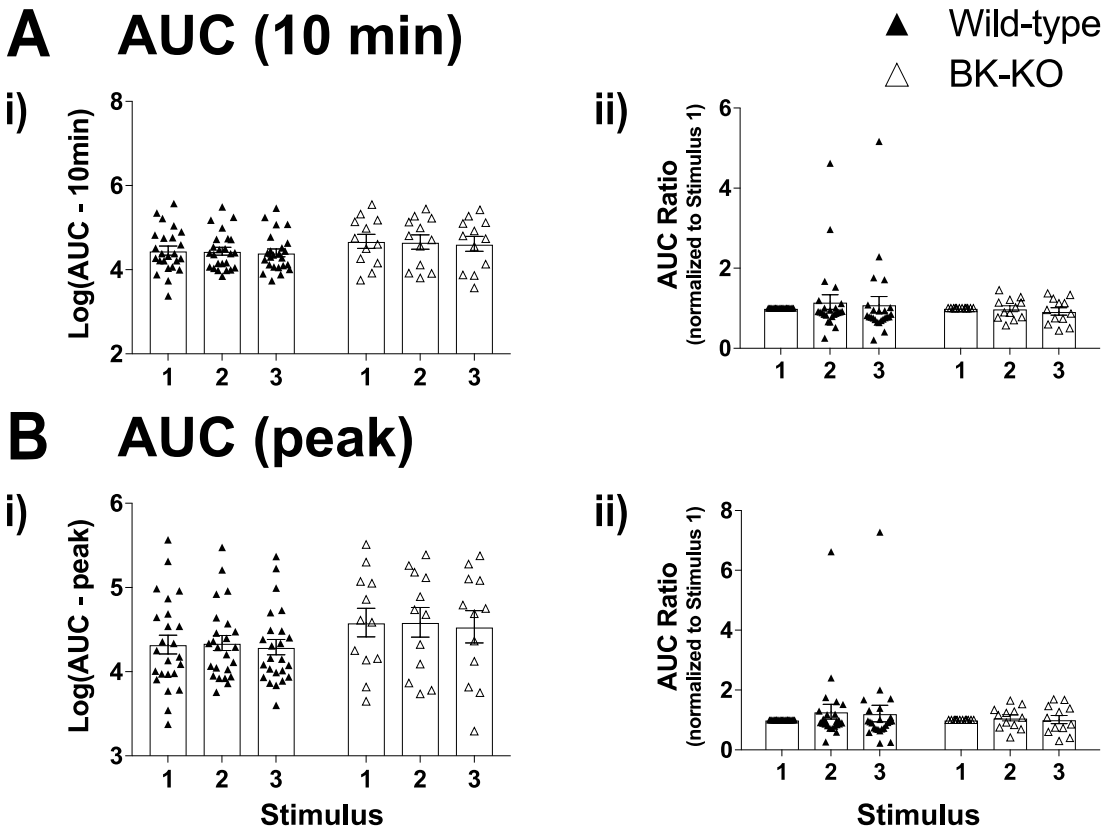


**Figure 4.45 No significant differences in AVP-induced AUC (10 min) and AUC (peak) of $[Ca^{2+}]_i$ responses between female wild-type and BK-KO corticotrophs.** Quantification of effects of repeated exposure to 2 nM AVP in **(A)** AUC (10 min) and **(B)** AUC (peak) (wild-type n = 24 from 8 experiments, BK-KO n = 12 from 5 experiments, mixed effects model). All data are means ± SEM.

## Figure 4.46

**Female BK-KO corticotrophs have longer response duration but not peak or time to peak of $[Ca^{2+}]_i$ responses to repeated AVP compared to female wild-type corticotrophs**

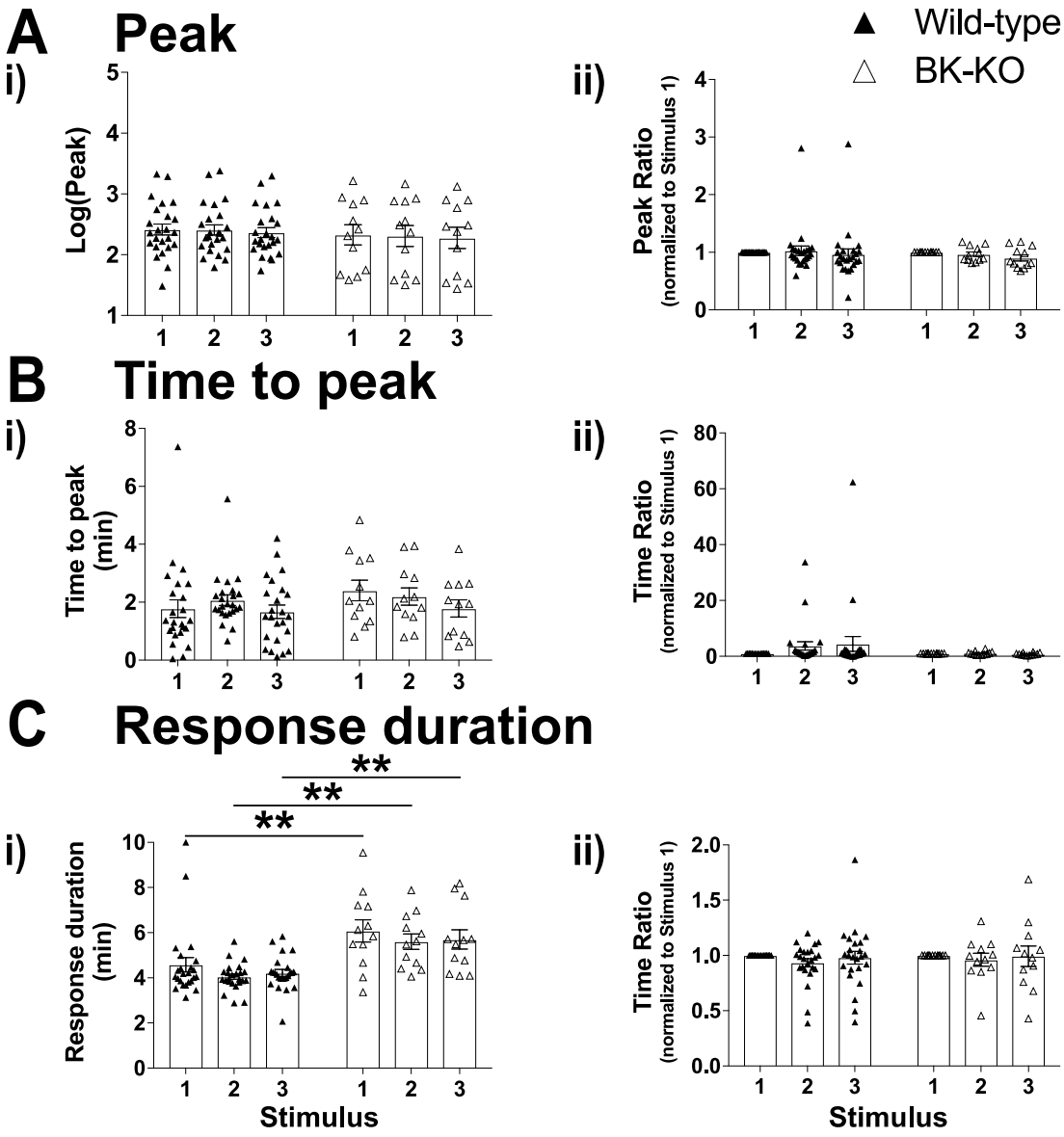


**Figure 4.46 Female BK-KO corticotrophs have longer response duration but not peak or time to peak of $[Ca^{2+}]_i$ responses to repeated AVP compared to female wild-type corticotrophs.** Quantification of effects of repeated exposure to 2 nM AVP in **(A)** peak **(B)** time to peak and **(C)** response duration. ** $p < 0.01$ (wild-type n = 24 from 8 experiments, BK-KO n = 12 from 5 experiments, mixed effects model). All data are means ± SEM.

## Figure 4.47

**Female BK-KO corticotrophs have longer peak duration but not time gap of $[Ca^{2+}]_i$ responses to repeated AVP compared to female wild-type corticotrophs**

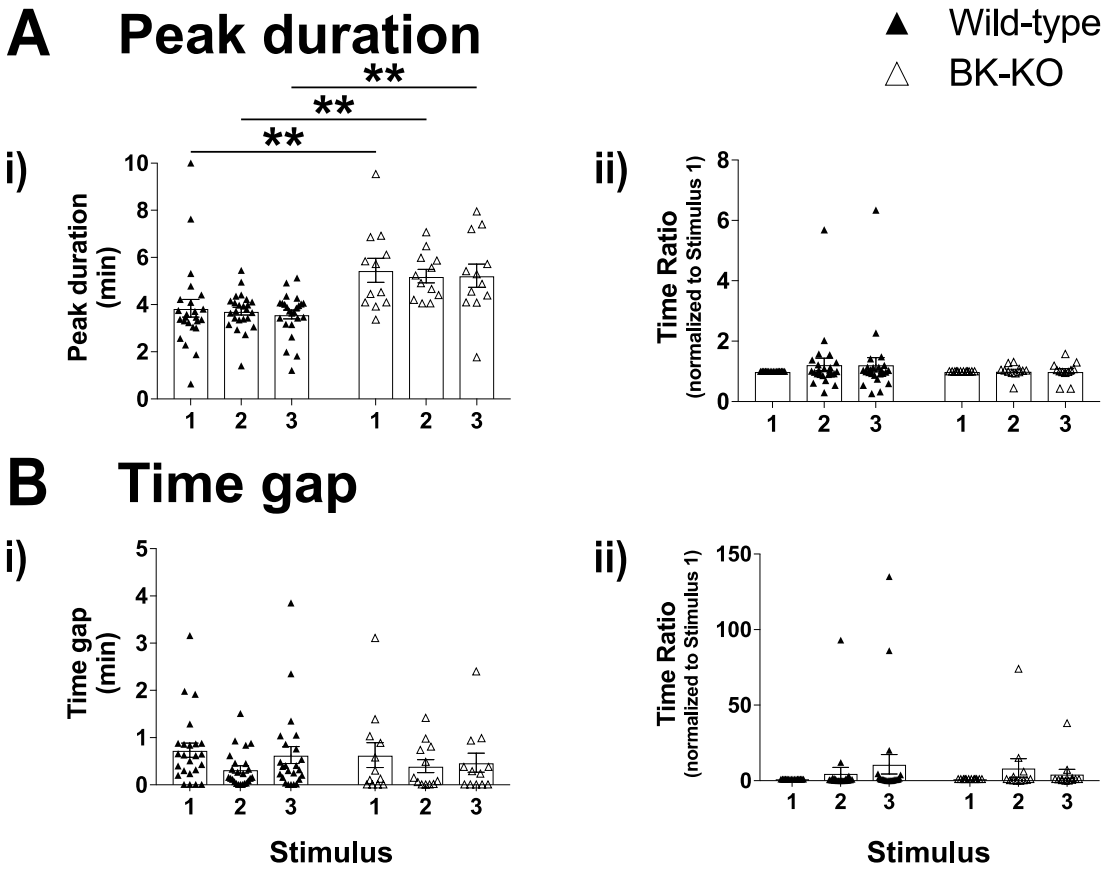


**Figure 4.47 Female BK-KO corticotrophs have longer peak duration but not time gap of $[Ca^{2+}]_i$ responses to repeated AVP compared to female wild-type corticotrophs.** Quantification of effects of repeated exposure to 2 nM AVP in **(A)** peak duration and **(B)** time gap (wild-type n = 24 from 8 experiments, BK-KO n = 12 from 5 experiments, mixed effects model). All data are means ± SEM.

$[Ca^{2+}]_i$ responses as female wild-type corticotrophs, genetic deletion of BK channels resulted in a significantly longer response duration and peak duration to repeated AVP stimulation in female corticotrophs.

Overall, both male and female BK-KO corticotrophs had robust and consistent $[Ca^{2+}]_i$ responses to repeated AVP stimulation as wild-type corticotrophs. Genetic deletion of BK channels had no significant effect on AVP-induced $[Ca^{2+}]_i$ responses in male corticotrophs. However, response duration and peak duration were significantly increased in female BK-KO corticotrophs in all three stimuli. Stable AUC (10 min), AUC (peak) and peak suggest that AVP-induced $[Ca^{2+}]_i$ responses are independent of BK channels and genetic deletion of BK channels may affect male and female corticotrophs differently.

### 4.2.4 Do BK-KO corticotrophs display synergy between CRH and AVP at the level of intracellular free calcium?

Previous study in Chapter Three indicated that there was no synergistic $[Ca^{2+}]_i$ responses between CRH and AVP in male wild-type corticotrophs. Although no statistical synergy was observed in female wild-type corticotrophs at the population level, 26.7% (4 out of 15 cells) of cells displayed synergistic $[Ca^{2+}]_i$ responses to CRH and AVP at the single cell level. Thus, we investigated whether there were synergistic

$[Ca^{2+}]_i$ responses between CRH and AVP in BK-KO corticotrophs. The experiments were only performed on female BK-KO corticotrophs as synergy was only observed in female wild-type corticotrophs.

#### 4.2.4.1 No synergistic $[Ca^{2+}]_i$ response between CRH and AVP in female BK-KO corticotrophs at the population level

Calcium imaging experiments were performed on female BK-KO corticotrophs following the repeated stimulation protocol used in female wild-type corticotrophs (see 3.2.5.2). To counteract the possible influence due to the sequence of the two single stimuli, the order of CRH and AVP was randomized (CRH, AVP, combination, n = 10 or AVP, CRH, combination, n = 11 from 6 experiments).

All female BK-KO corticotrophs displayed sustained elevation of $[Ca^{2+}]_i$ to individual 0.2 nM CRH stimulation despite of the order of two single stimuli, which was similar to $[Ca^{2+}]_i$ responses to repeated CRH stimulation. When stimulated with 2 nM AVP alone, two phenotypes of $[Ca^{2+}]_i$ responses were observed as before. 61.9% (13 out of 21) of female BK-KO corticotrophs displayed sustained $[Ca^{2+}]_i$ elevation, which was more than female wild-type corticotrophs (53.3%). The remaining 8 cells (38.1%) responded with oscillatory $[Ca^{2+}]_i$ behaviour, which was slightly less than female wild-type corticotrophs (46.7%) showing oscillatory $[Ca^{2+}]_i$ behaviour. Stimulation

with the combination of 0.2 nM CRH and 2 nM AVP, female BK-KO corticotrophs exhibited sustained and significant $[Ca^{2+}]_i$ increase, no matter what the exposure order and AVP-induced $[Ca^{2+}]_i$ responding patterns were (Figure 4.48A & Figure 4.49A). Although AVP evoked two phenotypes of $[Ca^{2+}]_i$ responses, extracts of representative calcium imaging traces suggested that $[Ca^{2+}]_i$ changes were coincident when responding to two single stimuli and combined stimulus following either stimulation sequence (Figure 4.48B & Figure 4.49B).

The synergistic $[Ca^{2+}]_i$ responses and the effects of two single stimuli and combined stimulus on $[Ca^{2+}]_i$ responses were evaluated with the same parameters used in wild-type corticotrophs. As the comparison between the AUC of the combined stimulus and the sum of the AUC of the two single stimuli was used to determine synergistic $[Ca^{2+}]_i$ responses, AUC (10 min) and AUC (peak) were analysed between AVP-induced sustained elevation of $[Ca^{2+}]_i$ (n = 13) and oscillatory $[Ca^{2+}]_i$ behaviour (n = 8) first. Statistical analysis revealed that female BK-KO corticotrophs showed no significant differences between the two $[Ca^{2+}]_i$ response phenotypes in either AUC (10 min) or AUC (peak) (data not shown). Therefore, statistical analysis was performed on all female BK-KO corticotrophs together. The statistical calculation of AUC (10 min), AUC (peak) and peak was performed on log-transformed data and the others were performed on raw data.

# Figure 4.48

## CRH, AVP and CRH/AVP induce $[Ca^{2+}]_i$ responses in female BK-KO corticotrophs

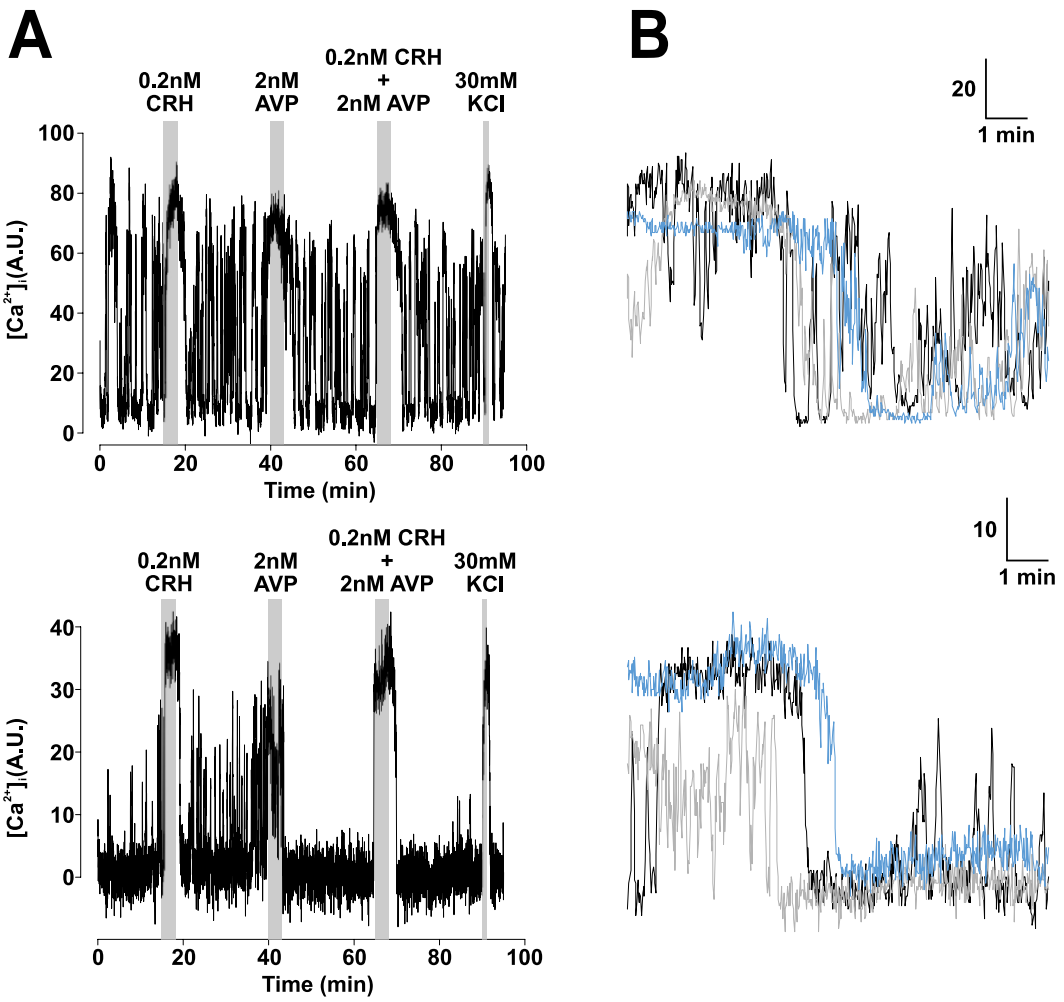


**Figure 4.48 CRH, AVP and CRH/AVP induce $[Ca^{2+}]_i$ responses in female BK-KO corticotrophs. (A)** Representative calcium imaging traces of female BK-KO corticotrophs exposed to 0.2 nM CRH, 2 nM AVP and 0.2 nM CRH together with 2 nM AVP at 25 minutes intervals. 30 mM potassium chloride was applied at the end for one minute. **(B)** Superposition of extracts of the two traces shown in A, showing $[Ca^{2+}]_i$ changes in female BK-KO corticotrophs with stimuli. Black line shows response to 0.2 nM CRH (starting at 15 min), grey line shows response to 2 nM AVP (starting at 40 min), and blue line shows response to the combined stimulus (starting at 65 min).

## Figure 4.49

### AVP, CRH and CRH/AVP induce $[Ca^{2+}]_i$ responses in female BK-KO corticotrophs

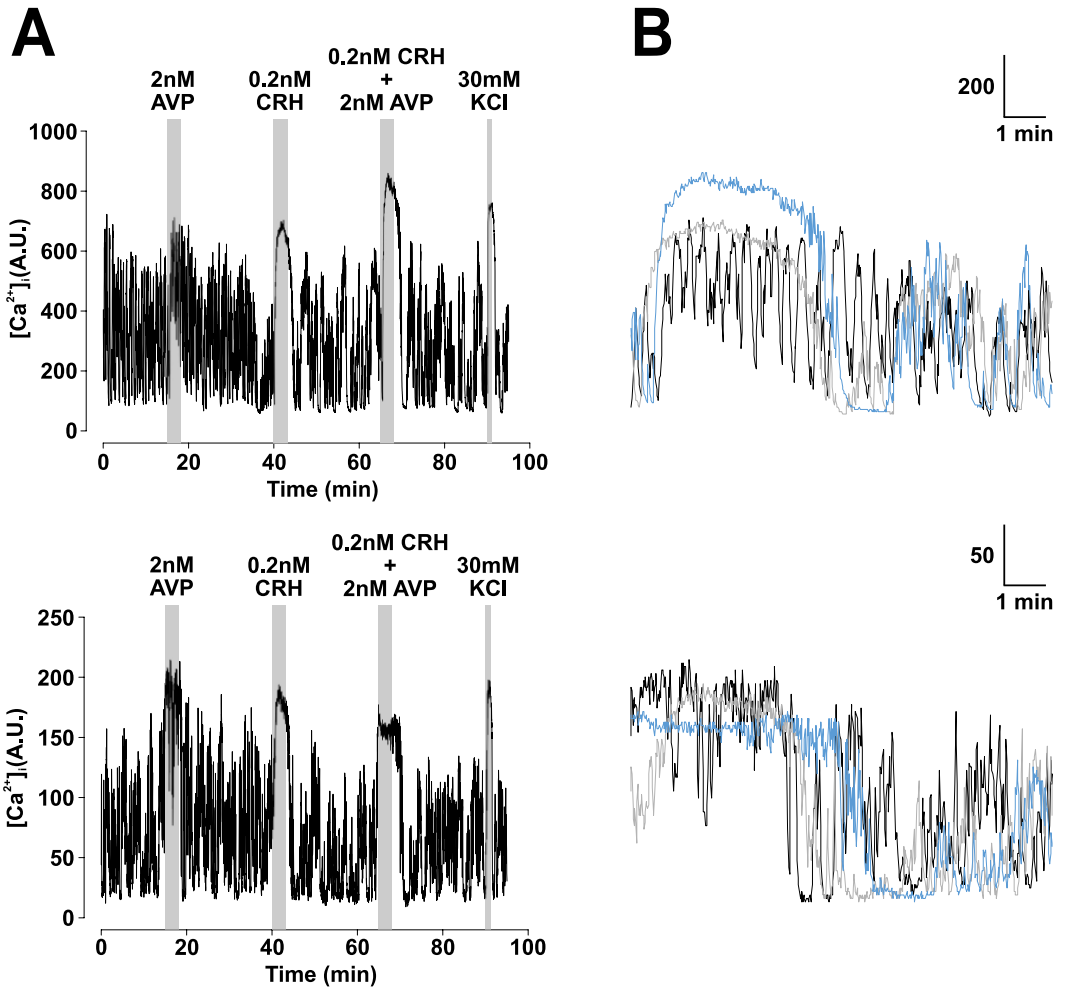


**Figure 4.49 AVP, CRH and CRH/AVP induce $[Ca^{2+}]_i$ responses in female BK-KO corticotrophs.** **(A)** Representative calcium imaging traces of female BK-KO corticotrophs exposed to 2 nM AVP, 0.2 nM CRH and 0.2 nM CRH together with 2 nM AVP at 25 minutes intervals. 30 mM potassium chloride was applied at the end for one minute. **(B)** Superposition of extracts of the two traces shown in A, showing $[Ca^{2+}]_i$ changes in female BK-KO corticotrophs with stimuli. Black line shows response to 2 nM CRH (starting at 15 min), grey line shows response to 0.2 nM AVP (starting at 40 min), and blue line shows response to the combined stimulus (starting at 65 min).

There were no statistically significant differences among the $[Ca^{2+}]_i$ responses induced by CRH, AVP and the combined stimulus in AUC (10 min) or AUC (peak). However, the combined stimulus was significantly ($p < 0.001$) smaller than the sum of the two single stimuli in both AUC (10 min) and AUC (peak). These data suggest that female BK-KO corticotrophs did not show synergy between CRH and AVP at the level of $[Ca^{2+}]_i$. Although the synergistic $[Ca^{2+}]_i$ responses were not observed at the population level, in 1 out of 21 cells (4.8%), AUC (10 min) as well as AUC (peak) of the combined stimulus was larger than the sum of the two single stimuli (Figure 4.50). Peak or time to peak were not significantly different between the two single stimuli and combined stimulus (Figure 4.51A&B). Stimulation with AVP resulted in a shorter response duration, which was significantly ($p < 0.05$) different from CRH stimulus but not combined stimulus (Figure 4.51C). There were no significant differences in peak duration or time gap among CRH-, AVP- and CRH/AVP-induced $[Ca^{2+}]_i$ responses either (Figure 4.52).

These results suggest that there were no synergistic $[Ca^{2+}]_i$ responses between CRH and AVP at the population level in female BK-KO corticotrophs. However, a reduced proportion of female BK-KO corticotrophs (4.8%) showed synergistic $[Ca^{2+}]_i$ responses at single cell level compared to wild-type female corticotrophs (26.7%).

## Figure 4.50

### No synergistic $[Ca^{2+}]_i$ responses to CRH/AVP in female BK-KO corticotrophs

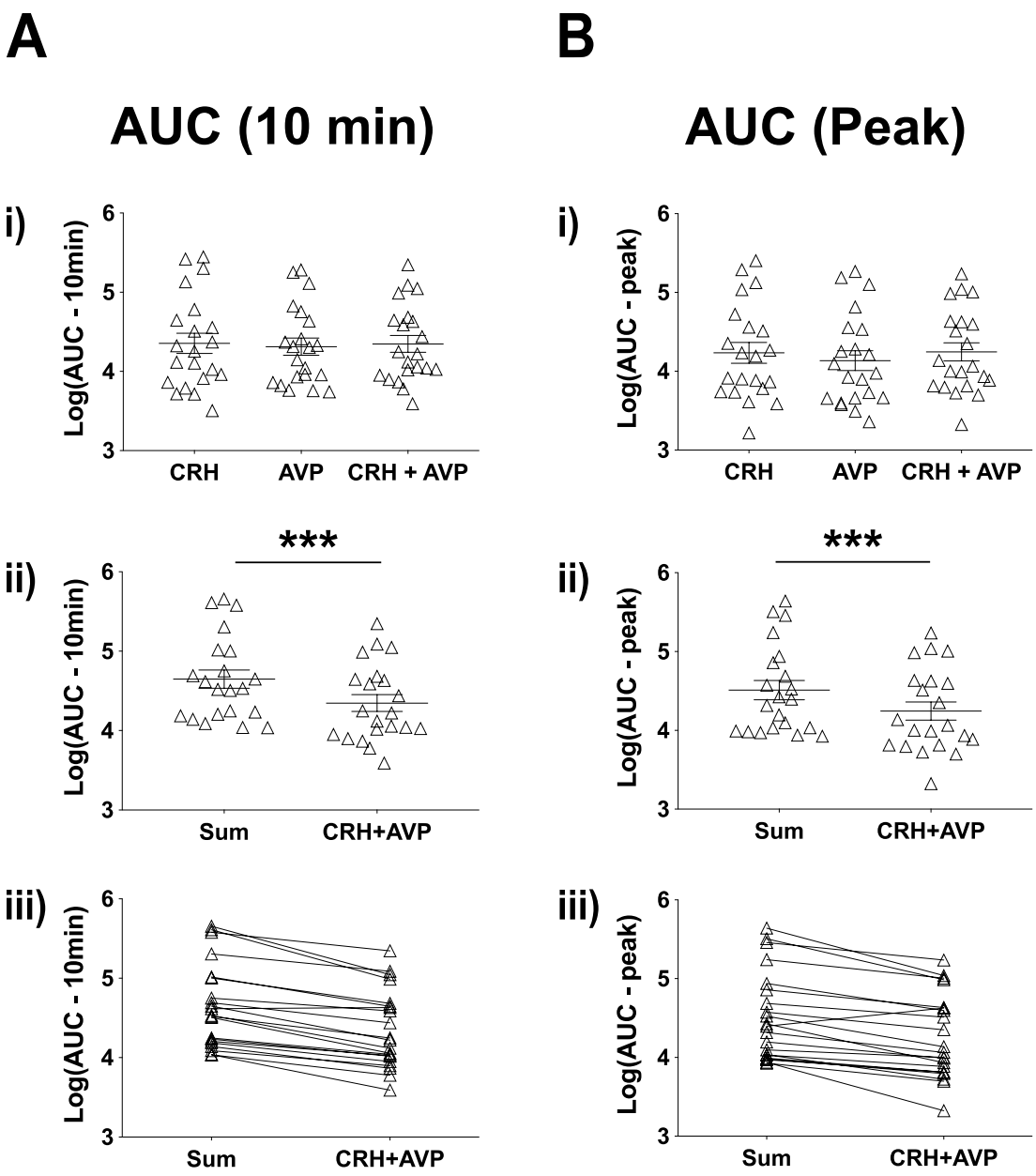


**Figure 4.50 No synergistic $[Ca^{2+}]_i$ responses to CRH/AVP in female BK-KO corticotrophs.** Quantification of effects of exposure to 0.2 nM CRH, 2 nM AVP and the combination of the two in **(A)** AUC (10 min) and **(B)** AUC (peak). The comparison of the AUC of the combined stimulus and the sum of the two single stimuli was used as a measurement of synergy. *** $p < 0.001$ ($n = 21$ from 6 experiments, mixed effects model). All data are means ± SEM.

## Figure 4.51

### CRH induces longer response duration but not peak or time to peak of $[Ca^{2+}]_i$ responses in female BK-KO corticotrophs

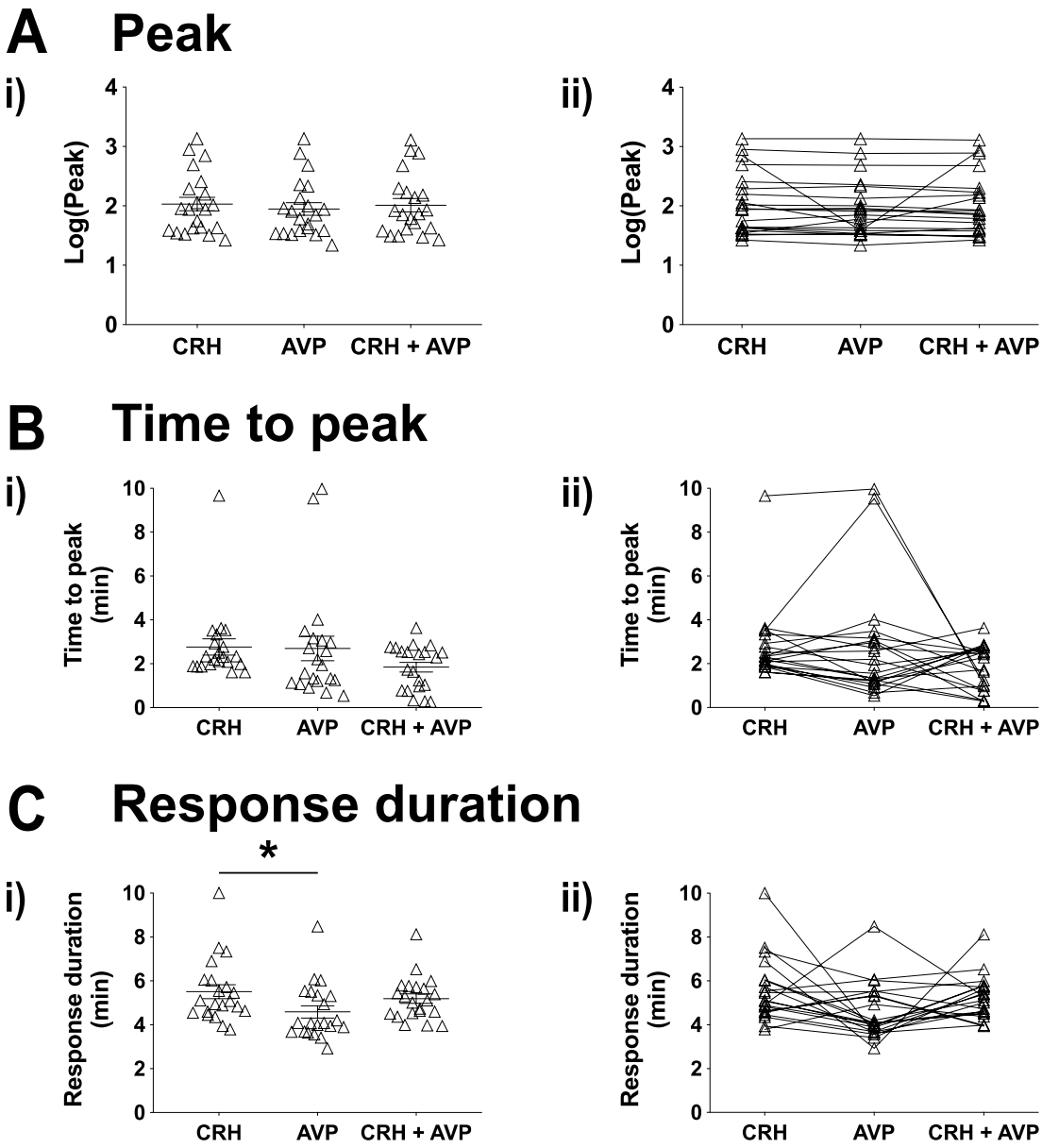


**Figure 4.51 CRH induces longer response duration but not peak or time to peak of $[Ca^{2+}]_i$ responses in female BK-KO corticotrophs.** Quantification of effects of exposure to 0.2 nM CRH, 2 nM AVP and the combination of the two in **(A)** peak, **(B)** time to peak and **(C)** response duration. * $p < 0.05$ ($n = 21$ from 6 experiments, mixed effects model). All data are means ± SEM.

## Figure 4.52

### Peak duration and time gap of $[Ca^{2+}]_i$ responses to CRH, AVP and CRH/AVP in female BK-KO corticotrophs

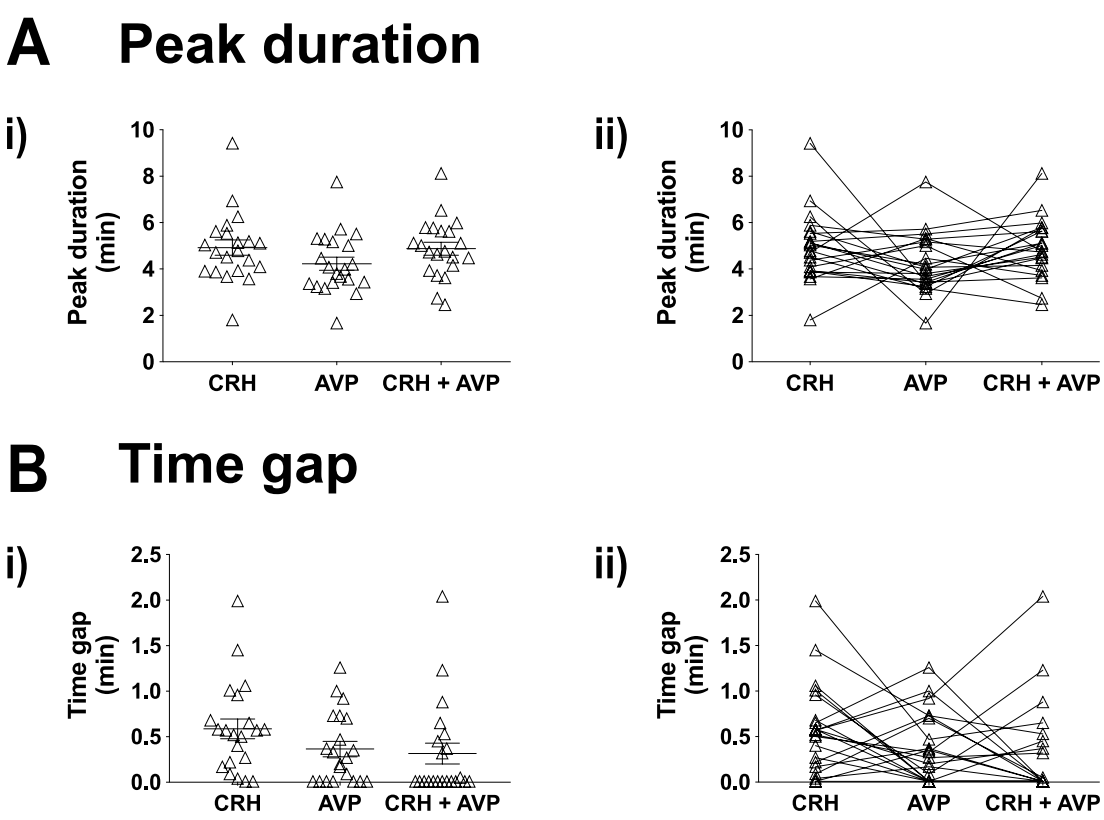


**Figure 4.52 Peak duration and time gap of $[Ca^{2+}]_i$ responses to CRH, AVP and CRH/AVP in female BK-KO corticotrophs.** Quantification of effects of exposure to 0.2 nM CRH, 2 nM AVP and the combination of the two in **(A)** peak duration and **(B)** time gap (n = 21 from 6 experiments, mixed effects model). All data are means ± SEM.

# Table 4.1

## Summary of major findings in results

| Genotype | Sex | Stimulus | AUC (10 min) | AUC (peak) | Peak | Time to peak | Response duration | Peak duration | Time gap |
|---|---|---|---|---|---|---|---|---|---|
| | | CRH | ↓↓ | ↓↓ | ↓↓↓ | ↔ | ↔ | ↔ | ↔ |
| | M | AVP | ↔ | ↔ | ↔ | ↔ | ↔ | ↔ | ↔ |
| BK-KO vs Wild-type | | CRH/AVP | | | | N/A | | | |
| | | CRH | ↔ | ↔ | ↔ | ↔ | ↔ | ↔ | ↔ |
| | F | AVP | ↔ | ↔ | ↔ | ↔ | ↑↑ | ↑↑ | ↔ |
| | | CRH/AVP | ↔ | ↔ | ↔ | ↔ | ↔ | ↔ | ↔ |

↓ decrease; ↑ increase; ↔ no significant difference (compared to wild-type)

↓ $p < 0.05$; ↓↓ $p < 0.01$; ↓↓↓ $p < 0.001$

## 4.3 Discussion

In this chapter, I investigated the role of BK channels in controlling spontaneous as well as CRH- and AVP-induced changes at the level of intracellular free calcium. Genetic deletion of BK channels differentially affects spontaneous $[Ca^{2+}]_i$ signalling in male and female corticotrophs. Compared to wild-type corticotrophs, stimulation with repeated CRH resulted in a significantly reduced $[Ca^{2+}]_i$ responses in male, but not female, BK-KO corticotrophs. In contrast, repeated AVP induced reproducible and consistent $[Ca^{2+}]_i$ responses in BK-KO corticotrophs from both sexes that were not significantly different from the $[Ca^{2+}]_i$ responses in wild-type corticotrophs. However, acute pharmacological inhibition of BK channels with paxilline had no significant effect on CRH-induced $[Ca^{2+}]_i$ responses in either male or female wild-type corticotrophs. Loss of BK channels did not significantly affect synergistic $[Ca^{2+}]_i$ responses to CRH and AVP.

### 4.3.1 CRH-induced $[Ca^{2+}]_i$ responses are suppressed in male BK-KO corticotrophs but not affected by acute pharmacological inhibition of BK channels in wild-type corticotrophs

The central finding in this Chapter is that $[Ca^{2+}]_i$ responses to repeated CRH stimulation in corticotrophs from male, but not female, BK-KO mice were

significantly attenuated compared to wild-type. However, surprisingly, CRH-induced $[Ca^{2+}]_i$ responses were not significantly attenuated following acute pharmacological inhibition of BK channels in wild-type corticotrophs using the specific BK channel inhibitor paxilline. Importantly, previous studies have shown that both genetic deletion, as well as acute pharmacological inhibition with paxilline, of BK channels in male corticotrophs prevents CRH-induced transition to electrical bursting (Duncan *et al.*, 2015). Taken together, these data suggest two potential important features of CRH-induced $[Ca^{2+}]_i$ responses: (i) CRH-induced electrical bursting observed on the millisecond to second timescale is not critical for controlling the longer (minutes) "global" $[Ca^{2+}]_i$ responses analysed in this Thesis; (ii) genetic deletion of BK channels results in compensatory changes in the ion channel and/or signalling landscape of male corticotrophs resulting in suppression of CRH-induced $[Ca^{2+}]_i$ responses.

At face value, the attenuation of CRH-induced $[Ca^{2+}]_i$ responses in male corticotrophs from BK-KO mice support the original hypothesis that lack of BK channels would decrease $[Ca^{2+}]_i$ responses due to a loss of CRH-induced bursting. Indeed, as indicated before, CRH regulates corticotrophs through cAMP/PKA pathway that results in a $Ca^{2+}$ influx via L-type $Ca^{2+}$ channels and CRH-induced transition to bursting is dependent on BK channels (Lee & Tse, 1997; Duncan *et al.*, 2015). In other pituitary cells, bursting has been suggested to have larger capacity to drive calcium influx than

spiking (Van Goor *et al.*, 2001*b*; Stojilkovic *et al.*, 2005) and this is dependent on BK channels. Electrical bursts are observed on the millisecond to second timescale whereas the $[Ca^{2+}]_i$ responses analysed here are on the second to minute timescale. However, as this effect was not observed in acute pharmacological inhibition of BK channels with paxilline, this suggest that there is not a direct link between electrical bursting and long-term changes in global $[Ca^{2+}]_i$ signalling induced by CRH.

It has been previously shown that CRH still significantly increases electrical spiking frequency in BK-KO, or paxilline treated, corticotrophs (Duncan *et al.*, 2015). As increased spiking events can still drive $Ca^{2+}$ into the cell, it is therefore proposed that blockade of BK channels with paxilline, or knockout of BK channels, prevents the transition to bursting but still enables significant elevation of global $Ca^{2+}$ influx through single spiking following stimulation with CRH. This suggests that increased spiking frequency may also deliver the similar total amount of global $Ca^{2+}$ as bursting behaviour with consequently similar level of global $[Ca^{2+}]_i$ signalling. Indeed, a recent study has suggested that spiking can be as effective as bursting for hormone release when release sites are located close to the channel, although bursting is generally more effective at evoking secretion (Tagliavini *et al.*, 2016). This study also revealed that bursting is not more effective than spiking if spiking frequency increases to a level where the active time of $Ca^{2+}$ influx is comparable to bursting. As indicated in Chapter

One, two distinct populations of BK channels have been implicated in the generation of bursting: BK-near channels, located close proximity to voltage-gated $Ca^{2+}$ channels, are rapidly activated by the high $Ca^{2+}$ concentration in the microdomains around the channels to facilitate bursting; BK-far channels, involve the termination of a burst that are located distantly from voltage-gated $Ca^{2+}$ channels (Tsaneva-Atanasova *et al.*, 2007; Duncan *et al.*, 2015). Since the activation of BK-near channels is necessary for the bursting, genetic deletion or pharmacological inhibition of BK channels may result in the loss of bursting behaviour but not affect the bulk $[Ca^{2+}]_i$ concentration. . Another potential explanation for the lack of effect of paxilline is that BK-near and BK-far channels expressed in corticotrophs might be differentially sensitive to paxilline. For example, if paxilline blocks more BK-far channels than BK-near channels this would be predicted to result in longer bursting and $[Ca^{2+}]_i$ responses in corticotrophs. Although there is some evidence that the molecular composition of BK channel can determine their sensitivity to different BK channel blockers, to date there is no evidence to suggest that BK channels are differentially responsive to paxilline. For example, BK channels assembled with β4 subunits are resistant to iberiotoxin but are inhibited similarly by paxilline (Meera *et al.*, 2000). In addition, paxilline displayed the same $IC_{50}$ for paxilline inhibition (~ 17nM) of different BK channel splice variants, including STREX and ZERO that are expressed in corticotrophs (Saleem *et al.*, 2009). Thus, while we cannot exclude that BK far and BK near may be differentially sensitive

to paxilline, there is no current evidence to suggest that BK channels are differentially regulated by paxilline and paxilline was used at saturating (1uM) concentrations in these assays. Furthermore, as the electrical activity is measured on the timescale of milliseconds to seconds which may not have impact on global $[Ca^{2+}]_i$ signalling over minutes. To address this question, it would be important to measure $[Ca^{2+}]_i$ responses and electrical activity in the same cells to address whether $[Ca^{2+}]_i$ responses measured on millisecond timescale correlate with electrical bursting in corticotrophs. Moreover, understanding whether the pattern of $[Ca^{2+}]_i$ responses on millisecond timescale rather than global $[Ca^{2+}]_i$ changes are more important for hormone secretion in corticotrophs will be important.

As CRH-induced $[Ca^{2+}]_i$ responses were significantly attenuated in male BK-KO corticotrophs, this also suggests that potential compensatory mechanisms are occurring in corticotrophs as a result of the global loss of BK channels. Considering the differences between BK-KO and paxilline treated corticotrophs, it is suspected the reduced $[Ca^{2+}]_i$ signalling in BK-KO corticotrophs has modified the landscape of ion channel expression and/or signalling pathways to compensate for the long-term lack of BK channels in mice. Increasing evidence have revealed compensatory mechanisms after deletion of BK channels. A previous study in murine bladder demonstrated that smooth muscle-specific deletion of the BK channel caused a more severe overactive

urinary bladder syndrome compared with constitutive BK channel knockout, which suggests the existence of compensatory mechanisms (Sprossmann *et al.*, 2009). Reduced L-type $Ca^{2+}$ current density, enhanced expression of PKA, activation of β-adrenergic signalling pathways independently of BK channels were identified in constitutive BK channel knockout detrusor muscle. Another study also reported a compensatory mechanism in the regulation of airway tone. Mice with genetic deletion of BK channel displayed a reduced sensitivity following cholinergic stimulation, which is caused by an up-regulation of cGMP/PKG signalling pathway to counterbalance the enhanced $Ca^{2+}$ influx via voltage-gated $Ca^{2+}$ channels even they were not up-regulated (Sausbier *et al.*, 2006). As $[Ca^{2+}]_i$ signalling was reduced in male BK-KO corticotrophs when stimulated with CRH, but not AVP (Section 4.2.3), it is likely that compensation specifically modifies the CRH-induced signalling pathway. Whether this involves down-regulation of signalling events between CRH receptor activation and L-type $Ca^{2+}$ channels or may involve up-regulation of $Ca^{2+}$ sequestration and removal of $Ca^{2+}$ remain unknown. However, compensation is unlikely to occur at the level of CRH receptors or cAMP/PKA signalling pathway, because addition of a fast activating BK current with dynamic clamp can induce CRH-dependent bursting in corticotrophs isolated from BK-KO mice or paxilline treated wild-type corticotrophs (Duncan *et al.*, 2015, 2016). Compensation is also supported by the fact that spontaneous $[Ca^{2+}]_i$ active time is reduced in male BK-KO,

but not paxilline-treated, corticotrophs, and this may also contribute to the attenuated CRH-induced $[Ca^{2+}]_i$ responses.

To address the compensation theory, analysis of changes in mRNA, protein and function levels of L-type calcium channel and other ion channels in BK-KO corticotrophs will be required. Fluorescence-activated cell sorting (FACS) would provide a method for sorting and purifying corticotrophs from the mixture of pituitary anterior hormone secretion cells to address more global mRNA and protein analysis. In addition, addressing whether similar changes in CRH-induced $[Ca^{2+}]_i$ responses were also observed in corticotrophs from mice in which BK channels have been conditionally deleted only in corticotrophs will allow us to address if this is a cell autonomous change.

Importantly, these results also revealed differences between male and female corticotrophs with respect to both spontaneous and CRH-induced $[Ca^{2+}]_i$ responses when BK channels were genetically deleted. Firstly, there was a reduction in spontaneous active time in male BK-KO corticotrophs (32.1 ± 6.1%) that approached statistical significance compared with controls (53.0 ± 3.1%). In contrast, female BK-KO corticotrophs (49.8 ± 3.6%) displayed a significant increase in spontaneous active time compared to wild-type corticotrophs (39.9 ± 3.0%). Moreover, in male, but

not female corticotrophs, CRH-induced $[Ca^{2+}]_i$ responses were attenuated in BK-KO corticotrophs compared to wild-type. This suggests that the functional role of BK channels and the ion channel/signalling pathways controlling spontaneous and CRH-induced $[Ca^{2+}]_i$ signalling is different between male and female corticotrophs. Previous data have reported differences between male and female corticotroph excitability. For example, corticotrophs from female mice express intermediate conductance (IK) $Ca^{2+}$-activated $K^+$ channels and inhibition of IK channels with specific IK channel blocker promoted bursting behaviour in female corticotrophs and mice genetic deletion of IK channels showed hyperresponsivenss to restraint stress (Liang *et al.*, 2011). However, unpublished data from the Shipston Lab (Dr Peter J. Duncan, personal communication) revealed a lack of effect of IK inhibition in male corticotrophs. Importantly, female wild-type corticotrophs displaying limited electrical bursting behaviour to CRH/AVP, with stimulation largely driven by increases in spike frequency even though BK channel mRNA, protein and single channel currents can be detected in corticotrophs from female mice. Intriguingly, loss of BK channels in corticotrophs from female mice also showed a lower percentage of cells that displayed synergy in $[Ca^{2+}]_i$ responses to the combination of CRH and AVP, ~ 30% of female wild-type corticotrophs showed synergistic $[Ca^{2+}]_i$ responses compared to only ~ 8% of female BK-KO corticotrophs. No significant synergistic $[Ca^{2+}]_i$ responses were seen in male corticotrophs isolated from both wild-type and BK-KO mice. This

sex difference further supports the existence of sexual dimorphism in the regulation of corticotroph $[Ca^{2+}]_i$ responses and physiological function.

The mechanism(s) underlying these differences remains to be explored although a potential mechanism may involve differential control by circulating sex steroids. For example, oestrogen and testosterone have both been reported to regulate the expression and/or properties of both BK channels as well as $Ca^{2+}$ channels in the pituitary (Xie & McCobb, 1998; Fiordelisio *et al.*, 2007). Cleary, further investigation of potential sex differences is warranted.

### 4.3.2 AVP-induced $[Ca^{2+}]_i$ responses are unaffected by genetic deletion of BK channels in both male and female corticotrophs

Stimulation with repeated 2 nM AVP resulted in a significant elevation of $[Ca^{2+}]_i$ in both male and female BK-KO corticotrophs. However, no significant differences were observed compared with corticotrophs isolated from both male and female wild-type mice, which suggests that BK channels play no major role in modulating AVP-evoked calcium signalling. This is consistent with the lack of a role for BK channels in regulating electrical activity. Stimulation with AVP results in an increase in single spiking frequency rather than a transition to bursting behaviour in male corticotrophs (Duncan *et al.*, 2015). This AVP-induced electrical activity is independent of BK

channel function, and thus is in agreement with the lack of effect predicted and observed in the absence of BK channels seen in 4.2.3. AVP regulates the activity of corticotrophs through $IP_3$/PKC pathway which results in the release of calcium from intracellular $IP_3$-sensitive calcium pool as well as influx via L-type calcium channels (Tse & Lee, 1998; Romanò *et al.*, 2017). This involves a biphasic pattern of $[Ca^{2+}]_i$ signalling with a transient and plateau phase that controls the exocytosis during the AVP-evoked elevation of $[Ca^{2+}]_i$ (Tse & Lee, 1998). This also suggests that the potential compensatory mechanisms observed in CRH-induced $[Ca^{2+}]_i$ responses in BK-KO corticotrophs are not involved in AVP-induced signalling pathways, perhaps also suggesting $Ca^{2+}$ influx is not a major component of AVP-induced $[Ca^{2+}]_i$ responses in murine corticotrophs as also observed in rat corticotrophs (Romanò *et al.*, 2017). Together, these data suggest that genetic deletion of BK channels has little impact on AVP-induced, $IP_3$-sensitive $[Ca^{2+}]_i$ signalling.

Interestingly, it is worth noting that although two phenotypes of $[Ca^{2+}]_i$ responses were observed in both wild-type and BK-KO corticotroph, ablation of BK channels results in the percentage of female corticotrophs displaying oscillatory $[Ca^{2+}]_i$ behaviour decreasing from 50.0% (12/24 cells) to 8.3% (1/12 cells) compared to female wild-type corticotrophs, while oscillatory $[Ca^{2+}]_i$ behaviour in male BK-KO corticotrophs increased from 25% (4/16 cells) to 50% (3/6 cells). In addition, wild-type

corticotrophs always responded to repeated AVP stimulation with consistent deterministic patterns of $[Ca^{2+}]_i$ responses: either sustained elevation of $[Ca^{2+}]_i$ or oscillatory $[Ca^{2+}]_i$ behaviour in any single cell from 40 calcium imaging recordings. However, 16.7% (1/6 cells) of male and 8.3% (1/12 cells) of female BK-KO corticotrophs displayed a mixture of two phenotypes of $[Ca^{2+}]_i$ response following repeated AVP stimulation. This oscillatory $[Ca^{2+}]_i$ behaviour is likely to result primarily from $IP_3$-sensitive calcium signalling and may suggest subtle roles of BK channels as has been reported for other calcium-activated potassium channels in pituitary cells (Shipston, 2018).

CRH is a more potent hypothalamic secretagogue in stimulating ACTH secretion compared to AVP, including in murine corticotrophs. Stimulation with CRH or AVP results in distinct patterns of electrical activity, transition from spiking into bursting and increasing spiking frequency respectively, in wild-type corticotrophs. However, the accompanied sustained "global" $[Ca^{2+}]_i$ responses measured over minutes is largely similar. This may also support the hypothesis that it is the pattern of $[Ca^{2+}]_i$ responses, rather than the global $[Ca^{2+}]_i$ responses that is important for secretion. Indeed, genetic deletion, or pharmacological inhibition, of BK channels, results in attenuation of CRH-evoked ACTH secretion in male corticotrophs (Brunton *et al.*, 2007; Duncan *et al.*, 2015). To address this question, simultaneous measurement of

electrical behaviour, $[Ca^{2+}]_i$ responses and secretion in the same timescale are required.

## 4.4 Chapter summary

Genetic deletion of BK channels revealed a sexual dimorphism in spontaneous $[Ca^{2+}]_i$ signalling with a significantly increased active time in female corticotrophs and a reduction of active time approached statistical significance in male corticotrophs compared to wild-type. Following CRH stimulation, male corticotrophs isolated from BK-KO mice showed a significant reduction in $[Ca^{2+}]_i$ responses compared to wild-type. In contrast, CRH-induced $[Ca^{2+}]_i$ responses were unaffected in corticotrophs from female BK-KO mice. However, acute pharmacological blockage of BK channels with paxilline had no significant impact on CRH-induced $[Ca^{2+}]_i$ responses in either male or female corticotrophs. This paradoxical result may suggest the existence of compensatory mechanisms in corticotrophs following global deletion of BK channels. Importantly, this suggests that CRH-induced changes in bursting behaviour, which are dependent on BK channels in male corticotrophs, is not important for the global changes in $[Ca^{2+}]_i$ responses measured over minutes. Rather, the patterns of $[Ca^{2+}]_i$ responses in the millisecond to second timescale may be more important for controlling CRH-evoked secretion. AVP-evoked $[Ca^{2+}]_i$ responses were largely unaffected by genetic deletion of BK channels in either male or female corticotrophs although the number of female BK-KO corticotrophs that displayed oscillatory $[Ca^{2+}]_i$

behaviour was decreased compared to wild-type controls.

The role of BK channels in the control of CRH-induced $[Ca^{2+}]_i$ responses and the correlation between the patterns of $[Ca^{2+}]_i$ signalling and secretion of ACTH warrant further study.

# Chapter Five:

# Calcium signalling in zDHHC23-KO corticotrophs

# Chapter 5: Calcium signalling in zDHHC23-KO corticotrophs

## 5.1 Introduction

In this chapter, the aim was to investigate the role of the S-acyl transferase zDHHC23, that controls surface expression of BK channels, in the modulation of spontaneous and secretagogue-induced intracellular free calcium ($[Ca^{2+}]_i$) signalling in corticotrophs. I first examined the effects of the deletion of zDHHC23 on spontaneous $[Ca^{2+}]_i$ signalling in corticotrophs. Calcium imaging experiments were then performed to investigate whether genetically deletion of zDHHC23 have an impact on corticotrophs following CRH or AVP stimulation as well as the synergy between CRH and AVP at the level of $[Ca^{2+}]_i$. All experiments were performed and analysed in male and female corticotrophs respectively.

### 5.1.1 S-acylation is regulated by zDHHCs

Cellular proteins are regulated by a wide variety of post-translational modifications (PTMs), such as lipid modifications and phosphorylation. In particular, protein S-acylation, the only fully reversible lipid PTM, provides a ubiquitous and dynamic mechanism to regulate the properties and functions of various proteins and physiological processes (Resh, 2006*a*; Chamberlain & Shipston, 2015). S-acylation of

most proteins is enzymatically controlled by a large family of transmembrane zinc-finger containing protein acyl-transferases (zDHHC family, 23/24 zDHHCs genes in mammals). zDHHCs have a highly conserved Asp-His-His-Cys (DHHC) signature sequence across species from yeast to humans that is important for catalytic activity (Shipston, 2011; Chamberlain & Shipston, 2015). In addition, distinct zDHHC enzymes display substrate specificity (Greaves & Chamberlain, 2011) and specific subcellular localization and tissue distribution (Ohno *et al.*, 2006).

### 5.1.2 BK channels are modulated by S-acylation

S-acylation has been implicated in the regulation of a diverse array of ion channels, such as the function of L-type $Ca^{2+}$ channels (Chien *et al.*, 1996), the voltage sensing of the voltage-gated Kv1.1 channels (Gubitosi-Klug *et al.*, 2005) and the phosphorylation of BK channels (Tian *et al.*, 2008). Importantly, recent studies suggest that S-acylation of BK channels plays an important role in controlling the properties and function including surface expression, trafficking and channel activity (Shipston, 2014*b*; Chamberlain & Shipston, 2015).

The BK channel pore-forming α-subunit is S-acylated at two distinct sites: cysteine residues within the intracellular loop between transmembrane domains S0 and S1 (S0-S1 loop) and the alternatively spliced STREX insert in the intracellular linker

between the two RCK domains in the C-terminus (Shipston, 2013). Of particular interest is the S-acylation of the S0-S1 loop of BK channels that has been suggested to be crucial in cell surface expression (Jeffries *et al.*, 2010). S-acylation of S0-S1 loop allows the interaction between S0-S1 loop and the plasma membrane to regulate surface expression (Jeffries *et al.*, 2010). It has been shown that distinct S-acylation sites of the same ion channel could be modulated by different subsets of zDHHCs, where the S-acylation of the S0-S1 loop is predominately controlled by zDHHC22 and zDHHC23 and overexpression of zDHHC23 increases the surface expression of the S0-S1 loop (Tian *et al.*, 2010, 2012). In addition, the zDHHCs controlling the S-acylation of BK channels are also expressed at ER, Golgi and/or plasma membrane suggesting that the regulation of BK channel function may occur at various sites and multiple phases in the ion channel life cycle (Shipston, 2014*a*).

In this chapter, calcium imaging experiments were performed to determine whether deletion of zDHHC23 had an effect on $[Ca^{2+}]_i$ responses in corticotrophs. As zDHHC23 is highly expressed in murine corticotrophs and controls cell surface expression of BK channels, it was predicted that zDHHC23-mediated S-acylation plays an important role in controlling BK channel-dependent excitability and accompanied modulation of $[Ca^{2+}]_i$ signalling in corticotrophs. Importantly, a previous study suggested that knockdown of zDHHC23 resulted in a significant reduction in

surface expression of BK channel as well as S-acylation of the BK channel (Tian *et al.*, 2012). As BK channels are essential in CRH-induced transition to bursting but not AVP-evoked spiking frequency increase, it was hypothesised that corticotrophs isolated from zDHHC23 knockout mice would show a reduction in $[Ca^{2+}]_i$ responses to CRH but not AVP.

## 5.2 Results

### 5.2.1 Genetic deletion of zDHHC23 has no effect on spontaneous $[Ca^{2+}]_i$ in corticotrophs

Before investigating the role of zDHHC23-mediated S-acylation in secretagogue-evoked corticotroph $[Ca^{2+}]_i$ signalling, the spontaneous $[Ca^{2+}]_i$ signalling in zDHHC23-KO corticotrophs was examined. Calcium imaging was performed on corticotrophs isolated from zDHHC23-KO mice and the active time of spontaneous $[Ca^{2+}]_i$ signalling over a five minute "baseline" period was analysed in males and females respectively. All data were analysed together, only data from zDHHC23-KO corticotrophs and the comparison between wild-type and zDHHC23-KO corticotrophs are presented in this chapter. The analysis of these data was done in conjunction with the analyses for Chapters Three and Four (see 2.6.3). Overall, the mean active time of spontaneous $[Ca^{2+}]_i$ signalling across all zHHDC23-KO corticotrophs was 51.1 ± 2.8% (n = 87 from 47 experiments) with a negative skewed distribution. The active time was

## Figure 5.1

**The active time of spontaneous $[Ca^{2+}]_i$ signalling is not different between male and female zDHHC23-KO corticotrophs**

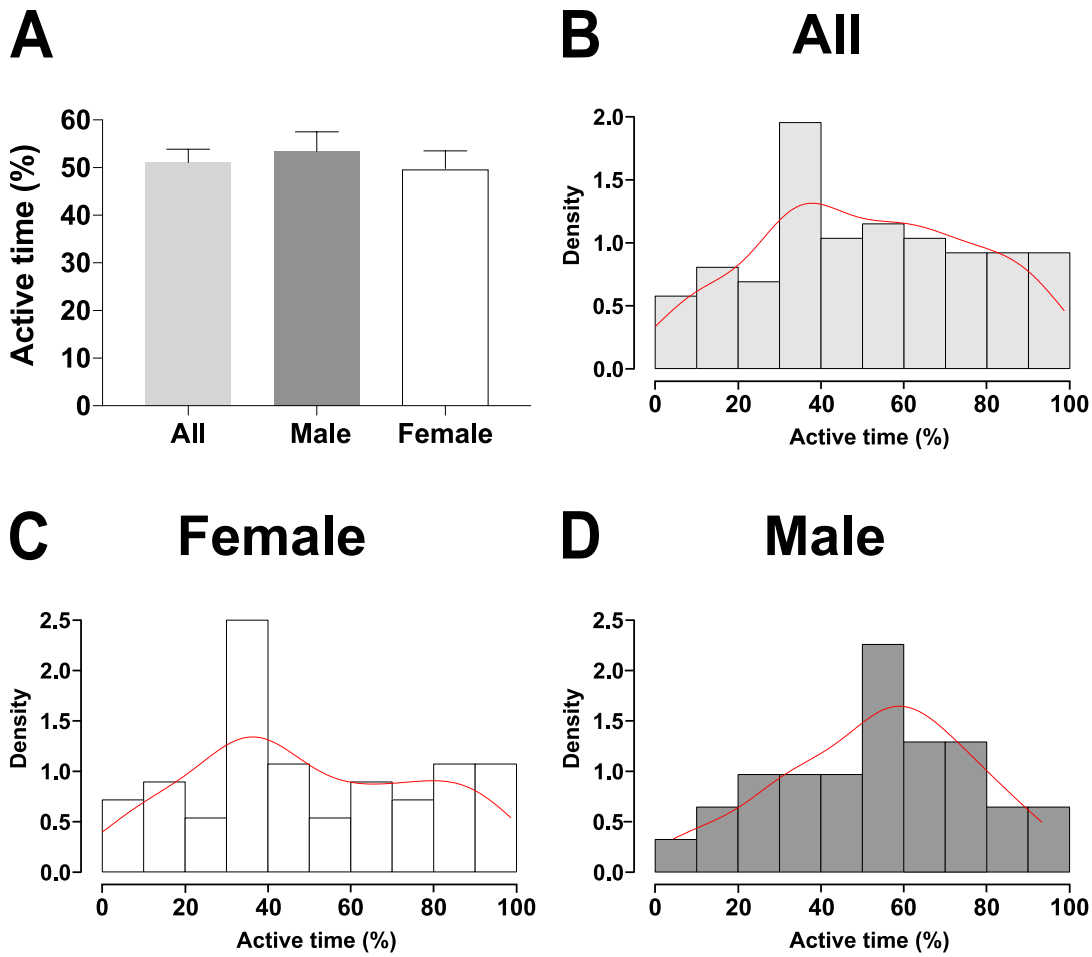


**Figure 5.1 The active time of spontaneous $[Ca^{2+}]_i$ signalling is not different between male and female zDHHC23-KO corticotrophs. (A)** The mean active time of spontaneous $[Ca^{2+}]_i$ signalling in all zDHHC23-KO corticotrophs. **(B)** The distribution of spontaneous $[Ca^{2+}]_i$ active time in all zDHHC23-KO corticotrophs. The distribution of spontaneous $[Ca^{2+}]_i$ active time in **(C)** female and **(D)** male zDHHC23-KO corticotrophs (female n = 56, male n = 31, mixed effects model). Red line indicates the fit of distribution density. All data are means ± SEM, N > 3 independent experiments.

not significantly different between male and female corticotrophs with 53.4 ± 4.1% in male corticotrophs (n = 31 from 21 experiments) and 49.8 ± 3.7% in female corticotrophs (n = 56 form 26 experiments) (Figure 5.1). Calcium imaging traces were normalized between 0 and 1 (the peak of the response to stimulus) to compare the relative change in maximum amplitude of spontaneous $[Ca^{2+}]_i$ signalling between zDHHC23-KO corticotrophs. All patterns of spontaneous $[Ca^{2+}]_i$ signalling were observed in zDHHC23-KO corticotrophs, including $[Ca^{2+}]_i$ oscillation (33.3%), sustained $[Ca^{2+}]_i$ elevation (52.9%) as well as low amplitude, complex patterns of $[Ca^{2+}]_i$ behaviour (12.6%), and only 1 out of 87 cells was quiescent under basal conditions (Figure 5.3A). zDHHC23-KO corticotrophs had a spontaneous $[Ca^{2+}]_i$ maximum amplitude of 69.7 ± 2.1% (n = 87 from 47 experiments) which was positively skewed (Figure 5.2A&B). The maximum amplitude of spontaneous $[Ca^{2+}]_i$ signalling in female corticotrophs was 64.9 ± 2.7% (n = 56 from 26 experiments), which was not significantly different from male corticotrophs with a mean of 78.2 ± 2.8% (n = 31 from 21 experiments) (Figure 5.2A). In addition, no low amplitude $[Ca^{2+}]_i$ was seen in male corticotrophs and the distribution of maximum amplitude was heavily skewed to the right in both male and female zDHHC23-KO corticotrophs (Figure 5.2C&D). These results suggest that there were no significant sex differences in the maximum amplitude of spontaneous $[Ca^{2+}]_i$ signalling.

## Figure 5.2

**The maximum amplitude of spontaneous $[Ca^{2+}]_i$ signalling is not different between male and female zDHHC23-KO corticotrophs**

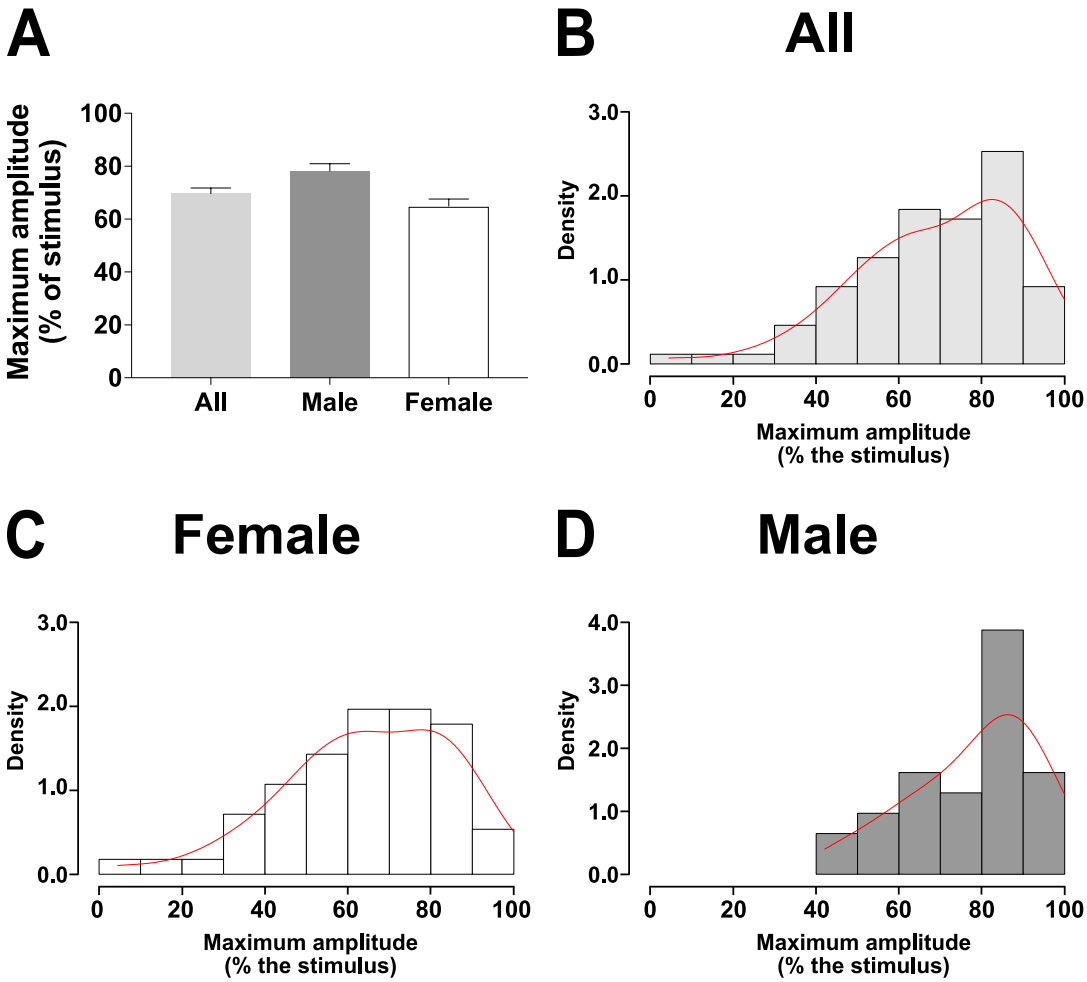


**Figure 5.2 The maximum amplitude of spontaneous $[Ca^{2+}]_i$ signalling is not different between male and female zDHHC23-KO corticotrophs. (A)** The mean maximum amplitude of spontaneous $[Ca^{2+}]_i$ signalling in all zDHHC23-KO corticotrophs. **(B)** The distribution of spontaneous $[Ca^{2+}]_i$ maximum amplitude in all zDHHC23-KO corticotrophs. The distributions of spontaneous $[Ca^{2+}]_i$ maximum amplitude in **(C)** female and **(D)** male zDHHC23-KO corticotrophs (female n = 56, male n = 31, mixed effects model). Red line indicates the fit of distribution density. All data are means ± SEM, N > 3 independent experiments.

Statistical calculation was performed to compare spontaneous $[Ca^{2+}]_i$ signalling between wild-type and zDHHC23-KO corticotrophs in terms of active time and maximum amplitude. Overall, analysis of active time revealed a mean of 45.2 ± 2.2% in wild-type corticotrophs (n = 121 from 56 experiments) with no significant differences compared to corticotrophs from zDHHC23-KO mice (n = 87 from 47 experiments) with the active time of 51.1 ± 2.8% (Figure 5.3B). The maximum amplitude in wild-type and zDHHC23-KO corticotrophs was not significantly different either, being 69.8 ± 1.7% and 69.7 ± 2.1% respectively (Figure 5.3C). Moreover, there were no significant differences between wild-type and zDHHC23-KO corticotrophs in active time or maximum amplitude of spontaneous $[Ca^{2+}]_i$ signalling when analysing male or female corticotrophs separately.

These results suggest that genetic deletion of zDHHC23 had no significant effect on spontaneous $[Ca^{2+}]_i$ signalling in male or female corticotrophs.

### 5.2.2 Progressive attenuation of $[Ca^{2+}]_i$ responses to repeated CRH stimulation in zDHHC23-KO corticotrophs

After determining that genetic deletion of zDHHC23 had no significant effect on spontaneous $[Ca^{2+}]_i$ signalling of corticotrophs, the role of zDHHC23 in controlling $[Ca^{2+}]_i$ responses induced by CRH was investigated in male corticotrophs first.

# Figure 5.3

## Genetic deletion of zDHHC23 has no effect on spontaneous $[Ca^{2+}]_i$ signalling in corticotrophs

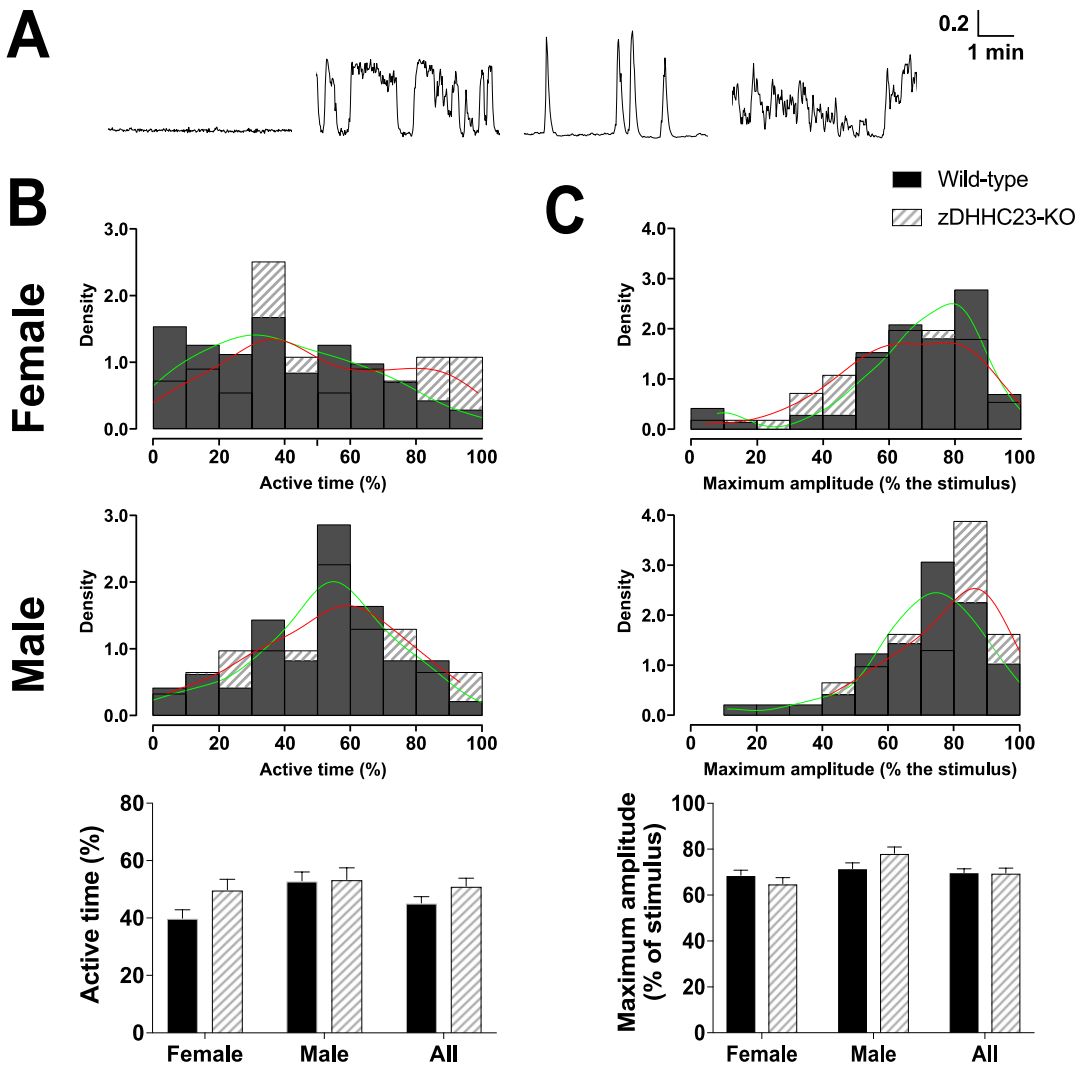


**Figure 5.3 Genetic deletion of zDHHC23 has no effect on spontaneous $[Ca^{2+}]_i$ signalling in corticotrophs. (A)** All patterns of spontaneous $[Ca^{2+}]_i$ signalling were seen in zDHHC23-KO corticotrophs. **(B)** The distribution and mean of spontaneous $[Ca^{2+}]_i$ active time in male and female wild-type and zDHHC23-KO corticotrophs. **(C)** The distribution and mean of spontaneous $[Ca^{2+}]_i$ maximum amplitude in male and female wild-type and zDHHC23-KO corticotrophs (wild-type n = 121, zDHHC23-KO n = 87, mixed effects model). Green line and red line indicate the fit of distribution density of wild-type and zDHHC23-KO corticotrophs respectively. All data are means ± SEM, N > 3 independent experiments.

#### 5.2.2.1 Repeated CRH stimulation results in progressively attenuated $[Ca^{2+}]_i$ responses in male zDHHC23-KO corticotrophs

Calcium imaging recordings were obtained from male zDHHC23-KO corticotrophs (n = 11 from 6 experiments) following the same repeated stimulation protocol used previously for wild-type corticotrophs (see 3.2.3.1).

In response to a three minute exposure to 0.2 nM CRH stimulation, all zDHHC23-KO male corticotrophs responded rapidly with a significant and sustained $[Ca^{2+}]_i$ elevation that returned to baseline after a few minutes (Figure 5.4A). Superposition of extracts of the calcium imaging traces shown indicated that $[Ca^{2+}]_i$ changes were stable in some cells (Figure 5.4B, bottom), whereas the others displayed a progressive attenuation of $[Ca^{2+}]_i$ responses following repeated CRH stimulation (Figure 5.4B, top).

The effects of 0.2 nM CRH on $[Ca^{2+}]_i$ in zDHHC23-KO corticotrophs were evaluated using the same parameters as for wild-type corticotrophs including AUC (10min), AUC (peak), peak, time to peak, response duration, peak duration and time gap. Log transformation was performed on AUC (10min), AUC (peak) and peak as before. Statistical analysis revealed that AUC (10 min) and AUC (peak) were significantly attenuated between Stimulus 1 and Stimulus 3 ($p < 0.001$). AUC (10 min) was also significantly decreased ($p < 0.05$) between Stimulus 2 and Stimulus 3 (Figure 5.5).

# Figure 5.4

## Progressive attenuation of $[Ca^{2+}]_i$ responses in male zDHHC23-KO corticotrophs to repeated CRH

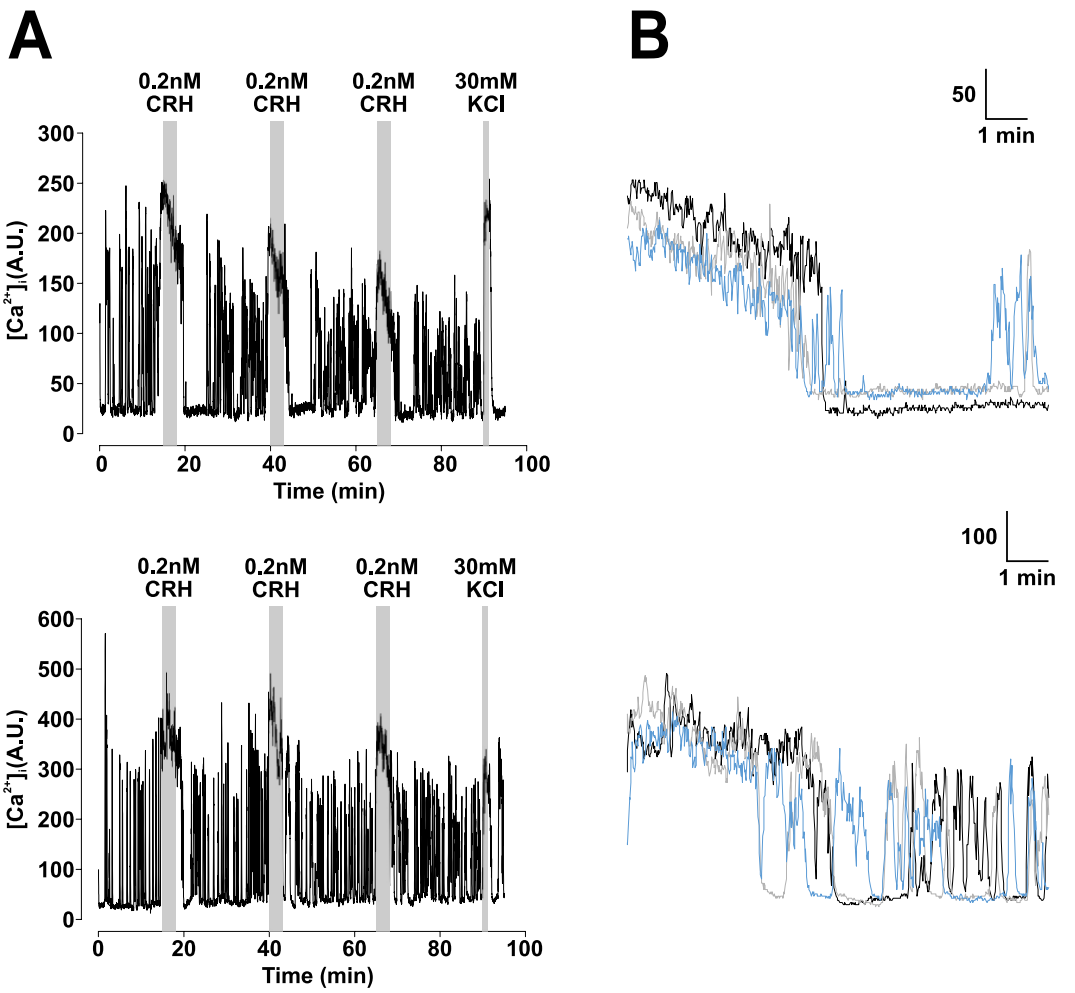


**Figure 5.4 Progressive attenuation of $[Ca^{2+}]_i$ responses in male zDHHC23-KO corticotrophs to repeated CRH. (A)** Representative calcium imaging traces of male zDHHC23-KO corticotrophs exposed to 0.2 nM CRH for three minutes and repeated three times at 25 minutes intervals. 30 mM potassium chloride was applied at the end for one minute. **(B)** Superposition of extracts of the two traces shown in A, showing $[Ca^{2+}]_i$ changes in male zDHHC23-KO corticotrophs with repeated 0.2 nM CRH stimulation. Black line shows response to the first stimulus (starting at 15 min), grey line shows response to the second stimulus (starting at 40 min), and blue line shows response to the third stimulus (starting at 65 min).

Peak showed significantly reduction between Stimulus 1 and Stimulus 3 ($p < 0.001$), Stimulus 2 and Stimulus 3 ($p < 0.001$) (Figure 5.6A). However, there were no statistically significant differences in time to peak, (Figure 5.6B), response duration, peak duration (Figure 5.7) or time gap (Figure 5.8) following repeated CRH stimulation.

The progressive attenuation in AUC (10 min), AUC (peak) and peak suggest that zDHHC23 is important for allowing sustained $[Ca^{2+}]_i$ responses to repeated CRH stimulation in male zDHHC23-KO corticotrophs.

#### 5.2.2.2 Repeated CRH stimulation results in progressively attenuated $[Ca^{2+}]_i$ responses in zDHHC23-KO female corticotrophs

Calcium imaging experiments were performed on female corticotrophs isolated from zDHHC23-KO mice (n = 19 from 11 experiments) following the same protocol used in male zDHHC23-KO corticotrophs.

Representative calcium imaging traces shown in Figure 5.9A revealed that stimulation with 0.2 nM CRH for three minutes resulted in a rapid and sustained increase of $[Ca^{2+}]_i$ in female zDHHC23-KO corticotrophs. Importantly, there was a similar attenuation of $[Ca^{2+}]_i$ responses upon repeated CRH stimulation as observed in male zDHHC23-KO

## Figure 5.5

**Attenuation of AUC (10 min) and AUC (peak) of $[Ca^{2+}]_i$ responses in male zDHHC23-KO corticotrophs to repeated CRH**

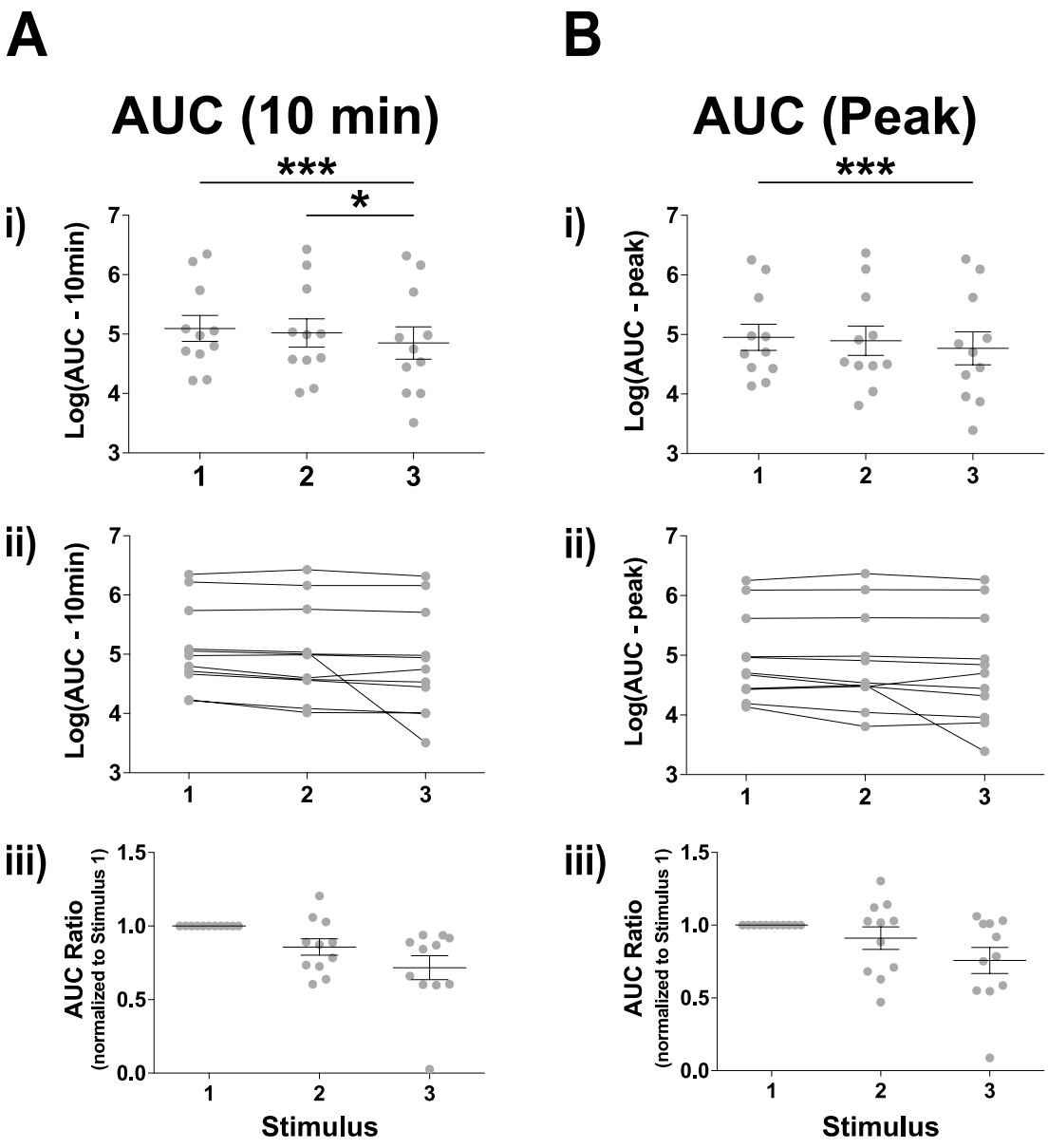


**Figure 5.5 Attenuation of AUC (10 min) and AUC (peak) of $[Ca^{2+}]_i$ responses in male zDHHC23-KO corticotrophs to repeated CRH.** Quantification of effects of repeated exposure to 0.2 nM CRH in **(A)** AUC (10 min) and **(B)** AUC (peak). *** $p < 0.001$, * $p < 0.05$ ($n = 11$ from 6 experiments, mixed effects model). All data are means ± SEM.

## Figure 5.6

### Attenuation of peak but not time to peak of $[Ca^{2+}]_i$ responses in male zDHHC23-KO corticotrophs to repeated CRH

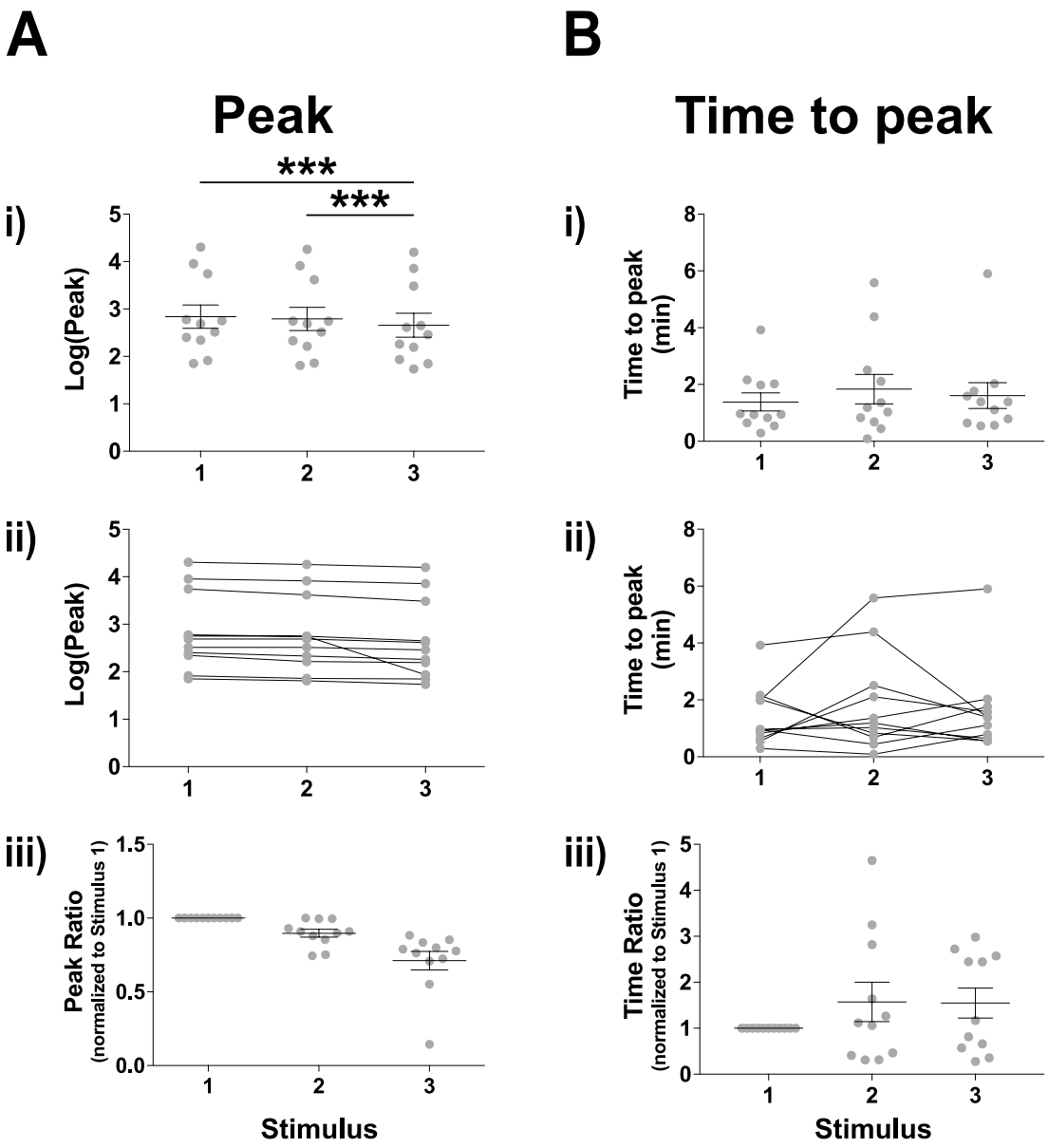


**Figure 5.6 Attenuation of peak but not time to peak of $[Ca^{2+}]_i$ responses in male zDHHC23-KO corticotrophs to repeated CRH.** Quantification of effects of repeated exposure to 0.2 nM CRH in **(A)** peak and **(B)** time to peak. *** $p < 0.001$ (n = 11 from 6 experiments, mixed effects model). All data are means ± SEM.

## Figure 5.7

### Response duration and peak duration of $[Ca^{2+}]_i$ responses in male zDHHC23-KO corticotrophs to repeated CRH

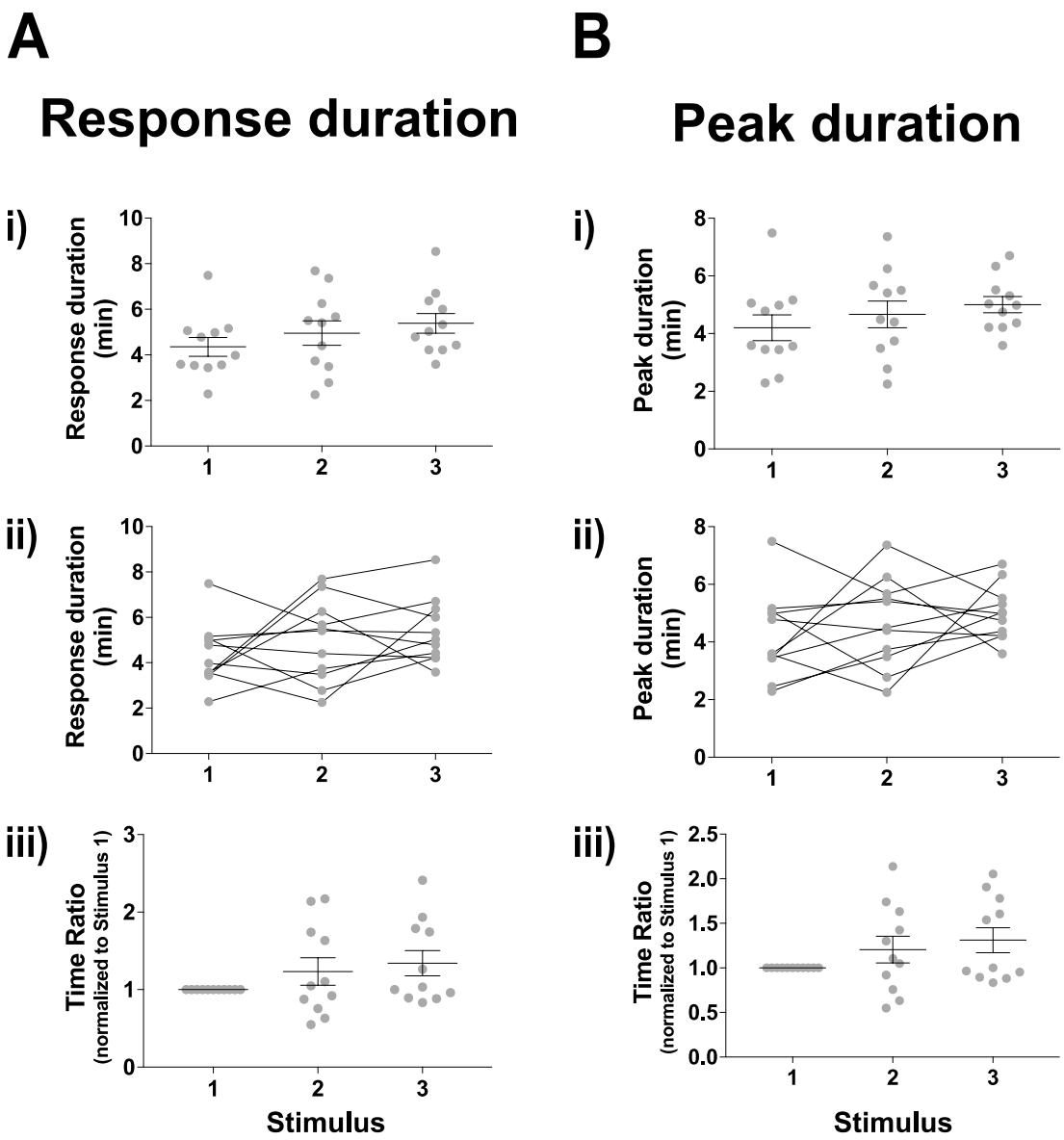


**Figure 5.7 Response duration and peak duration of $[Ca^{2+}]_i$ responses in male zDHHC23-KO corticotrophs to repeated CRH.** Quantification of effects of repeated exposure to 0.2 nM CRH in **(A)** response duration and **(B)** peak duration (n = 11 from 6 experiments, mixed effects model). All data are means ± SEM.

## Figure 5.8

### Time gap of $[Ca^{2+}]_i$ responses in male zDHHC23-KO corticotrophs to repeated CRH

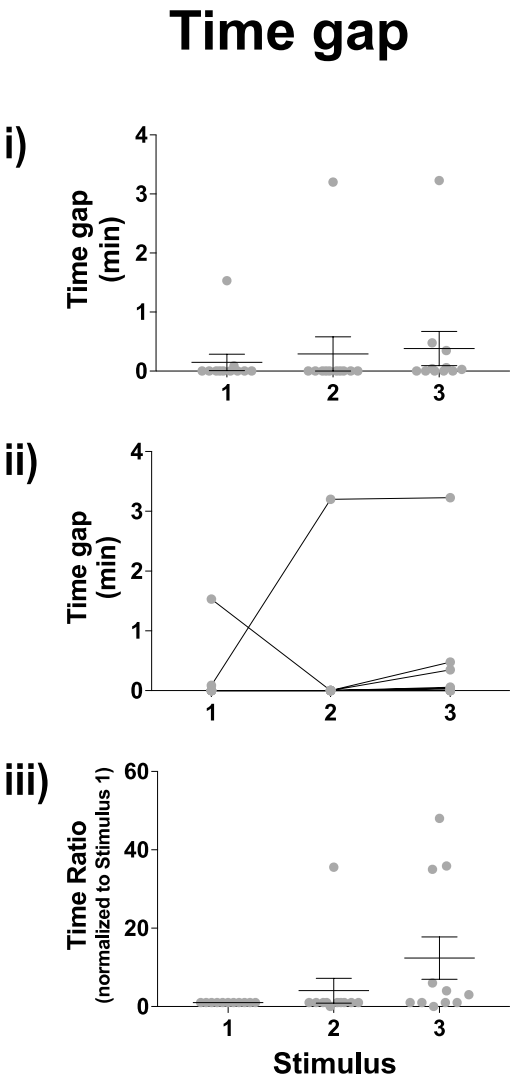


**Figure 5.8 Time gap of $[Ca^{2+}]_i$ responses in male zDHHC23-KO corticotrophs to repeated CRH.** Quantification of effects of repeated exposure to 0.2 nM CRH in time gap (n = 11 from 6 experiments, mixed effects model). All data are means ± SEM.

corticotrophs (Figure 5.9B).

Repeated CRH stimulation significantly reduced AUC (10 min) and AUC (peak) of Stimulus 3 ($p < 0.001$) and Stimulus 2 ($p < 0.05$) compared to Stimulus 1(Figure 5.10). Peak was also displayed significantly attenuation between Stimulus 1 and Stimulus 3 ($p < 0.001$), Stimulus 2 and Stimulus 3 ($p < 0.01$) as well as Stimulus 2 and Stimulus 3 ($p < 0.01$) (Figure 5.11A). Time to peak (Figure 5.11B), response duration, peak duration (Figure 5.12) and time gap (Figure 5.13) showed no statistically significant differences following repeated 0.2 nM CRH stimulation.

These data suggest that female zDHHC23-KO corticotrophs were also less able to sustain robust $[Ca^{2+}]_i$ responses to repeated CRH stimulation.

#### 5.2.2.3 Genetic deletion of zDHHC23 differentially controls AUC (peak) and response duration of $[Ca^{2+}]_i$ responses in male and female corticotrophs

Although corticotrophs from both male and female zDHHC23-KO mice displayed progressive attenuation of $[Ca^{2+}]_i$ responses to repeated CRH stimulation, we investigated whether there were differences between male and female zDHHC23-KO corticotrophs.

## Figure 5.9

### Progressive attenuation of $[Ca^{2+}]_i$ responses in female zDHHC23-KO corticotrophs to repeated CRH

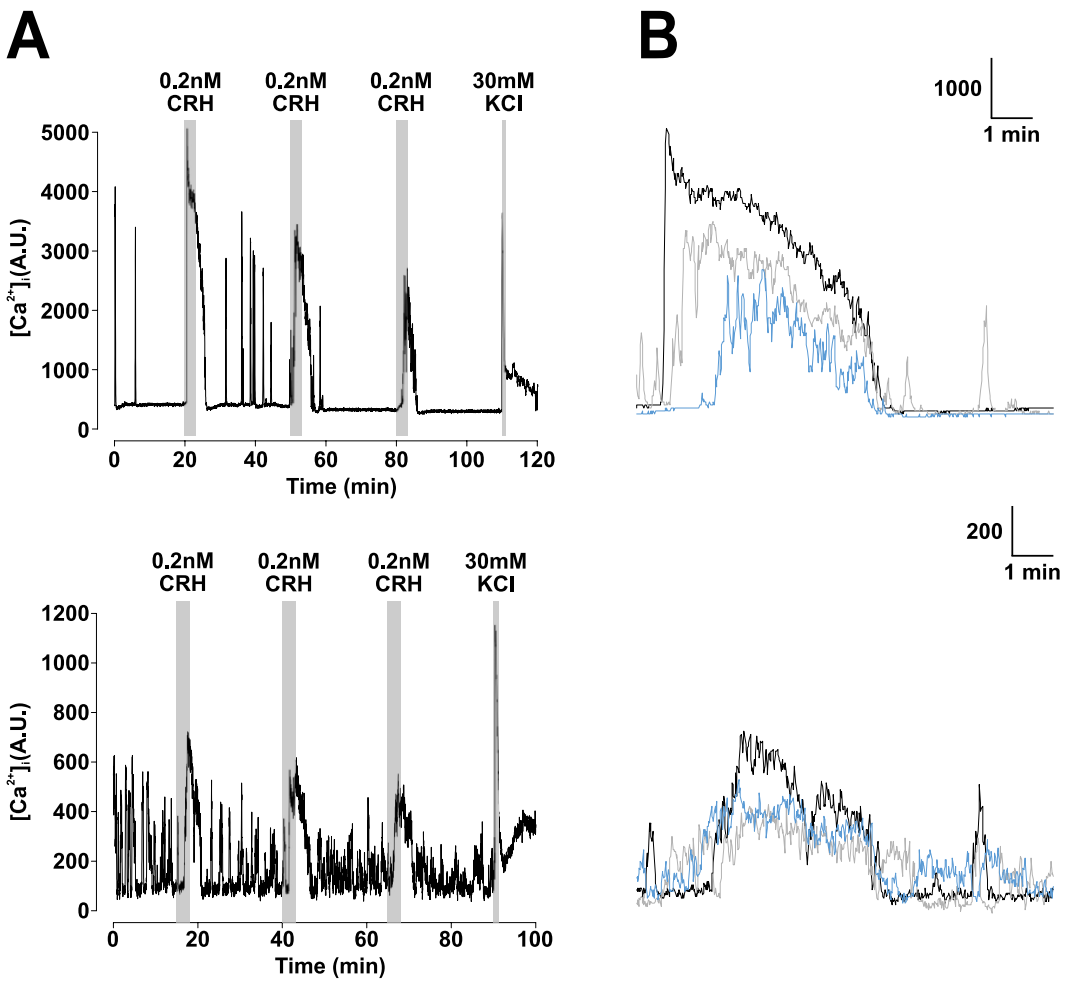


**Figure 5.9 Progressive attenuation of $[Ca^{2+}]_i$ responses in female zDHHC23-KO corticotrophs to repeated CRH. (A)** Representative calcium imaging traces of female zDHHC23-KO corticotrophs exposed to 0.2 nM CRH for three minutes and repeated three times at 25 minutes intervals. 30 mM potassium chloride was applied at the end for one minute. **(B)** Superposition of extracts of the two traces shown in A, showing $[Ca^{2+}]_i$ changes in female zDHHC23-KO corticotrophs with repeated 0.2 nM CRH stimulation. Black line shows response to the first stimulus (starting at 15 min), grey line shows response to the second stimulus (starting at 40 min), and blue line shows response to the third stimulus (starting at 65 min).

## Figure 5.10

**Attenuation of AUC (10 min) and AUC (peak) of $[Ca^{2+}]_i$ responses in female zDHHC23-KO corticotrophs to repeated CRH**

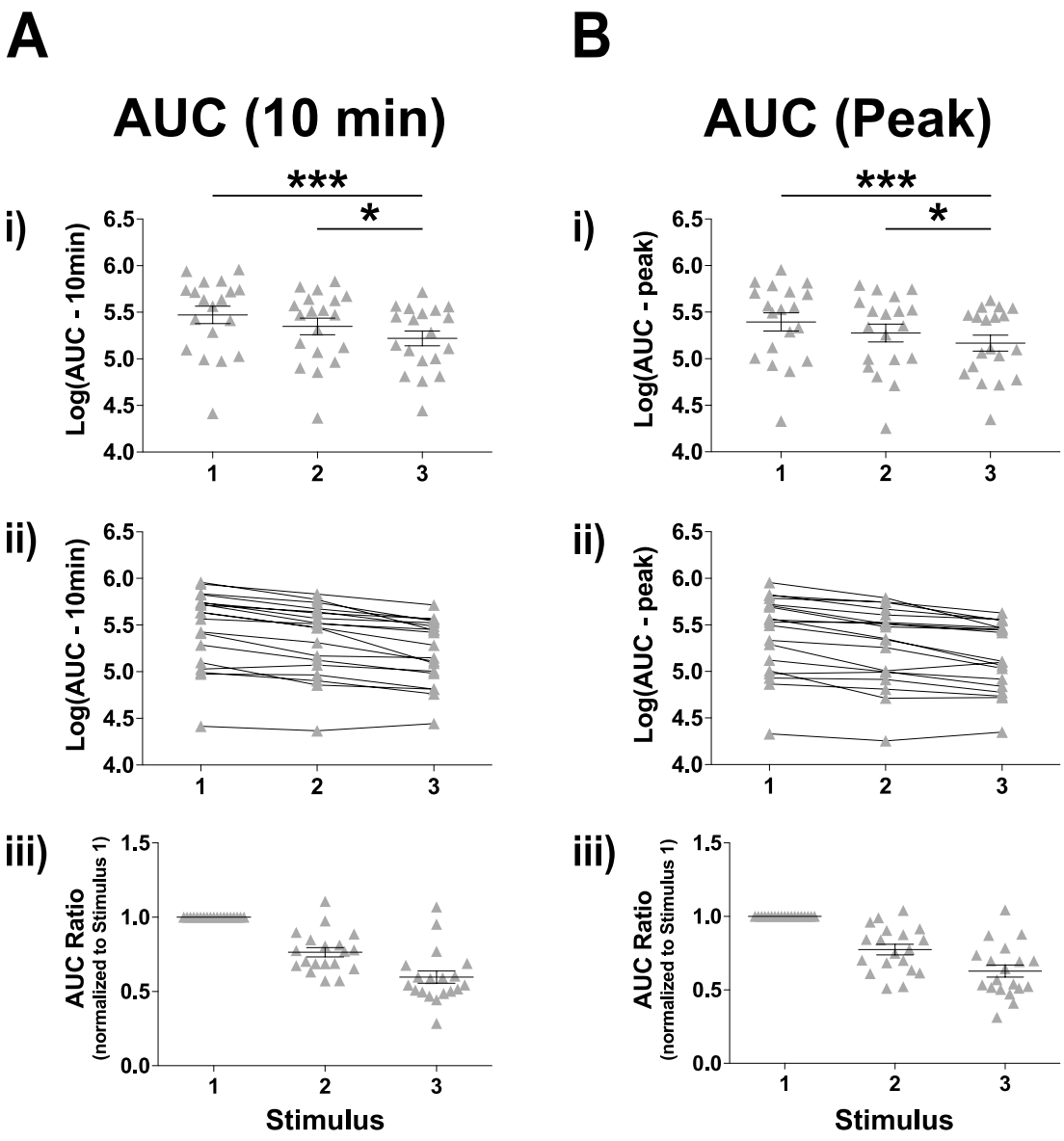


**Figure 5.10 Attenuation of AUC (10 min) and AUC (peak) of $[Ca^{2+}]_i$ responses in female zDHHC23-KO corticotrophs to repeated CRH.** Quantification of effects of repeated exposure to 0.2 nM CRH in **(A)** AUC (10 min) and **(B)** AUC (peak). *** $p < 0.001$, * $p < 0.05$ ($n = 19$ from 11 experiments, mixed effects model). All data are means ± SEM.

## Figure 5.11

### Attenuation of peak but not time to peak of $[Ca^{2+}]_i$ responses in female zDHHC23-KO corticotrophs to repeated CRH

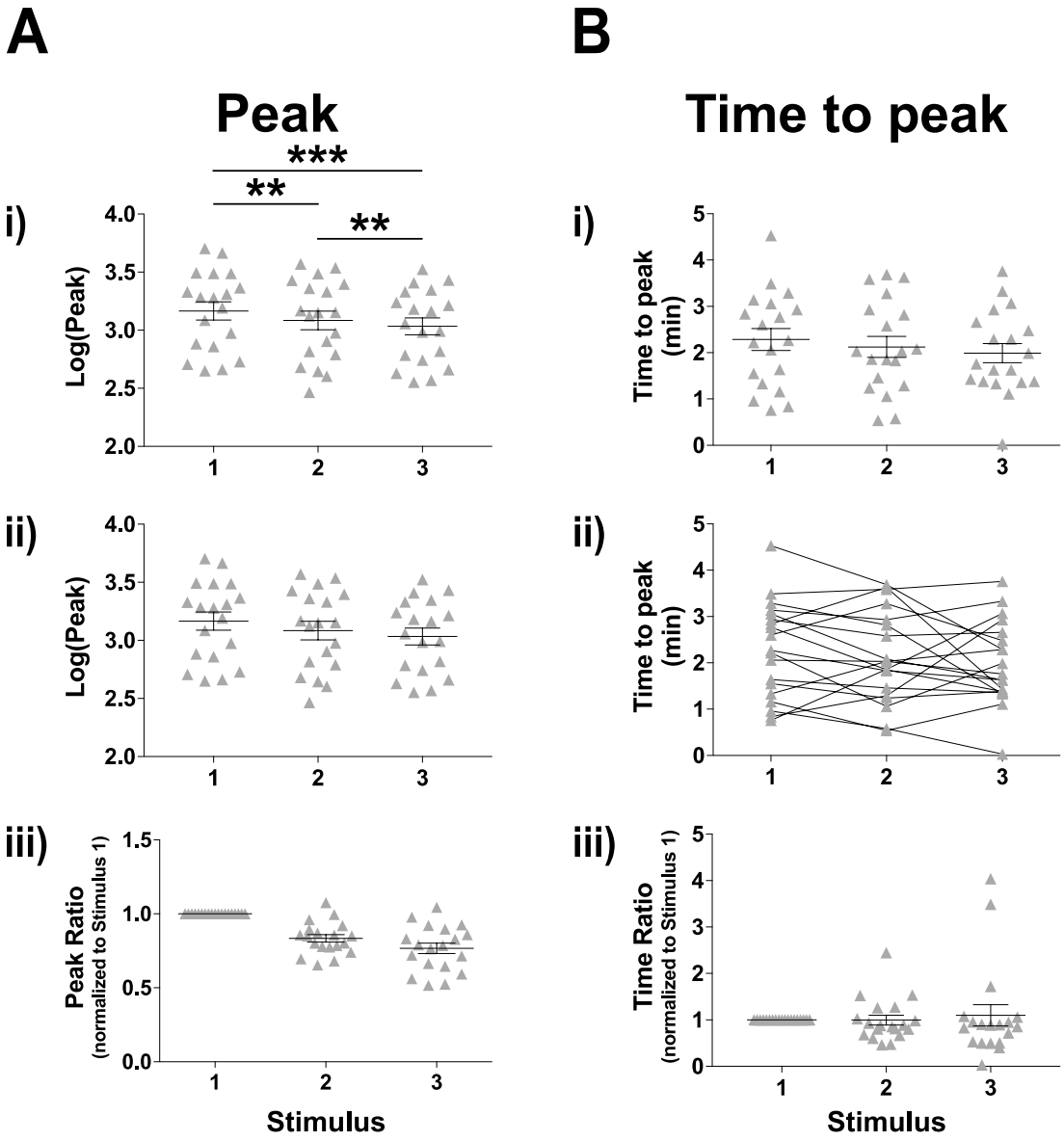


**Figure 5.11 Attenuation of peak but not time to peak of $[Ca^{2+}]_i$ responses in female zDHHC23-KO corticotrophs to repeated CRH.** Quantification of effects of repeated exposure to 0.2 nM CRH in **(A)** peak and **(B)** time to peak. *** $p < 0.001$, ** $p < 0.01$ ($n = 19$ from 11 experiments, mixed effects model). All data are means ± SEM.

## Figure 5.12

### Response duration and peak duration of $[Ca^{2+}]_i$ responses in female zDHHC23-KO corticotrophs to repeated CRH

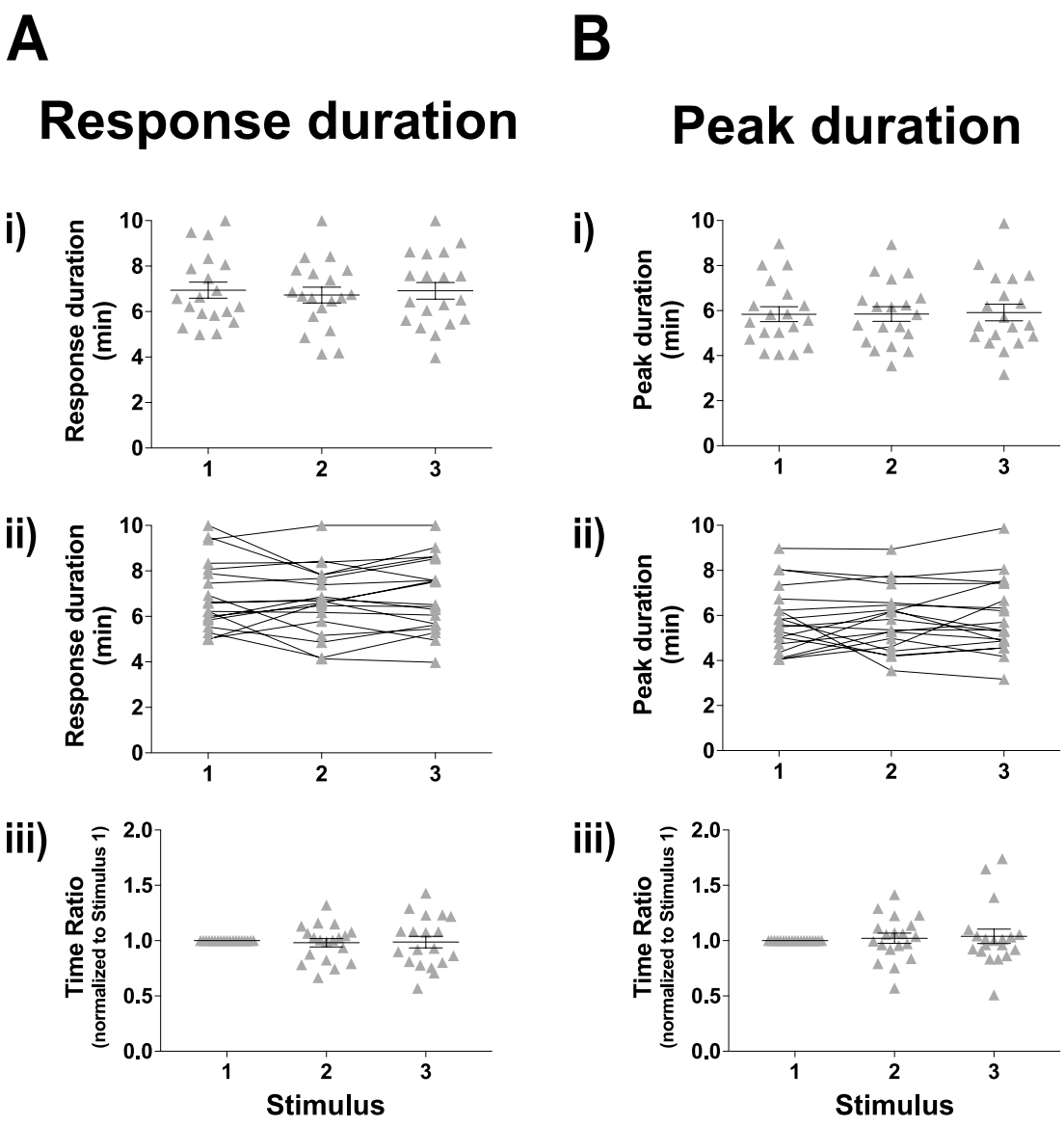


**Figure 5.12 Response duration and peak duration of $[Ca^{2+}]_i$ responses in female zDHHC23-KO corticotrophs to repeated CRH.** Quantification of effects of repeated exposure to 0.2 nM CRH in **(A)** response duration and **(B)** peak duration (n = 19 from 11 experiments, mixed effects model). All data are means ± SEM.

## Figure 5.13

### Time gap of $[Ca^{2+}]_i$ responses in female zDHHC23-KO corticotrophs to repeated CRH

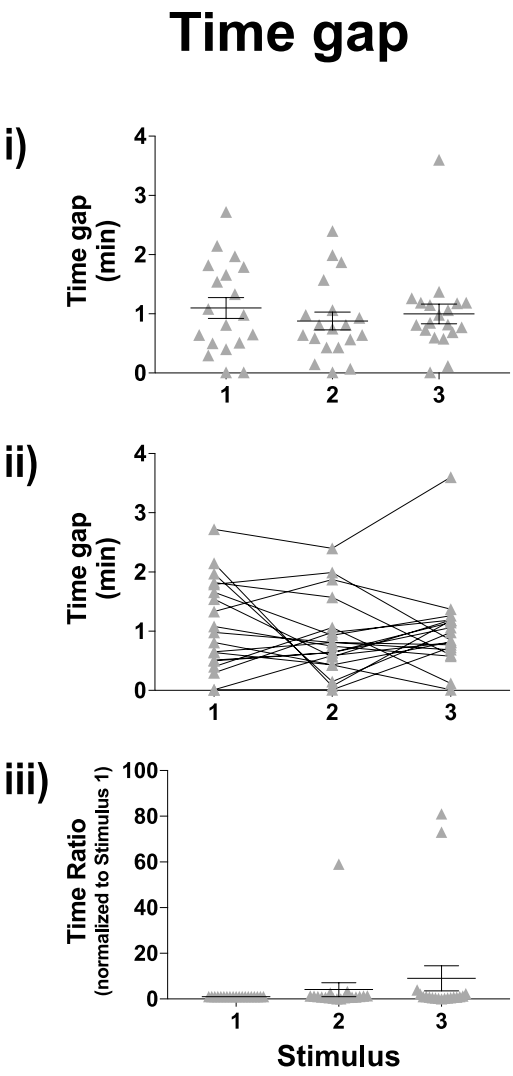


**Figure 5.13 Time gap of $[Ca^{2+}]_i$ responses in female zDHHC23-KO corticotrophs to repeated CRH.** Quantification of effects of repeated exposure to 0.2 nM CRH in time gap (n = 19 from 11 experiments, mixed effects model). All data are means ± SEM.

Statistical analysis revealed that AUC (peak) but not AUC (10 min) was significantly ($p < 0.05$) different between male and female zDHHC23-KO corticotrophs at each CRH stimulus (Figure 5.14). There were no significant differences in peak or time to peak although male corticotrophs tended to have higher variability (Figure 5.15A&B). However, female corticotrophs displayed significantly ($p < 0.05$) longer response duration in Stimulus 3 compared to males (Figure 5.15C). Peak duration and time gap were not significantly different following repeated CRH stimulation (Figure 5.16).

In summary, progressive attenuation of $[Ca^{2+}]_i$ responses to repeated CRH stimulation was observed in both male and female zDHHC23-KO corticotrophs with sex differences in AUC (peak) and response duration.

#### 5.2.2.4 No significant difference in $[Ca^{2+}]_i$ responses to repeated CRH stimulation between male wild-type and zDHHC23-KO corticotrophs

To investigate whether the attenuation of CRH-induced $[Ca^{2+}]_i$ responses with each stimulus in male zDHHC23-KO corticotrophs were significantly different from the $[Ca^{2+}]_i$ responses in male wild-type corticotrophs, comparison and statistical analysis of each parameter was performed.

Although there was a significant reduction in AUC (10 min) and AUC (peak) with

## Figure 5.14

**AUC (peak) but not AUC (10 min) of $[Ca^{2+}]_i$ responses to repeated CRH are significantly different between female and male zDHHC23-KO corticotrophs**

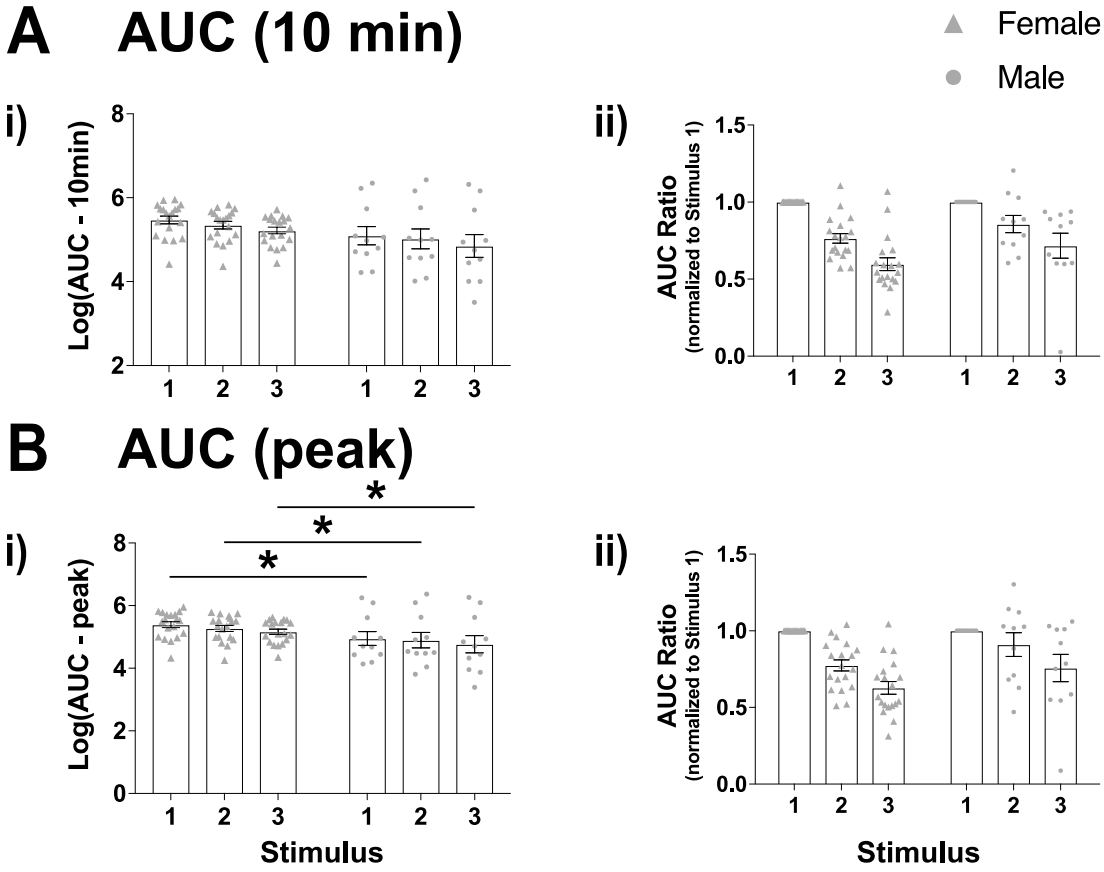


**Figure 5.14 AUC (peak) but not AUC (10 min) of $[Ca^{2+}]_i$ responses to repeated CRH are significantly different between female and male zDHHC23-KO corticotrophs.** Quantification of effects of repeated exposure to 0.2 nM CRH in **(A)** AUC (10 min) and **(B)** AUC (peak) (male n = 11 from 6 experiments, female n = 19 from 11 experiments, mixed effects model). All data are means ± SEM.

## Figure 5.15

**Female zDHHC23-KO corticotrophs have higher response duration but not peak or time to peak of $[Ca^{2+}]_i$ responses to repeated CRH compared to males**

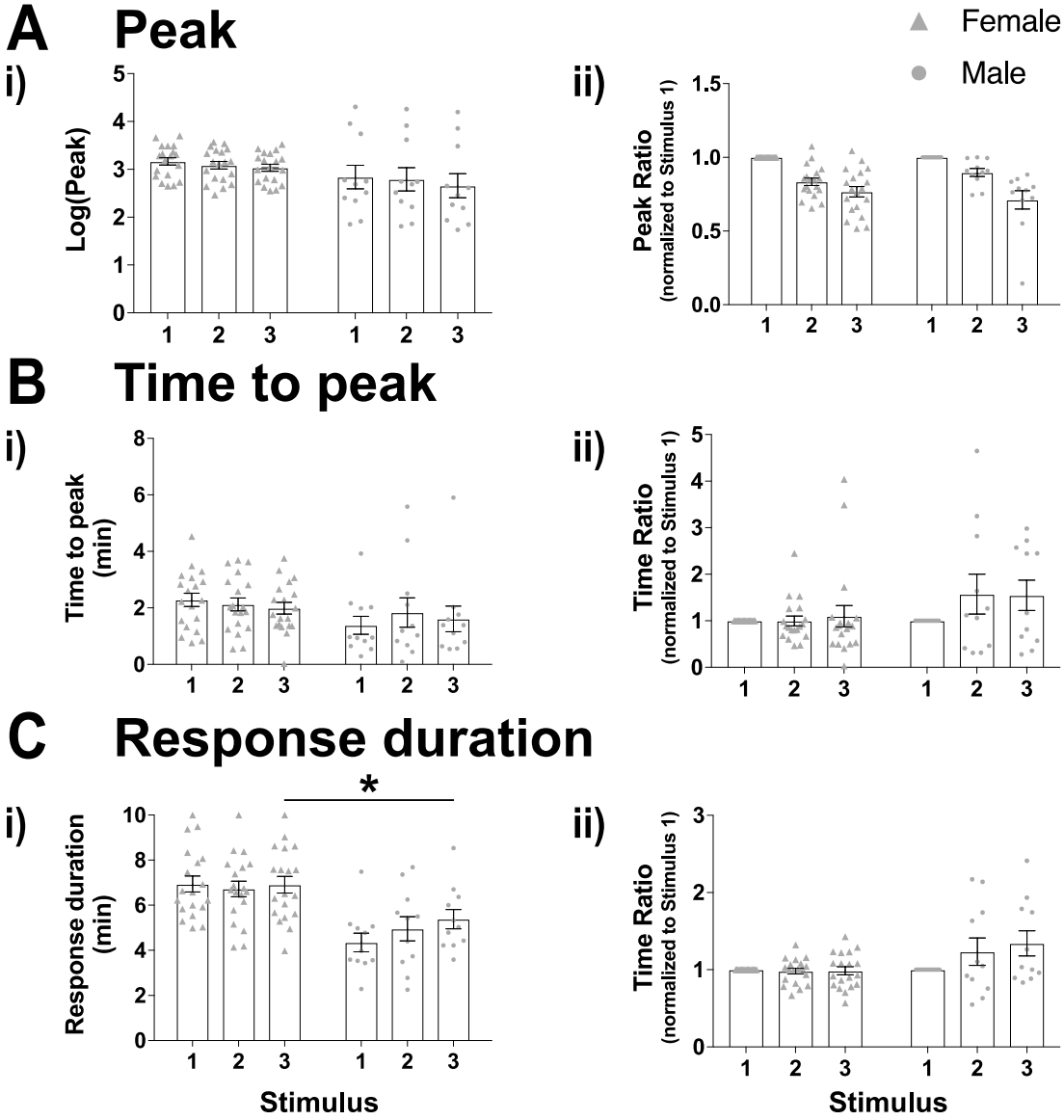


**Figure 5.15 Female zDHHC23-KO corticotrophs have higher response duration but not peak or time to peak of $[Ca^{2+}]_i$ responses to repeated CRH compared to males.** Quantification of effects of repeated exposure to 0.2 nM CRH in **(A)** peak, **(B)** time to peak and **(C)** response duration. * $p < 0.05$ (male n = 11 from 6 experiments, female n = 19 from 11 experiments, mixed effects model). All data are means ± SEM.

## Figure 5.16

### No significant sex difference in CRH-induced peak duration or time gap $[Ca^{2+}]_i$ responses in zDHHC23-KO corticotrophs

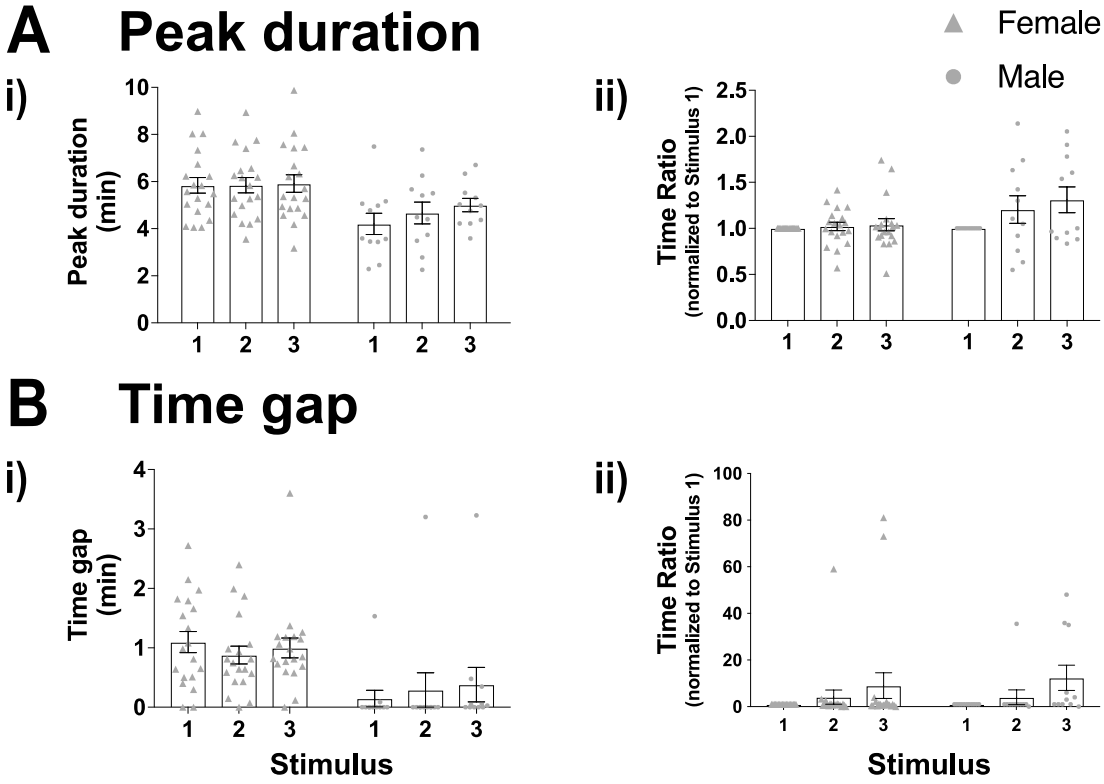


**Figure 5.16 No significant sex difference in CRH-induced peak duration or time gap $[Ca^{2+}]_i$ responses in zDHHC23-KO corticotrophs.** Quantification of effects of repeated exposure to 0.2 nM CRH in **(A)** peak duration and **(B)** time gap (male n = 11 from 6 experiments, female n = 19 from 11 experiments, mixed effects model). All data are means ± SEM.

repeated exposure to CRH in male zDHHC23-KO, but not wild-type, corticotrophs, comparison of each stimulus to the comparable response in wild-type corticotrophs revealed no significant statistical differences (Figure 5.17). Peak was significantly attenuated in both wild-type and zDHHC23-KO male corticotrophs following repeated CRH stimulation, however, no significant differences were observed between them at each stimulus (Figure 5.18A). This may in part reflect the higher variability in male corticotrophs. In addition, there were no significant differences between male wild-type and zDHHC23-KO corticotrophs in time to peak, response duration (Figure 5.18B&C), peak duration or time gap (Figure 5.19).

Overall, these results suggest that genetic deletion of zDHHC23 had no effect on CRH-induced $[Ca^{2+}]_i$ signalling in male corticotrophs compared to wild-type.

#### 5.2.2.5 No significant difference in $[Ca^{2+}]_i$ responses to repeated CRH stimulation between female wild-type and zDHHC23-KO corticotrophs

As observed in male zDHHC23-KO corticotrophs, female zDHHC23-KO corticotrophs also showed significant decline in AUC (peak), AUC (10 min) and peak with repeated exposure to CRH. However, as for male wild-type and zDHHC23-KO corticotrophs, there were no statistically significant differences in these parameters at each CRH stimulus between female wild-type and zDHHC23-KO corticotrophs either

## Figure 5.17

**No significant differences in CRH-induced AUC (10 min) or AUC (peak) of $[Ca^{2+}]_i$ responses between male wild-type and zDHHC23-KO corticotrophs**

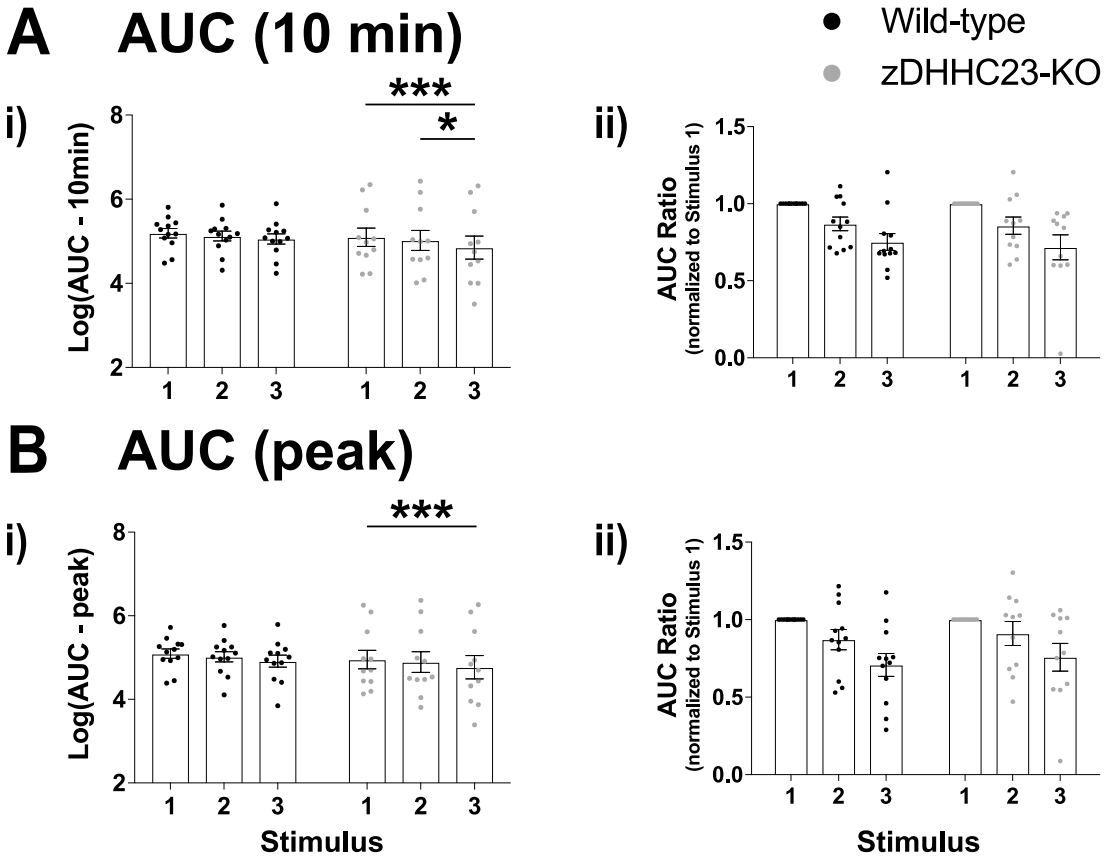


**Figure 5.17 No significant differences in CRH-induced AUC (10 min) or AUC (peak) of $[Ca^{2+}]_i$ responses between male wild-type and zDHHC23-KO corticotrophs.** Quantification of effects of repeated exposure to 0.2 nM CRH in **(A)** AUC (10 min) and **(B)** AUC (peak). *** $p < 0.001$, * $p < 0.05$ (wild-type n = 12 from 8 experiments, zDHHC23-KO n = 11 from 6 experiments, mixed effects model). All data are means ± SEM.

## Figure 5.18

**No significant differences in CRH-induced peak, time to peak or response duration of $[Ca^{2+}]_i$ responses between male wild-type and zDHHC23-KO corticotrophs**

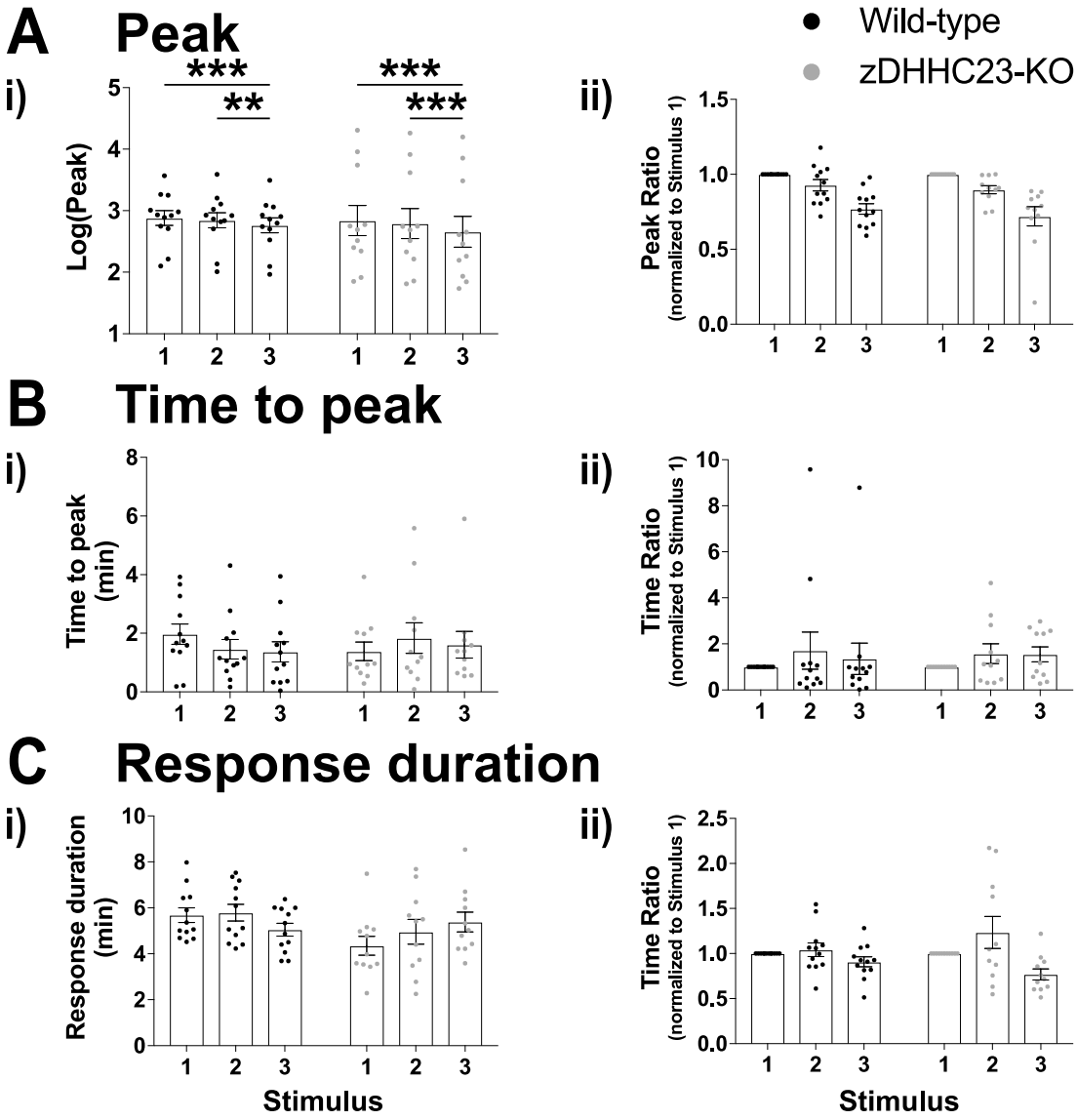


**Figure 5.18 No significant differences in CRH-induced peak, time to peak or responses duration of $[Ca^{2+}]_i$ responses between male wild-type and zDHHC23-KO corticotrophs.** Quantification of effects of repeated exposure to 0.2 nM CRH in **(A)** peak, **(B)** time to peak and **(C)** response duration. *** $p < 0.001$, ** $p < 0.01$ (wild-type n = 12 from 8 experiments, zDHHC23-KO n = 11 from 6 experiments, mixed effects model). All data are means ± SEM.

## Figure 5.19

**No significant differences in CRH-induced peak duration or time gap of $[Ca^{2+}]_i$ responses between male wild-type and zDHHC23-KO corticotrophs**

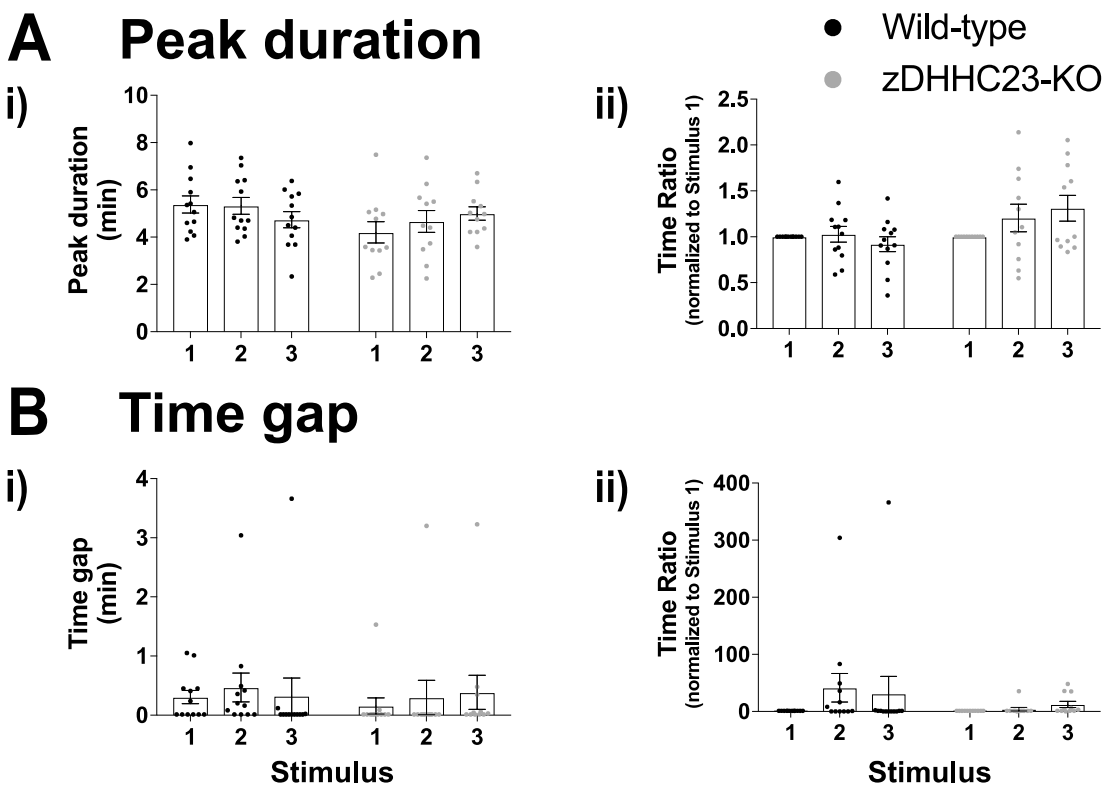


**Figure 5.19 No significant differences in CRH-induced peak duration or time gap of $[Ca^{2+}]_i$ responses between male wild-type and zDHHC23-KO corticotrophs.** Quantification of effects of repeated exposure to 0.2 nM CRH in **(A)** peak duration and **(B)** time gap (wild-type n = 12 from 8 experiments, zDHHC23-KO n = 11 from 6 experiments, mixed effects model). All data are means ± SEM.

(Figure 5.20 & Figure 5.21A). Female wild-type and zDHHC23-KO corticotrophs had no significant differences in time to peak, response duration (Figure 5.21B&C), peak duration or time gap (Figure 5.22) to repeated CRH stimulation either.

This suggests that genetic deletion of zDHHC23 did not affect $[Ca^{2+}]_i$ responses to repeated CRH stimulation in female corticotrophs.

In summary, genetic deletion of zDHHC23 significantly reduced the ability to respond consistently to repeated CRH stimulation in both male and female corticotrophs. However, there were no significant sex differences in CRH-induced $[Ca^{2+}]_i$ responses and there were no statistically significant differences between $[Ca^{2+}]_i$ responses at each CRH stimulus when comparing wild-type and zDHHC23-KO corticotrophs. Thus, while zDHHC23 may play a subtle role in controlling the stability of $[Ca^{2+}]_i$ responses to repeated CRH stimulation, zDHHC23 does not play a major role to control CRH-induced $[Ca^{2+}]_i$ signalling in murine corticotrophs.

### 5.2.3 Genetic deletion of zDHHC23 has no significant effect on AVP-induced $[Ca^{2+}]_i$ responses in male and female corticotrophs

The above data suggest that zDHHC23 is not a major mechanism to control

## Figure 5.20

**No significant differences in CRH-induced AUC (10 min) and AUC (peak) of $[Ca^{2+}]_i$ responses between female wild-type and zDHHC23-KO corticotrophs**

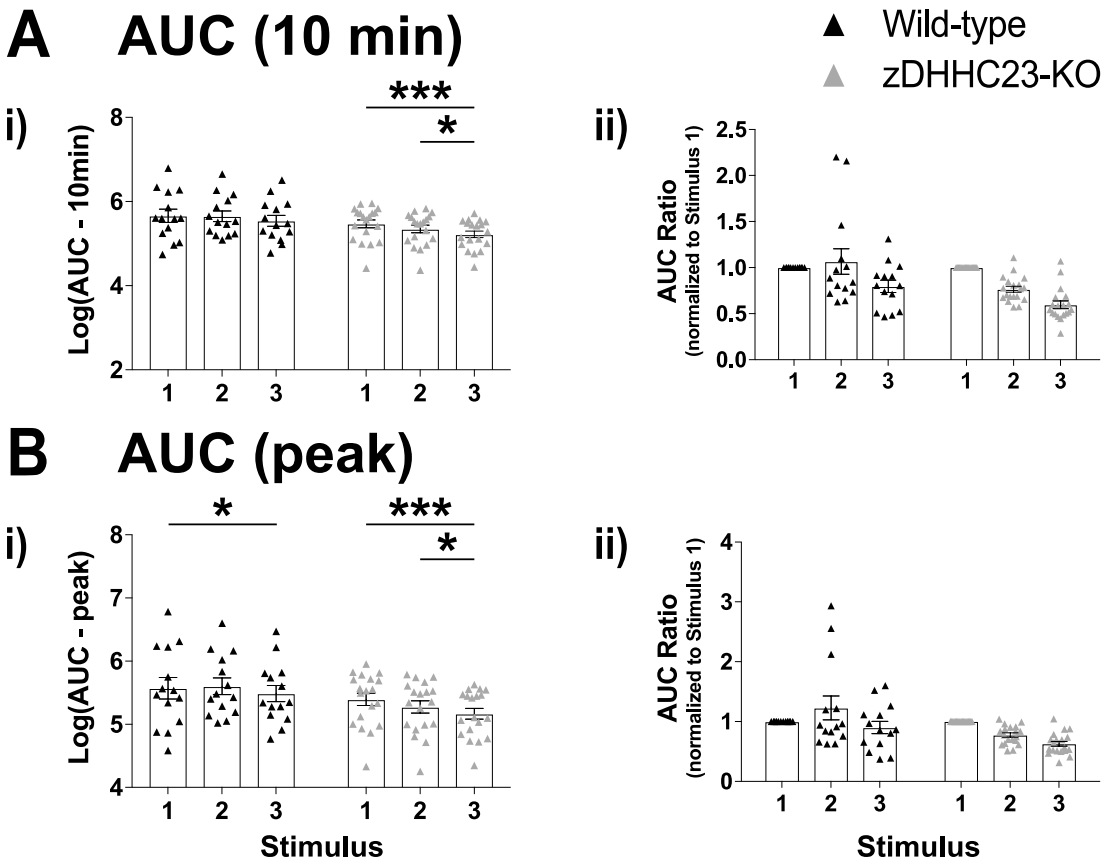


**Figure 5.20 No significant differences in CRH-induced AUC (10 min) and AUC (peak) of $[Ca^{2+}]_i$ responses between female wild-type and zDHHC23-KO corticotrophs.** Quantification of effects of repeated exposure to 0.2 nM CRH in **(A)** AUC (10 min) and **(B)** AUC (peak). *** $p < 0.001$, ** $p < 0.01$, * $p < 0.05$ (wild-type n = 14 from 7 experiments, zDHHC23-KO n = 19 from 11 experiments, mixed effects model). All data are means ± SEM.

## Figure 5.21

**No significant differences in CRH-induced peak, time to peak or response duration of $[Ca^{2+}]_i$ responses between female wild-type and zDHHC23-KO corticotrophs**

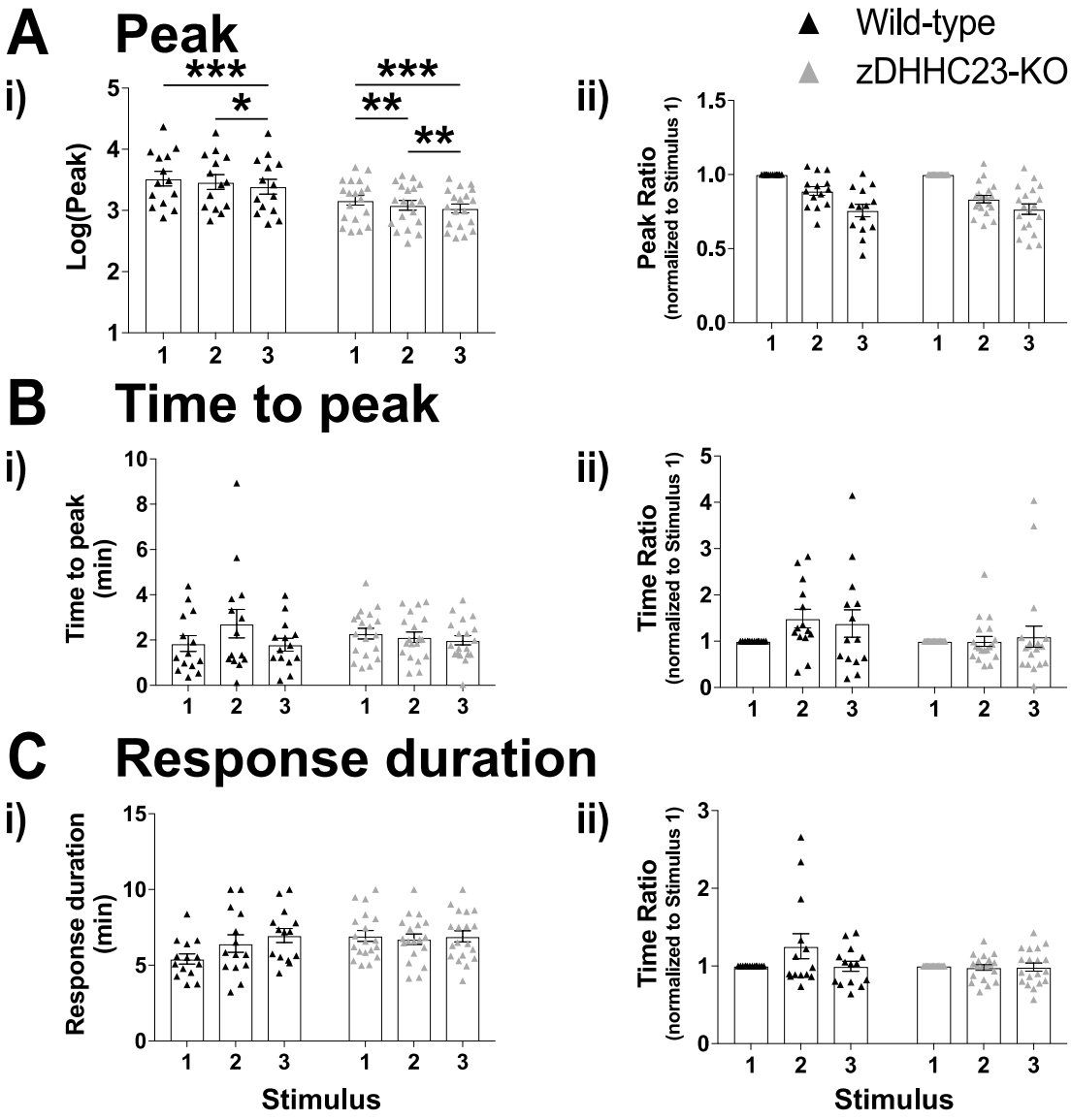


**Figure 5.21 No significant differences in CRH-induced peak, time to peak or response duration of $[Ca^{2+}]_i$ responses between female wild-type and zDHHC23-KO corticotrophs.** Quantification of effects of repeated exposure to 0.2 nM CRH in **(A)** peak, **(B)** time to peak and **(C)** response duration. *** $p < 0.001$ (wild-type n = 14 from 7 experiments, zDHHC23-KO n = 19 from 11 experiments, mixed effects model). All data are means ± SEM.

## Figure 5.22

**No significant differences in CRH-induced peak duration or time gap of $[Ca^{2+}]_i$ responses between female wild-type and zDHHC23-KO corticotrophs**

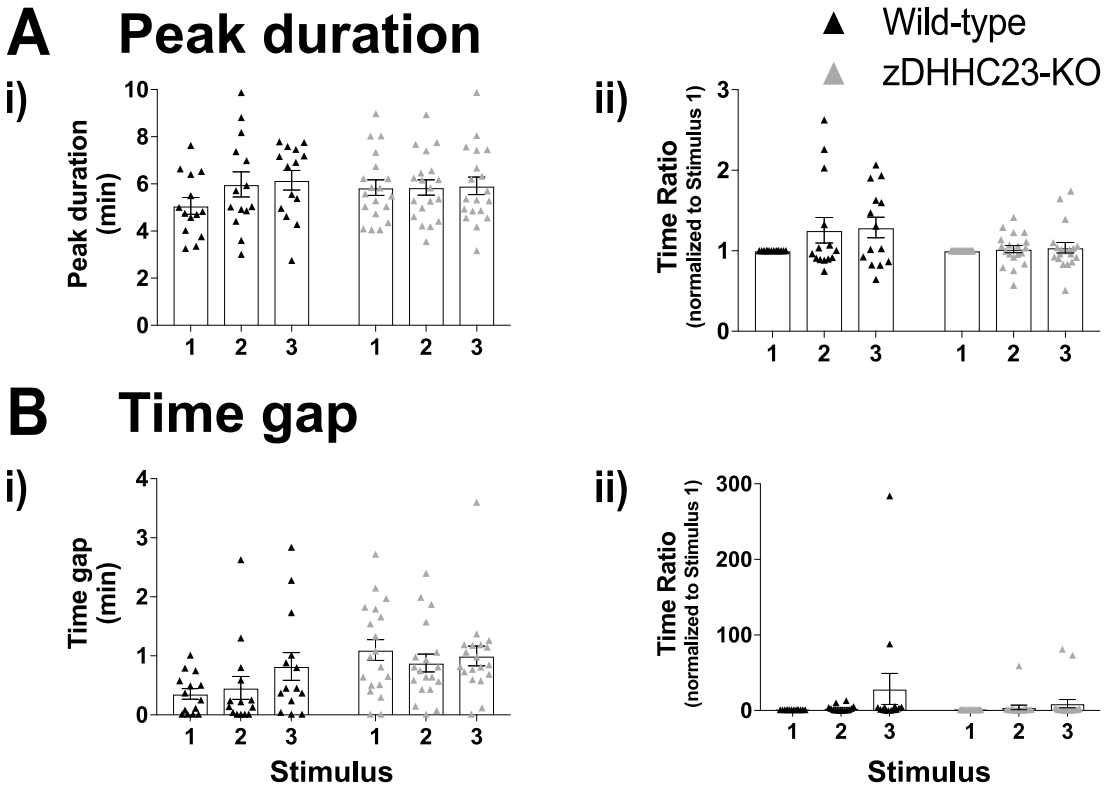


**Figure 5.22 No significant differences in CRH-induced peak duration or time gap of $[Ca^{2+}]_i$ responses between female wild-type and zDHHC23-KO corticotrophs.** Quantification of effects of repeated exposure to 0.2 nM CRH in **(A)** peak duration and **(B)** time gap (wild-type n = 14 from 7 experiments, zDHHC23-KO n = 19 from 11 experiments, mixed effects model). All data are means ± SEM.

spontaneous or CRH-induced $[Ca^{2+}]_i$ responses in murine corticotrophs. Experiments were also performed to investigate whether knockout of zDHHC23 controlled $[Ca^{2+}]_i$ responses to repeated 2 nM AVP stimulation in corticotrophs.

As observed in wild-type corticotrophs, zDHHC23-KO corticotrophs also displayed two phenotypes of $[Ca^{2+}]_i$ responses. Following repeated 2 nM AVP stimulation, 79.2% (19 out of 24) of cells always exhibited sustained elevation of $[Ca^{2+}]_i$; 8.3% of (2 out of 24) cells showed oscillatory $[Ca^{2+}]_i$ behaviour. In the remaining 3 cells (12.5%), both sustained increase of $[Ca^{2+}]_i$ and oscillatory $[Ca^{2+}]_i$ behaviour were found in one cell upon repeated AVP stimulation. This was different from wild-type corticotrophs, with 60% of cells showing sustained $[Ca^{2+}]_i$ elevation and the rest showing oscillatory $[Ca^{2+}]_i$ behaviour. Importantly, the mixture of the two phenotypes of $[Ca^{2+}]_i$ responses was not observed in the same corticotroph from wild-type mice. This suggests that genetic deletion of zDHHC23 may affect the pattern of $[Ca^{2+}]_i$ responses to AVP in corticotrophs. Next, AVP-induced $[Ca^{2+}]_i$ responses were examined in male and female zDHHC23-KO corticotrophs separately and quantified using the same parameters for wild-type corticotrophs.

#### 5.2.3.1 Repeated AVP evokes robust $[Ca^{2+}]_i$ responses in male zDHHC23-KO corticotrophs

Calcium imaging experiments were performed on male zDHHC23-KO corticotrophs (n = 10 from 8 experiments) following the same repeated stimulation protocol used for wild-type corticotrophs (see 3.2.4.1).

When exposed to repeated 2 nM AVP, 8 out of 10 cells showed sustained elevation of $[Ca^{2+}]_i$ (Figure 5.23A, top) and the other 2 cells displayed both sustained $[Ca^{2+}]_i$ increase and oscillatory $[Ca^{2+}]_i$ behaviour (Figure 5.23A, bottom). No cell showed repetitive oscillatory $[Ca^{2+}]_i$ responses to AVP. It's interesting to note that two phenotypes of $[Ca^{2+}]_i$ responses did not appear in one cell in male wild-type corticotrophs. The dynamics of $[Ca^{2+}]_i$ responses to repeated AVP stimulation was similar to each other when corticotrophs showed sustained $[Ca^{2+}]_i$ increase (Figure 5.23B, top). Although some corticotrophs displayed two phenotypes of $[Ca^{2+}]_i$ responses between repeated AVP stimulation, $[Ca^{2+}]_i$ responses were still consistent in response duration (Figure 5.23B, bottom).

All parameters were examined between the two response phenotypes to examine whether they had significant differences. Statistical analysis revealed that there were no significant differences between sustained increase of $[Ca^{2+}]_i$ and the mixture of

# Figure 5.23

## Repeated AVP induces repeatable $[Ca^{2+}]_i$ responses in male zDHHC23-KO corticotrophs

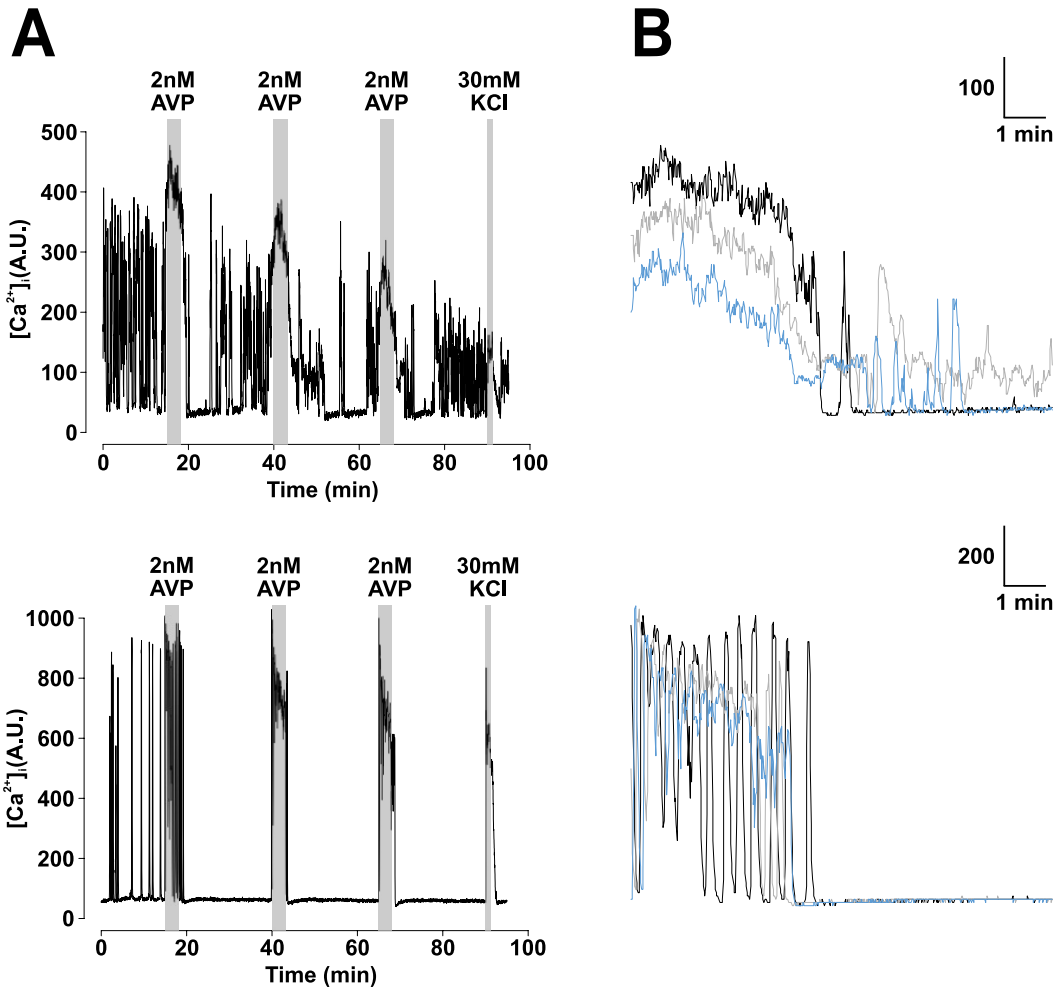


**Figure 5.23 Repeated AVP induces repeatable $[Ca^{2+}]_i$ responses in male zDHHC23-KO corticotrophs. (A)** Representative calcium imaging traces of male zDHHC23-KO corticotrophs exposed to 2 nM AVP for three minutes and repeated three times at 25 minutes intervals. 30 mM potassium chloride was applied at the end for one minute. **(B)** Superposition of extracts of the two traces shown in A, showing $[Ca^{2+}]_i$ changes in male zDHHC23-KO corticotrophs with repeated 2 nM AVP stimulation. Black line shows response to the first stimulus (starting at 15 min), grey line shows response to the second stimulus (starting at 40 min), and blue line shows response to the third stimulus (starting at 65 min).

sustained and oscillatory $[Ca^{2+}]_i$ behaviour (data not shown). Therefore, statistical analysis was performed on all male zDHHC23-KO corticotrophs together. There were no significant differences in AUC (10 min), AUC (peak) (Figure 5.24), peak, time to peak (Figure 5.25), responses duration, peak duration (Figure 5.26) or time gap (Figure 5.27) in male zDHHC23-KO corticotrophs following repeated AVP stimulation.

This suggests that repeated 2 nM AVP stimulation evokes robust and consistent $[Ca^{2+}]_i$ responses in male zDHHC23-KO corticotrophs.

#### 5.2.3.2 Repeated AVP evokes robust $[Ca^{2+}]_i$ responses in female zDHHC23-KO corticotrophs

The calcium imaging experiments were performed on corticotrophs isolated from female zDHHC23-KO mice (n = 14 from 7 experiments) following the same protocol used in male zDHHC23-KO corticotrophs.

When stimulated with 2 nM AVP, all female zDHHC23-KO corticotrophs showed two different phenotypes of $[Ca^{2+}]_i$ responses as male zDHHC23-KO corticotrophs. 11 out of 14 cells displayed sustained elevation of $[Ca^{2+}]_i$ and oscillatory $[Ca^{2+}]_i$ behaviour was observed in 2 cells (Figure 5.28A). Only 1 cell showed both sustained $[Ca^{2+}]_i$ increase and oscillatory $[Ca^{2+}]_i$ behaviour following repeated AVP stimulation.

## Figure 5.24

**Stable AUC (10 min) and AUC (peak) of $[Ca^{2+}]_i$ responses in male zDHHC23-KO corticotrophs to repeated AVP**

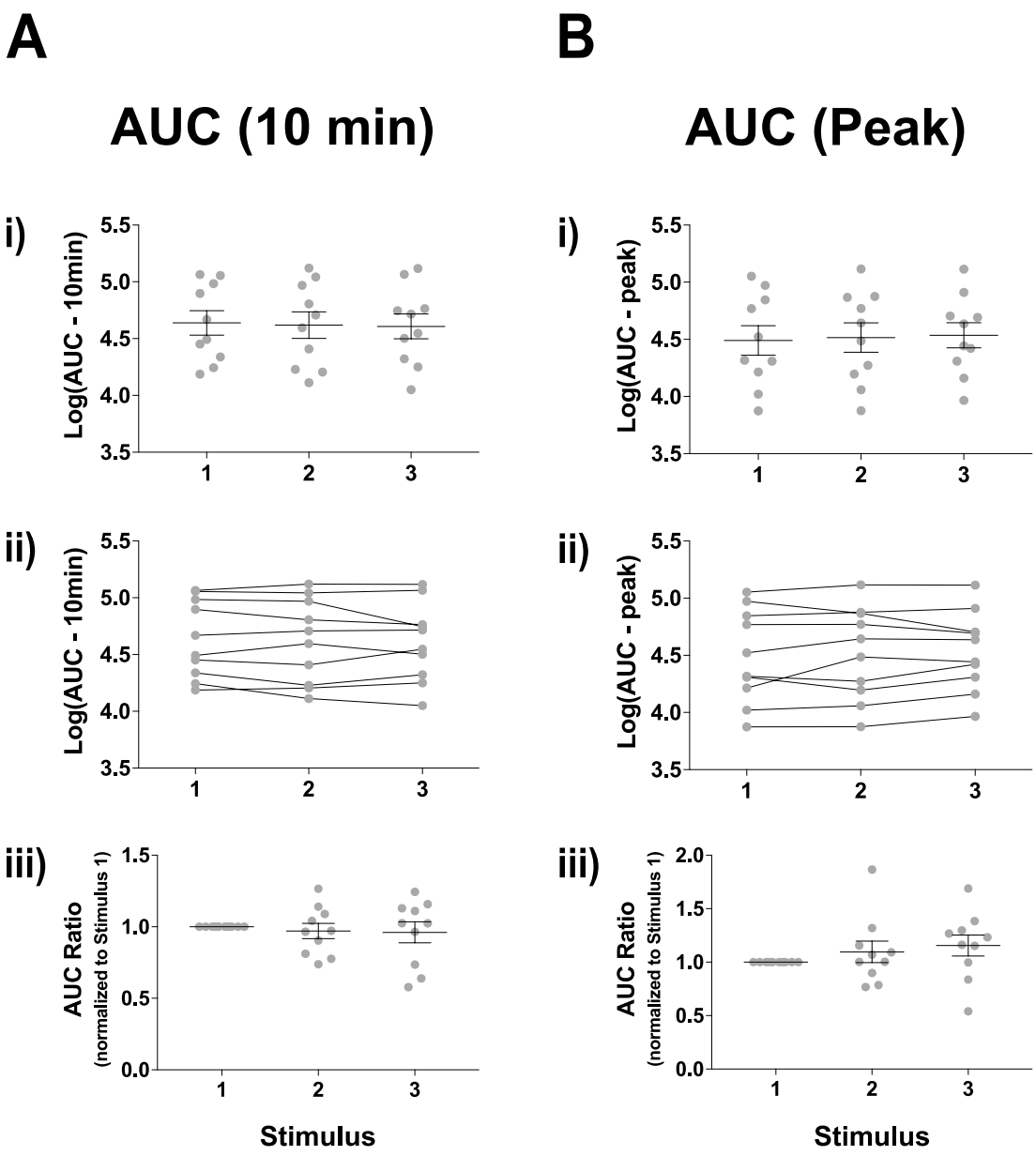


**Figure 5.24 Stable AUC (10 min) and AUC (peak) of $[Ca^{2+}]_i$ responses in male zDHHC23-KO corticotrophs to repeated AVP.** Quantification of effects of repeated exposure to 2 nM AVP in **(A)** AUC (10 min) and **(B)** AUC (peak) (n = 10 from 8 experiments, mixed effects model). All data are means ± SEM.

## Figure 5.25

**Peak and time to peak of $[Ca^{2+}]_i$ responses in male zDHHC23-KO corticotrophs to repeated AVP**

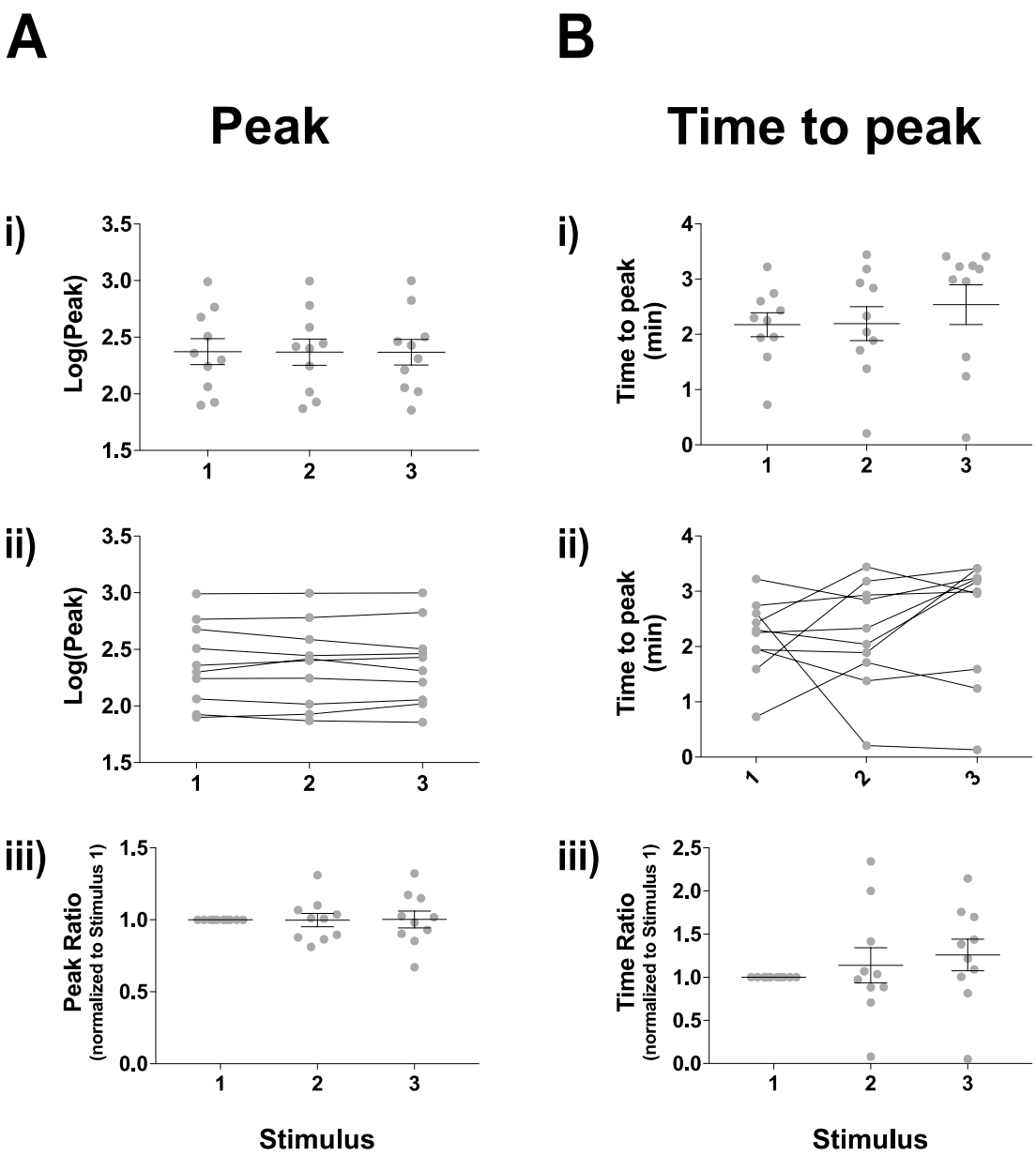


**Figure 5.25 Peak and time to peak of $[Ca^{2+}]_i$ responses in male zDHHC23-KO corticotrophs to repeated AVP.** Quantification of effects of repeated exposure to 2 nM AVP in **(A)** peak and **(B)** time to peak (n = 10 from 8 experiments, mixed effects model). All data are means ± SEM.

## Figure 5.26

### Response duration and peak duration of $[Ca^{2+}]_i$ responses in male zDHHC23-KO corticotrophs to repeated AVP

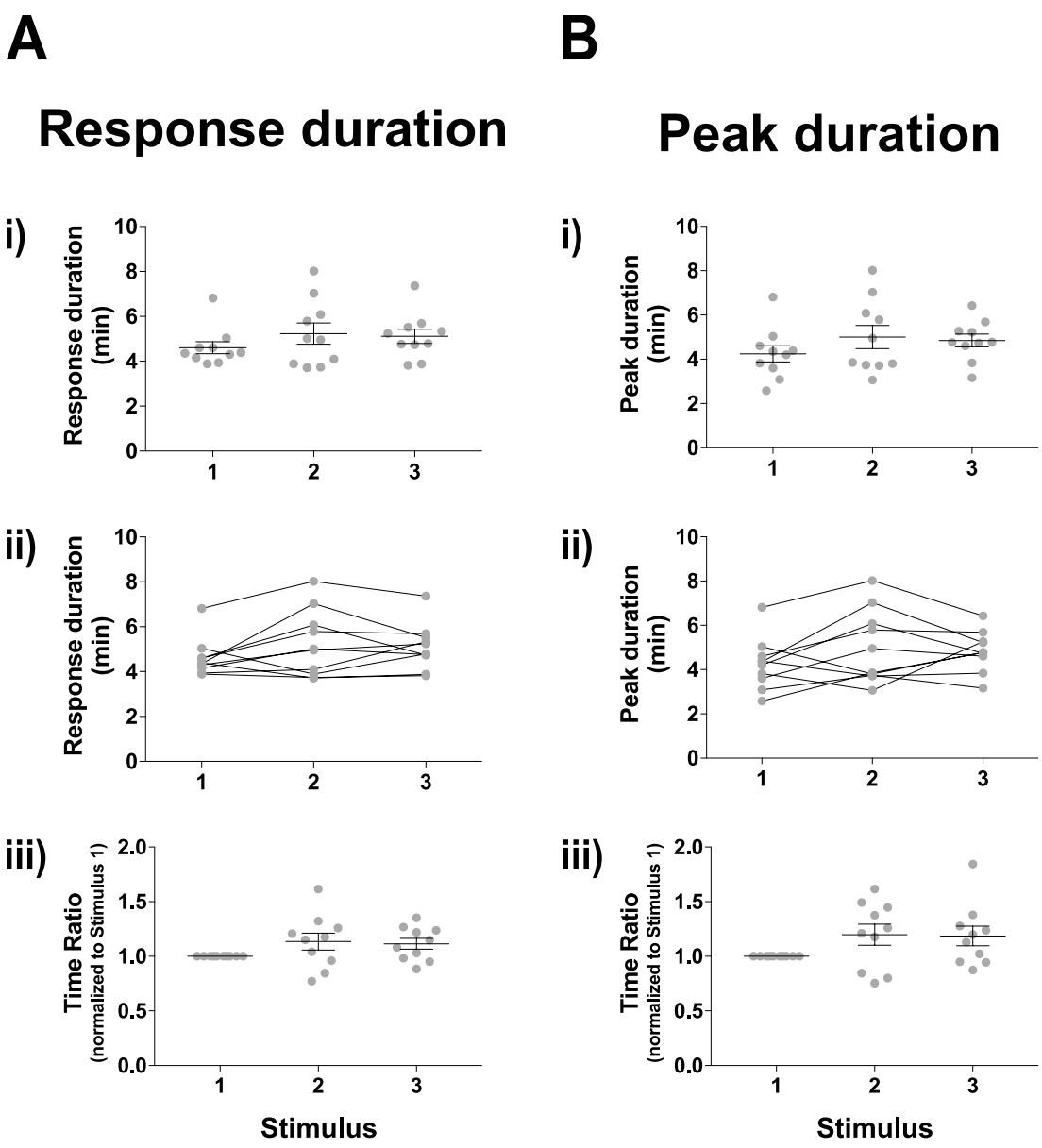


**Figure 5.26 Response duration and peak duration of $[Ca^{2+}]_i$ responses in male zDHHC23-KO corticotrophs to repeated AVP.** Quantification of effects of repeated exposure to 2 nM AVP in **(A)** response duration and **(B)** peak duration (n = 10 from 8 experiments, mixed effects model). All data are means ± SEM.

## Figure 5.27

**Time gap of $[Ca^{2+}]_i$ responses in male zDHHC23-KO corticotrophs to repeated AVP**

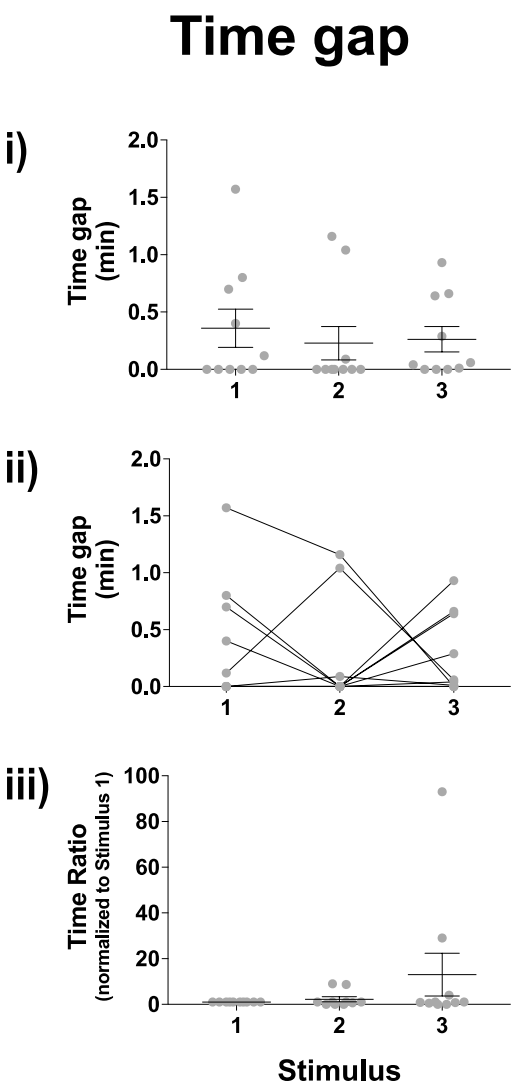


**Figure 5.27 Time gap of $[Ca^{2+}]_i$ responses in male zDHHC23-KO corticotrophs to repeated AVP.** Quantification of effects of repeated exposure to 2 nM AVP in time gap (n = 10 from 8 experiments, mixed effects model). All data are means ± SEM.

However, this was different from female wild-type corticotrophs where each response phenotype accounted for 50% respectively and the mixture of the two phenotypes did not appear in one single cell. As the differences were observed in both male and female zDHHC23-KO corticotrophs compared to wild-type controls, this suggests that zDHHC23 may play a role in controlling the patterns of $[Ca^{2+}]_i$ responses induced by AVP in corticotrophs. Extracts of calcium imaging traces were highly coincidental in both phenotypes indicated that $[Ca^{2+}]_i$ responses to repeated 2 nM AVP stimulus were reproducible in female zDHHC23-KO corticotrophs (Figure 5.28B).

The comparison and analysis of all parameters were performed between AVP-induced two phenotypes of $[Ca^{2+}]_i$ responses to examine whether they were different. These parameters failed to show any significant difference between sustained elevation and oscillatory $[Ca^{2+}]_i$ behaviour (data not shown), thus statistical analysis was performed on all female zDHHC23-KO corticotrophs together. As observed in male zDHHC23-KO corticotrophs, AUC (10 min), AUC (peak) (Figure 5.29), peak, time to peak (Figure 5.30), response duration, peak duration (Figure 5.31) and time gap (Figure 5.32) showed no significant differences following repeated AVP stimulation.

These results suggest that repeated 2 nM AVP stimulation induced highly repeatable and stable $[Ca^{2+}]_i$ responses in female zDHHC23-KO corticotrophs.

## Figure 5.28

### Repeated AVP induces repeatable $[Ca^{2+}]_i$ responses in female zDHHC23-KO corticotrophs

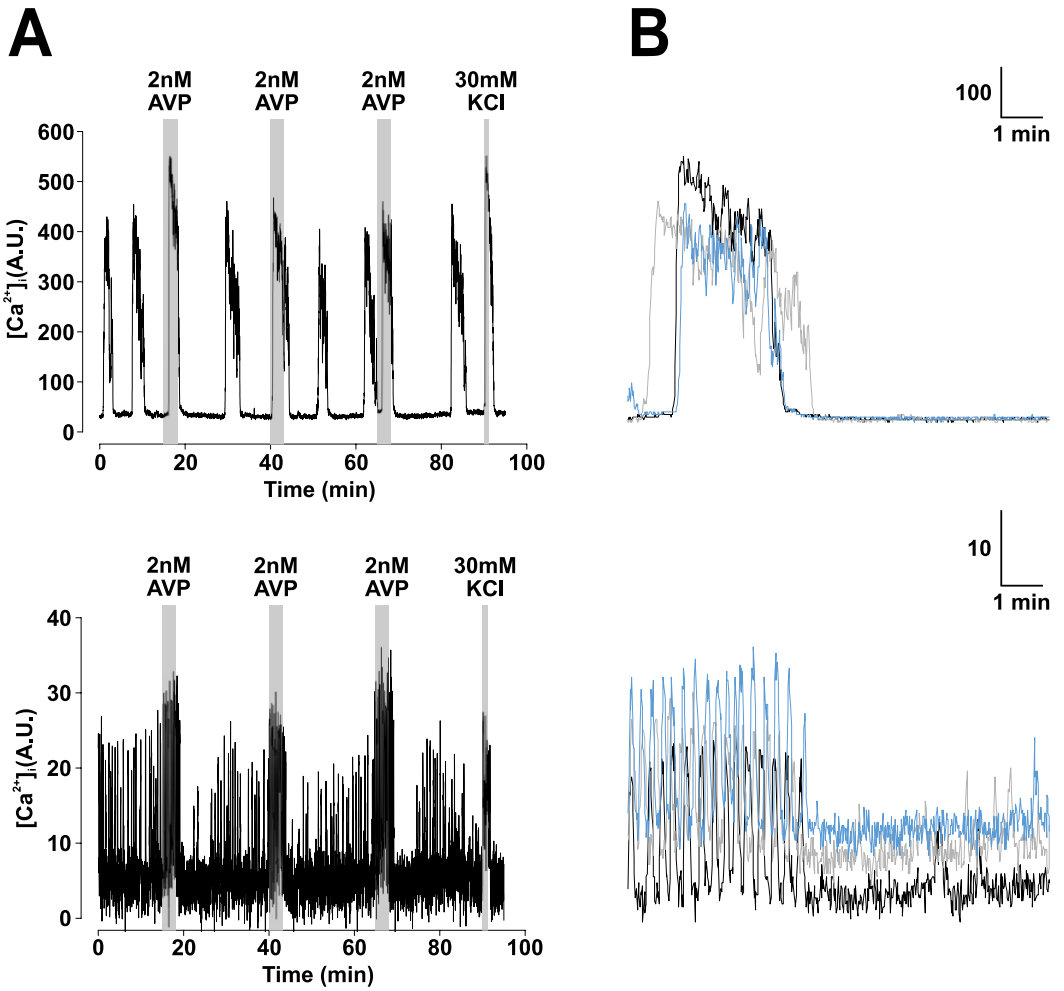


**Figure 5.28 Repeated AVP induces repeatable $[Ca^{2+}]_i$ responses in female zDHHC23-KO corticotrophs. (A)** Representative calcium imaging traces of female zDHHC23-KO corticotrophs exposed to 2 nM AVP for three minutes and repeated three times at 25 minutes intervals. 30 mM potassium chloride was applied at the end for one minute. **(B)** Superposition of extracts of the two traces shown in A, showing $[Ca^{2+}]_i$ changes in female zDHHC23-KO corticotrophs with repeated three times 2 nM AVP stimulation. Black line shows response to the first stimulus (starting at 15 min), grey line shows response to the second stimulus (starting at 40 min), and blue line shows response to the third stimulus (starting at 65 min).

## Figure 5.29

**Stable AUC (10 min) and AUC (peak) of $[Ca^{2+}]_i$ responses in female zDHHC23-KO corticotrophs to repeated AVP**

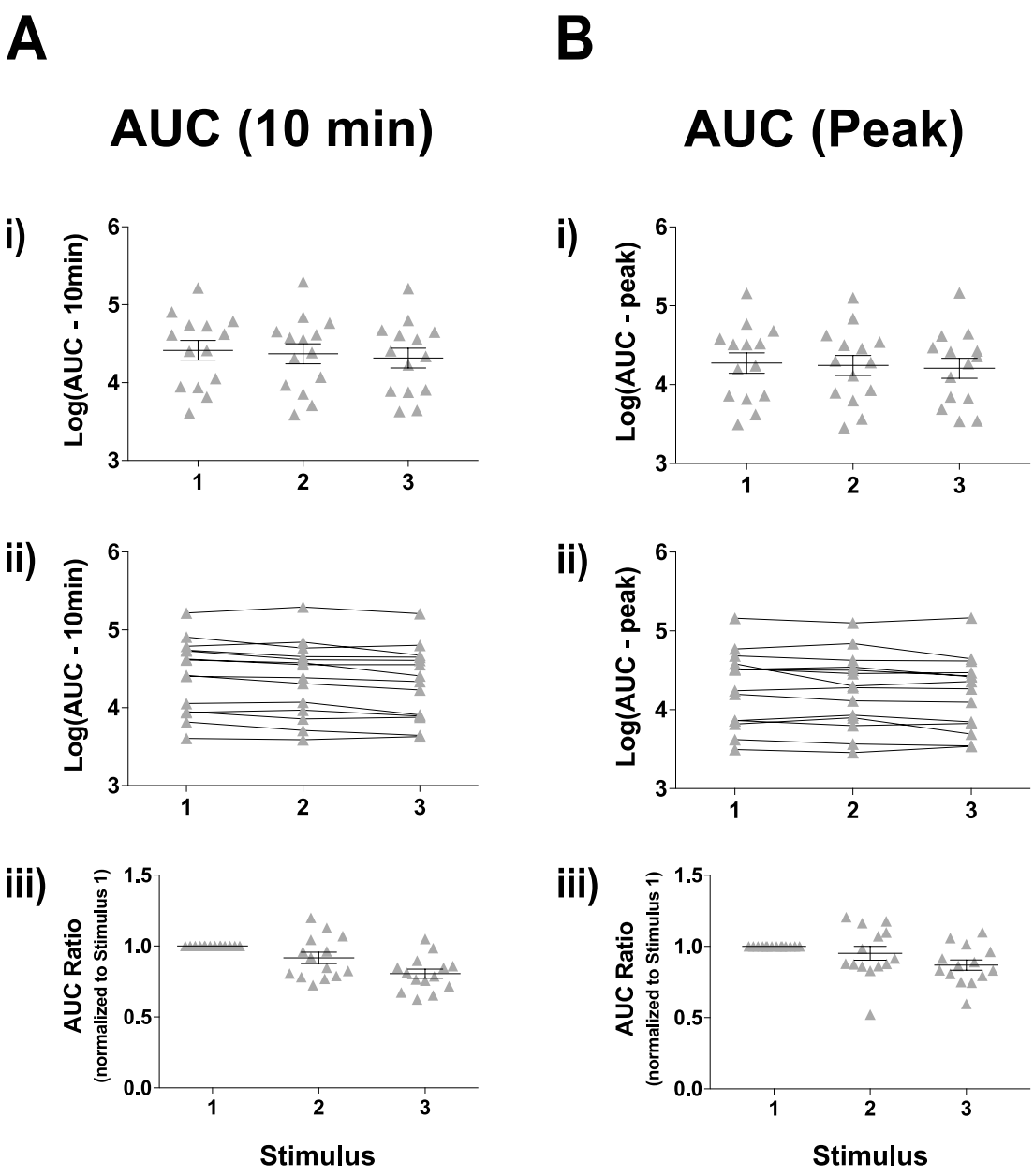


**Figure 5.29 Stable AUC (10 min) and AUC (peak) of $[Ca^{2+}]_i$ responses in female zDHHC23-KO corticotrophs to repeated AVP.** Quantification of effects of repeated exposure to 2 nM AVP in **(A)** AUC (10 min) and **(B)** AUC (peak) (n = 14 from 7 experiments, mixed effects model). All data are means ± SEM.

## Figure 5.30

**Peak and time to peak of $[Ca^{2+}]_i$ responses in female zDHHC23-KO corticotrophs to repeated AVP**

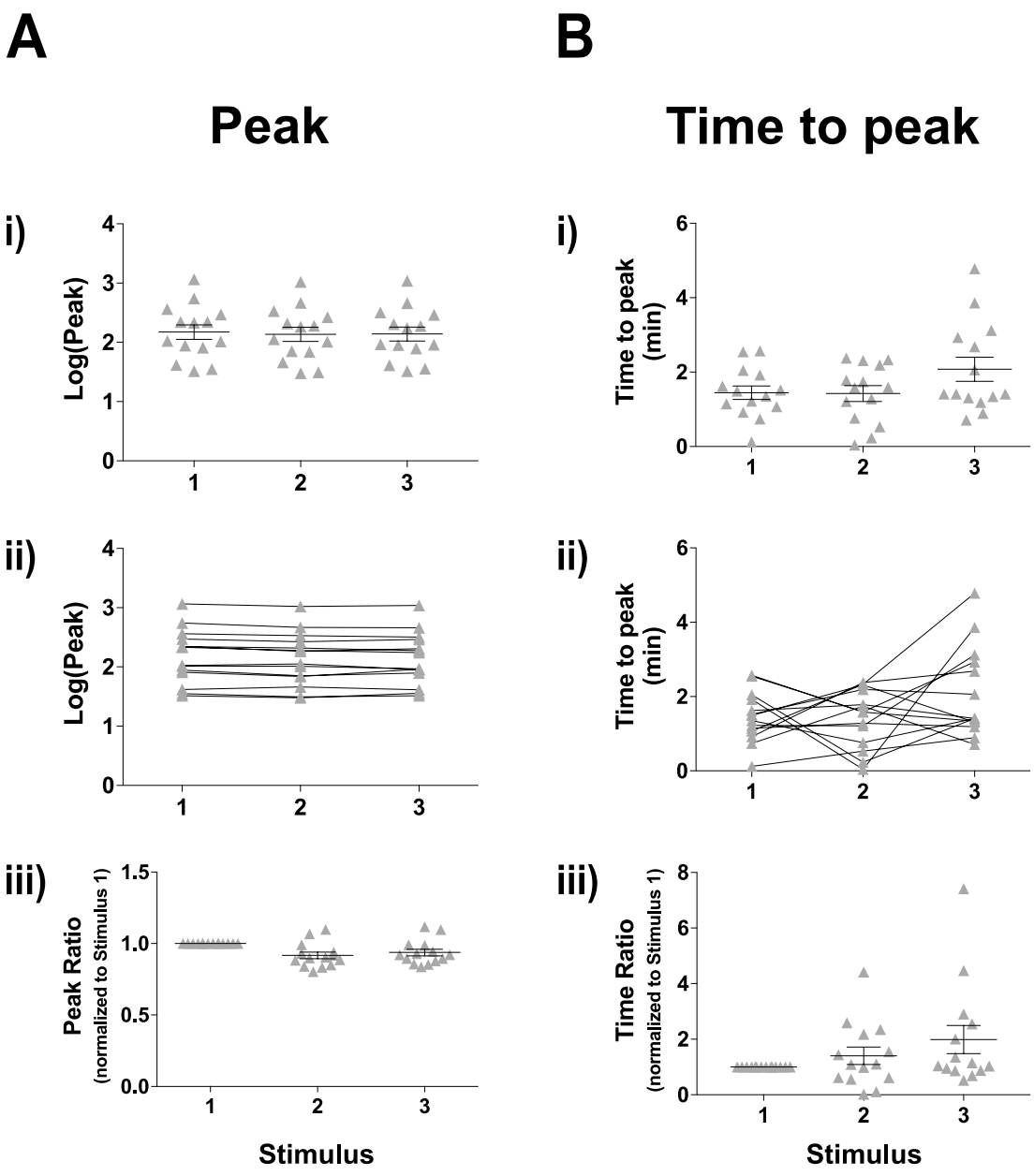


**Figure 5.30 Peak and time to peak of $[Ca^{2+}]_i$ responses in female zDHHC23-KO corticotrophs to repeated AVP.** Quantification of effects of repeated exposure to 2 nM AVP in **(A)** peak and **(B)** time to peak (n = 14 from 7 experiments, mixed effects model). All data are means ± SEM.

## Figure 5.31

### Response duration and peak duration of $[Ca^{2+}]_i$ responses in female zDHHC23-KO corticotrophs to repeated AVP

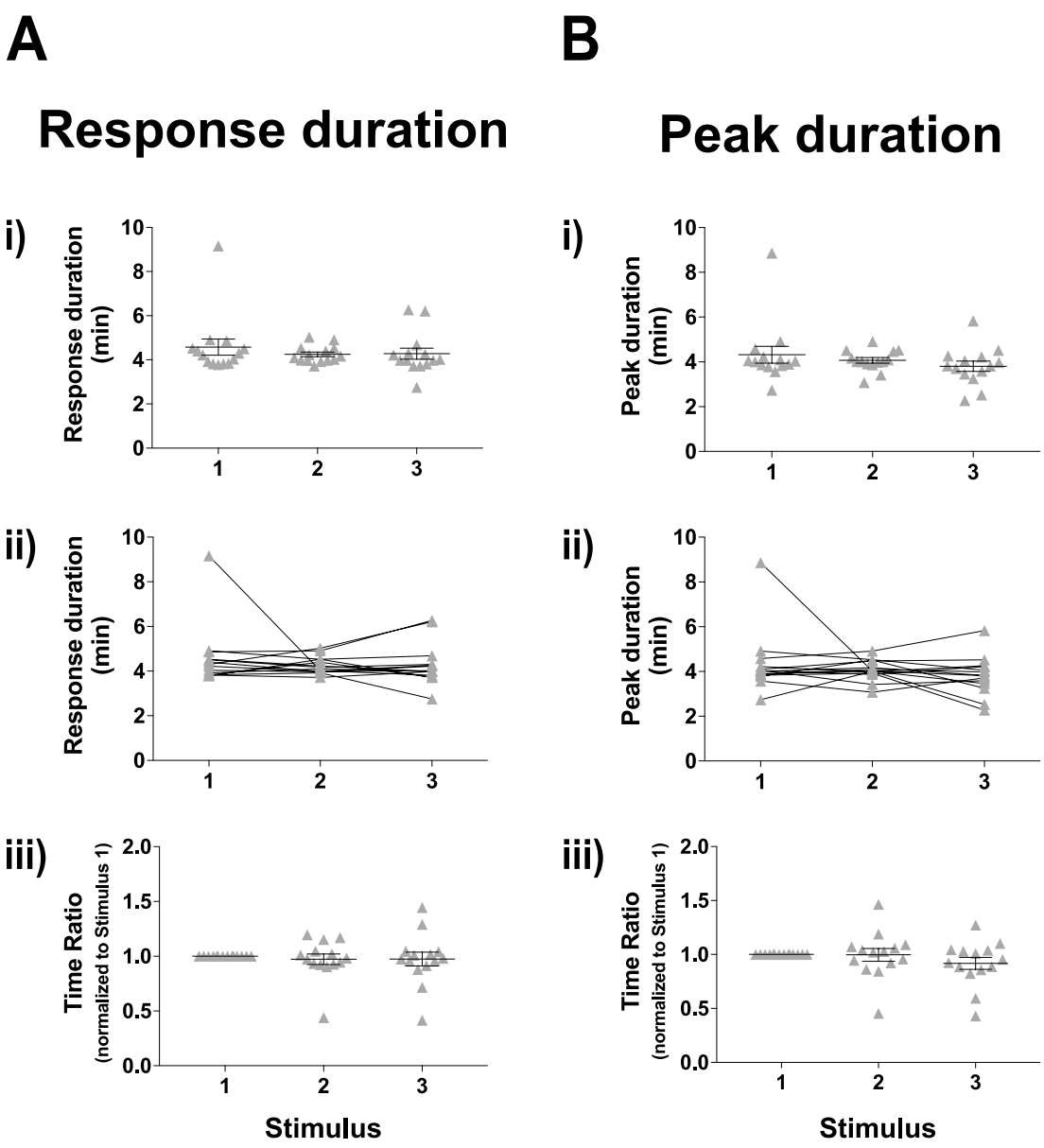


**Figure 5.31 Response duration and peak duration of $[Ca^{2+}]_i$ responses in female zDHHC23-KO corticotrophs to repeated AVP.** Quantification of effects of repeated exposure to 2 nM AVP in **(A)** response duration and **(B)** peak duration (n = 14 from 7 experiments, mixed effects model). All data are means ± SEM.

## Figure 5.32

### Time gap of $[Ca^{2+}]_i$ responses in female zDHHC23-KO corticotrophs to repeated AVP

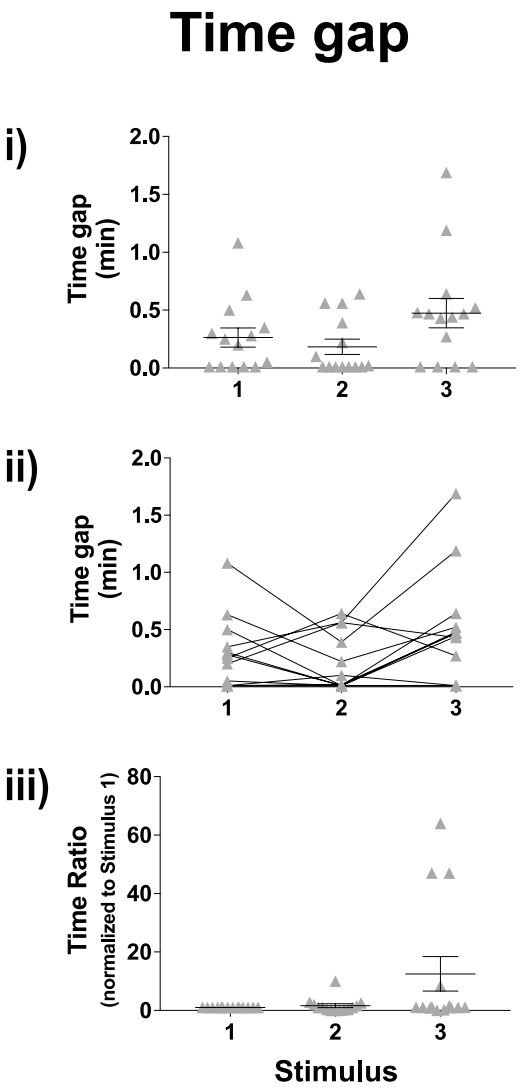


**Figure 5.32 Time gap of $[Ca^{2+}]_i$ responses in female zDHHC23-KO corticotrophs to repeated AVP.** Quantification of effects of repeated exposure to 2 nM AVP in time gap (n = 14 from 7 experiments, mixed effects model). All data are means ± SEM.

### 5.2.3.3 AVP-induced $[Ca^{2+}]_i$ responses are not significantly different between male and female zDHHC23-KO corticotrophs

Both male and female zDHHC23-KO corticotrophs had robust and consistent $[Ca^{2+}]_i$ responses to repeated AVP stimulation, we investigated whether there were differences between male and female zDHHC23-KO corticotrophs. Previous results indicated that there were no significant differences between AVP-evoked two phenotypes of $[Ca^{2+}]_i$ responses in both male and female zDHHC23-KO corticotrophs. Thus, the comparison and statistical analysis of AVP-induced $[Ca^{2+}]_i$ responses were performed on all calcium imaging experiments to examine whether there were sex differences in zDHHC23-KO corticotrophs.

Statistically analysis revealed that there were no significant differences in AUC (10min), AUC (peak) (Figure 5.33), peak, time to peak, response duration (Figure 5.34), peak duration or time gap (Figure 5.35) at each AVP stimulus between male and female zDHHC23-KO corticotrophs, although male zDHHC23-KO corticotrophs tended to have higher $[Ca^{2+}]_i$ responses in AUC (peak), AUC (10 min) and peak.

In conclusion, $[Ca^{2+}]_i$ responses to repeated 2 nM AVP stimulation were highly consistent and reproducible in both male and female zDHHC23-KO corticotrophs. Genetic deletion of zDHHC23 had no significant sex differences in AVP-induced

## Figure 5.33

### No significant sex difference in AVP-induced AUC (10 min) or AUC (peak) of $[Ca^{2+}]_i$ responses in zDHHC23-KO corticotrophs

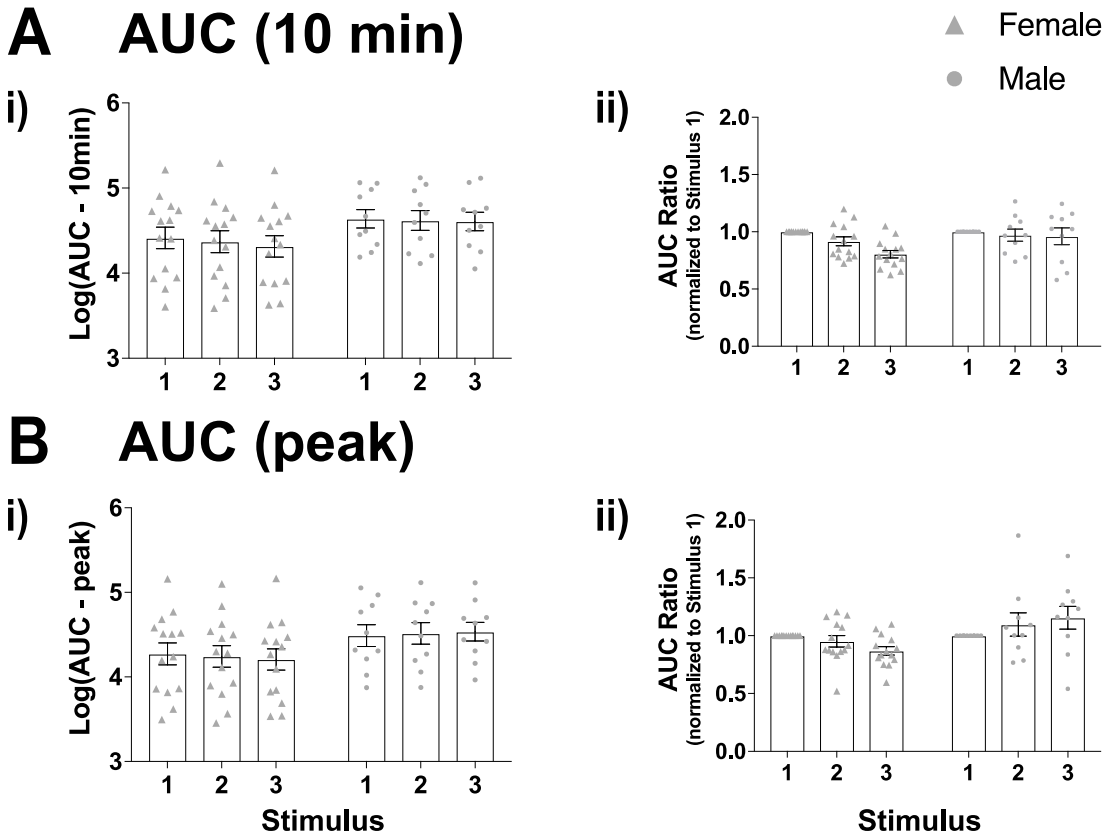


**Figure 5.33 No significant sex difference in AVP-induced AUC (10 min) or AUC (peak) of $[Ca^{2+}]_i$ responses in zDHHC23-KO corticotrophs.** Quantification of effects of repeated exposure to 2 nM AVP in **(A)** AUC (10 min) and **(B)** AUC (peak) (male n = 10 from 8 experiments, female n = 14 from 7 experiments, mixed effects model). All data are means ± SEM.

## Figure 5.34

**No significant sex difference in AVP-induced peak, time to peak or response duration of $[Ca^{2+}]_i$ responses in zDHHC23-KO corticotrophs**

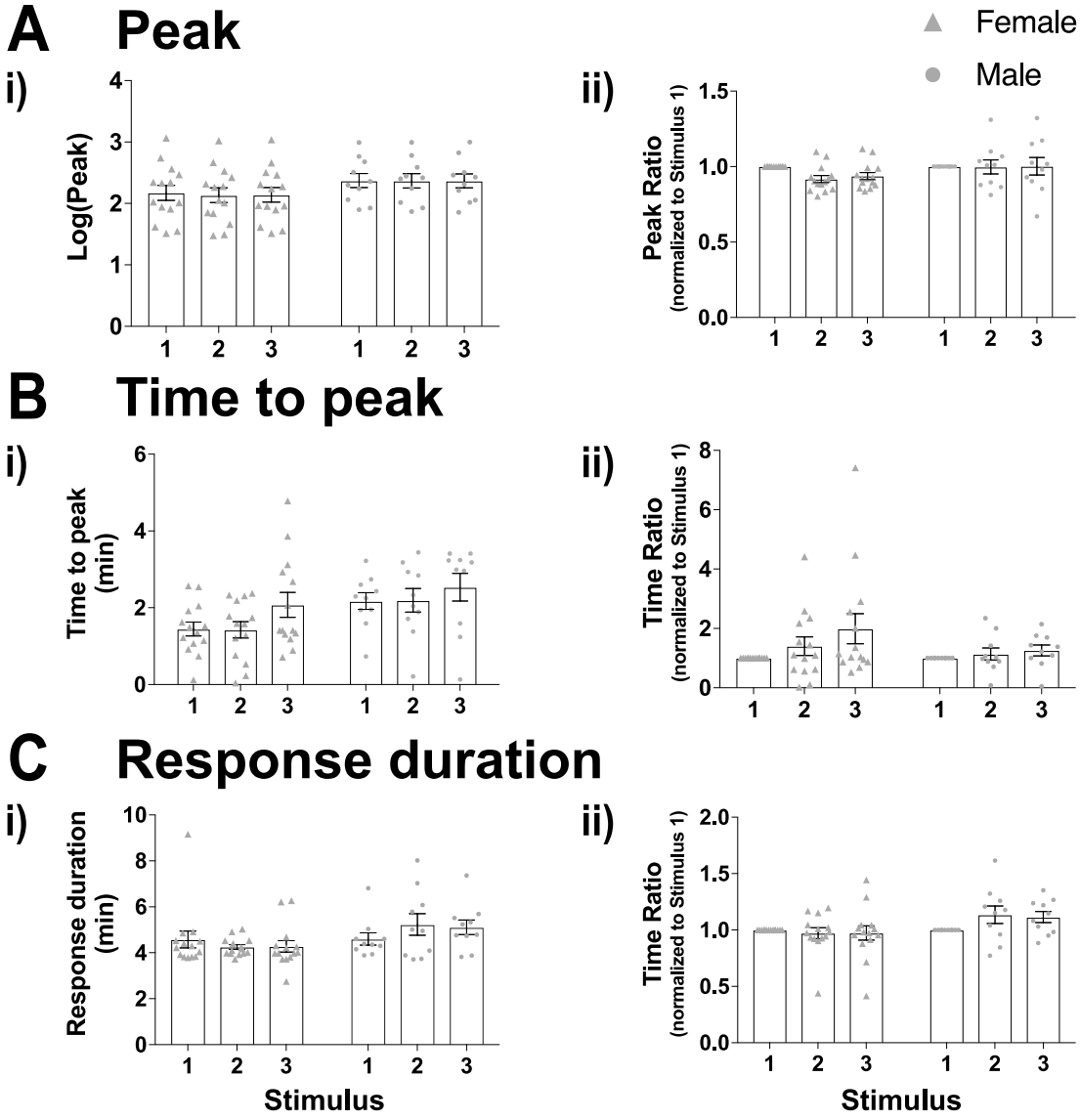


**Figure 5.34 No significant sex difference in AVP-induced peak, time to peak or response duration of $[Ca^{2+}]_i$ responses in zDHHC23-KO corticotrophs.** Quantification of effects of repeated exposure to 2 nM AVP in **(A)** peak, **(B)** time to peak and **(C)** response duration (male n = 10 from 8 experiments, female n = 14 from 7 experiments, mixed effects model). All data are means ± SEM.

## Figure 5.35

### No significant sex difference in AVP-induced peak duration or time gap of $[Ca^{2+}]_i$ responses in zDHHC23-KO corticotrophs

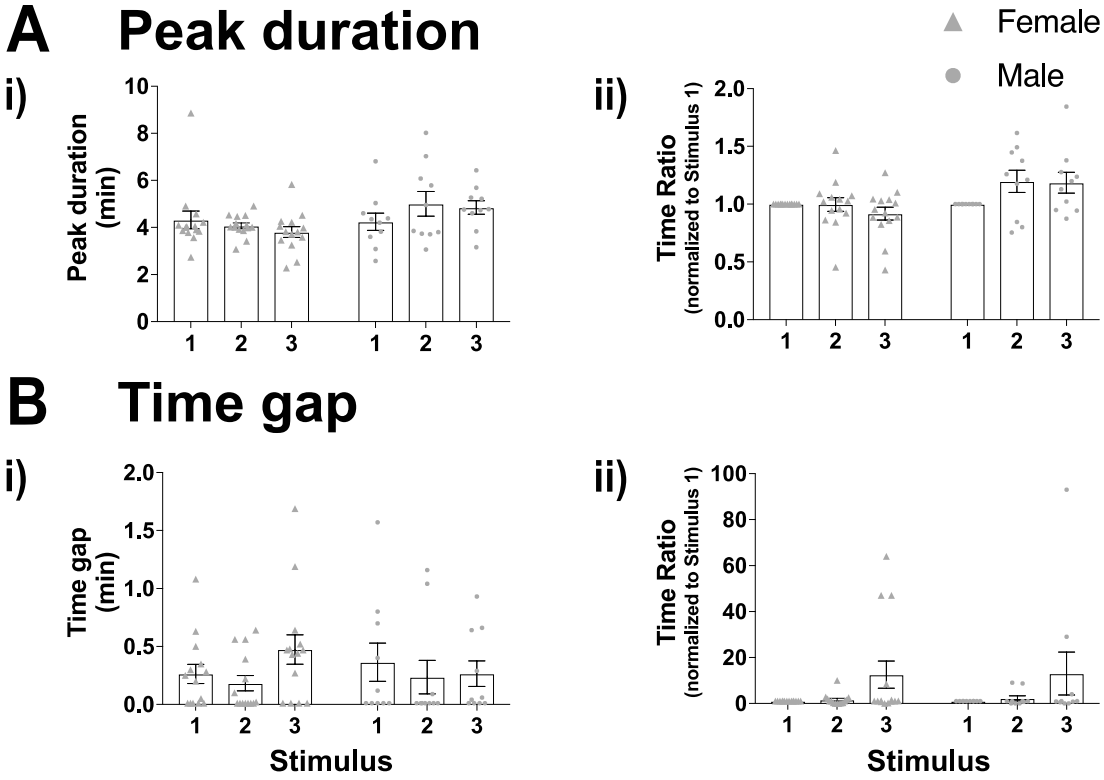


**Figure 5.35 No significant sex difference in AVP-induced peak duration or time gap of $[Ca^{2+}]_i$ responses in zDHHC23-KO corticotrophs.** Quantification of effects of repeated exposure to 2 nM AVP in **(A)** peak duration and **(B)** time gap (male n = 10 from 8 experiments, female n = 14 from 7 experiments, mixed effects model). All data are means ± SEM.

$[Ca^{2+}]_i$ responses.

#### 5.2.3.4 Genetic deletion of zDHHC23 has no significant effect on AVP-induced $[Ca^{2+}]_i$ responses in male corticotrophs

Male wild-type and zDHHC23-KO corticotrophs showed consistent $[Ca^{2+}]_i$ responses to repeated AVP stimulation. Each parameter was then compared between male wild-type and zDHHC23-KO corticotrophs to examine whether genetic deletion of zDHHC23 had effect on AVP-induced $[Ca^{2+}]_i$ responses.

Following repeated AVP stimulation, male zDHHC23-KO corticotrophs showed no statistically significant differences in AUC (10 min), AUC (peak) (Figure 5.36), peak, time to peak, response duration (Figure 5.37), peak duration or time gap (Figure 5.38) at each stimulus compared to male wild-type corticotrophs.

These results suggest that genetic deletion of zDHHC23 had no significant effect on $[Ca^{2+}]_i$ responses evoked by repeated 2 nM AVP stimulation in male corticotrophs.

#### 5.2.3.5 Genetic deletion of zDHHC23 has no significant effect on AVP-induced $[Ca^{2+}]_i$ responses in female corticotrophs

Next, the same statistical analysis was performed between female wild-type and zDHHC23-KO corticotrophs. Genetic deletion of zDHHC23 showed no statistically

## Figure 5.36

**No significant differences in AVP-induced AUC (10 min) or AUC (peak) $[Ca^{2+}]_i$ responses between male wild-type and zDHHC23-KO corticotrophs**

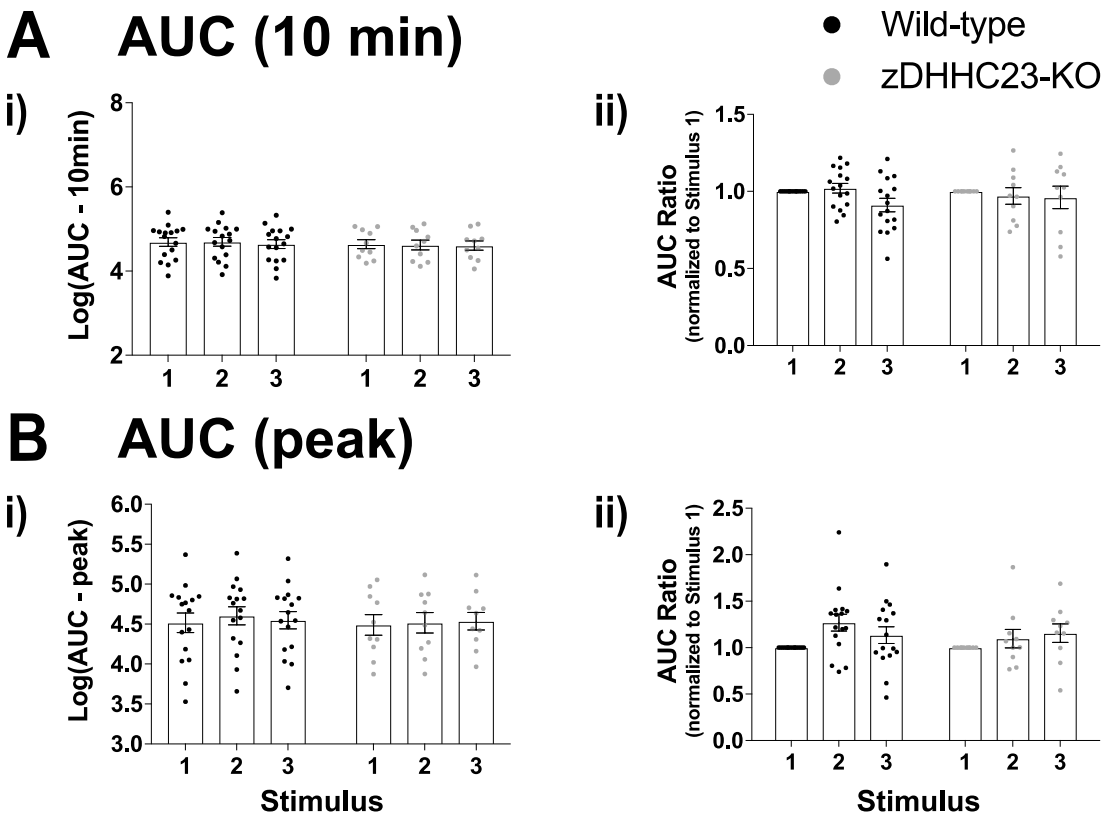


**Figure 5.36 No significant differences in AVP-induced AUC (10 min) or AUC (peak) $[Ca^{2+}]_i$ responses between male wild-type and zDHHC23-KO corticotrophs.** Quantification of effects of repeated exposure to 2 nM AVP in **(A)** AUC (10 min) and **(B)** AUC (peak) (wild-type n = 16 from 9 experiments, zDHHC23-KO n = 10 from 8 experiments, mixed effects model). All data are means ± SEM.

## Figure 5.37

**No significant differences in AVP-induced peak, time to peak or response duration $[Ca^{2+}]_i$ responses between male wild-type and zDHHC23-KO corticotrophs**

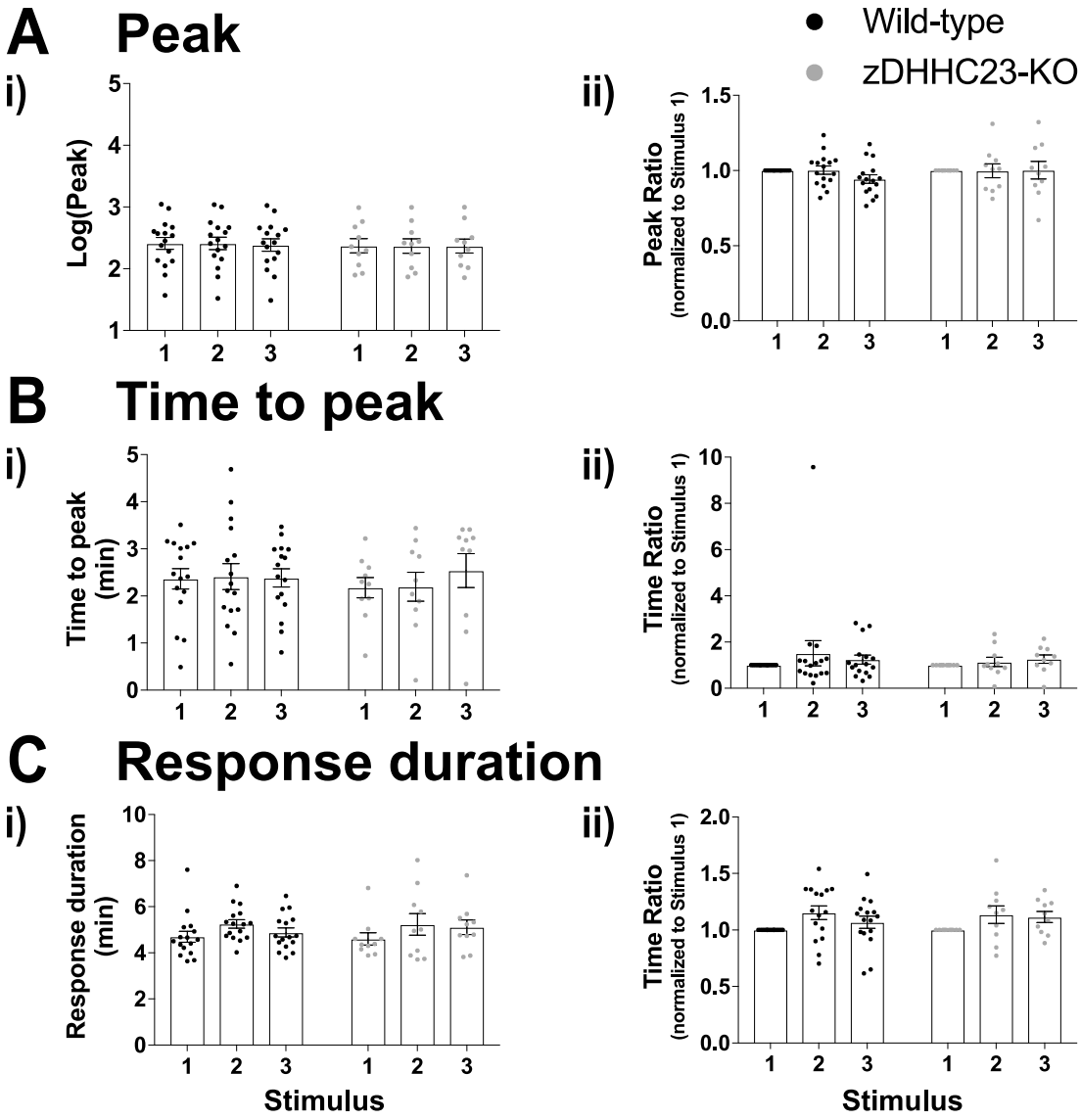


**Figure 5.37 No significant differences in AVP-induced peak, time to peak or response duration $[Ca^{2+}]_i$ responses between male wild-type and zDHHC23-KO corticotrophs.** Quantification of effects of repeated exposure to 2 nM AVP in **(A)** peak, **(B)** time to peak and **(C)** response duration (wild-type n = 16 from 9 experiments, zDHHC23-KO n = 10 from 8 experiments, mixed effects model). All data are means ± SEM.

## Figure 5.38

**No significant differences in AVP-induced peak duration or time gap $[Ca^{2+}]_i$ responses between male wild-type and zDHHC23-KO corticotrophs**

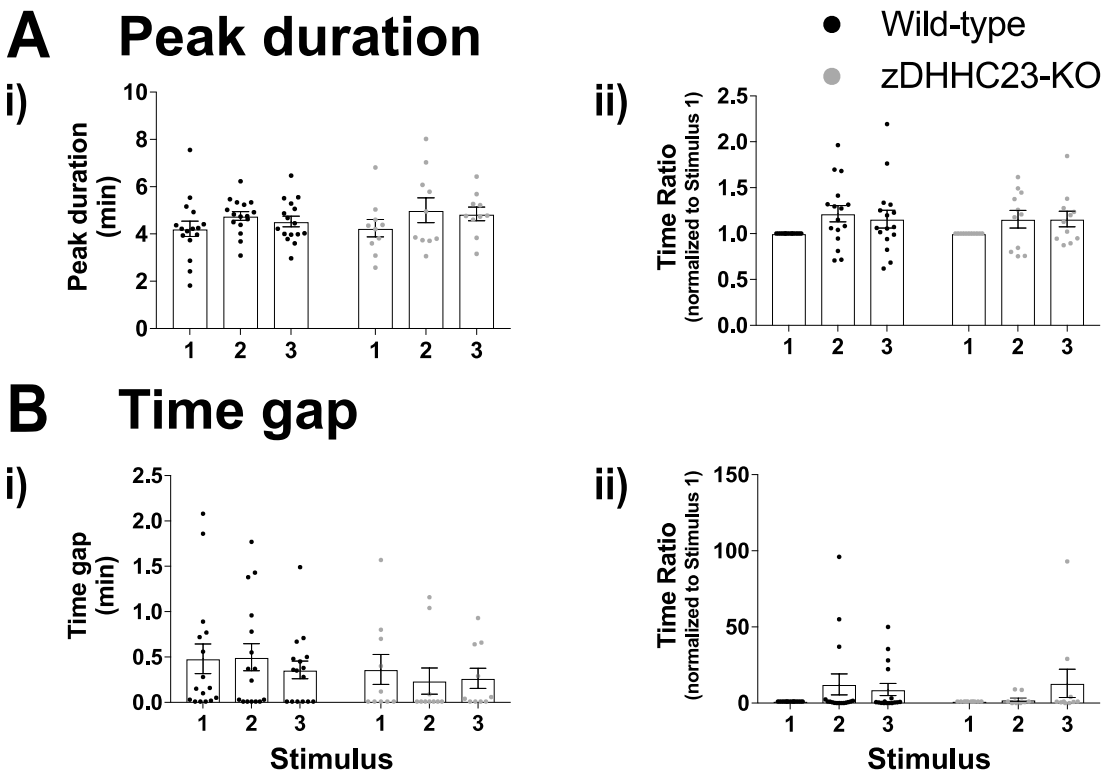


**Figure 5.38 No significant differences in AVP-induced peak duration or time gap $[Ca^{2+}]_i$ responses between male wild-type and zDHHC23-KO corticotrophs.** Quantification of effects of repeated exposure to 2 nM AVP in **(A)** peak duration and **(B)** time gap (wild-type n = 16 from 9 experiments, zDHHC23-KO n = 10 from 8 experiments, mixed effects model). All data are means ± SEM.

significant differences in AUC (10 min), AUC (peak) (Figure 5.39), peak, time to peak, responses duration (Figure 5.40), peak duration or time gap (Figure 5.41) compared to female wild-type corticotrophs.

This suggest that female zDHHC23-KO corticotrophs, as female wild-type corticotrophs, could also evoke robust and consistent $[Ca^{2+}]_i$ responses to repeated AVP stimulation.

In summary, repeated AVP stimulation evoked robust and reproducible $[Ca^{2+}]_i$ responses in both male and female zDHHC23-KO corticotrophs, which was similar to wild-type corticotrophs. Some differences were observed between male and female zDHHC23-KO corticotrophs in AVP-induced $[Ca^{2+}]_i$ responses, however, they were not considered statistically significant different. Thus, zDHHC23 does not play a role in controlling AVP-induced $[Ca^{2+}]_i$ signalling in murine corticotrophs.

### 5.2.4 Do zDHHC23-KO corticotrophs show synergy between CRH and AVP at the level of intracellular free calcium?

Previous study in Chapter Three suggested that there were no significant synergistic $[Ca^{2+}]_i$ responses between CRH and AVP in wild-type corticotrophs at the population level, but a proportion of (26.7%) female, but not male, wild-type corticotrophs

## Figure 5.39

**No significant differences in AVP-induced AUC (10 min) or AUC (peak) of $[Ca^{2+}]_i$ responses between female wild-type and zDHHC23-KO corticotrophs**

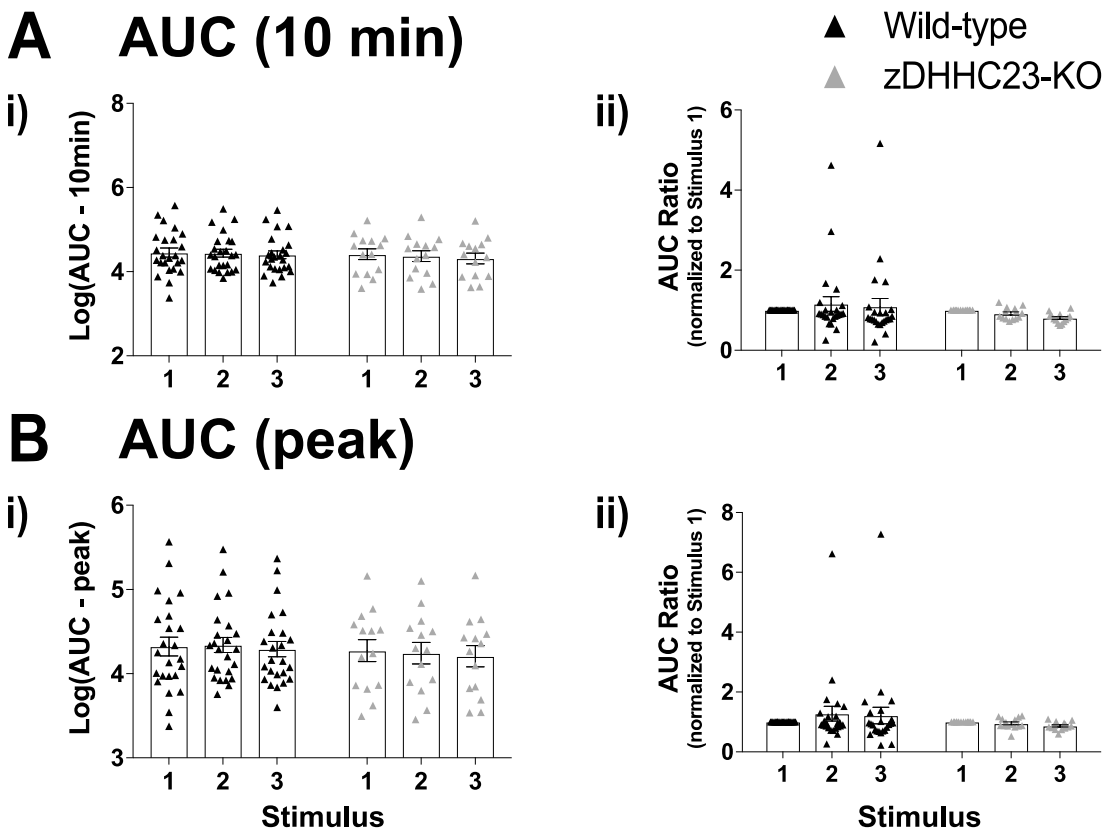


**Figure 5.39 No significant differences in AVP-induced AUC (10 min) or AUC (peak) of $[Ca^{2+}]_i$ responses between female wild-type and zDHHC23-KO corticotrophs.** Quantification of effects of repeated exposure to 2 nM AVP in **(A)** AUC (10 min) and **(B)** AUC (peak) (wild-type n = 24 from 8 experiments, zDHHC23-KO n = 14 from 7 experiments, mixed effects model). All data are means ± SEM.

## Figure 5.40

**No significant differences in AVP-induced peak, time to peak or response duration of $[Ca^{2+}]_i$ responses between female wild-type and zDHHC23-KO corticotrophs**

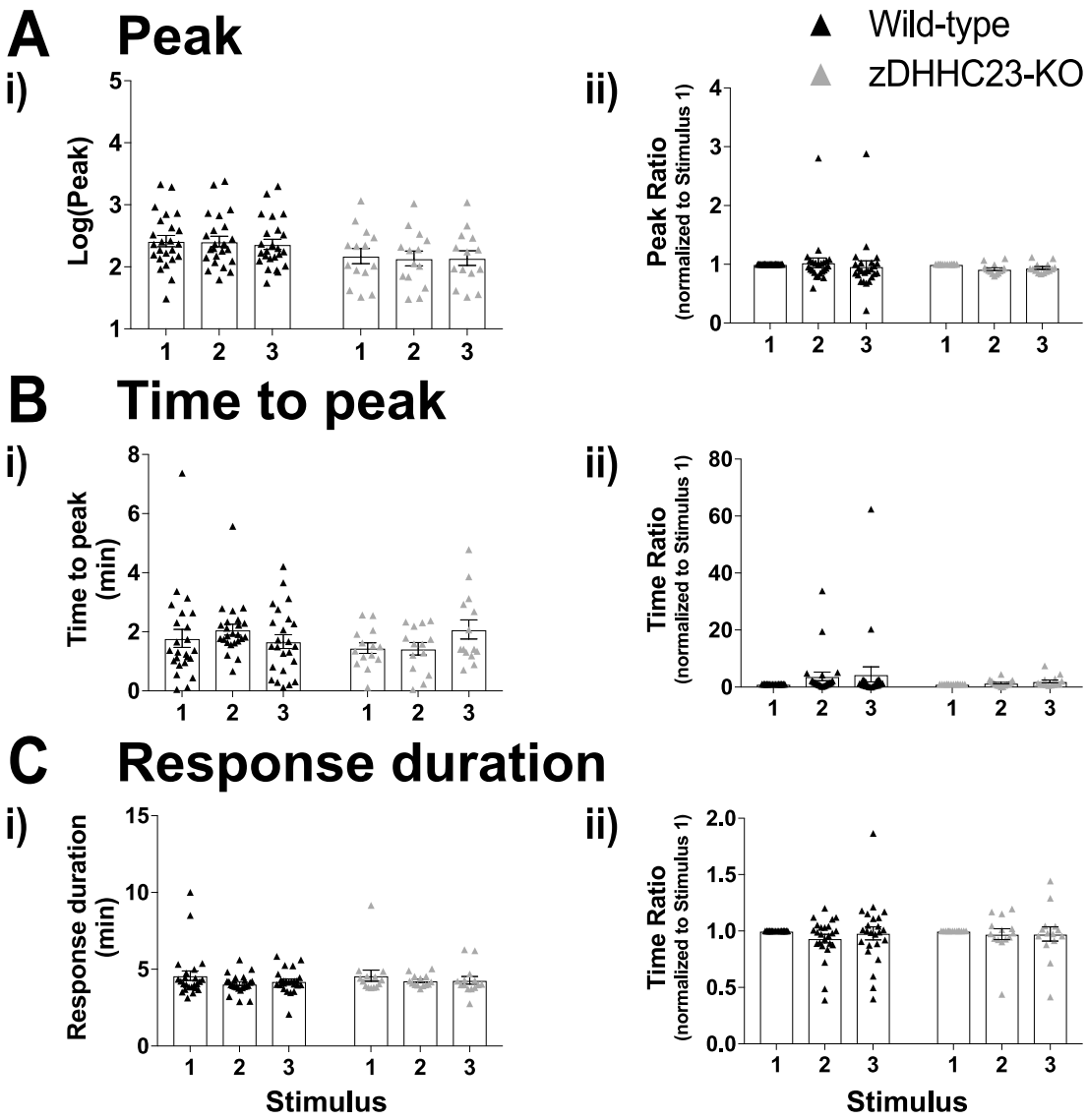


**Figure 5.40 No significant differences in AVP-induced peak, time to peak or response duration $[Ca^{2+}]_i$ responses between female wild-type and zDHHC23-KO corticotrophs.** Quantification of effects of repeated exposure to 2 nM AVP in **(A)** peak, **(B)** time to peak and **(C)** response duration (wild-type n = 24 from 8 experiments, zDHHC23-KO n = 14 from 7 experiments, mixed effects model). All data are means ± SEM.

## Figure 5.41

**No significant differences in AVP-induced peak duration or time gap of $[Ca^{2+}]_i$ responses between female wild-type and zDHHC23-KO corticotrophs**

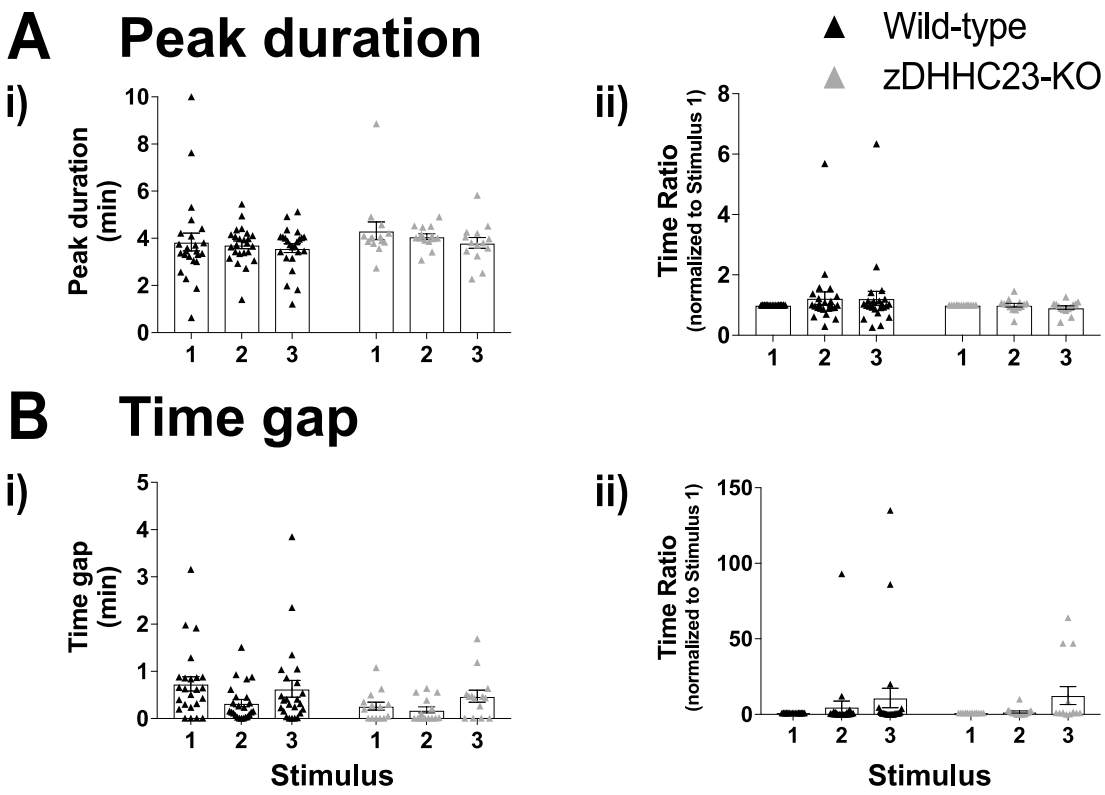


**Figure 5.41 No significant differences in AVP induced peak duration or time gap of $[Ca^{2+}]_i$ responses between female wild-type and zDHHC23-KO corticotrophs.** Quantification of effects of repeated exposure to 2 nM AVP in **(A)** peak duration and **(B)** time gap (wild-type n = 24 from 8 experiments, zDHHC23-KO n = 14 from 7 experiments, mixed effects model). All data are means ± SEM.

showed synergy at the single cell level. Thus, following experiments were performed to determine whether deletion of zDHHC23 had an effect on synergistic $[Ca^{2+}]_i$ responses to CRH and AVP in corticotrophs.

#### 5.2.4.1 No synergistic $[Ca^{2+}]_i$ response between CRH and AVP in male zDHHC23-KO corticotrophs at the population level

Calcium imaging recordings were obtained from male corticotrophs isolated from zDHHC23-KO mice following the repeated stimulation protocol used in male wild-type corticotrophs (see 3.2.5.1). The order of two single stimuli was randomized to minimize the possible effect due to the order of exposure to CRH and AVP (CRH, AVP, combination, n = 5 or AVP, CRH, combination, n = 5 from 8 experiments).

When stimulated with 0.2 nM CRH, male zDHHC23-KO corticotrophs always had sustained elevation of $[Ca^{2+}]_i$ irrespective of the stimulus order. Two phenotypes of $[Ca^{2+}]_i$ responses observed before were also found when exposed to 2 nM AVP. However, only 1 out of 10 cells showed the oscillatory $[Ca^{2+}]_i$ behaviour and the other 9 cells had sustained $[Ca^{2+}]_i$ responses regardless of the sequence of stimulus. The sustained elevation and oscillatory of $[Ca^{2+}]_i$ responses were 54.5% and 45.5% respectively when investigating the synergistic $[Ca^{2+}]_i$ responses in male wild-type corticotrophs. However, AVP-induced oscillatory calcium behaviour tended to be rare

in male zDHHC23-KO corticotrophs suggesting that deletion of zDHHC23 may have effect on $[Ca^{2+}]_i$ responding patterns in corticotrophs when stimulation with AVP. Stimulation with 0.2 nM CRH and 2 nM AVP together resulted in significant and sustained increase of $[Ca^{2+}]_i$ (Figure 5.42A & Figure 5.43A). The extracts of calcium imaging traces of typical experiments for male zDHHC23-KO corticotrophs were shown in Figure 5.42B and Figure 5.43B. The $[Ca^{2+}]_i$ responses to two single stimuli and combined stimulus were coincident in spite of the stimulus order and the phenotypes of $[Ca^{2+}]_i$ responses elicited by AVP.

The AUC of the combined stimulus was compared to the sum of the AUC of the two single stimuli to examine whether there were synergistic $[Ca^{2+}]_i$ responses in male zDHHC23-KO corticotrophs. Comparison and analysis of each parameter between AVP-induced sustained elevation of $[Ca^{2+}]_i$ (n = 9) and oscillatory $[Ca^{2+}]_i$ behaviour (n = 1) revealed that there were no significant differences between the two phenotypes of $[Ca^{2+}]_i$ responses. Therefore, statistical analysis was performed on all male zDHHC23-KO corticotrophs together. The statistical calculation of AUC (10 min), AUC (peak) and peak was performed on log-transformed data and the others were performed on raw data.

## Figure 5.42

### CRH, AVP and CRH/AVP induce $[Ca^{2+}]_i$ responses in male zDHHC23-KO corticotrophs

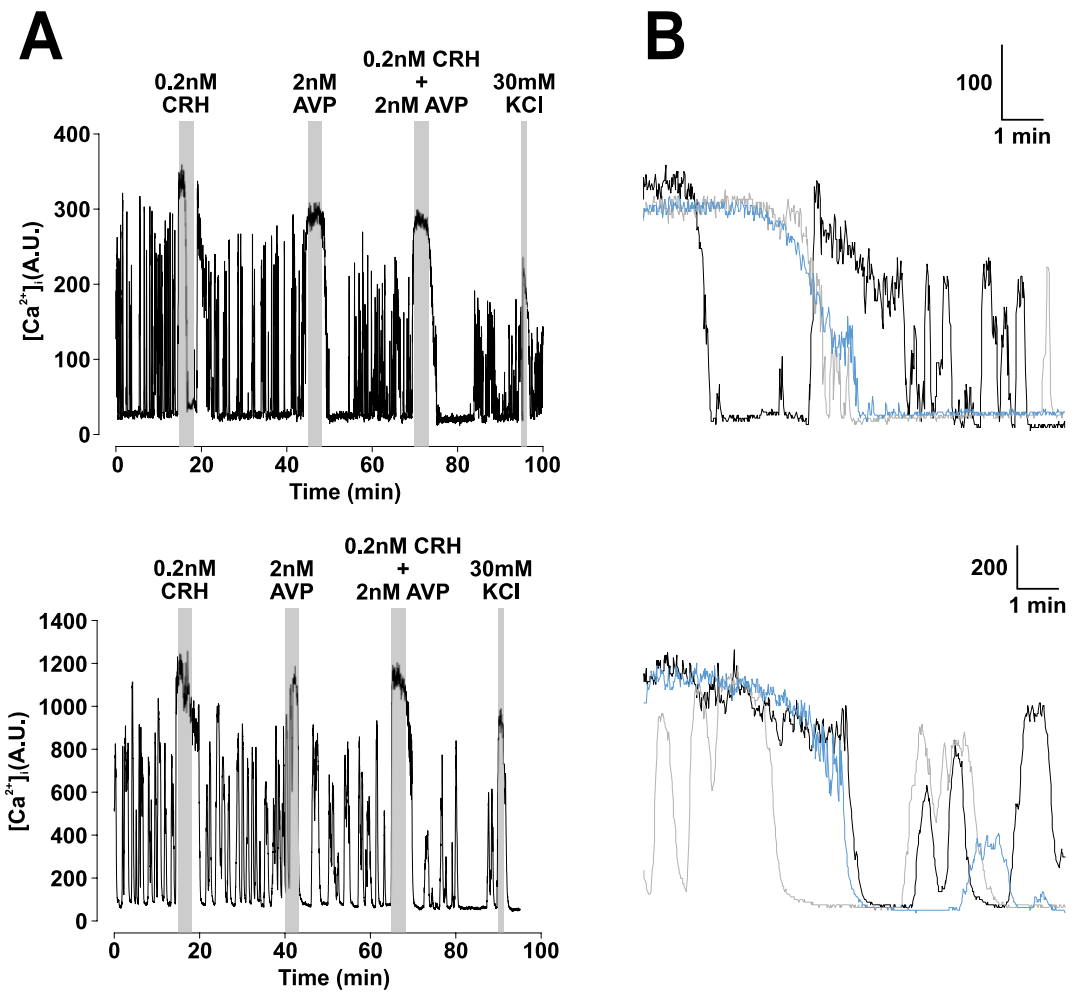


**Figure 5.42 CRH, AVP and CRH/AVP induce $[Ca^{2+}]_i$ responses in male zDHHC23-KO corticotrophs. (A)** Representative calcium imaging traces of male zDHHC23-KO corticotrophs exposed to 0.2 nM CRH, 2 nM AVP and 0.2 nM CRH together with 2 nM AVP at 25 minutes intervals. 30 mM potassium chloride was applied at the end for one minute. **(B)** Superposition of extracts of the two traces shown in A, showing $[Ca^{2+}]_i$ changes in male zDHHC23-KO corticotrophs with stimuli. Black line shows response to 0.2 nM CRH (starting at 15 min), grey line shows response to 2 nM AVP (starting at 40 min), and blue line shows response to the combined stimulus (starting at 65 min).

## Figure 5.43

### AVP, CRH and CRH/AVP induce $[Ca^{2+}]_i$ responses in male zDHHC23-KO corticotrophs

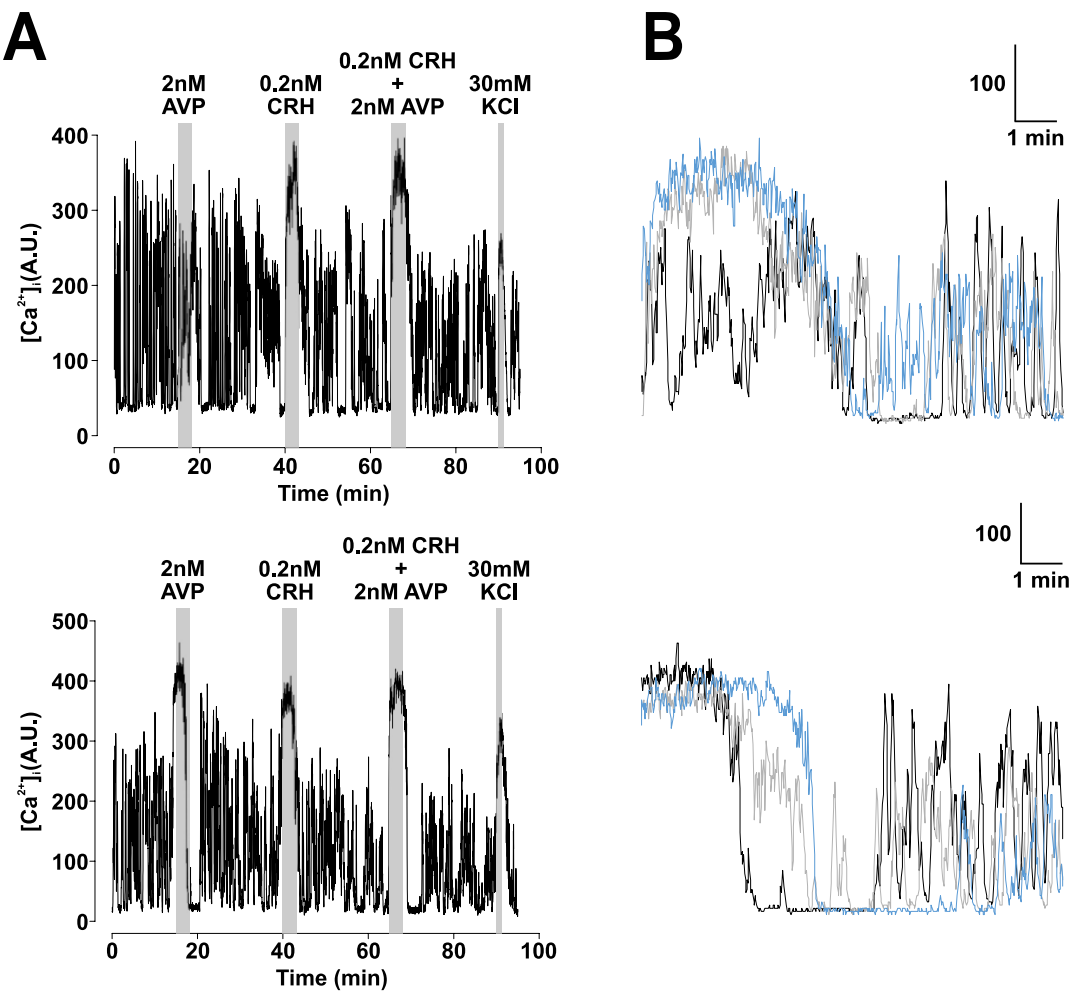


**Figure 5.43 AVP, CRH and CRH/AVP induce $[Ca^{2+}]_i$ responses in male zHDHC23-KO corticotrophs. (A)** Representative calcium imaging traces of male zDHHC23-KO corticotrophs exposed to 2 nM AVP, 0.2 nM CRH, 0.2 nM CRH together with 2 nM AVP at 25 minutes intervals. 30 mM potassium chloride was applied at the end for one minute. **(B)** Superposition of extracts of the two traces shown in A, showing $[Ca^{2+}]_i$ changes in male zDHHC23-KO corticotrophs with stimuli. Black line shows response to 2 nM AVP (starting at 15 min), grey line shows response to 0.2 nM CRH (starting at 40 min), and blue line shows response to the combined stimulus (starting at 65 min).

$[Ca^{2+}]_i$ responses evoked by the combined stimulus were significantly ($p < 0.05$) larger than AVP-induced $[Ca^{2+}]_i$ responses in AUC (peak) but not AUC (10 min). However, the combined stimulus was significantly ($p < 0.001$) smaller than the sum of the two single stimuli in both AUC (10 min) and AUC (peak) (Figure 5.44). This suggests that male zDHHC23-KO corticotrophs did not show synergistic $[Ca^{2+}]_i$ responses to CRH and AVP. Peak, time to peak, response duration (Figure 5.45), peak duration and time gap (Figure 5.46) showed no statistically significant differences between CRH-, AVP- and CRH/AVP-induced $[Ca^{2+}]_i$ responses.

These results suggest that there was no synergy between CRH and AVP in male zDHHC23-KO corticotrophs at the level of $[Ca^{2+}]_i$.

#### 5.2.4.2 No synergistic $[Ca^{2+}]_i$ response between CRH and AVP in female zDHHC23-KO corticotrophs at the population level

Calcium imaging experiments were performed on female zDHHC23-KO corticotrophs following the same protocol used in male zDHHC23-KO corticotrophs. The order of 0.2 nM CRH and 2 nM AVP was randomized to counteract the possible effect caused by exposure sequence (CRH, AVP, combination, n = 6 or AVP, CRH, combination, n = 7 from 5 experiments).

## Figure 5.44

**No synergistic $[Ca^{2+}]_i$ response to CRH/AVP in male zDHHC23-KO corticotrophs**

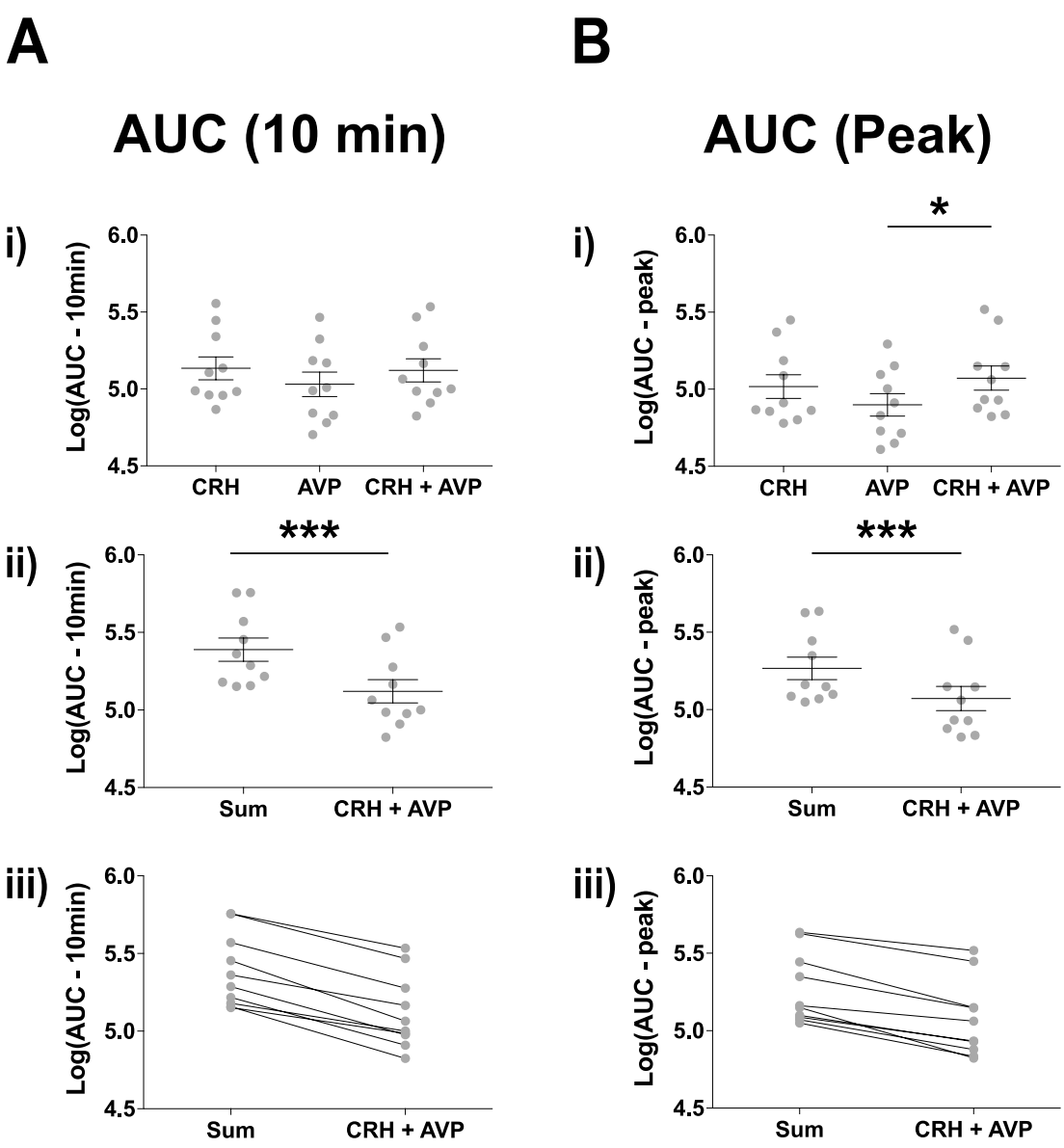


**Figure 5.44 No synergistic $[Ca^{2+}]_i$ responses to CRH/AVP in male zDHHC23-KO corticotrophs.** Quantification of effects of exposure to 0.2 nM CRH, 2 nM AVP and the combination of the two in **(A)** AUC (10 min) and **(B)** AUC (peak). The comparison of the AUC of the combined stimulus and the sum of the two single stimuli was used as a measurement of synergy. *** $p < 0.001$, * $p < 0.05$ ($n = 10$ from 8 experiments, mixed effects model). All data are means ± SEM.

## Figure 5.45

### Peak, time to peak and response duration of $[Ca^{2+}]_i$ responses to CRH, AVP and CRH/AVP in male zDHHC23-KO corticotrophs

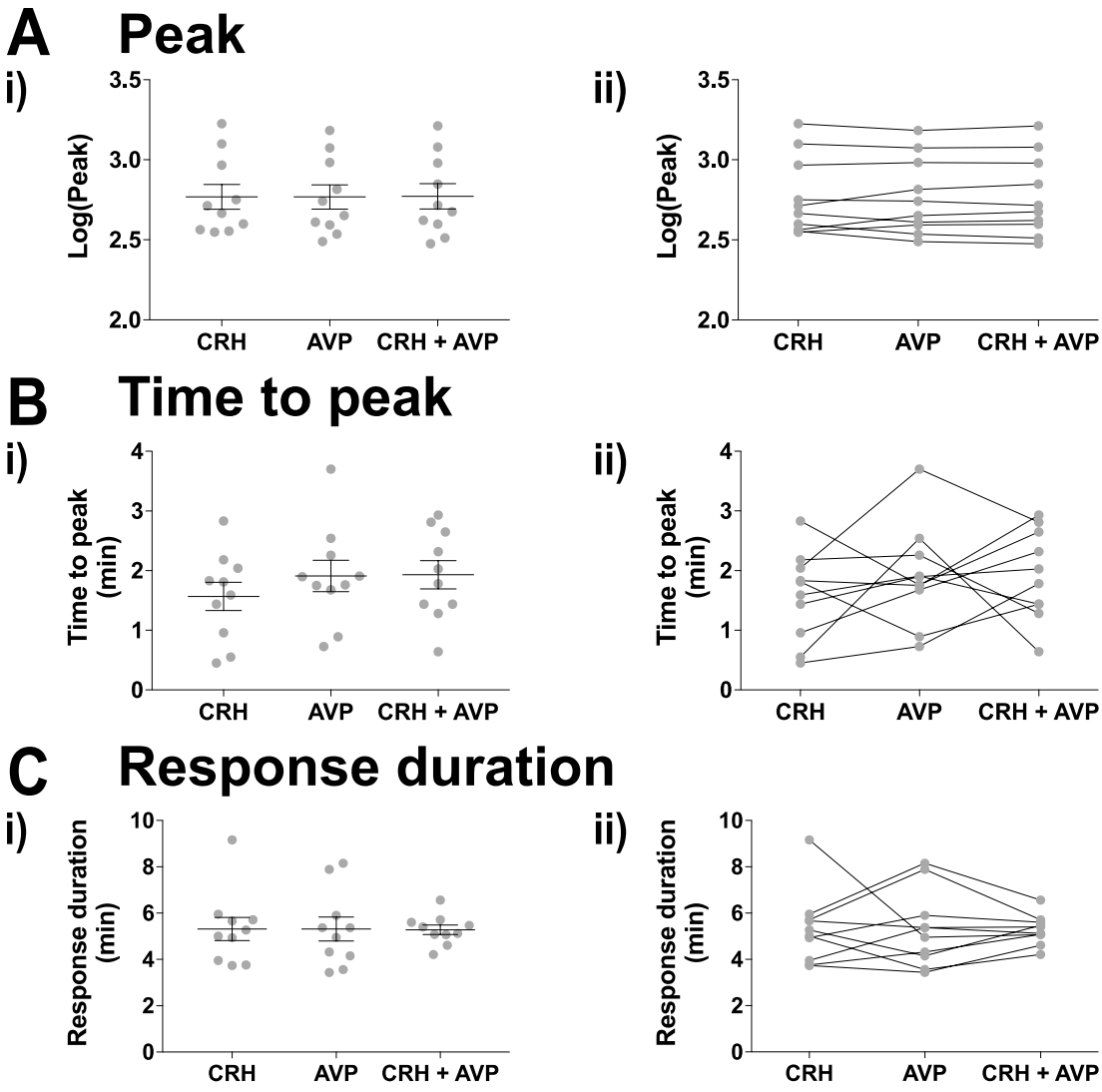


**Figure 5.45 Peak, time to peak and response duration of $[Ca^{2+}]_i$ responses to CRH, AVP and CRH/AVP in male zDHHC23-KO corticotrophs.** Quantification of effects of exposure to 0.2 nM CRH, 2 nM AVP and the combination of the two in **(A)** peak, **(B)** time to peak and **(C)** response duration (n = 10 from 8 experiments, mixed effects model). All data are means ± SEM.

## Figure 5.46

### Peak duration and time gap of $[Ca^{2+}]_i$ responses to CRH, AVP and CRH/AVP in male zDHHC23-KO corticotrophs

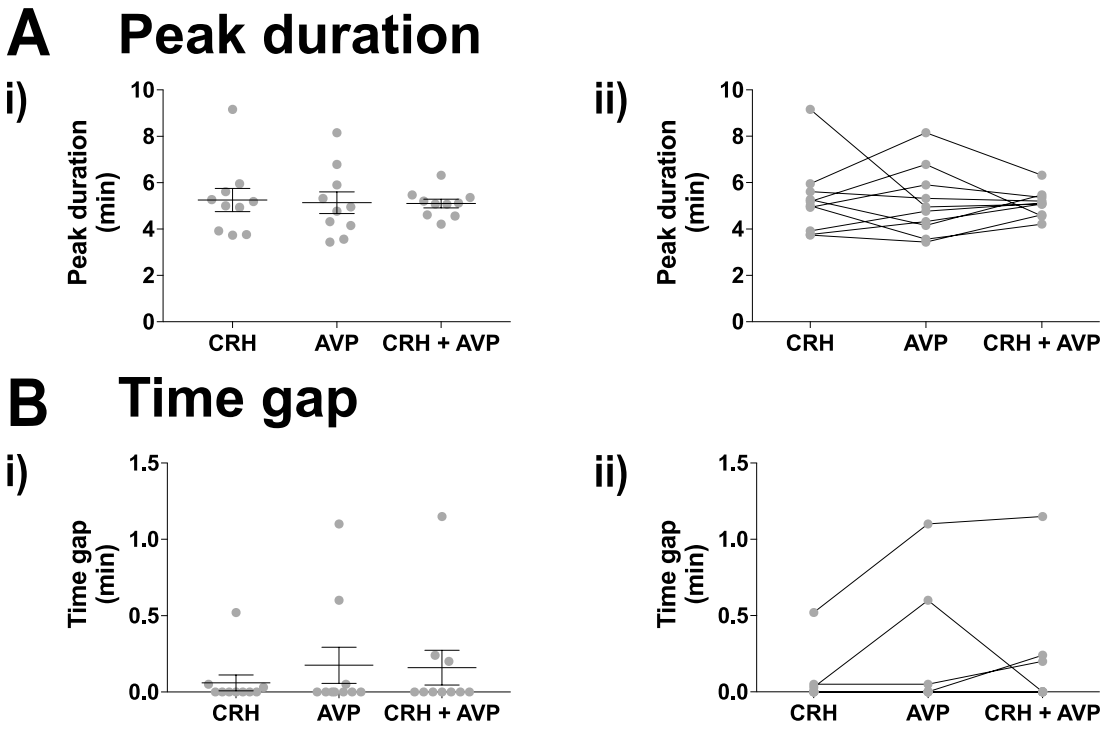


**Figure 5.46 Peak duration and time gap of $[Ca^{2+}]_i$ responses to CRH, AVP and CRH/AVP in male zDHHC23-KO corticotrophs.** Quantification of effects of exposure to 0.2 nM CRH, 2 nM AVP and the combination of the two in **(A)** peak duration and **(B)** time gap (n = 10 from 8 experiments, mixed effects model). All data are means ± SEM.

When stimulated with 0.2 nM CRH, 2 nM AVP and the combined stimulus in order, all 6 cells responded to CRH with sustained $[Ca^{2+}]_i$ increase; 2 out of 6 cells displayed sustained elevation of $[Ca^{2+}]_i$ to AVP and the other 4 cells showed oscillatory $[Ca^{2+}]_i$ behaviour; the combination of CRH and AVP resulted in significant increase of $[Ca^{2+}]_i$ in all cells (Figure 5.47A). When exposed to 2 nM AVP, 0.2 nM CRH and the combined stimulus sequentially, all 7 cells showed sustained increase of $[Ca^{2+}]_i$ when responding to CRH and the combined stimulus; AVP induced high frequency of oscillatory $[Ca^{2+}]_i$ responses in 1 cell while the other 6 cells showed sustained $[Ca^{2+}]_i$ elevation to AVP (Figure 5.48A). Compared to female wild-type corticotrophs, AVP-induced oscillatory $[Ca^{2+}]_i$ behaviour was less likely to appear in female zDHHC23-KO corticotrophs suggesting that zDHHC23 probably play a role in controlling AVP-evoked $[Ca^{2+}]_i$ response patterns in corticotrophs. Overlapping calcium traces seen in two different stimulation sequences indicated that $[Ca^{2+}]_i$ responses to two single stimuli and combined stimulus were coincident regardless of AVP-induced phenotypes of $[Ca^{2+}]_i$ responses (Figure 5.47B & Figure 5.48B).

The synergistic $[Ca^{2+}]_i$ responses and the effects of two single stimuli and combined stimulus on $[Ca^{2+}]_i$ responses were evaluated with the same parameters used in male zDHHC23-KO corticotrophs. Sustained increase of $[Ca^{2+}]_i$ (n = 8) and oscillatory $[Ca^{2+}]_i$ behaviour (n = 5) showed no statistically significant differences in either AUC

## Figure 5.47

### CRH, AVP and CRH/AVP induce $[Ca^{2+}]_i$ responses in female zDHHC23-KO corticotrophs

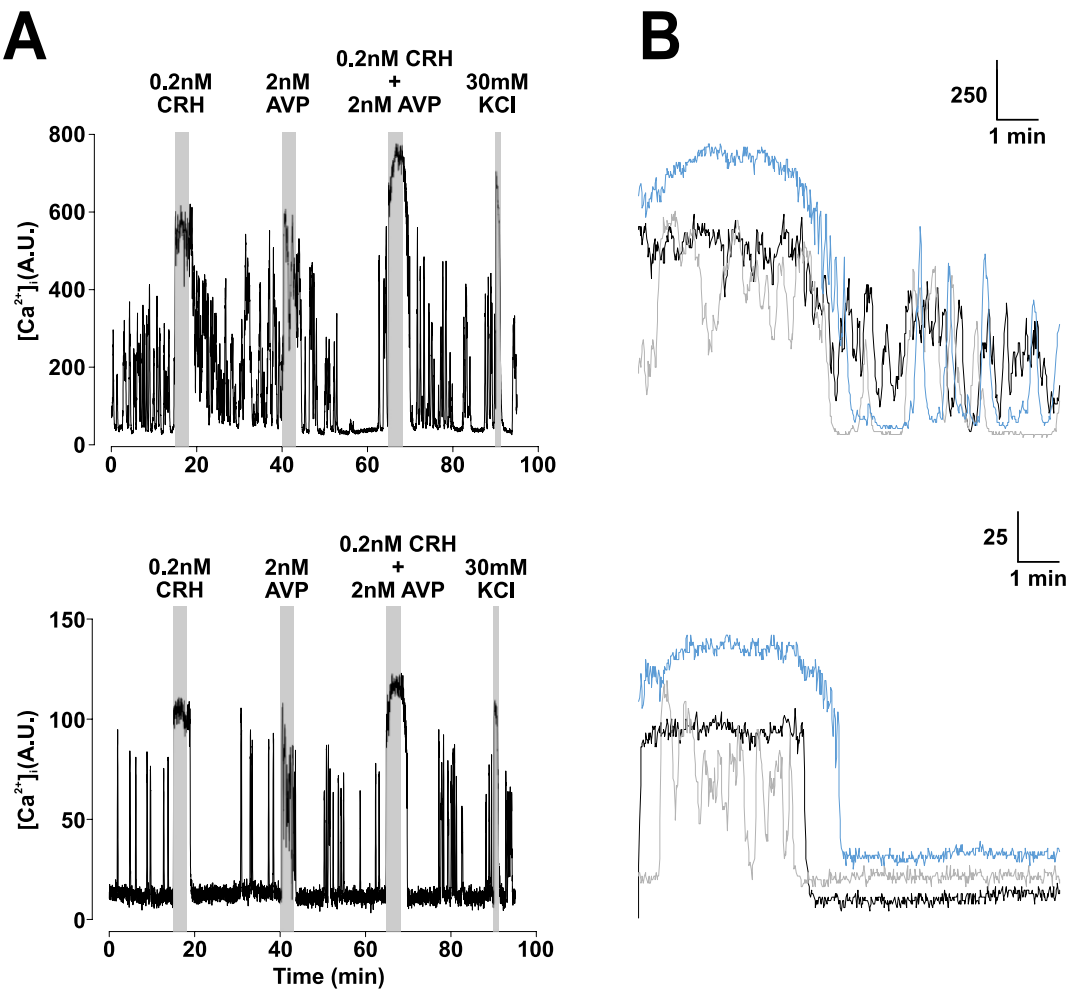


**Figure 5.47 CRH, AVP and CRH/AVP induce $[Ca^{2+}]_i$ responses in female zDHHC23-KO corticotrophs. (A)** Representative calcium imaging traces of female zDHHC23-KO corticotrophs exposed to 0.2 nM CRH, 2 nM AVP and 0.2 nM CRH together with 2 nM AVP at 25 minutes intervals. 30 mM potassium chloride was applied at the end for one minute. **(B)** Superposition of extracts of the two traces shown in A, showing $[Ca^{2+}]_i$ changes in female zDHHC23-KO corticotrophs with stimuli. Black line shows response to 0.2 nM CRH (starting at 15 min), grey line shows response to 2 nM AVP (starting at 40 min), and blue line shows response to the combined stimulus (starting at 65 min).

# Figure 5.48

## AVP, CRH and CRH/AVP induce $[Ca^{2+}]_i$ responses in female zDHHC23-KO corticotrophs

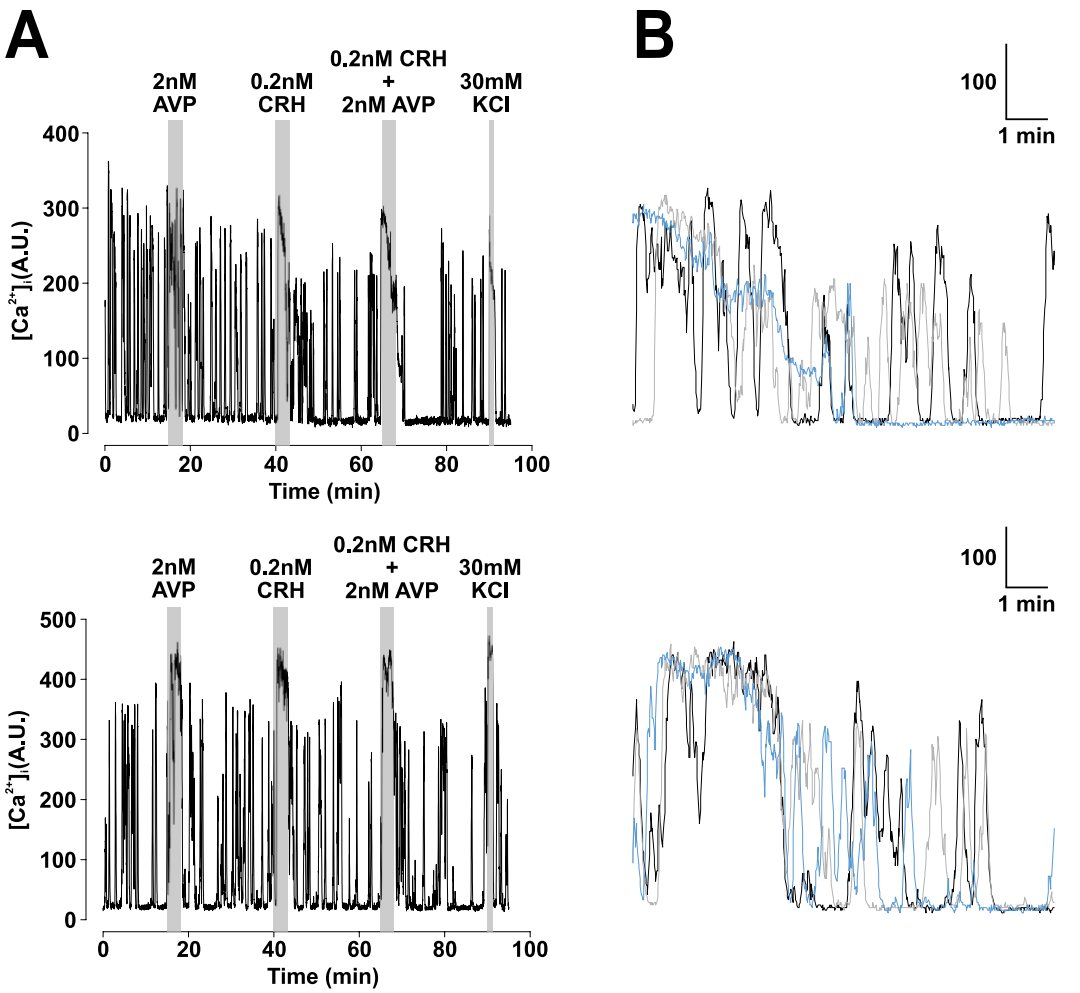


**Figure 5.48 AVP, CRH and CRH/AVP induce $[Ca^{2+}]_i$ responses in female zHDHC23-KO corticotrophs. (A)** Representative calcium imaging traces of female zDHHC23-KO corticotrophs exposed to 2 nM AVP, 0.2 nM CRH and 0.2 nM CRH together with 2 nM AVP at 25 minutes intervals. 30 mM potassium chloride was applied at the end for one minute. **(B)** Superposition of extracts of the two traces shown in A, showing $[Ca^{2+}]_i$ changes in female zDHHC23-KO corticotrophs with stimuli. Black line shows response to 2 nM AVP (starting at 15 min), grey line shows response to 0.2 nM CRH (starting at 40 min), and blue line shows response to the combined stimulus (starting at 65 min).

(10 min) or AUC (peak) (data not shown). Therefore, statistical analysis was performed on all female zDHHC23-KO corticotrophs together.

There were no significant differences in $[Ca^{2+}]_i$ responses induced by CRH, AVP and combined stimulus in AUC (10 min), but AUC (peak) displayed significant differences between CRH and AVP ($p < 0.05$), AVP and combined stimulus ($p < 0.05$). Importantly, combined stimulus was significantly ($p < 0.001$) smaller than the sum of the two single stimuli in both AUC (10 min) and AUC (peak). This suggests that there was no synergy between CRH and AVP at the level of $[Ca^{2+}]_i$ when considering the population. However, in 1 out of 13 cells (7.7%) the AUC (10 min) and AUC (peak) of combined stimulus were larger than the sum of the two single stimuli (Figure 5.49). CRH-, AVP- and CRH/AVP-induced $[Ca^{2+}]_i$ responses were not significantly different in peak, time to peak, response duration (Figure 5.50), peak duration or time gap (Figure 5.51).

These results suggest that there was no synergistic $[Ca^{2+}]_i$ response between CRH and AVP in female zDHHC23-KO corticotrophs when considering the population. However, a small portion of female zDHHC23-KO corticotrophs (7.7%) showed synergistic $[Ca^{2+}]_i$ response at the single cell level.

## Figure 5.49

**No synergistic $[Ca^{2+}]_i$ responses to CRH/AVP in female zDHHC23-KO corticotrophs**

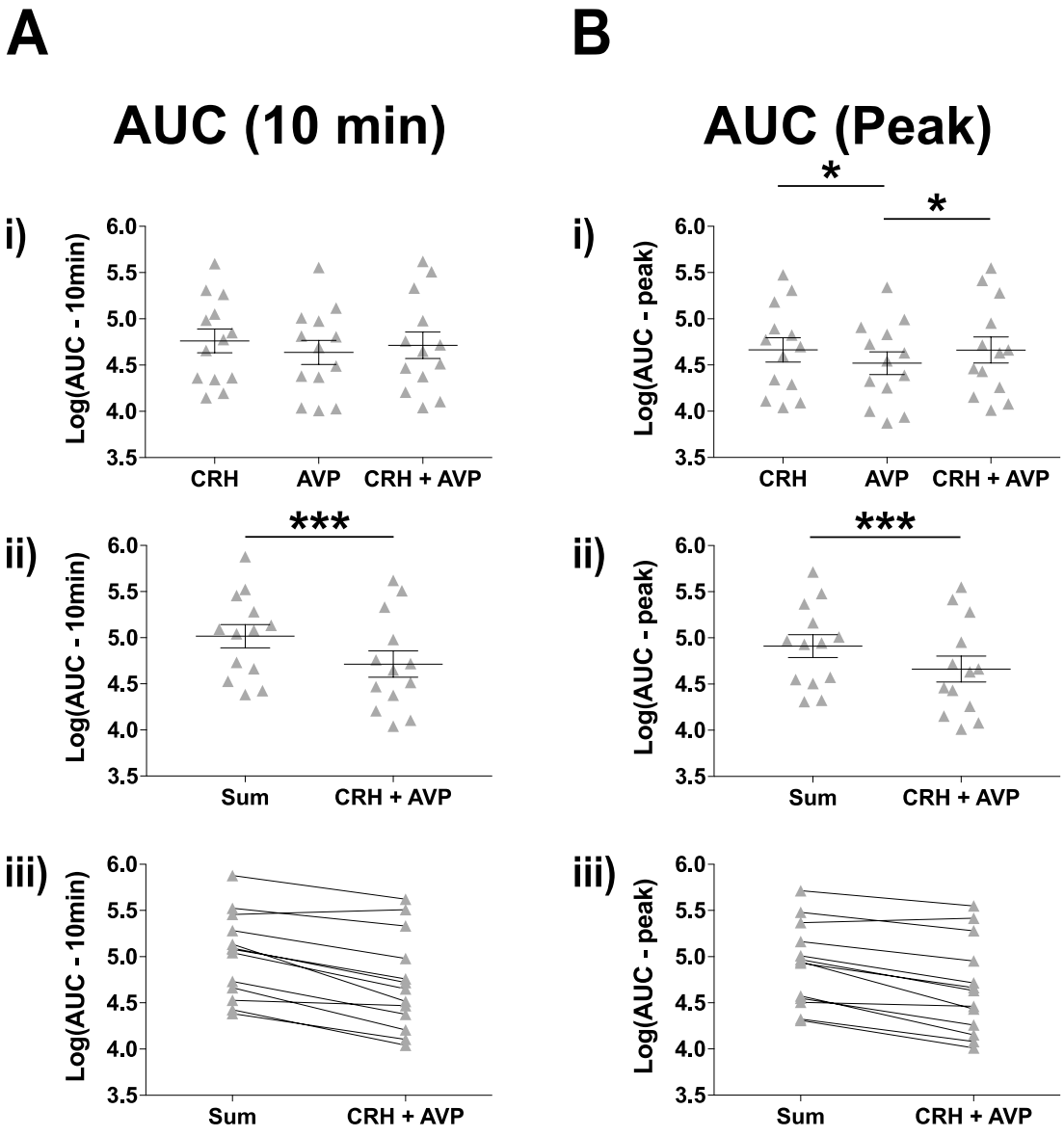


**Figure 5.49 No synergistic $[Ca^{2+}]_i$ responses to CRH/AVP in female zDHHC23-KO corticotrophs.** Quantification of effects of exposure to 0.2 nM CRH, 2 nM AVP and the combination of the two in **(A)** AUC (10 min) and **(B)** AUC (peak). The comparison of the AUC of the combined stimulus and the sum of the two single stimuli was used as a measurement of synergy. *** $p < 0.001$, * $p < 0.05$ ($n = 13$ from 5 experiments, mixed effects model). All data are means ± SEM.

## Figure 5.50

**Peak, time to peak and response duration of $[Ca^{2+}]_i$ responses to CRH, AVP and CRH/AVP in female zDHHC23-KO corticotrophs**

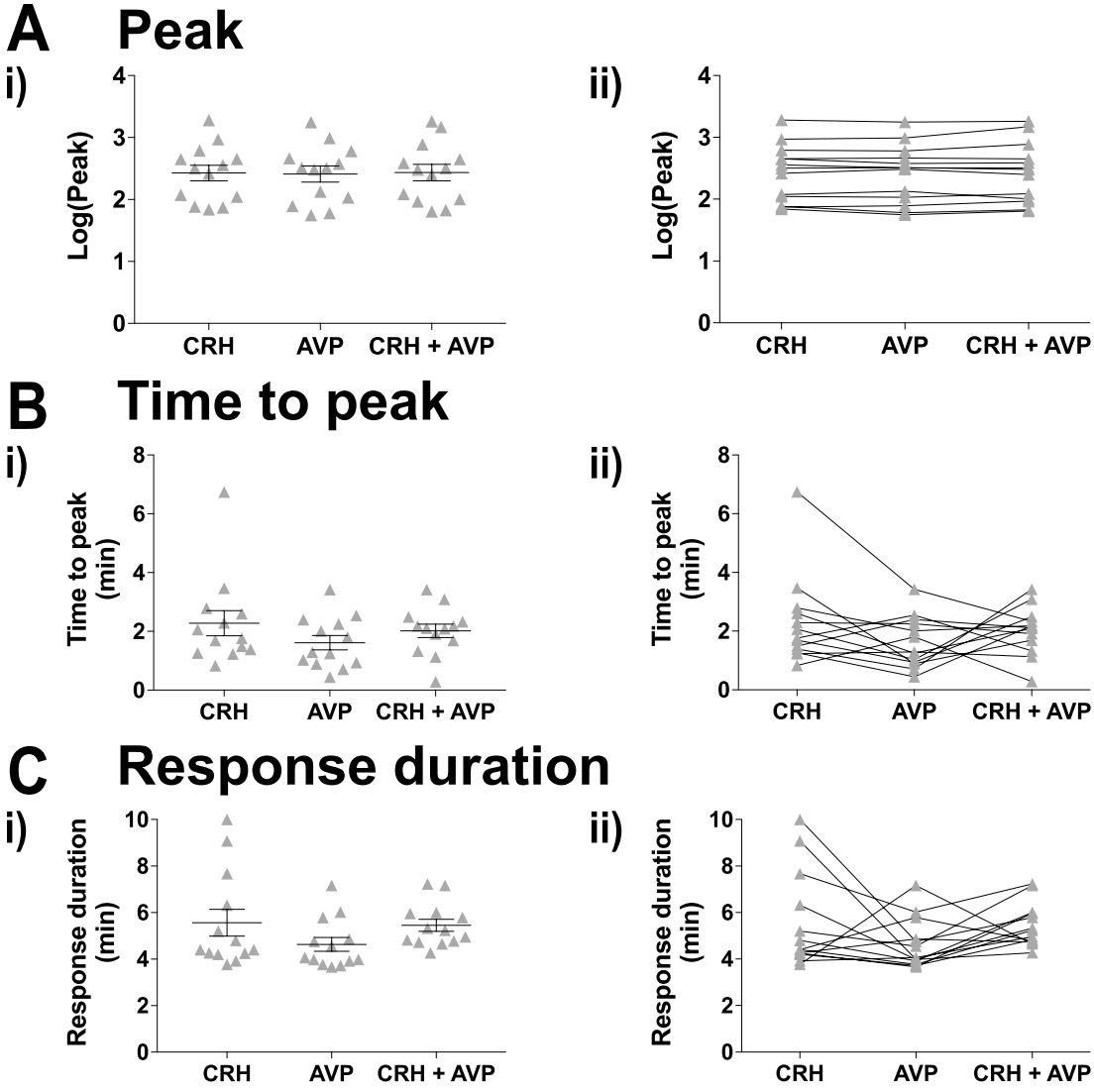


**Figure 5.50 Peak, time to peak and response duration of $[Ca^{2+}]_i$ responses to CRH, AVP and CRH/AVP in female zDHHC23-KO corticotrophs.** Quantification of effects of exposure to 0.2 nM CRH, 2 nM AVP and the combination of the two in **(A)** peak, **(B)** time to peak and **(C)** response duration (n = 13 from 5 experiments, mixed effects model). All data are means ± SEM.

## Figure 5.51

### Peak duration and time gap of $[Ca^{2+}]_i$ responses to CRH, AVP and CRH/AVP in female zDHHC23-KO corticotrophs

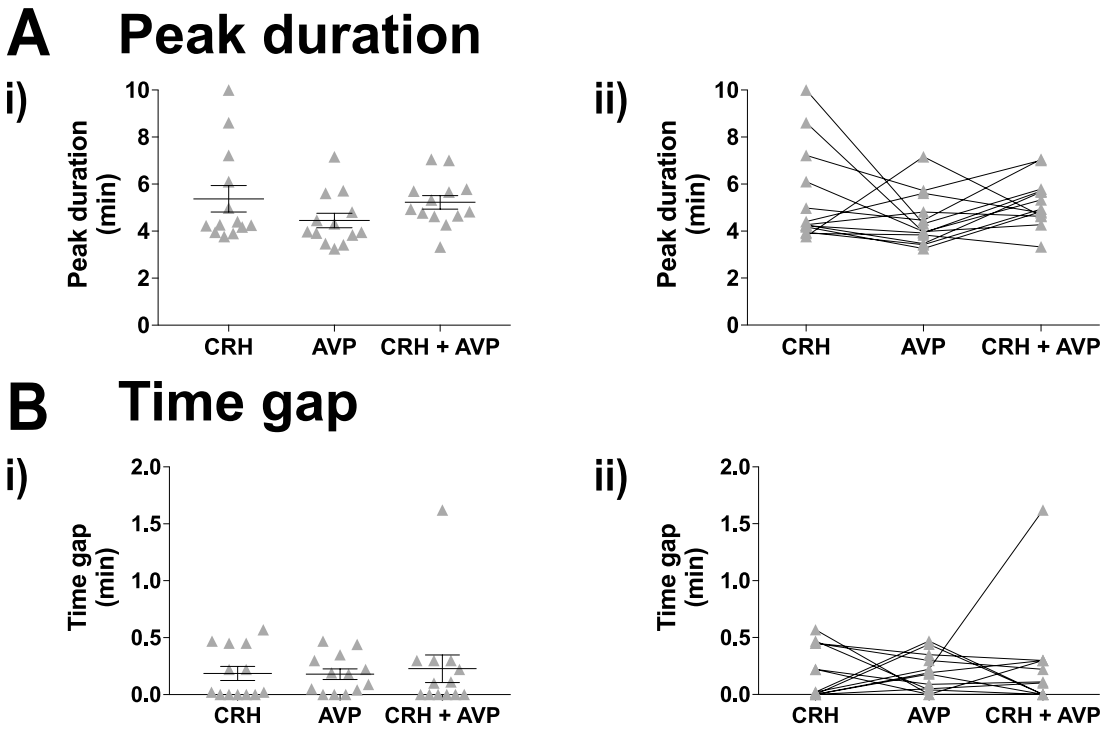


**Figure 5.51 Peak duration and time gap of $[Ca^{2+}]_i$ responses to CRH, AVP and CRH/AVP in female zDHHC23-KO corticotrophs.** Quantification of effects of exposure to 0.2 nM CRH, 2 nM AVP and the combination of the two in **(A)** peak duration and **(B)** time gap (n = 13 from 5 experiments, mixed effects model). All data are means ± SEM.

### 5.2.4.3 CRH/AVP-induced $[Ca^{2+}]_i$ responses are not significantly different between male and female zDHHC23-KO corticotrophs

Although there were no synergistic $[Ca^{2+}]_i$ responses to CRH/AVP in either male or female zDHHC23-KO corticotrophs at the level of population, we examined whether there were differences between male and female zDHHC23-KO corticotrophs.

Statistical analysis revealed that there were no significant differences between male and female zDHHC23-KO corticotrophs in AUC (10 min) or AUC (peak), although male zDHHC23-KO corticotrophs tended to have larger $[Ca^{2+}]_i$ responses to two single stimuli and combined stimulus compared to females (Figure 5.52). In addition, CRH-, AVP-, CRH/AVP-induced $[Ca^{2+}]_i$ responses showed no significant differences between male and female zDHHC23-KO corticotrophs in peak, time to peak, response duration, response duration (Figure 5.53) or time gap (Figure 5.54) either.

In summary, there were no statistically significant differences between male and female zDHHC23-KO corticotrophs in $[Ca^{2+}]_i$ responses induced by CRH, AVP and the combination of the two.

## Figure 5.52

**No significant sex difference in AUC (10 min) or AUC (peak) of $[Ca^{2+}]_i$ responses to CRH, AVP and CRH/AVP in zDHHC23-KO corticotrophs**

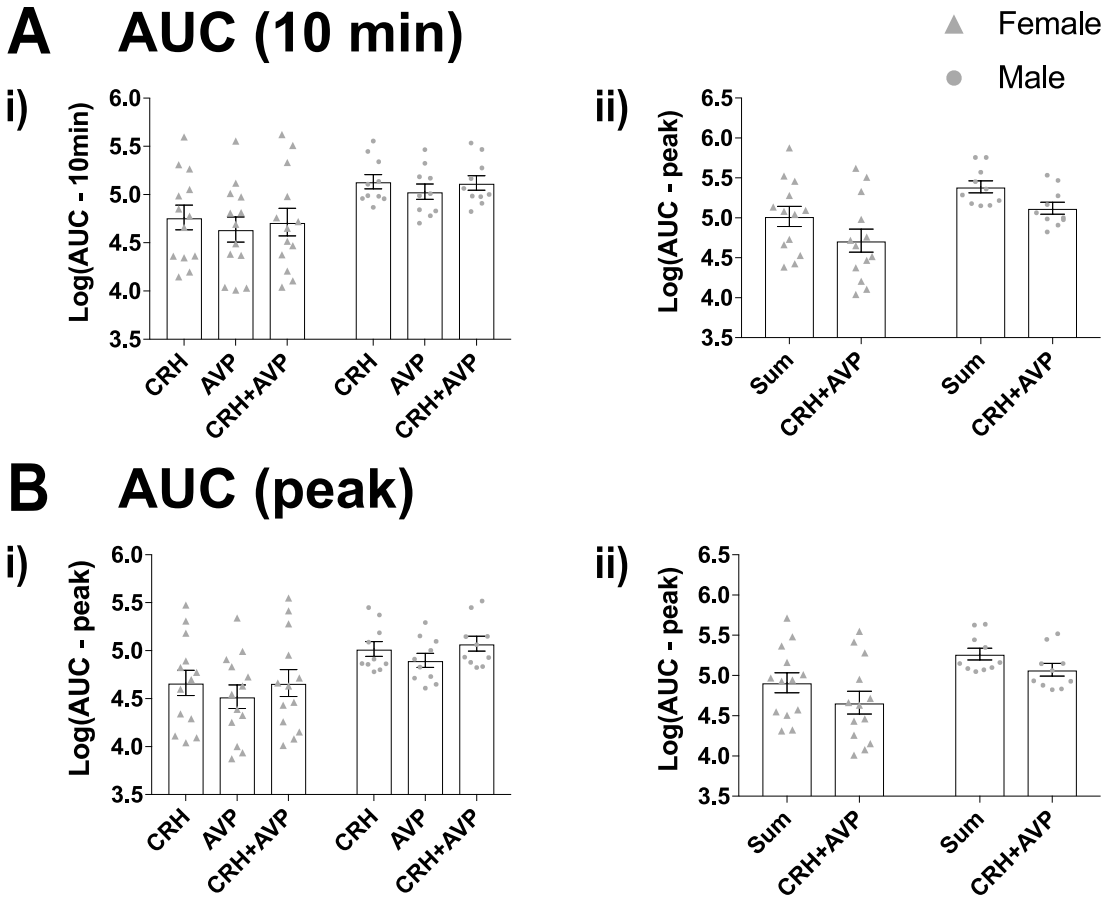


**Figure 5.52 No significant sex difference in AUC (10 min) or AUC (peak) of $[Ca^{2+}]_i$ responses to CRH, AVP and CRH/AVP in zDHHC23-KO corticotrophs.** Quantification of effects of exposure to 0.2 nM CRH, 2 nM AVP and the combination of the two in **(A)** AUC (10 min) and **(B)** AUC (peak) (male n = 10 from 8 experiments, female n = 13 from 5 experiments, mixed effects model). All data are means ± SEM.

## Figure 5.53

**No significant sex difference in peak, time to peak, response duration or peak duration of $[Ca^{2+}]_i$ responses to CRH, AVP and CRH/AVP in zDHHC23-KO corticotrophs**

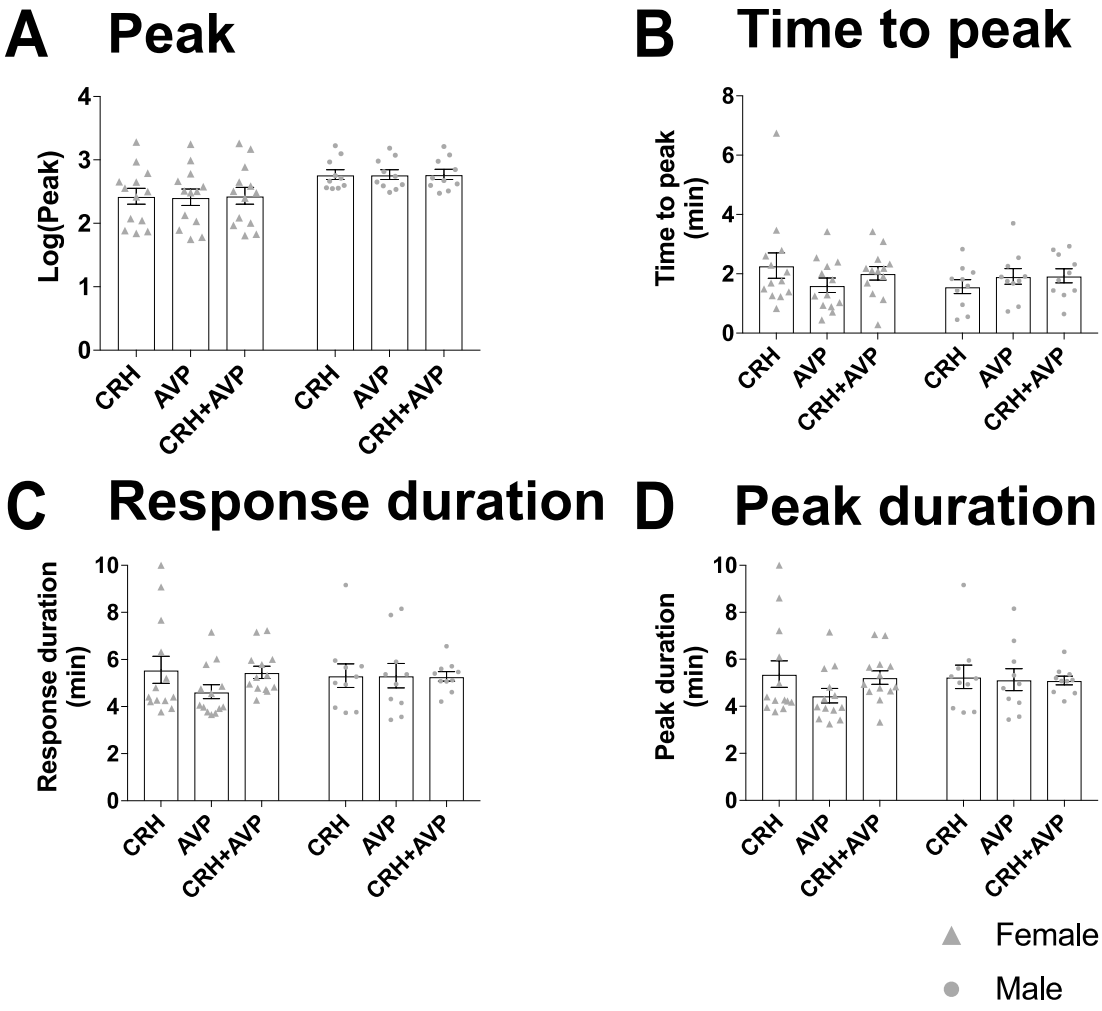


**Figure 5.53 No significant sex difference in peak, time to peak, response duration or peak duration of $[Ca^{2+}]_i$ responses to CRH, AVP and CRH/AVP in zDHHC23-KO corticotrophs.** Quantification of effects of exposure to 0.2 nM CRH, 2 nM AVP and the combination of the two in **(A)** peak, **(B)** time to peak, **(C)** response duration and **(D)** peak duration (male n = 10 from 8 experiments, female n = 13 from 5 experiments, mixed effects model). All data are means ± SEM.

# Figure 5.54

## No significant sex difference in time gap of $[Ca^{2+}]_i$ responses to CRH, AVP and CRH/AVP in zDHHC23-KO corticotrophs

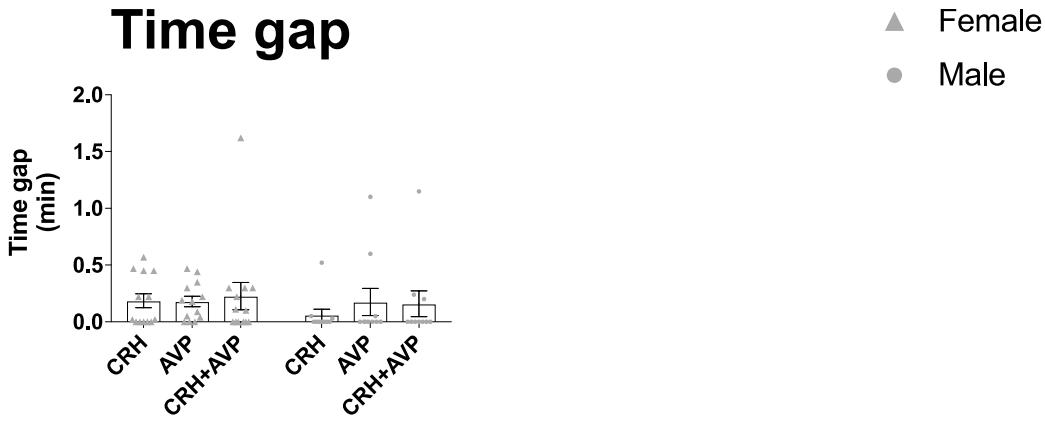


**Figure 5.54 No significant sex difference in time gap of $[Ca^{2+}]_i$ responses to CRH, AVP and CRH/AVP in zDHHC23-KO corticotrophs.** Quantification of effects of exposure to 0.2 nM CRH, 2 nM AVP and the combination of the two in time gap (male n = 10 from 8 experiments, female n = 13 from 5 experiments, mixed effects model). All data are means ± SEM.

## 5.3 Discussion

In this chapter, calcium imaging experiments were performed on zDHHC23-KO corticotrophs to investigate the role of zDHHC23 in controlling calcium signalling in murine corticotrophs. Global genetic deletion of zDHHC23 resulted in progressively attenuated $[Ca^{2+}]_i$ responses to repeated CRH stimulation in both male and female corticotrophs. However, there were no significant differences when compared to $[Ca^{2+}]_i$ responses induced by CRH in wild-type corticotrophs. Overall, loss of zDHHC23 had no significant effect on spontaneous or AVP-induced $[Ca^{2+}]_i$ responses in murine corticotrophs. Interestingly, in a small proportion of zDHHC23-KO corticotrophs, the $[Ca^{2+}]_i$ responses to repeated AVP stimulation in the same cell showed a mixture of sustained and oscillatory $[Ca^{2+}]_i$ responses. This was never observed in wild-type corticotrophs that always showed deterministic responses to AVP. This suggests zDHHC23 may play a role in controlling the pattern of AVP-induced $[Ca^{2+}]_i$ signalling rather than effects on global or peak of $[Ca^{2+}]_i$ responses. Loss of zDHHC23 did not significantly affect synergistic $[Ca^{2+}]_i$ responses to CRH and AVP. Thus, while zDHHC23 may play a role in the ability of corticotrophs to sustain repeated $[Ca^{2+}]_i$ responses to CRH and control the pattern of AVP-induced $[Ca^{2+}]_i$ signalling, overall zDHHC23 plays a relatively minor role in controlling $[Ca^{2+}]_i$ responses to either CRH or AVP in murine corticotrophs.

### 5.3.1 Progressive attenuation of CRH-induced $[Ca^{2+}]_i$ responses in zDHHC23-KO corticotrophs

Genetic deletion of zDHHC23 did not affect spontaneous $[Ca^{2+}]_i$ active time or maximum amplitude compared to wild-type corticotrophs. This suggests a limited role of zDHHC23 in controlling $[Ca^{2+}]_i$ signalling under basal conditions.

Compared to the robust and consistent $[Ca^{2+}]_i$ responses in wild-type corticotrophs, repeated CRH stimulation resulted in a progressive attenuation of $[Ca^{2+}]_i$ responses in both male and female zDHHC23-KO corticotrophs. However, $[Ca^{2+}]_i$ responses were not significantly different from $[Ca^{2+}]_i$ responses to CRH in wild-type corticotrophs. Genetic deletion of zDHHC23 is predicted to reduce cell surface expression of BK channels in corticotrophs as it controls BK channel trafficking. Previous studies in HEK293 cells reported that S-acylation of the S0-S1 loop of BK channels was mainly controlled by zDHHC23, which was involved in controlling BK channel surface trafficking (Tian *et al.*, 2012). Loss of S0-S1 loop S-acylation reduces BK channel cell surface expression by ~ 50% and thus represents a partial loss of function. Thus, the progressive attenuation of CRH-, but not AVP-induced $[Ca^{2+}]_i$ responses in zDHHC23-KO corticotrophs may represent a partial loss of BK channel function. However, it remains unclear whether BK channel surface expression is reduced in murine corticotrophs lacking zDHHC23. This represents a significant technical

challenge as zDHHC23 and BK channels are expressed in other anterior pituitary cells such as somatotrophs and gonadotrophs (Van Goor *et al.*, 2001*a*). Thus, purification of corticotrophs will be required to allow proteomic analysis of BK channel S-acylation in zDHHC23-KO corticotrophs and BK channel cell surface expression is hampered by a lack of antibodies to external epitopes of BK channels. Clearly, voltage clamp recordings are required to determine whether loss of zDHHC23 results in reduced BK channel currents in corticotrophs.

Ablation of BK channels resulted in a significant reduction in $[Ca^{2+}]_i$ responses in male corticotrophs whereas genetic deletion of zDHHC23 only induce minor differences that are not statistically significant different. These results may suggest that zDHHC23 is not an important determinant in the regulation of CRH-induced $[Ca^{2+}]_i$ responses or regulate corticotroph calcium signalling through a BK-independent pathway. In addition, the gradually declining calcium signals may also suggest the role of zDHHC23 in maintaining appropriate responses to repeated stressors on a longer timescale.

However, as CRH-induced $[Ca^{2+}]_i$ responses were progressively reduced in both male and female corticotrophs from zDHHC23-KO mice, whereas genetic ablation of BK channels only attenuated CRH-induced $[Ca^{2+}]_i$ responses in male corticotrophs, this

suggest that the small effects of zDHHC23 may result from controlling of S-acylation of other components of the CRH-signalling pathway. To date relatively few targets for zDHHC23 have been identified, although the STRING database (Szklarczyk *et al.*, 2017) suggests zDHHC23 may interact with other proteins such as zinc finger protein Zfp69, Zfp84 and S-acyl transferase zDHHC22 (String-db.org, 2019). zDHHC22 has also been shown to control S-acylation of BK channels and regulate the localization of BK channels at the plasma membrane (Tian *et al.*, 2012). In addition, G-protein coupling receptors (GPCRs), including CRH receptors, adenylate cyclases (ACs) (Naumenko & Ponimaskin, 2018) and L-type $Ca^{2+}$ channels (Chien *et al.*, 1996) have been shown or predicted to be S-acylated. Taken together, genetic deletion of zDHHC23 may modify multiple pathways in corticotrophs although importantly these would appear to be important for CRH-, but not AVP-induced $[Ca^{2+}]_i$ responses. To address whether zDHHC23 controls CRHR1 signalling pathway, PRESTO-Tango (parallel receptorome expression and screening via transcriptional output, with transcriptional activation following arrestin translocation) assay may provide a viable approach (Kroeze *et al.*, 2015).

### 5.3.2 Does zDHHC23 control the pattern of AVP-evoked $[Ca^{2+}]_i$ responses in corticotrophs?

Genetic deletion of zDHHC23 did not result in significant differences in $[Ca^{2+}]_i$

responses to repeated AVP stimulation compared to wild-type controls. However, loss of zDHHC23 did result in a reduction in the percentage of corticotrophs that displayed oscillatory $[Ca^{2+}]_i$ behaviour decreasing from 50.0% (12/24 cells) to 14.3% (2/14 cells) in female corticotrophs, while oscillatory $[Ca^{2+}]_i$ behaviour was not observed in male zDHHC23-KO corticotrophs compared to 25.0% (4/16 cells) of male wild-type corticotrophs showing oscillatory $[Ca^{2+}]_i$ behaviour. Moreover, repeated stimulation with AVP in wild-type corticotrophs always evoked consistent deterministic patterns of $[Ca^{2+}]_i$ responses: either sustained elevation of $[Ca^{2+}]_i$ or oscillatory $[Ca^{2+}]_i$ behaviour was only observed in any single cell from 40 calcium imaging recordings. However, 20.0% (2/10 cells) of male and 7.1% (1/14 cells) of female zDHHC23-KO corticotrophs displayed a mixture of two phenotypes of $[Ca^{2+}]_i$ response following repeated AVP stimulation. Previous studies in gonadotrophs revealed that gonadotropin-releasing hormone (GnRH) induced an oscillatory release of $Ca^{2+}$ through $IP_3$-sensitive intracellular calcium stores, which activates SK channels causing the hyperpolarization of gonadotrophs (Tse & Hille, 1992; Tse *et al.*, 1993). Thus, a plausible explanation for the decreased oscillatory $Ca^{2+}$ release in zDHHC23-KO corticotrophs, together with the mixture of $[Ca^{2+}]_i$ response patterns, may indicate that zDHHC23 plays a role in the coupling between $IP_3$-mediated $Ca^{2+}$ release and membrane ion channels that is important for the control of $Ca^{2+}$ oscillations.

## 5.4 Chapter summary

Genetic deletion of the S-acyl transferase zDHHC23 had no significant effect on spontaneous $[Ca^{2+}]_i$ signalling. Repeated CRH stimulation resulted in a progressive attenuation of $[Ca^{2+}]_i$ responses in both male and female zDHHC23-KO corticotrophs, although this was not significantly different from wild-type controls. This suggests that zDHHC23 may have a minor role in supporting $[Ca^{2+}]_i$ responses to repeated CRH stimulation but is unlikely to be due to control of BK channels *per se* as this was observed in both male and female corticotrophs. Following repeated AVP stimulation, corticotrophs isolated from zDHHC23-KO mice induced consistent and reproducible $[Ca^{2+}]_i$ responses. However, AVP-induced oscillatory $[Ca^{2+}]_i$ behaviour was reduced in both male and female zDHHC23-KO corticotrophs compared to wild-type corticotrophs and a small proportion of cells responded with both sustained and oscillatory $[Ca^{2+}]_i$ responses — something never observed in wild-type corticotrophs. In addition, female zDHHC23-KO corticotrophs showed a reduced proportion of cells that showed synergistic $[Ca^{2+}]_i$ responses compared to wild-type. Taken together, this suggests that zDHHC23 may be important for controlling the pattern of AVP-induced $[Ca^{2+}]_i$ signalling perhaps by controlling coupling between $IP_3$-mediated $Ca^{2+}$ release and membrane ion channels.

# Chapter Six:

# General discussion and future work

# Chapter 6: General discussion and future work

## 6.1 Hypothesis and aims

The central hypothesis of this Thesis was that CRH-, but not AVP-induced intracellular free calcium ($[Ca^{2+}]_i$) responses are dependent on functional BK channels in murine corticotrophs. To address this hypothesis, the primary aims of this thesis were to: (i) exploit a new POMC-GCaMP6s reporter using lentivirus-mediated transduction to allow specific labelling of live murine corticotrophs *in vitro*; (ii) characterise the spontaneous and secretagogue-induced $[Ca^{2+}]_i$ responses in wild-type corticotrophs; (iii) investigate the role of BK channels in regulating $[Ca^{2+}]_i$ signalling in corticotrophs; (iv) identify the regulation of corticotroph $[Ca^{2+}]_i$ signalling by S-acyl transferase zDHHC23.

## 6.2 Discussion and future work

### 6.2.1 CRH-induced $[Ca^{2+}]_i$ responses are suppressed in male BK-KO corticotrophs

The GCaMP6s calcium reporter was specifically expressed in murine corticotrophs by using lentiviral-mediated transduction under the control of a minimal rat *Pomc* promoter. This allowed robust real-time identification of live murine corticotrophs *in*

*vitro* for calcium imaging experiments to examine spontaneous and secretagogue-induced $[Ca^{2+}]_i$ responses. In most previous studies, CRH and/or AVP-induced $[Ca^{2+}]_i$ responses were examined in response to a single supraphysiological concentration of secretagogue in corticotrophs. However, *in vivo* corticotrophs must respond to repeated changes in CRH and AVP at physiologically relevant concentrations. To address this, a repeated stimulation protocol was established in this study to allow robust and repeatable $[Ca^{2+}]_i$ responses to pulses of secretagogue at physiological concentrations with frequency of pulses similar to those reported *in vivo*.

Repeated CRH stimulation resulted in significant and rapid sustained elevation of global $[Ca^{2+}]_i$ in wild-type corticotrophs with no significant differences between male and female wild-type corticotrophs. $[Ca^{2+}]_i$ responses to repeated CRH stimulation in corticotrophs from male, but not female, BK-KO mice were significantly attenuated compared to wild-type. Surprisingly, CRH-induced $[Ca^{2+}]_i$ responses were not significantly attenuated following acute pharmacological inhibition of BK channels in both male and female wild-type corticotrophs with the specific BK channel inhibitor paxilline. Previous studies have revealed that both genetic deletion and pharmacological inhibition of BK channels with paxilline prevents CRH-induced transition to bursting in male corticotrophs (Duncan *et al.*, 2015). Taken together, these results suggest two potential mechanisms: (i) CRH-induced transition to bursting

observed on the millisecond to second timescale, which are dependent on BK channels, is not important for the global $[Ca^{2+}]_i$ responses measured over minutes in male corticotrophs (Figure 6.1); (ii) potential compensatory changes are occurring in male corticotrophs following global deletion of BK channels in ion channel landscape and/or CRH-induced signalling pathway.

At face value, genetic deletion of BK channels resulted in the attenuation of CRH-induced $[Ca^{2+}]_i$ responses in male corticotrophs suggest that loss of BK channels would decrease $[Ca^{2+}]_i$ responses due to a loss of CRH-induced transition to bursting. However, surprisingly, acute pharmacological blockade of BK channels with paxilline did not show the same effect. This suggests that CRH-induced electrical bursting measured on the millisecond to second timescale probably has no direct link to global $[Ca^{2+}]_i$ signalling measured over minutes. Genetic deletion or pharmacological inhibition of BK channels may result in the loss of bursting but have no impact on global $[Ca^{2+}]_i$ signalling. Moreover, CRH has been shown to increases electrical spiking frequency in BK-KO, or paxilline treated, corticotrophs (Duncan *et al.*, 2015). As CRH regulates corticotrophs through cAMP/PKA pathway that drives $Ca^{2+}$ influx via L-type $Ca^{2+}$ channels (Lee & Tse, 1997; Duncan *et al.*, 2015), it is likely that inhibition of BK channels with paxilline, or knockout of BK channels, prevents the transition to CRH-induced bursting but still enables significant accumulation of global

## Figure 6.1

### Schematic diagram of different timescale between global $[Ca^{2+}]_i$ signalling and electrical activity in corticotrophs

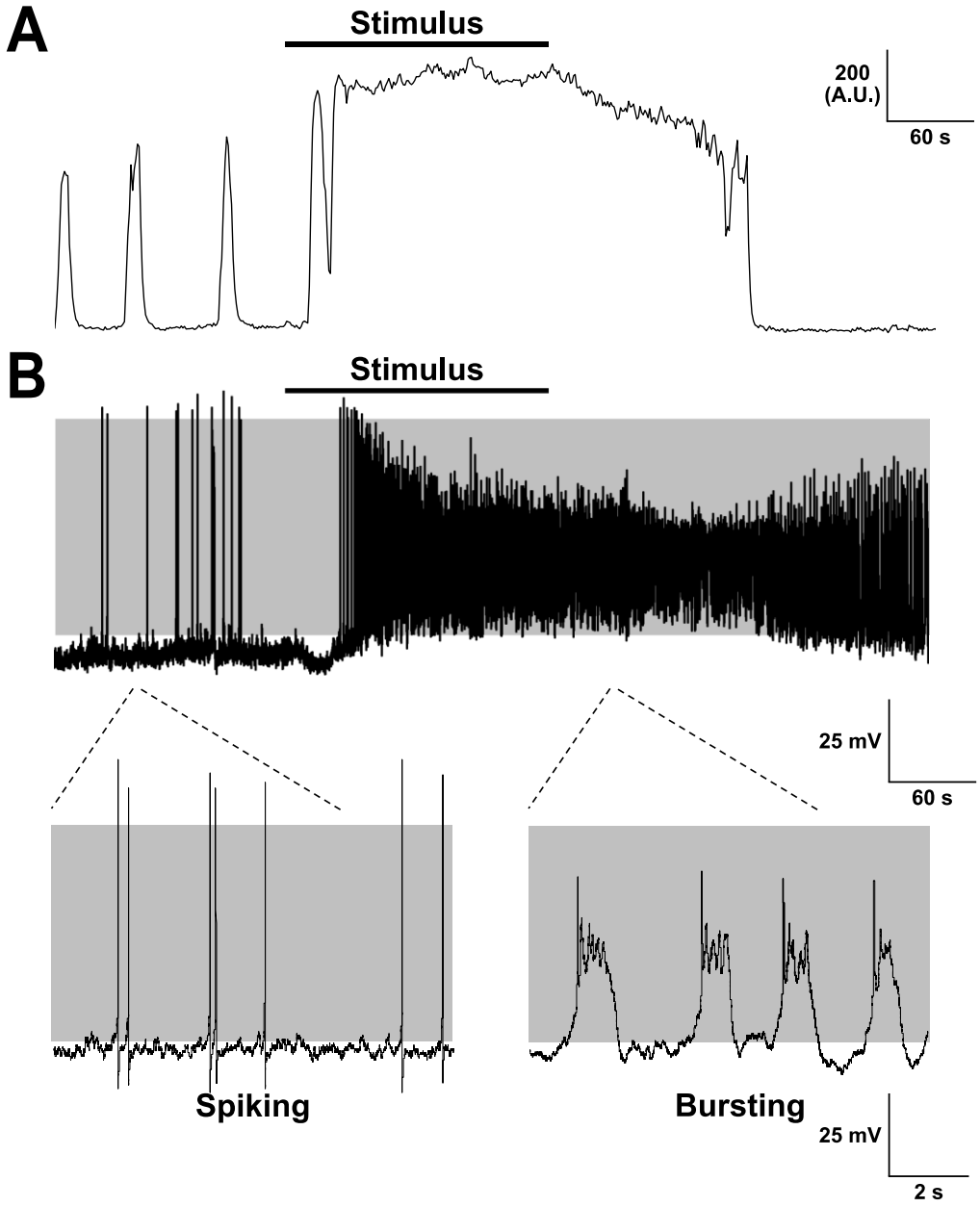


**Figure 6.1 Schematic diagram of different timescale between global $[Ca^{2+}]_i$ signalling and electrical activity in corticotrophs. (A)** Global $[Ca^{2+}]_i$ response is measured over minutes. **(B)** Electrical activity (spiking and bursting) is measured on the millisecond to second timescale. Grey shading indicates membrane potential between −50 mv to +10 mv. Electrical activity images are adapted from Duncan *et al.*, 2016.

$Ca^{2+}$ influx through single spiking. A recent study has also shown that electrical spiking can be as effective as bursting at evoking hormone secretion when release sites are located close to the channel or spiking frequency increases to a level to deliver the similar total amount of global $Ca^{2+}$ as bursting (Tagliavini *et al.*, 2016). To address these questions, it would be important to examine the correlation between $[Ca^{2+}]_i$ responses measured on millisecond timescale and electrical bursting behaviour in corticotrophs. Furthermore, it is important to understand what is more important for hormone secretion in corticotrophs: the global $[Ca^{2+}]_i$ signalling over minutes, the pattern of $[Ca^{2+}]_i$ responses on millisecond timescale or the pattern of electrical activity (bursting). In addition, a calcium indicator expressed at the plasma membrane or vesicles will allow us to measure calcium changes at the level of plasma membrane or vesicle, which will help to address the role of calcium in evoking hormone secretion.

As CRH-induced $[Ca^{2+}]_i$ responses were significantly attenuated in male, but not female, BK-KO corticotrophs, and paxilline-treated corticotrophs showed different $[Ca^{2+}]_i$ responses compared to BK-KO corticotrophs, the other potential mechanism is that compensation is occurring in corticotrophs. The ion channel landscape and/or signalling pathways have been modified to compensate for the long-term lack of BK channels in mice. Importantly, these compensatory changes specifically modify CRH, but not AVP-induced calcium signalling pathway and affect male and female

corticotrophs differentially. Differences were observed between male and female BK-KO corticotrophs in both spontaneous and CRH-induced $[Ca^{2+}]_i$ responses. Unpublished data from the Shipston Lab (Dr Peter J. Duncan, personal communication) revealed that female wild-type corticotrophs showed limited electrical bursting behaviour upon stimulation, with largely showing spiking frequency increases, which is different from male wild-type corticotrophs. This suggests that the functional role of BK channels and the ion channels/signalling pathways controlling spontaneous and CRH-induced $[Ca^{2+}]_i$ responses are different between male and female corticotrophs. The compensatory changes may regulate CRH-induced calcium signalling pathways differentially between male and female corticotrophs. In addition, genetic deletion of BK channels resulted in a reduction in spontaneous $[Ca^{2+}]_i$ active time in male corticotrophs whereas female BK-KO corticotrophs showed an increase compared to wild-type. The maximum amplitude of spontaneous $[Ca^{2+}]_i$ signalling was unaffected by genetic deletion of BK channels. However, acute pharmacological inhibition of BK channels had no effect on either active time or maximum amplitude of spontaneous $[Ca^{2+}]_i$ signalling, which may also reflect compensation. If the compensation really occurs in corticotrophs, how does the compensation modify the signalling pathway? Whether this down-regulates CRH receptor activation, the amount of L-type $Ca^{2+}$ channels or up-regulates the sequestration of $Ca^{2+}$ remain unknown. Analysis of changes in mRNA, protein and function levels of L-type $Ca^{2+}$ channel and other ion

channels in BK-KO corticotrophs will be required to address the compensation theory. As mice with global genetic deletion of BK channels were used in this study, the same calcium imaging experiments could be performed on corticotrophs from mice in which BK channels have been conditionally deleted only in corticotrophs to examine whether CRH induces similar $[Ca^{2+}]_i$ responses.

Genetic deletion of zDHHC23 had no effect on spontaneous $[Ca^{2+}]_i$ signalling in any corticotrophs. This suggests that BK channels *per se*, rather than zDHHC23 that controls S-acylation of BK channels, is partly responsible for controlling $[Ca^{2+}]_i$ signalling under basal conditions. Loss of zDHHC23 resulted in a progressive attenuation of $[Ca^{2+}]_i$ responses to repeated CRH stimulation in both male and female corticotrophs. However, CRH-induced $[Ca^{2+}]_i$ responses were not significantly different from wild-type. This suggests the limited role of zDHHC23 in the regulation of CRH-induced $[Ca^{2+}]_i$ responses or zDHHC23 regulates corticotroph $[Ca^{2+}]_i$ signalling through a BK-independent pathway. Voltage clamp recordings could be performed in zDHHC23-KO corticotrophs to determine whether loss of zDHHC23 leads to reduced BK channel currents in corticotrophs.

### 6.2.2 Genetic deletion of BK channels or zDHHC23 have no effect on AVP-induced $[Ca^{2+}]_i$ responses in corticotrophs

Following repeated AVP stimulation, two phenotypes of $[Ca^{2+}]_i$ response, sustained elevation of $[Ca^{2+}]_i$ and oscillatory $[Ca^{2+}]_i$ behaviour, were observed in wild-type corticotrophs. These distinct $[Ca^{2+}]_i$ response patterns were deterministic in wild-type corticotrophs and no sex differences were observed. Corticotrophs from both male and female BK-KO mice showed significant elevation of $[Ca^{2+}]_i$ following AVP stimulation and two phenotypes of $[Ca^{2+}]_i$ response were observed as well. However, there were no significant differences between wild-type and BK-KO corticotrophs in both sexes. This suggests that BK channels are not vital in controlling AVP-induced $[Ca^{2+}]_i$ responses in corticotrophs. This is in accord with the role of BK channels in regulating electrical activity. Genetic deletion of BK channels results in an increase in spiking frequency rather than a transition to bursting in male corticotrophs following AVP stimulation (Duncan *et al.*, 2015). AVP-induced electrical activity is independent of BK channels, which agrees with the lack of effect on $[Ca^{2+}]_i$ responses in BK-KO corticotrophs. As AVP regulates corticotrophs through $IP_3$/PKC pathway which results in the release of calcium from intracellular $IP_3$-sensitive calcium pool as well as influx via L-type $Ca^{2+}$ channels (Tse & Lee, 1998; Romanò *et al.*, 2017), this suggests that the potential compensatory changes observed in CRH-induced $[Ca^{2+}]_i$ responses in BK-KO corticotrophs are not involved in AVP-induced calcium signalling pathways.

It may also suggest that $Ca^{2+}$ influx via L-type $Ca^{2+}$ channels is not a major component in regulating AVP-induced $[Ca^{2+}]_i$ responses in murine corticotrophs. Loss of zDHHC23 had no significant effect on $[Ca^{2+}]_i$ responses to repeated AVP stimulation in either male or female corticotrophs compared to wild-type. Interestingly, genetic deletion of BK channels and zDHHC23 resulted in a reduction in the percentage of female corticotrophs displaying oscillatory $[Ca^{2+}]_i$ behaviour compared to female wild-type corticotrophs. Furthermore, both male and female corticotrophs from BK-KO and zDHHC23-KO mice displayed a mixture of two phenotypes of $[Ca^{2+}]_i$ responses following repeated AVP stimulation, which is different from wild-type corticotrophs always showing consistent deterministic patterns of $[Ca^{2+}]_i$ responses. Oscillatory $[Ca^{2+}]_i$ behaviour is likely to result primarily from $IP_3$-sensitive calcium signalling. These data suggest that BK channels and zDHHC23 play no major role in controlling AVP-induced $[Ca^{2+}]_i$ responses in corticotrophs, however, they may partly regulate the coupling between $IP_3$-mediated $Ca^{2+}$ release and membrane ion channels that is important for the control of $Ca^{2+}$ oscillations.

### 6.2.3 Lack of synergistic $[Ca^{2+}]_i$ responses to CRH and AVP

CRH and AVP have been shown to act synergistically to increase the secretion of ACTH in corticotrophs. This synergy has been considered to occur at multiple levels signalling in corticotrophs. However, whether the synergy also occurs at the level of

intracellular free calcium is largely unexplored. This study suggests that there was no synergistic $[Ca^{2+}]_i$ response in any male corticotrophs isolated from wild-type, BK-KO or zDHHC23-KO mice. Although female corticotrophs did not display synergistic $[Ca^{2+}]_i$ responses to CRH and AVP at the population level, ~ 30% of wild-type, ~ 5% of BK-KO and ~ 8% of zDHHC23-KO female corticotrophs showed synergistic $[Ca^{2+}]_i$ responses at the single cell level. It is unclear whether this proportion of female, but not male, corticotrophs that shows synergistic $[Ca^{2+}]_i$ responses reflects stochastic variability in corticotroph signalling pathways or represents distinct subpopulation of corticotrophs. In addition, the high degree of variability in spontaneous $[Ca^{2+}]_i$ signalling that can be roughly categorized into three subtypes may also reflect stochastic variability in corticotroph behaviour or implies potential distinct subpopulation of corticotrophs. To address this, corticotroph $[Ca^{2+}]_i$ signalling could be analysed in pituitary slices instead of pituitary cultures to determine whether there is a correlation between $[Ca^{2+}]_i$ responses and the location of corticotrophs within the pituitary gland. It is possible that synergistic $[Ca^{2+}]_i$ responses to CRH and AVP were not observed in this study because 0.2 nM CRH alone and 2 nM AVP alone have already induced maximal $[Ca^{2+}]_i$ responses. Although this was not been formally tested in these studies, these concentrations of CRH alone and AVP alone did not maximally stimulate ACTH secretion in primary isolated rodent corticotrophs *in vitro* and when administered together synergistic stimulation of ACTH release was measured (Vale *et*

*al.*, 1981; Gibbs & Vale, 1982; unpublished data from the Shipston Lab). To verify that the concentrations for both CHR and AVP were not maximal, a dose-response curve determining $[Ca^{2+}]_i$ responses to a wide range of both CRH alone and AVP alone concentrations is required for future studies. In addition, as the synergy between CRH and AVP does not occur at the level of $[Ca^{2+}]_i$ may suggest that synergistic secretion of ACTH is regulated through other signalling pathways rather than the intracellular free calcium.

$[Ca^{2+}]_i$ signalling has not been systematically analysed in mouse corticotrophs between males and females in previous studies, although sexual dimorphism has been shown to occur at multiple levels of HPA axis function. Sex differences observed in this study may suggest potential sexual dimorphism also occurs at the level of corticotroph calcium signalling. Thus, it is necessary to investigate the regulation of corticotroph calcium signalling in male and female corticotrophs respectively in further studies. The stage of the oestrous cycle of the female mice used in this study was not determined. As indicated in Chapter One, sex steroids can regulate the expression and function of ion channels expressed in the pituitary and the activity of the HPA stress axis varies during different stages of oestrous cycles (Fiordelisio *et al.*, 2007; Panagiotakopoulos & Neigh, 2014). In future studies, monitoring the oestrous cycles of the female animals used will be valuable to examine whether apparent differences

between male and female corticotrophs may, in part, be dependent on the stage of the oestrous cycle.

In the intact mouse anterior pituitary, 5-10% of the cells are corticotrophs; that is, representing approximately 4,000-5,000 cells. In the majority of the calcium imaging experiments done in this study, a minimum of 10 cells were randomly analysed under each condition, which thus represents less than 0.5% of the total population of corticotrophs in the anterior pituitary gland. However, in each group, the results were relatively consistent that might suggesting that they might be representative of the whole population. Further studies using larger numbers of cells to investigate the potential heterogeneity of corticotroph properties and regulation are required as well as in ex *vivo* experiments using the intact pituitaries to address whether location in the gland is also an important factor.

## 6.3 Conclusion

In conclusion, development of the POMC-GCaMP6s lentivirus allowed the specific identification of murine anterior pituitary corticotrophs *in vitro* and the examination of spontaneous and CRH- and/or AVP-induced $[Ca^{2+}]_i$ responses in corticotrophs. CRH induced sustained elevations of $[Ca^{2+}]_i$ whereas AVP evoked two phenotypes of $[Ca^{2+}]_i$ response: sustained $[Ca^{2+}]_i$ elevation and oscillatory $[Ca^{2+}]_i$ response. Genetic deletion

of BK channels significantly reduced CRH-, but not AVP-induced $[Ca^{2+}]_i$ responses in male, but not female, corticotrophs. However, acute pharmacological blockade of BK channels did not show the same effect in wild-type corticotrophs. This suggests potential compensatory mechanisms may occur in corticotrophs as a result of deletion of BK channels. Moreover, CRH-induced transition to bursting, which are dependent on BK channels, may be not important for the global changes in $[Ca^{2+}]_i$ responses measured over minutes. zDHHC23 plays a limited role in controlling $[Ca^{2+}]_i$ signalling in corticotrophs. There is no synergy between CRH and AVP in corticotrophs at the intracellular free calcium level.

Anterior pituitary corticotrophs, the central components of the HPA axis, are important for regulating the neuroendocrine responses to stress. Corticotrophs receive inputs from hypothalamic secretagogues with the negative feedback of glucocorticoids from the adrenal gland at the level of both the pituitary and the hypothalamus to keep the balance of HPA axis. The secretion of ACTH is regulated through an increase in electrical excitability in corticotrophs, which is associated with an increase in the level of intracellular free calcium. Therefore, it is important to characterise the role of specific ion channels and their signalling pathways in regulating electrical activity and $[Ca^{2+}]_i$ responses of corticotrophs. Further studies of the correlation between electrical excitability and $[Ca^{2+}]_i$ signalling in corticotrophs would suggest potential

mechanisms for ACTH secretion and HPA axis regulation. Glucocorticoid has been shown to suppress bursting activity following CRH/AVP stimulation in corticotrophs (Duncan *et al.*, 2016), thus it is important to further investigate the regulation of corticotroph $[Ca^{2+}]_i$ signalling by glucocorticoids which would provide new insight of negative feedback in controlling HPA axis function at the level of $[Ca^{2+}]_i$ signalling. The approach developed in this Thesis will allow us to explore the mechanisms of $[Ca^{2+}]_i$ signalling and its regulation that will lead to a greater understanding of the physiological role of corticotrophs and the control of the stress axis, which potentially leads to novel therapeutic targets and drugs for stress-related disorders.

# References

# References

Abou-Samra AB, Harwood JP, Manganiello VC, Catt KJ & Aguilera G (1987). Phorbol 12-myristate 13-acetate and vasopressin potentiate the effect of corticotropin-releasing factor in cyclic AMP production in rat anterior pituitary cells. Mechanisms of action. *J Biol Chem* **262,** 1129–1136.

Aguilera G (1998). Corticotropin releasing hormone, receptor regulation and the stress response. *Trends Endocrinol Metab* **9,** 329–336.

Akerboom J, Rivera JDV, Guilbe MMR, Malavé ECA, Hernandez HH, Tian L, Hires SA, Marvin JS, Looger LL & Schreiter ER (2009). Crystal structures of the GCaMP calcium sensor reveal the mechanism of fluorescence signal change and aid rational design. *J Biol Chem* **284,** 6455–6464.

Antoni FA (1993). Vasopressinergic control of pituitary adrenocorticotropin secretion comes of age. *Front Neuroendocrinol* **14,** 76–122.

Antoni FA (2012). Interactions between intracellular free $Ca^{2+}$ and cyclic AMP in neuroendocrine cells. *Cell Calcium* **51,** 260–266.

Antoni MH, Lutgendorf SK, Cole SW, Dhabhar FS, Sephton SE, McDonald PG, Stefanek M & Sood AK (2006). The influence of bio-behavioural factors on tumour biology: pathways and mechanisms. *Nat Rev Cancer* **6,** 240–248.

Autelitano DJ, Lundblad JR, Blum M & Roberts JL (1989). Hormonal Regulation of POMC Gene Expression. *Annu Rev Physiol* **51,** 715–726.

Bale TL & Vale WW (2004). CRF and CRF receptors : Role in stress responsivity and other behaviors. *Annu Rev Pharmacol Toxicol* **44,** 525–557.

Bangasser DA & Wiersielis KR (2018). Sex differences in stress responses: a critical role for corticotropin-releasing factor. *Hormones* **17,** 5–13.

Beery AK & Zucker I (2011). Sex bias in neuroscience and biomedical research. *Neurosci Biobehav Rev* **35,** 565–572.

Behrens R, Nolting A, Reimann FY, Schwarz M, Waldschu R & Pongs O (2000). hKCNMB3 and hKCNMB4, cloning and characterization of two members of the large-conductance calcium-activated potassium channel β subunit family. *FEBS Lett* **474,** 99–106.

Bourke CH, Harrell CS & Neigh GN (2012). Stress-induced sex differences: Adaptations mediated by the glucocorticoid receptor. *Horm Behav* **62,** 210–218.

Brenner R, Peréz GJ, Bonev AD, Eckman DM, Kosek JC, Wiler SW, Patterson AJ, Nelson MT & Aldrich RW (2000). Vasoregulation by the β1 subunit of the calcium-activated potassium channel. *Nature* **407,** 870–876.

Brunton PJ, Sausbier M, Wietzorrek G, Sausbier U, Knaus HG, Russell JA, Ruth P & Shipston MJ (2007). Hypothalamic-pituitary-adrenal axis hyporesponsiveness to restraint stress in mice deficient for large-conductance calcium- and voltage-activated potassium (BK) channels. *Endocrinology* **148,** 5496–5506.

Chamberlain LH & Shipston MJ (2015). The Physiology of Protein S-acylation. *Physiol Rev* **95,** 341–376.

Chen L, Bi D, Tian L, McClafferty H, Steeb F, Ruth P, Knaus HG & Shipston MJ (2013*a*). Palmitoylation of the β4-subunit regulates surface expression of large conductance calcium-activated potassium channel splice variants. *J Biol Chem* **288,** 13136–13144.

Chen L, Tian L, MacDonald SHF, McClafferty H, Hammond MSL, Huibant JM, Ruth P, Knaus HG & Shipston MJ (2005). Functionally diverse complement of large conductance calcium- and voltage-activated potassium channel (BK) α-subunits generated from a single site of splicing. *J Biol Chem* **280,** 33599–33609.

Chen TW, Wardill TJ, Sun Y, Pulver SR, Renninger SL, Baohan A, Schreiter ER, Kerr RA, Orger MB, Jayaraman V, Looger LL, Svoboda K & Kim DS (2013*b*). Ultrasensitive fluorescent proteins for imaging neuronal activity. *Nature* **499,** 295–300.

Chien AJ, Carr KM, Shirokov RE, Rios E & Hosey MM (1996). Identification of palmitoylation sites within the L-type calcium channel β2a subunit and effects on channel function. *J Biol Chem* **271,** 26465–26468.

Childs GV, Marchetti C & Brown AM (1987). Involvement of sodium channels and two types of calcium channels in the regulation of adrenocorticotropin release. *Endocrinology* **120,** 2059–2069.

Chrousos GP & Gold PW (1992). The concepts of stress and stress system disorders. *Jama* **267,** 1244–1252.

Coetzee WA, Amarillo Y, Chiu J, Chow A, Ozaita A, Pountney D & Saganich M (1999). Molecular diversity of $K^+$ Channels. *Ann N Y Acad Sci* **868,** 233–285.

Corcuff J, Guerineau C, Mariot P & Lussiers BT (1993). Multiple cytosolic calcium signals and membrane electrical events evoked in single arginine vasopressin-stimulated corticotrophs. *J Biol Chem* **268,** 22313–22321.

Ding JJ, Luo AF, Hu LY, Wang DC & Shao F (2014). Structural basis of the ultrasensitive calcium indicator GCaMP6. *Sci China Life Sci* **57,** 269–274.

Du W, Bautista JF, Yang H, Diez-Sampedro A, You SA, Wang L, Kotagal P, Lüders HO, Shi J, Cui J, Richerson GB & Wang QK (2005). Calcium-sensitive potassium channelopathy in human epilepsy and paroxysmal movement disorder. *Nat Genet* **37,** 733–738.

Duncan PJ, Şengül S, Tabak J, Ruth P, Bertram R & Shipston MJ (2015). Large conductance $Ca^{2+}$ -activated $K^{+}$ (BK) channels promote secretagogue-induced transition from spiking to bursting in murine anterior pituitary corticotrophs. *J Physiol* **5,** 1197–1211.

Duncan PJ, Tabak J, Ruth P, Bertram R & Shipston MJ (2016). Glucocorticoids inhibit CRH/AVP-evoked bursting activity of male murine anterior pituitary corticotrophs. *Endocrinology* **157,** 3108–3121.

Engler D, Redei E & Kola I (1999). The corticotropin-release inhibitory factor hypothesis: A review of the evidence for the existence of inhibitory as well as stimulatory hypophysiotropic regulation of adrenocorticotropin secretion and biosynthesis. *Endocr Rev* **20,** 460–500.

Favrod-Coune C, Raux-Demay MC, Proeschel MF, Bertagna X, Girard F & Luton JP (1993). Potentiation of the classic ovine corticotrophin releasing hormone stimulation test by the combined administration of small doses of lysine vasopressin. *Clin Endocrinol* **38,** 405–410.

Fiordelisio T, Jiménez N, Baba S, Shiba K & Hernández-Cruz A (2007). Immunoreactivity to neurofilaments in the rodent anterior pituitary is associated with the expression of α1A protein subunits of voltage-gated Ca2+channels. *J Neuroendocrinol* **19,** 870–881.

Fletcher PA, Zemkova H, Stojilkovic SS & Sherman A (2017). Modeling the diversity of spontaneous and agonist-induced electrical activity in anterior pituitary corticotrophs. *J Neurophysiol* **117,** 2298–2311.

Fury M, Marx SO & Marks AR (2002). Molecular BKology: The study of splicing and dicing. *Sci STKE* **2002,** pe12.

Garcia MI, Chen JJ & Boehning D (2017). Genetically encoded calcium indicators for studying long-term calcium dynamics during apoptosis. *Cell Calcium* **61,** 44–49.

Ghatta S, Nimmagadda D, Xu X & O'Rourke ST (2006). Large-conductance, calcium-activated potassium channels: Structural and functional implications. *Pharmacol Ther* **110,** 103–116.

Gibbs DM & Vale W (1982). Presence of corticotropin releasing factor-like immunoreactivity in hypophysial portal blood. *Endocrinology* **Ill,** 1418–1420.

Gillies GE, Linton EA & Lowry PJ (1982). Corticotropin releasing activity of the new CRF is potentiated several times by vasopressin. *Nature* **299,** 355–357.

Goncharova ND (2013). Stress responsiveness of the hypothalamic-pituitary-adrenal axis: Age-related features of the vasopressinergic regulation. *Front Endocrinol (Lausanne)* **4,** 4:26.

Van Goor F, Li YX & Stojilkovic SS (2001*a*). Paradoxical role of large-conductance

calcium-activated $K^+$ (BK) channels in controlling action potential-driven $Ca^{2+}$ entry in anterior pituitary cells. *J Neurosci* **21,** 5902–5915.

Van Goor F, Zivadinovic D, Martinez-Fuentes AJ & Stojilkovic SS (2001*b*). Dependence of pituitary hormone secretion on the pattern of spontaneus voltage-gated calcium influx. Cell type-specific action potential secretion coupling. *J Biol Chem* **276,** 33840–33846.0

Greaves J & Chamberlain LH (2011). DHHC palmitoyl transferases: Substrate interactions and (patho)physiology. *Trends Biochem Sci* **36,** 245–253.

Gubitosi-Klug RA, Mancuso DJ & Gross RW (2005). The human Kv1.1 channel is palmitoylated, modulating voltage sensing: Identification of a palmitoylation consensus sequence. *Proc Natl Acad Sci U S A* **102,** 5964–5968.

Guérineau N, Corcuff JB, Tabarin A & Mollard P (1991). Spontaneous and corticotropin-releasing factor-induced cytosolic calcium transients in corticotropin. *Endocrinology* **129,** 409–420.

Haleem DJ, Kennett G & Curzon G (1988). Adaptation of female rats to stress: Shift to male pattern by inhibition of corticosterone synthesis. *Brain Res* **458,** 339–347.

Hammer GD, Fairchild-Huntress V & Low MJ (1990). Pituitary-specific and hormonally regulated gene expression directed by the rat proopiomelanocortin promoter in transgenic mice. *Mol Endocrinol* **4,** 1689–1697.

Heffner KL, Loving TJ, Robles TF & Kiecolt-Glaser JK (2003). Examining psychosocial factors related to cancer incidence and progression: In search of the silver lining. *Brain Behav Immun* **17,** S109–S111.

Herman JP, Figueiredo H, Mueller NK, Ulrich-Lai Y, Ostrander MM, Choi DC & Cullinan WE (2003). Central mechanisms of stress integration: Hierarchical circuitry controlling hypothalamo–pituitary–adrenocortical responsiveness. *Front Neuroendocrinol* **24,** 151–180.

Hinz B & Hirschelmann R (2000). Rapid non-genomic feedback effects of glucocorticoids on CRF-induced ACTH secretion in rats. *Pharm Res* **17,** 1273–1277.

Horikawa K (2015). Recent progress in the development of genetically encoded $Ca^{2+}$ indicators. *J Med Investig* **62,** 24–28.

Huang MH, So EC, Liu YC & Wu SN (2006). Glucocorticoids stimulate the activity of large-conductance $Ca^{2+}$-activated $K^+$ channels in pituitary GH3 and AtT-20 cells via a non-genomic mechanism. *Steroids* **71,** 129–140.

Ixart G, Barbanel G & Assenmaeher I (1991). A quantitative study of the pulsatile parameters of CRH-41 secretion in unanesthetized free-moving rats. *Exp Brain Res* **87,** 153–158.

Jeffries O, Geiger N, Rowe ICM, Tian L, McClafferty H, Chen L, Bi D, Knaus HG, Ruth P & Shipston MJ (2010). Palmitoylation of the S0-S1 linker regulates cell surface expression of voltage- and calcium-activated potassium (BK) channels. *J Biol Chem* **285,** 33307–33314.

Jiao H, Arner P, Hoffstedt J, Brodin D, Dubern B, Czernichow S, Van'T Hooft F, Axelsson T, Pedersen O, Hansen T, Sørensen TI, Hebebrand J, Kere J, Dahlman-Wright K, Hamsten A, Clement K & Dahlman I (2011). Genome wide association study identifies KCNMA1 contributing to human obesity. *BMC Med Genomics* **4,** 4:51.

Joëls M & de Kloet ER (1992). Control of neuronal excitability by corticosteroid hormones. *Trends Neurosci* **15,** 25–30.

Kelberman D, Rizzoti K, Lovell-Badge R, Robinson ICAF & Dattani MT (2009). Genetic regulation of pituitary gland development in human and mouse. *Endocr Rev* **30,** 790–829.

Keller-Wood ME & Dallman MF (1984). Corticosteroid inhibition of ACTH secretion. *Endocr Rev* **5,** 1–24.

Konturek PC, Brzozowski T & Konturek SJ (2011). Stress and the gut : Pathophysiology, clinical consequences, diagnostic approach and treatment options. *J Physiol Pharmacol* **62,** 591–599.

Korbie DJ & Mattick JS (2008). Touchdown PCR for increased specificity and sensitivity in PCR amplification. *Nat Protoc* **3,** 1452–1456.

Krantz DS & McCeney MK (2002). Effects of psychological and social factors on organic disease: A critical assessment of research on coronary heart disease. *Annu Rev Psychol* **53,** 341–369.

Kroeze WK, Sassano MF, Huang XP, Lansu K, McCorvy JD, Giguère PM, Sciaky N & Roth BL (2015). PRESTO-Tango as an open-source resource for interrogation of the druggable human GPCRome. *Nat Struct Mol Biol* **22,** 362–369.

Kudielka BM & Kirschbaum C (2005). Sex differences in HPA axis responses to stress: A review. *Biol Psychol* **69,** 113–132.

Kuryshev YA, Childs GV. & Ritchie AK (1996). Corticotropin-releasing hormone stimulates $Ca^{2+}$ through L- and P-Type $Ca^{2+}$ Channels in Rat Corticotropes. *Endocrinology* **37,** 2269–2277.

Kuryshev YA, Childs GV & Ritchie AK (1995). Corticotropin-releasing hormone stimulation of $Ca^{2+}$ entry in corticotropes is partially dependent on protein kinase A. *Endocrinology* **136,** 3925–3935.

Kuryshev YA, Haak L, Childs GV. & Ritchie AK (1997). Corticotropin releasing hormone inhibits an inwardly rectifying potassium current in rat corticotropes. *J*

*Physiol* **502,** 265–279.

Labonté B et al. (2017). Sex-specific transcriptional signatures in human depression. **23,** 1102–1111.

Lagrutta A, Shen KZ, North RA & Adelman JP (1994). Functional differences among alternatively spliced variants of Slowpoke, a Drosophila calcium-activated potassium channel. *J Biol Chem* **269,** 20347–20351.

Lamberts SWJ, Verleun T, Oosterom R, de Jong F & Hackeng WHL (1984). Corticotropin-releasing factor (ovine) and vasopressin exert a synergistic effect on adrenocorticotropin release in man. *J Clin Endocrinol Metab* **58,** 298–303.

LeBeau AP, Robson AB, McKinnon AE, Donald RA & Sneyd J (1997). Generation of action potentials in a mathematical model of corticotrophs. *Biophys J* **73,** 1263–1275.

Lee AK, Smart JL, Rubinstein M, Low MJ & Tse A (2011). Reciprocal regulation of TREK-1 channels by arachidonic acid and CRH in mouse corticotropes. *Endocrinology* **152,** 1901–1910.

Lee AK & Tse A (1997). Mechanism underlying corticotropin-releasing hormone (CRH) triggered cytosolic $Ca^{2+}$ rise in identified rat corticotrophs. *J Physiol* **504,** 367–378.

Lee AK, Tse FW & Tse A (2015). Arginine vasopressin potentiates the stimulatory action of CRH on pituitary corticotropes via a protein kinase C-dependent reduction of the background TREK-1 current. *Endocrinology* **156,** 3661–3672.

Leong DA (1988). A complex mechanism of facilitation in pituitary ACTH cells: recent single-cell studies. *J Exp Biol* **139,** 151–168.

Liang Z, Chen L, McClafferty H, Lukowski R, MacGregor D, King JT, Rizzi S, Sausbier M, McCobb DP, Knaus H-G, Ruth P & Shipston MJ (2011). Control of hypothalamic-pituitary-adrenal stress axis activity by the intermediate conductance calcium-activated potassium channel, SK4. *J Physiol* **589,** 5965–5986.

Lock JT, Parker I & Smith IF (2015). A comparison of fluorescent $Ca^{2+}$indicators for imaging local $Ca^{2+}$ signals in cultured cells. *Cell Calcium* **58,** 638–648.

Loechner KJ, Knox RJ, McLaughlin JT & Dunlap K (1999). Dexamethasone-mediated inhibition of calcium transients and ACTH release in a pituitary cell line (AtT-20). *Steroids* **64,** 404–412.

Luine V (2002). Sex differences in chronic stress effects on memory in rats. *Stress* **5,** 205–216.

Lundblad JR & Roberts JL (1988). Regulation of proopiomelanocortin gene

expression in pituitary. *Endocr Rev* **9,** 135–158.

Maeng LY & Milad MR (2015). Sex differences in anxiety disorders: Interactions between fear, stress, and gonadal hormones. *Horm Behav* **76,** 106–117.

Majzoub JA (2006). Corticotropin-releasing hormone physiology. *Eur J Endocrinol* **155,** S71–S76.

Mao T, O'Connor DH, Scheuss V, Nakai J & Svoboda K (2008). Characterization and subcellular targeting of GCaMP-type genetically-encoded calcium indicators. *PLoS One* **3,** e1796.

Mazure CM (1998). Life stressors as risk factors in depression. *Clin Psychol Sci Pract* **5,** 291–313.

Meera P, Wallner M, Song M & Toro L (1997). Large conductance voltage- and calcium-dependent $K^+$ channel, a distinct member of voltage-dependent ion channels with seven N-terminal transmembrane segments (S0-S6), an extracellular N terminus, and an intracellular (S9-S10) C terminus. *Proc Natl Acad Sci U S A* **94,** 14066–14071.

Meera P, Wallner M & Toro L (2000). A neuronal β subunit (KCNMB4) makes the large conductance, voltage- and $Ca^{2+}$-activated $K^+$ channel resistant to charybdotoxin and iberiotoxin. *Proc Natl Acad Sci* **97,** 5562–5567.

Mental Health Foundation (2018). Research report: Stress are we coping. *Ment Heal Found*.

Mollard P, Vacher P, Guerin J, Rogawski MA & Dufy B (1987). Electrical properties of cultured human adrenocorticotropin-secreting adenoma cells: effects of high $K^+$, corticotropin-releasing factor, and angiotensin II. *Endocrinology* **121,** 395–405.

Morey JN, Boggero IA, Scott AB & Segerstrom SC (2015). Current directions in stress and human immune function. *Curr Opin Psychol* **5,** 13–17.

Murat B, Devost D, Andrés M, Mion J, Boulay V, Corbani M, Zingg HH & Guillon G (2012). V1b and CRHR1 receptor heterodimerization mediates synergistic biological actions of vasopressin and CRH. *Mol Endocrinol* **26,** 502–520.

Nakai J, Ohkura M & Imoto K (2001). A high signal-to-noise $Ca^{2+}$ probe composed of a single green fluorescent protein. *Nat Biotechnol* **19,** 137–141.

Naumenko VS & Ponimaskin E (2018). Palmitoylation as a functional regulator of neurotransmitter receptors. *Neural Plast* **2018,** 5701348.

Nieuwenhuizen AG & Rutters F (2008). The hypothalamic-pituitary-adrenal-axis in the regulation of energy balance. *Physiol Behav* **94,** 169–177.

Ohno Y, Kihara A, Sano T & Igarashi Y (2006). Intracellular localization and tissue-

specific distribution of human and yeast DHHC cysteine-rich domain-containing proteins. *Biochim Biophys Acta* **1761,** 474–483.

Ooi GT, Tawadros N & Escalona RM (2004). Pituitary cell lines and their endocrine applications. *Mol Cell Endocrinol* **228,** 1–21.

Orio P, Rojas P, Ferreira G & Latorre R (2002). New disguises for an old channel: MaxiK channel β-Subunits. *News Physiol Sci* **17,** 156–161.

Oster H, Challet E, Ott V, Arvat E, de Kloet ER, Dijk DJ, Lightman S, Vgontzas A & Van Cauter E (2017). The functional and clinical significance of the 24-hour rhythm of circulating glucocorticoids. *Endocr Rev* **38,** 3–45.

Palmer AE & Tsien RY (2006). Measuring calcium signaling using genetically targetable fluorescent indicators. *Nat Protoc* **1,** 1057–1065.

Panagiotakopoulos L & Neigh GN (2014). Development of the HPA axis: Where and when do sex differences manifest? *Front Neuroendocrinol* **35,** 285–302.

Papadimitriou A & Priftis KN (2009). Regulation of the hypothalamic-pituitary-adrenal axis. *Neuroimmunomodulation* **16,** 265–271.

Perry JL, Ramachandran NK, Utama B & Hyser JM (2015). Use of genetically-encoded calcium indicators for live cell calcium imaging and localization in virus-infected cells. *Methods* **90,** 28–38.

Pozzoli G, Bilezikjian LM, Perrin MH, Blount AL & Vale WW (1996). Corticotropin-releasing factor (CRF) and glucocorticoids modulate the expression of type 1 CRF receptor messenger ribonucleic acid in rat anterior pituitary cell cultures. *Endocrinology* **137,** 65–71.

Raffin-Sanson ML, de Keyzer Y & Bertagna X (2003). Proopiomelanocortin, a polypeptide precursor with multiple functions: From physiology to pathological conditions. *Eur J Endocrinol* **149,** 79–90.

Ratka A, Sutanto W, Bloemers M & de Kloet ER (1989). On the role of brain mineralocorticoid (type I) and glucocorticoid (type II) receptors in neuroendocrine regulation. *Neuroendocrinology* **50,** 117–123.

Regitz-Zagrosek V & Kararigas G (2017). Mechanistic pathways of sex differences in cardiovascular disease. *Physiol Rev* **97,** 1–37.

Resh MD (2006*a*). Use of analogs and inhibitors to study the functional significance of protein palmitoylation. *Methods* **40,** 191–197.

Resh MD (2006*b*). Trafficking and signaling by fatty-acylated and prenylated proteins. *Nat Chem Biol* **2,** 584–590.

Ritchie AK, Kuryshev YA & Childs GV (1996). Corticotropin-Releasing Hormone and Calcium Signaling in Corticotropes. *Trends Endocrinol Metab* **7,** 365–369.

Romanò N, McClafferty H, Walker JJ, Tissier P Le & Shipston MJ (2017). Heterogeneity of calcium responses to secretagogues in corticotrophs from male rats. *Endocrinology* **158,** 1849–1858.

Saito M, Nelson C, Salkoff L & Lingle CJ (1997). A cysteine-rich domain defined by a novel exon in a Slo variant in rat adrenal chromaffin cells and PC12 cells. *J Biol Chem* **272,** 11710–11717.

Saleem F, Rowe ICM & Shipston MJ (2009). Characterization of BK channel splice variants using membrane potential dyes. *Br J Pharmacol* **156,** 143–152.

Sausbier M et al. (2005). Elevated blood pressure linked to primary hyperaldosteronism and impaired vasodilation in BK channel-deficient mice. *Circulation* **112,** 60–68.

Sausbier M, Hu H, Arntz C, Feil S, Kamm S, Adelsberger H, Sausbier U, Sailer CA, Feil R, Hofmann F, Korth M, Shipston MJ, Knaus H-G, Wolfer DP, Pedroarena CM, Storm JF & Ruth P (2004). Cerebellar ataxia and Purkinje cell dysfunction caused by $Ca^{2+}$-activated $K^+$ channel deficiency. *Proc Natl Acad Sci U S A* **101,** 9474–9478.

Sausbier M, Zhou X-B, Caroline B, Sausbier U, Wolpers D, Sylvi M, Christian M, Alexander D, Anna-Rebekka R, Harald R, Jens S, Franz H, Winfried N, Thomas G, Stefan U, Michael K & Peter R (2006). Reduced rather than enhanced cholinergic airway constriction in mice with ablation of the large conductance $Ca^{2+}$-activated $K^+$ channel. *FASEB J* **21,** 812–822.

Schindelin J, Arganda-Carreras I, Frise E, Kaynig V, Longair M, Pietzsch T, Preibisch S, Rueden C, Saalfeld S, Schmid B, Tinevez J-Y, White DJ, Hartenstein V, Eliceiri K, Tomancak P & Cardona A (2012). Fiji: an open-source platform for biological-image analysis. *Nat Methods* **9,** 676–682.

Seibold MA, Wang B, Eng C, Kumar G, Beckman KB, Sen S, Choudhry S, Meade K, Lenoir M, Watson HG, Thyne S, Williams LK, Kumar R, Weiss KB, Grammer LC, Avila PC, Schleimer RP, Burchard EG & Brenner R (2008). An african-specific functional polymorphism in KCNMB1 shows sex-specific association with asthma severity. *Hum Mol Genet* **17,** 2681–2690.

Sheward WJ & Fink G (1991). Effects of corticosterone on the secretion of corticotrophin-releasing factor, arginine vasopressin and oxytocin into hypophysial portal blood in long-term hypophysectomized rats. *J Endocrinol* **129,** 91–98.

Shipston MJ (1995). Mechanism(s) of early glucocorticoid inhibition of adrenocorticotropin secretion from anterior pituitary corticotropes. *Elsevier Sci Inc* **6,** 261–266.

Shipston MJ (2011). Ion channel regulation by protein palmitoylation. *J Biol Chem* **286,** 8709–8716.

Shipston MJ (2013). Regulation of large conductance calcium- and voltage-activated potassium (BK) channels by S-palmitoylation. *Biochem Soc Trans* **41,** 67–71.

Shipston MJ (2014*a*). Ion channel regulation by protein S-acylation. *J Gen Physiol* **143,** 659–678.

Shipston MJ (2014*b*). S-acylation dependent post-translational cross-talk regulates large conductance calcium- and voltage- activated potassium (BK) channels. *Front Physiol* **5,** 281.

Shipston MJ (2018). Control of anterior pituitary cell excitability by calcium-activated potassium channels. *Mol Cell Endocrinol* **463,** 37–48.

Slavich GM & Irwin MR (2014). From stress to inflammation and major depressive disorder: A social signal transduction theory of depression. *Psychol Bull* **140,** 774–815.

Soares SM, Thompson M & Chini EN (2005). Role of the second-messenger cyclic-adenosine 5′-diphosphate-ribose on adrenocorticotropin secretion from pituitary cells. *Endocrinology* **146,** 2186–2192.

Sorge RE & Totsch SK (2017). Sex Differences in Pain. *J Neurosci Res* **95,** 1271–1281.

Spiga F, Walker JJ, Terry JR & Lightman SL (2014). HPA axis-rhythms. *Compr Physiol* **4,** 1273–1298.

Sprossmann F, Pankert P, Sausbier U, Wirth A, Zhou X-B, Madlung J, Zhao H, Bucurenciu I, Jakob A, Lamkemeyer T, Neuhuber W, Offermanns S, Shipston MJ, Korth M, Nordheim A, Ruth P & Sausbier M (2009). Inducible knockout mutagenesis reveals compensatory mechanisms elicited by constitutive BK channel deficiency in overactive murine bladder. *FEBS J* **276,** 1680–1697.

Steptoe A & Mika Kivimäki (2012). Stress and cardiovascular disease. *Nat Rev Cardiol* **9,** 360–370.

Stojilkovic SS (2008). Ion Channels, Transporters, and Electrical Signaling. In *Neuroscience in Medicine*, Third Edit., ed. Conn PM, pp. 53–89. Humana Press, Totowa, NJ. Available at: https://doi.org/10.1007/978-1-60327-455-5_3.

Stojilkovic SS (2012). Molecular mechanisms of pituitary endocrine cell calcium handling. *Cell Calcium* **51,** 212–221.

Stojilkovic SS, Tabak J & Bertram R (2010). Ion Channels and Signaling in the Pituitary Gland. *Endocr Rev* **31,** 845–915.

Stojilkovic SS, Zemkova H & Van Goor F (2005). Biophysical basis of pituitary cell type-specific $Ca^{2+}$ signaling-secretion coupling. *Trends Endocrinol Metab* **16,** 152–159.

String-db.org (2019). zDHHC23 protein (mouse) - STRING interaction network.

Stroud CB, Davila J & Moyer A (2008). The relationship between stress and depression in first onsets versus recurrences: A meta-analytic review. *J Abnorm Psychol* **117,** 206–213.

Surprenant A (1982). Correlation between electrical activity and ACTH/β-endorphin secretion in mouse pituitary tumor cells. *J Cell Biol* **95,** 559–566.

Suzuki J, Kanemaru K & Iino M (2016). Genetically encoded fluorescent indicators for organellar calcium imaging. *Biophys J* **111,** 1119–1131.

Szklarczyk D, Morris JH, Cook H, Kuhn M, Wyder S, Simonovic M, Santos A, Doncheva NT, Roth A, Bork P, Jensen LJ & Von Mering C (2017). The STRING database in 2017: Quality-controlled protein-protein association networks, made broadly accessible. *Nucleic Acids Res* **45,** D362–D368.

Tabak J, Tomaiuolo M, Gonzalez-Iglesias AE, Milescu LS & Bertram R (2011). Fast-activating voltage- and calcium-dependent potassium (BK) conductance promotes bursting in pituitary cells: A dynamic clamp study. *J Neurosci* **31,** 16855–16863.

Tagliavini A, Tabak J, Bertram R & Pedersen MG (2016). Is bursting more effective than spiking in evoking pituitary hormone secretion? A spatiotemporal simulation study of calcium and granule dynamics. *Am J Physiol Metab* **310,** E515–E525.

Takano K, Yasufuku-Takano J, Teramoto A & Fujita T (1996). Corticotropin-releasing hormone excites adrenocorticotropin-secreting human pituitary adenoma cells by activating a nonselective cation current. *J Clin Invest* **98,** 2033–2041.

Tasker JG, Di S & Malcher-Lopes R (2006). Minireview: Rapid glucocorticoid signaling via membrane-associated receptors. *Endocrinology* **147,** 5549–5556.

Tian L, Coghill LS, McClafferty H, MacDonald SH-F, Antoni FA, Ruth P, Knaus H-G & Shipston MJ (2004). Distinct stoichiometry of BKCa channel tetramer phosphorylation specifies channel activation and inhibition by cAMP-dependent protein kinase. *Proc Natl Acad Sci U S A* **101,** 11897–11902.

Tian L, Duncan RR, Hammond MSL, Coghill LS, Wen H, Rusinova R, Clark AG, Levitan IB & Shipston MJ (2001). Alternative splicing switches potassium channel sensitivity to protein phosphorylation. *J Biol Chem* **276,** 7717–7720.

Tian L, Jeffries O, McClafferty H, Molyvdas A, Rowe ICM, Saleem F, Chen L, Greaves J, Chamberlain LH, Knaus H-G, Ruth P & Shipston MJ (2008). Palmitoylation gates phosphorylation-dependent regulation of BK potassium channels. *Proc Natl Acad Sci U S A* **105,** 21006–21011.

Tian L, McClafferty H, Jeffries O & Shipston MJ (2010). Multiple

palmitoyltransferases are required for palmitoylation-dependent regulation of large conductance calcium- and voltage-activated potassium channels. *J Biol Chem* **285,** 23954–23962.

Tian L, McClafferty H, Knaus H-G, Ruth P & Shipston MJ (2012). Distinct acyl protein transferases and thioesterases control surface expression of calcium-activated potassium channels. *J Biol Chem* **287,** 14718–14725.

Truett GE, Heeger P, Mynatt RL, Truett AA, Walker JA & Warman ML (2000). Preparation of PCR-quality mouse genomic DNA with hot sodium hydroxide and tris (HotSHOT). *Biotechniques* **29,** 52–54.

Tsaneva-Atanasova K, Sherman A, Van Goor F & Stojilkovic SS (2007). Mechanism of spontaneous and receptor-controlled electrical activity in pituitary somatotrophs: Experiments and theory. *J Neurophysiol* **98,** 131–144.

Tse A & Hille B (1992). GnRH-induced $Ca^{2+}$ oscillations and rhythmic hyperpolarizations of pituitary gonadotropes. *Science* **255,** 462–464.

Tse A & Lee AK (1998). Arginine vasopressin triggers intracellular calcium release, a calcium-activated potassium current and exocytosis in identified rat corticotropes. *Endocrinology* **139,** 2246–2252.

Tse A, Tse FW, Almers W & Hille B (1993). Rhythmic exocytosis stimulated by GnRH-induced calcium oscillations in rat gonadotropes. *Science* **260,** 82–84.

Tseng-Crank J, Foster CD, Krause JD, Mertz R, Godinot N, DiChiara TJ & Reinhartt PH (1994). Cloning, expression, and distribution of functionally distinct $Ca^{2+}$-activated $K^+$ channel isoforms from human brain. *Neuron* **13,** 1315–1330.

Vale W, Rivier C, Brown MR, Spies J, Koob G, Swanson L, Bilezikjian L, Bloom F & Rivier J (1983). Chemical and biological characterization of corticotropin releasing factor. In *Recent Progress in Hormone Research*, pp. 245–270.

Vale W, Spies J, Rivier C & Rivier J (1981). Characterization of a 41-Residue Ovine Hypothalamic Peptide That Stimulates Secretion of Corticotropin and β-Endorphin. *Science* **213,** 1394–1397.

Walker JJ, Terry JR & Lightman SL (2010). Origin of ultradian pulsatility in the hypothalamic-pituitary-adrenal axis. *Proc R Soc B* **277,** 1627–1633.

Wang Z-W, Saifee O, Nonet ML & Salkoff L (2001). SLO-1 potassium channels control quantal content of neurotransmitter release at the C. elegans neuromuscular junction. *Neuron* **32,** 867–881.

Weich S, Sloggett A & Lewis G (2001). Social roles and the gender difference in rates of the common mental disorders in Britain: A 7-year, population-based cohort study. *Psychol Med* **31,** 1055–1064.

Wellman GC & Nelson MT (2003). Signaling between SR and plasmalemma in smooth muscle: Sparks and the activation of $Ca^{2+}$-sensitive ion channels. *Cell Calcium* **34,** 211–229.

Woods MD, Shipston MJ, Mullens EL & Antoni FA (1992). Pituitary corticotrope tumor (AtT20) cells as a model system for the study for early inhibition by glucorticoids. *Endocrinology* **131,** 2873–2880.

Xie J & McCobb DP (1998). Control of alternative splicing of potassium channels by stress hormones. *Science* **280,** 443–446.

Yamamori E, Iwasaki Y, Oki Y, Yoshida M, Asai M, Kambayashii M, Oiso Y & Nakashima N (2004). Possible involvement of ryanodine receptor-mediated intracellular calcium release in the effect of corticotropin-releasing factor on adrenocorticotropin seretion. *Endocrinology* **145,** 36–38.

Yan J & Aldrich RW (2012). BK potassium channel modulation by leucine-rich repeat-containing proteins. *Proc Natl Acad Sci U S A* **109,** 7917–7922.

Yan Y, Dominguez S, Fisher DW & Dong H (2018). Sex differences in chronic stress responses and Alzheimer's disease. *Neurobiol Stress* **8,** 120–126.

Yeung CM, Chan CB, Leung PS & Cheng CHK (2006). Cells of the anterior pituitary. *Int J Biochem Cell Biol* **38,** 1441–1449.

Yoshimura S, Sakamoto S, Kudo H, Sassa S, Kumai A & Okamoto R (2003). Sex-differences in adrenocortical responsiveness during development in rats. *Steroids* **68,** 439–445.

Zarei MM, Zhu N, Alioua A, Eghbali M, Stefani E & Toro L (2001). A novel MaxiK splice variant exhibits dominant-negative properties for surface expression. *J Biol Chem* **276,** 16232–16239.

Zhou X, Arntz C, Kamm S, Motejlek K, Sausbier U, Wang G-X, Ruth P & Korth M (2001). A molecular switch for specific stimulation of the BKCa channel by cGMP and cAMP kinase. *J Biol Chem* **276,** 43239–43245.

Zhou X, Wulfsen I, Korth M, McClafferty H, Lukowski R, Shipston MJ, Ruth P, Dobrev D & Wieland T (2012). Palmitoylation and membrane association of the stress axis regulated insert (STREX) controls BK channel regulation by protein kinase C. *J Biol Chem* **287,** 32161–32171.

Zhou X, Wulfsen I, Utku E, Sausbier U, Sausbier M, Wieland T, Ruth P & Korth M (2010). Dual role of protein kinase C on BK channel regulation. *Proc Natl Acad Sci U S A* **107,** 8005–8010.

# Appendices

# Appendices

## I. The UI script

```
library(shiny)

setwd("working directory")
files <- dir(pattern = "csv$")
files <- files[grep("treatments", files, invert = T)]

shinyUI(
  fluidPage
      (
      titlePanel("Calcium Imaging Analysis"),
      sidebarLayout
        (
        sidebarPanel
            (
            selectInput("experiment", "Experiment", choices = c("Select an
experiment", files)),
            selectInput("visualization", label = "Plot type", choices = c("All traces" =
"traces",
                                                "Single trace" = "single")),
            fluidRow(
              column(width = 3,numericInput("timeFrom", "Min time", min = 0, max
                          = 1000,                  step = 0.5, value = 0,width = 100)),
              column(width = 3, numericInput("timeTo", "Max time", min = 0, max =
                          1000,                    step = 0.5, value = 120, width = 100)),
              column(width = 3, numericInput("yFrom", "Min y", step = 0.5, value =
                          0, width                 = 100)),
              column(width = 3, numericInput("yTo", "Max y", step = 0.5, value =
                          1000, width                  = 100)),
              column(width = 5, checkboxInput("autoscaleY", "autoscale y", value =
TRUE)),
              column(width = 5, checkboxInput("normalise", "normalise y", value =
FALSE))
               ),
          downloadButton('downloadPlot', 'Download Plot (PDF)'),
          conditionalPanel(
             "(input.visualization == 'single' || input.visualization == 'peaks') &&
input.experiment != 'Select an experiment'",
            sliderInput("traceNum", label = "Trace #", min = 1, max = 10, step = 1,
value = 1, round = TRUE, ticks = FALSE),
            checkboxInput("bgSub", label = "Background subtracted", value =
TRUE),
            checkboxInput("showBase", label = "Show baseline", value = TRUE),
```

```
                checkboxInput("showActThr", label = "Show activity threshold", value
= FALSE),
                sliderInput("centile", label = "Centile", min = 1, max = 100, step = 1,
value = 10),
                sliderInput("span", label = "Span", value = 0.2, min = 0.01, max = 2, step
= 0.01),
                sliderInput("activityThresh", label = "Activity threshold", value = 0.15,
min = 0.01, max = 1, step = 0.01)
              ),
              conditionalPanel(
                 "input.visualization == 'single' && input.experiment != 'Select an
experiment'",
                  checkboxInput("showTreatments", "Show treatments", value =
TRUE),
                  checkboxInput("showStats", "Show statistics", value = TRUE)
                ),
              conditionalPanel(
                  "input.showStats == 1 && input.visualization == 'single'
                    && input.experiment != 'Select an experiment'",
                  verbatimTextOutput("plotStats")
                  )
              ),
            mainPanel
              (
                plotOutput("mainPlot", height = "500px", click = "plotClick", hover =
hoverOpts("plot_hover", delay = 100, delayType = "throttle")),
                conditionalPanel(
                    "input.visualization == 'single'
                    && input.experiment != 'Select an experiment'",
                    verbatimTextOutput("plotCoords")),
                conditionalPanel(
                    "input.visualization != 'peaks'
                    && input.experiment != 'Select an experiment'",
                    tableOutput("treatmentTable"))
                              )
        )
    )
  )
```

# II. The Sever script

```
library(shiny)

fmt <- function(num, dig = 2)
  {
  format(num, nsmall = dig, digits = dig, scientific = FALSE)
  }

shinyServer(function(input, output, clientData, session)
  {
  read.data <- reactive(
    {
    if (input$experiment != "Select an experiment")
      {
      tmp <- read.csv(input$experiment)
      calcium$traces <- as.matrix(tmp[, !(colnames(tmp) %in% c("Background",
"Time"))])
      if (is.null(tmp$Background))
        calcium$bg <- 1:nrow(calcium$traces)
      else
        calcium$bg <- tmp$Background
      if (is.null(tmp$Time))
        calcium$time <- rep(0, nrow(calcium$traces))
      else
        calcium$time <- tmp$Time
      treatments.file <- paste(substr(input$experiment, 1, nchar(input$experiment) -
4), "- treatments.csv")
      if (file.exists(treatments.file))
        calcium$treatments <- read.csv(treatments.file)
      else
        calcium$treatments <- NULL

      calcium$baseline <- NULL
      calcium$baselinesd <- NULL

      updateSliderInput(session, "traceNum", max = ncol(calcium$traces))
      updateNumericInput(session, "timeTo", value = max(calcium$time)/60)

      calcium$peaks.start <- NULL
      calcium$peaks.end <- NULL
      calcium$peaks <- NULL
      }
    })

  calcium <- reactiveValues()
  clicksValues <- reactiveValues(
```

```
    click1 = NULL,
    range = NULL
    )

  observeEvent(input$plotClick,
               {
               if (is.null(clicksValues$click1))
                    {
                    clicksValues$click1 <- max(1, input$plotClick$x) * 60
                    clicksValues$range <- NULL
                    }
               else
                    {
                    clicksValues$range <- range(clicksValues$click1, max(1,
input$plotClick$x) * 60)
                    clicksValues$click1 <- NULL
                    }
               })

  output$plotStats <- renderPrint(
    {
    trace <- calcium$traces[,input$traceNum]
    basecv <- trace[1:calcium$treatments$From[1]] -
              calcium$bg[1:calcium$treatments$From[1]]
    basecv <- (basecv - min(basecv)) / diff(range(basecv))
    basecv <- sd(basecv) / mean(basecv)

    if (is.null(clicksValues$range))
      {
      cat("Select a region of the plot (two clicks) to get stats.")
      }
    else
      {
      rg <- clicksValues$range

      region <- trace[rg[1]:rg[2]] - calcium$bg[rg[1]:rg[2]]
      region.scaled <- (region - min(trace-calcium$bg)) / diff(range(trace-
calcium$bg))

      output <- paste0("Length: ", fmt(diff(rg) / 60), " (", fmt(rg[1] / 60),
                       " to ", fmt(rg[2] / 60) ,")",
                       "\nMean value: ", fmt(mean(region)),
                       "\nMax value: ", fmt(max(region)),
                       " at ", fmt((which.max(region) + rg[1]) / 60),
                       "\nCV: ", fmt(sd(region)/mean(region)),
                       "\nAUC: ", fmt(sum(region) -
sum(calcium$baseline[rg[1]:rg[2]])),
                       "\n%Time active: ", fmt(sum(region.scaled >
```

```
input$activityThresh)/
                                                    length(region.scaled) * 100)
                          )
      cat(output)
      }
    })

  output$treatmentTable <- renderTable(
    {
    if (input$experiment == "Select an experiment")
      {
      NULL
      }
    else if (!is.null(calcium$treatments))
      {
      data.frame("Treatment" = calcium$treatments$Treatment,
                 "From" = calcium$treatments$From / 60,
                 "Duration" = calcium$treatments$Duration / 60)
      }
    else
      {
      NULL
      }
    })

  output$plotCoords <- renderPrint(
    if (!is.null(input$plot_hover) & input$visualization == "single")
      paste("X:", format(input$plot_hover$x, digits = 2, nsmall = 1),
            "- Y:", format(input$plot_hover$y, digits = 2, nsmall = 1))
    else
      cat(" ")
    )

  output$peakStats <- renderPrint(
    cat(paste("Number of peaks: ", length(calcium$peaks)))
    )

  plotTraceFn <- function()
      {
      read.data()

      if (input$experiment == "Select an experiment")
      {
        plot(0, 0, "n", axes = F, xlab = "", ylab = "")
      }
      else
      {
        if (!is.null(calcium$traces))
```

```
{

  if (input$visualization == "traces")
  {
    plot(0, 0, "n", ylim = c(1, ncol(calcium$traces) + 1), bty = "n",
         xlab = "Time (min)", ylab = "", yaxt = "n",
         xlim = c(input$timeFrom, input$timeTo)
    i <- 1
    apply(calcium$traces, 2, function(t)
    {
      t <- t - calcium$bg
      t <- (t - min(t)) / diff(range(t))
      lines(calcium$time / 60, t + i)
      i <<- i + 1
    })

    if (!is.null(calcium$treatments))
    {
      tr <- calcium$treatments
      rect(tr$From/60, 0, tr$From/60 + tr$Duration/60, ncol(calcium$traces)
* 2,
           border = 0, col = rgb(0, 0, 0, 0.2))
    }
  }

  else if (input$visualization == "single")
  {
    if (input$bgSub)
    {
      trace <- calcium$traces[,input$traceNum] - calcium$bg
    }
    else
    {
      trace <- calcium$traces[,input$traceNum]
    }
    times <- calcium$time / 60
    if (input$normalise)
    {
      plot(times, (trace-min(trace)) / (max(trace)-min(trace)), t = "l", las = 1,
xlim = c(input$timeFrom, input$timeTo), ylim = c(0, 1), xlab = "Time (min)", ylab =
"", bty = "n", yaxt = "n")
      axis(2, at = seq(0, 1, 0.2), las = 1)
    }
    else if (input$autoscaleY)
      plot(times, trace, t = "l", las = 1, xlim = c(input$timeFrom,
input$timeTo), xlab = "Time (min)", ylab = "", bty = "n")
    else
      plot(times, trace, t = "l", las = 1, xlim = c(input$timeFrom,
```

```
input$timeTo), xlab = "Time (min)", ylab = "", bty = "n", ylim = c(input$yFrom,
input$yTo))

        if (!is.null(calcium$treatments) & input$showTreatments)
        {
          tr <- calcium$treatments
          rect(tr$From/60, -100, tr$From/60 + tr$Duration/60, max(trace) * 2,
               border = 0, col = rgb(0, 0, 0, 0.2))
        }

        if (input$showBase)
        {
          q <- quantile(trace, input$centile/100)
          baseline <- trace
          baseline[baseline >= q] <- q
          ls <- loess(baseline ~ times, span = input$span)
          calcium$baseline <- predict(ls)
          lines(times, calcium$baseline, col = "darkgreen", lwd = 2)
        }

        if (input$showActThr)
        {
          if (input$normalise)
            abline(h = input$activityThresh, lty = "dashed", col = "orange")
          else
            abline(h = min(trace) + input$activityThresh * diff(range(trace)),
                   lty = "dashed", col = "orange")
        }

        if (input$showStats)
        {
          rn <- clicksValues$range

          if (!is.null(clicksValues$click1))
          {
            abline(v = clicksValues$click1/60, lwd = 2, col = "darkorange")
          }

          if (!is.null(rn))
          {
            rect(rn[1]/60, -100, rn[2]/60, max(trace) * 2,
                 col = rgb(.9, .4, 0, .1), border = "darkorange")

            region <- trace[rn[1]:rn[2]]

            if (!is.null(calcium$baseline))
              polygon(c(times[rn[1]:rn[2]], times[rn[2]:rn[1]]),
                      c(region, calcium$baseline[rn[2]:rn[1]]), col = rgb(0, 0.4,
```

```
0.8, 0.5),
                                border = NA)
                    }
                  }
                }

                else if (input$visualization == "peaks")
                {
                  if (input$bgSub)
                  {
                    trace <- calcium$traces[,input$traceNum] - calcium$bg
                  }
                  else
                  {
                    trace <- calcium$traces[,input$traceNum]
                  }
                  times <- calcium$time / 60
                  if (input$autoscaleY)
                    plot(times, trace, t = "l", las = 1, xlim = c(input$timeFrom,
input$timeTo), xlab = "Time (min)", ylab = "", bty = "n")
                  else
                    plot(times, trace, t = "l", las = 1, xlim = c(input$timeFrom,
input$timeTo), xlab = "Time (min)", ylab = "", bty = "n", ylim = c(input$yFrom,
input$yTo))

                  q <- quantile(trace, input$centile/100)
                  baseline <- trace
                  baseline[baseline >= q] <- q
                  ls <- loess(baseline ~ times, span = input$span)
                  calcium$baseline <- predict(ls)

                  if (input$showBase)
                  {
                    lines(times, calcium$baseline, col = "darkgreen", lwd = 2)
                  }

                  calcium$baselinesd <- sd(trace[trace <= quantile(trace,
input$centile/100)])

                  threshold <- baseline + input$minheight * calcium$baselinesd

                  calcium$peaks <- NULL
                  calcium$peaks.start <- NULL
                  calcium$peaks.end <- NULL

                  t <- 2
                  last.end <- 1
```

```
while (t < length(trace))
{
  if (trace[t] > threshold[t])
  {
    start <- which((trace[last.end:t] - baseline[last.end:t]) <= 0)
    if (length(start) > 0)
      start <- max(start) + last.end
    else
    {
      t <- t + 1
      next
    }
    end <- which((trace[-1:-t] - baseline[-1:-t]) <= 0)
    if (length(end) > 0)
      end <- min(end) + t
    else
    {
      t <- t + 1
      next
    }

    last.end <- end

    peak <- which.max(trace[start:last.end]) + start - 1

    if ((end - start) >= input$peakwidth[1] &
        (end - start) <= input$peakwidth[2])
    {
      calcium$peaks.start <- c(calcium$peaks.start, start)
      calcium$peaks.end <- c(calcium$peaks.end, end)
      calcium$peaks <- c(calcium$peaks, peak)

      t <- tail(calcium$peaks.end, 1) + 1
    }
  }

  t <- t + 1
}

if (input$showPeaks)
{
  points(times[calcium$peaks], trace[calcium$peaks], col = "purple", pch
= 20, cex = 2)
  points(times[calcium$peaks.start], trace[calcium$peaks.start], col =
"blue", pch = 20, cex = 1)
  points(times[calcium$peaks.end], trace[calcium$peaks.end], col =
"orange", pch = 20, cex = 1)
}
```

```
            }
          }
        }
    }

output$mainPlot <- renderPlot(
    {
    plotTraceFn()
    })

output$downloadPlot <- downloadHandler(
    contentType = "application/pdf",
    filename = "plot.pdf",
    content = function(file)
        {
        pdf(file, width = 10, height = 8)
        plotTraceFn()
        dev.off()
        }
    )

})
```